ISSN 1007-9327 (print)
ISSN 2219-2840 (online)

World Journal of *Gastroenterology*

World J Gastroenterol 2017 March 14; 23(10): 1735-1924

Published by Baishideng Publishing Group Inc

World Journal of Gastroenterology

A peer-reviewed, online, open-access journal of gastroenterology and hepatology

Editorial Board

2014-2017

The *World Journal of Gastroenterology* Editorial Board consists of 1375 members, representing a team of worldwide experts in gastroenterology and hepatology. They are from 68 countries, including Algeria (2), Argentina (7), Australia (31), Austria (9), Belgium (11), Brazil (20), Brunei Darussalam (1), Bulgaria (2), Cambodia (1), Canada (25), Chile (4), China (165), Croatia (2), Cuba (1), Czech (6), Denmark (2), Egypt (9), Estonia (2), Finland (6), France (20), Germany (58), Greece (31), Guatemala (1), Hungary (14), Iceland (1), India (33), Indonesia (2), Iran (10), Ireland (9), Israel (18), Italy (194), Japan (149), Jordan (1), Kuwait (1), Lebanon (7), Lithuania (1), Malaysia (1), Mexico (11), Morocco (1), Netherlands (5), New Zealand (4), Nigeria (3), Norway (6), Pakistan (6), Poland (12), Portugal (8), Puerto Rico (1), Qatar (1), Romania (10), Russia (3), Saudi Arabia (2), Singapore (7), Slovenia (2), South Africa (1), South Korea (69), Spain (51), Sri Lanka (1), Sudan (1), Sweden (12), Switzerland (5), Thailand (7), Trinidad and Tobago (1), Tunisia (2), Turkey (55), United Kingdom (49), United States (180), Venezuela (1), and Vietnam (1).

Gordon Stanley Howarth, *Roseworthy*
Seungha Kang, *Brisbane*
Alfred King Lam, *Gold Coast*
Ian C Lawrance, *PerthFremantle*
Barbara Anne Leggett, *Brisbane*
Daniel A Lemberg, *Sydney*
Rupert W Leong, *Sydney*
Finlay A Macrae, *Victoria*
Vance Matthews, *Melbourne*
David L Morris, *Sydney*
Reme Mountifield, *Bedford Park*
Hans J Netter, *Melbourne*
Nam Q Nguyen, *Adelaide*
Liang Qiao, *Westmead*
Rajvinder Singh, *Adelaide*
Ross Cyril Smith, *StLeonards*
Kevin J Spring, *Sydney*
Debbie Trinder, *Fremantle*
Daniel R van Langenberg, *Box Hill*
David Ian Watson, *Adelaide*
Desmond Yip, *Garran*
Li Zhang, *Sydney*

Austria

Felix Aigner, *Innsbruck*
Gabriela A Berlakovich, *Vienna*
Herwig R Cerwenka, *Graz*
Peter Ferenci, *Wien*
Alfred Gangl, *Vienna*
Kurt Lenz, *Linz*
Markus Peck-Radosavljevic, *Vienna*
Markus Raderer, *Vienna*
Stefan Riss, *Vienna*

Belgium

Michael George Adler, *Brussels*
Benedicte Y De Winter, *Antwerp*
Mark De Ridder, *Jette*
Olivier Detry, *Liege*
Denis Dufrane Dufrane, *Brussels*
Sven M Francque, *Edegem*
Nikos Kotzampassakis, *Liège*
Geert KMM Robaeys, *Genk*
Xavier Sagaert, *Leuven*
Peter Starkel, *Brussels*
Eddie Wisse, *Keerbergen*

Brazil

SMP Balzan, *Santa Cruz do Sul*
JLF Caboclo, *Sao jose do rio preto*
Fábio Guilherme Campos, *Sao Paulo*
Claudia RL Cardoso, *Rio de Janeiro*
Roberto J Carvalho-Filho, *Sao Paulo*
Carla Daltro, *Salvador*
José Sebastiao dos Santos, *Ribeirao Preto*
Eduardo LR Mello, *Rio de Janeiro*
Sthela Maria Murad-Regadas, *Fortaleza*
Claudia PMS Oliveira, *Sao Paulo*
Júlio C Pereira-Lima, *Porto Alegre*
Marcos V Perini, *Sao Paulo*
Vietla Satyanarayana Rao, *Fortaleza*
Raquel Rocha, *Salvador*
AC Simoes e Silva, *Belo Horizonte*
Mauricio F Silva, *Porto Alefre*
Aytan Miranda Sipahi, *Sao Paulo*
Rosa Leonôra Salerno Soares, *Niterói*
Cristiane Valle Tovo, *Porto Alegre*
Eduardo Garcia Vilela, *Belo Horizonte*

Brunei Darussalam

Vui Heng Chong, *Bandar Seri Begawan*

Bulgaria

Tanya Kirilova Kadiyska, *Sofia*
Mihaela Petrova, *Sofia*

Cambodia

Francois Rouet, *Phnom Penh*

Canada

Brian Bressler, *Vancouver*
Frank J Burczynski, *Winnipeg*
Wangxue Chen, *Ottawa*
Francesco Crea, *Vancouver*
Jane A Foster, *Hamilton*
Hugh J Freeman, *Vancouver*
Shahrokh M Ghobadloo, *Ottawa*
Yuewen Gong, *Winnipeg*
Philip H Gordon, *Quebec*
Rakesh Kumar, *Edmonton*
Wolfgang A Kunze, *Hamilton*
Patrick Labonte, *Laval*
Zhikang Peng, *Winnipeg*
Jayadev Raju, *Ottawa*
Maitreyi Raman, *Calgary*
Giada Sebastiani, *Montreal*
Maida J Sewitch, *Montreal*
Eldon A Shaffer, *Alberta*
Christopher W Teshima, *Edmonton*
Jean Sévigny, *Québec*
Pingchang Yang, *Hamilton*
Pingchang Yang, *Hamilton*
Eric M Yoshida, *Vancouver*
Bin Zheng, *Edmonton*

Chile

Marcelo A Beltran, *La Serena*
Flavio Nervi, *Santiago*
Adolfo Parra-Blanco, *Santiago*
Alejandro Soza, *Santiago*

China

Zhao-Xiang Bian, *Hong Kong*
San-Jun Cai, *Shanghai*
Guang-Wen Cao, *Shanghai*
Long Chen, *Nanjing*
Ru-Fu Chen, *Guangzhou*
George G Chen, *Hong Kong*
Li-Bo Chen, *Wuhan*
Jia-Xu Chen, *Beijing*
Hong-Song Chen, *Beijing*
Lin Chen, *Beijing*
Yang-Chao Chen, *Hong Kong*
Zhen Chen, *Shanghai*
Ying-Sheng Cheng, *Shanghai*
Kent-Man Chu, *Hong Kong*
Zhi-Jun Dai, *Xi'an*
Jing-Yu Deng, *Tianjin*
Yi-Qi Du, *Shanghai*
Zhi Du, *Tianjin*
Hani El-Nezami, *Hong Kong*
Bao-Ying Fei, *Hangzhou*
Chang-Ming Gao, *Nanjing*
Jian-Ping Gong, *Chongqing*
Zuo-Jiong Gong, *Wuhan*
Jing-Shan Gong, *Shenzhen*
Guo-Li Gu, *Beijing*
Yong-Song Guan, *Chengdu*
Mao-Lin Guo, *Luoyang*
Jun-Ming Guo, *Ningbo*
Yan-Mei Guo, *Shanghai*
Xiao-Zhong Guo, *Shenyang*
Guo-Hong Han, *Xi'an*
Ming-Liang He, *Hong Kong*
Peng Hou, *Xi'an*
Zhao-Hui Huang, *Wuxi*
Feng Ji, *Hangzhou*
Simon Law, *Hong Kong*
Yan-Chang Lei, *Hangzhou*
Yu-Yuan Li, *Guangzhou*
Meng-Sen Li, *Haikou*
Shu-De Li, *Shanghai*
Zong-Fang Li, *Xi'an*
Qing-Quan Li, *Shanghai*
Kang Li, *Lasa*
Han Liang, *Tianjin*
Xing'e Liu, *Hangzhou*
Zheng-Wen Liu, *Xi'an*
Xiao-Fang Liu, *Yantai*
Bin Liu, *Tianjin*
Quan-Da Liu, *Beijing*
Hai-Feng Liu, *Beijing*
Fei Liu, *Shanghai*
Ai-Guo Lu, *Shanghai*
He-Sheng Luo, *Wuhan*
Xiao-Peng Ma, *Shanghai*
Yong Meng, *Shantou*
Ke-Jun Nan, *Xi'an*
Siew Chien Ng, *Hong Kong*
Simon SM Ng, *Hong Kong*
Zhao-Shan Niu, *Qingdao*
Di Qu, *Shanghai*
Ju-Wei Mu, *Beijing*
Rui-Hua Shi, *Nanjing*
Bao-Min Shi, *Shanghai*
Xiao-Dong Sun, *Hangzhou*
Si-Yu Sun, *Shenyang*
Guang-Hong Tan, *Haikou*
Wen-Fu Tang, *Chengdu*
Anthony YB Teoh, *Hong Kong*
Wei-Dong Tong, *Chongqing*
Eric Tse, *Hong Kong*
Hong Tu, *Shanghai*

Stavros Gourgiotis, *Athens*
Leontios J Hadjileontiadis, *Thessaloniki*
Thomas Hyphantis, *Ioannina*
Ioannis Kanellos, *Thessaloniki*
Stylianos Karatapanis, *Rhodes*
Michael Koutsilieris, *Athens*
Spiros D Ladas, *Athens*
Theodoros K Liakakos, *Athens*
Emanuel K Manesis, *Athens*
Spilios Manolakopoulos, *Athens*
Gerassimos John Mantzaris, *Athens*
Athanasios D Marinis, *Piraeus*
Nikolaos Ioannis Nikiteas, *Athens*
Konstantinos X Papamichael, *Athens*
George Sgourakis, *Athens*
Konstantinos C Thomopoulos, *Patras*
Konstantinos Triantafyllou, *Athens*
Christos Triantos, *Patras*
Georgios Zacharakis, *Athens*
Petros Zezos, *Alexandroupolis*
Demosthenes E Ziogas, *Ioannina*

Guatemala

Carlos Maria Parellada, *Guatemala*

Hungary

Mihaly Boros, *Szeged*
Tamás Decsi, *Pécs*
Gyula Farkas, *Szeged*
Andrea Furka, *Debrecen*
Y vette Mandi, *Szeged*
Peter L Lakatos, *Budapest*
Pal Miheller, *Budapest*
Tamás Molnar, *Szeged*
Attila Olah, *Gyor*
Maria Papp, *Debrecen*
Ferenc Sipos, *Budapest*
Miklós Tanyi, *Debrecen*
Tibor Wittmann, *Szeged*

Iceland

Tryggvi Bjorn Stefánsson, *Reykjavík*

Indiad

Brij B Agarwal, *New Delhi*
Deepak N Amarapurkar, *Mumbai*
Shams ul Bari, *Srinagar*
Sriparna Basu, *Varanasi*
Runu Chakravarty, *Kolkata*
Devendra C Desai, *Mumbai*
Nutan D Desai, *Mumbai*
Suneela Sunil Dhaneshwar, *Pune*
Radha K Dhiman, *Chandigarh*
Pankaj Garg, *Mohali*
Uday C Ghoshal, *Lucknow*
Kalpesh Jani, *Vadodara*
Premashis Kar, *New Delhi*
Jyotdeep Kaur, *Chandigarh*
Rakesh Kochhar, *Chandigarh*
Pradyumna K Mishra, *Mumbai*
Asish K Mukhopadhyay, *Kolkata*
Imtiyaz Murtaza, *Srinagar*
P Nagarajan, *New Delhi*
Samiran Nundy, *Delhi*
Gopal Pande, *Hyderabad*
Benjamin Perakath, *Vellore*
Arun Prasad, *New Delhi*
D Nageshwar Reddy, *Hyderabad*
Lekha Saha, *Chandigarh*
Sundeep Singh Saluja, *New Delhi*
Mahesh Prakash Sharma, *New Delhi*
Sadiq Saleem Sikora, *Bangalore*
Sarman Singh, *New Delhi*
Rajeev Sinha, *Jhansi*
Rupjyoti Talukdar, *Hyderabad*
Rakesh Kumar Tandon, *New Delhi*
Narayanan Thirumoorthy, *Coimbatore*

Indonesia

David Handojo Muljono, *Jakarta*
Andi Utama, *Jakarta*

Iran

Arezoo Aghakhani, *Tehran*
Seyed Mohsen Dehghani, *Shiraz*
Ahad Eshraghian, *Shiraz*
Hossein Khedmat, *Tehran*
Sadegh Massarrat, *Tehran*
Marjan Mohammadi, *Tehran*
Roja Rahimi, *Tehran*
Farzaneh Sabahi, *Tehran*
Majid Sadeghizadeh, *Tehran*
Farideh Siavoshi, *Tehran*

Ireland

Gary Alan Bass, *Dublin*
David J Brayden, *Dublin*
Ronan A Cahill, *Dublin*
Glen A Doherty, *Dublin*
Liam J Fanning, *Cork*
Barry Philip McMahon, *Dublin*
RossMcManus, *Dublin*
Dervla O'Malley, *Cork*
Sinead M Smith, *Dublin*

Israel

Dan Carter, *Ramat Gan*
Jorge-Shmuel Delgado, *Metar*
Eli Magen, *Ashdod*
Nitsan Maharshak, *Tel Aviv*
Shaul Mordechai, *Beer Sheva*
Menachem Moshkowitz, *Tel Aviv*
William Bahij Nseir, *Nazareth*
Shimon Reif, *Jerusalem*
Ram Reifen, *Rehovot*
Ariella Bar-Gil Shitrit, *Jerusalem*
Noam Shussman, *Jerusalem*
Igor Sukhotnik, *Haifa*
Nir Wasserberg, *Petach Tiqwa*
Jacob Yahav, *Rehovot*
Doron Levi Zamir, *Gedera*
Shira Zelber-Sagi, *Haifa*
Romy Zemel, *Petach-Tikva*

Italy

Ludovico Abenavoli, *Catanzaro*
Luigi Elio Adinolfi, *Naples*
Carlo Virginio Agostoni, *Milan*
Anna Alisi, *Rome*
Piero Luigi Almasio, *Palermo*
Donato Francesco Altomare, *Bari*
Amedeo Amedei, *Florence*
Pietro Andreone, *Bologna*
Imerio Angriman, *Padova*
Vito Annese, *Florence*
Paolo Aurello, *Rome*
Salavtore Auricchio, *Naples*
Gian Luca Baiocchi, *Brescia*
Gianpaolo Balzano, *Milan*
Antonio Basoli, *Rome*
Gabrio Bassotti, *San Sisto*
Mauro Bernardi, *Bologna*
Alberto Biondi, *Rome*
Ennio Biscaldi, *Genova*
Massimo Bolognesi, *Padua*
Luigi Bonavina, *Milano*
Aldo Bove, *Chieti*
Raffaele Bruno, *Pavia*
Luigi Brusciano, *Napoli*
Giuseppe Cabibbo, *Palermo*
Carlo Calabrese, *Bologna*
Daniele Calistri, *Meldola*
Vincenza Calvaruso, *Palermo*
Lorenzo Camellini, *Reggio Emilia*
Marco Candela, *Bologna*
Raffaele Capasso, *Naples*
Lucia Carulli, *Modena*
Renato David Caviglia, *Rome*
Luigina Cellini, *Chieti*
Giuseppe Chiarioni, *Verona*
Claudio Chiesa, *Rome*
Michele Cicala, *Roma*
Rachele Ciccocioppo, *Pavia*
Sandro Contini, *Parma*
Gaetano Corso, *Foggia*
Renato Costi, *Parma*
Alessandro Cucchetti, *Bologna*
Rosario Cuomo, *Napoli*
Giuseppe Currò, *Messina*
Paola De Nardi, *Milano*
Giovanni D De Palma, *Naples*
Raffaele De Palma, *Napoli*
Giuseppina De Petro, *Brescia*
Valli De Re, *Aviano*
Paolo De Simone, *Pisa*
Giuliana Decorti, *Trieste*
Emanuele Miraglia del Giudice, *Napoli*
Isidoro Di Carlo, *Catania*
Matteo Nicola Dario Di Minno, *Naples*
Massimo Donadelli, *Verona*
Mirko D'Onofrio, *Verona*
Maria Pina Dore, *Sassari*
Luca Elli, *Milano*
Massimiliano Fabozzi, *Aosta*
Massimo Falconi, *Ancona*

Ezio Falletto, *Turin*
Silvia Fargion, *Milan*
Matteo Fassan, *Verona*
Gianfranco Delle Fave, *Roma*
Alessandro Federico, *Naples*
Francesco Feo, *Sassari*
Davide Festi, *Bologna*
Natale Figura, *Siena*
Vincenzo Formica, *Rome*
Mirella Fraquelli, *Milan*
Marzio Frazzoni, *Modena*
Walter Fries, *Messina*
Gennaro Galizia, *Naples*
Andrea Galli, *Florence*
Matteo Garcovich, *Rome*
Eugenio Gaudio, *Rome*
Paola Ghiorzo, *Genoa*
Edoardo G Giannini, *Genova*
Luca Gianotti, *Monza*
Maria Cecilia Giron, *Padova*
Alberto Grassi, *Rimini*
Gabriele Grassi, *Trieste*
Francesco Greco, *Bergamo*
Luigi Greco, *Naples*
Antonio Grieco, *Rome*
Fabio Grizzi, *Rozzano*
Laurino Grossi, *Pescara*
Simone Guglielmetti, *Milan*
Tiberiu Hershcovici, *Jerusalem*
Calogero Iacono, *Verona*
Enzo Ierardi, *Bari*
Amedeo Indriolo, *Bergamo*
Raffaele Iorio, *Naples*
Paola Iovino, *Salerno*
Angelo A Izzo, *Naples*
Loreta Kondili, *Rome*
Filippo La Torre, *Rome*
Giuseppe La Torre, *Rome*
Giovanni Latella, *L'Aquila*
Salvatore Leonardi, *Catania*
Massimo Libra, *Catania*
Anna Licata, *Palermo*
C armela Loguercio, *Naples*
Amedeo Lonardo, *Modena*
Carmelo Luigiano, *Catania*
Francesco Luzza, *Catanzaro*
Giovanni Maconi, *Milano*
Antonio Macrì, *Messina*
Mariano Malaguarnera, *Catania*
Francesco Manguso, *Napoli*
Tommaso Maria Manzia, *Rome*
Daniele Marrelli, *Siena*
Gabriele Masselli, *Rome*
Sara Massironi, *Milan*
Giuseppe Mazzarella, *Avellino*
Michele Milella, *Rome*
Giovanni Milito, *Rome*
Antonella d'Arminio Monforte, *Milan*
Fabrizio Montecucco, *Genoa*
Giovanni Monteleone, *Rome*
Mario Morino, *Torino*
Vincenzo La Mura, *Milan*
Gerardo Nardone, *Naples*
Riccardo Nascimbeni, *Brescia*
Gabriella Nesi, *Florence*
Giuseppe Nigri, *Rome*
Erica Novo, *Turin*
Veronica Ojetti, *Rome*
Michele Orditura, *Naples*
Fabio Pace, *Seriate*
Lucia Pacifico, *Rome*
Omero Alessandro Paoluzi, *Rome*
Valerio Pazienza, *San Giovanni Rotondo*
Rinaldo Pellicano, *Turin*
Adriano M Pellicelli, *Rome*
Nadia Peparini, *Ciampino*
Mario Pescatori, *Rome*
Antonio Picardi, *Rome*
Alberto Pilotto, *Padova*
Alberto Piperno, *Monza*
Anna Chiara Piscaglia, *Rome*
Maurizio Pompili, *Rome*
Francesca Romana Ponziani, *Rome*
Cosimo Prantera, *Rome*
Girolamo Ranieri, *Bari*
Carlo Ratto, *Tome*
Barbara Renga, *Perugia*
Alessandro Repici, *Rozzano*
Maria Elena Riccioni, *Rome*
Lucia Ricci-Vitiani, *Rome*
Luciana Rigoli, *Messina*
Mario Rizzetto, *Torino*
Ballarin Roberto, *Modena*
Roberto G Romanelli, *Florence*
Claudio Romano, *Messina*
Luca Roncucci, *Modena*
Cesare Ruffolo, *Treviso*
L ucia Sacchetti, *Napoli*
Rodolfo Sacco, *Pisa*
Lapo Sali, *Florence*
Romina Salpini, *Rome*
Giulio Aniello, *Santoro Treviso*
Armando Santoro, *Rozzano*
Edoardo Savarino, *Padua*
Marco Senzolo, *Padua*
Annalucia Serafino, *Rome*
Giuseppe S Sica, *Rome*
Pierpaolo Sileri, *Rome*
Cosimo Sperti, *Padua*
Vincenzo Stanghellini, *Bologna*
Cristina Stasi, *Florence*
Gabriele Stocco, *Trieste*
Roberto Tarquini, *Florence*
Mario Testini, *Bari*
Guido Torzilli, *Milan*
Guido Alberto Massimo, *Tiberio Brescia*
Giuseppe Toffoli, *Aviano*
Alberto Tommasini, *Trieste*
Francesco Tonelli, *Florence*
Cesare Tosetti Porretta, *Terme*
Lucio Trevisani, *Cona*
Guglielmo M Trovato, *Catania*
Mariapia Vairetti, *Pavia*
Luca Vittorio Valenti, *Milano*
Mariateresa T Ventura, *Bari*
Giuseppe Verlato, *Verona*
Marco Vivarelli, *Ancona*
Giovanni Li Volti, *Catania*
Giuseppe Zanotti, *Padua*
Vincenzo Zara, *Lecce*
Gianguglielmo Zehender, *Milan*
Anna Linda Zignego, *Florence*
Rocco Antonio Zoccali, *Messina*
Angelo Zullo, *Rome*

Japan

Yasushi Adachi, *Sapporo*
Takafumi Ando, *Nagoya*
Masahiro Arai, *Tokyo*
Makoto Arai, *Chiba*
Takaaki Arigami, *Kagoshima*
Itaru Endo,*Yokohama*
Munechika Enjoji, *Fukuoka*
Shunji Fujimori, *Tokyo*
Yasuhiro Fujino, *Akashi*
Toshiyoshi Fujiwara, *Okayama*
Yosuke Fukunaga, *Tokyo*
Toshio Fukusato, *Tokyo*
Takahisa Furuta, *Hamamatsu*
Osamu Handa, *Kyoto*
Naoki Hashimoto, *Osaka*
Yoichi Hiasa, *Toon*
Masatsugu Hiraki, *Saga*
Satoshi Hirano, *Sapporo*
Keiji Hirata, *Fukuoka*
Toru Hiyama, *Higashihiroshima*
Akira Hokama, *Nishihara*
Shu Hoteya, *Tokyo*
Masao Ichinose, *Wakayama*
Tatsuya Ide, *Kurume*
Masahiro Iizuka, *Akita*
Toshiro Iizuka, *Tokyo*
Kenichi Ikejima, *Tokyo*
Tetsuya Ikemoto, *Tokushima*
Hiroyuki Imaeda, *Saitama*
Atsushi Imagawa, *Kan-onji*
Hiroo Imazu, *Tokyo*
Shuji Isaji, *Tsu*
Toru Ishikawa, *Niigata*
Toshiyuki Ishiwata, *Tokyo*
Soichi Itaba, *Kitakyushu*
Yoshiaki Iwasaki, *Okayama*
Tatehiro Kagawa, *Isehara*
Satoru Kakizaki, *Maebashi*
Naomi Kakushima, *Shizuoka*
Terumi Kamisawa, *Tokyo*
Akihide Kamiya, *Isehara*
Osamu Kanauchi, *Tokyo*
Tatsuo Kanda, *Chiba*
Shin Kariya, *Okayama*
Shigeyuki Kawa, *Matsumoto*
Takumi Kawaguchi, *Kurume*
Takashi Kawai, *Tokyo*
Soo Ryang Kim, *Kobe*
Shinsuke Kiriyama, *Gunma*
Tsuneo Kitamura, *Urayasu*
Masayuki Kitano, *Osakasayama*
Hirotoshi Kobayashi, *Tokyo*
Hironori Koga, *Kurume*
Takashi Kojima, *Sapporo*
Satoshi Kokura, *Kyoto*
Shuhei Komatsu, *Kyoto*
Tadashi Kondo, *Tokyo*
Yasuteru Kondo, *Sendai*
Yasuhiro Kuramitsu, *Yamaguchi*
Yukinori Kurokawa, *Osaka*
Shin Maeda, *Yokohama*
Koutarou Maeda, *Toyoake*

Hitoshi Maruyama, *Chiba*
Atsushi Masamune, *Sendai*
Hiroyuki Matsubayashi, *Suntogun*
Akihisa Matsuda, *Inzai*
Hirofumi Matsui, *Tsukuba*
Akira Matsumori, *Kyoto*
Yoichi Matsuo, *Nagoya*
Y Matsuzaki, *Ami*
Toshihiro Mitaka, *Sapporo*
Kouichi Miura, *Akita*
Shinichi Miyagawa, *Matumoto*
Eiji Miyoshi, *Suita*
Toru Mizuguchi, *Sapporo*
Nobumasa Mizuno, *Nagoya*
Zenichi Morise, *Nagoya*
Tomohiko Moriyama, *Fukuoka*
Kunihiko Murase, *Tusima*
Michihiro Mutoh, *Tsukiji*
Akihito Nagahara, *Tokyo*
Hikaru Nagahara, *Tokyo*
Hidenari Nagai, *Tokyo*
Koichi Nagata, *Shimotsuke-shi*
Masaki Nagaya, *Kawasaki*
Hisato Nakajima, *Nishi-Shinbashi*
Toshifusa Nakajima, *Tokyo*
Hiroshi Nakano, *Kawasaki*
Hiroshi Nakase, *Kyoto*
Toshiyuki Nakayama, *Nagasaki*
Takahiro Nakazawa, *Nagoya*
Shoji Natsugoe, *Kagoshima City*
Tsutomu Nishida, *Suita*
Shuji Nomoto, *Naogya*
Sachiyo Nomura, *Tokyo*
Takeshi Ogura, *Takatsukishi*
Nobuhiro Ohkohchi, *Tsukuba*
Toshifumi Ohkusa, *Kashiwa*
Hirohide Ohnishi, *Akita*
Teruo Okano, *Tokyo*
Satoshi Osawa, *Hamamatsu*
Motoyuki Otsuka, *Tokyo*
Michitaka Ozaki, *Sapporo*
Satoru Saito, *Yokohama*
Naoaki Sakata, *Sendai*
Ken Sato, *Maebashi*
Toshiro Sato, *Tokyo*
Tomoyuki Shibata, *Toyoake*
Tomohiko Shimatani, *Kure*
Yukihiro Shimizu, *Nanto*
Tadashi Shimoyama, *Hirosaki*
Masayuki Sho, *Nara*
Ikuo Shoji, *Kobe*
Atsushi Sofuni, *Tokyo*
Takeshi Suda, *Niigata*
M Sugimoto, *Hamamatsu*
Ken Sugimoto, *Hamamatsu*
Haruhiko Sugimura, *Hamamatsu*
Shoichiro Sumi, *Kyoto*
Hidekazu Suzuki, *Tokyo*
Masahiro Tajika, *Nagoya*
Hitoshi Takagi, *Takasaki*
Toru Takahashi, *Niigata*
Yoshihisa Takahashi, *Tokyo*
Shinsuke Takeno, *Fukuoka*
Akihiro Tamori, *Osaka*
Kyosuke Tanaka, *Tsu*
Shinji Tanaka, *Hiroshima*
Atsushi Tanaka, *Tokyo*
Yasuhito Tanaka, *Nagoya*
Shinji Tanaka, *Tokyo*
Minoru Tomizawa, *Yotsukaido City*
Kyoko Tsukiyama-Kohara, *Kagoshima*
Takuya Watanabe, *Niigata*
Kazuhiro Watanabe, *Sendai*
Satoshi Yamagiwa, *Niigata*
Takayuki Yamamoto, *Yokkaichi*
Hiroshi Yamamoto, *Otsu*
Kosho Yamanouchi, *Nagasaki*
Ichiro Yasuda, *Gifu*
Yutaka Yata, *Maebashi-city*
Shin-ichi Yokota, *Sapporo*
Norimasa Yoshida, *Kyoto*
Hiroshi Yoshida, *Tama-City*
Hitoshi Yoshiji, *Kashihara*
Kazuhiko Yoshimatsu, *Tokyo*
Kentaro Yoshioka, *Toyoake*
Nobuhiro Zaima, *Nara*

Jordan
Khaled Ali Jadallah, *Irbid*

Kuwait
Islam Khan, *Kuwait*

Lebanon
Bassam N Abboud, *Beirut*
Kassem A Barada, *Beirut*
Marwan Ghosn, *Beirut*
Iyad A Issa, *Beirut*
Fadi H Mourad, *Beirut*
AIa Sharara, *Beirut*
Rita Slim, *Beirut*

Lithuania
Antanas Mickevicius, *Kaunas*

Malaysia
Huck Joo Tan, *Petaling Jaya*

Mexico
Richard A Awad, *Mexico City*
Carlos R Camara-Lemarroy, *Monterrey*
Norberto C Chavez-Tapia, *Mexico City*
Wolfgang Gaertner, *Mexico City*
Diego Garcia-Compean, *Monterrey*
Arturo Panduro, *Guadalajara*
OT Teramoto-Matsubara, *Mexico City*
Felix Tellez-Avila, *Mexico City*
Omar Vergara-Fernandez, *Mexico City*
Saúl Villa-Trevino, *Cuidad de México*

Morocco
Samir Ahboucha, *Khouribga*

Netherlands
Robert J de Knegt, *Rotterdam*
Tom Johannes Gerardus Gevers, *Nijmegen*
Menno Hoekstra, *Leiden*
BW Marcel Spanier, *Arnhem*
Karel van Erpecum, *Utrecht*

New Zealand
Leo K Cheng, *Auckland*
Andrew Stewart Day, *Christchurch*
Jonathan Barnes Koea, *Auckland*
Max Petrov, *Auckland*

Nigeria
Olufunmilayo Adenike Lesi, *Lagos*
Jesse Abiodun Otegbayo, *Ibadan*
Stella Ifeanyi Smith, *Lagos*

Norway
Trond Berg, *Oslo*
Trond Arnulf Buanes, *Krokkleiva*
Thomas de Lange, *Rud*
Magdy El-Salhy, *Stord*
Rasmus Goll, *Tromso*
Dag Arne Lihaug Hoff, *Aalesund*

Pakistan
Zaigham Abbas, *Karachi*
Usman A Ashfaq, *Faisalabad*
Muhammad Adnan Bawany, *Hyderabad*
Muhammad Idrees, *Lahore*
Saeed Sadiq Hamid, *Karachi*
Yasir Waheed, *Islamabad*

Poland
Thomas Brzozowski, *Cracow*
Magdalena Chmiela, *Lodz*
Krzysztof Jonderko, *Sosnowiec*
Anna Kasicka-Jonderko, *Sosnowiec*
Michal Kukla, *Katowice*
Tomasz Hubert Mach, *Krakow*
Agata Mulak, *Wroclaw*
Danuta Owczarek, *Kraków*
Piotr Socha, *Warsaw*
Piotr Stalke, *Gdansk*
Julian Teodor Swierczynski, *Gdansk*
Anna M Zawilak-Pawlik, *Wroclaw*

Portugal
Marie Isabelle Cremers, *Setubal*
Ceu Figueiredo, *Porto*
Ana Isabel Lopes, *LIsbon*
M Paula Macedo, *Lisboa*
Ricardo Marcos, *Porto*
Rui T Marinho, *Lisboa*
Guida Portela-Gomes, *Estoril*

Filipa F Vale, *Lisbon*

Puerto Rico

Caroline B Appleyard, *Ponce*

Qatar

Abdulbari Bener, *Doha*

Romania

Mihai Ciocirlan, *Bucharest*
Dan LucianDumitrascu, *Cluj-Napoca*
Carmen Fierbinteanu-Braticevici, *Bucharest*
Romeo G Mihaila, *Sibiu*
Lucian Negreanu, *Bucharest*
Adrian Saftoiu, *Craiova*
Andrada Seicean, *Cluj-Napoca*
Ioan Sporea, *Timisoara*
Letiţia Adela Maria Streba, *Craiova*
Anca Trifan, *Iasi*

Russia

Victor Pasechnikov, *Stavropol*
Vasiliy Ivanovich Reshetnyak, *Moscow*
Vitaly Skoropad, *Obninsk*

Saudi Arabia

Abdul-Wahed N Meshikhes, *Dammam*
M Ezzedien Rabie, *Khamis Mushait*

Singapore

Brian KP Goh, *Singapore*
Richie Soong, *Singapore*
Ker-Kan Tan, *Singapore*
Kok-Yang Tan, *Singapore*
Yee-Joo Tan, *Singapore*
Mark Wong, *Singapore*
Hong Ping Xia, *Singapore*

Slovenia

Matjaz Homan, *Ljubljana*
Martina Perse, *Ljubljana*

South Korea

Sang Hoon Ahn, *Seoul*
Seung Hyuk Baik, *Seoul*
Soon Koo Baik, *Wonju*
Soo-Cheon Chae, *Iksan*
Byung-Ho Choe, *Daegu*
Suck Chei Choi, *Iksan*
Hoon Jai Chun, *Seoul*
Yeun-Jun Chung, *Seoul*
Young-Hwa Chung, *Seoul*
Ki-Baik Hahm, *Seongnam*
Sang Young Han, *Busan*
Seok Joo Han, *Seoul*
Seung-Heon Hong, *Iksan*
Jin-Hyeok Hwang, *Seoungnam*
Jeong Won Jang, *Seoul*
Jin-Young Jang, *Seoul*
Dae-Won Jun, *Seoul*
Young Do Jung, *Kwangju*
Gyeong Hoon Kang, *Seoul*
Sung-Bum Kang, *Seoul*
Koo Jeong Kang, *Daegu*
Ki Mun Kang, *Jinju*
Chang Moo Kang, *Seodaemun-gu*
Gwang Ha Kim, *Busan*
Sang Soo Kim, *Goyang-si*
Jin Cheon Kim, *Seoul*
Tae Il Kim, *Seoul*
Jin Hong Kim, *Suwon*
Kyung Mo Kim, *Seoul*
Kyongmin Kim, *Suwon*
Hyung-Ho Kim, *Seongnam*
Seoung Hoon Kim, *Goyang*
Sang Il Kim, *Seoul*
Hyun-Soo Kim, *Wonju*
Jung Mogg Kim, *Seoul*
Dong Yi Kim, *Gwangju*
Kyun-Hwan Kim, *Seoul*
Jong-Han Kim, *Ansan*
Sang Wun Kim, *Seoul*
Ja-Lok Ku, *Seoul*
Kyu Taek Lee, *Seoul*
Hae-Wan Lee, *Chuncheon*
Inchul Lee, *Seoul*
Jung Eun Lee, *Seoul*
Sang Chul Lee, *Daejeon*
Song Woo Lee, *Ansan-si*
Hyuk-Joon Lee, *Seoul*
Seong-Wook Lee, *Yongin*
Kil Yeon Lee, *Seoul*
Jong-Inn Lee, *Seoul*
Kyung A Lee, *Seoul*
Jong-Baeck Lim, *Seoul*
Eun-Yi Moon, *Seoul*
SH Noh, *Seoul*
Seung Woon Paik, *Seoul*
Won Sang Park, *Seoul*
Sung-Joo Park, *Iksan*
Kyung Sik Park, *Daegu*
Se Hoon Park, *Seoul*
Yoonkyung Park, *Gwangju*
Seung-Wan Ryu, *Daegu*
Il Han Song, *Cheonan*
Myeong Jun Song, *Daejeon*
Yun Kyoung Yim, *Daejeon*
Dae-Yeul Yu *Daejeon*

Spain

Mariam Aguas, *Valencia*
Raul J Andrade, *Málaga*
Antonio Arroyo, *Elche*
Josep M Bordas, *Barcelona*
Lisardo Boscá, *Madrid*
Ricardo Robles Campos, *Murcia*
Jordi Camps, *Reus*
Carlos Cervera *Barcelona*
Alfonso Clemente, *Granada*
Pilar Codoner-Franch, *Valencia*
Fernando J Corrales, *Pamplona*
Fermin Sánchez de Medina, *Granada*
Alberto Herreros de Tejada, *Majadahonda*
Enrique de-Madaria, *Alicante*
JE Dominguez-Munoz, *Santiago de Compostela*
Vicente Felipo, *Valencia*
CM Fernandez-Rodriguez, *Madrid*
Carmen Frontela-Saseta, *Murcia*
Julio Galvez, *Granada*
Maria Teresa García, *Vigo*
MI Garcia-Fernandez, *Málaga*
Emilio Gonzalez-Reimers, *La Laguna*
Marcel Jimenez, *Bellaterra*
Angel Lanas, *Zaragoza*
Juan Ramón Larrubia, *Guadalajara*
Antonio Lopez-Sanroman, *Madrid*
Vicente Lorenzo-Zuniga, *Badalona*
Alfredo J Lucendo, *Tomelloso*
Vicenta Soledad Martinez-Zorzano, *Vigo*
José Manuel Martin-Villa, *Madrid*
Julio Mayol, *Madrid*
Manuel Morales-Ruiz, *Barcelona*
Alfredo Moreno-Egea, *Murcia*
Albert Pares, *Barcelona*
Maria Pellise, *Barcelona*
José Perea, *Madrid*
Miguel Angel Plaza, *Zaragoza*
María J Pozo, *Cáceres*
Enrique Quintero, *La Laguna*
Jose M Ramia, *Madrid*
Francisco Rodriguez-Frias, *Barcelona*
Silvia Ruiz-Gaspa, *Barcelona*
Xavier Serra-Aracil, *Barcelona*
Vincent Soriano, *Madrid*
Javier Suarez, *Pamplona*
Carlos Taxonera, *Madrid*
M Isabel Torres, *Jaén*
Manuel Vazquez-Carrera, *Barcelona*
Benito Velayos, *Valladolid*
Silvia Vidal, *Barcelona*

Sri Lanka

Arjuna Priyadarsin De Silva, *Colombo*

Sudan

Ishag Adam, *Khartoum*

Sweden

Roland G Andersson, *Lund*
Bergthor Björnsson, *Linkoping*
Johan Christopher Bohr, *Örebro*
Mauro D'Amato, *Stockholm*
Thomas Franzen, *Norrkoping*
Evangelos Kalaitzakis, *Lund*
Riadh Sadik, *Gothenburg*
Per Anders Sandstrom, *Linkoping*
Ervin Toth, *Malmö*
Konstantinos Tsimogiannis, *Vasteras*
Apostolos V Tsolakis, *Uppsala*

Switzerland

Gieri Cathomas, *Liestal*
Jean Louis Frossard, *Geneve*
Christian Toso, *Geneva*
Stephan Robert Vavricka, *Zurich*
Dominique Velin, *Lausanne*

Thailand

Thawatchai Akaraviputh, *Bangkok*
P Yoysungnoen Chintana, *Pathumthani*
Veerapol Kukongviriyapan, *Muang*
Vijittra Leardkamolkarn, *Bangkok*
Varut Lohsiriwat, *Bangkok*
Somchai Pinlaor, *Khaon Kaen*
D Wattanasirichaigoon, *Bangkok*

Trinidad and Tobago

B Shivananda Nayak, *Mount Hope*

Tunisia

Ibtissem Ghedira, *Sousse*
Lilia Zouiten-Mekki, *Tunis*

Turkey

Inci Alican, *Istanbul*
Mustafa Altindis, *Sakarya*
Mutay Aslan, *Antalya*
Oktar Asoglu, *Istanbul*
Yasemin Hatice Balaban, *Istanbul*
Metin Basaranoglu, *Ankara*
Yusuf Bayraktar, *Ankara*
Süleyman Bayram, *Adiyaman*
Ahmet Bilici, *Istanbul*
Ahmet Sedat Boyacioglu, *Ankara*
Züleyha Akkan Cetinkaya, *Kocaeli*
Cavit Col, *Bolu*
Yasar Colak, *Istanbul*
Cagatay Erden Daphan, *Kirikkale*
Mehmet Demir, *Hatay*
Ahmet Merih Dobrucali, *Istanbul*
Gülsüm Ozlem Elpek, *Antalya*
Ayse Basak Engin, *Ankara*
Eren Ersoy, *Ankara*
Osman Ersoy, *Ankara*
Yusuf Ziya Erzin, *Istanbul*
Mukaddes Esrefoglu, *Istanbul*
Levent Filik, *Ankara*
Ozgur Harmanci, *Ankara*
Koray Hekimoglu, *Ankara*
Abdurrahman Kadayifci, *Gaziantep*
Cem Kalayci, *Istanbul*
Selin Kapan, *Istanbul*
Huseyin Kayadibi, *Adana*
Sabahattin Kaymakoglu, *Istanbul*
Metin Kement, *Istanbul*
Mevlut Kurt, *Bolu*
Resat Ozaras, *Istanbul*
Elvan Ozbek, *Adapazari*
Cengiz Ozcan, *Mersin*
Hasan Ozen, *Ankara*
Halil Ozguc, *Bursa*
Mehmet Ozturk, *Izmir*
Orhan V Ozkan, *Sakarya*
Semra Paydas, *Adana*
Ozlem Durmaz Suoglu, *Istanbul*
Ilker Tasci, *Ankara*
Müge Tecder-ünal, *Ankara*
Mesut Tez, *Ankara*
Serdar Topaloglu, *Trabzon*
Murat Toruner, *Ankara*
Gokhan Tumgor, *Adana*
Oguz Uskudar, *Adana*
Mehmet Yalniz, *Elazig*
Mehmet Yaman, *Elazig*
Veli Yazisiz, *Antalya*
Yusuf Yilmaz, *Istanbul*
Ozlem Yilmaz, *Izmir*
Oya Yucel, *Istanbul*
Ilhami Yuksel, *Ankara*

United Kingdom

Nadeem Ahmad Afzal, *Southampton*
Navneet K Ahluwalia, *Stockport*
Yeng S Ang, *Lancashire*
Ramesh P Arasaradnam, *Coventry*
Ian Leonard Phillip Beales, *Norwich*
John Beynon, *Swansea*
Barbara Braden, *Oxford*
Simon Bramhall, *Birmingham*
Geoffrey Burnstock, *London*
Ian Chau, *Sutton*
Thean Soon Chew, *London*
Helen G Coleman, *Belfast*
Anil Dhawan, *London*
Sunil Dolwani, *Cardiff*
Piers Gatenby, *London*
Anil T George, *London*
Pasquale Giordano, *London*
Paul Henderson, *Edinburgh*
Georgina Louise Hold, *Aberdeen*
Stefan Hubscher, *Birmingham*
Robin D Hughes, *London*
Nusrat Husain, *Manchester*
Matt W Johnson, *Luton*
Konrad Koss, *Macclesfield*
Anastasios Koulaouzidis, *Edinburgh*
Simon Lal, *Salford*
John S Leeds, *Aberdeen*
JK K Limdi, *Manchester*
Hongxiang Liu, *Cambridge*
Michael Joseph McGarvey, *London*
Michael Anthony Mendall, *London*
Alexander H Mirnezami, *Southampton*
J Bernadette Moore, *Guildford*
Claudio Nicoletti, *Norwich*
Savvas Papagrigoriadis, *London*
Sylvia LF Pender, *Southampton*
David Mark Pritchard, *Liverpool*
James A Ross, *Edinburgh*
Kamran Rostami, *Worcester*
Xiong Z Ruan, *London*
Frank I Tovey, *London*
Dhiraj Tripathi, *Birmingham*
Vamsi R Velchuru, *Great Yarmouth*
Nicholas T Ventham, *Edinburgh*
Diego Vergani, *London*
Jack Westwood Winter, *Glasgow*
Terence Wong, *London*
Ling Yang, *Oxford*

United States

Daniel E Abbott, *Cincinnati*
Ghassan K Abou-Alfa, *New York*
Julian Abrams, *New York*
David William Adelson, *Los Angeles*
Jonathan Steven Alexander, *Shreveport*
Tauseef Ali, *Oklahoma City*
Mohamed R Ali, *Sacramento*
Rajagopal N Aravalli, *Minneapolis*
Hassan Ashktorab, *Washington*
Shashi Bala, *Worcester*
Charles F Barish, *Raleigh*
P Patrick Basu, *New York*
Robert L Bell, *Berkeley Heights*
David Bentrem, *Chicago*
Henry J Binder, *New Haven*
Joshua Bleier, *Philadelphia*
Wojciech Blonski, *Johnson City*
Kenneth Boorom, *Corvallis*
Brian Boulay, *Chicago*
Carla W Brady, *Durham*
Kyle E Brown, *Iowa City*
Adeel A Butt, *Pittsburgh*
Weibiao Cao, *Providence*
Andrea Castillo, *Cheney*
Fernando J Castro, *Weston*
Adam S Cheifetz, *Boston*
Xiaoxin Luke Chen, *Durham*
Ramsey Cheung, *Palo Alto*
Parimal Chowdhury, *Little Rock*
Edward John Ciaccio, *New York*
Dahn L Clemens, *Omaha*
Yingzi Cong, *Galveston*
Laura Iris Cosen-Binker, *Boston*
Joseph John Cullen, *Lowa*
Mark J Czaja, *Bronx*
Mariana D Dabeva, *Bronx*
Christopher James Damman, *Seattle*
Isabelle G De Plaen, *Chicago*
Punita Dhawan, *Nashville*
Hui Dong, *La Jolla*
Wael El-Rifai, *Nashville*
Sukru H Emre, *New Haven*
Paul Feuerstadt, *Hamden*
Josef E Fischer, *Boston*
Laurie N Fishman, *Boston*
Joseph Che Forbi, *Atlanta*
Temitope Foster, *Atlanta*
Amy E Foxx-Orenstein, *Scottsdale*
Daniel E Freedberg, *New York*
Shai Friedland, *Palo Alto*
Virgilio George, *Indianapolis*
Ajay Goel, *Dallas*
Oliver Grundmann, *Gainesville*
Stefano Guandalini, *Chicago*
Chakshu Gupta, *St. Joseph*
Grigoriy E Gurvits, *New York*

World Journal of Gastroenterology

Contents

Weekly Volume 23 Number 10 March 14, 2017

REVIEW

MINIREVIEWS

ORIGINAL ARTICLE

Basic Study

META-ANALYSIS

CASE REPORT

NAME OF JOURNAL
World Journal of Gastroenterology

ISSN
ISSN 1007-9327 (print)
ISSN 2219-2840 (online)

LAUNCH DATE
October 1, 1995

FREQUENCY
Weekly

EDITORIAL OFFICE
Jin-Lei Wang, Director
Yuan Qi, Vice Director
Ze-Mao Gong, Vice Director
World Journal of Gastroenterology
Baishideng Publishing Group Inc
8226 Regency Drive,
Pleasanton, CA 94588, USA
Telephone: +1-925-2238242
Fax: +1-925-2238243
E-mail: editorialoffice@wjgnet.com
Help Desk: http://www.wjgnet.com/esps/helpdesk.aspx
http://www.wjgnet.com

PUBLISHER
Baishideng Publishing Group Inc
8226 Regency Drive,
Pleasanton, CA 94588, USA
Telephone: +1-925-2238242
Fax: +1-925-2238243
E-mail: bpgoffice@wjgnet.com
Help Desk: http://www.wjgnet.com/esps/helpdesk.aspx
http://www.wjgnet.com

PUBLICATION DATE
March 14, 2017

INSTRUCTIONS TO AUTHORS
Full instructions are available online at http://www.wjgnet.com/bpg/gerinfo/204

ONLINE SUBMISSION
http://www.wjgnet.com/esps/

World Journal of Gastroenterology

Submit a Manuscript: http://www.wjgnet.com/esps/

World J Gastroenterol 2017 March 14; 23(10): 1735-1746

DOI: 10.3748/wjg.v23.i10.1735

ISSN 1007-9327 (print) ISSN 2219-2840 (online)

REVIEW

Portal hypertension: Imaging of portosystemic collateral pathways and associated image-guided therapy

Murad Feroz Bandali, Anirudh Mirakhur, Edward Wolfgang Lee, Mollie Clarke Ferris, David James Sadler, Robin Ritchie Gray, Jason Kam Wong

Murad Feroz Bandali, Anirudh Mirakhur, Mollie Clarke Ferris, David James Sadler, Robin Ritchie Gray, Jason Kam Wong, Department of Radiology, Foothills Medical Centre, University of Calgary, Calgary, Alberta T2N 2T9, Canada

Anirudh Mirakhur, Edward Wolfgang Lee, Division of Interventional Radiology, Department of Radiology, UCLA Medical Center, Los Angeles, CA 90095, United States

Author contributions: All authors contributed to this review article with conception, literature review and analysis, image preparation and editing, manuscript drafting and critical revision and editing, and approval of the final version; Bandali MF and Mirakhur A contributed equally and are trainees of Lee EW.

Conflict-of-interest statement: Authors declare no potential conflicts of interests. No financial support.

Manuscript source: Invited manuscript

Correspondence to: Edward Wolfgang Lee, MD, PhD, Division of Interventional Radiology, Department of Radiology, UCLA Medical Center, 757 Westwood Plaza, Suite 2125, Los Angeles, CA 90095, United States. edwardlee@mednet.ucla.edu
Telephone: +1-310-2678771
Fax: +1-310-2673631

Received: November 14, 2016
Peer-review started: November 15, 2016
First decision: January 10, 2017
Revised: January 26, 2017
Accepted: February 16, 2017

Article in press: February 17, 2017
Published online: March 14, 2017

Abstract

Portal hypertension is a common clinical syndrome, defined by a pathologic increase in the portal venous pressure. Increased resistance to portal blood flow, the primary factor in the pathophysiology of portal hypertension, is in part due to morphological changes occurring in chronic liver diseases. This results in rerouting of blood flow away from the liver through collateral pathways to low-pressure systemic veins. Through a variety of computed tomographic, sonographic, magnetic resonance imaging and angiographic examples, this article discusses the appearances and prevalence of both common and less common portosystemic collateral channels in the thorax and abdomen. A brief overview of established interventional radiologic techniques for treatment of portal hypertension will also be provided. Awareness of the various imaging manifestations of portal hypertension can be helpful for assessing overall prognosis and planning proper management.

Key words: Portal hypertension; Diagnostic imaging; Portosystemic collaterals; Image-guided therapy

Core tip: Pathologic resistance to portal venous blood flow results in elevated portal pressure, forcing blood to decompress through various portosystemic collaterals. Blood may circumvent the liver *via* intrathoracic, intraabdominal, abdominal wall and pelvic collateral pathways - resulting in variceal bleeding, ascites and encephalopathy. Our objective is to provide a

comprehensive review of the commonly recruited portosystemic collaterals in portal hypertension and demonstrate its multimodality appearance on ultrasound, computed tomography and magnetic resonance imaging. Additionally, we will review several image-guided therapies which either aim to decrease portal venous pressure or mitigate the sequelae of portal hypertension.

Bandali MF, Mirakhur A, Lee EW, Ferris MC, Sadler DJ, Gray RR, Wong JK. Portal hypertension: Imaging of portosystemic collateral pathways and associated image-guided therapy. *World J Gastroenterol* 2017; 23(10): 1735-1746 Available from: URL: http://www.wjgnet.com/1007-9327/full/v23/i10/1735.htm DOI: http://dx.doi.org/10.3748/wjg.v23.i10.1735

INTRODUCTION

The portal venous system is a unique circulatory system which connects two systems of capillary beds; one in the gastrointestinal tract and splenic parenchyma, and the second in the hepatic sinusoids. The portal vein transports blood from abdominal viscera and ramifies - much like an artery - at the liver, ending into the hepatic sinusoids. The main portal vein is typically formed by the confluence of splenic vein and the superior mesenteric vein, posterior to the neck of the pancreas. The inferior mesenteric vein usually drains into the splenic vein and does not directly connect to the main portal vein (Figure 1). Other tributaries of the portal vein that make up the portal venous system are the left gastric, right gastric, paraumbilical, and cystic veins.

Normal portal venous pressure is between 5 to 10 mmHg, while the normal pressure gradient between the portal vein and the inferior vena cava, known as the hepatovenous pressure gradient (HVPG), is typically 1 to 5 mmHg[1]. Pathologic increase in portal venous pressure is primarily caused by resistance to portal inflow, which can occur either at the level of the portal vein, hepatic sinusoids or hepatovenous outflow. In addition to an increase in hepatic vascular resistance to portal blood flow, there is progressive splanchnic vasodilatation that aggravates the portal hypertension syndrome by augmenting portal blood flow[2]. Recent updates in pathophysiologic understanding of portal hypertension have also highlighted the contribution of hepatic sinusoidal endothelial dysfunction elevating portal pressure[1]. Ongoing portal hypertension eventually leads to formation of collateral circulation that directly connects the portal blood vessels to systemic circulation, bypassing the liver and thus constituting the clinical syndrome of portal hypertension[3-5]. Clinically significant portal hypertension is defined as an increase in HVPG to $\geqslant$ 10 mmHg; above this threshold, the complications of portal hypertension may begin to appear[6]. Formation

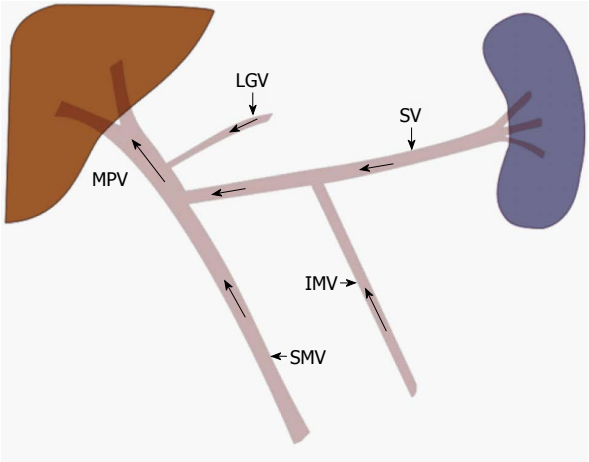

Figure 1 Normal portal venous anatomy and direction of blood flow. The main portal vein (MPV) is most commonly formed when the splenic vein (SV) and the superior mesenteric vein (SMV) join. While variable, the inferior mesenteric vein (IMV) most commonly drains in to the splenic vein, at the level of the pancreatic body. Other tributaries may also join the MPV, such as the left gastric vein (LGV) as depicted here.

of portosystemic collaterals is a complex process involving the opening, dilatation and hypertrophy of pre-existing vascular channels in order to decompress the portal system[2,4,5,7,8]. Some have also postulated that a component of angiogenesis is also involved in collateral formation[9].

In this review, we discuss the entire spectrum of portosystemic collateral pathways in the abdomen and thorax, through examples of computed tomography (CT), ultrasonography (US), magnetic resonance imaging (MRI) and angiographic examples. A brief overview of established interventional techniques for treatment of portal hypertension and related complications will also be provided.

IMAGING MODALITIES FOR THE ASSESSMENT OF PORTAL HYPERTENSION AND COLLATERAL PATHWAYS

A variety of imaging modalities are available to provide early diagnosis, prognostication and treatment planning for patients with advanced liver cirrhosis and portal hypertension. Catheter-based hepatic venography allows for measurement of HVPG which is the difference between the wedge and the free hepatic venous pressures. Measurement of HVPG is currently the best available method to evaluate the presence and severity of portal hypertension, however, this minimally invasive technique is not without risks - including bleeding, infection, possible contrast reaction, arrhythmias and need for intravenous sedation[8,10]. US, CT, and MRI offer diagnostic information complementary to catheter-based techniques.

US is typically the initial, first-line modality choice for the diagnosis and follow-up of portal

hypertension[8,11]. Spectral and colour Doppler US can provide accurate and specific detection of certain portosystemic collaterals (recanalized paraumbilical vein, splenorenal collaterals, dilated left and short gastric veins), as well as, directionality of flow within the portal vein[8,11]. US is also very accurate in the detection of portal and hepatic venous thrombosis and can be used for the surveillance of transjugular intrahepatic portosystemic shunt (TIPS) patency. In addition, US can provide cheap and readily accessible assessment of hepatic parenchymal nodularity, splenomegaly, provide screening for liver tumors including metastasis and hepatocellular carcinoma (HCC), as well as, detect the presence of abdominal ascites[8]. Unfortunately, the clinical usefulness of US in portal hypertension remains unsettled as it is plagued by the lack of reproducibility and accuracy secondary to intra- and interobserver variation and patient related factors (body habitus, respiratory motion, *etc*.). Transient elastography is a novel but well-validated sonographic technique that has emerged in the evaluation of hepatic fibrosis. The reported correlation between liver stiffness and HWVP makes elastography a potential helpful tool for the non-invasive evaluation of portal hypertension[12].

Both CT and MRI provide excellent cross-sectional visualization of the portal venous system with superior spatial and contrast resolution when combined with intravenous contrast agents (non-iodinated contrast and gadolinium chelate agents, respectively)[8]. CT and MRI can outline the full extent of portal vein thrombosis, portosystemic collateral mapping, and treatment planning in cases of complex anatomy. Although endoscopy is the gold standard, CT can also be useful in the detection of esophageal/gastric varices. In a prospective evaluation, Perri *et al*[13] demonstrated that CT had a 90% sensitivity in the identification of esophageal varices determined to be large on endoscopy, but only about 50% specific. The sensitivity of CT in detecting gastric varices was 87%. CT however carries with it the burden of ionizing radiation and there is a small risk of both allergic reaction and nephrotoxicity with both CT and MR contrast agents[8,14].

Four-dimensional flow MRI (4-D flow MR) with complete volumetric acquisition of the hepatic arterial and portal venous system also offers a promising non-invasive approach for characterization and follow-up of portal hypertension. Studies have demonstrated the utility of 4-D flow MR for the evaluation of the entire splanchnic system with high spatial resolution, as well as, validated the technique for quantification of flow velocities and volume using Doppler US data as reference standards[15-17]. Future clinical applications may include the evaluation of patients with portal hypertension for the purpose of interventional treatment planning, as well as, post-procedural TIPS assessment and follow-up[15].

ANATOMIC SITES OF PORTOSYSTEMIC CONFLUENCE

To ensure consistency in terminology, it should be noted that varices are dilated end-organ veins that have the propensity to bleed whereas shunts are dilated collateral channels that simply connect the portal and systemic vascular beds. The portosystemic collateral channels that can develop in portal hypertension are numerous, widespread and varied in appearance. Intrathoracic manifestations of portosystemic collateral vessels characteristically develop by way of the coronary vein into esophageal or paraesophageal (22%-38%) varices and cardiophrenic varices (18%)[10,18,19]. Other common pathways of portosystemic shunting involve gastroesophageal, paraumbilical, splenorenal, and inferior mesenteric collateral vessels. Pleuro-pericardial-peritoneal, pancreaticoduodenal, splenoazygos and mesocaval collaterals are less common pathways for decompression of portal vein (Figure 2).

CORONARY, ESOPHAGEAL, PARAESOPHAGEAL AND CARDIOPHRENIC VARICES

Coronary (or left gastric) veins within the lesser omentum are the most frequently depicted varices, seen in 80% of cross-sectional and 86% of angiographic studies in patients with portal hypertension[16,20,21]. With CT, the cephalic portion of the coronary vein is clearly delineated, often as multiple channels near the gastroesophageal junction. A coronary vein larger than 5-6 mm in diameter on Doppler sonograms or CT is considered abnormal and is an indicator of portal hypertension[20,22-24].

Coronary venous collaterals are usually accompanied by esophageal or paraesophageal varices. Esophageal varices are usually supplied by the anterior branch of the left gastric vein, whereas the posterior branch of this vein supplies paraesophageal varices[25]. On CT, varices appear as well-defined round, tubular, or serpentine structures that are smooth, have homogeneous attenuation, and enhance with contrast material to the same degree as adjacent portal and mesenteric veins (Figure 3).

Esophageal varices, the most common and clinically important collateral vessels, consist of dilated subepithelial and submucosal veins in the wall of the lower esophagus (Figure 4). They usually drain into the azygos or the hemiazygos system[20]. The reported rate of variceal hemorrhage in patients with esophageal varices is estimated at 10%-30% per year, with the mortality from variceal hemorrhage high at 20%-35%[26]. CT is useful for detection and grading of esophageal varices, with a detection rate of more than 92% of large varices which have an elevated

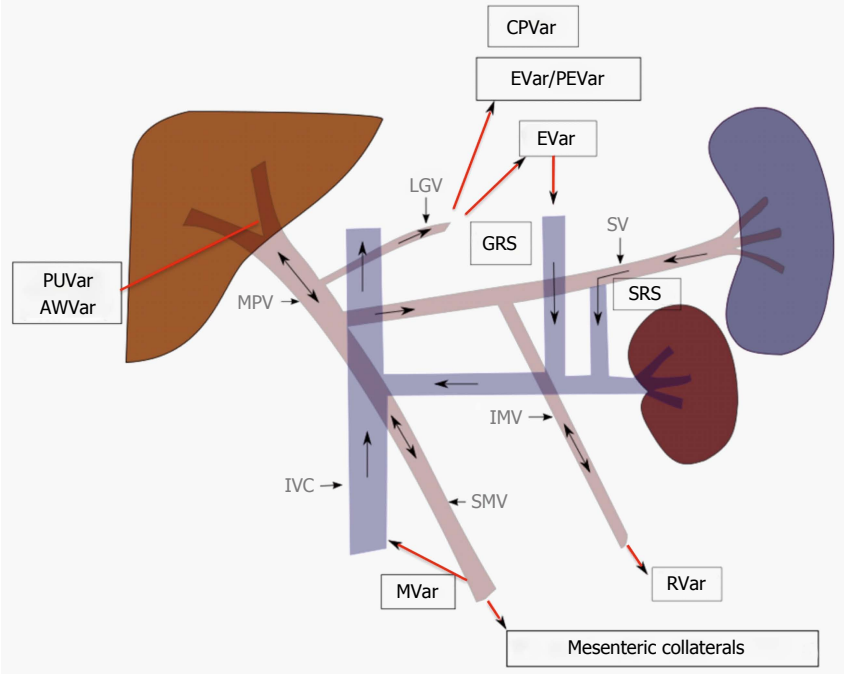

Figure 2 Portosystemic collateral pathways and direction of blood flow in portal hypertension. Progressive resistance to hepatopetal flow results in slowed and eventually reversed flow in the main portal vein (MPV). Portal venous system decompresses by recruiting several pre-exiting collateral pathways, the selection of which is partly dictated by the location of the portal venous resistance. Paraumbilical (PUVar), abdominal wall varices (AWVar), esophageal (EVar), paraesophageal (PEVar), gastric (GVar), cardiophrenic (CPVar), mesenteric (MVar) and rectal (RVar) varices may be created in order to allow the passage the portal venous blood into systemic circulation. LGV: Left gastric vein; SV: Splenic vein; IMV: Inferior mesenteric vein; IVC: Inferior vena cava; SRS: Splenorenal shunt; GRS: Gastrorenal shunt.

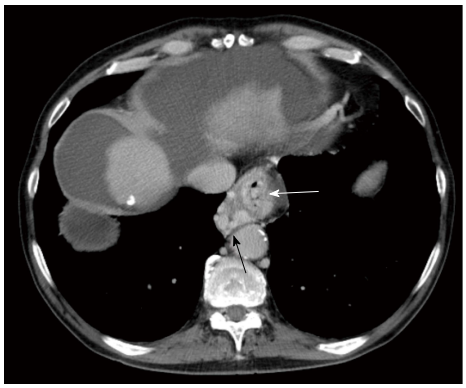

Figure 3 Axial enhanced computed tomography of the upper abdomen in portal venous phase demonstrates multiple large tubular and serpiginous esophageal (white arrow) and paraesophageal (black arrow) varices at the level of the esophageal hiatus of the diaphragm.

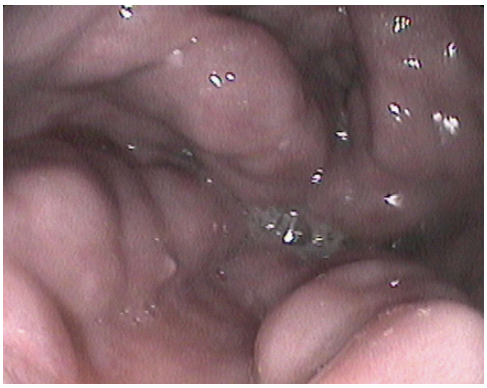

Figure 4 Endoscopic image of large tortuous submucosal esophageal varices protruding into the esophageal lumen.

risk of bleeding[18]. Typical CT appearance is nodular thickening of the esophageal wall and enhancing nodular intraluminal protrusions with scalloped borders[18].

Paraesophageal varices are venous collaterals surrounding the esophagus through a network of multiple veins and connect the coronary vein with the azygos, hemiazygos veins and the vertebral plexus. They are seen in 22%-38% of CT scans as dilated collateral vessels surrounding the esophagus and the descending thoracic aorta (Figure 5)[10,18,19]. They are located outside the walls of the esophagus and thus cannot be seen with endoscopy. Their clinical significance is not entirely clear, however, Lin *et al*[27] demonstrated that paraesophageal varices revealed on chest CT suggested a poor prognosis for patients with esophageal variceal hemorrhage who underwent sclerotherapy.

Cardiophrenic angle varices consist of dilated pericardiacophrenic veins, which frequently occur in patients with cirrhosis caused by membranous obstruction of the inferior vena cava (IVC). Their reported prevalence is estimated at 18%[10]. At radiography, they may manifest as undulating masses

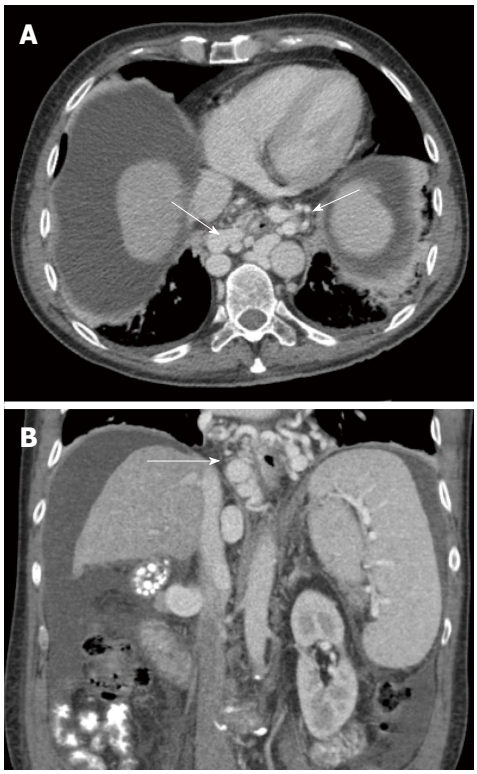

Figure 5 Axial (A) and coronal (B) cross-sectional enhanced computed tomography images show large paraesophageal varices (white arrow) surrounding the esophagus circumferentially in a patient with liver cirrhosis and portal hypertension. Note the nodular and shrunken liver, low-density abdominal ascites and splenomegaly.

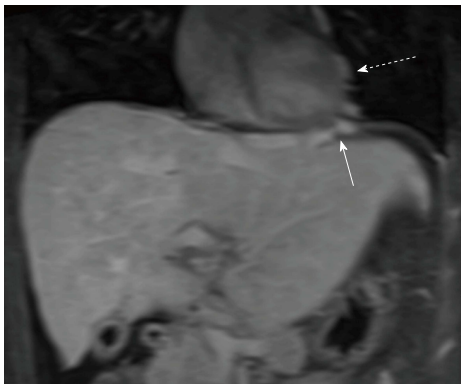

Figure 6 Coronal post-gadolinium T1-weighted fat-suppressed magnetic resonance image shows prominent cardiophrenic (white arrow) and pericardial collateral veins (dashed white arrow) in a patient with Budd-Chiari syndrome.

along the cardiac borders, simulating a tumor (Figure 6).

GASTRIC VARICES AND GASTRORENAL SHUNTS

Gastric varices, along with esophageal varices, are by far the most common portosystemic pathways seen in portal hypertension[21]. The reported prevalence of gastric varices ranges from 2% to 70%. Esophageal

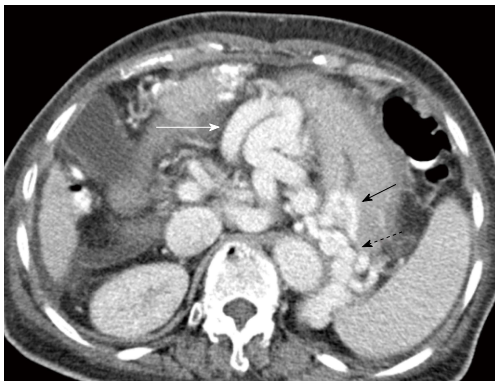

Figure 7 Enhanced axial computed tomography image acquired in portal venous phase demonstrates large upper abdominal omental varices (white arrow). Additionally, several enlarged submucosal gastric (black arrow) and short gastric varices (dashed black arrow).

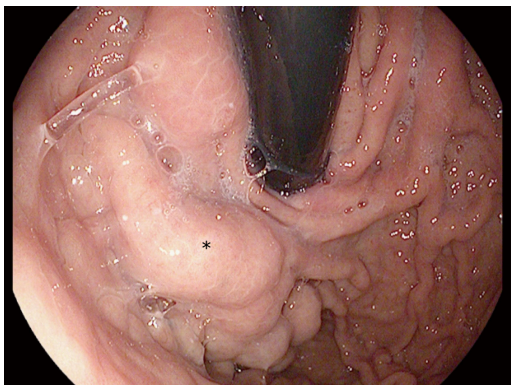

Figure 8 Retroflexed endoscopic image of large tortuous submucosal gastric varices (black star).

and gastric varices frequently coexist, as noted in the widely used Sarin endoscopic grading classification for gastric varices (Table 1)[28]. Esophageal varices are more likely to be supplied by the left gastric or the coronary vein, whereas gastric varices are more likely to be supplied by the short gastric and posterior gastric veins[29]. Dilated short gastric veins appear as a tangle of vessels along the medial aspect of the spleen near the hilum, making it often difficult to distinguish between the gastric fundus and individual vessels (Figure 7). Gastric varices are known to simulate tumors or thickened rugae at endoscopy or barium radiography (Figure 8).

Gastric varices that usually drain into the esophageal or paraesophageal veins but can occasionally drain into the left renal vein *via* a gastrorenal shunt (Figure 9). A gastrorenal shunt appears as a large left-sided retroperitoneal venous channel, associated with dilatation of the left renal vein[30]. These shunts may arise from pre-existing tiny portosystemic communications or from the adrenal and periadrenal venous system[30]. In patients with gastrorenal shunts, large gastric varices may be encountered in the absence of esophageal varices.

Table 1 Sarin endoscopic grading classification for gastric varices

Category	Description
Gastroesophageal varix type 1	Continuation from esophageal varices which extend along the lesser curve
Gastroesophageal varix type 2	Continuation from esophageal varices which extend along the lesser curve but are more tortuous than GOV-1
Isolated gastric varix type 1	Occur in the absence of esophageal varices and are located at the gastric fundus. Varices are tortuous and complex
Isolated gastric varix type 2	Occur in the absence of esophageal varices and are located at the gastric body, antrum or pylorus

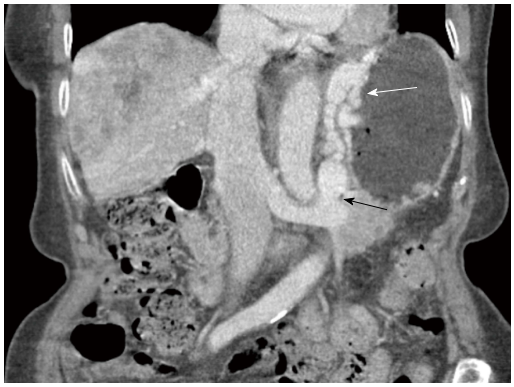

Figure 9 Coronal enhanced computed tomography image demonstrates a large gastrorenal shunt (black arrow) and perigastric, as well as, gastric submucosal varices (white arrow) in a patient with liver cirrhosis and portal hypertension.

PERISPLENIC VARICES AND SPLENORENAL AND SPLENOCAVAL/SPLENOAZYGOS SHUNTS

Splenic varices usually traverse the splenocolic ligament and are seen as dilated veins in the anteroinferior aspect of the spleen[20]. Perisplenic collaterals can communicate with the gastric veins. It should be noted that the tortuous splenic veins frequently seen at the hilum of the enlarged spleen should not be called perisplenic varices.

A spontaneous splenorenal shunt can also develop, which on CT, is seen as large, tortuous veins in the region of the splenic and left renal hilum that drain into an enlarged left renal vein (Figure 10)[30]. These shunts can be so tortuous that the exact origin of the connection along the splenic vein is sometimes difficult to discern.

In the rare case of a splenocaval shunt, large veins may be seen extending from the inferior aspect of the spleen to the pelvis and draining into the inferior vena cava *via* the left internal iliac vein or gonadal vein[20]. Splenoazygos shunts involve portal decompression *via* splenic vein to hemiazygos vein or posterior abdominal wall veins[20]. CT is the best modality for demonstrating these deep portosystemic collateral shunts[20].

PARAUMBILICAL AND ABDOMINAL WALL COLLATERALS

The paraumbilical vein arises from the left portal vein and usually courses between the lateral and medial segments of the left hepatic lobe, along the anterior edge of the falciform ligament. The course and number of the paraumbilical collaterals is variable[31,32]. On cross-sectional imaging, paraumbilical varices appear as tubular structures more than 2-3 mm in diameter (Figure 11) and usually anastomose with the superior epigastric or internal thoracic veins. From there, drainage is typically either into the superior vena cava or anastomose with inferior epigastric vein and then drain into the inferior vena cava through the external iliac vein[31]. Occasionally, the paraumbilical vein drains into the abdominal veins, creating a "Medusa's head" appearance (Figure 12). The paraumbilical system is considered a frequent abdominal portosystemic pathway, with reported prevalence of 30%-35%[20,22].

OMENTAL AND MESENTERIC COLLATERALS

Omental collateral vessels are infrequently included in list of common portosystemic pathways because they are not well visualized with angiography or other modalities. However, Cho *et al*[20] demonstrated a 20% prevalence of omental varices in their series of 60 patients with cirrhosis. Omental varices tend to be small but are usually numerous throughout the greater omentum and should not be mistaken for metastases on CT imaging.

Mesenteric collateral vessels usually appear as dilated and tortuous branches of the superior mesenteric vein within the mesenteric fat[20]. These collateral vessels ultimately drain into the systemic venous system *via* the retroperitoneal or pelvic veins[32]. Mesenterorenal shunts also exist, although rare. They manifest as communication between superior mesenteric vein and the right renal vein[33]. The presence of collateral vessels through the inferior mesenteric vein has also been documented, with authors theorizing that such vessels usually flow into systemic circulation *via* middle and inferior rectal (or hemorrhoidal) varices[34]. Occasionally, blood shunts from the inferior mesenteric vein directly into the inferior vena cava, which is called an inferior mesenteric-caval shunt (or mesocaval shunt) (Figure 13). This may cause encephalopathy, although there is less of a risk of hemorrhage from rectal varices[34].

OTHER COLLATERAL VESSELS

Intrahepatic portal veins may form collateral pathways

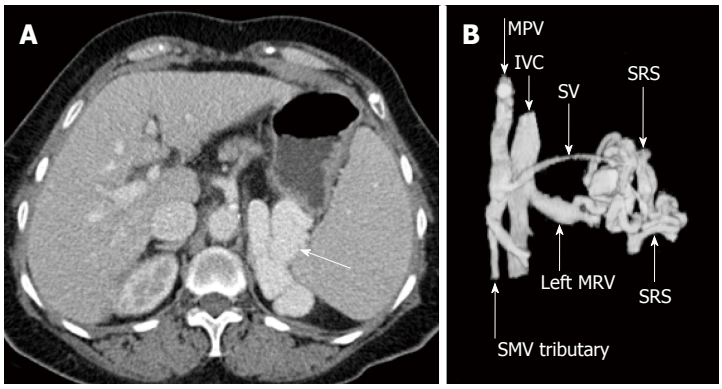

Figure 10 Axial enhanced computed tomography acquired in portal venous phase demonstrates a prominent splenorenal shunt (A, white arrow), left anterior oblique three dimensional computed tomography reconstruction re-demonstrates spontaneous splenorenal shunt draining portal venous blood into the left extra-hilar main renal vein (B). MPV: Main portal vein; SMV: Superior mesenteric vein; IVC: Inferior vena cava; SV: Splenic vein; SRS: Spontaneous splenorenal shunt; MRV: Main renal vein.

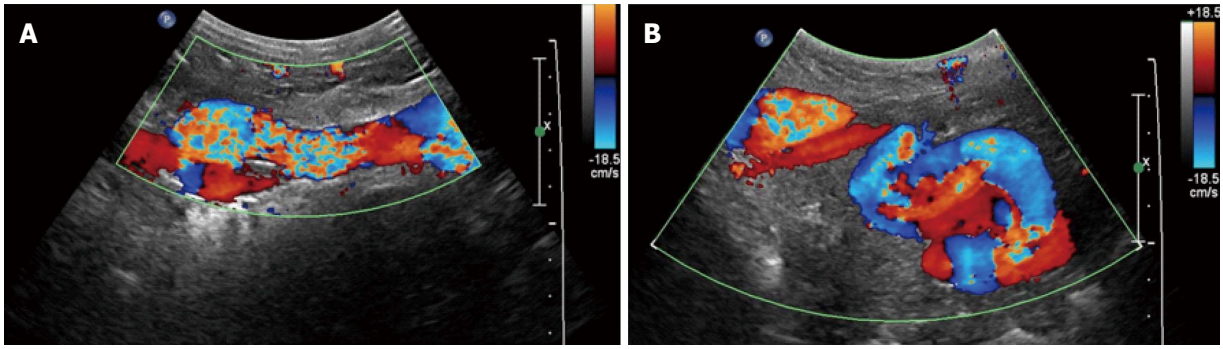

Figure 11 Sagittal (A) and transverse midline (B) Doppler sonographic images demonstrate turbulent flow within a recanalized paraumbilical vein.

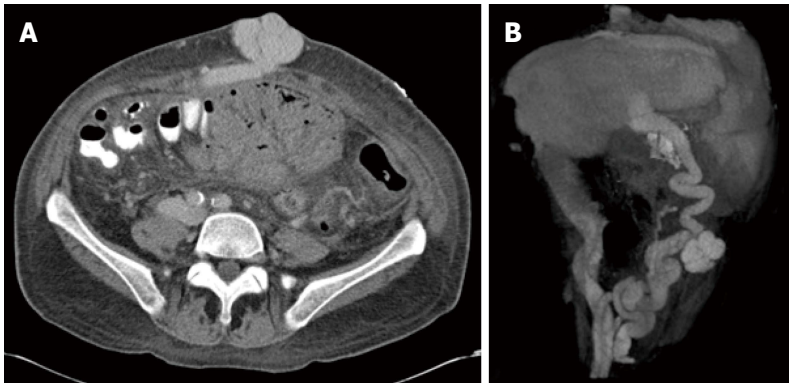

Figure 12 Axial enhanced computed tomography image acquired in portal venous phase (A) and coronal-oblique three-dimensional computed tomography reconstruction (B) demonstrating large paraumbilical varices with large associated caput medusa.

with hepatic venous branches or direct communication with the left gastric vein, usually in the left lobe[32]. A loose collateral plexus over the hepatic surfaces sometimes is widely distributed over the parietal peritoneum, with branches piercing the diaphragm to join pericardial, pleural, and pulmonary veins (pleuropericardial-peritoneal collaterals)[35]. The term vein of Sappey has been used in the past to indicate these small diaphragmatic collaterals, but is now regarded as synonymous for the paraumbilical vein[36,37].

RADIOLOGIC INTERVENTIONS IN PORTAL HYPERTENSION

Interventions involving the portal venous system were conceived as early as 1969, when Rosch and colleagues reported creating a portosystemic shunt within the liver parenchyma in a series of dog experiments using Teflon tubes as stents[38]. Subsequent decades have seen an expansion in the variety of therapeutic interventions to treat portal hypertension. The primary goal in treating portal hypertension is reduction in

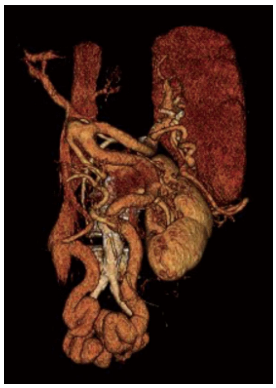

Figure 13 Right anterior oblique three-dimensional computed tomography reconstruction shows mesocaval collateral veins shunting blood from the inferior mesenteric vein to the inferior vena cava *via* the right ovarian vein.

the portal venous pressure itself, in order to mitigate complications such as variceal hemorrhage, congestive gastroenteropathy, refractory ascites, hepatic hydrothorax, and hepatorenal syndrome[39]. In cases where it is not possible to achieve this primary goal, various procedures can be offered to palliate or control the symptoms related to portal hypertension.

REDUCING PORTAL VENOUS PRESSURE: TRANSJUGULAR INTRAHEPATIC PORTOSYSTEMIC SHUNT

Transjugular intrahepatic portosystemic shunt (TIPS) is an image-guided, minimally invasive procedure in which polytetrafluoroethylene (PTFE)-covered stents are deployed through the hepatic parenchyma, bridging the hepatic vein and portal vein[40]. Briefly, frequently under general anaesthesia, the right internal jugular vein is accessed and under fluoroscopic guidance, a catheter-trocar set is typically advanced from the right hepatic vein to the right portal vein. Once appropriate position is confirmed, angioplasty and a PTFE-covered stent is deployed - bridging the portal venous system with the system venous system (Figure 14)[39].

TIPS reduces the portosystemic pressure gradient by functioning as a side-to-side portocaval shunt. The strongest evidence in favor of performing a TIPS procedure exists for the secondary prevention of the onset or recurrence of variceal bleeding[41,42]. A recent meta-analysis published in 2008 found more than threefold decrease in the risk of recurrent bleeding after insertion of a TIPS compared with various forms of endoscopic therapy[43]. TIPS is also indicated for treatment of refractory ascites[44]. A recent trial also showed improved survival in the group of patients who received a TIPS, on top of reduced risk of recurrent ascites[44,45]. Despite limited evidence, TIPS has also found a wider clinical use than just secondary prevention of variceal bleeding and treatment of refractory ascites. Additional indications include: hydrothorax, acute gastropathy, hepatorenal syndrome, Budd-Chiari Syndrome and hepatorenal syndrome[39].

Disadvantages of TIPS include: deterioration of hepatic function caused by diversion of portal venous blood flow and shunt dysfunction, requiring routine imaging surveillance and shunt maintenance procedures. TIPS is contraindicated in patients with congestive heart failure, severe pulmonary hypertension, severe tricuspid regurgitation, and hepatic failure[39]. Moreover, creating an unimpeded shunt to carry un-detoxified blood to systemic circulation may result in worsening of existing hepatic encephalopathy[46].

Direct intrahepatic portocaval shunt (DIPS) is a variation of the TIPS procedure, where intravascular ultrasound (IVUS) is utilized to assist in the transhepatic puncture, passing directly from the IVC to the portal vein, through the caudate lobe[47]. DIPS may be helpful in cases of hepatic vein thrombosis, challenging anatomy or in the presence of an ill-suited hepatic parenchymal tract (presence of hepatocellular carcinoma for example) [47].

PALLIATING SYMPTOMS OF PORTAL HYPERTENSION: BRTO AND VARIANTS

For the past two decades, balloon-occluded retrograde transvenous obliteration of varices (BRTO) has become common practice in Asia for the management of gastric varices. Studies have shown that gastric varices may bleed despite HVPG being less than 12 mmHg, below the treatment target pressure for TIPS[48,49]. The conventional technique involves advancing a catheter from the femoral vein into the outlet of the gastrorenal shunt, typically in the region of the left renal vein. Following balloon occlusion of the shunt, a sclerosant is injected retrograde to fill the gastric varices (Figure 15). Balloon-catheter and sclerosing agent are typically left in place from 4-48 h before completing the procedure[39,48-50].

BRTO has been shown to be effective in controlling gastric variceal bleeding with low re-bleed rates[48,50]. The efficacy of BRTO for treating gastric varices has been described as excellent and some authors have insisted that the procedure could be used as a prophylactic treatment technique before the rupture of gastric varices[49]. BRTO is also thought to improve portal venous flow as it diverts the blood flow from a collateral shunt pathway to the liver. As such, BRTO is also an effective treatment for those patients with refractory hepatic encephalopathy[46,48-51].

BRTO is advantageous to TIPS in that it does not require general anesthesia and can be performed on patients with poor hepatic reserve or those with encephalopathy[49]. However, occlusion of the natural shunts results in increase hepatopetal flow through

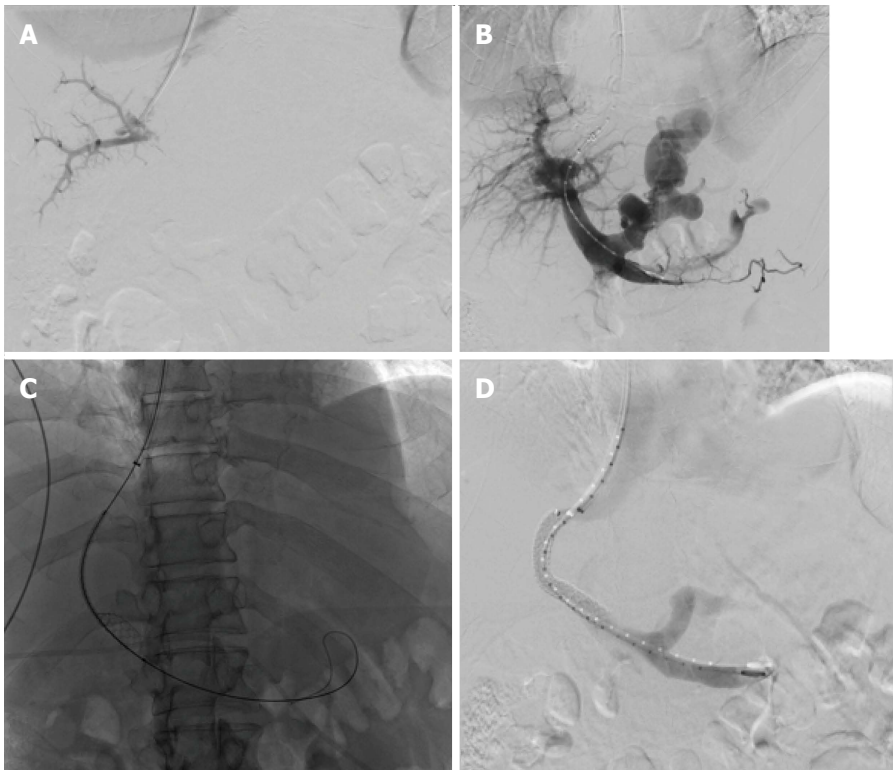

Figure 14 Transjugular intrahepatic portosystemic shunt procedure performed on a 54-year-old male with alcohol-induced cirrhosis and portal hypertension who presents with intractable ascites. A: Rosch-Uchida transjugular intrahepatic portosystemic shunt (TIPS) trochar-needle set (Cook Medical, Bloomington, United States) was advanced into an anterior branch of the right portal vein successfully after four attempts; B: Subsequently a wire and pigtail catheter were advanced into the main portal vein and subtraction angiography was performed demonstrating large dilated left gastric varices; C: Viatorr polytetrafluoroethylene (PTFE)-covered self-expanding stent (Gore Medical, Flagstaff, United States) was deployed over the tract; D: Completion portography demonstrates patency of the TIPS with decreased overall flow into the gastric varices.

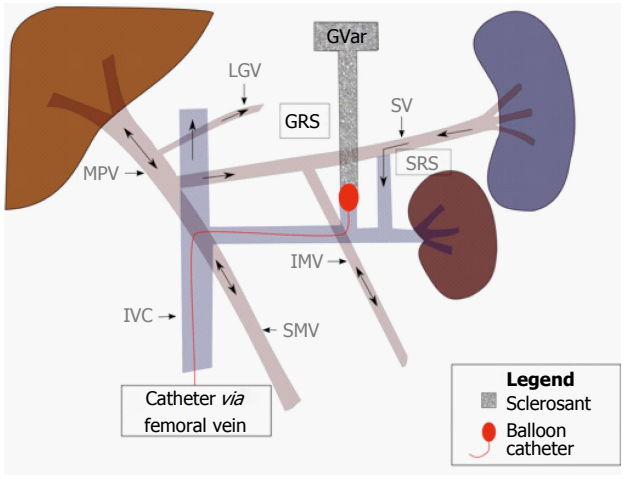

Figure 15 Retrograde balloon occlusion of gastro-renal shunt *via* femoral venous approach coursing through the inferior vena cava and left renal vein. After balloon occlusion, a sclerosing agent is injected into the gastric varices (GVar). Black arrows indicate directional blood flow. MPV: Main portal vein; IMV: Inferior mesenteric vein; IVC: Inferior vena cava; GRS: Gastrorenal shunt.

the portal vein, increasing portal venous pressure. This may inadvertently aggravate esophageal varices and ascites. In patients with poor hepatic reserve, risks and benefits of BRTO should be weighted very carefully[39,49]. Additionally, the sclerosing agents themselves also have a potential serious side effects including, pulmonary edema, disseminated intravascular coagulopathy, portal vein thrombosis, renal dysfunction and anaphylaxis[49,50,52].

Coil-assisted retrograde transvenous obliteration (CARTO) of gastric varices is a modified version of the original BRTO procedure. Utilizing dual microcatheter technique, one microcatheter is placed within the proximal shunt while the second is advanced and placed distally closer to gastric varices. Coil embolization is performed *via* the proximally placed microcatheter, while gelfoam embolization of the gastric varices is performed *via* the distal microcatheter. After variceal embolization is complete, the entire microcatheter system is removed[52]. A recent study has demonstrated similar procedural efficacy to BRTO, while alleviating the complications related to an indwelling balloon catheter (balloon-rupture, access site complication, intensive care admission and monitoring), as well as, avoiding the potential systemic side-effects of the sclerosing agent[52]. A similar procedure, using a vascular plug instead of a coil pack (vascular plug-assisted transvenous obliteration of gastric varices or "PARTO"), has also been validated demonstrating high technical success and clinical efficacy for the treatment of gastric

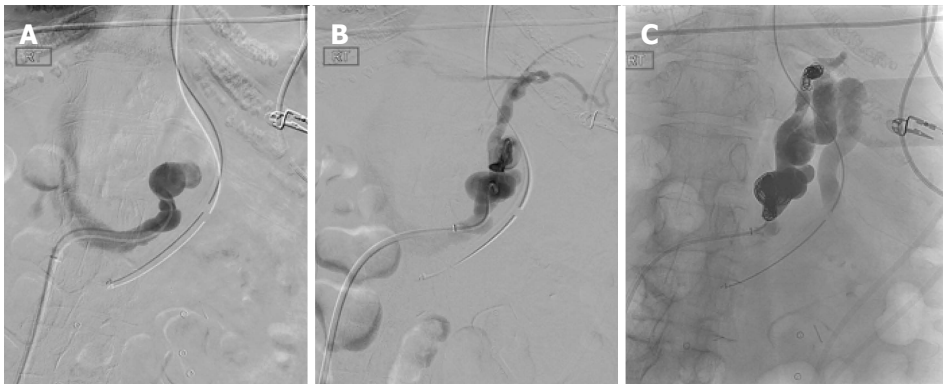

Figure 16 Coil-assisted retrograde transvenous obliteration of gastric varices in a 55-year-old patient who presented with recurrent gastric variceal bleeding refractory to endoscopic therapy. A: Angled catheter was navigated into the left gastrorenal shunt after obtaining access from the right common femoral vein and advancing 5-french sheath into the inferior vena cava; B: Digital subtraction angiography performed through the gastrorenal shunt demonstrating large dilated shunt vessels, as well as, secondary outflow through pericardiophrenic collaterals; C: Both the proximal and distal shunts were coil-occluded and gelfoam was utilized to embolize and thrombose the gastric varices.

varices and hepatic encephalopathy[53] (Figure 16).

CONCLUSION

Portal hypertension is a common clinical syndrome characterized by pathologic increase in portal venous pressure and the formation of portosystemic collaterals that divert blood away from the liver. The imaging appearance can be quite variable and knowledge of the various collateral pathways is essential for diagnosis and treatment planning. The role of radiology continues to evolve with increased utilization of advanced imaging techniques in detecting and diagnosing portal hypertension and liver disease, as well as, image-guided interventions to treat complications of portal hypertension.

REFERENCES

1 **Bosch J**, Groszmann RJ, Shah VH. Evolution in the understanding of the pathophysiological basis of portal hypertension: How changes in paradigm are leading to successful new treatments. *J Hepatol* 2015; **62**: S121-S130 [PMID: 25920081 DOI: 10.1016/j.jhep.2015.01.003]

2 **Bosch J**, Abraldes JG, Fernández M, García-Pagán JC. Hepatic endothelial dysfunction and abnormal angiogenesis: new targets in the treatment of portal hypertension. *J Hepatol* 2010; **53**: 558-567 [PMID: 20561700 DOI: 10.1016/j.jhep.2010.03.021]

3 **Plessier A**, Darwish-Murad S, Hernandez-Guerra M, Consigny Y, Fabris F, Trebicka J, Heller J, Morard I, Lasser L, Langlet P, Denninger MH, Vidaud D, Condat B, Hadengue A, Primignani M, Garcia-Pagan JC, Janssen HL, Valla D. Acute portal vein thrombosis unrelated to cirrhosis: a prospective multicenter follow-up study. *Hepatology* 2010; **51**: 210-218 [PMID: 19821530 DOI: 10.1002/hep.23259]

4 **Schuppan D**, Afdhal NH. Liver cirrhosis. *Lancet* 2008; **371**: 838-851 [PMID: 18328931 DOI: 10.1016/S0140-6736(08)60383-9]

5 **Bosch J**, Navasa M, Garcia-Pagán JC, DeLacy AM, Rodés J. Portal hypertension. *Med Clin North Am* 1989; **73**: 931-953 [PMID: 2657268]

6 **Bosch J**, Abraldes JG, Berzigotti A, García-Pagan JC. The clinical use of HVPG measurements in chronic liver disease. *Nat Rev Gastroenterol Hepatol* 2009; **6**: 573-582 [PMID: 19724251 DOI: 10.1038/nrgastro.2009.149]

7 **Harmanci O**, Bayraktar Y. Clinical characteristics of idiopathic portal hypertension. *World J Gastroenterol* 2007; **13**: 1906-1911 [PMID: 17461489 DOI: 10.3748/wjg.v13.i13.1906]

8 **Berzigotti A**, Seijo S, Reverter E, Bosch J. Assessing portal hypertension in liver diseases. *Expert Rev Gastroenterol Hepatol* 2013; **7**: 141-155 [PMID: 23363263 DOI: 10.1586/egh.12.83]

9 **Thabut D**, Shah V. Intrahepatic angiogenesis and sinusoidal remodeling in chronic liver disease: new targets for the treatment of portal hypertension? *J Hepatol* 2010; **53**: 976-980 [PMID: 20800926 DOI: 10.1016/j.jhep.2010.07.004]

10 **Wachsberg RH**, Yaghmai V, Javors BR, Levine CD, Simmons MZ, Maldjian PD. Cardiophrenic varices in portal hypertension: evaluation with CT. *Radiology* 1995; **195**: 553-556 [PMID: 7724782 DOI: 10.1148/radiology.195.2.7724782]

11 **Berzigotti A**, Piscaglia F. Ultrasound in portal hypertension--part 2--and EFSUMB recommendations for the performance and reporting of ultrasound examinations in portal hypertension. *Ultraschall Med* 2012; **33**: 8-32; quiz 30-31 [PMID: 22322479 DOI: 10.1055/s-0031-1299145]

12 **Castera L**, Pinzani M, Bosch J. Non invasive evaluation of portal hypertension using transient elastography. *J Hepatol* 2012; **56**: 696-703 [PMID: 21767510 DOI: 10.1016/j.jhep.2011.07.005]

13 **Perri RE**, Chiorean MV, Fidler JL, Fletcher JG, Talwalkar JA, Stadheim L, Shah ND, Kamath PS. A prospective evaluation of computerized tomographic (CT) scanning as a screening modality for esophageal varices. *Hepatology* 2008; **47**: 1587-1594 [PMID: 18393388 DOI: 10.1002/hep.22219]

14 **Bosch J**, Berzigotti A, Garcia-Pagan JC, Abraldes JG. The management of portal hypertension: rational basis, available treatments and future options. *J Hepatol* 2008; **48** Suppl 1: S68-S92 [PMID: 18304681 DOI: 10.1016/j.jhep.2008.01.021]

15 **Stankovic Z**, Allen BD, Garcia J, Jarvis KB, Markl M. 4D flow imaging with MRI. *Cardiovasc Diagn Ther* 2014; **4**: 173-192 [PMID: 24834414 DOI: 10.3978/j.issn.2223-3652.2014.01.02]

16 **Stankovic Z**, Csatari Z, Deibert P, Euringer W, Blanke P, Kreisel W, Abdullah Zadeh Z, Kallfass F, Langer M, Markl M. Normal and altered three-dimensional portal venous hemodynamics in patients with liver cirrhosis. *Radiology* 2012; **262**: 862-873 [PMID: 22357888 DOI: 10.1148/radiol.11110127]

17 **Roldán-Alzate A**, Frydrychowicz A, Niespodzany E, Landgraf BR, Johnson KM, Wieben O, Reeder SB. In vivo validation of 4D flow MRI for assessing the hemodynamics of portal hypertension. *J Magn Reson Imaging* 2013; **37**: 1100-1108 [PMID: 23148034 DOI: 10.1002/jmri.23906]

18 **Kim YJ**, Raman SS, Yu NC, To'o KJ, Jutabha R, Lu DS. Esophageal varices in cirrhotic patients: evaluation with liver CT. *AJR Am J Roentgenol* 2007; **188**: 139-144 [PMID: 17179356 DOI: 10.2214/AJR.05.1737]

19 **Lee SJ**, Lee KS, Kim SA, Kim TS, Hwang JH, Lim JH. Computed radiography of the chest in patients with paraesophageal varices: diagnostic accuracy and characteristic findings. *AJR Am J Roentgenol* 1998; **170**: 1527-1531 [PMID: 9609167 DOI: 10.2214/ajr.170.6.9609167]

20 **Cho KC**, Patel YD, Wachsberg RH, Seeff J. Varices in portal hypertension: evaluation with CT. *Radiographics* 1995; **15**: 609-622 [PMID: 7624566 DOI: 10.1148/radiographics.15.3.7624566]

21 **Hoevels J**, Lunderquist A, Tylén U, Simert G. Porto-systemic collaterals in cirrhosis of the liver. Selective percutaneous transhepatic catheterization of the portal venous system in portal hypertension. *Acta Radiol Diagn* (Stockh) 1979; **20**: 865-877 [PMID: 546069]

22 **Subramanyam BR**, Balthazar EJ, Madamba MR, Raghavendra BN, Horii SC, Lefleur RS. Sonography of portosystemic venous collaterals in portal hypertension. *Radiology* 1983; **146**: 161-166 [PMID: 6849040 DOI: 10.1148/radiology.146.1.6849040]

23 **Wachsberg RH**, Simmons MZ. Coronary vein diameter and flow direction in patients with portal hypertension: evaluation with duplex sonography and correlation with variceal bleeding. *AJR Am J Roentgenol* 1994; **162**: 637-641 [PMID: 8109512 DOI: 10.2214/ajr.162.3.8109512]

24 **Lafortune M**, Marleau D, Breton G, Viallet A, Lavoie P, Huet PM. Portal venous system measurements in portal hypertension. *Radiology* 1984; **151**: 27-30 [PMID: 6701328 DOI: 10.1148/radiology.151.1.6701328]

25 **Takahashi N**, Kuroki K, Yanaga K. Percutaneous Transhepatic Mechanical Thrombectomy for Acute Mesenteric Venous Thrombosis. *J Endovasc Ther* 2005; **12**: 508-511 [PMID: 16048384 DOI: 10.1583/04-1335MR.1]

26 **Garcia-Tsao G**. Current Management of the Complications of Cirrhosis and Portal Hypertension: Variceal Hemorrhage, Ascites, and Spontaneous Bacterial Peritonitis. *Dig Dis* 2001; **34**: 382-386 [PMID: 27170392 DOI: 10.1053/gast.2001.22580]

27 **Lin CY**, Lin PW, Tsai HM, Lin XZ, Chang TT, Shin JS. Influence of paraesophageal venous collaterals on efficacy of endoscopic sclerotherapy for esophageal varices. *Hepatology* 1994; **19**: 602-608 [PMID: 8119684 DOI: 10.1002/hep.1840190310]

28 **Sarin SK**, Lahoti D, Saxena SP, Murthy NS, Makwana UK. Prevalence, classification and natural history of gastric varices: a long-term follow-up study in 568 portal hypertension patients. *Hepatology* 1992; **16**: 1343-1349 [PMID: 1446890 DOI: 10.1002/hep.1840160607]

29 **Feldman M**, Feldman M. Gastric varices. *Gastroenterology* 1956; **30**: 318-321 [PMID: 13294324]

30 **Mitty HA**, Cohen BA, Sprayregen S, Schwartz K. Adrenal pseudotumors on CT due to dilated portosystemic veins. *AJR Am J Roentgenol* 1983; **141**: 727-730 [PMID: 6604425 DOI: 10.2214/ajr.141.4.727]

31 **Morin C**, Lafortune M, Pomier G, Robin M, Breton G. Patent paraumbilical vein: anatomic and hemodynamic variants and their clinical importance. *Radiology* 1992; **185**: 253-256 [PMID: 1523319 DOI: 10.1148/radiology.185.1.1523319]

32 **Okuda K**, Matsutani S. Portal-systemic collaterals: anatomy and clinical implications. 1st ed. Tokyo, Japan: Springer Japan, 1991

33 **Gould H**, Benjamin S, Alter A. Retroperitoneal varices simulating masses. *Gastrointest Radiol* 1982;**7**:335-9 [PMID: 7141186]

34 **Malde H**, Nagral A, Shah P, Joshi MS, Bhatia SJ, Abraham P. Detection of rectal and pararectal varices in patients with portal hypertension: efficacy of transvaginal sonography. *AJR Am J Roentgenol* 1993; **161**: 335-337 [PMID: 8333372 DOI: 10.2214/ajr.161.2.8333372]

35 **Kim M**, Mitchell DG, Ito K. Portosystemic collaterals of the upper abdomen: review of anatomy and demonstration on MR imaging. *Abdom Imaging* 2000; **25**: 462-470 [PMID: 10931979 DOI: 10.1007/s002610000014]

36 **William P**. Veins of the abdomen and pelvis: hepatic portal system. In: Grey's Anatomy. New York, NY: Churchill Livingstone, 1999: 1602-1604

37 **Uflacker R**. Veins of the abdomen and pelvis. In: Atlas of vascular anatomy. Baltimore, MA: Lippincott Williams & Wilson, 1997: 699-803

38 **Rösch J**, Hanafee WN, Snow H. Transjugular portal venography and radiologic portacaval shunt: an experimental study. *Radiology* 1969; **92**: 1112-1114 [PMID: 5771827 DOI: 10.1148/92.5.1112]

39 **Kirby JM**, Cho KJ, Midia M. Image-guided intervention in management of complications of portal hypertension: more than TIPS for success. *Radiographics* 2013; **33**: 1473-1496 [PMID: 24025936 DOI: 10.1148/rg.335125166]

40 **Fidelman N**, Kwan SW, LaBerge JM, Gordon RL, Ring EJ, Kerlan RK. The transjugular intrahepatic portosystemic shunt: an update. *AJR Am J Roentgenol* 2012; **199**: 746-755 [PMID: 22997364 DOI: 10.2214/AJR.12.9101]

41 **Rössle M**, Haag K, Ochs A, Sellinger M, Nöldge G, Perarnau JM, Berger E, Blum U, Gabelmann A, Hauenstein K. The transjugular intrahepatic portosystemic stent-shunt procedure for variceal bleeding. *N Engl J Med* 1994; **330**: 165-171 [PMID: 8264738 DOI: 10.1056/NEJM199401203300303]

42 **García-Pagán JC**, Caca K, Bureau C, Laleman W, Appenrodt B, Luca A, Abraldes JG, Nevens F, Vinel JP, Mössner J, Bosch J. Early use of TIPS in patients with cirrhosis and variceal bleeding. *N Engl J Med* 2010; **362**: 2370-2379 [PMID: 20573925 DOI: 10.1056/NEJMoa0910102]

43 **Zheng M**, Chen Y, Bai J, Zeng Q, You J, Jin R, Zhou X, Shen H, Zheng Y, Du Z. Transjugular intrahepatic portosystemic shunt versus endoscopic therapy in the secondary prophylaxis of variceal rebleeding in cirrhotic patients: meta-analysis update. *J Clin Gastroenterol* 2000; **42**: 507-516 [PMID: 18344888 DOI: 10.1097/MCG.0b013e31815576e6]

44 **Rössle M**, Ochs A, Gülberg V, Siegerstetter V, Holl J, Deibert P, Olschewski M, Reiser M, Gerbes AL. A comparison of paracentesis and transjugular intrahepatic portosystemic shunting in patients with ascites. *N Engl J Med* 2000; **342**: 1701-1707 [PMID: 10841872 DOI: 10.1056/NEJM200006083422303]

45 **Narahara Y**, Kanazawa H, Fukuda T, Matsushita Y, Harimoto H, Kidokoro H, Katakura T, Atsukawa M, Taki Y, Kimura Y, Nakatsuka K, Sakamoto C. Transjugular intrahepatic portosystemic shunt versus paracentesis plus albumin in patients with refractory ascites who have good hepatic and renal function: a prospective randomized trial. *J Gastroenterol* 2011; **46**: 78-85 [PMID: 20632194 DOI: 10.1007/s00535-010-0282-9]

46 **Uflacker R**, Silva Ade O, d'Albuquerque LA, Piske RL, Mourão GS. Chronic portosystemic encephalopathy: embolization of portosystemic shunts. *Radiology* 1987; **165**: 721-725 [PMID: 3685350 DOI: 10.1148/radiology.165.3.3685350]

47 **Petersen BD**, Clark TW. Direct intrahepatic portocaval shunt. *Tech Vasc Interv Radiol* 2008; **11**: 230-234 [PMID: 19527850 DOI: 10.1053/j.tvir.2009.04.006]

48 **Saad WE**, Khaja MS, Hirota S. Balloon-occluded retrograde transvenous obliteration of gastric varices: conception, evolution, and history. *Tech Vasc Interv Radiol* 2012; **15**: 160-164 [PMID: 23021830 DOI: 10.1053/j.tvir.2012.07.002]

49 **Cho SK**, Shin SW, Lee IH, Do YS, Choo SW, Park KB, Yoo BC. Balloon-occluded retrograde transvenous obliteration of gastric varices: outcomes and complications in 49 patients. *AJR Am J Roentgenol* 2007; **189**: W365-W372 [PMID: 18029851 DOI: 10.2214/AJR.07.2266]

50 **Ninoi T**, Nishida N, Kaminou T, Sakai Y, Kitayama T, Hamuro M, Yamada R, Nakamura K, Arakawa T, Inoue Y. Balloon-occluded retrograde transvenous obliteration of gastric varices with gastrorenal shunt: long-term follow-up in 78 patients. *AJR Am J Roentgenol* 2005; **184**: 1340-1346 [PMID: 15788621 DOI: 10.2214/ajr.184.4.01841340]

51 **Fukuda T**, Hirota S, Sugimura K. Long-term results of balloon-occluded retrograde transvenous obliteration for the treatment of gastric varices and hepatic encephalopathy. *J Vasc Interv Radiol* 2001; **12**: 327-336 [PMID: 11287510]

52 **Lee EW**, Saab S, Gomes AS, Busuttil R, McWilliams J, Durazo F, Han SH, Goldstein L, Tafti BA, Moriarty J, Loh CT, Kee ST. Coil-Assisted Retrograde Transvenous Obliteration (CARTO) for the Treatment of Portal Hypertensive Variceal Bleeding: Preliminary

Results. *Clin Transl Gastroenterol* 2014; **5**: e61 [PMID: 25273155 DOI: 10.1038/ctg.2014.12]

53 **Gwon DI**, Kim YH, Ko GY, Kim JW, Ko HK, Kim JH, Shin JH, Yoon HK, Sung KB. Vascular Plug-Assisted Retrograde Transvenous Obliteration for the Treatment of Gastric Varices and Hepatic Encephalopathy: A Prospective Multicenter Study. *J Vasc Interv Radiol* 2015; **26**: 1589-1595 [PMID: 26316136 DOI: 10.1016/j.jvir.2015.07.011]

P- Reviewer: Guo XZ, Kreisel W **S- Editor**: Yu J **L- Editor**: A
E- Editor: Wang CH

World Journal of Gastroenterology

Submit a Manuscript: http://www.wjgnet.com/esps/

World J Gastroenterol 2017 March 14; 23(10): 1747-1757

DOI: 10.3748/wjg.v23.i10.1747

ISSN 1007-9327 (print) ISSN 2219-2840 (online)

REVIEW

Non-alcoholic fatty liver disease connections with fat-free tissues: A focus on bone and skeletal muscle

Eleonora Poggiogalle, Lorenzo Maria Donini, Andrea Lenzi, Claudio Chiesa, Lucia Pacifico

Eleonora Poggiogalle, Lorenzo Maria Donini, Andrea Lenzi, Department of Experimental Medicine- Medical Pathophysiology, Food Science and Endocrinology Section, Sapienza University of Rome, 00185 Rome, Italy

Claudio Chiesa, Institute of Translational Pharmacology, National Research Council, 00133 Rome, Italy

Lucia Pacifico, Policlinico Umberto I Hospital, Sapienza University of Rome, 00161 Rome, Italy

Author contributions: Poggiogalle E, Donini LM, Lenzi A, Chiesa C and Pacifico L designed the study, analyzed the data and wrote the manuscript; all authors participated in the critical review and in the final approval of the manuscript.

Conflict-of-interest statement: There are no potential conflicts of interest relevant to this article.

Manuscript source: Invited manuscript

Correspondence to: Lucia Pacifico, MD, Policlinico Umberto I Hospital, Sapienza University of Rome, Rome, Viale Regina Elena, 324, 00161 Rome, Italy. lucia.pacifico@uniroma1.it
Telephone: +39-6-49979215
Fax: +39-6-49979216

Received: October 28, 2016
Peer-review started: November 22, 2016
First decision: January 19, 2017
Revised: January 30, 2017
Accepted: February 16, 2017
Article in press: February 17, 2017
Published online: March 14, 2017

Abstract

The estimates of global incidence and prevalence of non-alcoholic fatty liver disease (NAFLD) are worrisome, due to the parallel burden of obesity and its metabolic complications. Indeed, excess adiposity and insulin resistance represent two of the major risk factors for NAFLD; interestingly, in the last years a growing body of evidence tended to support a novel mechanistic perspective, in which the liver is at the center of a complex interplay involving organs and systems, other than adipose tissue and glucose homeostasis. Bone and the skeletal muscle are fat- free tissues which appeared to be independently associated with NAFLD in several cross-sectional studies. The deterioration of bone mineral density and lean body mass, leading to osteoporosis and sarcopenia, respectively, are age-related processes. The prevalence of NAFLD also increases with age. Beyond physiological aging, the three conditions share some common underlying mechanisms, and their elucidations could be of paramount importance to design more effective treatment strategies for the management of NAFLD. In this review, we provide an overview on epidemiological data as well as on potential contributors to the connections of NAFLD with bone and skeletal muscle.

Key words: Non-alcoholic fatty liver disease; Bone; Skeletal muscle; Osteoporosis; Sarcopenia

Core tip: Novel epidemiological findings open new avenues for a thorough understanding of the pathogenesis of non-alcoholic fatty liver disease (NAFLD). Liver appears to participate in a fascinating cross- talk with fat-free tissue, mainly bone and skeletal muscle. The identification of contributors other than the classic roles played by excess fat and insulin resistance may

be relevant for the design of more effective treatment strategies for NAFLD.

Poggiogalle E, Donini LM, Lenzi A, Chiesa C, Pacifico L. Non-alcoholic fatty liver disease connections with fat-free tissues: A focus on bone and skeletal muscle. *World J Gastroenterol* 2017; 23(10): 1747-1757 Available from: URL: http://www.wjgnet.com/1007-9327/full/v23/i10/1747.htm DOI: http://dx.doi.org/10.3748/wjg.v23.i10.1747

INTRODUCTION

In the last decades, a wealth of studies have focused on non-alcoholic fatty liver disease (NAFLD), given that the rising prevalence of this clinical condition has paralleled the obesity epidemic in Western and developing countries[1,2]. The intrahepatic triglyceride accumulation is the hallmark of NAFLD[3]; energy imbalance and insulin resistance are considered the most relevant determinants leading to ectopic fat deposition in the liver, and NAFLD has been described as the hepatic manifestation of the metabolic syndrome[3,4]. Hence, evidence regarding NAFLD is undoubtedly strictly related to excess adiposity and its metabolic consequences[2-4]. However, in recent years, NAFLD has been associated to diseases and clinical conditions which typically have a natural history that is independent of obesity, such as osteoporosis and the decline of lean body mass, namely sarcopenia[5,6]. Similar to osteoporosis and sarcopenia, which are notably linked to age-related processes[7], the prevalence of NAFLD also tends to increase with aging in men and in both premenopausal and postmenopausal women[8,9]. Furthermore, the association between fatty liver and poor bone mineralization has been also revealed in the pediatric population[5], expanding the constellation of mechanistic hypotheses other than the known potential contributors characterizing the aging process (*e.g.,* changes in sex steroids)[8,10]. Therefore, NAFLD appears to be at the center of an intriguing cross- talk involving fat-free tissues, in a new fascinating scenario in which obesity could be only marginally present. In the extant studies, the relationships between NAFLD and bone health, as well as between NAFLD and sarcopenia, have been separately examined. The aim of the present review is to summarize epidemiological evidence and potential underlying mechanisms in the complex interplay among NAFLD, bone, and skeletal muscle. Relevant peer- reviewed journal articles published in English were identified in the MEDLINE database (the last search was conducted on August 31, 2016); different combinations of the following search terms were used: "nonalcoholic fatty liver disease", "bone", "skeletal muscle mass", "lean body mass".

Also the following exclusion criteria were used: any paper dealing with viral or autoimmune hepatic disease, inherited metabolic disorders, excessive alcohol intake; any paper including the definition of NAFLD based on clinical chemistry data only (*e.g.,* elevated aminotransferase levels); any paper on sarcopenia associated to cancer cachexia or neurological diseases, inflammatory or autoimmune diseases, corticosteroids for systemic use; any paper including bedridden subjects; any paper concerning osteoporosis as secondary disease; any paper in which fractures and not bone mineral density (BMD), were the main outcome; any paper evaluating markers of bone turnover without data on BMD; and any study conducted in animals. Review articles and secondary data analyses, letters in response to published articles, editorials, commentaries and conference abstracts were excluded.

NAFLD AND BONE MINERAL DENSITY

Most studies dealing with BMD in subjects with fatty liver were conducted in the Asian population, and liver ultrasonography was the most used method for the diagnosis of NAFLD. BMD was assessed by dual energy X-ray absorptiometry (DXA) in all studies, but different sites of the skeleton, or whole body BMD, were examined (Table 1)[11-22]. The association between NAFLD and decreased BMD has been reported in both genders, and also confirmed in children and adolescents, in the majority of the studies, with few exceptions[13,16,20].

Xia *et al*[11] reported a negative association between NAFLD and any site of the skeleton examined in Chinese men and postmenopausal women aged 46-93 years. Similarly, Cui *et al*[12] described a negative association between NAFLD and BMD (as average of BMD at the femoral neck, hip, and lumbar spine) in Chinese men and postmenopausal women (aged 40-70 years). However, both genders with NAFLD showed lower BMD at the hip than controls, whereas no difference was found at the lumbar level. In a large Korean cohort including men aged 40 years and older, and postmenopausal women, Lee *et al*[13] observed a negative association between NAFLD and the femoral neck BMD in men, whereas a positive relationship emerged between NAFLD and lumbar spine BMD in women. Moon *et al*[14] reported that a negative association between NAFLD and lumbar spine BMD was present in postmenopausal, but not premenopausal women. However, in these studies liver ultrasound was used to diagnose NAFLD. It is well known that sonography is highly operator-dependent, and has limited repeatability and reproducibility because it evaluates liver fat content on the basis of subjective qualitative features of liver echogenicity[23]. In addition, just a few studies examined thoroughly multiple sites or whole body bone mineral density. Bhatt and coll. assessed BMD in different skeletal segments, and surprisingly, found higher BMD values

Table 1 Studies exploring the association between non-alcoholic fatty liver disease and bone mineral density

Ref.	Study population and sample size	Race/ethnicity	NAFLD assessment	Skeleton: segments	Main findings: BMD
Xia *et al*[11], 2016	Elderly men (n = 755) and postmenopausal women (n = 904) divided into quartiles of liver fat content (LFC)	Chinese	Liver quantitative US	Lumbar spine, hip, whole body	BMD in any skeletal segment was lower in the highest LFC quartile compared to the lowest quartile. LFC inversely correlated with BMD (all skeletal segments)
Cui *et al*[12], 2013	Men with NAFLD (n = 46) *vs* male controls (n = 53); postmenopausal women with NAFLD (n = 73) *vs* female controls (n = 52)	Chinese	Liver US	Lumbar spine, right hip, femoral neck	Lower BMD at the right hip in participants with NAFLD than controls (in both genders); lower BMD at the femoral neck in men with NAFLD *vs* controls. Negative association between NAFLD and BMD
Lee *et al*[13], 2016	Men with NAFLD (n = 1288) *vs* male controls (n = 2018); postmenopausal women with NAFLD (n = 1217) *vs* female controls (n = 2112)	Korean	Liver US	Lumbar spine and femoral neck	Negative association between femoral neck BMD and NAFLD in men; positive correlation between lumbar spine BMD and NAFLD in postmenopausal women
Moon *et al*[14], 2012	Premenopausal women with NAFLD (n = 162) *vs* controls (n = 54), and postmenopausal with NAFLD (n = 102) *vs* controls (n = 163)	Korean	Liver US	Lumbar spine	Higher BMD in the control group than postmenopausal women NAFLD; NAFLD negatively associated with BMD in postmenopausal women, but not premenopausal women
Purnak *et al*[15], 2012	Men (n = 52) and women (n = 50) with NAFLD *vs* healthy men (n = 28) and women (n = 26)	Caucasian	Liver US	Femur (neck, trochanter, intertrochanteric region and total femur) and lumbar spine	Lower lumbar spine and femoral neck BMD Z-scores in women with high ALT levels
Bhatt *et al*[16], 2013	Men (n = 129) and women (n = 33) with NAFLD *vs* controls (men, n = 109; women, n = 64)	Indian	Liver US	Trunk, pelvis, spine, whole body	Higher BMD values in NAFLD subjects than controls
Yang *et al*[17], 2016	Men with NAFLD (n = 249) *vs* male controls (n = 610)	Korean	Liver US	Right Hip	NAFLD negatively associated with right-hip BMD
Pacifico *et al*[18], 2013	Obese children with NAFLD (boys, n = 24, and girls, n = 20) *vs* obese controls (boys, n = 24, and girls, n = 20)	Caucasian	MRI + liver biopsy	Lumbar spine and whole body	Lower lumbar BMD Z-score in NAFLD children than controls. Negative association of lumbar BMD and whole-body BMD Z-scores with NASH
Pardee *et al*[19], 2012	Obese children(10-17 yr) with (n = 38) or without (n = 38) NAFLD	Mixed (89.5% Hipanic, 10.5% non-Hispanic, White)	Liver biopsy	Whole body	Lower whole body BMD Z-score in children with NAFLD than children without NAFLD. Lower whole body BMD Z-score in children with NASH than children without NASH
Chang *et al*[20], 2015	Obese children and adolescents with NAFLD (n = 15) *vs* obese children and adolescents with NASH (n = 47) *vs* controls (n = 32)	Korean	Liver US (NAFLD); liver US + elevated serum aminotransferase levels (NASH)	Arm, leg, trunk, whole body	Age-matched BMD Z-scores were not different between groups
Pirgon *et al*[21], 2011	Obese children with NAFLD (boys, n = 19, and girls, n = 23) *vs* obese children (boys, n = 18, and girls, n = 22) and lean children (boys, n = 15, and girls, n = 15)	Caucasian (Turkish)	Liver US	Lumbar spine	Lower lumbar BMD-SDS in obese adolescents with NAFLD compared with obese and lean adolescents without NAFLD
Campos *et al*[22], 2012	Obese adolescents with NAFLD (n = 18) *vs* obese adolescents without NAFLD (n = 22)	Brazilian	Liver US	Whole body	Obese adolescents with NAFLD had a significantly lower values of BMC than their counterparts without NAFLD. No differences in BMD Z-scores

BMC: Bone mineral content; BMD-SDS: Bone mineral density-standard deviation score; BMD: Bone mineral density; LFC: Liver fat content; MRI: Magnetic resonance imaging; NAFLD: Non-alcoholic fatty liver disease; NASH: Non-alcoholic steatohepatitis; US: Ultrasound; ALT: Alanine aminotransferase.

in some bone sites (namely, trunk, pelvis, spine, and also whole body BMD) in adult subjects with NAFLD compared to controls[16]. In this study, participants with NAFLD had a higher BMI and a higher body fat than controls, and any adjustments for either BMI or body fat were not considered in the comparison of BMD between groups: this may account for the discrepant results obtained[16]. Currently it is unclear if the presence of NAFLD is associated to a higher susceptibility to bone mass deterioration in any specific segment of the skeleton, and this research question, together with a more in-depth investigation of gender differences, needs to be addressed in future studies. However, evidence from pediatric studies, in which NAFLD was biopsy-proven, suggests that the effects of the interrelationship between fatty liver and bone is

already present in the first decades of life, and whole body bone mass seems to be affected[18,19]. Pacifico *et al*[18] evaluated lumbar spine BMD and whole body BMD in obese children with fatty infiltration of the liver, as assessed through MRI (two-point Dixon method) and liver biopsy. Compared to controls, children with NAFLD had lower whole body BMD and lumbar spine BMD; similarly, whole body BMD Z-score and lumbar segmental BMD Z-score were significantly lower according to histological staging. The association between NAFLD and BMD was maintained even after adjustment for fat mass or high-sensitivity C-reactive protein levels. Conversely, Chang *et al*[20] described no difference in age-matched BMD Z-scores in Korean children with simple steatosis or NASH, compared to controls; in that study, the diagnosis of NAFLD was based on liver ultrasonography, and NASH was defined as the presence of elevated transaminase levels in children with NAFLD. These observations need to be consolidated by further research in larger cohorts, using gold-standard methods for the evaluation of fatty liver.

NAFLD AND SKELETAL MUSCLE

Growing interest has been directed to the involvement of skeletal muscle mass in chronic liver disease, especially in cirrhosis. The decline in lean body mass, namely sarcopenia, has been recognized as one of the comorbidities accompanying liver cirrhosis, likely related to malnutrition occurring in cirrhotic patients[24]. Beyond chronic liver disease of viral or auto-immune origin, several studies have described the phenotype of sarcopenia in subjects with NAFLD (Table 2)[25-31]. Evidence concerning the deterioration of skeletal muscle in NAFLD is scarce, and data from pediatric studies are lacking, due to several reasons. First, sarcopenia is an age-related process, with prevalence increasing in late life[7]. However, the coexistence of risk factors such as obesity and physical inactivity may be responsible for a more precocious onset of this clinical condition. Second, contrary to osteoporosis and reduction of the BMD in the pregeriatric population, universally accepted criteria for the diagnosis of sarcopenia are lacking and are still under debate[32]. In the extant studies investigating the relationship between sarcopenia and NAFLD, the skeletal muscle mass was assessed by DXA or bioimpedance analysis (BIA), and different indices of sarcopenia were used. The majority of studies relied on the use of surrogate indices to identify NAFLD and fibrosis in NAFLD. Moreover, the Asian population has been mainly investigated, whereas evidence from other ethnic groups is scarce to date. In the Korean Sarcopenic Obesity Study, Hong *et al*[6] demonstrated that participants in the lowest skeletal muscle index quartile exhibited a higher odds ratio of having NAFLD (defined by the liver attenuation index from abdominal computed tomography) than subjects in the higher quartiles. Interestingly, this association was maintained even after adjustment for potential confounders such as age, sex, physical activity level, homeostasis model assessment of insulin resistance (HOMA-IR), C-reactive protein, and vitamin D levels. In a different cohort of Korean subjects with a biopsy-proven diagnosis of NAFLD, Koo *et al*[25] found that the prevalence of sarcopenia [defined by the appendicular skeletal muscle mass divided by body weight or normalized to body mass index (BMI)], increased according to NAFLD histological grades (steatosis and ballooning) and fibrosis stage. In addition, the odds ratio of having NASH was increased in sarcopenic subjects compared to their nonsarcopenic counterparts, independent of obesity and HOMA-IR. In the remaining studies, the assessment of NAFLD or liver fibrosis was based on the calculation of surrogate indices (Table 2). In a large population- based study, namely the KHANES 2008-2011, Lee *et al*[26] observed an approximately two-fold higher risk of liver fibrosis in sarcopenic subjects with NAFLD, independent of obesity and insulin resistance. Analogous observations were provided by other studies carried out in Korean, Japanese and Italian cohorts[27-31], showing that the relationship linking NAFLD and sarcopenia was independent of the classic risk factors such as obesity, insulin resistance or other metabolic covariates. Notably, the aforementioned studies included mainly middle-aged and elderly participants. As such, the reciprocal influence of NAFLD and skeletal muscle in the first decades of life remains to be clarified.

POTENTIAL MECHANISMS UNDERLYING THE INTERPLAY BETWEEN NAFLD, BONE, AND SKELETAL MUSCLE

Growth hormone/insulin-like growth factor 1 axis

The growth hormone/insulin-like growth factor 1 (GH/IGF1) axis is involved in protein metabolism in the skeletal muscle as well as bone growth and remodeling[33,34]. The age-related decline of the somatotropic axis activity, namely the somato-pause, represents an important determinant of the development of osteoporosis and sarcopenia[34]. Recent evidence highlights the crucial role of IGF1 signaling in the cross-talk linking striated muscle and bone[35]. Furthermore, NAFLD is a frequent comorbidity observed in patients with GH deficiency, with a more rapid progression to NASH[36]. Several studies have also reported decreased levels of IGF1, that is the major mediator of GH action, in subjects with NAFLD[37]. GH and IGF1 influence carbohydrate and lipid metabolism, with opposite actions: IGF1 stimulates glucose uptake, favoring insulin signaling, whereas GH induces lipolysis, determining insulin resistance mediated by elevated free fatty acid levels[38,39]. However, the association between NAFLD and IGF1 appears to be independent of insulin resistance[40]. Sumida *et al*[41]

Table 2 Studies exploring the association between non-alcoholic fatty liver disease and skeletal muscle mass

Ref.	Study population and sample size	Race/ ethnicity	NAFLD assessment	Skeletal muscle mass assessment	Main findings: skeletal muscle
Hong *et al*[6], 2014	Men (n = 32) and women (n = 96) with sarcopenia *vs* men (n = 135) and women (n = 189) without sarcopenia	Korean	LAI	DXA: -SMI = SMM/ weight (%)	Increased ORs of NAFLD in individuals with SMI value in the lower quartiles
Koo *et al*[25], 2016	Adults with NAFLD (n = 117) *vs* adults with NASH (n = 123) *vs* controls (n = 69)	Korean	Liver biopsy, Fibroscan	BIA: -ASM (kg) -ASM/weight (%) -ASM/BMI	Lower ASM (%) and ASM/BMI in NAFLD and NASH than controls; higher prevalence of sarcopenia in NAFLD and NASH groups than control group
Lee *et al*[26], 2015	Men (n = 5617) and women (n = 9515) divided into four groups: sarcopenic obese (n = 2455) *vs* non-sarcopenic obese subjects (n = 2198); sarcopenic non-obese (n = 2004) *vs* non-sarcopenic non-obese subjects (n = 8475)	Korean	For NAFLD: HSI, CNS For fibrosis: BARD, FIB-4	DXA: -ASMI = ASM/ weight (%)	Inverse correlation between all indices of NAFLD and SMI Increased ORs of NAFLD and advanced fibrosis in subjects with sarcopenia
Hashimoto *et al*[27], 2016	Diabetic men with NAFLD (n = 58) *vs* controls (n = 21), and diabetic women with NAFLD (n = 39) *vs* controls (n = 27)	Japanese	CAP FIB-4	BIA: -SMM (kg) -SMI = SMM/ weight (%)	Negative association between CAP and SMI in men; no significant association in women
Moon *et al*[28], 2013	Low FLI group (men = 1641, and women, n = 1180) *vs* intermediate FLI group (men, n = 2600, and women, n = 2296) *vs* high FLI group (men, n = 1052, and women, n = 796)	Korean	FLI	BIA: -SMI = SMM/ weight (%) -SVR = SMM/VFA	Lower SMI in the high FLI group and the intermediate FLI group than the low FLI group. Negative correlation between FLI and SMI, and between FLI and SVR. The highest SVR quartile had a lower OR for FLI ⩾ 60
Kim *et al*[29], 2016	FLI ⩾ 60 group (men, n = 208, and women, n = 181) *vs* FLI < 60 group (men, n = 976, and women, n = 2374)	Korean	FLI	DXA: -ASM (kg) -SMI = ASM/ weight (%)	Lower SMI in the high FLI group than the low FLI group in both genders. Increased ORs for FLI-defined NAFLD in men and women with low SMI
Lee *et al*[30], 2016	Men (n = 1241) and women (n = 1520) with NFLS-based NAFLD divided into two groups: sarcopenic subjects (n = 337) v. non-sarcopenic subjects (n = 2424)	Korean	For NAFLD: NLFS, CNS,HSI; For fibrosis: NFS, FIB-4, Forns index	DXA: -SI = ASM/BMI	Higher NFS, FIB-4, and Forns index in the sarcopenic group that the non-sarcopenic group; negative association of SI with NFS, FIB-4, and Forns index
Poggiogalle *et al*[31], 2016	Obese men (n = 81) and women (n = 346) divided into 2 groups: FLI 20 ⩽ FLI < 60 (n = 61) and FLI ⩾ 60 (n = 359) (FLI ⩽ 20 in 7 subjects only, excluded from the analysis)	Caucasian (Italian)	FLI	DXA: -TrFM/ASM ratio	Positive association between FLI and TrFM/ASM ratio (indicating high visceral adiposity and low appendicular muscularity)

ASM: Appendicular skeletal mass; ASMI: Appendicular skeletal mass index; BMI: Body mass index; CAP: Controlled attenuation parameter; CNS: Comprehensive NAFLD score; CT: Computed tomography; FLI: Fatty liver index; HIS: Hepatic steatosis index; LAI: Liver attenuation index; NAFLD: Non-alcoholic fatty liver disease; NASH: Nonalcoholic steatohepatitis; NFS: NAFLD fibrosis score; SI: Sarcopenia index; NLFS: NAFLD liver fat score; SMI: Skeletal muscle index; SMM: Skeletal muscle mass; SVR: Skeletal muscle to visceral fat ratio; TrFM: Truncal fat mass; VFA: Visceral fat area.

found that IGF1 levels and IGF1-standard deviation score (SDS) values were lower in Japanese subjects with NAFLD at the histological examination when compared to controls; moreover, IGF1-SDS values were associated with the histological severity of NAFLD, independent of insulin resistance. Similarly, in a large population- based study, Völzke *et al*[42] described an association between low IGF1 and IGF1/IGFBP3 ratio and liver hyperechogenicity, independent of BMI and diabetes. Though the prevalence of hepatic steatosis, and the deterioration of lean body mass and BMD tend to increase with age[7,8], paralleling the somatopause, the GH/IGF1 axis affects the liver, the skeletal muscle and bone health even in earlier stages of life. In fact, IGF1 is known to stimulate longitudinal bone growth[43], and recently an analogous action has been attributed also to GH, independent of IGF1[44]. A robust correlation between IGF1 levels and bone mass has been shown to occur in early pubertal stages in both genders[45]. Cianfarani *et al*[46] found that IGF1 levels were associated with NAFLD activity score and histological patterns in obese children with biopsy-proven NAFLD. A recent study by Cabrera and coll. shed light on the underlying mechanisms linking IGF1, NAFLD and sarcopenia[47]. In mice NAFLD was induced by an American Lifestyle-Induced Obesity Syndrome (ALIOS) diet model, based on a Western dietary pattern combined to fructose excess. Muscle fiber size and muscle strength, as well as IGF1 levels decreased in animals with diet-induced NAFLD. Interestingly, the phenotypic aspects of sarcopenia were observed prior to the development of liver fibrosis, indicating that they could occur in early stages of NAFLD natural history[47].

Vitamin D deficiency

Vitamin D deficiency has been postulated to play a role in the pathogenesis of NAFLD. Two recent quantitative

meta-analysis (including twenty-three and nine studies, respectively) concluded that 25(OH)D levels were lower in subjects with NAFLD or NASH than in individuals without fatty liver[48,49]. If cross-sectional studies support the potential influence of vitamin D status on NAFLD[50], limited evidence exists proving the effectiveness of vitamin D supplementation in NAFLD patients[51,52]. However, findings from animal models revealed that vitamin D interferes with the activation of hepatic stellate cell, which are responsible for collagen deposition and extracellular matrix remodeling, leading to fibrosis[53]. Vitamin D seems to inhibit hepatic stellate cell proliferation[53], and clinical trials are needed to demonstrate that vitamin D supplementation could slow down the progression from NAFLD to NASH. Vitamin D is well known to exert pleiotropic effects. Vitamin D plays a relevant role in bone homeostasis: vitamin D deficiency determines secondary hyperparathyroidism and accelerated bone turnover[54]. Inadequate vitamin D levels have been reported in subjects with osteoporosis, even if only modest beneficial effects of vitamin D supplementation have been shown in fracture prevention[55]. In the last years mounting interest has been addressed to vitamin D action in skeletal muscle. Reduced vitamin D levels have been associated with sarcopenia, disability, and falls in the elderly[56,57]. In adults with vitamin D deficiency, histological alterations in muscle fiber composition and diameter have been described[58]. In disagreement with the above mentioned data, among the studies included in the present review, Hong *et al*[6] found no significant association between 25(OH)D levels and skeletal muscle index or liver attenuation index in Korean men and women. Methodological issues exist in the studies which explored vitamin D status, especially related to seasonality, variability in sun exposure, coexistence of obesity and physical inactivity. The presence of these potential confounders limits the interpretation of the available data.

Osteocalcin

Osteocalcin is a bone-derived hormone, mainly produced by the osteoblasts, and is a non-collagenous matrix protein. Osteocalcin is considered as a serum biomarker of bone formation. In a number of studies a negative association has been described between serum osteocalcin levels and decreased bone mineral density in postmenopausal women[59,60]. Emerging evidence from animal and human studies unveiled that osteocalcin is involved in many homeostatic mechanisms other than those specific for bone health[61,62]. Notably, osteocalcin is able to interfere with energy and glucose metabolism, modulating pancreatic beta-cell activity. Undercarboxylated osteocalcin is the active isoform of the hormone, responsible for inducing insulin secretion and favoring insulin sensitivity in skeletal muscle and adipose tissue[61,62]. Accumulating evidence suggests that osteocalcin is also involved in liver disease; low serum osteocalcin levels have been related to NAFLD. In a case-control study, Yilmaz and coworkers found that osteocalcin was inversely associated with histological features of NAFLD[63]. Moreover, this inverse association linking osteocalcin and NAFLD has been also reported in male and female participants with normal bone mineral density[64-66]. In an experimental model of diet- induced NAFLD, the administration of osteocalcin was demonstrated to be effective in reversing metabolic changes and reducing markedly hepatic triglyceride content, suggesting a protective role of osteocalcin in NAFLD development[67]. Interestingly, osteocalcin has been shown to play a crucial role also in the inter-organ cross-talk between the skeleton and skeletal muscle. Osteocalcin signaling in myofibers seems to be an important mediator of metabolic adaptive mechanisms to exercise[68]. In addition, recently Mera and coll. showed that in mice exogenous osteocalcin administration promoted protein synthesis in myotubes, preventing the age-related muscle loss[69]. Further evidence is required to establish if osteocalcin may represent a suitable candidate for counteracting muscle wasting and liver fat infiltration.

Insulin resistance

NAFLD is known to be the hepatic manifestation of the metabolic syndrome, due to the remarkable effects of insulin resistance in the pathogenesis of hepatic steatosis[70]. Intrahepatic lipid accumulation has been related to the deterioration of insulin sensitivity at the level of liver, skeletal muscle, and adipose tissue[71]. Furthermore, the presence of NAFLD predicts the risk of developing type 2 diabetes, independent of age and obesity[72]. Furthermore, insulin resistance is a key factor also in anabolic processes taking place in the skeletal muscle and bone. The skeletal muscle is the major target tissue of insulin action[73]. On one hand, insulin resistance interferes with the effectiveness of protein synthesis, leading to the age-related reduction of lean body mass[74]. In nondiabetic elderly subjects, Guillet *et al*[75] reported that insulin ability to counteract whole body protein break down was decreased. On the other hand, the presence of reduced lean mass can further favor the development of insulin resistance[74]. In vitro and in vivo studies demonstrated that insulin plays an important role in bone homeostasis. Insulin promotes osteoblast proliferation and differentiation, the generation of anabolic signals and collagen synthesis, influencing microarchitecture and mechanical properties of bone[76]. A complex connection exists between bone metabolism and insulin resistance, with the frequent overlap of insulin resistance and excess adiposity being the major confounding factor. Due to the increased mechanical load on the skeleton, obesity appeared to confer protection against bone mass deterioration. In addition, bone turnover seemed to

be lower in subjects with the metabolic syndrome and type 2 diabetes[77]. Even if evidence is not conclusive, especially for the prevention of fragility fractures[78], this assumption has been weakened by a number of studies in which the relationship between metabolic syndrome and bone outcomes, such as bone strength or areal BMD, became negative in models adjusted for BMI[79]. In fact, several studies reported a negative association between insulin resistance and bone mineral density as well as bone strength indices and markers of bone formation[80-82]. Novel findings from animal studies unveiled that bone represents a site of insulin resistance, and osteoblasts are primarily involved in insulin signaling in bone. In more detail, in mice fed a high-fat diet, insulin resistance in osteoblasts was responsible for the reduced production of osteocalcin, which in turn affected detrimentally whole body insulin sensitivity[83,84]. Furthermore, in a model of high-fat diet induced obesity in rats, the development of insulin resistance led to reduced osteoblast proliferation and differentiation, and increased osteoblast apoptosis, resulting in decreased jaw bone density[85].

Chronic inflammation

A proinflammatory milieu represents another common soil favoring the development of the three conditions examined in the present review. Systemic inflammation is one of the major actors in the progression from NAFLD to NASH[86]. Liver resident cells, like hepatic stellate cells, Kupffer cells, and dendritic cells, generate pro-inflammatory signals involved in the cascade leading to cell death[86]. In addition, tumor necrosis factor-alpha (TNF-a) is another relevant mediator and inducer of hepatocyte death[87]. Also in aged skeletal muscle, TNF-alpha signaling is involved in the activation of apoptosis, leading to muscle fiber loss and sarcopenia[88]. Though the role of proinflammatory cytokines, IL-6, in protein breakdown in skeletal muscle is controversial[89,90], epidemiological evidence underpins the relationship between chronic low-grade inflammation and age-related sarcopenia[91]. The interplay between TNF-alpha and the RANKL/RANK/osteoprotegerin system is crucial for the modulation of osteoclast activity and bone resorption and remodeling[92]. Recently, reduced osteoprotegerin levels have been described in NAFLD, independent of potential confounders[93,94]. Taken together, these observation emphasize the connections linking immune response, inflammation, and bone physiology to NAFLD.

Physical inactivity

Sedentariness is a well- known risk factor for weight gain and the consequences related to excess fat, including the onset of fatty liver[95]. Indeed, lifestyle interventions, combining dietary interventions and physical activity, have been demonstrated to be beneficial in terms of liver fat reduction, due to weight loss. Interestingly, mounting evidence supports an exercise effect and a physical fitness role *per se* in the pathophysiology of NAFLD[96]. In fact, based on pooled data from six studies, a recent meta-analysis revealed that exercise alone (*vs* non-exercise control, without any dietary intervention) was sufficient to determine a significant decrease of the intrahepatic lipid content, even in the absence of weight change, or minimal weight loss[97].

Physical inactivity represents also a well- established risk factor for both sarcopenia and osteoporosis. The lack of physical activity favors the decline of lean body mass, triggering a vicious cycle leading to both progressive inactivity and sarcopenia[98]. Similarly, physical activity is recognized as a relevant factor in promoting bone health across the lifespan[99,100]. According to the mechanostat theory, bone and skeletal muscle are connected by mechanical interactions. In the last years, skeletal muscle and bone have been demonstrated to act as endocrine organs, producing several factors responsible for this intriguing inter-organ cross-talk[101].

Among a number of factors involved in the above mentioned interplay, irisin is a recently described hormone- like myokine. Plasma irisin levels increase in response to exercise; moreover, irisin is able to increase energy expenditure. Irisin autocrinally modulates some metabolic functions in the skeletal muscle, and it also exerts endocrine effects on adipocytes and osteoblasts. In fact irisin can induce browning of white adipose tissue, and can regulate the expression of osteogenic genes as well as it is able to induce differentiation of osteoblasts[102]. Zhang *et al*[103] reported that circulating irisin was negatively associated with intrahepatic triglyceride content in Chinese obese adults with NAFLD, independent of other metabolic factors. Due to the pleiotropic effects on energy metabolism, glucose homeostasis, insulin resistance, and obesity, irisin may represent a pivotal mediator in the complex communication among the liver, skeletal muscle and bone[104,105].

CONCLUSION

Emerging evidence supports the crucial role played by new contributors in the pathogenesis of NAFLD in a complex inter-organ communication, widening the classic paradigm centered on insulin resistance and excess fat. In this emerging perspective, fat-free tissues like bone and skeletal muscle appear to be relevant actors. Though the novel findings are fascinating, the roles of fat-free tissues, independent of obesity and classic risk factors for NAFLD, need to be further investigated. More rigorous methods for the diagnosis of NAFLD and sarcopenia should be used. The extant evidence needs to be confirmed in different races and ethnicities, and further research should be prompted in order to narrow the gap in the literature, especially with regard to the connection between

NAFLD and skeletal muscle in the early stages of the aging process.

REFERENCES

1 **Li L**, Liu DW, Yan HY, Wang ZY, Zhao SH, Wang B. Obesity is an independent risk factor for non-alcoholic fatty liver disease: evidence from a meta-analysis of 21 cohort studies. *Obes Rev* 2016; **17**: 510-519 [PMID: 27020692 DOI: 10.1111/OBR.12407]

2 **Dietrich P**, Hellerbrand C. Non-alcoholic fatty liver disease, obesity and the metabolic syndrome. *Best Pract Res Clin Gastroenterol* 2014; **28**: 637-653 [PMID: 25194181 DOI: 10.1016/J.PBG.2014.07.008]

3 **Fabbrini E**, Sullivan S, Klein S. Obesity and nonalcoholic fatty liver disease: biochemical, metabolic, and clinical implications. *Hepatology* 2010; **51**: 679-689 [PMID: 20041406 DOI: 10.1002/HEP.23280]

4 **Lonardo A**, Bellentani S, Argo CK, Ballestri S, Byrne CD, Caldwell SH, Cortez-Pinto H, Grieco A, Machado MV, Miele L, Targher G. Epidemiological modifiers of non-alcoholic fatty liver disease: Focus on high-risk groups. *Dig Liver Dis* 2015; **47**: 997-1006 [PMID: 26454786 DOI: 10.1016/J.DLD.2015.08.004]

5 **Targher G**, Lonardo A, Rossini M. Nonalcoholic fatty liver disease and decreased bone mineral density: is there a link? *J Endocrinol Invest* 2015; **38**: 817-825 [PMID: 26003827 DOI: 10.1007/S40618-015-0315-6]

6 **Hong HC**, Hwang SY, Choi HY, Yoo HJ, Seo JA, Kim SG, Kim NH, Baik SH, Choi DS, Choi KM. Relationship between sarcopenia and nonalcoholic fatty liver disease: the Korean Sarcopenic Obesity Study. *Hepatology* 2014; **59**: 1772-1778 [PMID: 23996808 DOI: 10.1002/HEP.26716]

7 **Curtis E**, Litwic A, Cooper C, Dennison E. Determinants of Muscle and Bone Aging. *J Cell Physiol* 2015; **230**: 2618-2625 [PMID: 25820482 DOI: 10.1002/JCP.25001]

8 **Bertolotti M**, Lonardo A, Mussi C, Baldelli E, Pellegrini E, Ballestri S, Romagnoli D, Loria P. Nonalcoholic fatty liver disease and aging: epidemiology to management. *World J Gastroenterol* 2014; **20**: 14185-14204 [PMID: 25339806 DOI: 10.3748/WJG.V20.I39.14185]

9 **Hamaguchi M**, Kojima T, Ohbora A, Takeda N, Fukui M, Kato T. Aging is a risk factor of nonalcoholic fatty liver disease in premenopausal women. *World J Gastroenterol* 2012; **18**: 237-243 [PMID: 22294826 DOI: 10.3748/WJG.V18.I3.237]

10 **Polyzos SA**, Kountouras J, Tsatsoulis A, Zafeiriadou E, Katsiki E, Patsiaoura K, Zavos C, Anastasiadou VV, Slavakis A. Sex steroids and sex hormone-binding globulin in postmenopausal women with nonalcoholic fatty liver disease. *Hormones* (Athens) 2013; **12**: 405-416 [PMID: 24121382]

11 **Xia MF**, Lin HD, Yan HM, Bian H, Chang XX, Zhang LS, He WY, Gao X. The association of liver fat content and serum alanine aminotransferase with bone mineral density in middle-aged and elderly Chinese men and postmenopausal women. *J Transl Med* 2016; **14**: 11 [PMID: 26791408 DOI: 10.1186/S12967-016-0766-3]

12 **Cui R**, Sheng H, Rui XF, Cheng XY, Sheng CJ, Wang JY, Qu S. Low bone mineral density in chinese adults with nonalcoholic Fatty liver disease. *Int J Endocrinol* 2013; **2013**: 396545 [PMID: 23983685 DOI: 10.1155/2013/396545]

13 **Lee SH**, Yun JM, Kim SH, Seo YG, Min H, Chung E, Bae YS, Ryou IS, Cho B. Association between bone mineral density and nonalcoholic fatty liver disease in Korean adults. *J Endocrinol Invest* 2016; **39**: 1329-1336 [PMID: 27561910 DOI: 10.1007/S40618-016-0528-3]

14 **Moon SS**, Lee YS, Kim SW. Association of nonalcoholic fatty liver disease with low bone mass in postmenopausal women. *Endocrine* 2012; **42**: 423-429 [PMID: 22407492]

15 **Purnak T**, Beyazit Y, Ozaslan E, Efe C, Hayretci M. The evaluation of bone mineral density in patients with nonalcoholic fatty liver disease. *Wien Klin Wochenschr* 2012; **124**: 526-531 [PMID: 22850810 DOI: 10.1007/S00508-012-0211-4]

16 **Bhatt SP**, Nigam P, Misra A, Guleria R, Qadar Pasha MA. Independent associations of low 25 hydroxy vitamin D and high parathyroid hormonal levels with nonalcoholic fatty liver disease in Asian Indians residing in north India. *Atherosclerosis* 2013; **230**: 157-163 [PMID: 23958268 DOI: 10.1016/J.ATHEROSCLEROSIS.2013.07.006]

17 **Yang HJ**, Shim SG, Ma BO, Kwak JY. Association of non-alcoholic fatty liver disease with bone mineral density and serum osteocalcin levels in Korean men. *Eur J Gastroenterol Hepatol* 2016; **28**: 338-344 [PMID: 26636404 DOI: 10.1097/MEG.0000000000000535]

18 **Pacifico L**, Bezzi M, Lombardo CV, Romaggioli S, Ferraro F, Bascetta S, Chiesa C. Adipokines and C-reactive protein in relation to bone mineralization in pediatric nonalcoholic fatty liver disease. *World J Gastroenterol* 2013; **19**: 4007-4014 [PMID: 23840146 DOI: 10.3748/WJG.V19.I25.4007]

19 **Pardee PE**, Dunn W, Schwimmer JB. Non-alcoholic fatty liver disease is associated with low bone mineral density in obese children. *Aliment Pharmacol Ther* 2012; **35**: 248-254 [PMID: 22111971 DOI: 10.1111/J.1365-2036.2011.04924.X]

20 **Chang EJ**, Yi DY, Yang HR. Vitamin D Status and Bone Mineral Density in Obese Children with Nonalcoholic Fatty Liver Disease. *J Korean Med Sci* 2015; **30**: 1821-1827 [PMID: 26713058 DOI: 10.3346/JKMS.2015.30.12.1821]

21 **Pirgon O**, Bilgin H, Tolu I, Odabas D. Correlation of insulin sensitivity with bone mineral status in obese adolescents with nonalcoholic fatty liver disease. *Clin Endocrinol* (Oxf) 2011; **75**: 189-195 [PMID: 21521307 DOI: 10.1111/J.1365-2265.2011.04038.X]

22 **Henry CJ**, Sedjo RL, Rozhok A, Salstrom J, Ahnen D, Levin TR, D'Agostino R, Haffner S, DeGregori J, Byers T. Lack of significant association between serum inflammatory cytokine profiles and the presence of colorectal adenoma. *BMC Cancer* 2015; **15**: 123 [PMID: 25884547 DOI: 10.1186/s12885-015-1115-2]

23 **Strauss S**, Gavish E, Gottlieb P, Katsnelson L. Interobserver and intraobserver variability in the sonographic assessment of fatty liver. *AJR Am J Roentgenol* 2007; **189**: W320-W323 [PMID: 18029843 DOI: 10.2214/AJR.07.2123]

24 **Sinclair M**, Gow PJ, Grossmann M, Angus PW. Review article: sarcopenia in cirrhosis--aetiology, implications and potential therapeutic interventions. *Aliment Pharmacol Ther* 2016; **43**: 765-777 [PMID: 26847265 DOI: 10.1111/APT.13549]

25 **Koo BK**, Kim D, Joo SK, Kim JH, Chang MS, Kim BG, Lee KL, Kim W. Sarcopenia is an independent risk factor for non-alcoholic steatohepatitis and significant fibrosis. *J Hepatol* 2017; **66**: 123-131 [PMID: 27599824 DOI: 10.1016/J.JHEP.2016.08.019]

26 **Lee YH**, Jung KS, Kim SU, Yoon HJ, Yun YJ, Lee BW, Kang ES, Han KH, Lee HC, Cha BS. Sarcopaenia is associated with NAFLD independently of obesity and insulin resistance: Nationwide surveys (KNHANES 2008-2011). *J Hepatol* 2015; **63**: 486-493 [PMID: 25772036 DOI: 10.1016/J.JHEP.2015.02.051]

27 **Hashimoto Y**, Osaka T, Fukuda T, Tanaka M, Yamazaki M, Fukui M. The relationship between hepatic steatosis and skeletal muscle mass index in men with type 2 diabetes. *Endocr J* 2016; **63**: 877-884 [PMID: 27397679]

28 **Moon JS**, Yoon JS, Won KC, Lee HW. The role of skeletal muscle in development of nonalcoholic Fatty liver disease. *Diabetes Metab J* 2013; **37**: 278-285 [PMID: 23991406 DOI: 10.4093/DMJ.2013.37.4.278]

29 **Kim HY**, Kim CW, Park CH, Choi JY, Han K, Merchant AT, Park YM. Low skeletal muscle mass is associated with non-alcoholic fatty liver disease in Korean adults: the Fifth Korea National Health and Nutrition Examination Survey. *Hepatobiliary Pancreat Dis Int* 2016; **15**: 39-47 [PMID: 26818542]

30 **Lee YH**, Kim SU, Song K, Park JY, Kim do Y, Ahn SH, Lee BW, Kang ES, Cha BS, Han KH. Sarcopenia is associated with significant liver fibrosis independently of obesity and insulin resistance in nonalcoholic fatty liver disease: Nationwide surveys (KNHANES 2008-2011). *Hepatology* 2016; **63**: 776-786 [PMID: 26638128 DOI: 10.1002/HEP.28376]

31 **Poggiogalle E**, Lubrano C, Gnessi L, Mariani S, Lenzi A, Donini LM. Fatty Liver Index Associates with Relative Sarcopenia

and GH/ IGF- 1 Status in Obese Subjects. *PLoS One* 2016; **11**: e0145811 [PMID: 26741958 DOI: 10.1371/JOURNAL.PONE.0145811]
32 **Dawson-Hughes B**, Bischoff-Ferrari H. Considerations concerning the definition of sarcopenia: response to comments. *Osteoporos Int* 2016; **27**: 3147-3148 [PMID: 27503171]
33 **Tahimic CG**, Wang Y, Bikle DD. Anabolic effects of IGF-1 signaling on the skeleton. *Front Endocrinol* (Lausanne) 2013; **4**: 6 [PMID: 23382729 DOI: 10.3389/FENDO.2013.00006]
34 **Perrini S**, Laviola L, Carreira MC, Cignarelli A, Natalicchio A, Giorgino F. The GH/IGF1 axis and signaling pathways in the muscle and bone: mechanisms underlying age-related skeletal muscle wasting and osteoporosis. *J Endocrinol* 2010; **205**: 201-210 [PMID: 20197302 DOI: 10.1677/JOE-09-0431]
35 **Bikle DD**, Tahimic C, Chang W, Wang Y, Philippou A, Barton ER. Role of IGF-I signaling in muscle bone interactions. *Bone* 2015; **80**: 79-88 [PMID: 26453498 DOI: 10.1016/J.BONE]
36 **Loria P**, Carulli L, Bertolotti M, Lonardo A. Endocrine and liver interaction: the role of endocrine pathways in NASH. *Nat Rev Gastroenterol Hepatol* 2009; **6**: 236-247 [PMID: 19347015 DOI: 10.1038/NRGATRO.2009.33]
37 **Takahashi Y**. Essential roles of growth hormone (GH) and insulin-like growth factor-I (IGF-I) in the liver. *Endocr J* 2012; **59**: 955-962 [PMID: 22986486]
38 **Aguirre GA**, De Ita JR, de la Garza RG, Castilla-Cortazar I. Insulin-like growth factor-1 deficiency and metabolic syndrome. *J Transl Med* 2016; **14**: 3 [PMID: 26733412 DOI: 10.1186/S12967-015-0762-Z]
39 **Clemmons DR**. The relative roles of growth hormone and IGF-1 in controlling insulin sensitivity. *J Clin Invest* 2004; **113**: 25-27 [PMID: 14702105 DOI: 10.1172/JCI20660]
40 **Ichikawa T**, Nakao K, Hamasaki K, Furukawa R, Tsuruta S, Ueda Y, Taura N, Shibata H, Fujimoto M, Toriyama K, Eguchi K. Role of growth hormone, insulin-like growth factor 1 and insulin-like growth factor-binding protein 3 in development of non-alcoholic fatty liver disease. *Hepatol Int* 2007; **1**: 287-294 [PMID: 19669352 DOI: 10.1007/S12072-007-9007-4]
41 **Sumida Y**, Yonei Y, Tanaka S, Mori K, Kanemasa K, Imai S, Taketani H, Hara T, Seko Y, Ishiba H, Okajima A, Yamaguchi K, Moriguchi M, Mitsuyoshi H, Yasui K, Minami M, Itoh Y. Lower levels of insulin-like growth factor-1 standard deviation score are associated with histological severity of non-alcoholic fatty liver disease. *Hepatol Res* 2015; **45**: 771-781 [PMID: 25163357 DOI: 10.1111/HEPR.12408]
42 **Völzke H**, Nauck M, Rettig R, Dörr M, Higham C, Brabant G, Wallaschofski H. Association between hepatic steatosis and serum IGF1 and IGFBP-3 levels in a population-based sample. *Eur J Endocrinol* 2009; **161**: 705-713 [PMID: 19690083 DOI: 10.1530/EJE-09-0374]
43 **Wang J**, Zhou J, Bondy CA. Igf1 promotes longitudinal bone growth by insulin-like actions augmenting chondrocyte hypertrophy. *FASEB J* 1999; **13**: 1985-1990 [PMID: 10544181]
44 **Wu S**, Yang W, De Luca F. Insulin-Like Growth Factor-Independent Effects of Growth Hormone on Growth Plate Chondrogenesis and Longitudinal Bone Growth. *Endocrinology* 2015; **156**: 2541-2551 [PMID: 25910049 DOI: 10.1210/EN.2014-1983]
45 **Matar M**, Al-Shaar L, Maalouf J, Nabulsi M, Arabi A, Choucair M, Tamim H, El-Hajj Fuleihan G. The Relationship Between Calciotropic Hormones, IGF-1, and Bone Mass Across Pubertal Stages. *J Clin Endocrinol Metab* 2016; **101**: 4860-4870 [PMID: 27676398]
46 **Cianfarani S**, Inzaghi E, Alisi A, Germani D, Puglianiello A, Nobili V. Insulin-like growth factor-I and -II levels are associated with the progression of nonalcoholic fatty liver disease in obese children. *J Pediatr* 2014; **165**: 92-98 [PMID: 24607243 DOI: 10.1016/J.JPEDS]
47 **Cabrera D**, Ruiz A, Cabello-Verrugio C, Brandan E, Estrada L, Pizarro M, Solis N, Torres J, Barrera F, Arrese M. Diet-Induced Nonalcoholic Fatty Liver Disease Is Associated with Sarcopenia and Decreased Serum Insulin-Like Growth Factor-1. *Dig Dis Sci* 2016; **61**: 3190-3198 [PMID: 27572941 DOI: 10.1007/S10620-016-4285-0]
48 **Wang X**, Li W, Zhang Y, Yang Y, Qin G. Association between vitamin D and non-alcoholic fatty liver disease/non-alcoholic steatohepatitis: results from a meta-analysis. *Int J Clin Exp Med* 2015; **8**: 17221-17234 [PMID: 26770315]
49 **Eliades M**, Spyrou E, Agrawal N, Lazo M, Brancati FL, Potter JJ, Koteish AA, Clark JM, Guallar E, Hernaez R. Meta-analysis: vitamin D and non-alcoholic fatty liver disease. *Aliment Pharmacol Ther* 2013; **38**: 246-254 [PMID: 23786213 DOI: 10.1111/APT.12377]
50 **Kwok RM**, Torres DM, Harrison SA. Vitamin D and nonalcoholic fatty liver disease (NAFLD): is it more than just an association? *Hepatology* 2013; **58**: 1166-1174 [PMID: 23504808 DOI: 10.1002/HEP.26390]
51 **Foroughi M**, Maghsoudi Z, Askari G. The effect of vitamin D supplementation on blood sugar and different indices of insulin resistance in patients with non-alcoholic fatty liver disease (NAFLD). *Iran J Nurs Midwifery Res* 2016; **21**: 100-104 [PMID: 26985230 DOI: 10.4103/1735-9066.174759]
52 **Barchetta I**, Del Ben M, Angelico F, Di Martino M, Fraioli A, La Torre G, Saulle R, Perri L, Morini S, Tiberti C, Bertoccini L, Cimini FA, Panimolle F, Catalano C, Baroni MG, Cavallo MG. No effects of oral vitamin D supplementation on non-alcoholic fatty liver disease in patients with type 2 diabetes: a randomized, double-blind, placebo-controlled trial. *BMC Med* 2016; **14**: 92 [PMID: 27353492 DOI: 10.1186/S12916-016-0638-Y]
53 **Abramovitch S**, Sharvit E, Weisman Y, Bentov A, Brazowski E, Cohen G, Volovelsky O, Reif S. Vitamin D inhibits development of liver fibrosis in an animal model but cannot ameliorate established cirrhosis. *Am J Physiol Gastrointest Liver Physiol* 2015; **308**: G112-G120 [PMID: 25214398 DOI: 10.1152/AJPGI.00132.2013]
54 **Anderson PH**, Sawyer RK, Moore AJ, May BK, O'Loughlin PD, Morris HA. Vitamin D depletion induces RANKL-mediated osteoclastogenesis and bone loss in a rodent model. *J Bone Miner Res* 2008; **23**: 1789-1797 [PMID: 18597628 DOI: 10.1359/JBMR.080616]
55 **Reid IR**, Bolland MJ, Grey A. Effects of vitamin D supplements on bone mineral density: a systematic review and meta-analysis. *Lancet* 2014; **383**: 146-155 [PMID: 24119980 DOI: 10.1016/S0140-6736(13)61647-5]
56 **Kim MK**, Baek KH, Song KH, Il Kang M, Park CY, Lee WY, Oh KW. Vitamin D deficiency is associated with sarcopenia in older Koreans, regardless of obesity: the Fourth Korea National Health and Nutrition Examination Surveys (KNHANES IV) 2009. *J Clin Endocrinol Metab* 2011; **96**: 3250-3256 [PMID: 21832109 DOI: 10.1210/JC.2011-1602]
57 **Visser M**, Deeg DJ, Lips P. Low vitamin D and high parathyroid hormone levels as determinants of loss of muscle strength and muscle mass (sarcopenia): the Longitudinal Aging Study Amsterdam. *J Clin Endocrinol Metab* 2003; **88**: 5766-5772 [PMID: 14671166]
58 **Ceglia L**. Vitamin D and its role in skeletal muscle. *Curr Opin Clin Nutr Metab Care* 2009; **12**: 628-633 [PMID: 19770647 DOI: 10.1097/MCO.0B013E328331C707]
59 **Singh S**, Kumar D, Lal AK. Serum Osteocalcin as a Diagnostic Biomarker for Primary Osteoporosis in Women. *J Clin Diagn Res* 2015; **9**: RC04-RC07 [PMID: 26436008 DOI: 10.7860/JCDR/2015/14857.6318]
60 **Vs K**, K P, Ramesh M, Venkatesan V. The association of serum osteocalcin with the bone mineral density in post menopausal women. *J Clin Diagn Res* 2013; **7**: 814-816 [PMID: 23814717 DOI: 10.7860/JCDR/2013/5370.2946]
61 **Oldknow KJ**, MacRae VE, Farquharson C. Endocrine role of bone: recent and emerging perspectives beyond osteocalcin. *J Endocrinol* 2015; **225**: R1-R19 [PMID: 25655764 DOI: 10.1530/JOE-14-0584]
62 **Wei J**, Karsenty G. An overview of the metabolic functions of osteocalcin. *Curr Osteoporos Rep* 2015; **13**: 180-185 [PMID: 25809656 DOI: 10.1007/S11914-015-0267-Y]

63 **Yilmaz Y**, Kurt R, Eren F, Imeryuz N. Serum osteocalcin levels in patients with nonalcoholic fatty liver disease: association with ballooning degeneration. *Scand J Clin Lab Invest* 2011; **71**: 631-636 [PMID: 21859358 DOI: 10.3109/00365513.2011.604427]

64 **Liu JJ**, Chen YY, Mo ZN, Tian GX, Tan AH, Gao Y, Yang XB, Zhang HY, Li ZX. Relationship between serum osteocalcin levels and non-alcoholic fatty liver disease in adult males, South China. *Int J Mol Sci* 2013; **14**: 19782-19791 [PMID: 24084725 DOI: 10.3390/IJMS141019782]

65 **Dou J**, Ma X, Fang Q, Hao Y, Yang R, Wang F, Zhu J, Bao Y, Jia W. Relationship between serum osteocalcin levels and non-alcoholic fatty liver disease in Chinese men. *Clin Exp Pharmacol Physiol* 2013; **40**: 282-288 [PMID: 23369196 DOI: 10.1111/1440-1681.12063]

66 **Aller R**, Castrillon JL, de Luis DA, Conde R, Izaola O, Sagrado MG, Velasco MC, Alvarez T, Pacheco D. Relation of osteocalcin with insulin resistance and histopathological changes of non alcoholic fatty liver disease. *Ann Hepatol* 2011; **10**: 50-55 [PMID: 21301010]

67 **Du J**, Zhang M, Lu J, Zhang X, Xiong Q, Xu Y, Bao Y, Jia W. Osteocalcin improves nonalcoholic fatty liver disease in mice through activation of Nrf2 and inhibition of JNK. *Endocrine* 2016; **53**: 701-709 [PMID: 26994931 DOI: 10.1007/S12020-016-0926-5]

68 **Mera P**, Laue K, Ferron M, Confavreux C, Wei J, Galán-Díez M, Lacampagne A, Mitchell SJ, Mattison JA, Chen Y, Bacchetta J, Szulc P, Kitsis RN, de Cabo R, Friedman RA, Torsitano C, McGraw TE, Puchowicz M, Kurland I, Karsenty G. Osteocalcin Signaling in Myofibers Is Necessary and Sufficient for Optimum Adaptation to Exercise. *Cell Metab* 2016; **23**: 1078-1092 [PMID: 27304508 DOI: 10.1016/J.CMET.2016.05.004]

69 **Mera P**, Laue K, Wei J, Berger JM, Karsenty G. Osteocalcin is necessary and sufficient to maintain muscle mass in older mice. *Mol Metab* 2016; **5**: 1042-1047 [PMID: 27689017 DOI: 10.1016/J.MOLMET.2016.07.002]

70 **Bugianesi E**, Moscatiello S, Ciaravella MF, Marchesini G. Insulin resistance in nonalcoholic fatty liver disease. *Curr Pharm Des* 2010; **16**: 1941-1951 [PMID: 20370677]

71 **Gaggini M**, Morelli M, Buzzigoli E, DeFronzo RA, Bugianesi E, Gastaldelli A. Non-alcoholic fatty liver disease (NAFLD) and its connection with insulin resistance, dyslipidemia, atherosclerosis and coronary heart disease. *Nutrients* 2013; **5**: 1544-1560 [PMID: 23666091 DOI: 10.3390/NU5051544]

72 **Lallukka S**, Yki-Järvinen H. Non-alcoholic fatty liver disease and risk of type 2 diabetes. *Best Pract Res Clin Endocrinol Metab* 2016; **30**: 385-395 [PMID: 27432073]

73 **De Meyts P**. The Insulin Receptor and Its Signal Transduction Network. In: De Groot LJ, Chrousos G, Dungan K, Grossman A, Hershman JM, Koch C, Korbonits M, McLachlan R, New M, Purnell J, Rebar R, Singer F, Vinik A, editors. Endotext [Internet] South Dartmouth (MA): MDText.com, Inc., 2000-2016

74 **Cleasby ME**, Jamieson PM, Atherton PJ. Insulin resistance and sarcopenia: mechanistic links between common co-morbidities. *J Endocrinol* 2016; **229**: R67-R81 [PMID: 26931135 DOI: 10.1530/JOE-15-0533]

75 **Guillet C**, Zangarelli A, Gachon P, Morio B, Giraudet C, Rousset P, Boirie Y. Whole body protein breakdown is less inhibited by insulin, but still responsive to amino acid, in nondiabetic elderly subjects. *J Clin Endocrinol Metab* 2004; **89**: 6017-6024 [PMID: 15579753]

76 **Thrailkill KM**, Lumpkin CK, Bunn RC, Kemp SF, Fowlkes JL. Is insulin an anabolic agent in bone? Dissecting the diabetic bone for clues. *Am J Physiol Endocrinol Metab* 2005; **289**: E735-E745 [PMID: 16215165]

77 **Lerchbaum E**, Schwetz V, Nauck M, Völzke H, Wallaschofski H, Hannemann A. Lower bone turnover markers in metabolic syndrome and diabetes: the population-based Study of Health in Pomerania. *Nutr Metab Cardiovasc Dis* 2015; **25**: 458-463 [PMID: 25816734 DOI: 10.1016/J.NUMECD.2015.02.002]

78 **Esposito K**, Chiodini P, Capuano A, Colao A, Giugliano D. Fracture risk and bone mineral density in metabolic syndrome: a meta-analysis. *J Clin Endocrinol Metab* 2013; **98**: 3306-3314 [PMID: 23775355 DOI: 10.1210/JC.2013-1775]

79 **Laurent MR**, Cook MJ, Gielen E, Ward KA, Antonio L, Adams JE, Decallonne B, Bartfai G, Casanueva FF, Forti G, Giwercman A, Huhtaniemi IT, Kula K, Lean ME, Lee DM, Pendleton N, Punab M, Claessens F, Wu FC, Vanderschueren D, Pye SR, O'Neill TW. Lower bone turnover and relative bone deficits in men with metabolic syndrome: a matter of insulin sensitivity? The European Male Ageing Study. *Osteoporos Int* 2016; **27**: 3227-3237 [PMID: 27273111]

80 **Ishii S**, Cauley JA, Crandall CJ, Srikanthan P, Greendale GA, Huang MH, Danielson ME, Karlamangla AS. Diabetes and femoral neck strength: findings from the Hip Strength Across the Menopausal Transition Study. *J Clin Endocrinol Metab* 2012; **97**: 190-197 [PMID: 22072739 DOI: 10.1210/JC.2011-1883]

81 **Srikanthan P**, Crandall CJ, Miller-Martinez D, Seeman TE, Greendale GA, Binkley N, Karlamangla AS. Insulin resistance and bone strength: findings from the study of midlife in the United States. *J Bone Miner Res* 2014; **29**: 796-803 [PMID: 23983216 DOI: 10.1002/JBMR.2083]

82 **Szulc P**, Varennes A, Delmas PD, Goudable J, Chapurlat R. Men with metabolic syndrome have lower bone mineral density but lower fracture risk--the MINOS study. *J Bone Miner Res* 2010; **25**: 1446-1454 [PMID: 20200928 DOI: 10.1002/JBMR.13]

83 **Riddle RC**, Clemens TL. Insulin, osteoblasts, and energy metabolism: why bone counts calories. *J Clin Invest* 2014; **124**: 1465-1467 [PMID: 24642463 DOI: 10.1172/JCI75554]

84 **Wei J**, Ferron M, Clarke CJ, Hannun YA, Jiang H, Blaner WS, Karsenty G. Bone-specific insulin resistance disrupts whole-body glucose homeostasis via decreased osteocalcin activation. *J Clin Invest* 2014; **124**: 1-13 [PMID: 24642469 DOI: 10.1172/JCI72323]

85 **Pramojanee SN**, Phimphilai M, Kumphune S, Chattipakorn N, Chattipakorn SC. Decreased jaw bone density and osteoblastic insulin signaling in a model of obesity. *J Dent Res* 2013; **92**: 560-565 [PMID: 23569161 DOI: 10.1177/0022034513485600]

86 **Seki E**, Schwabe RF. Hepatic inflammation and fibrosis: functional links and key pathways. *Hepatology* 2015; **61**: 1066-1079 [PMID: 25066777 DOI: 10.1002/HEP.27332]

87 **Brenner C**, Galluzzi L, Kepp O, Kroemer G. Decoding cell death signals in liver inflammation. *J Hepatol* 2013; **59**: 583-594 [PMID: 23567086 DOI: 10.1016/J.JHEP.2013]

88 **Dirks AJ**, Leeuwenburgh C. Tumor necrosis factor alpha signaling in skeletal muscle: effects of age and caloric restriction. *J Nutr Biochem* 2006; **17**: 501-508 [PMID: 16517142]

89 **van Hall G**, Steensberg A, Fischer C, Keller C, Møller K, Moseley P, Pedersen BK. Interleukin-6 markedly decreases skeletal muscle protein turnover and increases nonmuscle amino acid utilization in healthy individuals. *J Clin Endocrinol Metab* 2008; **93**: 2851-2858 [PMID: 18430776 DOI: 10.1210/JC.2007-2223]

90 **van Hall G**. Cytokines: muscle protein and amino acid metabolism. *Curr Opin Clin Nutr Metab Care* 2012; **15**: 85-91 [PMID: 22123617 DOI: 10.1097/MCO.0B013E32834E6EA2]

91 **Beyer I**, Mets T, Bautmans I. Chronic low-grade inflammation and age-related sarcopenia. *Curr Opin Clin Nutr Metab Care* 2012; **15**: 12-22 [PMID: 22108098]

92 **Kwan Tat S**, Padrines M, Théoleyre S, Heymann D, Fortun Y. IL-6, RANKL, TNF-alpha/IL-1: interrelations in bone resorption pathophysiology. *Cytokine Growth Factor Rev* 2004; **15**: 49-60 [PMID: 14746813]

93 **Yilmaz Y**, Yonal O, Kurt R, Oral AY, Eren F, Ozdogan O, Ari F, Celikel CA, Korkmaz S, Ulukaya E, Imeryuz N, Kalayci C, Avsar E. Serum levels of osteoprotegerin in the spectrum of nonalcoholic fatty liver disease. *Scand J Clin Lab Invest* 2010; **70**: 541-546 [PMID: 20942739 DOI: 10.3109/00365513.2010.524933]

94 **Niu Y**, Zhang W, Yang Z, Li X, Fang W, Zhang H, Wang S, Zhou H, Fan J, Qin L, Su Q. Plasma osteoprotegerin levels are inversely associated with nonalcoholic fatty liver disease in patients with type 2 diabetes: A case-control study in China. *Metabolism* 2016; **65**: 475-481 [PMID: 26975539 DOI: 10.1016/J.METAB.2015.12.005]

95 **Rector RS**, Thyfault JP. Does physical inactivity cause

nonalcoholic fatty liver disease? *J Appl Physiol* (1985) 2011; **111**: 1828-1835 [PMID: 21565984 DOI: 10.1152/japplphysiol.00384]

96 **Johnson NA**, George J. Fitness versus fatness: moving beyond weight loss in nonalcoholic fatty liver disease. *Hepatology* 2010; **52**: 370-381 [PMID: 20578153 DOI: 10.1002/hep.23711]

97 **Keating SE**, Hackett DA, George J, Johnson NA. Exercise and non-alcoholic fatty liver disease: a systematic review and meta-analysis. *J Hepatol* 2012; **57**: 157-166 [PMID: 22414768 DOI: 10.1016/j.jhep.2012.02.023]

98 **Rolland Y**, Czerwinski S, Abellan Van Kan G, Morley JE, Cesari M, Onder G, Woo J, Baumgartner R, Pillard F, Boirie Y, Chumlea WM, Vellas B. Sarcopenia: its assessment, etiology, pathogenesis, consequences and future perspectives. *J Nutr Health Aging* 2008; **12**: 433-450 [PMID: 18615225]

99 **Kohrt WM**, Bloomfield SA, Little KD, Nelson ME, Yingling VR. American College of Sports Medicine Position Stand: physical activity and bone health. *Med Sci Sports Exerc* 2004; **36**: 1985-1996 [PMID: 15514517]

100 **Xu J**, Lombardi G, Jiao W, Banfi G. Effects of Exercise on Bone Status in Female Subjects, from Young Girls to Postmenopausal Women: An Overview of Systematic Reviews and Meta-Analyses. *Sports Med* 2016; **46**: 1165-1182 [PMID: 26856338 DOI: 10.1007/s40279-016-0494-0]

101 **Brotto M**, Bonewald L. Bone and muscle: Interactions beyond mechanical. *Bone* 2015; **80**: 109-114 [PMID: 26453500 DOI: 10.1016/j.bone.2015.02.010]

102 **Colaianni G**, Mongelli T, Colucci S, Cinti S, Grano M. Crosstalk Between Muscle and Bone Via the Muscle-Myokine Irisin. *Curr Osteoporos Rep* 2016; **14**: 132-137 [PMID: 27299471 DOI: 10.1007/s11914-016-0313-4]

103 **Zhang HJ**, Zhang XF, Ma ZM, Pan LL, Chen Z, Han HW, Han CK, Zhuang XJ, Lu Y, Li XJ, Yang SY, Li XY. Irisin is inversely associated with intrahepatic triglyceride contents in obese adults. *J Hepatol* 2013; **59**: 557-562 [PMID: 23665283 DOI: 10.1016/j.jhep.2013.04.030]

104 **Berzigotti A**, Saran U, Dufour JF. Physical activity and liver diseases. *Hepatology* 2016; **63**: 1026-1040 [PMID: 26313307 DOI: 10.1002/hep.28132]

105 **Arias-Loste MT**, Ranchal I, Romero-Gómez M, Crespo J. Irisin, a link among fatty liver disease, physical inactivity and insulin resistance. *Int J Mol Sci* 2014; **15**: 23163-23178 [PMID: 25514415 DOI: 10.3390/ijms151223163]

P- Reviewer: Kang H **S- Editor**: Yu J **L- Editor**: A
E- Editor: Wang CH

World Journal of Gastroenterology

Submit a Manuscript: http://www.wjgnet.com/esps/

World J Gastroenterol 2017 March 14; 23(10): 1758-1763

DOI: 10.3748/wjg.v23.i10.1758

ISSN 1007-9327 (print) ISSN 2219-2840 (online)

MINIREVIEWS

Ghrelin and gastrointestinal stromal tumors

Chang-Zhen Zhu, Dong Liu, Wei-Ming Kang, Jian-Chun Yu, Zhi-Qiang Ma, Xin Ye, Kang Li

Chang-Zhen Zhu, Dong Liu, Wei-Ming Kang, Jian-Chun Yu, Zhi-Qiang Ma, Xin Ye, Kang Li, Department of General Surgery, Peking Union Medical College Hospital, Chinese Academy of Medical Science and Peking Union Medical College, Beijing 100730, China

Author contributions: Zhu CZ and Liu D performed the majority of the writing and prepared the figures; Zhu CZ, Ma ZQ and Ye X performed the data acquisition and writing; Zhu CZ, Liu D and Li K provided input in writing the paper; Zhu CZ, Kang WM and Yu JC designed the outline and coordinated the writing of the paper.

Supported by the Capital Health Research and Development of Special Fund, No. 2014-3-4014.

Conflict-of-interest statement: The authors declare that there is no conflict of interest related to this study.

Manuscript source: Unsolicited manuscript

Correspondence to: Wei-Ming Kang, MD, Department of General Surgery, Peking Union Medical College Hospital, Chinese Academy of Medical Science and Peking Union Medical College, No. 1 Shuai Fu Yuan, Dong Cheng District, Beijing 100730, China. kangweiming@163.com
Telephone: +86-10-69152215
Fax: +86-10-69152213

Received: September 27, 2016
Peer-review started: September 28, 2016
First decision: October 10, 2016
Revised: November 28, 2016
Accepted: January 11, 2017
Article in press: January 11, 2017
Published online: March 14, 2017

Abstract

Ghrelin, as a kind of multifunctional protein polypeptide, is mainly produced in the fundus of the stomach and can promote occurrence and development of many tumors, including gastrointestinal tumors, which has been proved by the relevant researches. Most gastrointestinal stromal tumors (GISTs, about 80%), as the most common mesenchymal tumor, also develop in the fundus. Scientific research has confirmed that ghrelin, its receptors and mRNA respectively can be found in GISTs, which demonstrated the existence of a ghrelin autocrine/paracrine loop in GIST tissues. However, no reports to date have specified the mechanism whether ghrelin can promote the occurrence and development of GISTs. Studies of pulmonary artery endothelial cells in a low-oxygen environment and cardiac muscle cells in an ischemic environment have shown that ghrelin can activate the phosphatidylinositol 3-kinase/AKT/mammalian target of rapamycin (PI3K/AKT/mTOR) signaling pathway. Moreover, some studies of GISTs have confirmed that activation of the PI3K/AKT/mTOR pathway can indeed promote the growth and progression of GISTs. Whether ghrelin is involved in the development or progression of GISTs through certain pathways remains unknown. Can we find a new target for the treatment of GISTs? This review explores and summaries the relationship among ghrelin, the PI3K/AKT/mTOR pathway and the development of GISTs.

Key words: Gastrointestinal stromal tumor; PI3K/AKT/mTOR pathway; Ghrelin; Occurrence; Development

Core tip: Ghrelin has been proven to promote the occurrence and development of gastrointestinal tumors. Some gastrointestinal stromal tumors (GISTs) express ghrelin and its receptors. However, no previous reports have specified whether ghrelin is involved in the occurrence and development of GISTs. Through

a review of the literature, this paper is the first to summarize and discuss the correlation between ghrelin and GISTs.

Zhu CZ, Liu D, Kang WM, Yu JC, Ma ZQ, Ye X, Li K. Ghrelin and gastrointestinal stromal tumors. *World J Gastroenterol* 2017; 23(10): 1758-1763 Available from: URL: http://www.wjgnet.com/1007-9327/full/v23/i10/1758.htm DOI: http://dx.doi.org/10.3748/wjg.v23.i10.1758

INTRODUCTION

Gastrointestinal stromal tumors (GISTs) originate from pacemaker cells (interstitial cells of Cajal, or Cajal cells). They are the most common mesenchymal tumors in the gastrointestinal tract, with an annual incidence of approximately 10-20 per million. Although GISTs can occur in any part of the digestive tract, about 70% are found in the stomach, 10%-25% in the small intestine[1], and a small percentage in the rectum. However, GISTs rarely affect the esophagus or colon[2].

GISTs result from acquired functional changes caused by mutations in the *KIT* and *PDGFRA* genes located on chromosome 4q12. These mutations result in expression of activated forms of the protein products [c-KIT, which is a receptor tyrosine kinase (RTK), and platelet-derived growth factor receptor-α (PDGFRA)], leading to inhibition of apoptosis, activation of cell proliferation, and promotion of tumorigenesis[3,4].

At present, treatment strategies for GISTs mainly focused on the *KIT* and *PDGFRA* genes and their RTK products. Although introduction of the c-KIT and PDGFRA inhibitor imatinib (Gleevec®) has greatly improved treatment efficacy, the median progression-free survival time of patients with GISTs is only about 2 years. The incidence of secondary (acquired) drug resistance within the first 2 years of imatinib treatment is approximately 40%-50%[5]. Patients who display primary resistance to first-line therapy with imatinib can be treated with the multiple-kinase inhibitor sunitinib malate[6]. However, one trial revealed that the objective response rate to sunitinib malate was only 65% (7% partial response and 58% stable disease without progression)[7]. Moreover, the clinical effect is short and drug resistance soon appears. Therefore, although there are many advantages in the current targeted therapies for GISTs, there are also drawbacks, highlighting the urgent need for new ways to treat GISTs.

Clinical observations indicate that most GISTs originate at the base of the stomach, which is also the main secretion site of gastric ghrelin. As described in the following sections, ghrelin is a protein with a variety of functions[8]. Ghrelin receptors are expressed in several types of tumors, including gastric and colon cancer, and are able to promote tumor growth[9-11]. The Cajal cells from which GISTs arise both produce ghrelin and express the ghrelin receptor[12]. Whether ghrelin is involved in the development or progression of GISTs through certain pathways remains unknown. Can we find a new target for the treatment of GISTs? We herein review the relevant literature on this topic.

GHRELIN

Ghrelin is a 28-amino-acid peptide that also exists as des-Gln(14)-ghrelin[13-15]. Ghrelin is currently considered to be the main endogenous ligand of growth receptors[16]. The ghrelin coding gene is located on chromosome 3 (3p25-26)[17].

Approximately 80% of ghrelin in serum is produced by cells at the base of the stomach ("A-X-like" cells), most of which are distributed in acid-secreting glands[18]. These "A-X-like" cells constitute approximately 20% of gastric endocrine cells[19]. Ghrelin is also secreted by the hypothalamus, pituitary gland, kidneys[20], placenta[21], intestinal tract, thyroid[22], heart[13], Leydig cells[23], neutrophils, lungs[24,25], and ovarian tissues[26,27].

Some of the many functions of ghrelin include regulation of growth hormone secretion, energy balance, gastrointestinal motility, gastric acid secretion, cardiovascular activity, pancreatic hormone secretion, glucose metabolism, prolactin and adrenocorticotropic hormone secretion, sleep[15,23], and gonadal hormone secretion. Several studies[9-11] have shown that ghrelin can promote the development of malignant tumors through a variety of signaling pathways that increase cell proliferation and metastasis, including the phosphatidylinositol 3-kinase/AKT/mammalian target of rapamycin (PI3K/AKT/mTOR), Ras/RAF/extracellular signal-regulated kinases (ERK1/2), Janus kinase/signal transducers and activators of transcription (JAK/STAT), and Src kinase pathways.

GISTs EXPRESS GHRELIN AND GHRELIN RECEPTORS

To the best of our knowledge, the only study that has examined the expression of ghrelin and its receptors in GIST tissues is a Japanese study[28] in which ghrelin, ghrelin receptors, and their respective mRNA were detected in all 17 GIST tissues examined, although the extent of ghrelin and ghrelin receptor expression differed in each GIST tissue. The study demonstrated the existence of a ghrelin autocrine/paracrine loop in GIST tissues, suggesting that ghrelin may play a role in the occurrence and development of GISTs.

In contrast, the same study[28] found no statistically significant differences between positive ghrelin expression and tumor location (P = 0.426), tumor size (P = 0.590), KIT genotype (P = 0.935), a mitotic number of > 5 (P = 0.210), a Ki67 index of < 5 (P

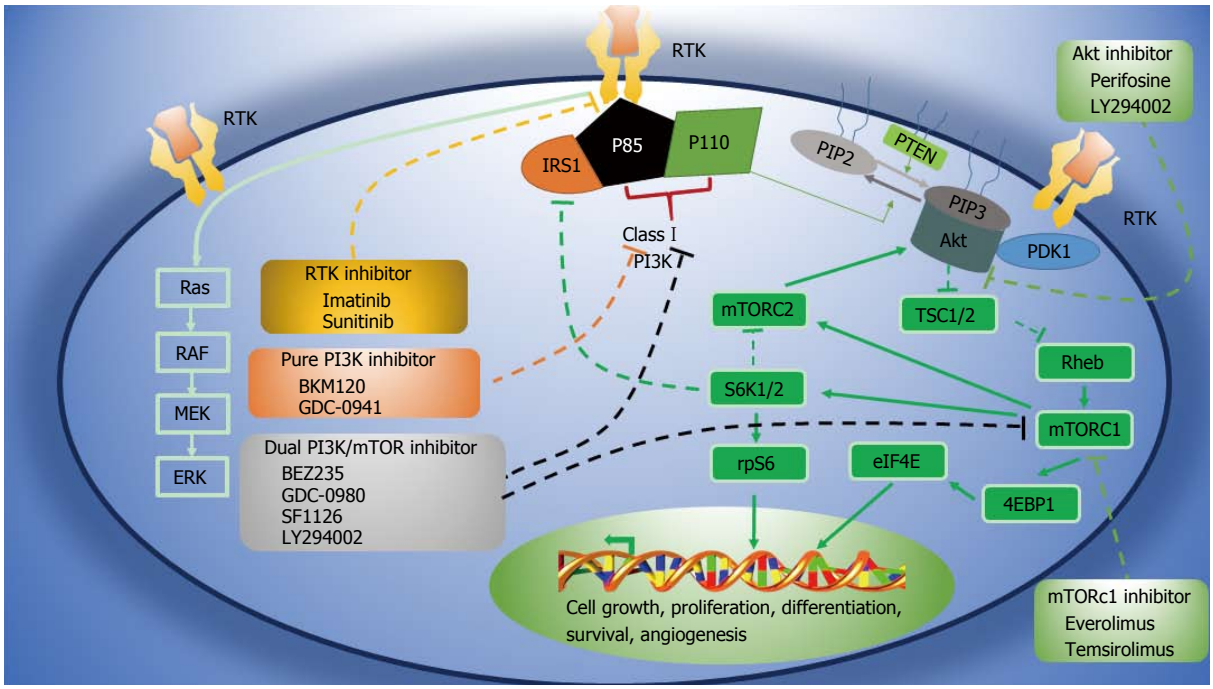

Figure 1 PI3K/AKT/mTOR pathway and inhibitors in clinical development[29]. Solid lines represent activating actions, and dotted lines represent inhibitory actions. 4EBP1: 4E-binding protein 1; PKB: Protein kinase B; ERK: Extracellular signal-related kinase; IRS1: Insulin receptor substrate 1; MEK: Mitogen-activated protein/ERK kinase; mTOR: Mammalian target of rapamycin; mTORC: mTOR complex; PDK1: Pyruvate dehydrogenase lipoamide kinase isozyme 1; PI3K: Phosphatidylinositol 3-kinase; PIP2: Phosphatidylinositol 4,5-bisphosphate; PIP3: Phosphatidylinositol 3,4,5-trisphosphate; PTEN: Phosphatase and tensin homolog; Rheb: Ras homolog enriched in brain; rpS6: Ribosomal protein S6; RTK: Receptor tyrosine kinase; S6K: Ribosomal S6 kinase; TSC1/2: Tuberous sclerosis protein.

= 0.659), or risk of stromal tumor recurrence (P = 0.420). Additionally, ghrelin receptor expression was not correlated with the tumor grade (P = 0.208), Ki67 index (P = 0.717), mitotic count (P = 0.264), tumor location (P = 0.392), tumor size (P = 1), or tumor morphological type (P = 0.223). However, because the study sample was small (17 cases), the significance of these results remains unclear.

ROLE OF PI3K/AKT/mTOR PATHWAY IN GISTs

RTKs such as c-KIT and PDGFRA can activate a variety of intracellular signaling pathways, such as PI3K/AKT/mTOR, Ras/RAF/ERK, JAK/STAT, and Src kinases, which can in turn activate signaling axes downstream of c-KIT. These RTKs are therefore key factors in the treatment of GISTs, especially refractory GISTs[29]. PI3K/AKT/mTOR pathway activation is associated with the development and invasion of a number of tumors[9-11]. Indeed, c-KIT activation *via* autophosphorylation leads to excessive activation of PI3K/AKT/mTOR, which promotes the development and progression of GISTs[29,30]. Thus, blocking excessive activation of this signaling pathway may provide a new therapeutic strategy for GISTs.

The PI3K/AKT/mTOR signaling pathway regulates cell growth, proliferation, and differentiation. The initiating signal molecule, PI3K[31], can be activated by RTKs, G protein-coupled receptors, and oncogenic Ras (Figure 1). Phosphorylation of the RTK recruits PI3K to the inner surface of the cell membrane, where it catalyzes the phosphorylation of phosphatidylinositol (4,5)-bisphosphate (PIP2) to phosphatidylinositol (3,4,5)-trisphosphate (PIP3). This reaction is reversed by phosphatase and tensin homolog (PTEN), which dephosphorylates PIP3 to PIP2[32]. Generation of PIP3 promotes translocation of the serine/threonine protein kinase AKT to the plasma membrane, and activated AKT indirectly leads to the accumulation of the Ras homology protein Rheb and activation of mTORC1[33]. mTORC1 then activates the downstream kinases S6 kinase 1 (S6K1) and S6K2, which stimulate protein synthesis, cell survival, and growth signal release[34-36]. This pathway is essential for the continued growth of tumors and it is therefore being intensely investigated as a source of new therapeutic strategies for GISTs.

The PI3K/AKT/mTOR signaling pathway is blocked by a number of inhibitors. Rapamycin derivatives such as temsirolimus, the first clinically applied inhibitor, mainly inhibit mTORC1. Dual inhibitors such as GDC-0980, BEZ235, and SF1126 inhibit PI3K and mTORC1/2[37], whereas BKM120 and GDC-0941 specifically inhibit PI3K but not mTOR[38]. In addition, Alkyl phosphoric acid choline compound can effectively inhibit AKT[39,40].

Studies have indicated that loss of the *PTEN* gene and dysregulation of the PI3K/ATK/mTOR signaling pathway may play an important role in the progression and drug resistance of GISTs. In cells

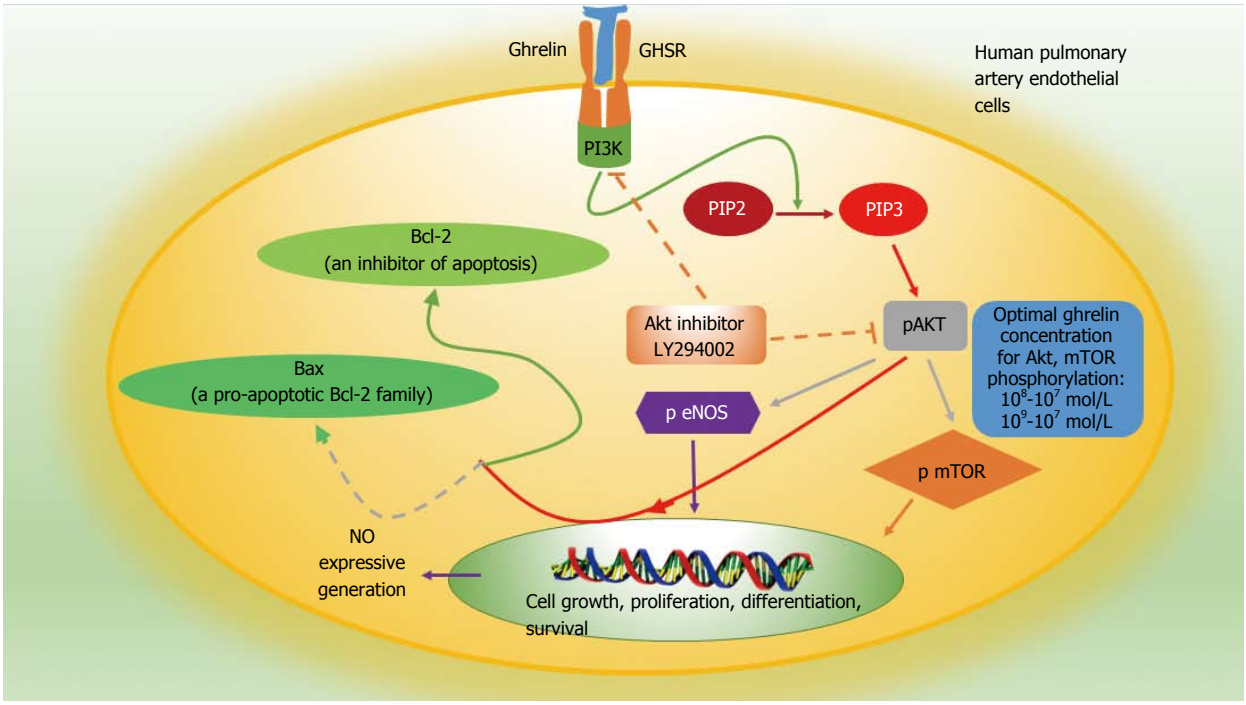

Figure 2 Specific mechanism of ghrelin involved in the protection of pulmonary artery endothelial cells and activation of the PI3K/AKT/mTOR pathway in human pulmonary artery endothelial cells[44-47]. Solid lines represent activating actions, and dotted lines represent inhibitory actions. PIP2: Phosphatidylinositol 4,5-bisphosphate; PIP3: Phosphatidylinositol 3,4,5-trisphosphate.

with absent or low-level expression of PTEN, tumor progression is more rapid[41]. *PTEN* gene silencing also leads to abnormal activation of the PI3K/AKT/mTOR pathway[42].

The expression of mTOR and phosphorylated mTOR is much higher in GISTs measuring > 5 cm in diameter with a medium to high risk of recurrence than in GISTs measuring < 5 cm in diameter with a low or very low recurrence risk[43]. However, few reports have focused on the role of mTOR in the pathogenesis of GISTs.

Collectively, these studies indicate that RTK-targeted therapy can benefit about 85% patients with GISTs, but drug resistance is a major hindrance to its application. The PI3K/ATK/mTOR pathway is believed to be an important pathway for the development and progression of GISTs, suggesting that signaling molecules in this pathway may be useful targets for the development of novel therapies.

GHRELIN ACTIVATES PI3K/ATK/mTOR PATHWAY

Ghrelin activates the PI3K/AKT/mTOR pathway through phosphorylation of AKT and mTOR. Two studies respectively investigated the protective effects of ghrelin on pulmonary artery endothelial cells in a low-oxygen environment and on cardiac muscle cells in an ischemic environment[44,45] and found that ghrelin could promote myocardial cell proliferation, inhibited apoptosis, reduced myocardial fibrosis, improved cardiac function, and significantly increased the survival rate of adipose-derived mesenchymal stem cells and pulmonary artery endothelial cells exposed to hypoxia. Western blot analysis showed that ghrelin reduced expression of the pro-apoptotic protein Bax, increased the level of the anti-apoptotic protein Bcl-2, and significantly increased phosphorylation of AKT and mTOR[44,45]. The PI3K inhibitor LY294002 suppressed phosphorylation events, indicating that ghrelin activates the PI3K/AKT/mTOR pathway through phosphorylation. Two other studies, one examined the modulatory effect of ghrelin on gastric mucosal prostaglandin and nitric oxide and another examined gastric mucosal inflammatory responses to *Helicobacter pylori*, also showed that ghrelin activates the PI3K/AKT/mTOR pathway in different ways[46,47] (Figure 2). Whether ghrelin promotes the development and progression of GISTs through this or other mechanisms remains unclear.

CONCLUSION

GISTs express ghrelin and ghrelin receptors. Ghrelin can activate the PI3K/ATK/mTOR signaling pathway in cardiac muscle cells and pulmonary artery endothelial cells, which plays an important role in the occurrence and development of GISTs. It is possible that ghrelin may promote GISTs by activating this pathway. However, this remains to be fully elucidated.

REFERENCES

1 **Fletcher CD**, Berman JJ, Corless C, Gorstein F, Lasota J, Longley

BJ, Miettinen M, O'Leary TJ, Remotti H, Rubin BP, Shmookler B, Sobin LH, Weiss SW. Diagnosis of gastrointestinal stromal tumors: A consensus approach. *Hum Pathol* 2002; **33**: 459-465 [PMID: 12094370 DOI: 10.1053/hupa.2002.123545]

2 **Dematteo RP**, Ballman KV, Antonescu CR, Maki RG, Pisters PW, Demetri GD, Blackstein ME, Blanke CD, von Mehren M, Brennan MF, Patel S, McCarter MD, Polikoff JA, Tan BR, Owzar K; American College of Surgeons Oncology Group (ACOSOG) Intergroup Adjuvant GIST Study Team. Adjuvant imatinib mesylate after resection of localised, primary gastrointestinal stromal tumour: a randomised, double-blind, placebo-controlled trial. *Lancet* 2009; **373**: 1097-1104 [PMID: 19303137 DOI: 10.1016/S0140-6736(09)60500-6]

3 **Hirota S**, Isozaki K, Moriyama Y, Hashimoto K, Nishida T, Ishiguro S, Kawano K, Hanada M, Kurata A, Takeda M, Muhammad Tunio G, Matsuzawa Y, Kanakura Y, Shinomura Y, Kitamura Y. Gain-of-function mutations of c-kit in human gastrointestinal stromal tumors. *Science* 1998; **279**: 577-580 [PMID: 9438854]

4 **Hirota S**, Ohashi A, Nishida T, Isozaki K, Kinoshita K, Shinomura Y, Kitamura Y. Gain-of-function mutations of platelet-derived growth factor receptor alpha gene in gastrointestinal stromal tumors. *Gastroenterology* 2003; **125**: 660-667 [PMID: 12949711 DOI: 10.1016/S0016-5085(03)01046-1]

5 **Gramza AW**, Corless CL, Heinrich MC. Resistance to Tyrosine Kinase Inhibitors in Gastrointestinal Stromal Tumors. *Clin Cancer Res* 2009; **15**: 7510-7518 [PMID: 20008851 DOI: 10.1158/1078-0432.CCR-09-0190]

6 **Goodman VL**, Rock EP, Dagher R, Ramchandani RP, Abraham S, Gobburu JV, Booth BP, Verbois SL, Morse DE, Liang CY, Chidambaram N, Jiang JX, Tang S, Mahjoob K, Justice R, Pazdur R. Approval summary: sunitinib for the treatment of imatinib refractory or intolerant gastrointestinal stromal tumors and advanced renal cell carcinoma. *Clin Cancer Res* 2007; **13**: 1367-1373 [PMID: 17332278 DOI: 10.1158/1078-0432.CCR-06-2328]

7 **Demetri GD**, van Oosterom AT, Garrett CR, Blackstein ME, Shah MH, Verweij J, McArthur G, Judson IR, Heinrich MC, Morgan JA, Desai J, Fletcher CD, George S, Bello CL, Huang X, Baum CM, Casali PG. Efficacy and safety of sunitinib in patients with advanced gastrointestinal stromal tumour after failure of imatinib: a randomised controlled trial. *Lancet* 2006; **368**: 1329-1338 [PMID: 17046465 DOI: 10.1016/S0140-6736(06)69446-4]

8 **De Ambrogi M**, Volpe S, Tamanini C. Ghrelin: central and peripheral effects of a novel peptydil hormone. *Med Sci Monit* 2003; **9**: RA217-RA224 [PMID: 12960936]

9 **Chopin L**, Walpole C, Seim I, Cunningham P, Murray R, Whiteside E, Josh P, Herington A. Ghrelin and cancer. *Mol Cell Endocrinol* 2011; **340**: 65-69 [PMID: 21616120 DOI: 10.1016/j.mce.2011.04.013]

10 **Nikolopoulos D**, Theocharis S, Kouraklis G. Ghrelin: a potential therapeutic target for cancer. *Regul Pept* 2010; **163**: 7-17 [PMID: 20382189 DOI: 10.1016/j.regpep.2010.03.011]

11 **Nikolopoulos D**, Theocharis S, Kouraklis G. Ghrelin's role on gastrointestinal tract cancer. *Surg Oncol* 2010; **19**: e2-e10 [PMID: 19328680 DOI: 10.1016/j.suronc.2009.02.011]

12 **Yang CG**, Liao ZF, Qiu WC, Yan J, Wang ZG. Function of ghrelin and ghrelin receptors in the network regulation of gastric motility. *Mol Med Rep* 2014; **10**: 2453-2458 [PMID: 25230765 DOI: 10.3892/mmr.2014.2571]

13 **Casanueva FF**, Dieguez C. Ghrelin: the link connecting growth with metabolism and energy homeostasis. *Rev Endocr Metab Disord* 2002; **3**: 325-338 [PMID: 12424434]

14 **Tschöp M**, Smiley DL, Heiman ML. Ghrelin induces adiposity in rodents. *Nature* 2000; **407**: 908-913 [PMID: 11057670 DOI: 10.1038/35038090]

15 **Muccioli G**, Tschöp M, Papotti M, Deghenghi R, Heiman M, Ghigo E. Neuroendocrine and peripheral activities of ghrelin: implications in metabolism and obesity. *Eur J Pharmacol* 2002; **440**: 235-254 [PMID: 12007539]

16 **Beaumont NJ**, Skinner VO, Tan TM, Ramesh BS, Byrne DJ, MacColl GS, Keen JN, Bouloux PM, Mikhailidis DP, Bruckdorfer KR, Vanderpump MP, Srai KS. Ghrelin can bind to a species of high density lipoprotein associated with paraoxonase. *J Biol Chem* 2003; **278**: 8877-8880 [PMID: 12531885 DOI: 10.1074/jbc.C200575200]

17 **Hosoda H**, Kojima M, Matsuo H, Kangawa K. Ghrelin and des-acyl ghrelin: two major forms of rat ghrelin peptide in gastrointestinal tissue. *Biochem Biophys Res Commun* 2000; **279**: 909-913 [PMID: 11162448 DOI: 10.1006/bbrc.2000.4039]

18 **Date Y**, Kojima M, Hosoda H, Sawaguchi A, Mondal MS, Suganuma T, Matsukura S, Kangawa K, Nakazato M. Ghrelin, a novel growth hormone-releasing acylated peptide, is synthesized in a distinct endocrine cell type in the gastrointestinal tracts of rats and humans. *Endocrinology* 2000; **141**: 4255-4261 [PMID: 11089560 DOI: 10.1210/endo.141.11.7757]

19 **Rindi G**, Necchi V, Savio A, Torsello A, Zoli M, Locatelli V, Raimondo F, Cocchi D, Solcia E. Characterisation of gastric ghrelin cells in man and other mammals: studies in adult and fetal tissues. *Histochem Cell Biol* 2002; **117**: 511-519 [PMID: 12107501 DOI: 10.1007/s00418-002-0415-1]

20 **Mori K**, Yoshimoto A, Takaya K, Hosoda K, Ariyasu H, Yahata K, Mukoyama M, Sugawara A, Hosoda H, Kojima M, Kangawa K, Nakao K. Kidney produces a novel acylated peptide, ghrelin. *FEBS Lett* 2000; **486**: 213-216 [PMID: 11119706]

21 **Horvath TL**, Diano S, Sotonyi P, Heiman M, Tschöp M. Minireview: ghrelin and the regulation of energy balance--a hypothalamic perspective. *Endocrinology* 2001; **142**: 4163-4169 [PMID: 11564668 DOI: 10.1210/endo.142.10.8490]

22 **Kanamoto N**, Akamizu T, Hosoda H, Hataya Y, Ariyasu H, Takaya K, Hosoda K, Saijo M, Moriyama K, Shimatsu A, Kojima M, Kangawa K, Nakao K. Substantial production of ghrelin by a human medullary thyroid carcinoma cell line. *J Clin Endocrinol Metab* 2001; **86**: 4984-4990 [PMID: 11600575 DOI: 10.1210/jcem.86.10.7891]

23 **Barreiro ML**, Gaytán F, Caminos JE, Pinilla L, Casanueva FF, Aguilar E, Diéguez C, Tena-Sempere M. Cellular location and hormonal regulation of ghrelin expression in rat testis. *Biol Reprod* 2002; **67**: 1768-1776 [PMID: 12444052]

24 **Volante M**, Allìa E, Gugliotta P, Funaro A, Broglio F, Deghenghi R, Muccioli G, Ghigo E, Papotti M. Expression of ghrelin and of the GH secretagogue receptor by pancreatic islet cells and related endocrine tumors. *J Clin Endocrinol Metab* 2002; **87**: 1300-1308 [PMID: 11889202 DOI: 10.1210/jcem.87.3.8279]

25 **Volante M**, Fulcheri E, Allìa E, Cerrato M, Pucci A, Papotti M. Ghrelin expression in fetal, infant, and adult human lung. *J Histochem Cytochem* 2002; **50**: 1013-1021 [PMID: 12133904]

26 **Gaytan F**, Barreiro ML, Chopin LK, Herington AC, Morales C, Pinilla L, Casanueva FF, Aguilar E, Diéguez C, Tena-Sempere M. Immunolocalization of ghrelin and its functional receptor, the type 1a growth hormone secretagogue receptor, in the cyclic human ovary. *J Clin Endocrinol Metab* 2003; **88**: 879-887 [PMID: 12574228 DOI: 10.1210/jc.2002-021196]

27 **Korbonits M**, Bustin SA, Kojima M, Jordan S, Adams EF, Lowe DG, Kangawa K, Grossman AB. The expression of the growth hormone secretagogue receptor ligand ghrelin in normal and abnormal human pituitary and other neuroendocrine tumors. *J Clin Endocrinol Metab* 2001; **86**: 881-887 [PMID: 11158061 DOI: 10.1210/jcem.86.2.7190]

28 **Ekeblad S**, Nilsson B, Lejonklou MH, Johansson T, Stålberg P, Nilsson O, Ahlman H, Skogseid B. Gastrointestinal stromal tumors express the orexigen ghrelin. *Endocr Relat Cancer* 2006; **13**: 963-970 [PMID: 16954444 DOI: 10.1677/erc.1.01201]

29 **Patel S**. Exploring novel therapeutic targets in GIST: focus on the PI3K/Akt/mTOR pathway. *Curr Oncol Rep* 2013; **15**: 386-395 [PMID: 23605780 DOI: 10.1007/s11912-013-0316-6]

30 **Bauer S**, Duensing A, Demetri GD, Fletcher JA. KIT oncogenic signaling mechanisms in imatinib-resistant gastrointestinal stromal tumor: PI3-kinase/AKT is a crucial survival pathway. *Oncogene* 2007; **26**: 7560-7568 [PMID: 17546049 DOI: 10.1038/sj.onc.1210558]

31 **Hollander MC**, Blumenthal GM, Dennis PA. PTEN loss in the continuum of common cancers, rare syndromes and mouse models. *Nat Rev Cancer* 2011; **11**: 289-301 [PMID: 21430697 DOI: 10.1038/nrc3037]

32 **Maehama T**, Dixon JE. The tumor suppressor, PTEN/MMAC1, dephosphorylates the lipid second messenger, phosphatidylinositol 3,4,5-trisphosphate. *J Biol Chem* 1998; **273**: 13375-13378 [PMID: 9593664 DOI: 10.1074/jbc.273.22.13375]

33 **Liu P**, Cheng H, Roberts TM, Zhao JJ. Targeting the phosphoinositide 3-kinase pathway in cancer. *Nat Rev Drug Discov* 2009; **8**: 627-644 [PMID: 19644473 DOI: 10.1038/nrd2926]

34 **Sridharan S**, Basu A. S6 kinase 2 promotes breast cancer cell survival via Akt. *Cancer Res* 2011; **71**: 2590-2599 [PMID: 21427355 DOI: 10.1158/0008-5472.CAN-10-3253]

35 **Pastor MD**, García-Yébenes I, Fradejas N, Pérez-Ortiz JM, Mora-Lee S, Tranque P, Moro MA, Pende M, Calvo S. mTOR/S6 kinase pathway contributes to astrocyte survival during ischemia. *J Biol Chem* 2009; **284**: 22067-22078 [PMID: 19535330 DOI: 10.1074/jbc.M109.033100]

36 **Glantschnig H**, Fisher JE, Wesolowski G, Rodan GA, Reszka AA. M-CSF, TNFalpha and RANK ligand promote osteoclast survival by signaling through mTOR/S6 kinase. *Cell Death Differ* 2003; **10**: 1165-1177 [PMID: 14502240 DOI: 10.1038/sj.cdd.4401285]

37 **Courtney KD**, Corcoran RB, Engelman JA. The PI3K pathway as drug target in human cancer. *J Clin Oncol* 2010; **28**: 1075-1083 [PMID: 20085938 DOI: 10.1200/JCO.2009.25.3641]

38 **Markman B**, Dienstmann R, Tabernero J. Targeting the PI3K/Akt/mTOR pathway--beyond rapalogs. *Oncotarget* 2010; **1**: 530-543 [PMID: 21317449 DOI: 10.18632/oncotarget.101012]

39 **Conley AP**, Araujo D, Ludwig J, Ravi V, Samuels BL, Choi H, Thall PF, Patel S, Benjamin R, Trent J. A randomized phase II study of perifosine (P) plus imatinib for patients with imatinib-resistant gastrointestinal stromal tumor (GIST). *J Clin Oncol* 2009; **27**: 10563 [PMID: 27963814 DOI: 10.1200/jco.2009.27.15s.10563]

40 **Kondapaka SB**, Singh SS, Dasmahapatra GP, Sausville EA, Roy KK. Perifosine, a novel alkylphospholipid, inhibits protein kinase B activation. *Mol Cancer Ther* 2003; **2**: 1093-1103 [PMID: 14617782]

41 **Ricci R**, Maggiano N, Castri F, Rinelli A, Murazio M, Pacelli F, Potenza AE, Vecchio FM, Larocca LM. Role of PTEN in gastrointestinal stromal tumor progression. *Arch Pathol Lab Med* 2004; **128**: 421-425 [PMID: 15043466 DOI: 10.1043/1543-2165(2004)128<421:ROPIGS>2.0.CO;2]

42 **Yang J**, Ikezoe T, Nishioka C, Takezaki Y, Hanazaki K, Taguchi T, Yokoyama A. Long-term exposure of gastrointestinal stromal tumor cells to sunitinib induces epigenetic silencing of the PTEN gene. *Int J Cancer* 2012; **130**: 959-966 [PMID: 21445973 DOI: 10.1002/ijc.26095]

43 **Li JC**, Zhu HY, Chen TX, Zou LY, Wang XY, Zhao HC, Xu J. Roles of mTOR and p-mTOR in gastrointestinal stromal tumors. *Asian Pac J Cancer Prev* 2013; **14**: 5925-5928 [PMID: 24289602]

44 **Yang D**, Liu Z, Zhang H, Luo Q. Ghrelin protects human pulmonary artery endothelial cells against hypoxia-induced injury via PI3-kinase/Akt. *Peptides* 2013; **42**: 112-117 [PMID: 23391508 DOI: 10.1016/j.peptides.2013.01.012]

45 **Han D**, Huang W, Ma S, Chen J, Gao L, Liu T, Zhang R, Li X, Li C, Fan M, Chen Y, Cao F. Ghrelin improves functional survival of engrafted adipose-derived mesenchymal stem cells in ischemic heart through PI3K/Akt signaling pathway. *Biomed Res Int* 2015; **2015**: 858349 [PMID: 25879037 DOI: 10.1155/2015/858349]

46 **Slomiany BL**, Slomiany A. Induction in gastric mucosal prostaglandin and nitric oxide by Helicobacter pylori is dependent on MAPK/ERK-mediated activation of IKK-β and cPLA2: modulatory effect of ghrelin. *Inflammopharmacology* 2013; **21**: 241-251 [PMID: 23563696 DOI: 10.1007/s10787-013-0169-5]

47 **Slomiany BL**, Slomiany A. Modulation of gastric mucosal inflammatory responses to Helicobacter pylori via ghrelin-induced protein kinase Cδ tyrosine phosphorylation. *Inflammopharmacology* 2014; **22**: 251-262 [PMID: 24840386 DOI: 10.1007/s10787-014-0206-z]

P- Reviewer: Hegardt FG, Navarrete A, Slomiany BL, Unger M
S- Editor: Gong ZM **L- Editor**: Ma JY **E- Editor**: Wang CH

World Journal of Gastroenterology

Submit a Manuscript: http://www.wjgnet.com/esps/

World J Gastroenterol 2017 March 14; 23(10): 1764-1770

DOI: 10.3748/wjg.v23.i10.1764

ISSN 1007-9327 (print) ISSN 2219-2840 (online)

ORIGINAL ARTICLE

Basic Study

Hyperplasia *vs* hypertrophy in tissue regeneration after extensive liver resection

Fabio Marongiu, Michela Marongiu, Antonella Contini, Monica Serra, Erika Cadoni, Riccardo Murgia, Ezio Laconi

Fabio Marongiu, Michela Marongiu, Antonella Contini, Monica Serra, Erika Cadoni, Riccardo Murgia, Ezio Laconi, Experimental Medicine Unit, Department of Biomedical Sciences, University of Cagliari, 09124 Cagliari, Italy

Author contributions: Marongiu F, Marongiu M and Laconi E substantially contributed to the conception and design of the study, critical analysis and interpretation of data; all authors designed and performed the experiments, and contributed to the acquisition and analysis of data, made critical revisions related to the intellectual content of the manuscript, and approved the final version of the article to be published.

Supported by Italian Association for Cancer Research, No. IG 14640.

Institutional review board statement: The study was reviewed and approved by the University of Cagliari Institutional Review Board.

Institutional animal care and use committee statement: All animal studies described in this manuscript were reviewed and approved by the Institutional Animal Care and Use Committee of the University of Cagliari.

Conflict-of-interest statement: To the best of our knowledge, no conflict of interest exists.

Data sharing statement: No additional data are available.

Manuscript source: Unsolicited manuscript

Correspondence to: Fabio Marongiu, PhD, Experimental Medicine Unit, Department of Biomedical Sciences, University of Cagliari, Via Porcell 4, IV floor, 09124 Cagliari, Italy. fabiomarongiu@unica.it
Telephone: +39-70-6758683
Fax: +39-70-662574

Received: November 10, 2016
Peer-review started: November 13, 2016
First decision: December 19, 2016
Revised: December 27, 2016
Accepted: January 11, 2017
Article in press: January 11, 2017
Published online: March 14, 2017

Abstract

AIM

To address to what extent hypertrophy and hyperplasia contribute to liver mass restoration after major tissue loss.

METHODS

The ability of the liver to regenerate is remarkable on both clinical and biological grounds. Basic mechanisms underlying this process have been intensively investigated. However, it is still debated to what extent hypertrophy and hyperplasia contribute to liver mass restoration after major tissue loss. We addressed this issue using a genetically tagged system. We were able to follow the fate of single transplanted hepatocytes during the regenerative response elicited by 2/3 partial surgical hepatectomy (PH) in rats. Clusters of transplanted cells were 3D reconstructed and their size distribution was evaluated over time after PH.

RESULTS

Liver size and liver DNA content were largely recovered 10 d post-PH, as expected (*e.g.*, total DNA/liver/100 g

b.w. was 6.37 ± 0.21 before PH and returned to 6.10 ± 0.36 10 d after PH). Data indicated that about 2/3 of the original residual hepatocytes entered S-phase in response to PH. Analysis of cluster size distribution at 24, 48, 96 h and 10 d after PH revealed that about half of the remnant hepatocytes completed at least 2 cell cycles. Average size of hepatocytes increased at 24 h (248.50 μm^2 ± 7.82 μm^2, P = 0.0015), but returned to control values throughout the regenerative process (up to 10 d post-PH, 197.9 μm^2 ± 6.44 μm^2, P = 0.11). A sizeable fraction of the remnant hepatocyte population does not participate actively in tissue mass restoration.

CONCLUSION

Hyperplasia stands as the major mechanism contributing to liver mass restoration after PH, with hypertrophy playing a transient role in the process.

Key words: Liver regeneration; Hypertrophy; Hyperplasia

Core tip: The ability of the liver to regenerate is remarkable on both clinical and biological grounds. It is still debated to what extent hypertrophy and hyperplasia contribute to liver mass restoration after major tissue loss. We addressed this issue using a genetically tagged system during the regenerative response elicited by 2/3 partial hepatectomy (PH) in rats. Analysis of cluster size distribution revealed that about half of the remnant hepatocytes completed at least 2 cell cycles. Average size of hepatocytes returned to control values throughout the regenerative process. Thus, hyperplasia stands as the major mechanism contributing to liver mass restoration after PH.

Marongiu F, Marongiu M, Contini A, Serra M, Cadoni E, Murgia R, Laconi E. Hyperplasia *vs* hypertrophy in tissue regeneration after extensive liver resection. *World J Gastroenterol* 2017; 23(10): 1764-1770 Available from: URL: http://www.wjgnet.com/1007-9327/full/v23/i10/1764.htm DOI: http://dx.doi.org/10.3748/wjg.v23.i10.1764

INTRODUCTION

The ability of the liver to regenerate is remarkable on both clinical and biological grounds. It allows this organ to maintain functional proficiency in spite of the multitude of food-born toxic insults it can be exposed to throughout life, given its anatomical position[1]. In addition, it represents one of the best systems for the mechanistic analysis of regulatory pathways controlling cell proliferation *in vivo*. Unsurprisingly, a vast scientific literature is dedicated to the detailed description of the process of liver regeneration, providing fundamental insights into its biological and molecular bases[2,3].

Partial (two/thirds) surgical hepatectomy (PH) is the most widely used experimental procedure to study liver regeneration. This model offers two important advantages: (1) it allows a relatively "clean" removal of hepatic parenchyma, due to the multilobular structure of the rodent liver, with no major interference of tissue necrosis and/or inflammation; and (2) The procedure is rapid (it can be performed in a few minutes) and the kinetics of the response is amenable to precise timing[4]. A large body of data is therefore available regarding the response of the liver following PH. The general consensus has been that, in order to restore the original mass, the majority of hepatocytes in the remaining lobes undergo one or two cell division cycles, resuming quiescence at the end of the process[2]. This conclusion is primarily based on reports describing the cumulative labelling of S phase cells[5-7], while direct data regarding the actual proportion of cells completing mitosis after S phase have been more difficult to obtain[6]. New insights into this issue were provided in an elegant study published a few years ago by Miyaoka *et al*[8], who followed the fate of single genetically tagged hepatocytes in the liver of mice during their response to PH. They reported that a significant fraction of hepatocytes (up to 40%) do not divide in the course of the regenerative response, while an increase in the size of single cells (hypertrophy) accounts for at least one third of the overall restoration of liver mass occurring after PH[8]. In spite of their challenging nature to current assumptions referred to above, to our knowledge these results have not been addressed so far. Taking advantage of an orthotopic system for rat hepatocyte transplantation that is utilized routinely by our research group[9], we probed into the hypothesis proposed by Miyaoka *et al*[8]. Our results support the conclusion that up to 1/3 of the remnant hepatocytes do not enter S-phase and/or divide in response to PH; however, hyperplasia is the main biological mechanism sustaining liver mass restoration in rats, while hypertrophy does not appear to contribute significantly to the process.

MATERIALS AND METHODS

Animals

The syngeneic Fischer 344 rat strain was used for transplantation experiments. All animals were maintained on daily cycles of alternating 12 h light-darkness with food and water available ad libitum. They were fed Purina Rodent Lab Chow diet throughout the experiment and received humane care according to the criteria outlined in the National Institutes of Health Publication 86-23, revised 1985. Animal studies were reviewed and approved by the Institutional Animal Care and Use Committee of the University of Cagliari.

Hepatocyte isolation and transplantation

Hepatocytes were isolated using a two-step collagenase

perfusion procedure as previously described[10,11]. To follow the fate of transplanted cells in the host liver, syngeneic donors expressing the green fluorescent protein (GFP^+) were used. Heterozygous rats expressing GFP under ubiquitin C promoter (line 307 F455 Chr5) were obtained from Rat Resource and Research Center (University of Missouri, Columbia, MO) and they were bred to homozygosity before being utilized. Isolated cells were transplanted (Tx) into the liver of recipient animals (2×10^6 cells per animal in 0.2 mL) *via* a mesenteric vein[9].

Transplanted hepatocytes were then allowed to engraft and integrate in the recipient liver and one month later 2/3 partial hepatectomy (PH) was performed; groups of 5 animals each were killed at various time points thereafter, including 24, 48, 72, 96 h and 10 d post-operation. One group of intact animals was kept as control. Each animal received multiple doses of 5'-bromo-deoxyUridine (BrdU, 50 mg/kg, i.p.), every 6 h, starting at 24 h before killing; the last injection was given 1 h prior to euthanasia. Livers were excised and tissue samples were either immediately frozen or fixed for further analysis. Liver DNA content was measured according to published techniques[12].

Immunofluorescence and Immunohistochemistry

For immunofluorescence analysis, liver tissues were fixed in 4% paraformaldehyde (PFA), cryoprotected in 30% sucrose solution for 24 h at 4 ℃, and then frozen. Five μm-thick sections were blocked for 30' with goat serum and incubated 1h at RT with Alexa Fluor 555®-conjugated Phalloidin (Thermo Fisher Scientific, Waltham, MA, United States). Nuclei were counterstained with DAPI (Abcam, Cambridge, MA, United States).

Immunohistochemical staining for GFP and BrdU, was performed on 5 μm-thick paraffin embedded sections, following de-wax and antigen retrieval with 0.01 mol/L pH 6 sodium citrate buffer. Slides were blocked for 30', incubated with the primary antibody (GFP, Thermo Fisher Scientific; BrdU, Santa Cruz, CA, United States) overnight at 4 ℃. Detection of specific signal was accomplished using an HRP/AEC detection IHC Kit (Abcam).

Cell imaging analysis

Three dimensional analysis of GFP^+ clusters was performed on 10 consecutive serial sections by scanning slides with a Pathscan Enabler IV scanner (Meyer Instruments, Houston, TX, United States). Acquired images were overlayed and analyzed using Image-Pro Premier Software (Media Cybernetics, Rockville, MD, United States). Cell and nuclear size was measured on fluorescence images acquired with an Axio Imager Fluorescence Microscope (Zeiss, Oberkochen, Germany) using Image-Pro Premier Software.

Statistical analysis

Data were analyzed and plotted using GraphPad Prism (GraphPad Software, La Jolla, CA, United States). Results are presented as mean ± SE. Two-tailed Student *t* test was used to evaluate results, with a lowest level of significance of $P < 0.05$. Statistical review of the study was performed by Prof. Giacomo Diaz from the University of Cagliari.

RESULTS

Recovery of liver mass and liver DNA content following PH

Relative liver weight increased gradually from day 1 to day 10 post-PH, returning to near-normal values at the latter time point (Figure 1A). A similar pattern was seen for the absolute and relative (*i.e.,* expressed as percent body weight) liver DNA content: both parameters had largely recovered between 72 and 96 h after PH and attained levels comparable to normal by 10 d post-surgery (Figure 1B and C).

Panels D, E and F report data on the cumulative S-phase entry of hepatocytes during the first 96 h after PH. Both the figure in panel E and the plot in panel F clearly indicate that about one third of the hepatocytes have not entered S-phase as late as 96 h post-PH. Furthermore, this proportion is possibly still higher if referred to the remnant liver prior to the initiation of the proliferative response, in that at least a fraction of S-phase cells have divided and are therefore over-represented at 96 h post-PH.

Size distribution of hepatocyte clusters originating from isolated transplanted cells in response to PH

As detailed the Experimental Procedures, hepatocytes isolated from a syngeneic Fischer 344 rat donor expressing the GFP were transplanted into the liver of GFP-negative recipients, *via* a mesenteric vein. Four weeks later, PH was performed and the fate of GFP^+ hepatocytes clusters was followed over time during the regenerative response of the liver. Each cluster was reconstructed in 3D through the analysis of 10 consecutive serial sections from each sample (see Experimental Procedures). Results are presented in Figure 2. At the time of PH, only single GFP^+ cells and doublets (about 60% and 40%, respectively) were seen (Figure 3A). This proportion remained virtually unchanged at 24 h post-PH, while it had significantly shifted at 48 h, with a relative decrease of single GFP^+ cells, an increase in doublets, a consistent appearance of triplets (about 20% of the total) and the first detection of four-cell sized clusters. Such progressive shift of GFP^+ clusters towards higher size categories continued at 96 h and was still more prominent at 10 d post-PH (Figure 3A and B). Clusters of 5 GFP^+ cells and larger were detected at 96 h (about 20% of the total, Figure 3C) and their proportion increased to approximately 35% at 10 d post-PH, when over 10%

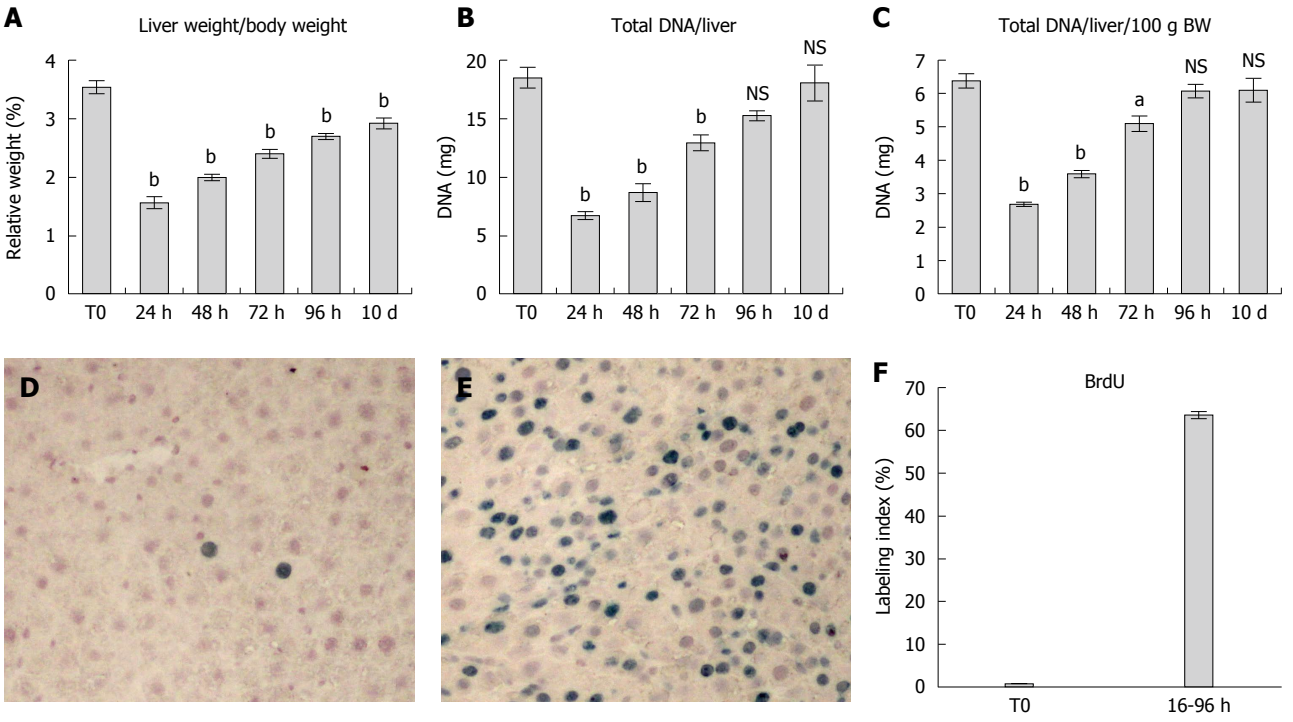

Figure 1 Kinetics of liver mass restoration following partial surgical hepatectomy. A: Showing the gradual increase in relative liver weight, which has almost returned to control values at 10 d post-surgery, albeit a small significant difference is still present; B and C: Reporting data on liver DNA content: both total liver DNA and the relative amount (expressed as % body weight) had largely recovered at 96 h post-PH and were back to normal values by 10 d after operation; D-F: Cumulative S-phase entry of hepatocytes in response to PH. Immunohistochemical staining for BrdU is shown in panels D (control rat liver) and E (cumulative labelling from 16 to 96 h post-PH). The histogram in panel F reports percent of hepatocytes that had incorporated BrdU in their nuclei between 16 and 96 h post PH (see Methods for details). Data are mean ± SE of 5 animals per group. $^{a}P < 0.05$, $^{b}P < 0.01$ *vs* control group. PH: Partial surgical hepatectomy.

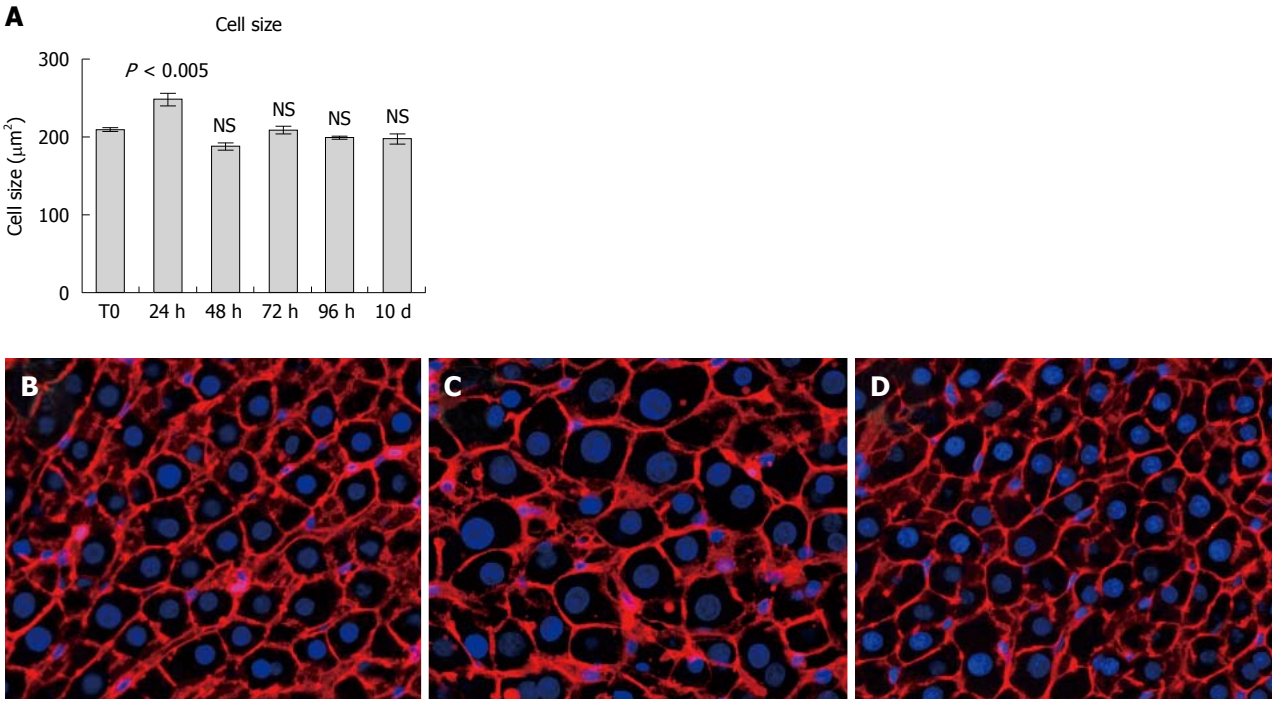

Figure 2 Hepatocyte size during the regenerative response to partial surgical hepatectomy. A: Reporting mean area of hepatocytes in control rat liver and at various time points after PH. At least five hundred hepatocytes per animal in each group were scored. Data are mean ± SE of 5 animals per group. Immunofluorescent staining for Phalloidin is shown in panels B (control rat liver), C (24 h post-PH) and D (10 d post-PH). Nuclei were counterstained with DAPI. PH: Partial surgical hepatectomy.

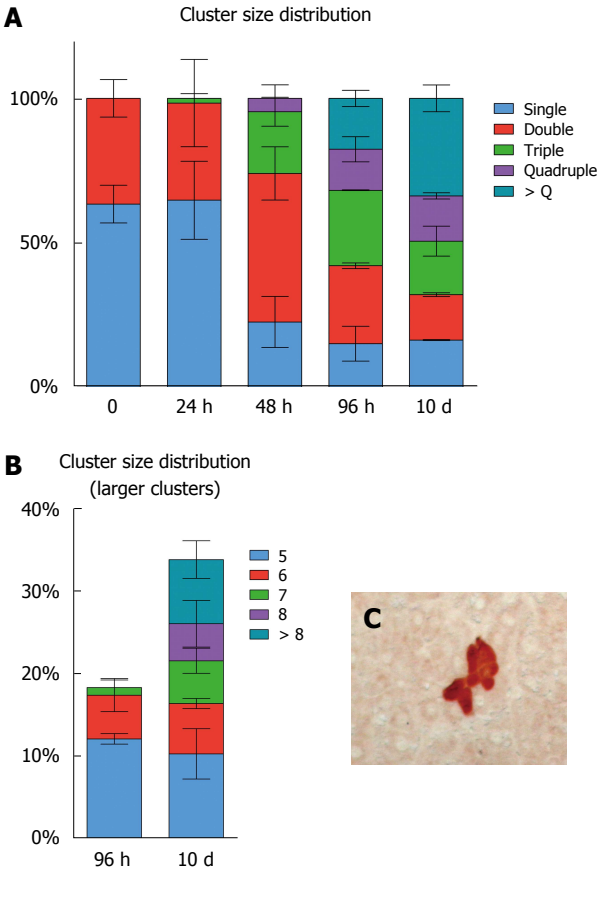

Figure 3 Size distribution of GFP$^+$ hepatocyte clusters at various time points after partial surgical hepatectomy. A: Each cluster was 3D reconstructed (see Methods for details) and number of hepatocytes was counted. Bars of the histogram report the frequency of each class size expressed as percent of the total number of clusters. At least one hundred clusters per group were computed; B: An expansion of panel A. It shows the class size distribution of largest clusters present at 96 h and 10 d after PH; C: An image of immunohistochemical staining for GFP. PH: Partial surgical hepatectomy; GFP$^+$: Green fluorescent protein.

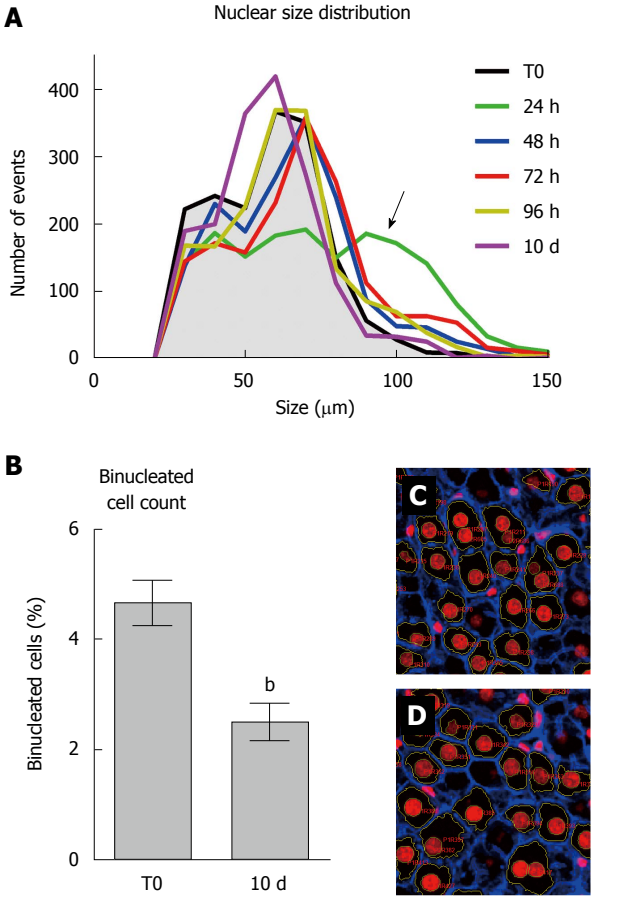

Figure 4 Size distribution of hepatocyte nuclei, the only evident change being detected after 24 h. A: Showing nuclear size distribution over time following PH. The most prominent change is observed at 24 h post-PH (green line), with the appearance of a larger nuclear class size (arrow), which is only marginally present at later time points; B: Reporting percent of binucleated hepatocytes detected on 2D sections in control rat liver and at 10 d post-PH. A relative decrease is observed after PH; C (control rat liver) and D (10 d post-PH) show immunofluorescent staining for Phalloidin with nuclei were counterstained with DAPI. Binucleated hepatocytes are easily discerned. Data are mean ± SE of 5 animals per group. $^bP < 0.01$, *vs* control group. PH: Partial surgical hepatectomy.

of GFP$^+$ clusters comprised 8 or more hepatocytes, indicating that they resulted from multiple cell cycles.

Size of hepatocytes during the regenerative response to PH

In Figure 4 (panels A through D) the average size of hepatocytes at various time points after PH, measured on 2D slides, is reported. The only evident change was observed at 24 h post-surgery, *i.e.,* prior to the first wave of mitosis, when hepatocytes were significantly enlarged compared to any other time point considered. Importantly, no differences in size were recorded between hepatocytes in resting liver and those present at the end of the regenerative phase.

Size distribution of hepatocyte nuclei during the regenerative response was also similar at various time points post-PH, the only evident change being detected after 24 h (Figure 4A). In fact, at 24 h hepatocyte nuclei appeared to distribute in three different size categories, including a larger one, which is absent or minimally present in either control rat liver or at later time points after PH.

Finally, we estimated the percent of binucleated hepatocytes on 2D liver sections obtained prior to PH and at 10 d post-surgery (Figure 4, panels B through D). Although this is clearly an underestimate of the absolute numbers, results did indicate a significant drop (about 50%) in the proportion of binuclear hepatocytes following PH, in agreement with previous studies[8,13]. Such decrease has been generally attributed to cell division occurring in response to PH[13].

DISCUSSION

The remarkable ability of the liver to regenerate has intrigued humankind ever since the dawn of civilization, as exemplified by Greek mythology[14]. However, it was the work of Higgins and Anderson[15], describing the surgical procedure to perform PH, that

set the stage for a detailed analysis of the process. Classical studies by Grisham[7], by Bucher's research group[5,16] and by Fabrikant[6] established fundamental parameters of hepatic regeneration, including the kinetics of DNA synthesis in parenchymal and littoral cells and its critical dependence on the extent of tissue removal. The general agreement that emerged from these observations was that, in order for the liver to recover its original mass after PH, the large majority of hepatocytes had to undergo one round of DNA synthesis and cell division, followed by a smaller percentage of cells entering a second replication cycle[3]. In retrospect, it is worth noting that irrefutable evidence in support of this paradigm was not present in the available literature. In fact, the seminal papers referred to above report levels of about 60% resident hepatocytes entering S phase within 36-40 h post-PH, and an additional 22% doing so between 36 and 72 h post-surgery[5,7], with the possibility that the latter population could represent, at least in part, a fraction of the former. Furthermore, Rabes *et al*[17] reported that up to 80% of hepatocytes initiated S-phase during the first 40 h after PH; however, those studies were performed under continuous infusion of hydroxyurea, an S-phase blocker that might have recruited additional cells into cycle. Thus, the postulation that all residual hepatocytes enter the cell cycle at least once after PH has been rather inferential in nature.

A direct challenge to this widely accepted concept came from work by Miyaoka *et al*[8] reported a few years ago. The authors followed the fate of tagged single hepatocytes during their response to PH in mouse. They were able to observe that a significant fraction of hepatocytes (about 40%) do not divide in the course of the regenerative response, while an increase in the size of single cells (hypertrophy) accounts for at least one third of the overall restoration of liver mass occurring after PH[8].

Given the relevance of these findings, in the present investigation we probed into this issue using an experimental system of hepatocyte transplantation in the rat that is conceptually similar to the one of Miyaoka *et al*[8]. Single hepatocytes expressing GFP were injected into the liver of syngeneic Fischer 344 rats and their fate was traced over time following PH. Our findings indicate that hyperplasia stands as the main biological mechanism sustaining restoration of liver mass following PH in the rat, while hypertrophy does not appear to contribute to the process to any measurable extent.

These conclusions stem from the following observations. First, restoration of liver weight and liver DNA content is already prominent at day 4 and is virtually complete at day 10 post PH, as expected[18]. Secondly, the size distribution of GFP^+ hepatocyte clusters at various time points post PH indicates that about 1 in 3 GFP^+ clusters detected at day 10 comprise more than 4 cells. Given that at time zero all clusters were only 1 or 2 cells in size, the only possibility is that clones containing 5 cells and higher resulted from at least two cell division cycles of the original residual hepatocytes.

On the other hand, we confirmed that a sizeable proportion of the original hepatocytes do not enter S phase and/or do not appear to divide (Figure 1, panel F) for up to 10 d post-PH, when hepatic mass is largely recovered, in agreement with previous results[5-8]. In fact, about 1/3 of GFP^+ clusters were still 1 to 2 cells in size at the end of the regenerative phase, indicating that they had not responded to the proliferative stimulus. Conversely, as already mentioned, a sub-population of the original hepatocytes divided at least twice, contributing substantially to the final liver mass. This is in line with data reported by Wu *et al*[19], documenting that at least 11% of residual hepatocytes divide thrice or more after PH[19,20]. Although S-phase and mitotic division are not necessarily coupled, neither in the liver or in other tissues[21], classical studies by Fabrikant indicated that at least the first wave of mitosis following PH in rat liver is preceded by DNA synthesis in virtually all dividing cells[6]. This implies that unconventional cell division, *i.e.,* mitosis without prior S-phase[15], is not of prominent occurrence, if any, under these conditions.

Furthermore, mean hepatocyte size, measured in 2D, increased at 24 h after PH (Figure 3); however, no significant changes were observed at later time points and till the end of the regenerative process, in agreement with previously published results[22], implying that cell hypertrophy is not a major contributor to liver mass reconstitution after PH.

The reason(s) for the discrepancies between our present data and those of Miyaoka *et al*[8] are not apparent at this point. One likely possibility is that there might exist species-specificities in the overall strategies set in motion to respond to liver tissue loss in mice as compared to rats. It is well known that the kinetics of response to PH are substantially different between the two species[3], and such peculiarities appear to be cell autonomous, as if they are part of the overall genetic program of each species[23]. By analogy, a similar concept might also extend to the threshold level of tissue loss involved in activation of hypertrophy as opposed to hyperplasia as compensatory mechanisms for functional tissue mass restoration. More investigations are required to address this fundamental issue in rats and mice and, possibly, in humans.

In conclusion, we present evidence to indicate that restoration of rat liver mass following PH is attained largely via a hyperplastic response of the residual tissue. However, such response does not involve the totality of the residual hepatocyte population.

ACKNOWLEDGMENTS

We thank Mrs. Anna Saba and Mr. Roberto Marras for their technical contribution.

COMMENTS

Background

The ability of the liver to regenerate is remarkable on both clinical and biological grounds. Basic mechanisms underlying this process have been intensively investigated. However, it is still debated to what extent hypertrophy and hyperplasia contribute to liver mass restoration after major tissue loss. We addressed this issue using a genetically tagged system.

Research frontiers

Liver regenerative capacity declines with aging and its preservation is one of aims of current research.

Innovations and breakthroughs

A better understanding of such fundamental physiological response of the liver is important to devise better therapeutic strategies (*e.g.,* through cell therapy of liver diseases).

Applications

The techniques described in this study can be applied to the field of regenerative medicine.

Peer-review

In this paper, the authors described the mechanism of hepatocyte regenerate the liver after acute liver injury model using partial hepatectomy as model. The authors clearly described hepatocytes undergo hypertrophy and hyperplasia after liver injury, with the occurrence of hypertrophy only observed within the first 24 h, and hepatocyte hyperplasia is mainly responsible for the remaining liver regeneration event. The authors use transplantation studies in rats as an alternative method to investigate the mechanism of hepatocyte regenerates the liver after acute liver injury.

REFERENCES

1 **Huang J**, Rudnick DA. Elucidating the metabolic regulation of liver regeneration. *Am J Pathol* 2014; **184**: 309-321 [PMID: 24139945 DOI: 10.1016/j.ajpath.2013.04.034]
2 **Fausto N**, Campbell JS, Riehle KJ. Liver regeneration. *Hepatology* 2006; **43**: S45-S53 [PMID: 16447274 DOI: 10.1002/hep.20969]
3 **Michalopoulos GK**. Liver regeneration. *J Cell Physiol* 2007; **213**: 286-300 [PMID: 17559071 DOI: 10.1002/jcp.21172]
4 **Michalopoulos GK**. Liver regeneration after partial hepatectomy: critical analysis of mechanistic dilemmas. *Am J Pathol* 2010; **176**: 2-13 [PMID: 20019184 DOI: 10.2353/ajpath.2010.090675]
5 **Bucher NL**, Swaffield MN. The rate of incorporation of labeled thymidine into the deoxyribonucleic acid of regenerating rat liver in relation to the amount of liver excised. *Cancer Res* 1964; **24**: 1611-1625 [PMID: 14234005]
6 **Fabrikant JI**. The kinetics of cellular proliferation in regenerating liver. *J Cell Biol* 1968; **36**: 551-565 [PMID: 5645547]
7 **Grisham JW**. A morphologic study of deoxyribonucleic acid synthesis and cell proliferation in regenerating rat liver; autoradiography with thymidine-H3. *Cancer Res* 1962; **22**: 842-849 [PMID: 13902009]
8 **Miyaoka Y**, Ebato K, Kato H, Arakawa S, Shimizu S, Miyajima A. Hypertrophy and unconventional cell division of hepatocytes underlie liver regeneration. *Curr Biol* 2012; **22**: 1166-1175 [PMID: 22658593 DOI: 10.1016/j.cub.2012.05.016]
9 **Serra MP**, Marongiu F, Marongiu M, Contini A, Laconi E. Cell-autonomous decrease in proliferative competitiveness of the aged hepatocyte. *J Hepatol* 2015; **62**: 1341-1348 [PMID: 25617502 DOI: 10.1016/j.jhep.2015.01.015]
10 **Berry MN**, Friend DS. High-yield preparation of isolated rat liver parenchymal cells: a biochemical and fine structural study. *J Cell Biol* 1969; **43**: 506-520 [PMID: 4900611]
11 **Seglen PO**. Preparation of isolated rat liver cells. *Methods Cell Biol* 1976; **13**: 29-83 [PMID: 177845]
12 **Laconi S**, Curreli F, Diana S, Pasciu D, De Filippo G, Sarma DS, Pani P, Laconi E. Liver regeneration in response to partial hepatectomy in rats treated with retrorsine: a kinetic study. *J Hepatol* 1999; **31**: 1069-1074 [PMID: 10604581]
13 **Gerlyng P**, Abyholm A, Grotmol T, Erikstein B, Huitfeldt HS, Stokke T, Seglen PO. Binucleation and polyploidization patterns in developmental and regenerative rat liver growth. *Cell Prolif* 1993; **26**: 557-565 [PMID: 9116122]
14 **Tiniakos DG**, Kandilis A, Geller SA. Tityus: a forgotten myth of liver regeneration. *J Hepatol* 2010; **53**: 357-361 [PMID: 20472318 DOI: 10.1016/j.jhep.2010.02.032]
15 **Higgins G**, Anderson GM. Experimental pathology of the liver. Restoration of the liver of the white rat following partial surgical removal. *Arch Pathol* 1931; **12**: 186-202
16 **Bucher NL**. Regeneration of mammalian liver. *Int Rev Cytol* 1963; **15**: 245-300 [PMID: 14283580]
17 **Rabes HM**, Iseler G, Czichos S, Tuczek HV. Synchronization of hepatocellular DNA synthesis in regenerating rat liver by continuous infusion of hydroxyurea. *Cancer Res* 1977; **37**: 1105-1111 [PMID: 844040]
18 **Bucher NL**. Experimental aspects of hepatic regeneration. *N Engl J Med* 1967; **277**: 738-746 concl [PMID: 5342856 DOI: 10.1056/NEJM196710052771405]
19 **Wu Y**, Guo F, Liu J, Xiao X, Huang L, He D. Triple labeling with three thymidine analogs reveals a well-orchestrated regulation of hepatocyte proliferation during liver regeneration. *Hepatol Res* 2011; **41**: 1230-1239 [PMID: 21917088 DOI: 10.1111/j.1872-034X.2011.00876.x]
20 **Fausto N**, Campbell JS, Riehle KJ. Liver regeneration. *J Hepatol* 2012; **57**: 692-694 [PMID: 22613006 DOI: 10.1016/j.jhep.2012.04.016]
21 **Tamori Y**, Deng WM. Compensatory cellular hypertrophy: the other strategy for tissue homeostasis. *Trends Cell Biol* 2014; **24**: 230-237 [PMID: 24239163 DOI: 10.1016/j.tcb.2013.10.005]
22 **Papp V**, Dezsö K, László V, Nagy P, Paku S. Architectural changes during regenerative and ontogenic liver growth in the rat. *Liver Transpl* 2009; **15**: 177-183 [PMID: 19177433 DOI: 10.1002/lt.21665]
23 **Weglarz TC**, Sandgren EP. Timing of hepatocyte entry into DNA synthesis after partial hepatectomy is cell autonomous. *Proc Natl Acad Sci USA* 2000; **97**: 12595-12600 [PMID: 11050176 DOI: 10.1073/pnas.220430497]

P- Reviewer: Lu WY **S- Editor**: Ma YJ **L- Editor**: A
E- Editor: Wang CH

World Journal of Gastroenterology

Submit a Manuscript: http://www.wjgnet.com/esps/

World J Gastroenterol 2017 March 14; 23(10): 1771-1779

DOI: 10.3748/wjg.v23.i10.1771

ISSN 1007-9327 (print) ISSN 2219-2840 (online)

ORIGINAL ARTICLE

Basic Study

Catheterization of the gallbladder: A novel mouse model of severe acute cholangitis

Jian-Hua Yu, Hai-Jun Tang, Wei-Guang Zhang, Zhi-Yang Zhu, Xin-Xian Ruan, Bao-Chun Lu

Jian-Hua Yu, Hai-Jun Tang, Zhi-Yang Zhu, Xin-Xian Ruan, Bao-Chun Lu, Department of Hepatobiliary Surgery, Shaoxing People's Hospital, Shaoxing Hospital of Zhejiang University, Shaoxing 312000, Zhejiang Province, China

Wei-Guang Zhang, Department of Molecular Medicine and Clinical Laboratory, Shaoxing Second Hospital, Shaoxing 312000, Zhejiang Province, China

Author contributions: Yu JH and Lu BC designed this study; Yu JH and Zhu ZY performed experiments of molecular biology; Zhang WG performed data analysis for this study; Tang HJ and Ruan XX performed animal study; Yu JH and Lu BC wrote this manuscript.

Supported by Zhejiang Provincial Natural Science Foundation of China under grant No. LY17H030001 and No. LQ14H160001; Zhejiang Provincial Public Welfare Technology Application Research Projects under grant No. 2015C33293, No. 2013C33214 and No. 2011C33023; and Research Foundation of Health Bureau of Zhejiang Province under grant No. 2014RCA031 and No. 2016KYB300.

Institutional review board statement: All blood samples from the patients were taken after informed consent and ethical permission was obtained for participation in the study. The institutional review board statement has been provided.

Institutional animal care and use committee statement: All procedures involving animals were reviewed and approved by the Institutional Animal Care and Use Committee of the Zhejiang University.

Conflict-of-interest statement: The authors declare that there are no other conflicts of interest.

Data sharing statement: Technical appendix, statistical code, and dataset available from the corresponding author at sygd_lbc@126.com. No additional data are available.

Manuscript source: Unsolicited manuscript

Correspondence to: Dr. Bao-Chun Lu, Department of Hepatobiliary Surgery, Shaoxing People's Hospital, Shaoxing Hospital of Zhejiang University, 568 North Zhongxing Road, Shaoxing 312000, Zhejiang Province, China. sygd_lbc@126.com
Telephone: +86-575-88229383

Received: November 22, 2016
Peer-review started: November 23, 2016
First decision: February 19, 2016
Revised: January 22, 2017
Accepted: February 7, 2017
Article in press: February 8, 2017
Published online: March 14, 2017

Abstract

AIM

To establish a severe acute cholangitis (SAC) model in mice.

METHODS

Cholecystic catheterization was performed under the condition of bile duct ligation (BDL). Trans-cholecystic injection of lipopolysaccharide (LPS) was defined as the SAC animal model. Sham operation group, intraperitoneal injection of LPS without BDL group, intraperitoneal injection of LPS with BDL group and trans-cholecystic injection of normal saline with BDL group were defined as control groups. The survival rates and tissue injuries in liver, lungs and kidney were evaluated.

RESULTS
Mice in the SAC group showed a time-dependent mortality and much more severe tissue injuries in liver, lungs and kidney, compared with other groups. However, relieving biliary obstruction could effectively reduce mortality and attenuate liver injury in the SAC mouse model.

CONCLUSION
Trans-cholecystic injection of LPS under the condition of biliary obstruction could establish a repeatable and reversible mouse model of SAC.

Key words: Severe acute cholangitis; Mouse model; Cholecystic catheterization; Lipopolysaccharide; Bile duct ligation

Core tip: Severe acute cholangitis (SAC) is a severe biliary tract infection. Although mice are the most common experimental animal and have a similar anatomical construction of bile ducts to humans, there is still no valid study on establishing a SAC model in mice. To study SAC more easily and exactly, we established a repeatable and reversible mouse model of SAC through cholecystic catheterization under the condition of bile duct ligation.

Yu JH, Tang HJ, Zhang WG, Zhu ZY, Ruan XX, Lu BC. Catheterization of the gallbladder: A novel mouse model of severe acute cholangitis. *World J Gastroenterol* 2017; 23(10): 1771-1779 Available from: URL: http://www.wjgnet.com/1007-9327/full/v23/i10/1771.htm DOI: http://dx.doi.org/10.3748/wjg.v23.i10.1771

INTRODUCTION

Severe acute cholangitis (SAC) is a severe biliary tract infection with rapid progressing and a high mortality rate. Septicemia, septic shock and multiple-organ failure are always induced by this severe disease and result in a poor prognosis. For SAC, complete biliary obstruction is the initiation factor, and secondary infection from Gram-negative pathogen is the aggravating destroyer[1]. Pro-inflammatory cytokines, such as interleukin 1 beta (IL-1β), interleukin-6 (IL-6) and tumor necrosis factor-α (TNF-α), have been reported to have a close relationship with the process of the severe infectious diseases[2-4]. According to Tokyo guidelines 2013, associating with one or more other organs dysfunction is regarded as the diagnostic criteria to distinguish SAC from mild or moderate acute cholangitis[5,6]. Explosive inflammatory and subsequent multiple organ dysfunction syndrome (MODS) are important causes of poor prognosis.

To study the pathological process of SAC more accurately, a typical, stable, repeatable animal model is required. A few animal models of acute cholangitis have been established in species such as rats and rabbits[3,7,8]. However, mice are the most common experimental animal, and there is still no valid study on establishing an acute cholangitis model in mice. In the current study, we established a repeatable model of SAC in mice, based on common bile duct ligation and an indwelling catheter through cholecystostomy, with the aim to better understand the process of SAC.

MATERIALS AND METHODS

Animal

Male C57Bl/6 mice weighing 20 to 25 g were purchased from the Zhejiang Province Experimental Animal Center. All procedures were approved by the Ethics Committee of Zhejiang University and conformed to the Care and Use of Laboratory Animals Guide published by the US National Institutes of Health (NIH Publication No. 85-23, revised 1996). All surgery was performed under ether anesthesia, and all efforts were made to minimize suffering.

Surgery procedures

Mice were randomly assigned to the following five groups: sham (sham), lipopolysaccharide (LPS), bile duct ligation plus LPS (BDL + LPS), bile duct ligation plus cholecystic catheterization (BDL + CC), and severe acute cholangitis (SAC). Surgeries were performed under ether anesthesia. In the BDL + CC and SAC groups, common bile ducts were dissociated and ligated with 6-0 silk. Three days later, the gallbladders were greatly enlarged and mice received cholecystostomy in the BDL + CC and SAC groups (Figure 1B). Epidural catheters (format F3, diameter = 0.9 mm) were used as gallbladder drainage tubes and were outstretched from the skin. 6-0 silk was used to suture the incision of gallbladders and fix the epidural catheters. The distal ends of epidural catheters traveled through subcutaneous tissue and were finally fixed at the back of mice. The abdominal cavity was closed and the epidural catheters remained closed after cholecystostomy. Five days after cholecystic catheterization, 0.5 μg of LPS (from *E. coli* O111: B4, Sigma, St Louis, MO, United States) dissolved in 0.1 mL of normal saline (NS) was injected to the gallbladder through the epidural catheter in the SAC groups. An equivalent amount of NS was injected to the gallbladder through the epidural catheter in the BDL + CC groups. Before the catheter was sealed with a sealing cap, 0.1 mL air was injected and then the abdominal cavity was closed with silk sutures. In the BDL + LPS group, common bile ducts were ligated with 6-0 silk. At 72 h after bile duct ligation, another laparotomy, but no further operation, was performed. Eight days after the first operation, mice were

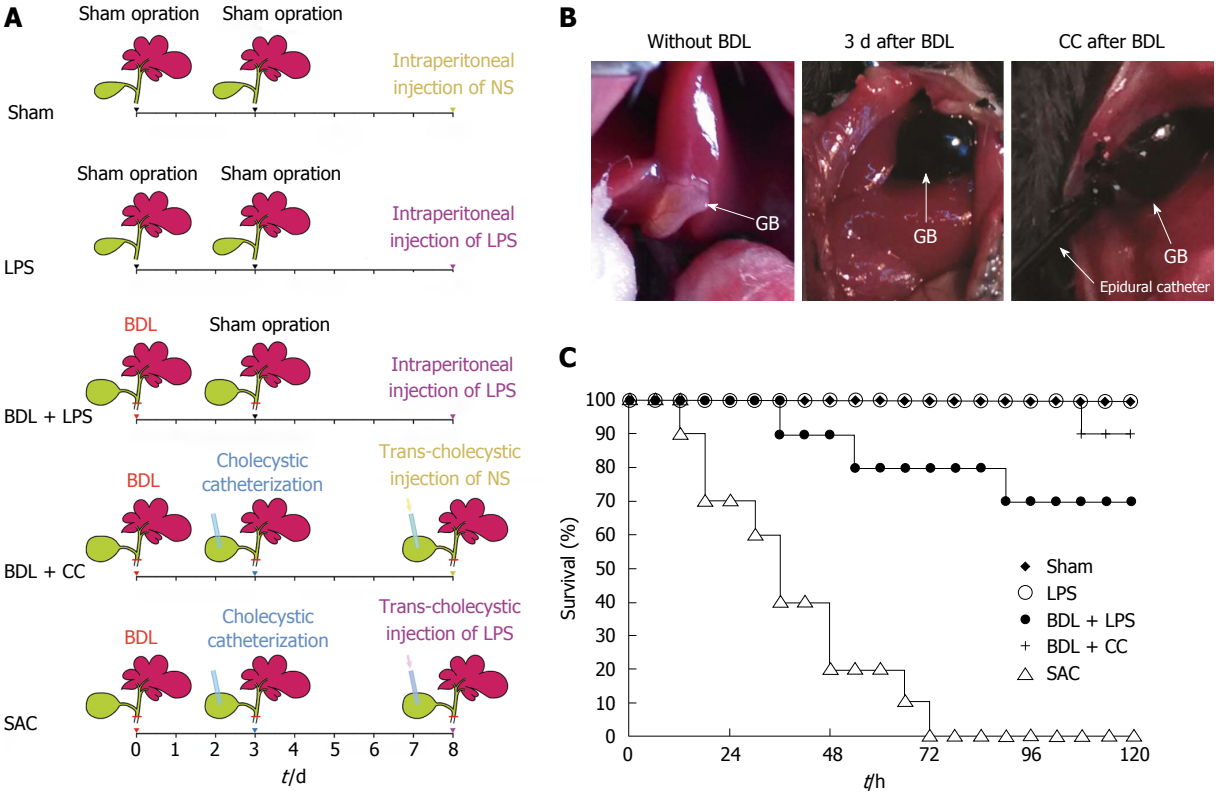

Figure 1 Cholecystostomy. A: Schematic description of experimental groups; B: Cholecystic catheterization under the condition of bile duct ligation; C: The survival rates of mice in five groups after intraperitoneal injection or trans-cholecystic injection (n = 10). BDL: Bile duct ligation; CC: Cholecystic catheterization; NS: Normal saline.

administrated with 0.5 μg of LPS intraperitoneally. In the LPS and sham groups, two sham laparotomies were performed at the same time points as described above. Eight days after the first operation, mice in the LPS and sham groups were intraperitoneally administrated with 0.5 μg of LPS or 0.1 mL of NS, respectively.

Ten mice in each group were used to observe the mortality rate after the last operation. The other animals were sacrificed at the 24 h and 48 h after the last injection. Blood collected from the inferior vena cava and the serum was stored at -80 ℃ before analysis. Bile samples in the BDL + CC and SAC groups were obtained through catheterization of the gallbladder. The tissue samples were snap-frozen in liquid nitrogen and then stored at -80 ℃.

Relief of biliary obstruction experiments

The mice in the SAC group were used for these experiments. At 6 h or 12 h after LPS injection through cholecystic catheterization, the sealing caps of catheters were removed and bile was allowed to outflow from catheters. The mortality rate was analyzed at 24 h and 48 h after LPS injection. Mice that survived were sacrificed at 48 h after LPS injection and serum samples were used to evaluate liver injury.

Laboratory data examination

Serum levels of aspartate aminotransferase (AST), alanine aminotransferase (ALT), total bilirubin (TBIL), blood urea nitrogen (BUN), and serum creatinine (SC) were quantitated by an Automated Chemical Analyzer (Abbott, Chicago, IL, United States). Alkaline phosphatase (ALP) and γ-gltamyltranspeptidase (γ-GGT) using kits (Jiancheng Bioengineering Institute, Nanjing, China) following the manufacturer's instruction.

RNA extraction and quantitative real-time polymerase chain reaction

Total RNA was isolated from tissues using TRIzol (Invitrogen Life Technologies, Carlsbad, CA, United States) and reverse transcribed into complementary DNA using the High-Capacity complementary DNA Reverse Transcription Kit (Applied Biosystems, Foster City, CA, United States), according to themanufacturer's instructions. Quantitative real-time polymerase chain reaction (PCR) was performed using SYBR Green PCRMasterMix and the ABI 7500 Real-time PCR system (Applied Biosystems). Specific primers were designed, respectively, for IL-1β, IL-6 and TNF-α (Table 1). Mouse β-actin was used as an endogenous control. PCR was performed according to the manufacturer's instructions. All assays were performed three times. Relative expression levels were then determined using the $2^{-\Delta\Delta Ct}$ method[9].

Caspase 3 activity detection

Caspase 3 activity in cells proteins was detected by

Table 1 Primer sequences

Name	Symbol	Forward (5'-3')	Reverse (5'-3')
β-actin	ACTB	CCACCATGTACCCAGGCATT	AGGGTGTAAAACGCAGCTCA
IL-6	IL6	TACCACTTCACAAGTCGGAGGC	CTGCAAGTGCATCATCGTTGTTC
TNF-α	TNF	GGTGCCTATGTCTCAGCCTCTT	GCCATAGAACTGATGAGAGGGAG
IL-1β	IL-1β	TGGACCTTCCAGGATGAGGACA	GTTCATCTCGGAGCCTGTAGTG

the Caspase 3 Activity Assay Kit (Beyotime, Nanjing, China), according to the manufacturer's protocol. The absorbance was measured at 405 nm, and the relative activity of Caspase 3 was determined.

Western blot analysis

Primary antibodies, for B-cell CLL/lymphoma 2 (Bcl2), BCL2-associated X protein (Bax) and β-actin, were purchased from Santa Cruz Biotechnology (Santa Cruz, CA, United States). On a 10% SDS-PAGE (sodium dodecyl sulfate-poly-acrylamide gel) gel, 20 mg of total protein was electrophoresed, transferred onto to a polyvinylidene fluoride membranes, blocked, and incubated with primary antibody and then with horseradish peroxidase-conjugated secondary antibody. Immunoreactive bands were visualized using a chemiluminescence solution. β-actin was used as an endogenous control.

Tissue staining

The formalin-fixed specimens were obtained from the mice which were sacrificed at the 48 h after the last injection. For histological evaluation, formalin-fixed specimens were stained with HE. Liver, lung and kidney tissues were examined for histopathological evidence of pathological damage.

Clinical samples

Serum and bile samples were obtained from 18 male patients at the Shaoxing People's Hospital from January 2014 to January 2016. Informed consent was obtained from patients and the tissue acquisition protocol was approved by the Shaoxing People' s Hospital Institutional Review Board. Among the patients, 6 patients in gallstone group suffered from gallstone and received cholecystectomy. Six patients in SAC group were diagnosed as SAC definitely, according to Tokyo guidelines 2013[6], with a condition characterized by fever, abdominal pain and jaundice (Charcot triad)[10]. Six patients in biliary obstruction group suffered from biliary obstructive disease (such as pancreaticobiliary tumour), with imaging findings of biliary dilation and elevated bilirubin, while without infection (such as fever or increase in leucocytes). Blood samples were obtained before surgery and bile samples were obtained during surgery.

Enzyme-linked immunosorbent assay

IL-1β, IL-6 and TNF-α in serum and bile samples were measured by ELISA kit (eBioscience&Bender, San Diego, CA, United States) according to the manufacturer's instructions. Each sample was tested in triplicate.

Immunohistochemistry staining

PCNA expression was detected immunohistochemistry (IHC) staining using paraffin-embedded specimens from different groups. After deparaffinization and rehydration of the sections, endogenous peroxidase activity was blocked using 0.3% hydrogen peroxide. The sections were incubated with primary anti-PCNA antibody (Santa Cruz) overnight at 4 ℃, followed by incubation with appropriate horseradish peroxidase-conjugated secondary antibody for 1.5 h. After a thorough washing, the sections were developed in 3,3'-diaminobenzidine and counterstained with hematoxylin. Each stained sample was observed under high power magnification (× 200).

Statistical analysis

Data were presented as means standard deviation. Statistical significance between two groups was determined using the Student *t*-test. One-way analysis of variance followed by the TukeyeKramer adjustment was used to examine differences among multiple groups. $P < 0.05$ was considered to be significant. All statistical analyses were conducted using SPSS 11.0.

RESULTS

Trans-cholecystic injection of LPS under the condition of biliary obstruction induces time-dependent mortality

The mortality rate of the mice in the SAC group was 80% (8/10 animals) at the point of 48 h and all mice died within 72 h after LPS injection (Figure 1C). Mice in the BDL + CC and BDL + LPS groups showed 90% and 70% survival, respectively, at 5 d after the last operation (Figure 1C). However, none of mice in the sham group or LPS group died during the same period (Figure 1C).

Trans-cholecystic injection of LPS under the condition of biliary obstruction induces progressive liver injury

Serum ALT, AST and TBIL levels were assessed to evaluate liver injury. Intraperitoneal injection with LPS induced a moderate rise in ALT and AST levels, but did not affect TBIL levels, compared with the sham group (Table 2). ALT, AST and TBIL levels in the BDL + LPS, BDL + CC and SAC groups were significantly higher because of bile duct ligation, compared with the sham group (Table 2). Interestingly, ALT, AST and TBIL levels

Table 2 Data of laboratory examination at 24 h after the last operation (n = 6)

	Sham	LPS	BDL + LPS	BDL + CC	SAC
TBIL (mg/dL)	0.81 ± 0.15	1.26 ± 0.72	14.21 ± 2.10^{a,c}	13.35 ± 1.71^{a,c}	17.68 ± 2.66^{a,c,e,f}
ALT (IU/L)	18.63 ± 1.46	106.4 ± 20.24^{a}	206.62 ± 25.92^{a,c}	197.48 ± 30.85^{a,c}	403.07 ± 74.92^{a,c,e,f}
AST (IU/L)	126.12 ± 34.39	558.97 ± 111.35^{a}	1693.17 ± 313.73^{a,c}	1462.85 ± 397.75^{a,c}	2332.32 ± 531.64^{a,c,e,f}
γ-GGT (U/L)	11.17 ± 2.27	24.67 ± 4.96^{a}	69.33 ± 9.74^{a,c}	70.00 ± 7.24^{a,c}	83.17 ± 9.08^{a,c,e,f}
ALP (U/L)	114.33 ± 19.68	229.67 ± 27.51^{a}	2765.33 ± 250.51^{a,c}	2544.17 ± 350.24^{a,c}	3470.83 ± 522.35^{a,c,e,f}
Creatinine (mg/dL)	0.27 ± 0.04	0.35 ± 0.07	0.32 ± 0.08	0.31 ± 0.08	0.45 ± 0.09^{a,e,f}
BUN (mg/dL)	20.18 ± 5.43	25.77 ± 4.52	26.82 ± 7.80	25.17 ± 5.04	42.78 ± 9.76^{a,c,e,f}

Values are expressed as mean ± SD. $^{a}P < 0.05$ *vs* sham group, $^{c}P < 0.05$ *vs* LPS group, $^{e}P < 0.05$ *vs* BDL + LPS group, $^{f}P < 0.05$ *vs* BDL + CC group.

in the SAC group were much higher compared with those in the BDL + LPS and BDL + CC groups (Table 2). However, although the data of BDL + LPS group were slightly higher than those of BDL + CC group, the differences were not significant. ALP and γ-GGT levels are regarded as important liver tests during acute cholangitis[10]. Our results also showed that ALP and γ-GGT levels in the SAC groups were significantly higher than those in the other groups (Table 2).

IL-1β, IL-6 and TNF-α are important pro-inflammatory cytokines in the process of liver injury and inflammation[4,11-14]. To evaluate the levels of inflammation and liver injury, the pro-inflammatory mediators' level in serum and liver tissues were examined. The results showed that biliary obstruction was an important inducement to increase the mRNA expression of IL-6 and TNF-α (Figure 2A). However, SAC group showed a further increasing and much higher IL-6 and TNF-α mRNA expression after exposed to LPS, compared with that of BDL + LPS and BDL + CC groups (Figure 2A). IL-1β mRNA expression in SAC group also showed a significant increase, compared with that of LPS and BDL + CC groups (Figure 2A). The serum levels of IL-1β, IL-6 and TNF-α were also significantly increased in the SAC group, compared with those of other groups (Figure 2B). And not only that, SAC group also showed a higher level of pro-inflammatory cytokines in bile, compared with BDL + CC groups (Figure 2C). These results indicated that the inflammatory response was further activated because of LPS injection into the biliary system.

Caspase 3, Bcl2 and Bax are common molecular hallmarks of apoptosis[15,16]. The activity of caspase 3 and the ratio of Bax to Bcl2 are often used to evaluate tissue apoptosis. Detection of caspase 3 activity and the ratio of Bax to Bcl2 showed that both intraperitoneal injection of LPS and biliary obstruction induced moderate apoptosis of hepatocytes (Figure 2D and H). Caspase 3 activity and the ratio of Bax to Bcl2 in the SAC group were prominently higher than those in the other groups (Figure 2D and H). This finding indicated that injection of LPS through cholecystic catheterization induced more serious apoptosis in the liver.

Morphology was examined to further evaluate the degree of injury in mouse liver tissues. Pathological examination showed that intraperitoneal injection of LPS induced considerable vacuolar degenerative changes (Figure 2F). In the BDL + CC group, biliary obstruction caused an obvious dilatation of bile capillaries and local necrosis (Figure 2F). In the BDL + LPS group, dilatation of bile capillaries, vacuolar degenerative changes and inflammatory cell infiltration could be found (Figure 2F). Notably, the liver in the SAC group showed obvious vacuolar changes, more inflammatory cell infiltration, and more broad areas of necrosis, compared with the BDL + LPS and BDL + CC groups (Figure 2F).

Proliferating cell nuclear antigen (PCNA) is common molecular biological hallmarks of regeneration[17]. We detected the expression of PCNA in specimens from different groups using immunohistochemistry. Compared with SAC groups, there were more PCNA-positive cells in BDL + LPS and BDL + CC groups (Figure 2F). It indicated that injection of LPS through cholecystic catheterization significantly suppressed the reparative live regeneration induced by biliary obstruction.

Trans-cholecystic injection of LPS under the condition of biliary obstruction induces obvious renal injury and acute lung injury

We also examined BUN and serum creatinine to evaluate renal injury. BUN and creatinine levels were significantly elevated in the SAC group after injection of LPS through catheters, compared with the other four groups (Table 2). Conversely, in the other treatment groups, including the LPS, BDL + LPS, and BDL + CC groups, BUN and creatinine levels tended to be evaluated after exposure to LPS or ligation of the bile duct, but the differences were not significant (Table 2). On HE-stained sections, the kidney in the SAC group showed glomerular and tubular injury with obvious tubular vacuolization (Figure 2F). However, none of the other groups showed these pathological changes.

We also investigated pathological changes in the lungs in the different groups. As shown in Figure 2F, lung tissue in the SAC group displayed obvious inflammatory cells exudation and fibroblasts proliferation in the pulmonary interstitium and alveolar spaces (Figure 2F). Although LPS was administrated at

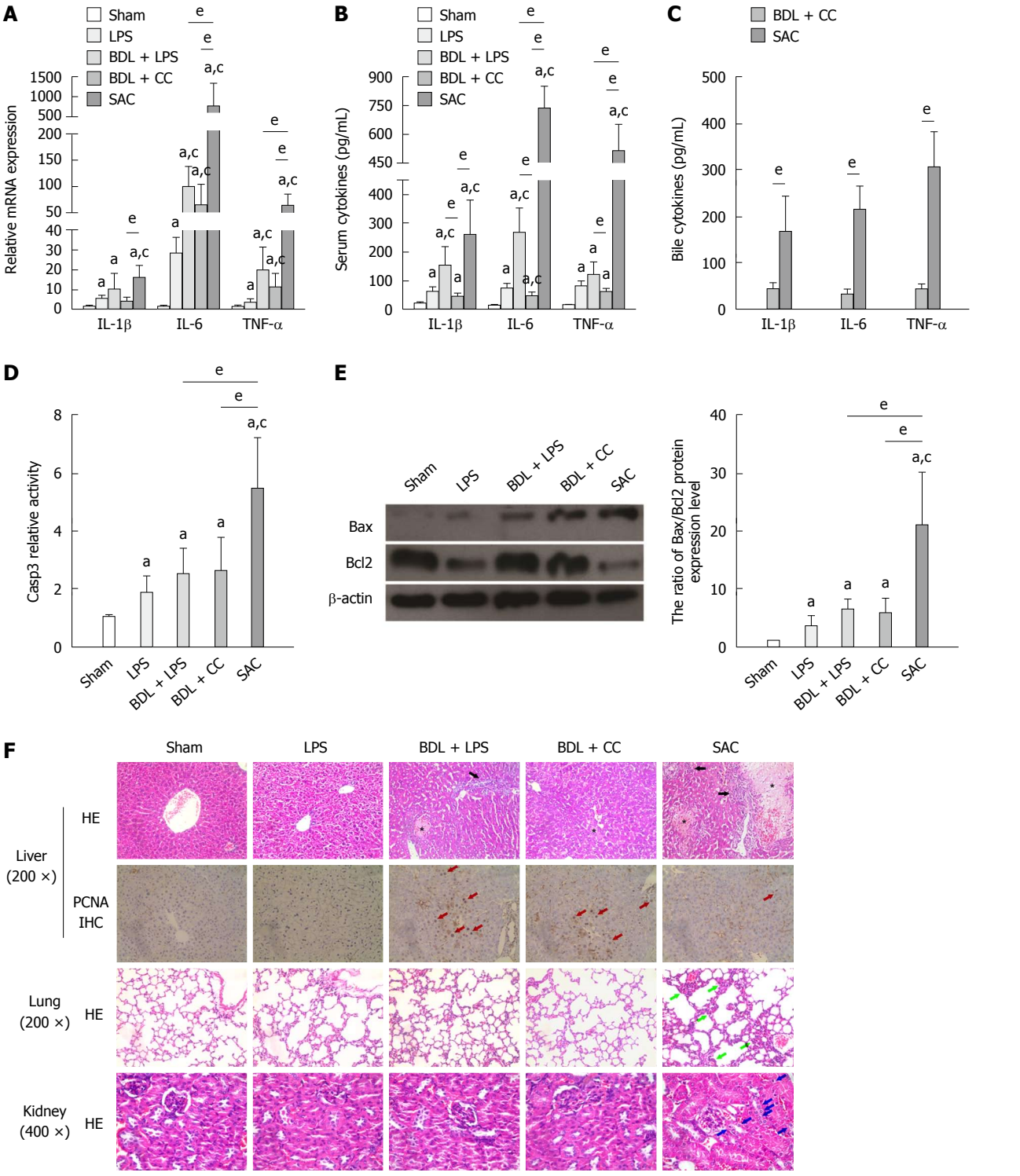

Figure 2 Liver injury is significantly facilitated in severe acute cholangitis mouse model. A: Relative expression levels of IL-1β, IL-6 and TNF-α in liver tissues were examined by real-time PCR at 24 h after the last operation (n = 6); B and C: Determination of pro-inflammatory cytokines in serum and bile of mice by ELISA at 48 h after the last operation (n = 6); D and E: The activity of Caspase 3 and the ratio of Bax to Bcl2 protein expression level were examined in different groups (n = 6); F: Histological examination of liver tissues (HE staining × 200, PCNA-IHC staining × 200), lung tissues (HE staining × 200) and kidney tissues (HE staining × 400) in different groups. Asterisk: necrosis. Black arrow: Inflammatory cell infiltration in liver tissue. Red arrow: PCNA-positive hepatocytes. Green arrow: abundant inflammatory cell infiltration in lung tissue. Blue arrow: The cells with vacuolization in kidney. $^{a}P < 0.05$ *vs* sham group; $^{c}P < 0.05$ *vs* LPS group; $^{e}P < 0.05$, difference between the two groups.

the same dose in the LPS and BDL + LPS groups, the pathological changes in the lungs in these groups were not as obvious as those in the SAC group.

Relieving biliary obstruction could reduce mortality and attenuate liver injury in the SAC mouse model

As shown in Figure 3A, relief of biliary obstruction at 6

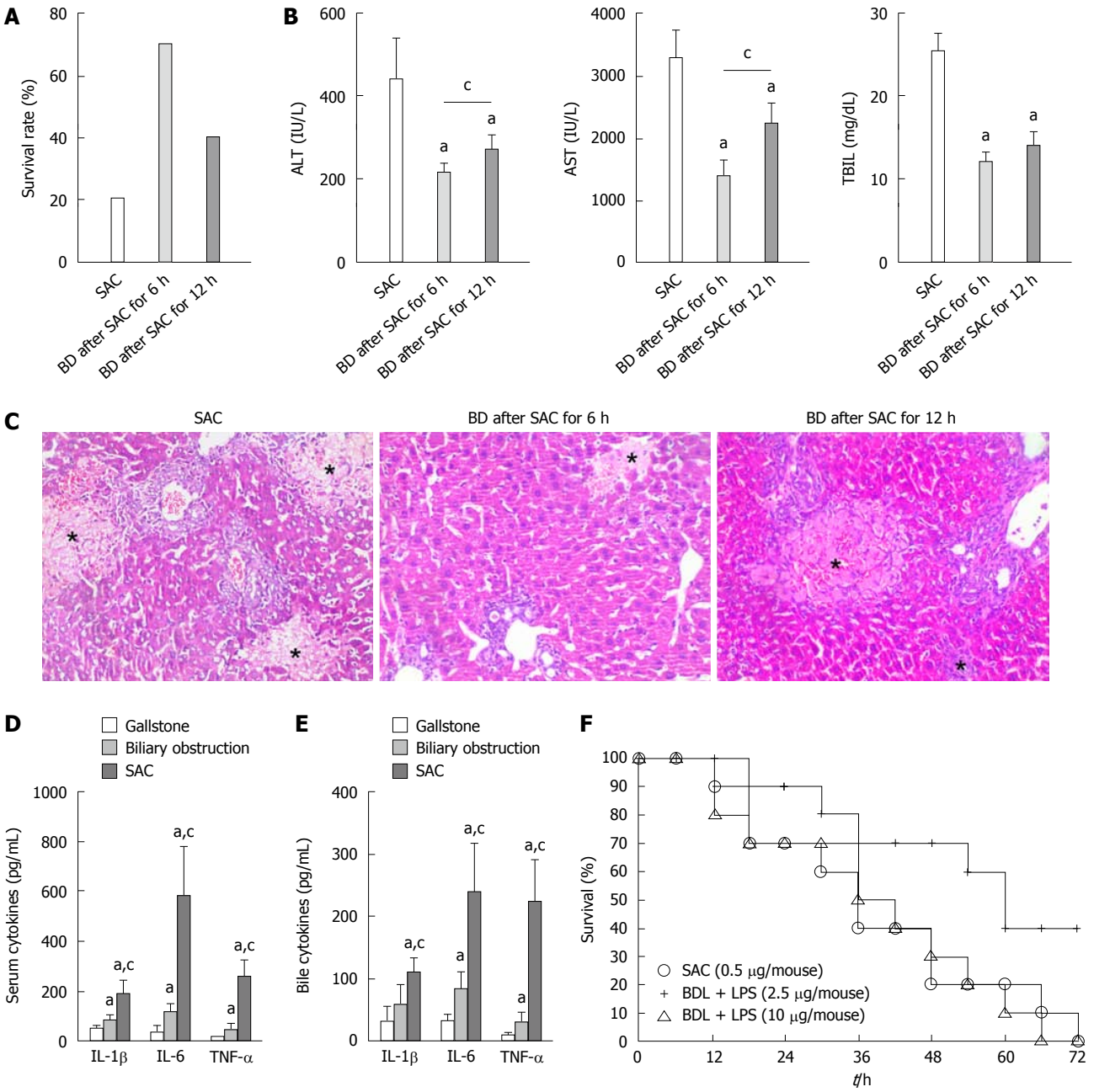

Figure 3 Relieving biliary obstruction reduces mortality and attenuates liver injury in the severe acute cholangitis mouse model. A: The survival rates of SAC mice with or without biliary drainage were determined at 48 h after model establishment (n = 10); B: ALT, AST, and TBIL of SAC mice with or without biliary drainage were examined at 48 h after model establishment (n = 6). $^{a}P < 0.05$ *vs* SAC group; $^{c}P < 0.05$, difference between the two groups; C: Histological analysis of liver tissues in mice after different treatments (HE × 200), asterisk: necrosis; D and E: Determination of pro-inflammatory cytokines in serum and bile of patients with or without SAC (n = 6). $^{a}P < 0.05$ *vs* gallstone group; $^{c}P < 0.05$ *vs* biliary obstruction group; F: The survival rates of mice which were intraperitoneally injected with high-dose of LPS under the condition of biliary obstruction. BD: Biliary drainage.

or 12 h after LPS injection resulted in a higher survival at 48 h after LPS injection compared with the non-decompressing SAC group. Examination of injury to the liver showed that ALT, AST, and TBIL levels were significantly decreased because of relieving biliary obstruction (Figure 3B). At the same time, histological analysis also indicated that biliary drainage could mitigate SAC-induced liver injury (Figure 3C).

DISCUSSION

SAC is a bacterial infection in the setting of complete biliary obstruction and leads to serious systemic signs of infection. To study this disease, the animal model of SAC has been established in rodents, such as rats[8,18,19]. As the most commonly used experimental animal[20], the anatomical construction of bile ducts in mice is more similar to that in humans because rats do not have a gallbladder. The gallbladder slows down the tremendous increase in biliary pressure at the beginning of biliary obstruction. However, a high-tension and exceedingly full gallbladder will aggravate biliary pressure at the middle and later periods of biliary obstruction[21]. Therefore, mice are a more

appropriate species to establish an animal model of SAC compared with rats. Nevertheless, the common bile duct of mice is too slim to complete successful injection. We performed cholecystic catheterization 3 d after ligation of the bile duct. At that time, the gallbladder was engorged and flexible enough to catheterize (Figure 1B). It's worth noting that subsequent infection always arises after a period of cholestasis in the SAC patients[1,5]. Our model also simulated this process exactly. Catheterization of the gallbladder is the other core operation for our model. Benefited from it, in the SAC and BDL + CC groups, bile sample could be got through catheters conveniently. More importantly, biliary drainage is the main therapeutic method for SAC[1,10,22]. Catheterization of the gallbladder provided a convenient method to relieve biliary obstruction. Our study also showed that timely relief of biliary obstruction reduced mortality and alleviated liver injury effectively. The mouse model shows a clear advantage to simulate the rehabilitation process of SAC.

To validate the reliability of model, more examinations were performed. Exploding ALT, AST, TBIL, ALP, γ-GGT and death detection indicated serious liver injury arose. Increasing pro-inflammatory cytokines indicated obvious inflammatory response arose. In clinical practice, SAC patients always have a higher level of pro-inflammatory cytokines in serum and bile, compared with the patients those suffered from chronic biliary obstruction or gallstone (Figure 3D and E). Our mouse model showed a similar change as SAC patients. According to the obvious pathologic change of histological examination and repressed liver regeneration, the liver injury of our animal model was consistent with the characteristics of SAC-induced liver injury[1,10].

In clinical practice, systemic inflammatory response syndrome (SIRS) and MODS would arise if patients with SAC did not obtain timely medical treatment[1,22,23]. In our study, time-dependent mortality and obvious injury of the liver, lungs and kidney were observed in the SAC group. These finding also indicated that our animal model displays a similar disease progression to SAC patients.

The barrier between blood and bile always is dysfunction because of biliary high-pressure. It is noteworthy that mice in the LPS, BDL + LPS and BDL + CC groups did not show severe tissue injuries in liver, lungs and kidney, compared with the SAC group. Injection of LPS into a high-pressure biliary system accelerated further breakdown of the bile-blood barrier and induced severe endotoxemia should be an adequate explanation. Compared with LPS and BDL groups, BDL + LPS group also had the two requirements of SAC (injection of LPS and biliary obstruction) in the same time. However, intraperitoneal injection with LPS (0.5 μg) under the condition of biliary obstruction did not induce organs injury as serious as trans-cholecystic injection with LPS (BDL + LPS group *vs* SAC group). We also found that if the dose of LPS was increased to 10 μg/mouse, the mortality rate in the BDL + LPS group (10 μg/mouse) reached a similar level to that in the SAC group (Figure 3F). The main reason for this finding may be that intraperitoneal endotoxin enters the bloodstream depending on absorption through the peritoneum. This manner is different from the special manner of endotoxin entering the bloodstream during SAC, and the absorbing ability of the peritoneum would be influenced by other factors, such as abnormal liver function. We also injected LPS (10 μg/mouse *i.p.*) to mice without any other operation. However, no mouse died within 72 h after LPS injection. It indicated that biliary obstruction for long enough is also an essential condition for SAC model and always leads to poor prognosis.

In summary, we established a repeatable and reversible mouse model of SAC through cholecystic catheterization. This animal model can be used to study disease progression and treatment of SAC.

COMMENTS

Background

Severe acute cholangitis (SAC) is a severe biliary tract infection. Although mice are the most common experimental animal, there is still no valid study on establishing a SAC model in mice.

Research frontiers

The animal model of SAC has been established in rodents, such as rats. However, the anatomical construction of bile ducts in mice is more similar to that in humans because rats do not have a gallbladder. To study SAC more easily and exactly, the authors established a repeatable and reversible mouse model of SAC.

Innovations and breakthroughs

This is the first study establishing a repeatable and reversible mouse model of SAC. To solve the technological difficulty that the common bile duct of mice is too slim to complete successful injection, the authors performed cholecystic catheterization 3 d after ligation of the bile duct. At that time, the gallbladder was engorged and flexible enough to catheterize.

Applications

The authors established a repeatable and reversible mouse model of SAC through cholecystic catheterization. This animal model can be used to study disease progression and treatment of SAC.

Terminology

SAC is a severe biliary tract infection with rapid progressing and a high mortality rate. According to Tokyo guidelines 2013, associating with one or more other organs dysfunction is regarded as the diagnostic criteria to distinguish SAC from mild or moderate acute cholangitis.

Peer-review

The authors developed a novel mouse model of severe acute cholangitis. It is very interesting.

REFERENCES

1 **Mosler P**. Diagnosis and management of acute cholangitis. *Curr Gastroenterol Rep* 2011; **13**: 166-172 [PMID: 21207254 DOI:

10.1007/s11894-010-0171-7]
2 **Guldiken N**, Kobazi Ensari G, Lahiri P, Couchy G, Preisinger C, Liedtke C, Zimmermann HW, Ziol M, Boor P, Zucman-Rossi J, Trautwein C, Strnad P. Keratin 23 is a stress-inducible marker of mouse and human ductular reaction in liver disease. *J Hepatol* 2016; **65**: 552-559 [PMID: 27151178]
3 **Watanabe K**, Yokoyama Y, Kokuryo T, Kawai K, Kitagawa T, Seki T, Nakagawa A, Nagino M. 15-deoxy-delta 12,14-prostaglandin J2 prevents inflammatory response and endothelial cell damage in rats with acute obstructive cholangitis. *Am J Physiol Gastrointest Liver Physiol* 2010; **298**: G410-G418 [PMID: 20056897 DOI: 10.1152/ajpgi.00233.2009]
4 **Plum W**, Tschaharganeh DF, Kroy DC, Corsten E, Erschfeld S, Dierssen U, Wasmuth H, Trautwein C, Streetz KL. Lack of glycoprotein 130/signal transducer and activator of transcription 3-mediated signaling in hepatocytes enhances chronic liver injury and fibrosis progression in a model of sclerosing cholangitis. *Am J Pathol* 2010; **176**: 2236-2246 [PMID: 20382701 DOI: 10.2353/ajpath.2010.090469]
5 **Kiriyama S**, Takada T, Strasberg SM, Solomkin JS, Mayumi T, Pitt HA, Gouma DJ, Garden OJ, Büchler MW, Yokoe M, Kimura Y, Tsuyuguchi T, Itoi T, Yoshida M, Miura F, Yamashita Y, Okamoto K, Gabata T, Hata J, Higuchi R, Windsor JA, Bornman PC, Fan ST, Singh H, de Santibanes E, Gomi H, Kusachi S, Murata A, Chen XP, Jagannath P, Lee S, Padbury R, Chen MF. New diagnostic criteria and severity assessment of acute cholangitis in revised Tokyo Guidelines. *J Hepatobiliary Pancreat Sci* 2012; **19**: 548-556 [PMID: 22825491 DOI: 10.1007/s00534-012-0537-3]
6 **Kiriyama S**, Takada T, Strasberg SM, Solomkin JS, Mayumi T, Pitt HA, Gouma DJ, Garden OJ, Büchler MW, Yokoe M, Kimura Y, Tsuyuguchi T, Itoi T, Yoshida M, Miura F, Yamashita Y, Okamoto K, Gabata T, Hata J, Higuchi R, Windsor JA, Bornman PC, Fan ST, Singh H, de Santibanes E, Gomi H, Kusachi S, Murata A, Chen XP, Jagannath P, Lee S, Padbury R, Chen MF, Dervenis C, Chan AC, Supe AN, Liau KH, Kim MH, Kim SW. TG13 guidelines for diagnosis and severity grading of acute cholangitis (with videos). *J Hepatobiliary Pancreat Sci* 2013; **20**: 24-34 [PMID: 23307001 DOI: 10.1007/s00534-012-0561-3]
7 **Higure A**, Okamoto K, Hirata K, Todoroki H, Nagafuchi Y, Takeda S, Katoh H, Itoh H, Ohsato K, Nakamura S. Macrophages and neutrophils infiltrating into the liver are responsible for tissue factor expression in a rabbit model of acute obstructive cholangitis. *Thromb Haemost* 1996; **75**: 791-795 [PMID: 8725725]
8 **Yang J**, Lu B. Establishment of a novel rat model of severe acute cholangitis. *Iran J Basic Med Sci* 2015; **18**: 1124-1129 [PMID: 26949501]
9 **Livak KJ**, Schmittgen TD. Analysis of relative gene expression data using real-time quantitative PCR and the 2(-Delta Delta C(T)) Method. *Methods* 2001; **25**: 402-408 [PMID: 11846609 DOI: 10.1006/meth.2001.1262]
10 **Lee JG**. Diagnosis and management of acute cholangitis. *Nat Rev Gastroenterol Hepatol* 2009; **6**: 533-541 [PMID: 19652653 DOI: 10.1038/nrgastro.2009.126]
11 **Yu H**, Wu SD. Activation of TLR-4 and liver injury via NF-kappa B in rat with acute cholangitis. *Hepatobiliary Pancreat Dis Int* 2008; **7**: 185-191 [PMID: 18397856]
12 **da Silva CG**, Studer P, Skroch M, Mahiou J, Minussi DC, Peterson CR, Wilson SW, Patel VI, Ma A, Csizmadia E, Ferran C. A20 promotes liver regeneration by decreasing SOCS3 expression to enhance IL-6/STAT3 proliferative signals. *Hepatology* 2013; **57**: 2014-2025 [PMID: 23238769 DOI: 10.1002/hep.26197]
13 **Bavia L**, de Castro ÍA, Cogliati B, Dettoni JB, Alves VA, Isaac L. Complement C5 controls liver lipid profile, promotes liver homeostasis and inflammation in C57BL/6 genetic background. *Immunobiology* 2016; **221**: 822-832 [PMID: 26896155]
14 **Szabo G**, Petrasek J. Inflammasome activation and function in liver disease. *Nat Rev Gastroenterol Hepatol* 2015; **12**: 387-400 [PMID: 26055245 DOI: 10.1038/nrgastro.2015.94]
15 **Vaughan AT**, Betti CJ, Villalobos MJ. Surviving apoptosis. *Apoptosis* 2002; **7**: 173-177 [PMID: 11865202]
16 **Zinkel S**, Gross A, Yang E. BCL2 family in DNA damage and cell cycle control. *Cell Death Differ* 2006; **13**: 1351-1359 [PMID: 16763616]
17 **Assy N**, Gong Y, Zhang M, Pettigrew NM, Pashniak D, Minuk GY. Use of proliferating cell nuclear antigen as a marker of liver regeneration after partial hepatectomy in rats. *J Lab Clin Med* 1998; **131**: 251-256 [PMID: 9523849]
18 **Huang YH**, Chuang JH, Yang YL, Huang CC, Wu CL, Chen CL. Cholestasis downregulate hepcidin expression through inhibiting IL-6-induced phosphorylation of signal transducer and activator of transcription 3 signaling. *Lab Invest* 2009; **89**: 1128-1139 [PMID: 19652645 DOI: 10.1038/labinvest.2009.82]
19 **Matsumoto Y**, Niimoto S, Katayama K, Hirose K, Yamaguchi A, Torigoe K. Effects of biliary drainage in obstructive jaundice on microcirculation, phagocytic activity, and ultrastructure of the liver in rats. *J Hepatobiliary Pancreat Surg* 2002; **9**: 360-366 [PMID: 12353147 DOI: 10.1007/s005340200040]
20 **Vaquer G**, Rivière F, Mavris M, Bignami F, Llinares-Garcia J, Westermark K, Sepodes B. Animal models for metabolic, neuromuscular and ophthalmological rare diseases. *Nat Rev Drug Discov* 2013; **12**: 287-305 [PMID: 23493083 DOI: 10.1038/nrd3831]
21 **Center SA**. Diseases of the gallbladder and biliary tree. *Vet Clin North Am Small Anim Pract* 2009; **39**: 543-598 [PMID: 19524793 DOI: 10.1016/j.cvsm.2009.01.004]
22 **Wada K**, Takada T, Kawarada Y, Nimura Y, Miura F, Yoshida M, Mayumi T, Strasberg S, Pitt HA, Gadacz TR, Büchler MW, Belghiti J, de Santibanes E, Gouma DJ, Neuhaus H, Dervenis C, Fan ST, Chen MF, Ker CG, Bornman PC, Hilvano SC, Kim SW, Liau KH, Kim MH. Diagnostic criteria and severity assessment of acute cholangitis: Tokyo Guidelines. *J Hepatobiliary Pancreat Surg* 2007; **14**: 52-58 [PMID: 17252297 DOI: 10.1007/s00534-006-1156-7]
23 **Zhang WZ**, Chen YS, Wang JW, Chen XR. Early diagnosis and treatment of severe acute cholangitis. *World J Gastroenterol* 2002; **8**: 150-152 [PMID: 11833092 DOI: 10.3748/wjg.v8.i1.150]

P- Reviewer: Abadi ATB, Nishino T **S- Editor**: Qi Y **L- Editor**: A
E- Editor: Wang CH

World Journal of Gastroenterology

Submit a Manuscript: http://www.wjgnet.com/esps/ *World J Gastroenterol* 2017 March 14; 23(10): 1780-1786

DOI: 10.3748/wjg.v23.i10.1780 ISSN 1007-9327 (print) ISSN 2219-2840 (online)

ORIGINAL ARTICLE

Basic Study

Clinicopathological significance of overexpression of interleukin-6 in colorectal cancer

Jun Zeng, Zhong-Hua Tang, Shuang Liu, Shan-Shan Guo

Jun Zeng, Zhong-Hua Tang, Shuang Liu, Shan-Shan Guo, College of Life Sciences, Chongqing Normal University, Chongqing 401331, China

Author contributions: Zeng J contributed to the design of the experiments, data acquisition and analysis, scientific discussion, and manuscript revision; Tang ZH, Liu S and Guo SS substantially contributed to the experimental preparation and the preparation of the manuscript; all authors approved the final version of the article to be published.

Supported by the National Natural Science Foundation of China, No. 81502131; the Natural Science Foundation of Chongqing, No. cstc2016jcyjA0405; and the Scientific and Technological Research Program of Chongqing Municipal Education Commission, No. KJ1500332.

Institutional review board statement: All colorectal cancer specimens from the patients were acquired after informed consent and ethical permission was obtained for participation in the study.

Conflict-of-interest statement: To the best of our knowledge, no conflict of interest exists.

Data sharing statement: No additional data are available.

Manuscript source: Unsolicited manuscript

Correspondence to: Jun Zeng, PhD, College of Life Sciences, Chongqing Normal University, 37 Daxuecheng Middle Road, Chongqing 401331, China. zengjun_2012@163.com
Telephone: + 86-187-23179063

Received: September 17, 2016
Peer-review started: September 19, 2016
First decision: October 20, 2016
Revised: November 6, 2016
Accepted: December 2, 2016
Article in press: December 2, 2016
Published online: March 14, 2017

Abstract

AIM

To compare the expression levels of interleukin (IL)-6 in colorectal cancer (CRC) tissues and adjacent non-cancerous tissues, and analyse the correlation of IL-6 expression with the clinicopathological parameters of CRC.

METHODS

Fifty CRC tissue specimens and 50 matched adjacent mucosa specimens were collected. The expression of IL-6 in these clinical samples was examined by immunohistochemical staining. The correlation between IL-6 expression and clinicopathological parameters was assessed by statistical analysis.

RESULTS

IL-6 expression was significantly elevated in CRC tissues compared with noncancerous tissues ($P < 0.001$). IL-6 expression was positively correlated with tumour TNM stage ($P < 0.001$), but a negative correlation was detected between IL-6 expression and tumor histological differentiation in CRC ($P < 0.05$). Furthermore, IL-6 expression was associated with invasion depth and lymph node metastasis in CRC.

CONCLUSION

IL-6 might be a useful marker for predicting a poor prognosis in patients with CRC and might be used as a potential therapeutic target in CRC.

Key words: Colorectal cancer; Interleukin-6; Invasion

depth; Lymph node metastases

Core tip: Colorectal cancer (CRC) is the fourth leading cause of cancer-related death worldwide. Previous studies have demonstrated that interleukin (IL)-6 is a critical tumor promoter during early CRC tumorigenesis. However, there have been few studies regarding the expression of IL-6 and its prognostic role in CRC. Therefore, we explored the correlation between the expression of IL-6 and the clinicopathological features in CRC. To the best of our knowledge, this is the first analysis of the expression of IL-6 in resected CRC samples using immunohistochemistry combined with biostatistics. The results showed that the expression of IL-6 was correlated with tumour TNM stage and histological differentiation. Furthermore, IL-6 in tumour cells showed stronger immunoreactivity as tumour cells invaded deeply. These data indicated that IL-6 might be used as a potential therapeutic target in patients with CRC.

Zeng J, Tang ZH, Liu S, Guo SS. Clinicopathological significance of overexpression of interleukin-6 in colorectal cancer. *World J Gastroenterol* 2017; 23(10): 1780-1786 Available from: URL: http://www.wjgnet.com/1007-9327/full/v23/i10/1780.htm DOI: http://dx.doi.org/10.3748/wjg.v23.i10.1780

INTRODUCTION

Colorectal cancer (CRC) is one of the most common malignancies and the fourth leading cause of cancer-related death worldwide[1-3]. Over one million new cases of CRC are diagnosed each year, and its incidence is second only to lung cancer[4,5]. CRC has been observed to be quite prevalent in Western industrialized countries in the past. In recent decades, a growing number of developing countries have exhibited an acute increase in the incidence of CRC. With the improvement in living conditions, the incidence rate of CRC in China has leapt, and CRC has become the fifth most common cancer. Despite radiotherapeutic and chemotherapeutic regimens and significantly improved surgical outcomes, approximately half of CRC patients will suffer from CRC again within five years of treatment and inevitably surrender to the disease[6]. The prognosis evaluation and treatment of CRC currently depend mostly on the pathologic stage of disease when diagnosed and primary surgical therapy. Unfortunately, no specific biomarker that allows for the accurate prediction of outcomes for individual patients currently exists.

Many previous studies have shown that neoplasms arise at sites of chronic inflammation[7]. The upregulation of inflammatory cytokines secreted by inflammatory cells, other mesenchymal cells and tumour cells could facilitate tumour initiation and enhance tumour cell proliferation and invasion[8-10]. Among the numerous inflammatory cytokines, interleukin (IL)-6 has continually attracted extensive attention.

IL-6 is a pleiotropic cytokine that is involved in tumour growth, invasion, and metastasis in human malignancies[11,12]. There is abundant mechanistic evidence suggesting a significant role of IL-6 in the tumour initiation and progression of a variety of cancers. For instance, Nguyen *et al*[13] demonstrated that IL-6 is a pivotal modulator in the initiation of prostate tumourigenesis, tumour growth, metastasis, and resistance to chemotherapy. Zhang *et al*[14] reported that IL-6 is necessary for pancreatic intraepithelial neoplasia (PanIN) maintenance and progression. Taniguchi *et al*[15] summarized that serum IL-6 levels correlate with poor prognosis, tumour burden, survival and advanced stages of disease in cancers of the lung, esophagus, mammary gland, ovary, and kidney, among others. In addition, several recent studies have suggested a potential role for IL-6 in colon cancer initiation and progression. It has been shown that serum levels of IL-6 are elevated in CRC patients[16]. Furthermore, IL-6 has been shown to promote the growth of colorectal cancer epithelial cells *in vitro*. However, there is relatively little understanding of the correlation between IL-6 expression and clinicopathological features in CRC.

The present study was designed to examine the difference in IL-6 expression between CRC tissues and matched adjacent normal mucosa tissues, and the association between IL-6 expression and clinicopathological features in CRC.

MATERIALS AND METHODS

Surgical specimens

Fifty primary CRC tissues and 50 matched adjacent normal mucosa tissues were collected from the patients who underwent surgical resection at the Sichuan Provincial People's Hospital (Chengdu, China). The original tumours were staged on the basis of the tumour-node-metastasis (TNM) classification system of the International Union Against Cancer[17]. Tumour differentiation was scored according to Edmondson Steiner scoring by senior pathologists. Detailed clinicopathological information was excerpted from the clinical data and a summary of the specific CRC demographics is displayed in Table 1. Informed prior to analysis, all patients consented to the tissue procurement, and the study was approved by the Institutional Ethics Committee of Sichuan Provincial People's Hospital.

Immunohistochemical staining

Human cancer tissue sections were subjected to

Table 1 Clinicopathological data of colorectal cancer patients in this study

Characteristic	Value
Total number of patients	50
Age (yr)	
Median	61
Range	25-88
Sex, *n*	
Male	28
Female	22
TNM stage	
Ⅰ / Ⅱ	29
Ⅲ / Ⅳ	21
Pathologic grade	
Well	14
Moderate	27
Poor	9

immunohistochemistry analysis using a Dako Envision System (Dako Cytomation GmbH, Hamburg, Germany Denmark) according to the manufacturer's instructions. In brief, tumour blocks were formalin-fixed, paraffin-embedded, and cut into 4-μm-thick sections. The sections were deparaffinized in xylene and rehydrated through diminishing concentrations of ethanol (100%, 95%, 85%, and 75%). This was followed by subsequent incubation in 3% H_2O_2 for 10 min in the dark at room temperature to eliminate endogenous peroxidase activity. Antigen-retrieval was performed by heating the sections for 5 min in citrate buffer (pH 6.0) using the autoclave sterilizer method. The sections were then allowed to cool at room temperature for 60 min, and rinsed twice for 5 min with fresh PBS. Thereafter, the slides were preincubated with healthy bovine or goat serum albumin diluted in PBS (pH 7.4) for 15 min at 37 ℃, and then incubated overnight at 4 ℃ with primary antibody specific for IL-6 (mouse anti-IL-6, dilution 1:100, Proteintech). After three rinses in fresh PBS, the slides were incubated for 40 min at 37 ℃ with horseradish peroxidase-coupled secondary antibody. Following three additional washes, all specimens were stained with 3,3'-diaminobenzidine (DAB) substrate chromogen system (Dako Cytomation GmbH). Finally, the sections were rinsed in distilled water, and counterstained with Mayer's haematoxylin according to the manufacturer's instructions. Non-immune rabbit IgG at the same dilution as the primary antibody was used as a negative control.

Evaluation of immunohistochemical staining

Cells with observable brown particles in the cytoplasm were taken as positive. All sections were assessed by two professional pathologists who were blinded to patient outcomes and all clinicopathologic data. The immunohistochemical staining was evaluated according to the intensity (weak = 1, intense = 2) of IL-6 immunostaining and the density (0% = 0, 1%-50% = 1, 51%-75% = 2, > 76% = 3) of positive carcinoma cells[5]. The eventual score of each specimen was calculated by multiplying intensity and density, and the tumours were finally determined as negative expression: score = 0; low expression: score ⩽ 3; or high expression: score > 3. If the two assessments did not agree for a sample, the sample was re-evaluated and classified based on the evaluations given most frequently by the experts.

Statistical analysis

The data were analysed with the SPSS 16.0 for Windows (SPSS Inc). Pearson χ^2 test and Fisher's exact test were used to compare qualitative variables, and quantitative variables were analysed by the *t*-test. The correlation between clinicopathological factors and IL-6 expression was evaluated by the Spearman test for non-parametric variables. *P*-values less than 0.05 were considered statistically significant.

RESULTS

IL-6 expression is elevated in CRC

To explore the underlying clinical role of IL-6 in CRC, the expression of IL-6 was examined by immunohistochemical staining in 50 CRC tissue samples and 50 matched adjacent normal mucosa tissue samples. Strong IL-6 staining was mostly located in the cytoplasm of CRC cells (Figure 1A), while partial IL-6 staining was observed in the normal mucosa. Strong IL-6 expression was observed in 8% (4/50) of the normal colorectal mucosa samples and in 46% (23/50) of primary CRC samples. IL-6 expression was significantly increased in the CRC tissues compared with the normal mucosa tissues ($P < 0.001$; Figure 1B).

IL-6 expression is associated with invasion depth and lymph node metastasis in CRC

When analysing the levels of IL-6 expression in colorectal tumour cells by immunohistochemistry, we observed that IL-6 in tumour cells showed stronger immunoreactivity as tumour cells invaded more deeply (Figure 2A). This means that the tumour regions that were closer to the invasion front showed higher IL-6 expression levels. In addition, the majority of tumor cells in lymph node metastases were also IL-6-immunopositive (Figure 2B).

IL-6 expression correlates with several clinicopathologic factors in CRC

We next analysed the association between the levels of IL-6 expression and clinicopathologic parameters in CRC, including TNM stage (stages Ⅰ, Ⅱ, Ⅲ, and Ⅳ) and histological differentiation (well, moderately, and poorly differentiated). The results showed that the levels of IL-6 expression were inversely associated with histological differentiation ($P < 0.05$, Figure 3A and B), but positively correlated with TNM stage ($P < 0.001$, Figure 3C and D). Of the 50 IL-6-positive CRC cases, 14 were well-differentiated, 27 moderately

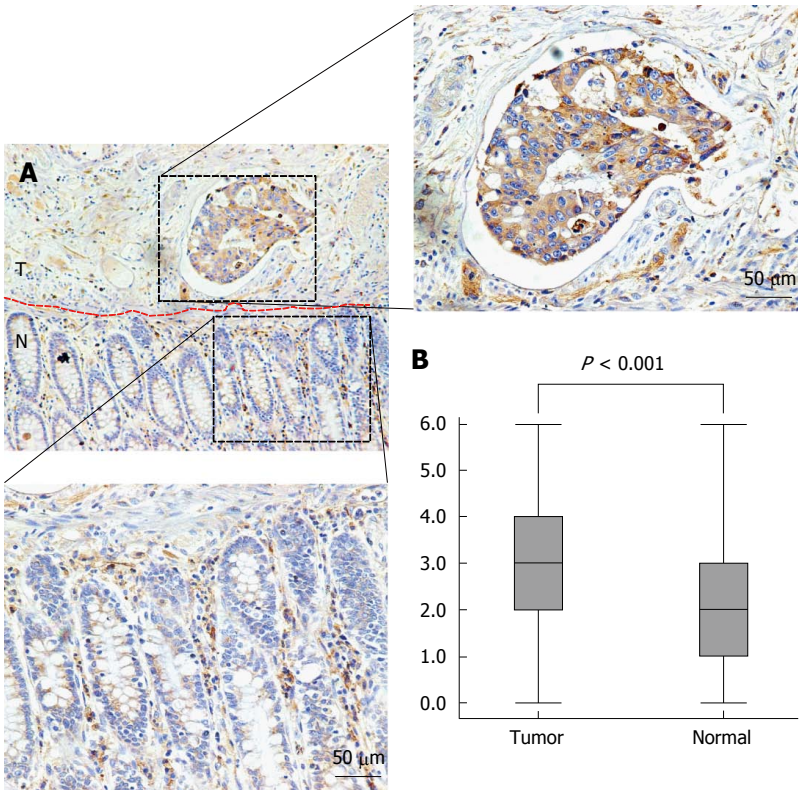

Figure 1 Interleukin-6 expression is elevated in human colorectal cancer tissue samples. A: Individual FFPE sections demonstrated that colorectal cancer cells had invaded underneath the colorectal mucosa. The IL-6 expression level was elevated in colorectal tumour tissues compared to adjacent non-tumour tissues. "T" refers to tumour tissue, and "N" indicates adjacent non-tumour tissue from the same patient; B: IL-6 expression scores are shown as box plots, with the horizontal lines representing the median, the bottom and top of the boxes representing the 25th and 75th percentiles, respectively, and the vertical bars representing the range of data.

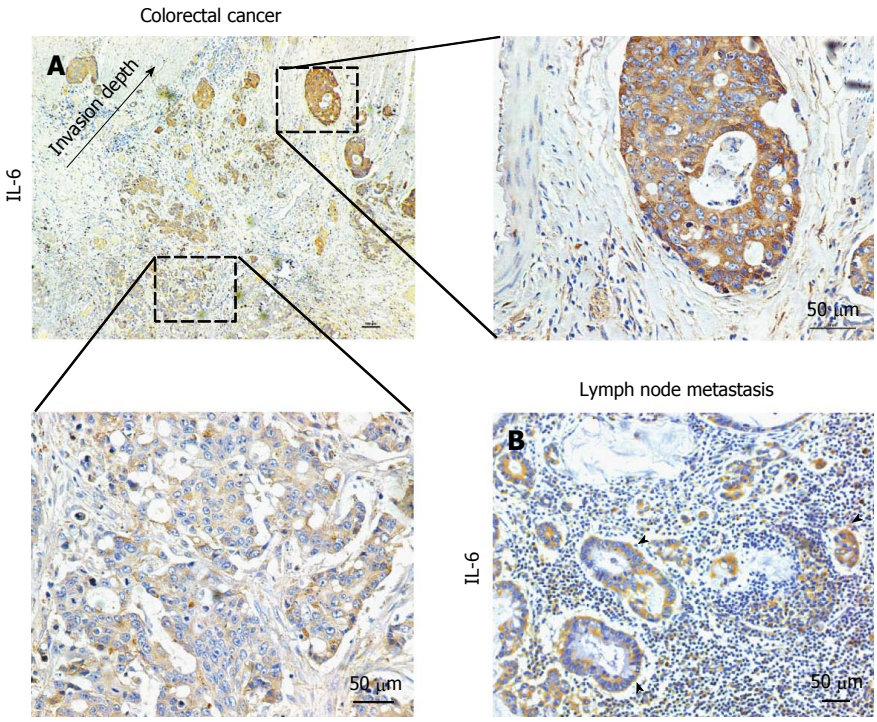

Figure 2 Interleukin-6 expression is associated with invasion depth and lymph node metastasis in colorectal cancer. A: Increased expression of IL-6 at the invasive front of human CRC samples compared with tumour centre; B: The tumor cells in lymph node metastases were also IL-6-immunopositive. IL: Interleukin.

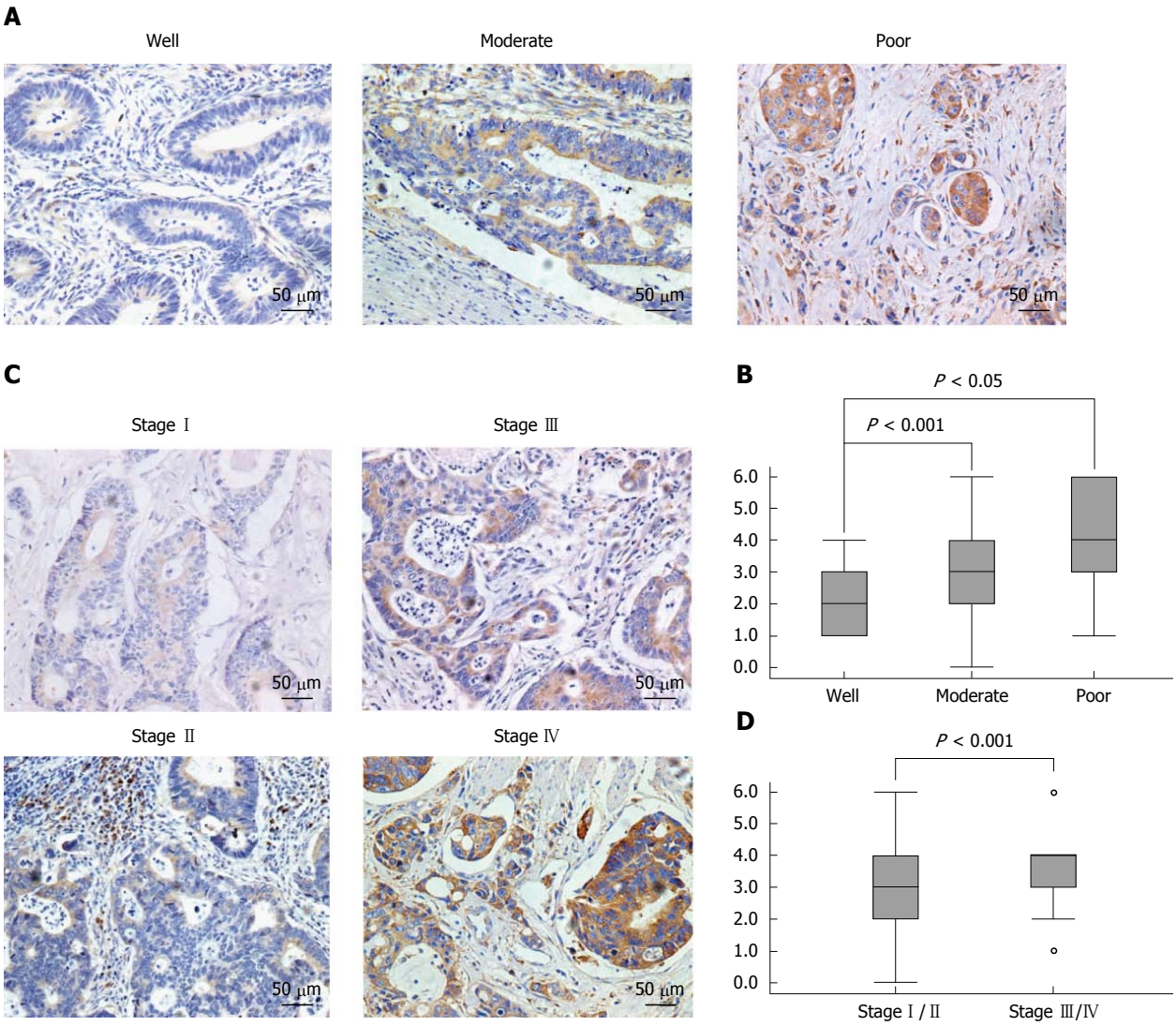

Figure 3 Interleukin-6 expression is significantly correlated with histological differentiation and TNM stage. A: Poorly differentiated colorectal tumours showed higher expression of IL-6 than moderately and well differentiated colorectal tumours; B: Comparison of immunohistochemical scores of IL-6 according to histological differentiation ($P < 0.05$); C: Strong immunoreactivity was more likely to present with advanced-stage (stage Ⅲ/Ⅳ) CRC compared to early-stage (stage Ⅰ/Ⅱ); D: Comparison of immunohistochemical scores of IL-6 according to TNM stage ($P < 0.001$).

differentiated and 9 poorly differentiated. In addition, 29 cases were classified as stage Ⅰ-Ⅱ, while 21 cases were classified as stage Ⅲ-Ⅳ. Taken together, these analyses indicated that the upregulation of IL-6 in CRC cells correlates with tumour progression.

DISCUSSION

Chronic inflammation is thought to be the leading cause of many human cancers including CRC[13]. In patients with inflammatory bowel disease, the risk of developing CRC is much higher than in the general population[18]. However, even in sporadic CRC with no preceding chronic inflammation, inflammatory cells infiltrate the tumour region and secrete inflammatory cytokines, which contribute to cancer development. Such "tumour-elicited inflammation" further emphasizes the importance of chronic inflammation in cancer progression. IL-6 is an NF-κB-regulated inflammatory cytokine that enforces proliferation and anti-apoptotic effects in tumour cells[2,13]. It has been reported that IL-6 expression in serum samples from patients was associated with an increased risk of colorectal adenoma[19,20]. Until now, to the best of our knowledge, there have been no relevant studies analysing the levels of IL-6 expression in resected CRC samples by immunohistochemistry combined with biostatistics. In this study, we found that IL-6 expression was elevated in CRC compared with normal mucosa, which is consistent with previous studies[21,22]. In addition, we found that the levels of IL-6 expression were inversely associated with histological differentiation, but positively associated with TNM stage. These results imply that IL-6 may be involved in CRC progression. Interestingly, the tumour regions that were closer to the invasion front showed higher IL-6 expression levels. Furthermore, the majority of cancer cells in lymph node metastases were also IL-

6-immunopositive. These results suggested that IL-6 might be associated with CRC invasion and metastasis.

The mechanisms underlying IL-6-mediated CRC initiation and development have been elucidated comprehensively. IL-6 is a critical tumour promoter during early CRC tumourigenesis[20]. In mice with colitis-associated cancer, anti-IL-6 receptor antibody treatment reduced the incidence of colitis-associated cancer (CAC) by decreasing the expression of key genes in aerobic glycolysis[23]. In an experimental CAC mouse model, researchers found that the expression levels of IL-6 protein were gradually increased after the induction of dysplastic lesions over time. These data suggested that IL-6 might be a therapeutic target in CAC[24]. Activation of the IL-6/Stat3 pathway *via* IL-6 trans-signaling plays an important role not only in CRC initiation but also in CRC development[25,26]. According to the growing evidence supporting a critical role for IL-6 signaling in the development of both sporadic and inflammation-associated CRC, therapeutics targeting this pathway could be promising options for CRC patients.

ACKNOWLEDGMENTS

The authors thank Professors Ke Xie and Dan-Dan Dong and Technician Fang-Hua Li at the Sichuan Provincial People's Hospital (Chengdu, China) for providing CRC tissue samples.

COMMENTS

Background

Colorectal cancer (CRC) is the fourth leading cause of cancer-related death worldwide. Previous studies have demonstrated that IL-6 is a critical tumour promoter during early CRC tumourigenesis. However, there have been few studies regarding the expression of IL-6 and its prognostic role in CRC. The correlation between the expression levels of IL-6 and the clinicopathological features of CRC specimens has not yet been investigated.

Research frontiers

Previous studies have demonstrated that IL-6 is a critical tumour promoter during early CRC tumourigenesis and that the IL-6/STAT3 signaling pathway plays an important role in the progression of CRC.

Innovations and breakthroughs

To the best of our knowledge, this is the first analysis of the expression of IL-6 in resected CRC samples and its prognostic role using immunohistochemistry combined with biostatistics.

Applications

The results showed that the expression levels of IL-6 were correlated with TNM stage and histological differentiation. Furthermore, IL-6 in tumour cells showed stronger immunoreactivity as tumour cells invaded more deeply. These data indicate that IL-6 might be used as a potential target for postoperative adjuvant therapy in patients with CRC.

Terminology

Invasion depth, also called the depth of tumour invasion, is the most significant histological predictor of lymph node metastasis in colorectal cancer. Increasing evidence indicates that colorectal cancer with submucosal deep invasion correlates with a poor prognosis.

Peer-review

This is an interesting paper. The method they used to quantify IL-6 in CRC specimens is only a qualitative method.

REFERENCES

1 **Khan S**, Cameron S, Blaschke M, Moriconi F, Naz N, Amanzada A, Ramadori G, Malik IA. Differential gene expression of chemokines in KRAS and BRAF mutated colorectal cell lines: role of cytokines. *World J Gastroenterol* 2014; **20**: 2979-2994 [PMID: 24659889 DOI: 10.3748/wjg.v20.i11.2979]

2 **Grivennikov S**, Karin E, Terzic J, Mucida D, Yu GY, Vallabhapurapu S, Scheller J, Rose-John S, Cheroutre H, Eckmann L, Karin M. IL-6 and Stat3 are required for survival of intestinal epithelial cells and development of colitis-associated cancer. *Cancer Cell* 2009; **15**: 103-113 [PMID: 19185845 DOI: 10.1016/j.ccr.2009.01.001]

3 **Lu CC**, Kuo HC, Wang FS, Jou MH, Lee KC, Chuang JH. Upregulation of TLRs and IL-6 as a marker in human colorectal cancer. *Int J Mol Sci* 2014; **16**: 159-177 [PMID: 25547486 DOI: 10.3390/ijms16010159]

4 **Jiang Q**, Li Q, Chen H, Shen A, Cai Q, Lin J, Peng J. Scutellaria barbata D. Don inhibits growth and induces apoptosis by suppressing IL-6-inducible STAT3 pathway activation in human colorectal cancer cells. *Exp Ther Med* 2015; **10**: 1602-1608 [PMID: 26622533 DOI: 10.3892/etm.2015.2692]

5 **Zeng J**, Yang X, Cheng L, Liu R, Lei Y, Dong D, Li F, Lau QC, Deng L, Nice EC, Xie K, Huang C. Chemokine CXCL14 is associated with prognosis in patients with colorectal carcinoma after curative resection. *J Transl Med* 2013; **11**: 6 [PMID: 23294544 DOI: 10.1186/1479-5876-11-6]

6 **Abajo A**, Bitarte N, Zarate R, Boni V, Lopez I, Gonzalez-Huarriz M, Rodriguez J, Bandres E, Garcia-Foncillas J. Identification of colorectal cancer metastasis markers by an angiogenesis-related cytokine-antibody array. *World J Gastroenterol* 2012; **18**: 637-645 [PMID: 22363134 DOI: 10.3748/wjg.v18.i7.637]

7 **Kraus S**, Arber N. Inflammation and colorectal cancer. *Curr Opin Pharmacol* 2009; **9**: 405-410 [PMID: 19589728 DOI: 10.1016/j.coph.2009.06.006]

8 **Knüpfer H**, Preiss R. Significance of interleukin-6 (IL-6) in breast cancer (review). *Breast Cancer Res Treat* 2007; **102**: 129-135 [PMID: 16927176 DOI: 10.1007/s10549-006-9328-3]

9 **Hyun YS**, Lee AR, Eun CS, Youn JH, Kim HY. This close link between IL-6 and cancer suggests that the IL-6 might be induce tumorigenesis. Carcinogenesis Advance Access, 2012: 1-25

10 **Wang K**, Kim Min K, Di Caro G, Wong J, Shalapour S, Wan J, Zhang W, Zhong Z, Sanchez-Lopez E, Wu L-W, Taniguchi K, Feng Y, Fearon E, Grivennikov Sergei I, Karin M. Interleukin-17 Receptor A Signaling in Transformed Enterocytes Promotes Early Colorectal Tumorigenesis. *Immunity* 2014; **41**: 1052-1063 [DOI: 10.1016/j.immuni.2014.11.009]

11 **Nie W**, Xue L, Sun G, Ning Y, Zhao X. Interleukin-6 -634C/G polymorphism is associated with lung cancer risk: a meta-analysis. *Tumour Biol* 2014; **35**: 4581-4587 [PMID: 24408019 DOI: 10.1007/s13277-013-1602-5]

12 **Esfandi F**, Mohammadzadeh Ghobadloo S, Basati G. Interleukin-6 level in patients with colorectal cancer. *Cancer Lett* 2006; **244**: 76-78 [PMID: 16442710 DOI: 10.1016/j.canlet.2005.12.003]

13 **Nguyen DP**, Li J, Tewari AK. Inflammation and prostate cancer: the role of interleukin 6 (IL-6). *BJU Int* 2014; **113**: 986-992 [PMID: 24053309 DOI: 10.1111/bju.12452]

14 **Zhang Y**, Yan W, Collins MA, Bednar F, Rakshit S, Zetter BR, Stanger BZ, Chung I, Rhim AD, di Magliano MP. Interleukin-6 is required for pancreatic cancer progression by promoting MAPK signaling activation and oxidative stress resistance. *Cancer Res* 2013; **73**: 6359-6374 [PMID: 24097820 DOI: 10.1158/0008-5472.CAN-13-1558-T]

15 **Taniguchi K**, Karin M. IL-6 and related cytokines as the critical lynchpins between inflammation and cancer. *Semin Immunol* 2014; **26**: 54-74 [PMID: 24552665 DOI: 10.1016/j.smim.2014.01.001]

16 **Galizia G**, Orditura M, Romano C, Lieto E, Castellano P, Pelosio L, Imperatore V, Catalano G, Pignatelli C, De Vita F. Prognostic significance of circulating IL-10 and IL-6 serum levels in colon cancer patients undergoing surgery. *Clin Immunol* 2002; **102**: 169-178 [PMID: 11846459 DOI: 10.1006/clim.2001.5163]
17 **Wittekind C**, Compton CC, Greene FL, Sobin LH. TNM residual tumor classification revisited. *Cancer* 2002; **94**: 2511-2516 [PMID: 12015777 DOI: 10.1002/cncr.10492]
18 **Langholz E**, Munkholm P, Davidsen M, Binder V. Colorectal cancer risk and mortality in patients with ulcerative colitis. *Gastroenterology* 1992; **103**: 1444-1451 [PMID: 1358741]
19 **Kim S**, Keku TO, Martin C, Galanko J, Woosley JT, Schroeder JC, Satia JA, Halabi S, Sandler RS. Circulating levels of inflammatory cytokines and risk of colorectal adenomas. *Cancer Res* 2008; **68**: 323-328 [PMID: 18172326 DOI: 10.1158/0008-5472.can-07-2924]
20 **Sasaki Y**, Takeda H, Sato T, Orii T, Nishise S, Nagino K, Iwano D, Yaoita T, Yoshizawa K, Saito H, Tanaka Y, Kawata S. Serum Interleukin-6, insulin, and HOMA-IR in male individuals with colorectal adenoma. *Clin Cancer Res* 2012; **18**: 392-399 [PMID: 22048241 DOI: 10.1158/1078-0432.ccr-11-0896]
21 **Kakourou A**, Koutsioumpa C, Lopez DS, Hoffman-Bolton J, Bradwin G, Rifai N, Helzlsouer KJ, Platz EA, Tsilidis KK. Interleukin-6 and risk of colorectal cancer: results from the CLUE II cohort and a meta-analysis of prospective studies. *Cancer Causes Control* 2015; **26**: 1449-1460 [PMID: 26220152 DOI: 10.1007/s10552-015-0641-1]
22 **Nagasaki T**, Hara M, Nakanishi H, Takahashi H, Sato M, Takeyama H. Interleukin-6 released by colon cancer-associated fibroblasts is critical for tumour angiogenesis: anti-interleukin-6 receptor antibody suppressed angiogenesis and inhibited tumour-stroma interaction. *Br J Cancer* 2014; **110**: 469-478 [PMID: 24346288 DOI: 10.1038/bjc.2013.748]
23 **Han J**, Meng Q, Xi Q, Zhang Y, Zhuang Q, Han Y, Jiang Y, Ding Q, Wu G. Interleukin-6 stimulates aerobic glycolysis by regulating PFKFB3 at early stage of colorectal cancer. *Int J Oncol* 2016; **48**: 215-224 [PMID: 26530697 DOI: 10.3892/ijo.2015.3225]
24 **Yang H**, Qi H, Ren J, Cui J, Li Z, Waldum HL, Cui G. Involvement of NF-κB/IL-6 Pathway in the Processing of Colorectal Carcinogenesis in Colitis Mice. *Int J Inflam* 2014; **2014**: 130981 [PMID: 25093140 DOI: 10.1155/2014/130981]
25 **Matsumoto S**, Hara T, Mitsuyama K, Yamamoto M, Tsuruta O, Sata M, Scheller J, Rose-John S, Kado S, Takada T. Essential roles of IL-6 trans-signaling in colonic epithelial cells, induced by the IL-6/soluble-IL-6 receptor derived from lamina propria macrophages, on the development of colitis-associated premalignant cancer in a murine model. *J Immunol* 2010; **184**: 1543-1551 [PMID: 20042582 DOI: 10.4049/jimmunol.0801217]
26 **Waldner MJ**, Foersch S, Neurath MF. Interleukin-6--a key regulator of colorectal cancer development. *Int J Biol Sci* 2012; **8**: 1248-1253 [PMID: 23136553 DOI: 10.7150/ijbs.4614]

P- Reviewer: Lakatos PL, Sterpetti AV **S- Editor**: Qi Y
L- Editor: Wang TQ **E- Editor**: Wang CH

World Journal of Gastroenterology

Submit a Manuscript: http://www.wjgnet.com/esps/

World J Gastroenterol 2017 March 14; 23(10): 1787-1795

DOI: 10.3748/wjg.v23.i10.1787

ISSN 1007-9327 (print) ISSN 2219-2840 (online)

ORIGINAL ARTICLE

Basic Study

Integrated analysis of microRNA and mRNA expression profiles in HBx-expressing hepatic cells

Ruo-Chan Chen, Juan Wang, Xu-Yuan Kuang, Fang Peng, Yong-Ming Fu, Yan Huang, Ning Li, Xue-Gong Fan

Ruo-Chan Chen, Juan Wang, Yong-Ming Fu, Yan Huang, Xue-Gong Fan, Hunan Key Laboratory of Viral Hepatitis, Department of Infectious Disease, Xiangya Hospital, Central South University, Changsha 410008, Hunan Province, China

Xu-Yuan Kuang, Department of Hyperbaric Oxygen, Xiangya Hospital, Central South University, Changsha 410008, Hunan Province, China

Fang Peng, Key Laboratory of Cancer Proteomics of Chinese Ministry of Health, Xiangya Hospital, Central South University, Changsha 410008, Hunan Province, China

Ning Li, Department of Blood Transfusion, Xiangya Hospital, Central South University, Changsha 410008, Hunan Province, China

Author contributions: Li N and Fan XG designed the study and contributed equally to this work; Li N is a co-corresponding author of this article; Chen RC, Wang J, Kuang XY, Peng F, Fu YM and Huang Y collected and analyzed the data; Chen RC and Li N wrote the manuscript; all authors read and approved the final manuscript.

Supported by the National Natural Sciences Foundation of China, No. 81272253, No. 81502098 and No. 81670538; and the Special National International Technology Cooperation of China, No. 2015DFA31490.

Conflict-of-interest statement: The authors declare that they have no competing interests.

Data sharing statement: All data generated or analyzed during this study are included in this published article (and its supplementary information files).

Manuscript source: Invited manuscript

Correspondence to: Xue-Gong Fan, MD, PhD, Professor of Infectious Disease, Hunan Key Laboratory of Viral Hepatitis, Department of Infectious Disease, Xiangya Hospital, Central South University, No.87 Xiangya Road, Changsha 410008, Hunan Province, China. xgfan@hotmail.com
Telephone: +86-13975163388

Received: November 15, 2016
Peer-review started: November 16, 2016
First decision: December 19, 2016
Revised: January 17, 2017
Accepted: February 16, 2017
Article in press: February 17, 2017
Published online: March 14, 2017

Abstract

AIM

To identify the miRNA-mRNA regulatory network in hepatitis B virus X (HBx)-expressing hepatic cells.

METHODS

A stable HBx-expressing human liver cell line L02 was established. The mRNA and miRNA expression profiles of L02/HBx and L02/pcDNA liver cells were identified by RNA-sequencing analysis. Kyoto Encyclopedia of Genes and Genomes pathway enrichment analysis was performed to investigate the function of candidate biomarkers, and the relationship between miRNA and mRNA was studied by network analysis.

RESULTS

Compared with L02/pcDNA cells, 742 unregulated genes and 501 downregulated genes were determined as differentially expressed in L02/HBx cells. Gene ontology analysis suggested that the differentially expressed genes were relevant to different biological

processes. Concurrently, 22 differential miRNAs were also determined in L02/HBx cells. Furthermore, integrated analysis of miRNA and mRNA expression profiles identified a core miRNA-mRNA regulatory network that is correlated with the carcinogenic role of HBx.

CONCLUSION

Collectively, the miRNA-mRNA network-based analysis could be useful to elucidate the potential role of HBx in liver cell malignant transformation and shed light on the underlying molecular mechanism and novel therapy targets for hepatocellular carcinoma.

Key words: Hepatitis B virus X protein; Hepatocellular carcinoma; miRNA; mRNA; miRNA-mRNA network

Core tip: A number of miRNAs have been identified to be substantially involved in hepatocellular carcinoma cell proliferation, migration and invasion. Thus, an integrated analysis of the expression and function of miRNA and mRNA makes it possible to successfully identify the predicted miRNA-target network pattern and functional candidates of miRNA-mRNA pairs associated with HBx-related hepatocarcinogenesis.

Chen RC, Wang J, Kuang XY, Peng F, Fu YM, Huang Y, Li N, Fan XG. Integrated analysis of microRNA and mRNA expression profiles in HBx-expressing hepatic cells. *World J Gastroenterol* 2017; 23(10): 1787-1795 Available from: URL: http://www.wjgnet.com/1007-9327/full/v23/i10/1787.htm DOI: http://dx.doi.org/10.3748/wjg.v23.i10.1787

INTRODUCTION

Hepatocellular carcinoma (HCC) is one of the most common malignancies around the world, accounting for more than 745000 deaths per year[1,2]. As a typical inflammation-driven tumor, approximately 53% of HCC cases happen in the setting of chronic virus infection (mostly the hepatitis B virus (HBV) and hepatitis C virus), especially in Asia[3]. The HBV genome has 4 open reading frames (ORFs), namely X, S, C and P genes. The X gene, which encodes hepatitis B virus X (HBx) protein, correlates most with HCC occurrence and development[4,5]. Mounting evidence indicates that the integration of HBx into the host genome in hepatocytes could lead to gene transcription, cell proliferation, cell signaling transduction, protein degradation and apoptosis[6-9]. Moreover, several studies *in vivo* have confirmed the high morbidity of HCC in HBx-expressing transgenic mice[10-13]. However, the exact mechanism of HBx-induced hepatocarcinogenesis remains relatively poorly defined.

The miRNAs are a group of endogenously expressed RNAs with small molecular length, which play vital roles in various biological and pathological processes[14]. Mounting evidence has suggested the importance of miRNAs in the modulation of gene expression, cellular proliferation, cellular mobility, cellular differentiation, apoptosis and tumorigenesis[15]. A number of miRNAs have been identified to be substantially involved in HCC cell proliferation, migration and invasion, among which miR-122, miR-125, miR-199 family members and so on are closely related with HBV-associated HCC, especially[16]. As has been widely interpreted, the expression of miRNAs and their corresponding target genes are often inversely modulated in different backgrounds[17]. Meanwhile, increasing evidence has highlighted the success of a combined approach to investigate the miRNA-mediated mRNA regulation in various diseases[18,19]. Thus, an integrated analysis of the expression and functional interaction involving miRNA and mRNA makes it possible to successfully identify the predicted miRNA-target network pattern and functional candidates of miRNA-mRNA pairs associated with HBx-related hepatocarcinogenesis.

In this study, we conducted a comprehensive analysis for the first time to identify the functional miRNA-mRNA interactive network in HBx-transfected liver cells. By integrating the transcriptome and miRNAome, our study shed light on the potential molecular mechanism of HBx-related liver cell malignant transformation.

MATERIALS AND METHODS

Cell culture

The human liver cell line L02 (purchased from the China Center for Type Culture Collection, China) was cultured in Dulbecco's Modified Eagle's Medium (DMEM) supplemented with 100 U/mL penicillin, 100 μg/mL streptomycin and 10% fetal bovine serum (Gibco, Thermo Fisher, Waltham, MA, United States) in a cell incubator with 5% CO_2 at 37 ℃. L02 cells were then transfected with empty plasmids pcDNA3.0 (as a control) and pcDNA/HBx (the experiment group) by Lipofectamine™ 2000 (Invitrogen, Carlsbad, CA, United States) and cell clones were selected with Geneticin® (G418) according to the manufacturer's instructions (Gibco). The efficiency of transfection with empty vector (termed L02/pcDNA) or pcDNA/HBx (termed L02/HBx) was validated by Western blot.

miRNA and gene expression profiling

L02/pcDNA and L02/HBx cells were cultured and grown to 70%-90% confluency. Total cell RNA was extracted by using Trizol reagents (Invitrogen) following the manufacturer's instructions. The RNA quality was validated by agarose gel electrophoresis. The mRNA and miRNA expression profile was identified through RNA-sequencing (RNA-seq) analysis of the total RNA sample (Novel Bioinformatics, China).

As a fast splice junction mapper for RNA-seq reads,

Table 1 The primer sequence of selected genes

Real-time PCR primer	Primer sequence (5'-3')
Alpha-2-macroglobulin (*A2M*)	F: CGGAGAATGACGTACTCCACT
	R: TGGGTTGGTCCTTTCACTTGG
KIAA1522 (*KIAA1522*)	F: CCAGGACAACGTCTTCTTTCC
	R: CAGCCACCCTTGTTCAGTTTC
Procollagen C-endopeptidase enhancer (*PCOLCE*)	F: GTGCGGAGGGGATGTGAAG
	R: CGAAGACTCGGAATGAGAGGG
Solute carrier family 22, member 14 (*SLC22A14*)	F: TGGAGATGCTGTTACGCAGAT
	R: CTGGAATGTGCCAAACTCCC
Asparagine synthetase (glutamine-hydrolyzing) (*ASNS*)	F: GGAAGACAGCCCCGATTTACT
	R: AGCACGAACTGTTGTAATGTCA
Claudine 1 (*CLDN1*)	F: CCTCCTGGGAGTGATAGCAAT
	R: GGCAACTAAAATAGCCAGACCT
Origin recognition complex, subunit 4 (*ORC4*)	F: AGGTGACCGAACTAGCAGTG
	R: CTGCCGGTGAGAAAATCTTGA
Forkhead box C1 (*FOXC1*)	F: GGCGAGCAGAGCTACTACC
	R: TGCGAGTACACGCTCATGG
Spermatid perinuclear RNA binding protein (*STRBP*)	F: GTGTGGTGTAATGAGGATTGGC
	R: GTGGGCTCTTTTGTATTCCGAA

TopHat was used for RNA-seq alignment in our study. Based on the ultra-high throughput short read aligner Bowtie, TopHat aligns RNA-Seq reads to reference genomes and further analyzes the mapping reads to determine the possible splice junctions between exons. In contrast, the unmapped reads are separated into small parts, which enable them to align to the reference genome and define splice junctions[20].

Differentially expressed mRNAs and miRNAs definition

Limma algorithm was used to filter the differentially expressed mRNAs and miRNAs, according to the significant analysis and false discovery rate (FDR) analysis[21]. All data analysis meets the following two criteria: (1) fold-change > 2 or < 0.5; and (2) FDR < 0.05[22].

Identification of miRNA-targeted genes and mRNA-miRNA regulatory network

TargetScan and miRnada were utilized as analysis tools for miRNA target prediction based on the differentially expressed mRNAs and miRNAs[20]. The complex relationship between mRNAs and miRNAs was elucidated to build the miRNA-mRNA network according to differential expression values as well as the interactions of miRNA and their target genes listed in the Sanger MicroRNA database. In the miRNA-mRNA interaction network, the shape of square represents miRNAs and the circle represents target genes. The key genes and miRNAs usually possess the biggest degrees in the entire network.

Gene ontology category and pathway analysis

We then performed gene ontology (GO) analysis to help elucidate the concrete biological functions of specific genes with significant differences in the representative profiles of the miRNA target genes[23]. GO annotations were downloaded from Gene Ontology (http://www.geneontology.org/), UniProt (http://www.uniprot.org/), and NCBI (http://www.ncbi.nlm.nih.gov/). Fisher's exact test was employed to determine the significant GO categories and *P* values were corrected by FDR.

Pathway analysis was employed to identify the critical signal pathways of the differential expressed genes based on the resources from Kyoto Encyclopedia of Genes and Genomes (KEGG) database[24]. Fisher's exact test was used to pick out the significant pathways according to *P* value and FDR.

Quantitative real-time PCR analysis

The cDNA was synthesized using primers with the PrimeScript Real-Time Reagent Kit (TaKaRa, Shiga, Japan) in accordance with the manufacturer's instructions. Quantitative real-time PCR (Q-PCR) reactions were conducted with an Applied Biosystem-7500 Real-Time PCR System, using *Taq* PCR Master Mix (Zhongtai, China). Human glyceraldehyde-3-phosphate dehydrogenase (GAPDH) was used as an internal control. The Ct values of different mRNAs and miRNAs were normalized to GAPDH and analyzed *via* the Applied Biosystems 7500 Fast Software. The primers of miRNAs were purchased from Yingrun Biotechnologies Inc. (Changsha, China). The primer sequences of selected genes are shown in Table 1.

Statistical analysis

Two-way ANOVA test was performed for statistical analysis, using SPSS16.0 software. $P < 0.05$ was considered to be statistically significant.

RESULTS

Differential gene expression profiles of L02/HBx cells

To elucidate the molecular mechanism underlying HBx-mediated hepatocarcinogenesis, we first conducted the RNA-seq analysis to compare the mRNA expression profile of L02/HBx cells with that of L02/pcDNA L02 cells. Of 1243 differentially expressed genes, the expression of 742 genes were upregulated and 501 genes expression were downregulated (fold-change $\geqslant$ 2, $P < 0.05$) in L02/HBx cells (Figure 1A). The 20 top-ranking differentially expressed genes were subjected to a cluster analysis (Figure 1B), which determined several groups of genes with identical expression patterns. According to comparison with the control L02/pcDNA cells, the expression of GPR6, KLHL31, FOXC1, UGT1A7 and MAGEA4 was most upregulated and of SLC22A14, HBG2, PCOLCE, A2M and KIAA1522 was most significantly downregulated in L02/HBx cells. These differentially expressed genes were diversely involved in DNA replication, cell cycle, cell proliferation, cell adhesion, cell-cell signaling, metabolic process, tumor transformation and several other signaling pathways.

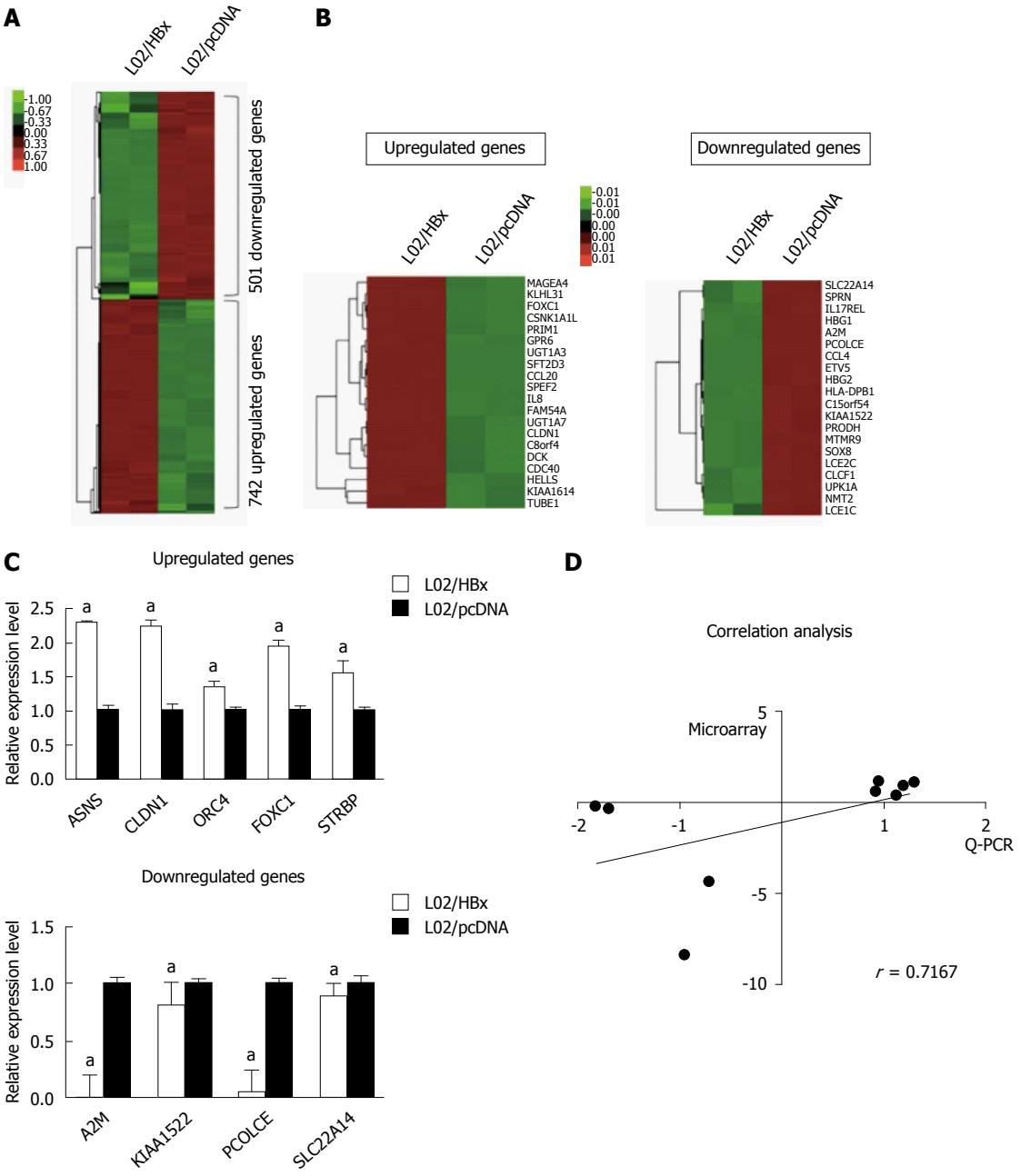

Figure 1 Differential mRNA expression between L02/HBx and L02/pcDNA cells. A: The global expression profile of L02/HBx and L02/pcDNA cells was analyzed by RNA-sequencing analysis. Heat map shows the differential gene expression patterns (fold-change > 2 or $P < 0.5$); B: The 20 top-ranking upregulated (left) and downregulated (right) genes represented on a heat map; C: Quantitative real-time PCR (Q-PCR) verification of selected differential gene expression in L02/HBx and L02/pcDNA cells. The relative expression levels of these genes were normalized to GAPDH; D: Correlation analysis of mRNA expression data detected by microarray and Q-PCR respectively ($P = 0.0369$). $^{a}P < 0.05$.

Next, we performed Q-PCR to confirm the relative mRNA expression of the 9 selected genes in which we were interested for further study. As shown in Figure 1C, the relative mRNA expression levels of 5 upregulated and 4 downregulated genes measured by Q-PCR were totally consistent with the RNA-seq results. Taking the sensitivity of two methods into consideration, the gene expression changes in RNA-seq were not exactly the same with that in Q-PCR analysis; however, there was a highly similar tendency between the two groups (Figure 1D; $r = 0.7167$, $P = 0.0369$).

GO and KEGG pathway analyses of putative target genes

In order to elucidate the correlation between differentially expressed genes and HBx-related hepatocarcigenesis, GO and signaling pathway analyses were applied respectively. GO analyses demonstrated that the 1243 annotated genes displayed diverse biological functions. The 742 upregulated genes were majorly correlated with the response to gene expression, DNA replication, DNA repair, cell cycle, cell division, and cellular response to DNA damage stimulus, while 501 downregulated genes were mainly related to

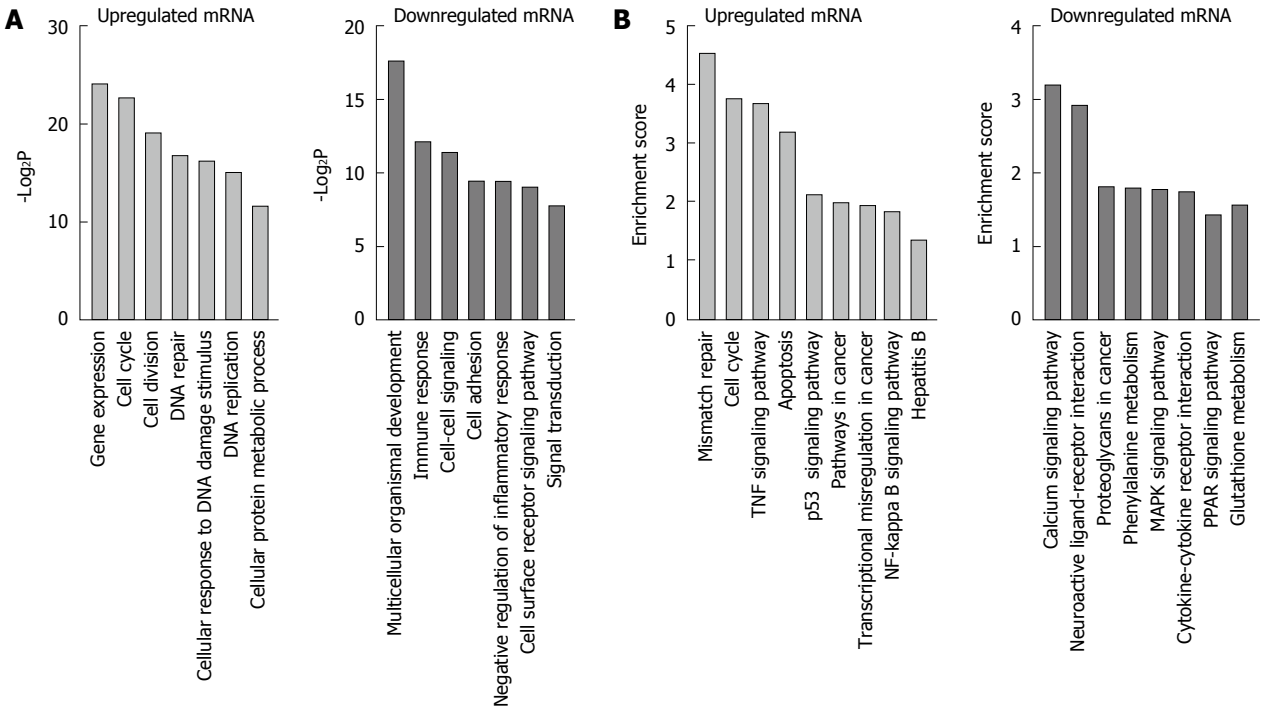

Figure 2 Gene ontology and Kyoto Encyclopedia of Genes and Genomes pathway analyses of differentially expressed mRNAs. A: Gene ontology analysis of differentially expressed genes; B: Kyoto Encyclopedia of Genes and Genomes pathway analysis of differentially expressed genes.

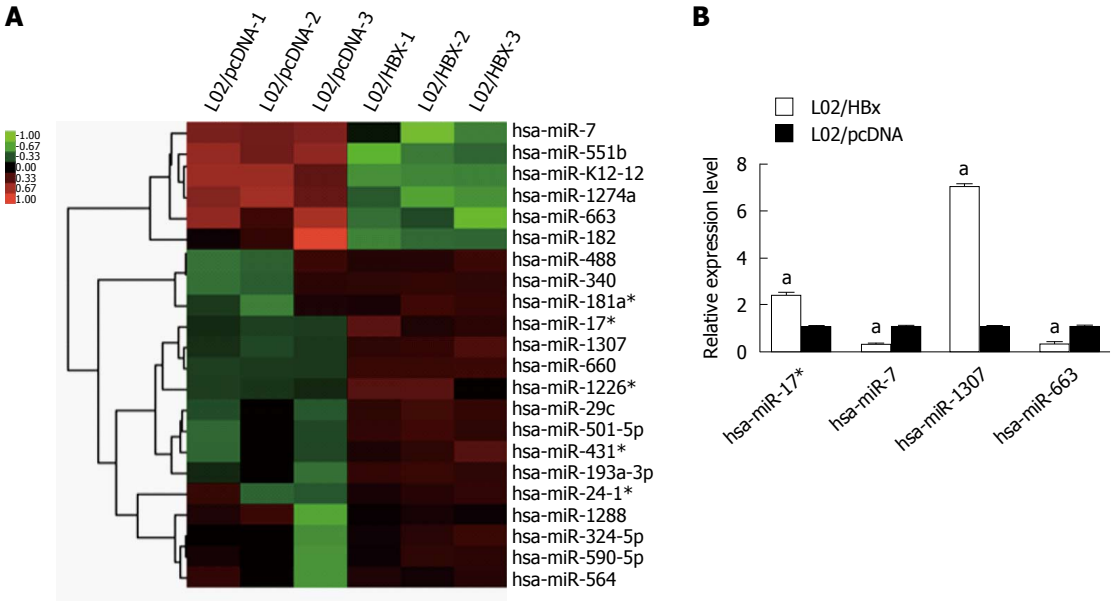

Figure 3 Differential miRNA expression between L02/HBx and L02/pcDNA cells. A: Global analysis of differentially expressed miRNAs between L02/HBx and L02/pcDNA cells; B: The relative expression of 4 differentially expressed miRNAs determined by Q-PCR analysis. The relative expression levels of miRNAs were normalized to U6 RNA ($^aP < 0.05$).

immune response, cell-cell signaling, cell adhesion, signal transduction and cell surface receptor signaling pathway (Figure 2A). Of note, further KEGG signal pathway analysis revealed that upregulated genes were briefly related to hepatitis B, mismatch repair, cell cycle, NF-κB signaling pathway and p53 signaling pathway, while downregulated genes were mostly involved in glutathione metabolism, PPAR signaling pathway, cytokine-cytokine receptor interaction, proteoglycans in cancer and MAPK signaling pathway (Figure 2B).

Analysis of miRNA expression patterns of L02/HBx cells

Compared with L02/pcDNA cells, 6 miRNAs were decreased and 16 miRNAs were upregulated in L02/HBx cells (Figure 3A). Specially, hsa-miR-7, hsa-miR-551b, hshv-miR-K12-12, hsa-miR-1274a, hsa-miR-663 and hsa-miR-182 were found to be downregulated;

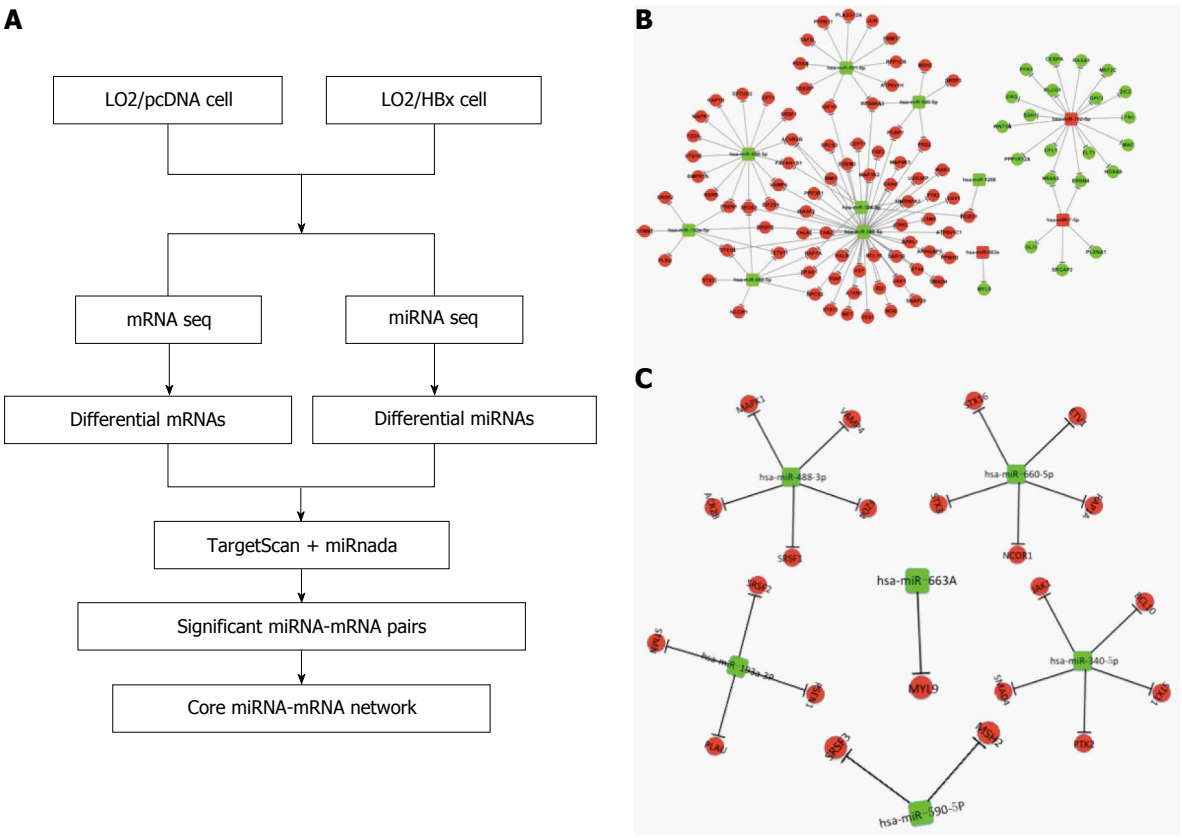

Figure 4 The miRNA-mRNA regulatory network in HBx-expressing cells. A: The strategy for constructing the miRNA-mRNA network associated with HBx integration; B: Hub miRNA-target network associated with HBx integration determined by bioinformatics analysis; C: A core miRNA-mRNA network was constructed by integrating the expression change of predicted target genes in L02/HBx cells.

meanwhile, hsa-miR-488, hsa-miR-340, hsa-miR-181a*, hsa-miR-17*, hsa-miR-1307, hsa-miR-660, hsa-miR-1226*, hsa-miR-29c, hsa-miR-501-5p, hsa-miR-431, hsa-miR-193a-3p, hsa-miR-24-1*, hsa-miR-1288, hsa-miR-324-5p, hsa-miR-590-5p and hsa-miR-564 were upregulated in L02/HBx cells. Then, the expression of 4 differentially expressed miRNAs was further validated through Q-PCR analysis, namely hsa-miR-17*, hsa-miR-7, hsa-miR-1307 and hsa-miR-663. As shown in Figure 3B, there was a consistent tendency of expression changes between miRNA-seq and Q-PCR data.

Integrated analysis of miRNA and mRNA expression profiles

It is generally believed that the network-based identification of hub miRNA patterns possesses higher accuracy compared with non-network-based methods. Thus, we employed the strategy illustrated in Figure 4A to identify the miRNA-mRNA regulatory network in L02 cells transfected with HBx. Through analysis using miRnada and TargetScan software, potential miRNA targets were successfully predicted. In combination with the expression pattern of target genes (Figure 1A), we generated several significant miRNA-mRNA pairs, which exhibited opposite expression patterns in L02/pcDNA and L02/HBx cells.

Hubs refer to the central parts of a network, and they play a substantial role in biological system progression. Hub miRNAs are generally defined as the top 10%-15% of the nodes by degree. Eleven differentially expressed miRNAs were identified as hub miRNAs in our study (Figure 4B). We found that miR340-5p is the one that regulates the most genes, as many as 51 predicted target genes. Furthermore, we also found that several miRNAs modulate a few common target genes through a combinational manner (Figure 4B). In order to identify the core miRNA-mRNA regulatory network, which is most functionally related to HCC development, the functional enrichment of these predicted target genes was analyzed. Genes closely related with cancer-associated pathways, such as DNA replication, gene expression, cell cycle, cell division, metabolic processes, signal transduction and so on, were especially picked out to build up the essential miRNA-mRNA regulatory network. Significantly, the miRNAs and their target genes displayed opposite expression patterns in L02/pcDNA and L02/HBx cells. As an example, the increased miRNAs in L02/HBx cells, such as hsa-miR-182-5p and hsa-miR-7-5p, may repress the expression of negative modulators, for instance, MEF2C and GLI3, to promote the cell transformation (Figure 4C). In contrast, the decreased miRNAs, including hsa-miR-501-5p, hsa-miR-340-5p, has-miR324-5p and has-miR-488-3p, may release the suppression of their target genes,

for example, JAK1, MAPK1, STX3 and BCL10, whose expression was upregulated in L02/HBx cells. The activation of these potential miRNA target genes might help to establish HBx-induced HCC progression.

Summarizing all the results, we have demonstrated that these core miRNAs may function as crucial regulators by modulating DNA replication, gene expression, cell cycle, cell division, metabolic processes and signal transduction, thus playing vital roles in tumorigenesis.

DISCUSSION

HCC is one of the deadliest malignancies, with dismal prognosis around the world. In southeast Africa and China, chronic HBV infection is the most important cause of HCC. At present, the molecular mechanism of HBV-related HCC development is not fully understood, and the *HBx* gene is frequently regarded as a vital regulator in HBV-related hepatocarcinogenesis[25,26]. Due to being integrated into the host genome, the HBx gene can act as a transactivator of numerous host cellular genes related with growth control, cell cycle and malignant transformation[10]. Therefore, a better understanding of the specific role of HBx in hepatocarcinogenesis is vital to the advancement of HCC treatment. Although a number of studies have been investigating the molecular mechanism underlying HBx-associated HCC development, the conclusions from different groups have varied from among each other[8,27-29]. Thus, a more reliable strategy was employed in our study to help improve the understanding of gene regulations on HBX-related progression on the basis of the combined analysis of the miRNA-mRNA regulatory network.

Of all the differentially expressed genes, a substantial proportion were associated with gene expression, DNA repair, cell cycle, cell division, metabolic processes, cell-cell signaling, cell adhesion and signal transduction (Figure 1C and D). These differentially expressed mRNA might vigorously participate in the hepatic malignant cell transformation through regulating multiple cellular processes. We further obtained the associated signal pathways modulated by the differential expressed genes with KEGG analysis. Among the 52 pathways mediated by the upregulated genes, 5 pathways have been confirmed to be HBx-related, including the hepatitis B pathway, cell cycle, apoptosis, and NF-kappa B and p53 signaling pathways. There is only one HBx-related signaling pathway among the 21 pathways mediated by downregulated genes, namely MAPK signal pathway[7]. Through regulating these 6 pathways and possibly other potential pathways as well, HBx might play a crucial role in hepatocarcinogenesis *via* modulating chromosome integrity[30], cell proliferation[29], cell cycle[8], apoptosis and oncogene expression[27,28]. Combining the function and pathway analysis for differentially expressed genes in L02/HBx cells, we may arrive at a conclusion that liver cells might develop various cellular responses and gain malignant potentials given the transfection of HBx.

With regard to the altered miRNAs, we successfully identified 6 downregulated and 16 upregulated miRNAs in L02/HBx cells by the application of custom microarray. Of these altered miRNAs, several, such as hsa-miR-338-3p and hsa-miR-29c, have been previously reported to be involved in HBx-associated HCC development[31]. Despite the fact that several research groups have independently established the HBx-regulated mRNA or miRNA expression pattern by identifying different mRNAs as well as miRNAs in the presence of HBx[31-34], few studies have focused on the miRNA-mRNA modulation and interaction.

Actually, hepatocarcinogenesis is a complex process in response to external and internal stimuli, and miRNA-target gene modulation is a crucial means of cellular response. Therefore, identification of miRNA-target with opposite expression patterns facilitated our selection of the potential miRNA as well as their corresponding target genes in HBx-related cell transformation. Bioinformatics analysis demonstrated that 11 hub miRNAs participated in constructing the miRNA-mRNA regulatory network (Figure 4B). Next, we will carry out more specific research on the function of those hub miRNAs in order to gain a better understanding of their role in HCC. Moreover, in this study, we also acquired an understanding of the essential miRNA-mRNA interactive network on the basis of functional enrichment (Figure 4C). The corresponding target genes for the 11 hub miRNAs, including JAK1, MAPK1, STX3 and BCL10, are crucial regulators in cell cycle, gene expression, signal transduction and apoptosis[35-37]. Thus, identification of the target genes modulated by the dysregulated miRNAs will greatly promote our understanding of HBx-associated hepatocarcinogenesis and facilitate design of new targeted therapeutic agents.

Collectively, we not only identified the mRNAs and miRNAs that may become the potential predictors and diagnostically valuable biomarkers of HBV-related HCC but we also established a core functional miRNA-mRNA regulatory network in the context of HBx-induced cell transformation. This study shows that HBx transfection of liver cells is correlated with gene expression, cell cycle, signal transduction and apoptosis disturbance. The established network might reveal the regulation from miRNAs to target genes in the development of HBx-induced malignant transformation in HCC cells. Thus, it will be helpful to further investigate the novel function of HBx in hepatocarcinogenesis with the selection of miRNA-mRNA pairs.

ACKNOWLEDGMENTS

We thank Novel Bioinformatics Co. Ltd. for providing technical assistance in deep sequencing and bioinformatics analysis.

COMMENTS

Background

Chronic hepatitis B virus (HBV) infection is one of the leading causes of hepatocellular carcinoma (HCC), especially in Asia. Accumulated evidence has suggested that hepatitis B virus X (HBx) protein plays a potentially oncogenic role in hepatocarcinogenesis; however, the exact mechanism remains exclusive.

Research frontiers

Mounting evidence indicates that the integration of HBx into the host genome in hepatocytes could lead to gene transcription, cell proliferation, cell signaling transduction, protein degradation and apoptosis.

Innovations and breakthroughs

In this study, the authors conducted a comprehensive analysis for the first time to identify the functional miRNA-mRNA interactive network in HBx-transfected liver cells. This study shows that HBx transfection of liver cells is correlated with gene expression, cell cycle, signal transduction and apoptosis disturbance.

Applications

By integrating the transcriptome and miRNAome, this study shed light on the potential molecular mechanism of HBx-related liver cell malignant transformation.

Terminology

Kyoto Encyclopedia of Genes and Genomes is a database resource for understanding high-level functions and utilities of the biological system, such as the cell, the organism and the ecosystem, from molecular-level information, especially large-scale molecular datasets generated by genome sequencing and other high throughput experimental technologies.

Peer-review

The authors' approach to clarify the association of miRNA and mRNA in HBx-carcinogenesis using software seems interesting.

REFERENCES

1 **Jemal A**, Bray F, Center MM, Ferlay J, Ward E, Forman D. Global cancer statistics. *CA Cancer J Clin* 2011; **61**: 69-90 [PMID: 21296855 DOI: 10.3322/caac.20107]

2 **Ma L**, Wang X, Jia T, Wei W, Chua MS, So S. Tankyrase inhibitors attenuate WNT/β-catenin signaling and inhibit growth of hepatocellular carcinoma cells. *Oncotarget* 2015; **6**: 25390-25401 [PMID: 26246473 DOI: 10.18632/oncotarget.4455]

3 **Okuda K**. Hepatocellular carcinoma. *J Hepatol* 2000; **32**: 225-237 [PMID: 10728807 DOI: 10.1016/S0168-8278(00)80428-6]

4 **Yang ST**, Yen CJ, Lai CH, Lin YJ, Chang KC, Lee JC, Liu YW, Chang-Liao PY, Hsu LS, Chang WC, Hung WC, Tang TK, Liu YW, Hung LY. SUMOylated CPAP is required for IKK-mediated NF-κB activation and enhances HBx-induced NF-κB signaling in HCC. *J Hepatol* 2013; **58**: 1157-1164 [PMID: 23369793 DOI: 10.1016/j.jhep.2013.01.025]

5 **Shi L**, Peng F, Tao Y, Fan X, Li N. Roles of long noncoding RNAs in hepatocellular carcinoma. *Virus Res* 2016; **223**: 131-139 [PMID: 27374059 DOI: 10.1016/j.virusres.2016.06.008]

6 **Murakami S**. Hepatitis B virus X protein: a multifunctional viral regulator. *J Gastroenterol* 2001; **36**: 651-660 [PMID: 11686474]

7 **Matsuda Y**, Ichida T. Impact of hepatitis B virus X protein on the DNA damage response during hepatocarcinogenesis. *Med Mol Morphol* 2009; **42**: 138-142 [PMID: 19784739 DOI: 10.1007/s00795-009-0457-8]

8 **Cheng P**, Li Y, Yang L, Wen Y, Shi W, Mao Y, Chen P, Lv H, Tang Q, Wei Y. Hepatitis B virus X protein (HBx) induces G2/M arrest and apoptosis through sustained activation of cyclin B1-CDK1 kinase. *Oncol Rep* 2009; **22**: 1101-1107 [PMID: 19787227 DOI: 10.3892/or_00000542]

9 **Ma NF**, Lau SH, Hu L, Xie D, Wu J, Yang J, Wang Y, Wu MC, Fung J, Bai X, Tzang CH, Fu L, Yang M, Su YA, Guan XY. COOH-terminal truncated HBV X protein plays key role in hepatocarcinogenesis. *Clin Cancer Res* 2008; **14**: 5061-5068 [PMID: 18698024 DOI: 10.1158/1078-0432.CCR-07-5082]

10 **Yu DY**, Moon HB, Son JK, Jeong S, Yu SL, Yoon H, Han YM, Lee CS, Park JS, Lee CH, Hyun BH, Murakami S, Lee KK. Incidence of hepatocellular carcinoma in transgenic mice expressing the hepatitis B virus X-protein. *J Hepatol* 1999; **31**: 123-132 [PMID: 10424292 DOI: 10.1016/S0168-8278(99)80172-X]

11 **Kim JH**, Alam MM, Park DB, Cho M, Lee SH, Jeon YJ, Yu DY, Kim TD, Kim HY, Cho CG, Lee DH. The Effect of Metformin Treatment on CRBP-I Level and Cancer Development in the Liver of HBx Transgenic Mice. *Korean J Physiol Pharmacol* 2013; **17**: 455-461 [PMID: 24227948 DOI: 10.4196/kjpp.2013.17.5.455]

12 **Wang C**, Yang W, Yan HX, Luo T, Zhang J, Tang L, Wu FQ, Zhang HL, Yu LX, Zheng LY, Li YQ, Dong W, He YQ, Liu Q, Zou SS, Lin Y, Hu L, Li Z, Wu MC, Wang HY. Hepatitis B virus X (HBx) induces tumorigenicity of hepatic progenitor cells in 3,5-diethoxycarbonyl-1,4-dihydrocollidine-treated HBx transgenic mice. *Hepatology* 2012; **55**: 108-120 [PMID: 21932402 DOI: 10.1002/hep.24675]

13 **Koff RS**. Hepatocellular carcinoma in transgenic mice: a consequence of continued expression of the HBx gene? *Gastroenterology* 1992; **102**: 1081-1082 [PMID: 1371486]

14 **Carrington JC**, Ambros V. Role of microRNAs in plant and animal development. *Science* 2003; **301**: 336-338 [PMID: 12869753 DOI: 10.1126/science.1085242]

15 **Bartel DP**. MicroRNAs: genomics, biogenesis, mechanism, and function. *Cell* 2004; **116**: 281-297 [PMID: 14744438]

16 **Meng F**, Henson R, Wehbe-Janek H, Ghoshal K, Jacob ST, Patel T. MicroRNA-21 regulates expression of the PTEN tumor suppressor gene in human hepatocellular cancer. *Gastroenterology* 2007; **133**: 647-658 [PMID: 17681183 DOI: 10.1053/j.gastro.2007.05.022]

17 **Djuranovic S**, Nahvi A, Green R. miRNA-mediated gene silencing by translational repression followed by mRNA deadenylation and decay. *Science* 2012; **336**: 237-240 [PMID: 22499947 DOI: 10.1126/science.1215691]

18 **Li Y**, Xu J, Chen H, Bai J, Li S, Zhao Z, Shao T, Jiang T, Ren H, Kang C, Li X. Comprehensive analysis of the functional microRNA-mRNA regulatory network identifies miRNA signatures associated with glioma malignant progression. *Nucleic Acids Res* 2013; **41**: e203 [PMID: 24194606 DOI: 10.1093/nar/gkt1054]

19 **Monzo M**, Navarro A, Bandres E, Artells R, Moreno I, Gel B, Ibeas R, Moreno J, Martinez F, Diaz T, Martinez A, Balagué O, Garcia-Foncillas J. Overlapping expression of microRNAs in human embryonic colon and colorectal cancer. *Cell Res* 2008; **18**: 823-833 [PMID: 18607389 DOI: 10.1038/cr.2008.81]

20 **Shen Y**, Pan Y, Xu L, Chen L, Liu L, Chen H, Chen Z, Meng Z. Identifying microRNA-mRNA regulatory network in gemcitabine-resistant cells derived from human pancreatic cancer cells. *Tumour Biol* 2015; **36**: 4525-4534 [PMID: 25722110 DOI: 10.1007/s13277-015-3097-8]

21 **Wettenhall JM**, Simpson KM, Satterley K, Smyth GK. affylmGUI: a graphical user interface for linear modeling of single channel microarray data. *Bioinformatics* 2006; **22**: 897-899 [PMID: 16455752 DOI: 10.1093/bioinformatics/btl025]

22 **Benjamini Y**, Drai D, Elmer G, Kafkafi N, Golani I. Controlling the false discovery rate in behavior genetics research. *Behav Brain Res* 2001; **125**: 279-284 [PMID: 11682119]

23 **Ashburner M**, Ball CA, Blake JA, Botstein D, Butler H, Cherry JM, Davis AP, Dolinski K, Dwight SS, Eppig JT, Harris MA, Hill DP, Issel-Tarver L, Kasarskis A, Lewis S, Matese JC, Richardson JE, Ringwald M, Rubin GM, Sherlock G. Gene ontology: tool for the unification of biology. The Gene Ontology Consortium. *Nat Genet* 2000; **25**: 25-29 [PMID: 10802651 DOI: 10.1038/75556]

24 **Draghici S**, Khatri P, Tarca AL, Amin K, Done A, Voichita C, Georgescu C, Romero R. A systems biology approach for pathway level analysis. *Genome Res* 2007; **17**: 1537-1545 [PMID:

17785539 DOI: 10.1101/gr.6202607]
25 **Feitelson MA**, Duan LX. Hepatitis B virus X antigen in the pathogenesis of chronic infections and the development of hepatocellular carcinoma. *Am J Pathol* 1997; **150**: 1141-1157 [PMID: 9094970]
26 **Su Q**, Schröder CH, Hofmann WJ, Otto G, Pichlmayr R, Bannasch P. Expression of hepatitis B virus X protein in HBV-infected human livers and hepatocellular carcinomas. *Hepatology* 1998; **27**: 1109-1120 [PMID: 9537452 DOI: 10.1002/hep.510270428]
27 **Shukla R**, Yue J, Siouda M, Gheit T, Hantz O, Merle P, Zoulim F, Krutovskikh V, Tommasino M, Sylla BS. Proinflammatory cytokine TNF-α increases the stability of hepatitis B virus X protein through NF-κB signaling. *Carcinogenesis* 2011; **32**: 978-985 [PMID: 21459755 DOI: 10.1093/carcin/bgr057]
28 **Park SG**, Min JY, Chung C, Hsieh A, Jung G. Tumor suppressor protein p53 induces degradation of the oncogenic protein HBx. *Cancer Lett* 2009; **282**: 229-237 [PMID: 19375220 DOI: 10.1016/j.canlet.2009.03.019]
29 **Bouchard MJ**, Wang LH, Schneider RJ. Calcium signaling by HBx protein in hepatitis B virus DNA replication. *Science* 2001; **294**: 2376-2378 [PMID: 11743208 DOI: 10.1126/science.294.5550.2376]
30 **Haruki K**, Shiba H, Fujiwara Y, Furukawa K, Iwase R, Uwagawa T, Misawa T, Ohashi T, Yanaga K. Inhibition of nuclear factor-κB enhances the antitumor effect of tumor necrosis factor-α gene therapy for hepatocellular carcinoma in mice. *Surgery* 2013; **154**: 468-478 [PMID: 23972653 DOI: 10.1016/j.surg.2013.05.037]
31 **Lamontagne J**, Steel LF, Bouchard MJ. Hepatitis B virus and microRNAs: Complex interactions affecting hepatitis B virus replication and hepatitis B virus-associated diseases. *World J Gastroenterol* 2015; **21**: 7375-7399 [PMID: 26139985 DOI: 10.3748/wjg.v21.i24.7375]
32 **Xu G**, Gao Z, He W, Ma Y, Feng X, Cai T, Lu F, Liu L, Li W. microRNA expression in hepatitis B virus infected primary treeshrew hepatocytes and the independence of intracellular miR-122 level for de novo HBV infection in culture. *Virology* 2014; **448**: 247-254 [PMID: 24314655 DOI: 10.1016/j.virol.2013.10.016]
33 **Gao P**, Wong CC, Tung EK, Lee JM, Wong CM, Ng IO. Deregulation of microRNA expression occurs early and accumulates in early stages of HBV-associated multistep hepatocarcinogenesis. *J Hepatol* 2011; **54**: 1177-1184 [PMID: 21145831 DOI: 10.1016/j.jhep.2010.09.023]
34 **Liu Y**, Zhao JJ, Wang CM, Li MY, Han P, Wang L, Cheng YQ, Zoulim F, Ma X, Xu DP. Altered expression profiles of microRNAs in a stable hepatitis B virus-expressing cell line. *Chin Med J* (Engl) 2009; **122**: 10-14 [PMID: 19187610]
35 **Wu S**, Xue J, Yang Y, Zhu H, Chen F, Wang J, Lou G, Liu Y, Shi Y, Yu Y, Xia C, Hu Y, Chen Z. Isoliquiritigenin Inhibits Interferon-γ-Inducible Genes Expression in Hepatocytes through Down-Regulating Activation of JAK1/STAT1, IRF3/MyD88, ERK/MAPK, JNK/MAPK and PI3K/Akt Signaling Pathways. *Cell Physiol Biochem* 2015; **37**: 501-514 [PMID: 26315837 DOI: 10.1159/000430372]
36 **Yiwei T**, Hua H, Hui G, Mao M, Xiang L. HOTAIR Interacting with MAPK1 Regulates Ovarian Cancer skov3 Cell Proliferation, Migration, and Invasion. *Med Sci Monit* 2015; **21**: 1856-1863 [PMID: 26117268 DOI: 10.12659/MSM.893528]
37 **Chiarini A**, Liu D, Armato U, Dal Prà I. Bcl10 crucially nucleates the pro-apoptotic complexes comprising PDK1, PKCζ and caspase-3 at the nuclear envelope of etoposide-treated human cervical carcinoma C4-I cells. *Int J Mol Med* 2015; **36**: 845-856 [PMID: 26202083 DOI: 10.3892/ijmm.2015.2290]

P- Reviewer: Ohkoshi S, Rojas E **S- Editor**: Yu J
L- Editor: Filipodia **E- Editor**: Wang CH

World Journal of Gastroenterology

Submit a Manuscript: http://www.wjgnet.com/esps/

World J Gastroenterol 2017 March 14; 23(10): 1796-1803

DOI: 10.3748/wjg.v23.i10.1796

ISSN 1007-9327 (print) ISSN 2219-2840 (online)

ORIGINAL ARTICLE

Basic Study

ECRG2 enhances the anti-cancer effects of cisplatin in cisplatin-resistant esophageal cancer cells *via* upregulation of *p53* and downregulation of *PCNA*

Xin-Fang Hou, Lin-Ping Xu, Hai-Yan Song, Shuai Li, Chen Wu, Ju-Feng Wang

Xin-Fang Hou, Shuai Li, Chen Wu, Ju-Feng Wang, Department of Medical Oncology, Affiliated Cancer Hospital of Zhengzhou University, Henan Cancer Hospital, Zhengzhou 450008, Henan Province, China

Lin-Ping Xu, Department of Science and Research, Affiliated Cancer Hospital of Zhengzhou University, Henan Cancer Hospital, Zhengzhou 450008, Henan Province, China

Hai-Yan Song, Key Laboratory for Medical Tissue Regeneration of Henan Province, College of Basic Medicine, Xinxiang Medical University, Xinxiang 453003, Henan Province, China

Supported by the Public Welfare Project Foundation of Henan Province, No. 20130010.

Institutional review board statement: The study was reviewed and approved by the Henan Cancer Hospital Institutional Review Board.

Conflict-of-interest statement: To the best of our knowledge, no conflict of interest exists.

Data sharing statement: There are no additional data available in relation to this manuscript.

Manuscript source: Unsolicited manuscript

Correspondence to: Dr. Ju-Feng Wang, Professor, Department of Medical Oncology, Affiliated Cancer Hospital of Zhengzhou University, Henan Cancer Hospital, 127 Dongming Road, Zhengzhou 450008, Henan Province, China. 13783583966@163.com

Telephone: +86-371-65587598
Fax: +86-371-65587598

Received: November 30, 2016
Peer-review started: December 2, 2016
First decision: December 19, 2016
Revised: January 6, 2017
Accepted: January 18, 2017
Article in press: January 18, 2017
Published online: March 14, 2017

Abstract

AIM

To explore the anti-tumor effects of esophageal cancer-related gene 2 (ECRG2) in combination with cisplatin (DDP) in DDP-resistant esophageal cancer cells (EC9706/DDP).

METHODS

A drug-resistant cell model was established, with EC9706/DDP cells being treated with ECRG2 and/or DDP. Cell viability was examined by MTT assay. The rate of cell apoptosis was determined by flow cytometry. The mRNA expression levels of proliferating cell nuclear antigen (PCNA), metallothionein (MT), and p53 were determined by RT-PCR and PCNA, while MT and p53 protein expression levels were determined by western blotting.

RESULTS

The anti-proliferative effect of ECRG2 in combination with DDP was superior when compared to ECRG2 or DDP alone. The inhibition rate for the combination reached its peak (51.33%) at 96 h. The early apoptotic rates of the control, ECRG2 alone, DDP alone, and ECRG2 plus DDP groups were 5.71% ± 0.27%, 12.68% ± 0.61%, 14.15% ± 0.87%, and 27.96% ±

0.36%, respectively. Although all treatment groups were significantly different from the control group (P < 0.05), the combination treatment of ECRG2 plus DDP performed significantly better when compared to either ECRG2 or DDP alone (P < 0.05). The combination of ECRG2 and DDP significantly upregulated p53 mRNA and protein levels and downregulated PCNA mRNA and protein levels compared to ECRG2 or DDP alone (P < 0.05). However, no changes were seen in the expression of MT mRNA or protein.

CONCLUSION

ECRG2 in combination with DDP can inhibit viability and induce apoptosis in esophageal cancer DDP-resistant cells, possibly *via* upregulation of *p53* expression and downregulation of *PCNA* expression. These findings suggest that the combination of ECRG2 and DDP may be a promising strategy for the clinical treatment of esophageal cancers that are resistant to DDP.

Key words: Esophageal cancer related-gene 2; Cisplatin; Resistance; p53; Proliferating cell nuclear antigen

Core tip: Cisplatin (DDP) is one of the most effective agents in treating esophageal cancer, but drug resistance poses a major impediment. Combination therapy has become an important method for overcoming drug resistance. This study showed that esophageal cancer-related gene 2 (ECRG2) in combination with DDP can inhibit viability and induce apoptosis in DDP-resistant esophageal cancer cells, possibly *via* upregulation of p53 expression and downregulation of proliferating cell nuclear antigen expression. These findings suggest that the combination of ECRG2 and DDP may be a promising strategy for the clinical treatment of esophageal cancers that are resistant to DDP.

Hou XF, Xu LP, Song HY, Li S, Wu C, Wang JF. *ECRG2* enhances the anti-cancer effects of cisplatin in cisplatin-resistant esophageal cancer cells *via* upregulation of *p53* and downregulation of *PCNA*. *World J Gastroenterol* 2017; 23(10): 1796-1803 Available from: URL: http://www.wjgnet.com/1007-9327/full/v23/i10/1796.htm DOI: http://dx.doi.org/10.3748/wjg.v23.i10.1796

INTRODUCTION

Esophageal cancer is a severe global health problem with an incidence that ranks eighth among all of the malignant cancers[1]. In spite of improvements in early-stage detection, most tumors are already at an advanced stage upon initial diagnosis[2]. Cisplatin (DDP)-based doublets have been the most commonly used treatment regimen for most patients with locally advanced or metastatic esophageal cancer[3-6]. Unfortunately, DDP resistance and dose-limiting side effects have been a challenge to any further improvement of this treatment's efficacy. These obstacles call for a novel combination of therapeutic approaches in order to achieve high therapeutic efficacy at a lower drug dose[7].

Esophageal cancer related gene 2 (ECRG2) was first separated and identified, using the mRNA technique of differential display, in normal esophageal tissues and esophageal cancer tissues in 1998[8]. It has been reported that ECRG2 inhibits tumor cell growth and promotes cell apoptosis *in vivo* and *in vitro*[9,10]. In our previous study, we found that ECRG2 combined with DDP had an enhanced inhibitory effect on EC9706 cell proliferation and an increased inductive effect on EC9706 cell apoptosis when compared to ECRG2 alone[11]. This suggests that ECRG2 may be involved in the drug resistance of esophageal cancer. There are currently no known studies in the literature examining the effects of ECRG2 on the drug resistance of esophageal cancer. In the present study, we established a drug-resistant cell model to explore the effects of ECRG2 on drug resistant cells.

MATERIALS AND METHODS

Cell culture and reagents

PCNA, p53, and MT primers and ECRG2 protein were manufactured by Sangon Biological Engineering Co., Ltd. (Shanghai, China). DDP was bought from Qilu Pharmaceutical Co., Ltd. (Jinan, China). RPMI 1640 medium and fetal bovine serum (FBS) were purchased from HyClone (Logan, UT, United States). 3-[4,5-Dimethylthiazol-2-yl]-2,5-diphenyl tetrazolium bromide (MTT), TRIzol, and annexin V-FITC apoptosis detection kits were purchased from Sigma Co. (St. Louis, MO, United States). The reverse transcription and amplification kits were purchased from Promega Co. (Madison, WI, United States). The rabbit anti-human PCNA and p53 antibodies were purchased from Santa Cruz Biotechnology (Santa Cruz, CA, United States). The rabbit anti-human MT and goat anti-rabbit IgG antibodies were purchased from Abcam (Cambridge, United Kingdom). The human esophageal cancer cell line EC9706 was provided by the tumor cell library of the Academy of Medical Sciences in China.

Establishment of a drug-resistant cell line

We shocked EC9706 cells in the logarithmic phase with a final concentration of 2 mg/L of DDP. We discarded the culture solution after 48 h, washing 3 times with PBS. The cells were cultured in a fresh nutrient solution and washed every 2 d to remove dead cells. When the cells reached stable growth, we increased the DDP concentration, and repeated until the cells maintained growth in a medium with a concentration of 0.5 mg/L of DDP. The cells were cultured in a RPMI-1640 medium containing 10% fetal bovine serum, 100 U/m penicillin,

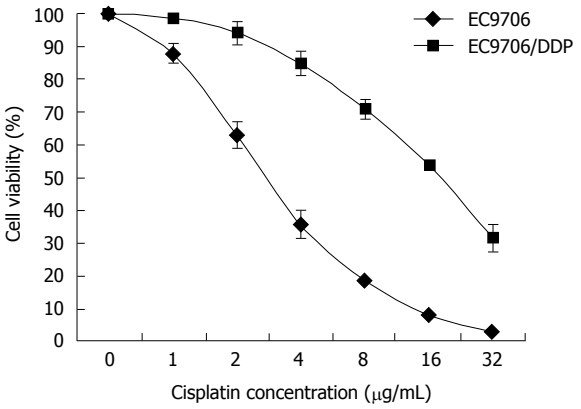

Figure 1 Survival rate of EC9706 and EC9706/cisplatin (DDP) cells treated with various concentrations of DDP. A dose-dependent association between the survival rate of EC9706 and EC9706/DDP cells and the concentration of DDP can be observed. The survival of EC9706 cells was significantly lower compared to EC9706/DDP cells following treatment with various concentrations of DDP. The IC50 of DDP in EC9706 cells is 3.34 ± 0.27 μg/mL, while the IC50 of DDP in EC9706/DDP cells is 16.83 ±1.46 μg/mL.

100 U/mL streptomycin, and 0.5 mL/L DDP in a humidified incubator at 37 ℃ with 5% CO_2.

Cell viability

Drug sensitivity was analyzed by MTT assay. The cells were plated at 1 × 10^3 cells/mL in 96-well plates in a volume of 100 μL and incubated for 24 h. The media were discarded and cells were treated with various concentrations of DDP or ECRG2 for 72 h. A total of 20 μL of 5 g/L MTT solution was added to each well, with cells then being incubated for 4 h at 37 ℃. The medium was discarded and 150 μL of dimethyl sulfoxide was added to each well, which was then shaken to completely dissolve the blue-purple precipitate from the MTT. A microplate reader was used to test the absorbance (OD) of each well at 490 nm and average values were obtained. Cell viability was calculated using the formula: (OD treated well-OD blank)/(OD control well-OD blank) × 100.

Cell apoptosis assay using annexin-V FITC/PI

The cells were seeded in a 6-well plate at a density of 4 × 10^5 cells per well. After overnight attachment, cells were treated with ECRG2 and/or DDP for 24 h. The cells were then harvested by trypsinization, washed with cold PBS, centrifuged at 1 × 10^3 rpm for 5 min, and resuspended in 1 × binding buffer. 500 μL of each sample solution was then added to 5 μL of FITC-conjugated annexin-V and 10 μL of PI, followed by incubation for 15 min in the dark at room temperature. The samples were then measured by flow cytometry.

RNA isolation and RT-PCR

Each group of cells was collected after 24 h of drug treatment. The total RNA was extracted from each group of cells using TRIzol reagent according to the manufacturer's protocol. The cDNA was made *via* the protocol for the Reverse Transcription System for RT-PCR. The primers for PCNA were 5'-ACCGCTGCGACC GCAATTTG-3'(forward) and 5'-ACGTGCAAATTCACC AGAAGGCATC-3'(reverse). The primers for MT were 5'-CGGATCCAGACTCAAACAGGCTTTTAT-3' (forward) and 5'-CGGATCCCGGAATGGACCCCAACTGCT-3' (reverse). The primers for p53 were 5'-ATTTGCGTGTG GAGTATTTGG-3' (forward) and 5'-GCTGTTCCGTCCCAGT AGATTA-3' (reverse). The primers for GAPDH were 5'-TCATGGGTGTGAACCATGAGAA-3' (forward) and 5'-GGCATGGACTGTGGTCATGAG-3' (reverse). PCR amplification was performed using a kit under the following conditions: 95 ℃ for 5 min, followed by 30 cycles at 95 ℃ for 40 s, 55 ℃ for 40 s, and 72 ℃ for 1 min. The expression level of mRNA encoding the p53, PCNA, and MT genes were evaluated and normalized relative to that of GAPDH.

Western blot

The cells were collected from each group and lysed in 200 μL of 1% Tween 20 in PBS by five cycles of freezing and thawing. The insoluble proteins were removed by centrifugation. After quantification of the total protein, the protein was separated on 8% polyacrylamide gel (PAGE), and transferred to a PVDF membrane (Millipore). The membranes were then blocked with 5% non-fat dry milk in PBS-Tween 20 for 1 h at room temperature. After incubation with polyclonal rabbit anti-human MT, PCNA, or p53 antibody overnight at 4 ℃ at a 1:500 dilution, the membranes were incubated with a secondary HRP-conjugated anti-rabbit antibody at a 1:1000 dilution and then washed again three times with PBST buffer. The transferred proteins were visualized using an ECL detection kit according to the manufacturer's protocol.

Statistical analysis

The SPSS 13.0 software system (SPSS, Inc., Chicago, IL, United States) was used for statistical evaluation. The data are expressed as the mean ± SD for at least 3 independent experiments. Statistical significance was evaluated by analysis of variance (ANOVA) with Tukey's post hoc test. A P value of < 0.05 was considered to indicate a statistically significant result.

RESULTS

Establishment of drug-resistant, EC9706/DDP cells

The EC9706/DDP cell line was established after several months of intermittent exposure by the parental cells to a gradually increasing concentration of drugs. After the EC9706 and EC9706/DDP cells were treated with DDP at various concentrations (1, 2, 4, 8, 16, 32 μg/mL) for 48 h, the cell viability rate was examined by MTT assay. As shown in Figure 1, the IC50 for 48 h of DDP in the EC9706/DDP cells was 16.83 ± 1.46 μg/mL and the IC50 for 48 h of DDP in the parental EC9706 cells was 3.34 ± 0.27 μg/mL. Therefore, the EC9706/DDP cells were five times more resistant to DDP compared to the parental cells.

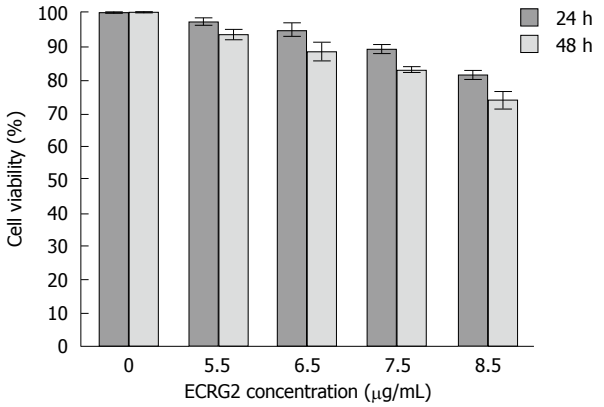

Figure 2 Survival rate at various concentrations of esophageal cancer-related gene 2. A dose- and time- dependent association between the survival rate of the EC9706/cisplatin (DDP) cells and the concentration of ECRG2. A longer incubation time with ECRG2 significantly decreased the survival rate of EC9706/DDP cells. The same was found for treatments with a higher concentration of ECRG2.

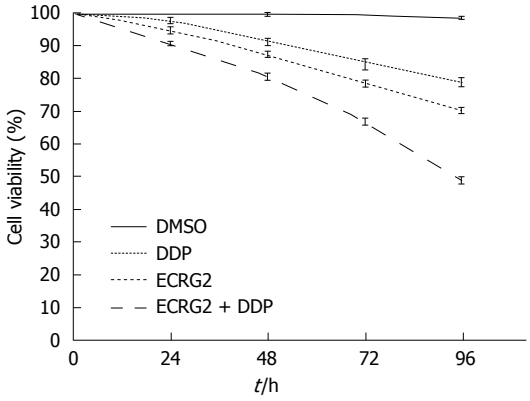

Figure 3 Effects of esophageal cancer-related gene 2 combined with cisplatin (DDP) on cell viability in EC9706/DDP cells. Cells were treated with dimethyl sulfoxide, ECRG2 (6.5 μg/mL) alone, DDP (3 μg/mL) alone, or a combination of ECRG2 (6.5 μg/mL) and DDP (3 μg/mL) for 24 h, 48 h, 72 h, and 96 h. Cell viability was detected *via* MTT assay.

Effects of ECRG2 on the EC9706/DDP cells

To evaluate the effects of ECRG2 on the growth and viability of the cells, the EC9706/DDP cells were treated with various concentrations of ECRG2 (5.5, 6.5, 7.5, 8.5 μg/mL). The growth rate of the cells was found to be inhibited in a dose- and time- dependent manner by the ECRG2 protein (Figure 2).

Effects of combination treatment of ECRG2 and DDP on the EC9706/DDP cells

Based on the results above, we used 3 μg/mL of DDP and 6.5 μg/mL of ECRG2 for 48 h in EC9706/DDP cells for further experiments. As shown in Figure 3, the anti-proliferative effect of ECRG2 in combination with DDP was better compared to ECRG2 or DDP alone. These results suggest that a combination treatment of ECRG2 and DDP resulted in a synergistic decrease in cell viability compared to each treatment alone. The inhibition rate for the combination reached its peak (51.33%) at 96 h (Figure 3).

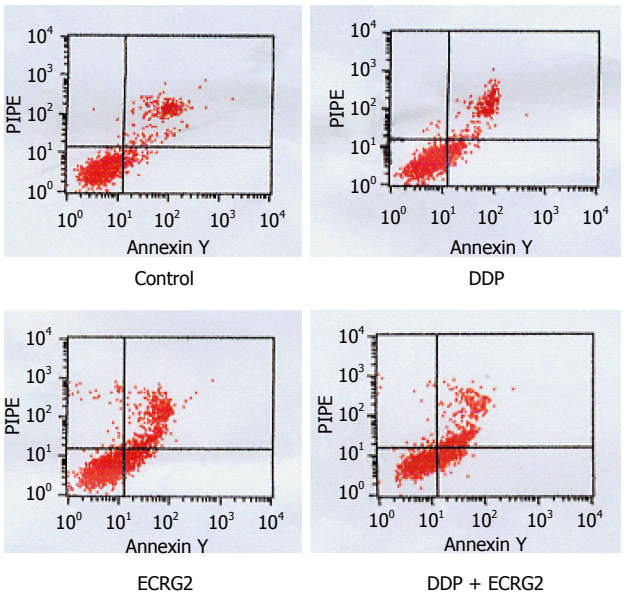

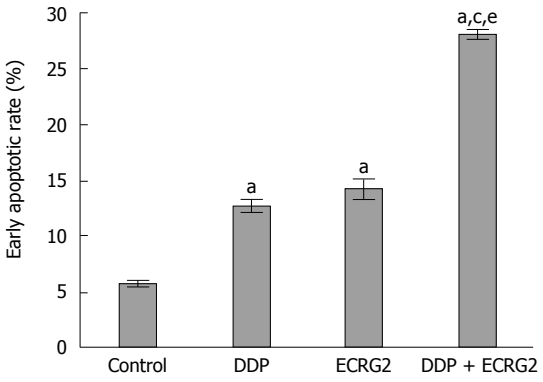

Figure 4 Effects of esophageal cancer-related gene 2 combined with cisplatin (DDP) on cell apoptosis in EC9706/DDP cells. Cells were treated with esophageal cancer-related gene 2 (ECRG2) (6.5 μg/mL) alone, DDP (3 μg/mL) alone, or a combination of ECRG2 and DDP for 24 h. Early apoptosis was determined by flow cytometry using annexin V/PI staining. Annexin V was set as the horizontal axis and PI was set as the vertical axis. Mechanically-damaged cells are located in the upper left quadrant, apoptotic or necrotic cells in the upper right quadrant, dual negative and normal cells in the lower left quadrant, and early apoptotic cells in the lower right quadrant of the flow cytometry dot plot. Data are shown as the mean ± SD. $^{a}P < 0.05$ *vs* control group; $^{c}P < 0.05$ ECRG2 +DDP *vs* DDP; $^{e}P < 0.05$ ECRG2 + DDP *vs* ECRG2.

Effects of ECRG2 and DDP on apoptosis of the EC9706/DDP cells

We next examined the effect of ECRG2 and DDP on cell apoptosis by performing annexin V/PI staining. The early apoptotic rates of the control, ECRG2 alone, DDP alone, and ECRG2 plus DDP groups were 5.71% ± 0.27%, 12.68% ± 0.61%, 14.15% ± 0.87%, and 27.96% ± 0.36%, respectively. Although all treatment groups were significantly different from the control group ($P < 0.05$), the combination treatment of ECRG2 plus DDP performed significantly better when compared to either ECRG2 or DDP alone ($P < 0.05$) (Figure 4).

Effects of ECRG2 and DDP on the expression of PCNA, p53, and MT mRNA

To further elucidate the mechanisms involved in ECRG2

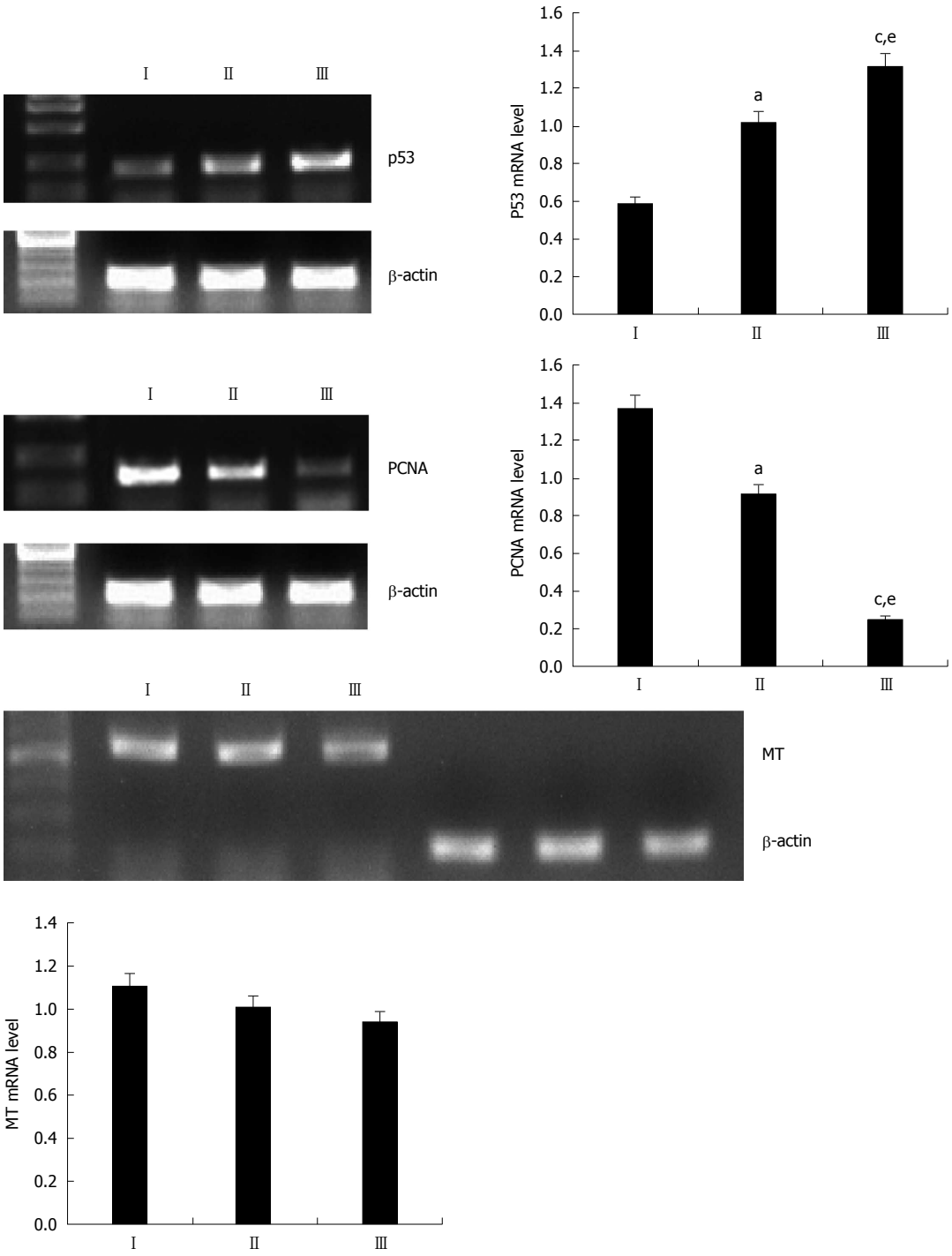

Figure 5 Effects of esophageal cancer-related gene 2 and cisplatin (DDP) on the expression of proliferating cell nuclear antigen, p53, and metallothionein mRNA. Ⅰ: Drug-resistant cell group; Ⅱ: DDP group; Ⅲ: DDP + esophageal cancer-related gene 2 (ECRG2) group. Data were expressed as the mean ± SD, n = 3. $^{a}P < 0.05$ *vs* control; $^{c}P < 0.05$ *vs* control; $^{e}P < 0.05$ *vs* DDP groups.

in combination with DDP on the anti-proliferative effects in drug-resistant cells, the expression of p53, PCNA, and MT mRNA were evaluated in cells using RT-PCR analysis. As shown in Figure 5, 3 μg/mL of DDP upregulated the expression of p53 and downregulated the expression of PCNA ($P < 0.05$). When ECRG2 protein was combined with DDP, p53 mRNA expression significantly increased and PCNA mRNA expression decreased compared to DDP alone ($P < 0.05$). However, changes in the expression of MT mRNA were not observed (Figure 5).

Effects of ECRG2 and DDP on the expression of the PCNA, p53, and MT proteins

As shown in Figure 6, the results of the western blot were consistent with RT-PCR; 3 μg/mL of DDP upregulated the expression of p53 protein and downregulated the expression of PCNA protein. When

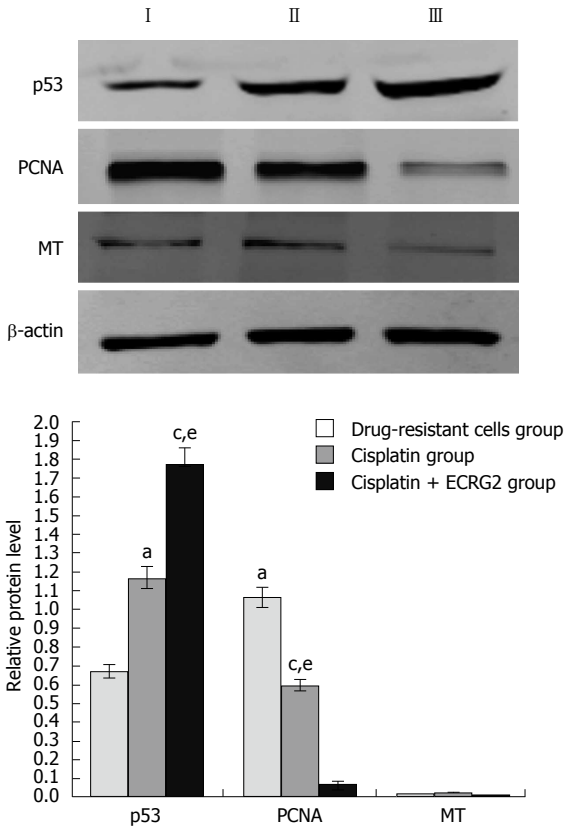

Figure 6 Effects of esophageal cancer-related gene 2 and cisplatin (DDP) on the expression of proliferating cell nuclear antigen, p53, and metallothionein proteins. Ⅰ: Drug-resistant cell group; Ⅱ: DDP group; Ⅲ: DDP + esophageal cancer-related gene 2 (ECRG2) group. Data were expressed as the mean ± SD, $n = 3$. $^{a}P < 0.05$ *vs* control; $^{c}P < 0.05$ *vs* control; $^{e}P < 0.05$ *vs* DDP groups.

ECRG2 protein was combined with DDP, expression of p53 protein was significantly increased and expression of PCNA protein was decreased compared to DDP alone ($P < 0.05$). However, no changes were seen in the expression of MT protein (Figure 6).

DISCUSSION

DDP is one of the most effective anti-cancer agents widely used in the treatment of solid tumors, including esophageal cancer. Despite a consistent rate of initial response, DDP treatment often results in the development of chemoresistance, leading to therapeutic failure. Combination therapy has become an important method of overcoming drug resistance. There have been many attempts to overcome DDP resistance in esophageal cancer cells. Lee *et al*[12] reported that the novel oxygen carrier YQ23 enhanced the DDP response of chemoresistant esophageal tumor xenografts, as well as reducing tumor size and the number of animals with invasive tumors. Lai *et al*[13] provided evidence that 14-3-3σ, or its related DNA repair molecule, is a promising therapeutic target for counteracting DDP resistance in esophageal squamous cell carcinoma. Furthermore, Yu *et al*[14] suggested autophagy is a novel target to improve the efficiency of DDP in human esophageal cancers with acquired resistance.

In this study, we first established an EC9706/DDP cell line derived from *in vitro* treatment of sensitive cells as a model to examine the effect of ECRG2 on DDP resistance. The results demonstrated that a combination of ECRG2 and DDP had synergistic inhibitory effects on the proliferation of EC9706/DDP cells. The inhibition rate was significantly higher in EC9706/DDP cells treated with ECRG2 and DDP compared to cells treated with ECRG2 or DDP alone. This suggests ECRG2 may reduce or inhibit DDP resistance.

The mechanism through which cancer cells develop resistance to chemotherapy is associated with increased resistance to apoptosis. Agents that induce apoptosis have been reported to sensitize tumor cells to DDP[15]. Cui *et al*[9,10] reported that ECRG2 promoted cell apoptosis *in vivo* and *in vitro*. Here, we provided experimental evidence showing the combination of ECRG2 and DDP promoted the apoptosis of esophageal DDP-resistant cancer cells. A study by Li *et al*[16] showed that ECRG2-overexpressing cells had a higher expression of p53. We therefore compared the p53 expression levels of the control, DDP alone, and ECRG2 plus DDP groups. Our results proved that p53 was involved in this process. The pivotal role of p53 pro-apoptotic function in sensitivity to DDP has also recently been reported[17,18]. The tumor suppressor protein p53 has been shown to mediate the cellular stress response, as well as initiate DNA repair, cell-cycle arrest, senescence, and, most notably, apoptosis. However, p53 can also induce DNA-damage, thereby further promoting cell death. Therefore, we believe the combination of ECRG2 and DDP induced overexpression of p53 and then increased the response to DDP by the p53 pro-apoptotic function in esophageal DDP-resistant cancer cells.

In addition to p53, there are other molecules involved in DDP resistance. Dillehay *et al*[19] reported a novel small molecule targeting PCNA-induced DNA damage and apoptosis in prostate cancer cells, as well as enhancing DNA damage and apoptosis triggered by DDP in a p53-independent manner. Expression of PCNA genes in all organisms is traditionally associated with cell proliferation and thus with DNA synthesis during genome replication in the S phase of the cell cycle[20]. However, recent developments in PCNA protein interactions, trimer formation, and signaling regulation allow for the potential of possible therapeutic targeting of PCNA[21]. Both peptides and small molecules targeting PCNA signaling have been reported to sensitize cancer cells to chemotherapeutic agents[22,23]. A PCNA inhibitor can increase DNA double-strand breaks and cause the accumulation of DNA damage, which will eventually lead to cell death in cells that lack the ability to repair this damage[19]. In the present study, we demonstrated that the small

molecule ECRG2 combined with DDP reversed DDP resistance by downregulating PCNA expression in esophageal DDP-resistant cancer cells. However, the underlying molecular mechanisms of this phenomenon require further future exploration.

MT is a low molecular weight protein that is rich in cysteine[24]. In recent years, the relationship between MT and tumors has received increasing attention, including the role of MT in tumor formation and the differentiation, proliferation, and apoptosis of tumor cells and tumor tissue in ammonia chloride DDP chemotherapy drug resistance[25,26]. *In vitro* and *in vivo* studies show that overexpression of MT involved in DDP resistance, MT expression level, and DDP resistance level are related, with MT increasing DDP resistance[27,28]. However, another study demonstrated that the expression of MT was not related to resistance in DDP treatment[29-31]. In this present study, we found no significant change in the expression of MT after increasing DDP and ECRG2. ECRG2 in combination with DDP promotes cell apoptosis and inhibits cell proliferation, but not by reducing the expression of MT.

In conclusion, we showed in the present study that ECRG2 in combination with DDP reduces or inhibits DDP resistance and induces cell apoptosis by upregulating p53 expression and downregulating PCNA expression, but not MT expression. Our results suggest that the combination of ECRG2 and DDP may be a promising strategy for the clinical treatment of esophageal cancers that are resistant to DDP. The effects of combined ECRG2 and DDP treatment on DDP-resistant cancer cells should be further investigated and confirmed in other human cancer cell lines, as well as animal models of cancers.

COMMENTS

Background

Cisplatin (DDP) is one of the most effective agents in esophageal cancer, but drug resistance poses a major impediment. Combination therapy has become an important method of overcoming drug resistance. It has been reported that esophageal cancer-related gene 2 (ECRG2) inhibits tumor cell growth and promotes cell apoptosis. In our previous study, we found ECRG2, in combination with DDP, had an enhanced inhibitory effect on EC9706 cell proliferation and an increased inductive effect on EC9706 cell apoptosis. This suggests that ECRG2 may be involved in the drug resistance of esophageal cancer. Currently, there are no known studies in the literature examining the effects of ECRG2 on the drug resistance of esophageal cancer.

Research frontiers

Drug resistance and dose-limiting side effects have been a challenge to the further improvement of chemotherapy efficacy. These obstacles call for a novel combination of therapeutic approaches. Anticancer drugs may be combined with a broad spectrum of molecules such as small-molecule inhibitors, interfering RNA molecules, microRNA, oncolytic viruses, and naturally occurring substances. The ECRG2/DDP combination presents a very promising treatment approach.

Innovations and breakthroughs

This is the first known study to investigate the synergistic effect of ECRG2 in combination with DDP. In addition, the current study also explores the synergy mechanisms of ECRG2 and DDP in DDP-resistant esophageal cancer cells.

Applications

This study shows that ECRG2 in combination with DDP can inhibit viability and induce apoptosis in esophageal cancer DDP-resistant cells, possibly through upregulation of p53 expression and downregulation of PCNA expression. These findings suggest that the combination of ECRG2 and DDP may be a promising strategy for the clinical treatment of esophageal cancers that are resistant to DDP.

Peer-review

This is an interesting study about ECRG2 enhancing the anticancer effects of DDP in DDP-resistant esophageal cancer cells.

REFERENCES

1 **Torre LA**, Bray F, Siegel RL, Ferlay J, Lortet-Tieulent J, Jemal A. Global cancer statistics, 2012. *CA Cancer J Clin* 2015; **65**: 87-108 [PMID: 25651787 DOI: 10.3322/caac.21262]

2 **Rustgi AK**, El-Serag HB. Esophageal carcinoma. *N Engl J Med* 2014; **371**: 2499-2509 [PMID: 25539106 DOI: 10.1056/NEJMra1314530]

3 **Kim M**, Keam B, Kim TM, Kim HG, Kim JS, Lee SS, Shin SH, Kim MK, Park KU, Kim DW, Yun HJ, Lee JS, Heo DS. Phase II Study of Irinotecan and Cisplatin Combination Chemotherapy in Metastatic, Unresectable Esophageal Cancer. *Cancer Res Treat* 2016; Epub ahead of print [PMID: 27488873 DOI: 10.4143/crt.2016.121]

4 **Millar J**, Scullin P, Morrison A, McClory B, Wall L, Cameron D, Philips H, Price A, Dunlop D, Eatock M. Phase II study of gemcitabine and cisplatin in locally advanced/metastatic oesophageal cancer. *Br J Cancer* 2005; **93**: 1112-1116 [PMID: 16278660 DOI: 10.1038/sj.bjc.6602842]

5 **Almhanna K**, Hoffe S, Strosberg J, Dinwoodie W, Meredith K, Shridhar R. Concurrent chemoradiotherapy with protracted infusion of 5-fluorouracil (5-FU) and cisplatin for locally advanced resectable esophageal cancer. *J Gastrointest Oncol* 2015; **6**: 39-44 [PMID: 25642336 DOI: 10.3978/j.issn.2078-6891.2014.101]

6 **Chang H**, Shin SK, Cho BC, Lee CG, Kim CB, Kim DJ, Lee JG, Hur J, Lee CY, Bae MK, Kim HR, Lee SK, Park JC, Lee H, Kim HI, Chung H, Cha J, Lee YC, Kim JH. A prospective phase II trial of S-1 and cisplatin-based chemoradiotherapy for locoregionally advanced esophageal cancer. *Cancer Chemother Pharmacol* 2014; **73**: 665-671 [PMID: 24562525 DOI: 10.1007/s00280-013-2371-y]

7 **Pavelic J**. Editorial: combined cancer therapy. *Curr Pharm Des* 2014; **20**: 6511-6512 [PMID: 25341927 DOI: 10.2174/1381612820666140826154834]

8 **Su T**, Liu H, Lu S. [Cloning and identification of cDNA fragments related to human esophageal cancer]. *Zhonghua Zhong Liu Za Zhi* 1998; **20**: 254-257 [PMID: 10920976]

9 **Cui YP**, Wang JB, Zhang XY, Bi MX, Guo LP, Lu SH. Using yeast two-hybrid system to identify ECRG2 associated proteins and their possible interactions with ECRG2 gene. *World J Gastroenterol* 2003; **9**: 1892-1896 [PMID: 12970870 DOI: 10.3748/wjg.v9.i9.1892]

10 **Cui Y**, Wang J, Zhang X, Lang R, Bi M, Guo L, Lu SH. ECRG2, a novel candidate of tumor suppressor gene in the esophageal carcinoma, interacts directly with metallothionein 2A and links to apoptosis. *Biochem Biophys Res Commun* 2003; **302**: 904-915 [PMID: 12646258 DOI: 10.1016/S0006-291X(03)00122-0]

11 **Song HY**, Deng XH, Yuan GY, Hou XF, Zhu ZD, Zhou L, Ren MX. Expression of bcl-2 and p53 in induction of esophageal cancer cell apoptosis by ECRG2 in combination with cisplatin. *Asian Pac J Cancer Prev* 2014; **15**: 1397-1401 [PMID: 24606472 DOI: 10.7314/APJCP.2014.15.3.1397]

12 **Lee NP**, Chan KT, Choi MY, Lam HY, Tung LN, Tzang FC, Han H, Lam IP, Kwok SY, Lau SH, Man C, Tong DK, Wong BL, Law S. Oxygen carrier YQ23 can enhance the chemotherapeutic drug responses of chemoresistant esophageal tumor xenografts. *Cancer Chemother Pharmacol* 2015; **76**: 1199-1207 [PMID: 26553104 DOI: 10.1007/s00280-015-2897-2]

13 **Lai KK**, Chan KT, Choi MY, Wang HK, Fung EY, Lam HY, Tan W, Tung LN, Tong DK, Sun RW, Lee NP, Law S. 14-3-3σ confers cisplatin resistance in esophageal squamous cell carcinoma cells via regulating DNA repair molecules. *Tumour Biol* 2016; **37**: 2127-2136 [PMID: 26346170 DOI: 10.1007/s13277-015-4018-6]

14 **Yu L**, Gu C, Zhong D, Shi L, Kong Y, Zhou Z, Liu S. Induction of autophagy counteracts the anticancer effect of cisplatin in human esophageal cancer cells with acquired drug resistance. *Cancer Lett* 2014; **355**: 34-45 [PMID: 25236911 DOI: 10.1016/j.canlet.2014.09.020]

15 **Zhang R**, Li Y, Dong X, Peng L, Nie X. MiR-363 sensitizes cisplatin-induced apoptosis targeting in Mcl-1 in breast cancer. *Med Oncol* 2014; **31**: 347 [PMID: 25416050 DOI: 10.1007/s12032-014-0347-3]

16 **Li MN**, Huang G, Guo LP, Lu SH. [Inhibitory effects of esophageal cancer related gene 2 on proliferation of human esophageal cancer cell EC9706]. *Zhonghua Yi Xue Za Zhi* 2005; **85**: 2785-2788 [PMID: 16324322]

17 **Huang H**, Chen AY, Ye X, Li B, Rojanasakul Y, Rankin GO, Chen YC. Myricetin inhibits proliferation of cisplatin-resistant cancer cells through a p53-dependent apoptotic pathway. *Int J Oncol* 2015; **47**: 1494-1502 [PMID: 26315556 DOI: 10.3892/ijo.2015.3133]

18 **Li X**, Huang JM, Wang JN, Xiong XK, Yang XF, Zou F. Combination of chrysin and cisplatin promotes the apoptosis of Hep G2 cells by up-regulating p53. *Chem Biol Interact* 2015; **232**: 12-20 [PMID: 25770930 DOI: 10.1016/j.cbi.2015.03.003]

19 **Dillehay KL**, Lu S, Dong Z. Antitumor effects of a novel small molecule targeting PCNA chromatin association in prostate cancer. *Mol Cancer Ther* 2014; **13**: 2817-2826 [PMID: 25253786 DOI: 10.1158/1535-7163.MCT-14-0522]

20 **Strzalka W**, Ziemienowicz A. Proliferating cell nuclear antigen (PCNA): a key factor in DNA replication and cell cycle regulation. *Ann Bot* 2011; **107**: 1127-1140 [PMID: 21169293 DOI: 10.1093/aob/mcq243]

21 **Wang SC**. PCNA: a silent housekeeper or a potential therapeutic target? *Trends Pharmacol Sci* 2014; **35**: 178-186 [PMID: 24655521 DOI: 10.1016/j.tips.2014.02.004]

22 **Inoue A**, Kikuchi S, Hishiki A, Shao Y, Heath R, Evison BJ, Actis M, Canman CE, Hashimoto H, Fujii N. A small molecule inhibitor of monoubiquitinated Proliferating Cell Nuclear Antigen (PCNA) inhibits repair of interstrand DNA cross-link, enhances DNA double strand break, and sensitizes cancer cells to cisplatin. *J Biol Chem* 2014; **289**: 7109-7120 [PMID: 24474685 DOI: 10.1074/jbc.M113.520429]

23 **Yu YL**, Chou RH, Liang JH, Chang WJ, Su KJ, Tseng YJ, Huang WC, Wang SC, Hung MC. Targeting the EGFR/PCNA signaling suppresses tumor growth of triple-negative breast cancer cells with cell-penetrating PCNA peptides. *PLoS One* 2013; **8**: e61362 [PMID: 23593472 DOI: 10.1371/journal.pone.0061362]

24 **Mehus AA**, Muhonen WW, Garrett SH, Somji S, Sens DA, Shabb JB. Quantitation of human metallothionein isoforms: a family of small, highly conserved, cysteine-rich proteins. *Mol Cell Proteomics* 2014; **13**: 1020-1033 [PMID: 24493013 DOI: 10.1074/mcp.M113.033373]

25 **Tian ZQ**, Xu YZ, Zhang YF, Ma GF, He M, Wang GY. Effects of metallothionein-3 and metallothionein-1E gene transfection on proliferation, cell cycle, and apoptosis of esophageal cancer cells. *Genet Mol Res* 2013; **12**: 4595-4603 [PMID: 24222235 DOI: 10.4238/2013]

26 **Zamirska A**, Matusiak Ł, Dziegiel P, Szybejko-Machaj G, Szepietowski JC. Expression of metallothioneins in cutaneous squamous cell carcinoma and actinic keratosis. *Pathol Oncol Res* 2012; **18**: 849-855 [PMID: 22407324 DOI: 10.1007/s12253-012-9513-0]

27 **Kelley SL**, Basu A, Teicher BA, Hacker MP, Hamer DH, Lazo JS. Overexpression of metallothionein confers resistance to anticancer drugs. *Science* 1988; **241**: 1813-1815 [PMID: 3175622 DOI: 10.1126/science.3175622]

28 **Kennette W**, Collins OM, Zalups RK, Koropatnick J. Basal and zinc-induced metallothionein in resistance to cadmium, cisplatin, zinc, and tertbutyl hydroperoxide: studies using MT knockout and antisense-downregulated MT in mammalian cells. *Toxicol Sci* 2005; **88**: 602-613 [PMID: 16150881 DOI: 10.1093/toxsci/kfi318]

29 **Surowiak P**, Kaplenko I, Spaczyński M, Zabel M. The expression of metallothionein (MT) and proliferation intensity in ovarian cancers treated with cisplatin and paclitaxel. *Folia Morphol* (Warsz) 2003; **62**: 493-495 [PMID: 14655150]

30 **Tuzel E**, Yorukoglu K, Ozkara E, Kirkali Z. Association of metallothionein expression and clinical response to cisplatin based chemotherapy in testicular germ cell tumors. *Cent European J Urol* 2015; **68**: 45-50 [PMID: 25914837 DOI: 10.5173/ceju.2015.01.486]

31 **Gansukh T**, Donizy P, Halon A, Lage H, Surowiak P. In vitro analysis of the relationships between metallothionein expression and cisplatin sensitivity of non-small cellular lung cancer cells. *Anticancer Res* 2013; **33**: 5255-5260 [PMID: 24324058]

P- Reviewer: Kantsevoy S, Ong J, Tokunaga Y **S- Editor**: Qi Y
L- Editor: Rutherford A **E- Editor**: Wang CH

World Journal of Gastroenterology

Submit a Manuscript: http://www.wjgnet.com/esps/

World J Gastroenterol 2017 March 14; 23(10): 1804-1815

DOI: 10.3748/wjg.v23.i10.1804

ISSN 1007-9327 (print) ISSN 2219-2840 (online)

ORIGINAL ARTICLE

Basic Study

Therapeutic effect of curcumin on experimental colitis mediated by inhibiting $CD8^+CD11c^+$ cells

Hai-Mei Zhao, Fei Han, Rong Xu, Xiao-Ying Huang, Shao-Min Cheng, Min-Fang Huang, Hai-Yang Yue, Xin Wang, Yong Zou, Han-Lin Xu, Duan-Yong Liu

Hai-Mei Zhao, Shao-Min Cheng, School of Basic Medical Sciences, Jiangxi University of Traditional Chinese Medicine, Nanchang 330004, Jiangxi Province, China

Fei Han, College of Pharmacy, Jiangxi University of Traditional Chinese Medicine, Nanchang 330004, Jiangxi Province, China

Fei Han, Han-Lin Xu, College of Pharmacy, Hubei University of Traditional Chinese Medicine, Wuhan 430065, Hubei Province, China

Rong Xu, Min-Fang Huang, Hai-Yang Yue, Xin Wang, Yong Zou, Department of Postgraduate, Jiangxi University of Traditional Chinese Medicine, Nanchang 330004, Jiangxi Province, China

Xiao-Ying Huang, Key Laboratory of Modern Preparation of TCM, Ministry of Education, Jiangxi University of Traditional Chinese Medicine, Nanchang 330004, Jiangxi Province, China

Han-Lin Xu, Collaborative Innovation Center of TCM of New Products for Geriatrics, Wuhan 430065, Hubei Province, China

Duan-Yong Liu, Science and Technology College, Jiangxi University of Traditional Chinese Medicine, Nanchang 330004, Jiangxi Province, China

Author contributions: Zhao HM and Han F contributed equally to this work as joint first authors; Zhao HM and Liu DY designed the research; Zhao HM, Han F, Xu R, Huang XY, Cheng SM, Huang MF, Yue HY, Wang X and Zou Y performed the research; Liu DY contributed the new reagents and analytic tools; Zhao HM, Huang XY, Xu HL and Liu DY analyzed the data; Zhao HM and Liu DY wrote the paper.

Supported by the National Natural Science Foundation of China, No. 81260595 and No. 81460679; Chinese Scholarship Council and Jiangxi Province as visiting scholar, No. 201408360106 and No. 201408360110; the Traditional Chinese Medicine Project of Health Department of Jiangxi Province, No. 2015B049; and Jiangxi University of Traditional Chinese Medicine, No. JZYC15S13.

Institutional animal care and use committee statement: All animals were housed in a pathogen-free environment at the animal facilities [No. SYXK (Gan) 2005-0001] of Jiangxi University of Traditional Chinese Medicine. The experimental protocols (JZ2015-16) were approved by Biomedical Ethics Committee of Jiangxi University of Traditional Chinese Medicine, Nanchang, China.

Conflict-of-interest statement: All authors have declared that there is no conflict of interest related to this study.

Data sharing statement: No additional unpublished data are available.

Manuscript source: Invited manuscript

Correspondence to: Duan-Yong Liu, Associate Professor, Science and Technology College, Jiangxi University of Traditional Chinese Medicine, 819 Xingwan Road, Nanchang 330004, Jiangxi Province, China. liuduanyong@163.com
Telephone: +86-791-83769126
Fax: +86-791-83769126

Received: October 22, 2016
Peer-review started: October 25, 2016
First decision: December 2, 2016
Revised: December 25, 2016
Accepted: January 17, 2017
Article in press: January 17, 2017
Published online: March 14, 2017

Abstract

AIM

To verify whether curcumin (Cur) can treat inflammatory bowel disease by regulating $CD8^+CD11c^+$ cells.

METHODS

We evaluated the suppressive effect of Cur on $CD8^+CD11c^+$ cells in spleen and Peyer's patches (PPs) in colitis induced by trinitrobenzene sulfonic acid. Mice with colitis were treated by 200 mg/kg Cur for 7 d. On day 8, the therapeutic effect of Cur was evaluated by visual assessment and histological examination, while co-stimulatory molecules of $CD8^+CD11c^+$ cells in the spleen and PPs were measured by flow cytometry. The levels of interleukin (IL)-10, interferon (IFN)-γ and transforming growth factor (TGF)-β1 in spleen and colonic mucosa were determined by ELISA.

RESULTS

The disease activity index, colon weight, weight index of colon and histological score of experimental colitis were obviously decreased after Cur treatment, while the body weight and colon length recovered. After treatment with Cur, $CD8^+CD11c^+$ cells were decreased in the spleen and PPs, and the expression of major histocompatibility complex Ⅱ, CD205, CD40, CD40L and intercellular adhesion molecule-1 was inhibited. IL-10, IFN-γ and TGF-β1 levels were increased compared with those in mice with untreated colitis.

CONCLUSION

Cur can effectively treat experimental colitis, which is realized by inhibiting $CD8^+CD11c^+$ cells.

Key words: CD8; CD11c; Curcumin; Experimental colitis; Therapeutic effect

Core tip: CD11c is highly expressed in $CD8^+$ and $CD8^-$ dendritic cells (DCs). Overaccumulation of $CD8^+$ DCs is seen in colonic mucosa in experimental colitis and patients with inflammatory bowel disease (IBD). $CD8^+CD11c^+$ cells may be a potential strategy to explore the mechanism of action of drugs in IBD. The immunosuppressant curcumin (Cur) plays a therapeutic role in various immune diseases, including IBD and rheumatoid arthritis. However, it is unclear whether Cur regulates level of $CD8^+CD11c^+$ cells to treat IBD. We found that the therapeutic effect of Cur in experimental colitis was closely related to decreased levels of $CD8^+CD11c^+$ cells.

Zhao HM, Han F, Xu R, Huang XY, Cheng SM, Huang MF, Yue HY, Wang X, Zou Y, Xu HL, Liu DY. Therapeutic effect of curcumin on experimental colitis mediated by inhibiting $CD8^+CD11c^+$ cells. *World J Gastroenterol* 2017; 23(10): 1804-1815 Available from: URL: http://www.wjgnet.com/1007-9327/full/v23/i10/1804.htm DOI: http://dx.doi.org/10.3748/wjg.v23.i10.1804

INTRODUCTION

As one of integrin family, CD11c is a type Ⅰ transmembrane protein that mediates adherence between leukocytes and endothelial cells, and participates in exudation and phagocytosis of leukocytes. It is suggested that CD11c induces tissue injury and the inflammatory response[1]. Importantly, CD11c is a specific marker in dendritic cells (DCs) and is highly expressed in $CD8^+$ and $CD8^-$ DCs[2].

As professional antigen-presenting cells, DC precursors capture antigens and promote T-cell migration to regions of the draining lymph nodes where they can mature into functional DCs and present antigens to initiate T-cell-mediated immune responses[3]. Increasingly, it has been reported that DCs are critical to maintaining intestinal immunity and mucosal immune tolerance to resist the pathogenicity of commensal microorganisms, which is one of the pivotal inflammatory etiologies of induced inflammatory bowel diseases (IBD)[4].

High expression of co-stimulatory molecules and major histocompatibility complex (MHC) Ⅱ of DCs, which is a known marker of DC maturation, and a "danger signal" of induced inflammatory mucosal damage in the gut, occurs in the colonic mucosa of animal models of colitis[5,6]. Moreover, DCs can develop from both myeloid and lymphoid progenitors. In mice, $CD8^+$ DCs have been designated as lymphoid DCs, and $CD8^-$ DCs as myeloid DCs[7]. More importantly, $CD8^+$ DCs predominantly stimulate T helper (Th)1-inducing cytokines such as interleukin (IL)-12p70 and IL-12p40, which can lead to Th1 differentiation[8], and have been reported to play a key role in controlling viral infection[3,9,10]. Overaccumulation of $CD8^+$ DCs induces inflammatory injury in the colonic mucosa when they migrate into Peyer's patches (PPs) in experimental colitis and IBD patients[11,12]. Thus, $CD8^+$ DCs may be a potential therapeutic target to explore the mechanisms of clinical treatment of IBD.

Many studies have indicated that CD11c expressed in DCs can promote maturation and activation of DCs; present antigen for $CD4^+$ or $CD8^+$ T cells; accelerate T-cell activation and proliferation; and produce various cytokines[13-15]. $CD11c^+$ DCs are depleted by diphtheria toxin during treatment of experimental colitis, induced indirectly by $CD4^+$ $CD62L^+$ T cells, with oligodeoxynucleotides containing unmethylated cytosine-guanosine[16]. These results suggest that $CD11c^+$ DCs play an important role in the pathogenetic process of IBD.

Curcumin (Cur) is the major constituent of turmeric powder that is extracted from the rhizomes of *Curcuma longa* L. Cur has a long history of

Table 1 Scoring of disease activity index

Score	Decrease in growth or weight loss	Stool consistency	Occult/gross rectal bleeding
0	0%	Normal	Normal
1	1%-5%	Normal	Occult blood+
2	5%-10%	Loose stools	Occult blood++
3	10%-15%	Loose stools	Occult blood+++
4	> 15%	Diarrhea	Gross bleeding

effectively treating chronic colitis by blocking nuclear factor-κB signaling in human IBD and experimental colitis, including trinitrobenzene sulfonic acid (TNBS)-induced and dextran sulfate sodium (DSS)-induced experimental colitis[17-19]. Multifunctional Cur has exhibited antioxidant, anti-inflammatory, antimutagenic, and anticarcinogenic activities, as well as antiplatelet, hypoglycemic, cholesterol-lowering, antibacterial, wound-healing and antifungal effects[17,20-22]. In addition, Shirley *et al*[23], have shown that Cur prevents DCs from responding to immunostimulants and DC-mediated induction of $CD4^+$ T-cell proliferation by blocking maturation marker expression, cytokine and chemokine expression, and reducing migration and endocytosis. Shirley *et al*[23] also concluded that Cur might play a therapeutic role as an immunosuppressant in the treatment of various immune diseases including IBD and rheumatoid arthritis. In our previous study, we found that Cur repaired colonic structure, decreased colonic weight and histological injury score, and recovered colonic length, indicating that Cur restored damaged colonic mucosa in mice with TNBS-induced colitis[24]. However, it is unclear whether Cur can regulate the expression levels of $CD8^+CD11c^+$ cells to treat IBD.

In the present study, we investigated the effects of Cur on $CD8^+CD11c^+$ cells in the spleen and PPs in a murine model of TNBS-induced colitis to explore the possible therapeutic mechanisms of Cur in experimentally induced IBD.

MATERIALS AND METHODS

Mice

Nine to twelve-week-old male C57BL/6 mice (20-24 g) were purchased from the Animal Center of Peking University Health Science Center (Animal Certificate No.: SCXK 2012-0001). Mice were housed in a special room with a humidity of 50% ± 5% and an equal 12-h light/dark cycle at 20 ± 2 ℃ throughout the experimental period. Animals were allowed free access to a commercial diet and clean water *ad libitum*. All animals were allowed to acclimatize for 4 d before the start of the experiment. The experimental protocols (JZ2015-016) were approved by the Biomedical Ethics Committee Experimental Animal Ethics Branch of Jiangxi University of Traditional Chinese Medicine.

Induction of experimental colitis

Colitis was induced according to the procedure described previously by Huang *et al*[25], Sałaga *et al*[26], Fina *et al*[27] and Bai *et al*[28]. Mice were fasted for 12 h. Each mouse was anesthetized with pentobarbital sodium (40 mg/kg), following which, 100 mg/kg TNBS (Sigma-Aldrich, St. Louis, MO, United States; 100 g/L dissolved in 0.3 mL 50% ethanol) was instilled *via* a rubber catheter that was inserted approximately 4 cm into the colon *via* the anus. The rubber catheter was modified with numerous holes positioned over the final 4 cm of its length. The instillation procedure required only a few seconds, following which the mice were maintained in a head-down position for 5 min to prevent solution leakage. Mice in the Normal group received 50% ethanol of the same volume that was delivered using the same technique as described above.

Treatment protocols

To explore the effect of Cur (purity ⩾ 95% by HPLC; Gangrun Biotechnology, Nanjing, China) on $CD8^+CD11c^+$ cells in colitis mice, C57BL/6 mice (20-24 g) were randomized into four groups of eight with comparable average body weight: Normal group (receiving ethanol only, and not treated); TNBS group (received TNBS and were not treated); TNBS + Cur group [received TNBS and 100 mg/kg/d Cur intragastrically (i.g.)]; and TNBS + mesalazine (Mes) group (received TNBS and mesalazine at 300 mg/kg/d i.g.). Before administration, Cur was dissolved in 5% dimethylsulfoxide (DMSO) in physiological saline, which was used as a vehicle. Twenty-four hours after colitis was induced, mice in the TNBS + Cur group were administered Cur, and in the TNBS + Mes group, they were administered Mes for 7 d until the mice were killed. Mice in the Normal and TNBS groups received the same volume of 5% DMSO in physiological saline daily (which was the vehicle for Cur) until the end of the experiment.

Assessment of severity of colitis: disease activity index

Disease activity index (DAI) was analyzed according to the previous study[29,30], which was the combined score of weight loss, stool consistency, and bleeding. The criteria for DAI scores are described in Table 1. The changes in growth rate, stool consistency, and gross bleeding or occult blood in the feces were scored daily from 0 to 4 for each animal after TNBS treatment.

Evaluation of colonic damage

On day 8, all mice were killed after being anesthetized with pentobarbital sodium (40 mg/kg) by intraperitoneal injection. The colon was removed rapidly and its length was measured, opened longitudinally, rinsed with phosphate-buffered saline (PBS), assessed immediately for weight, and the weight index of the colon was calculated (colonic

weight/body weight × 100%). Segments of the colon were fixed in 4% paraformaldehyde for at least 7 d. Subsequently, colon tissues were dehydrated, embedded in paraffin, sectioned at 5 μm and mounted onto slides. These sections were stained with hematoxylin and eosin.

A histological damage score was determined according to the criteria of Nicole and Schmidt *et al*[31]. The histological score included inflammatory cell infiltration and tissue damage. Scores for infiltration were as follows: 0: no infiltration; 1: increased number of inflammatory cells in the lamina propria; 2: inflammatory cells extending into the submucosa; and 3: transmural inflammatory cell infiltration. The scores of tissue damage were as follows: 0: no mucosal damage; 1: discrete epithelial lesions; 2: erosions or focal ulcerations; and 3: severe mucosal damage with extensive ulceration extending into the bowel wall.

Isolation of lymphocyte from spleen and PPs

PPs were separated and collected from the small intestine to the terminal rectum. To prepare single-cell suspensions, spleens or PPs were minced and digested in 2 mg/mL collagenase D (Roche Diagnostics, Basel Switzerland) in 1% fetal calf serum (FCS)/RPMI 1640 for 15 min at 37 ℃. Next, 10 mM EDTA was added for the last 5 min, and the cell suspensions were then pipetted up and down several times and filtered through a fine-mesh sieve. The cell suspensions were centrifuged at 380 × *g* at 4 ℃ for 5 min and suspended at a density of 10^6-10^7/mL in 3% FCS/PBS. Remnant supernatants of spleen and PPs were used separately to analyze the levels of cytokines by ELISA.

Assay of $CD8^+CD11c^+$ cells by flow cytometry

After removal of RBC, splenic and PPs cells were labeled with V450-anti-mouse $CD8a^+$antibody (0.125 μg/100 μL; BD Biosciences, San Jose, CA, United States) and APC/Cy7 anti-mouse CD11c (eBioscience, San Diego, CA, United States), respectively, at 37 ℃ in the dark. Cells were centrifuged at 380 × *g* at 4 ℃ for 5 min, and fixed in 1% paraformaldehyde/PBS. In addition, fluorescence-activated cell sorting analysis was performed on a FACSCalibur flow cytometer (BD Biosciences).

Measurement of co-stimulatory molecules of $CD8^+CD11c^+$ cells by flow cytometry

Cell suspensions were stained according to the appropriate isotypic control antibody match of different fluorochromes and incubated for 30 min with V450-anti-mouse $CD8a^+$ antibody (0.125 μg/100 μL; BD Biosciences), APC/Cy7 anti-mouse CD11c (eBioscience), PerCP/Cy5.5 anti-mouse I-A/I-E (MHC Ⅱ), PE anti-mouse CD40, APC anti-mouse CD154 (*i.e.*, CD40 ligand), FITC anti-mouse CD54, and PerCP/Cy5.5 anti-mouse CD205. Limits for the quadrant markers were based on negative populations and isotype controls.

ELISA

The levels of IL-10, IFN-γ and TGF-β1 in spleen and colonic mucosa supernatants were measured using ELISA (eBioscience).

Statistical analysis

Data were expressed as mean ± SEM. The statistical significance was evaluated by analysis of variance followed by Tukey's test for multiple comparisons using GraphPad Prism version 5.0 (La Jolla, CA, United States). Nonparametric data were analyzed with the Mann-Whitney *U* test. $P < 0.05$ was considered statistically significant.

RESULTS

Cur attenuated TNBS-induced colitis

The body weight of mice and the disease activity index of experimental colitis in the TNBS group were significantly decreased compared with the Normal, TNBS + Cur and TNBS + Mes groups (Figure 1B and C). Colonic weight and the weight index of the colon from the TNBS groups were higher than those in the Normal group, but lower than in the TNBS + Cur and TNBS + Mes groups (Figure 1D and E). However, the colonic length in the colitis mice was shorter in the TNBS group compared with the Normal, TNBS + Cur, and TNBS + Mes groups (Figure 1A and G). Histological evaluation of colonic sections from untreated mice with colitis showed that TNBS-induced colitis was characterized by a loss of mucosal architecture, thickening of the colon wall, cryptic abscesses, ulcer formation, and extensive inflammatory cell infiltration in the colonic mucosa (Figure 1F). Treatment with Cur and Mes inhibited these pathological symptoms and and kept histo-progressive restoration, reduced inflammatory cell infiltration in the mucosa and submucosa, and maintained the integrity of colonic mucosa (Figure 1F). We observed visually ulceration, hyperemia and edema in the colonic mucosa in colitis mice without treatment, which were ameliorated in mice treated with Cur and Mes (Figure 1A). Moreover, the histological scores in the colon of mice from the Normal, TNBS + Cur, and TNBS + Mes groups were significantly lower than those in untreated mice with colitis (Figure 1F and H). All results demonstrated that Cur effectively treated experimental colitis.

Cur inhibited levels of $CD8^+CD11c^+$ cells in spleen and PPs in colitis mice

We analyzed the numbers of $CD8^+CD11c^+$ cells in the spleen and PPs of mice with colitis (Figure 2). Data clearly indicated a significantly increased tendency in this parameter in the spleen (Figure 2A and D) and PPs (Figure 2A and C) in the TNBS group as compared with the Normal group. Significantly, after 7 d treatment

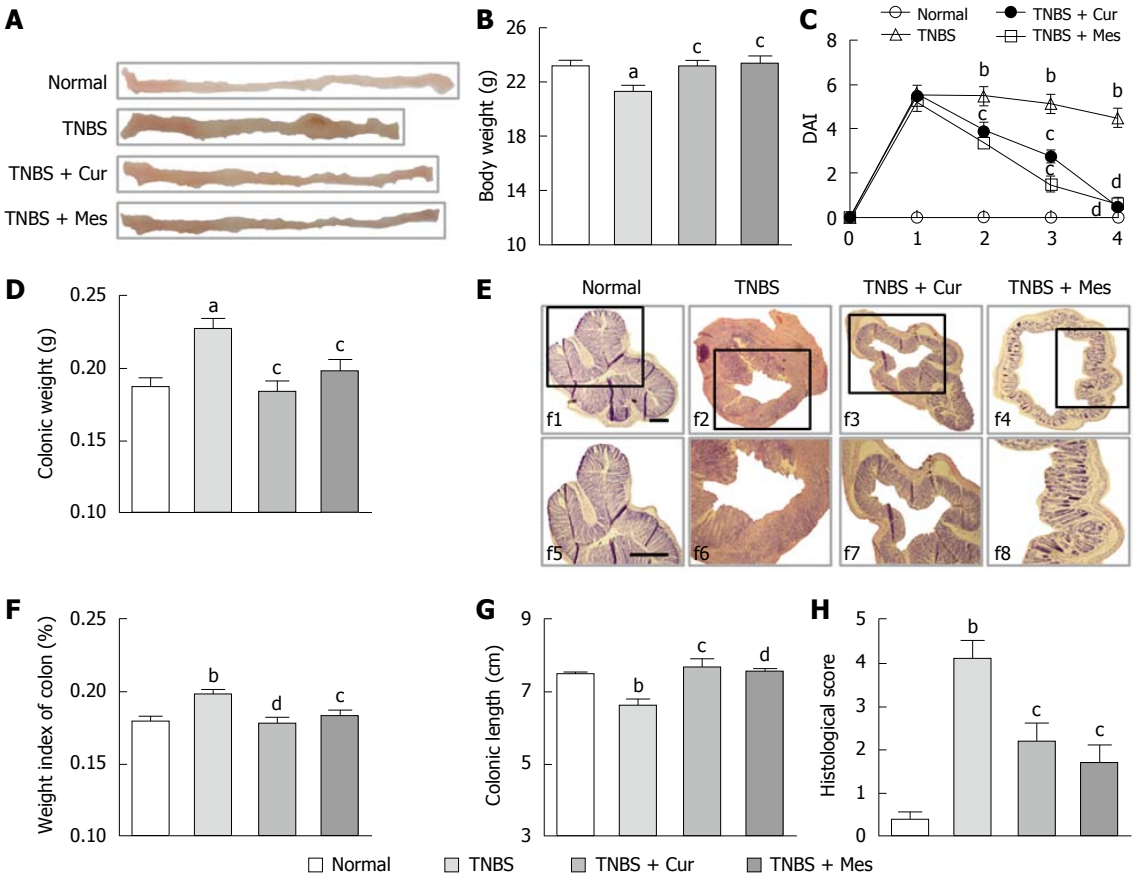

Figure 1 Macroscopic and microscopic observation. A: Macrography of the opened colon; B: Body weight; C: DAI score; D: Colonic weight; E: Weight index of the colon; F: Typical histological images stained by hematoxylin and eosin, f1-4: Bar = 40 μm, f5-8: Bar = 100 μm; G: Colonic length; H: Histological scores. Data are presented as mean ± SEM (n = 8). $^aP < 0.05$ and $^bP < 0.01$ *vs* Normal group; $^cP < 0.05$ and $^dP < 0.01$ *vs* TNBS group.

with Cur, the numbers of CD8$^+$CD11c$^+$ cells in the spleen and PPs in the TNBS + Cur and TNBS + Mes groups were decreased dramatically as compared with the TNBS group.

Cur increased IL-10, IFN-γ and TGF-β1 secretion in spleen and colonic mucosa in colitis mice

To understand the effects of activated CD8$^+$CD11c$^+$ cells in the development of murine colitis, the secretion of IL-10, IFN-γ and TGF-β1 was determined (Figure 3). There was significantly increased expression of TGF-β1 in the colonic mucosa of untreated colitis mice (Figure 3B). In addition, the secretion of TGF-β1 in the colonic mucosa in the TNBS + Cur and TNBS + Mes groups was lower than that in the TNBS group. However, expression of TGF-β1 in the spleen of mice treated with Cur and Mes was higher than that in the TNBS group compared with the Normal group, levels of IFN-γ (Figure 3B and E) and IL-10 (Figure 3C and F) in the spleen and colonic mucosa in untreated colitis mice were decreased 7 d after TNBS-induced colitis. In the colonic mucosa and spleen, the expression of both IL-10 and IFN-γ was increased in colitis mice treated with Cur and Mes as compared with untreated colitis mice.

Cur suppressed expression of co-stimulatory molecules of CD8$^+$CD11c$^+$ cells in colitis mice

Expression of co-stimulatory molecules of CD8$^+$CD11c$^+$ cells, including CD40 (Figure 4), CD40L (Figure 5), CD54 (Figure 6), CD205 (Figure 7) and MHC Ⅱ (Figure 8), was detected in normal spleen and PPs. Expression increased after TNBS-induced colitis. Treatment with Cur decreased expression of CD40 (Figure 4), CD40L (Figure 5), CD54 (Figure 6), CD205 (Figure 7) and MHC Ⅱ (Figure 8) in the spleen and PPs.

DISCUSSION

In the present study, the DAI, colonic weight, weight index of the colon, and histological score of colonic of experimental colitis were significantly decreased after Cur treatment, while the body weight and colonic length were recovered. The results indicate that Cur can effectively treat experimental colitis. The numbers of CD8$^+$CD11C$^+$ cells in the spleen and PPs were decreased, which showed that the therapeutic effect of Cur on colitis was related to the number of CD8$^+$CD11C$^+$ cells.

As a positive regulatory factor, CD11c, which is an adhesion molecule in the CD11/CD18 family,

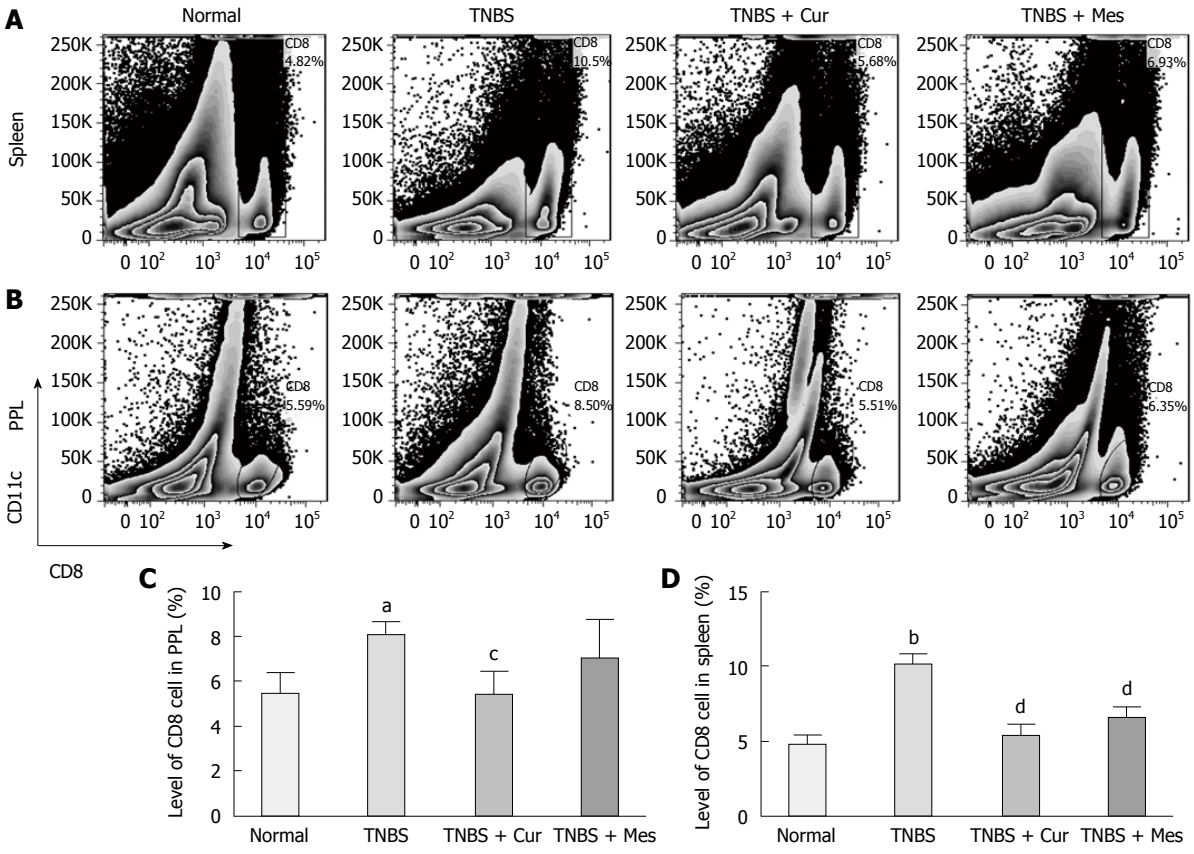

Figure 2 Typical histograms and levels of CD8⁺CD11c⁺ cells in the spleen and PPs. A: Typical graphs and mean fluorescence intensity (MFI) levels of CD8⁺CD11c⁺ cells in the spleen; B: Typical graphs and MFI levels of CD8⁺CD11c⁺ cells in PPs; C: MFI levels of CD8⁺CD11c⁺ cells in the spleen; D: MFI levels of CD8⁺CD11c⁺ cells in PPs. Data are shown as mean ± SEM (n = 8). $^{a}P < 0.05$ and $^{b}P < 0.01$ *vs* Normal group; $^{c}P < 0.05$ and $^{d}P < 0.01$ *vs* TNBS group.

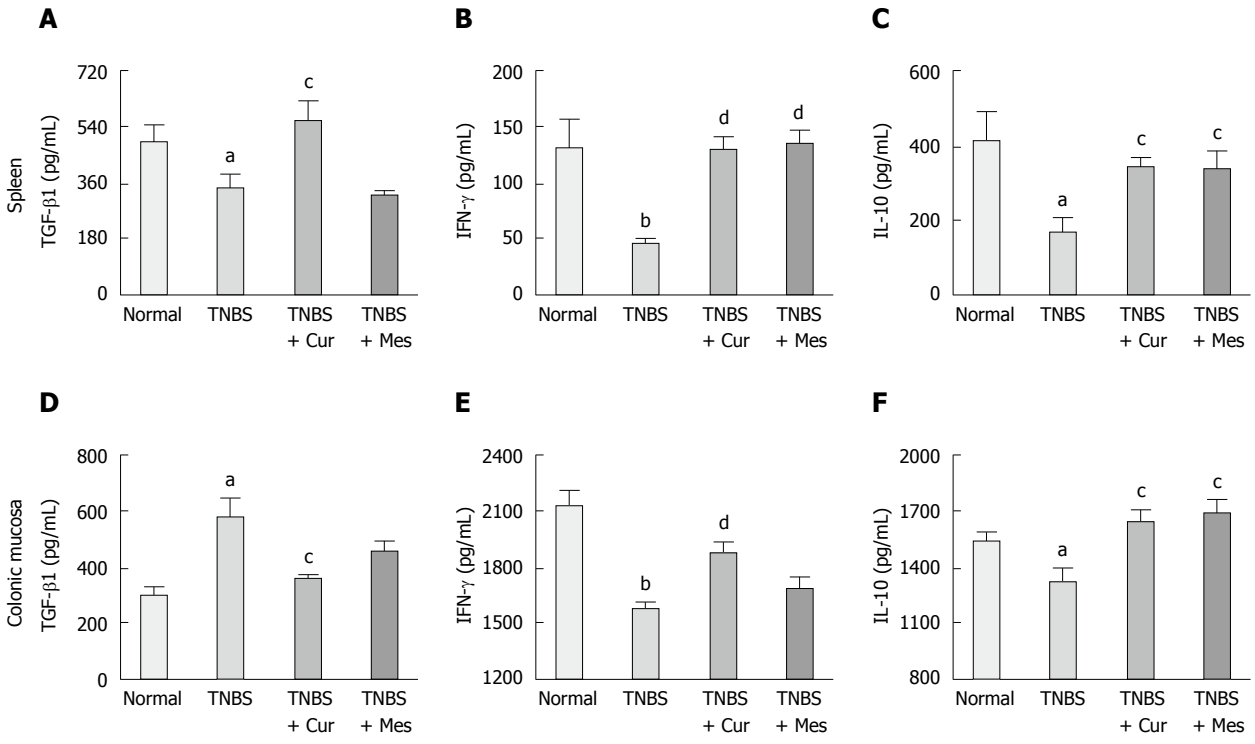

Figure 3 Levels of TGF-β1, IFN-γ and IL-10 in spleen and colonic mucosal supernatants. A-C: Concentration of TGF-β1, IFN-γ and IL-10 in the spleen from different groups; D-F: Concentration of TGF-β1, IFN-γ and IL-10 in the colonic mucosa from different groups. Data are shown as mean ± SEM (n = 8). $^{a}P < 0.05$ and $^{b}P < 0.01$ *vs* Normal group; $^{c}P < 0.05$ and $^{d}P < 0.01$ *vs* TNBS group.

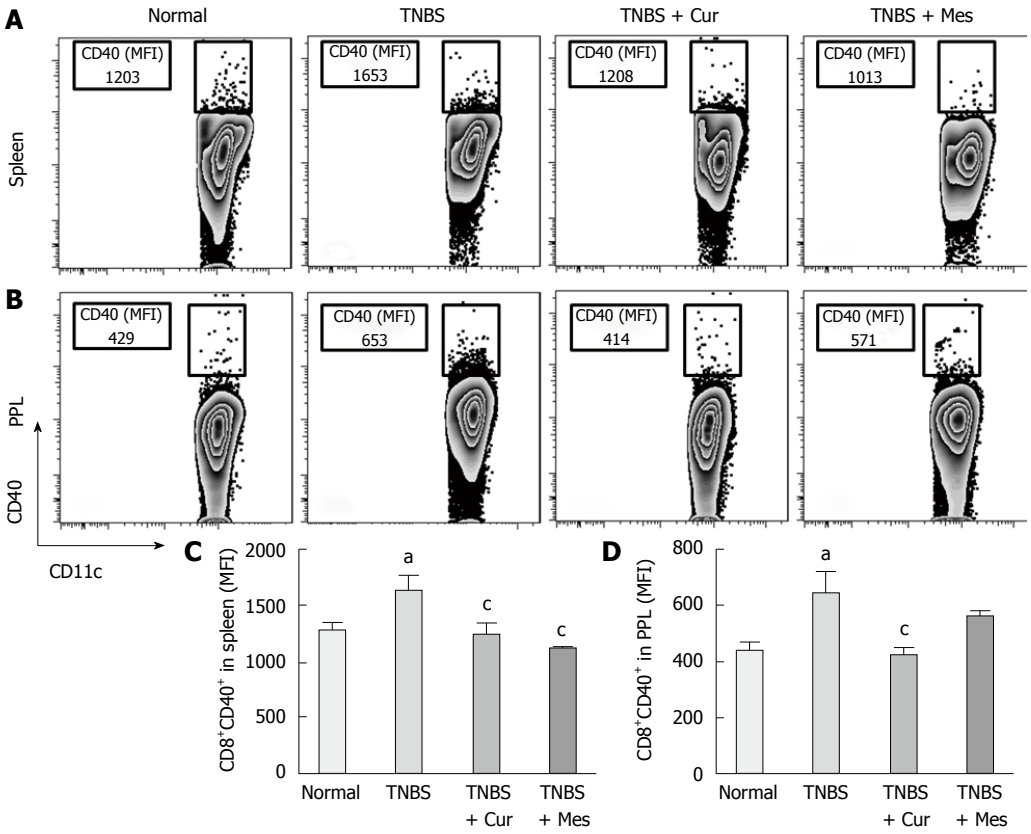

Figure 4 Typical histograms and levels of CD11c$^+$CD40$^+$ cells in spleen and PPs. A: Typical graphs of CD11c$^+$CD40$^+$ cells in the spleen; B: Typical graphs of CD11c$^+$CD40$^+$ cells in the PPs; C: MFI levels of CD11c$^+$CD40$^+$ cells in the spleen; D: MFI levels of CD11c$^+$CD40$^+$ cells in the PPs. Data are described as mean ± SEM (n = 8). $^aP < 0.05$ *vs* Normal control group; $^cP < 0.05$ *vs* TNBS group.

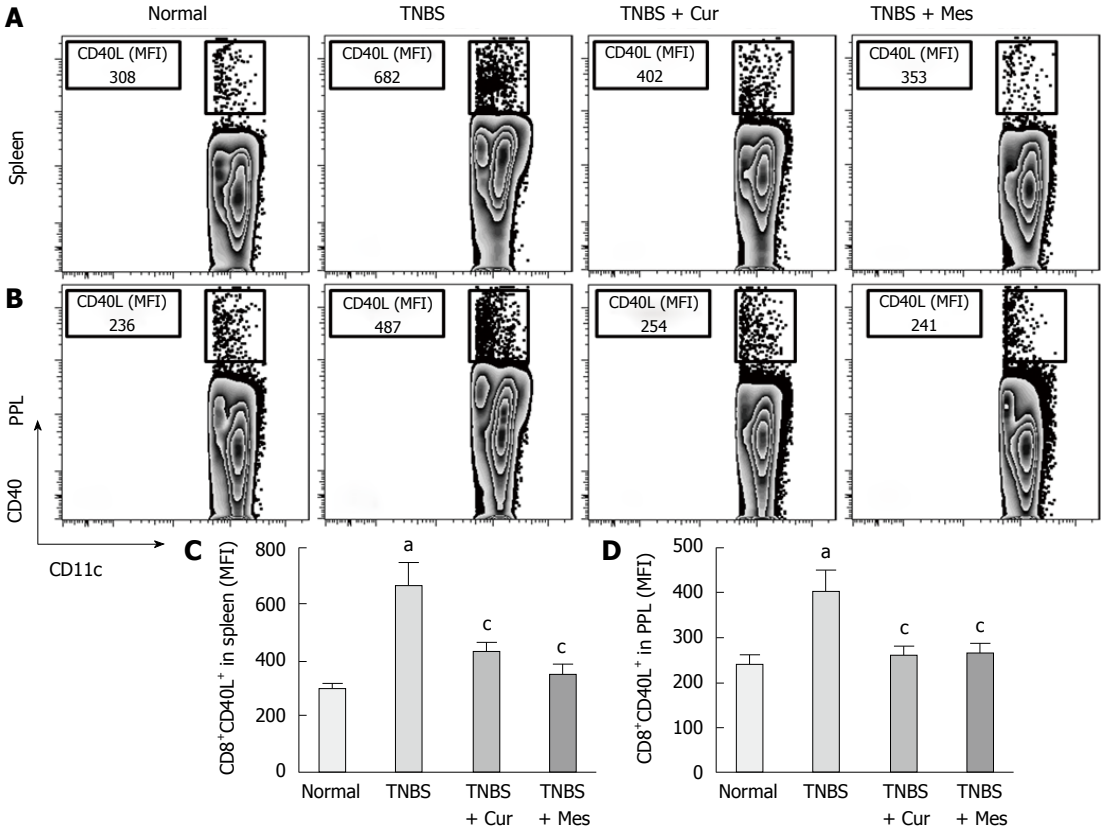

Figure 5 Typical histograms and levels of CD11c$^+$CD40L$^+$ cell in spleen and PPs. A: Typical graphs of CD11c$^+$CD40L$^+$ cells in the spleen; B: Typical graphs of CD11c$^+$ CD40L$^+$ cells in PPs; C: Levels (MFI) of CD11c$^+$CD40L$^+$ cells in the spleen; D: Levels (MFI) of CD11c$^+$CD40L$^+$ cells in PPs. Data are described as mean ± SEM (n = 8). $^aP < 0.05$ *vs* Normal control group; $^cP < 0.05$ *vs* TNBS group.

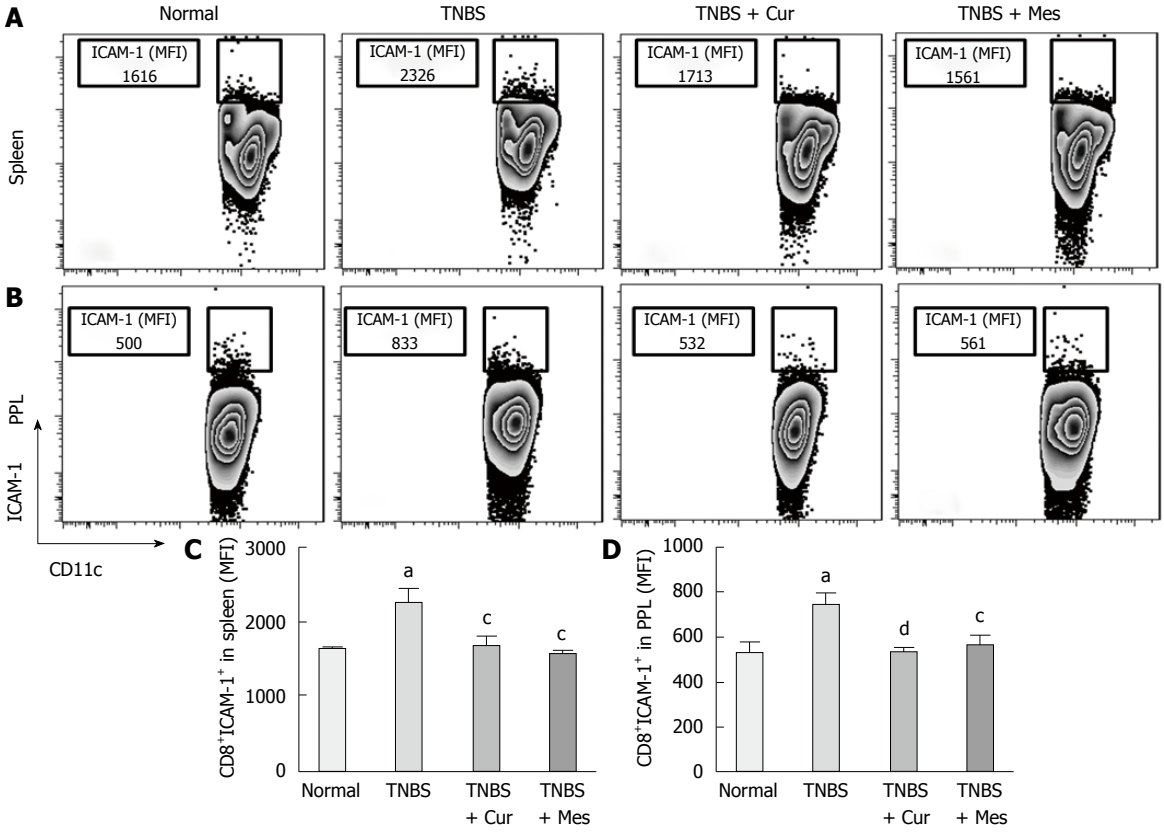

Figure 6 Typical histograms and levels of CD11c⁺ ICAM-1⁺ cells in spleen and PPs. A: Typical graphs of CD11c⁺ICAM-1⁺ cells in the spleen; B: Typical graphs of CD11c⁺ICAM-1⁺ cells in PPs; C: Levels (MFI) of CD11c⁺ ICAM-1⁺ cells in the spleen; D: Levels (MFI) of CD11c⁺ICAM-1⁺ cells in the PPs. Data are shown as mean ± SEM (n = 8). [a]P < 0.05 *vs* Normal control group; [c]P < 0.05 and [d]P < 0.01 *vs* TNBS group.

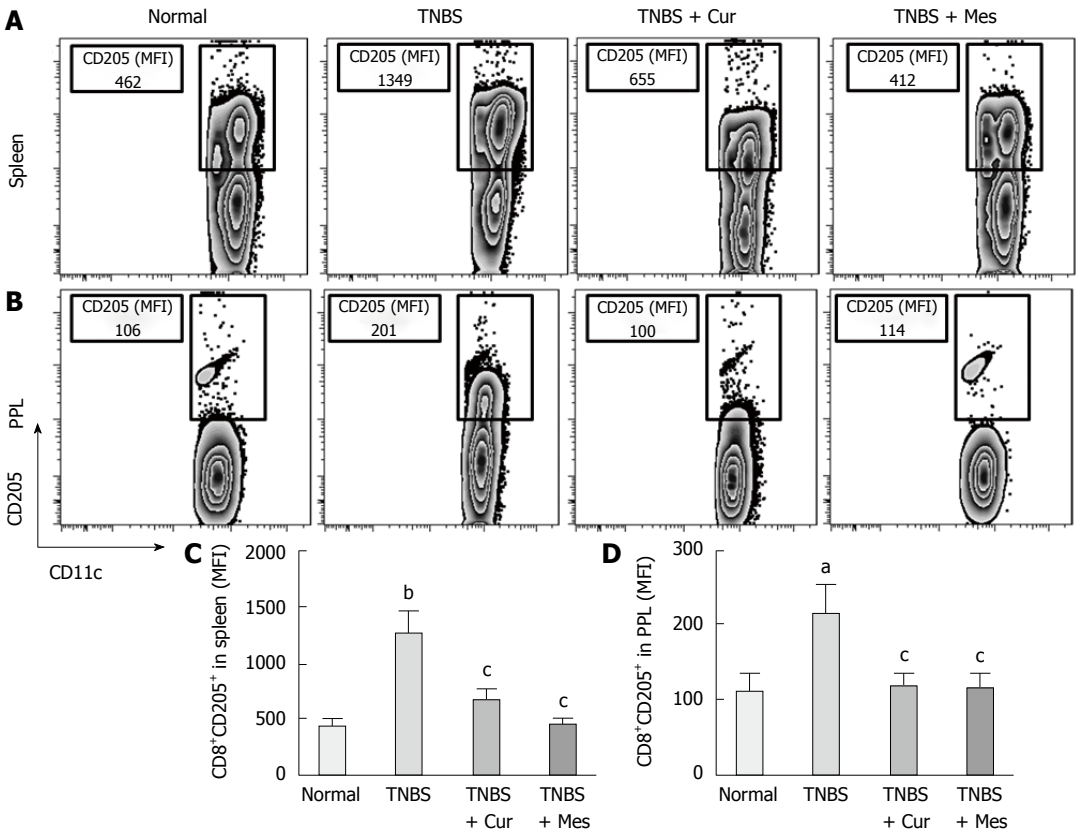

Figure 7 Typical histograms and levels of CD11c⁺CD205⁺ cells in the spleen and PPs. A: Typical graphs of CD11c⁺ CD205 ⁺ cells in the spleen; B: Typical graphs of CD11c⁺CD205⁺ cells in the PPs; C: Levels (MFI) of CD11c⁺CD205⁺ cells in the spleen; D: Levels (MFI) of CD11c⁺CD205⁺ cells in PPs. Data are mean ± SEM (n = 8). [a]P < 0.05 and [b]P < 0.01 *vs* Normal group; [c]P < 0.05 *vs* TNBS group.

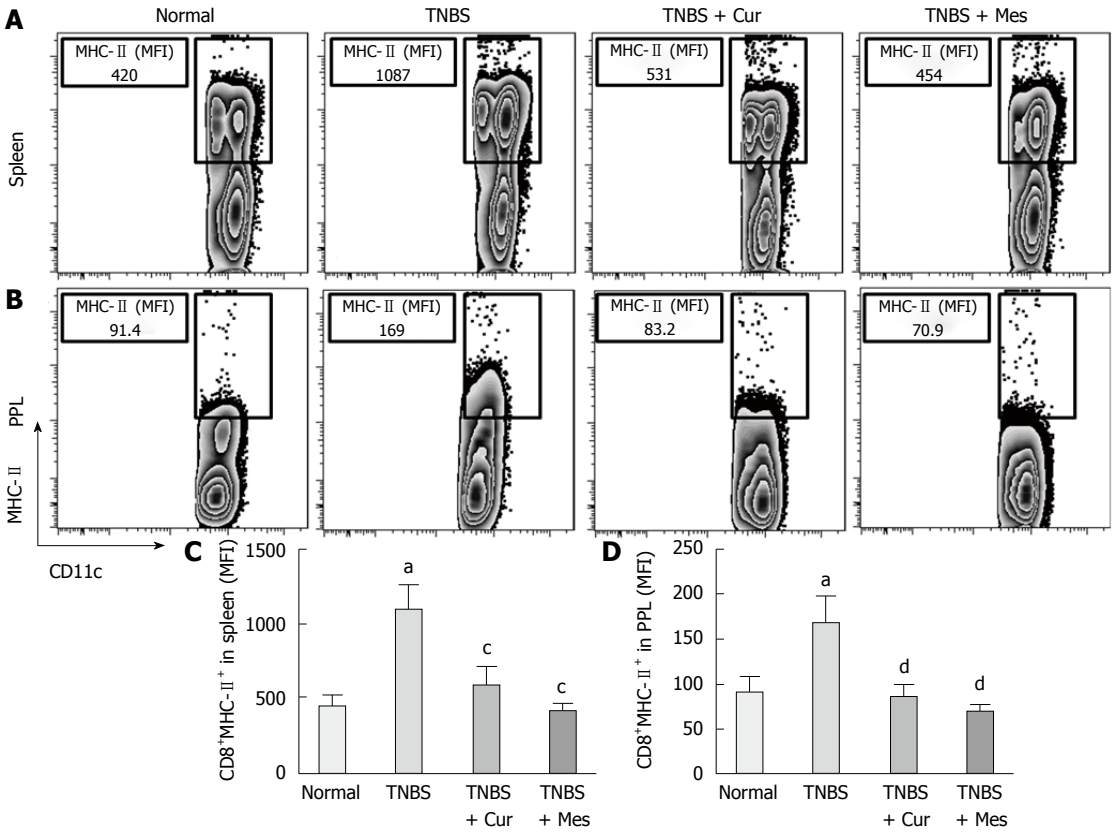

Figure 8 Typical histograms and levels of CD11c$^+$MHC II$^+$ cells in the spleen and PPs. A: Typical graphs of CD11c$^+$ MHC II$^+$ cells in the spleen; B: Typical graphs of CD11c$^+$ MHC II$^+$ cells in the PPs; C: Levels (MFI) of CD11c$^+$ MHC II$^+$ cells in the spleen; D: Levels (MFI) of CD11c$^+$ MHC II$^+$ cells in the PPs. Data are mean ± SEM (n = 8). $^aP < 0.05$ *vs* Normal control group; $^cP < 0.05$ and $^dP < 0.01$ *vs* TNBS group.

participates in conglutination, migration, antigenic recognition and presence of DCs, and activates CD4$^+$, CD8$^+$ T cells to regulate the immune response. CD11c can promote DC activation and maturity by elevating expression of co-stimulatory molecules[32,33]. Activated CD11c$^+$ DCs secrete a large number of inflammatory factors (including IL-1β, IL-6, IL-12 and IL-20) and promote CD4$^+$ T cells transformation into Th 1 cells, inducing inflammatory injury[34]. In the present study, the total number of CD8$^+$CD11c$^+$ cells in the spleen and PPs increased in colitis mice, which decreased with Cur treatment. Our previous study indicated that Cur alleviated inflammatory injury in the colonic mucosa of colitis mice, using the same model as in the present study[24]. These results show that Cur exerts its therapeutic effect on TNBS-induced colitis by decreasing the number of CD8$^+$CD11c$^+$ cells.

Previous research has shown that CD8$^+$ DCs play an important role in the development of experimental colitis and human IBD[11,12]. Our study showed that co-stimulatory molecules of DCs were increased in the spleen and PPs in untreated colitis mice, and Cur attenuated expression of MHC Ⅱ, CD205, CD40, CD40L and CD54 (ICAM-1) in CD8$^+$ DCs in the spleen and PPs. Our previous and present studies show that Cur can treat experimental colitis induced by TNBS or DSS[35,36]. The present study proves that Cur regulates the levels of CD8$^+$ DCs to treat TNBS-induced colitis.

DCs are essential in the activation of the adaptive immune system[37], and can be distinguished into myeloid and lymphoid DCs based on the cell-surface expression of CD8[8,9], which is one of the most important DC subset markers. Research has previously demonstrated that lymphoid DCs express CD8 in mice, whereas myeloid DCs do not[38-40]. Thus, DCs in the spleen and PPs of mice are considered to be CD8$^+$ DCs, which were identified in the present study[39,41].

Overwhelming evidence suggests that activation of CD8$^+$ DCs is a significant pathway to generate specific CD8$^+$ T-cell immune responses[42,43]. The complex pathway includes activation of Toll-like receptor 3[44], MHC and co-stimulatory molecule expression. MHC can promote DCs to migrate into lymphoid tissues such as the spleen and PPs, and accelerate antigen presentation, activation and maturation of DCs.

Researchers have previously incorporated MHC Ⅱ as a phenotypic segregation marker for *ex vivo* analysis of DCs under inflammatory settings such as influenza[44]. Waithman *et al*[45] have shown that many of the CD8$^+$ DC subpopulations undergo a phenotypic change from CD11c^{high} MHC Ⅱ^{int} in naïve mice to CD11c^{int} MHC Ⅱ^{high} mice infected with influenza A virus. According to MHC Ⅱ and CD11c expression levels, CD8$^+$ DCs, which are a classic migratory DC phenotype, could be segregated into both lymphoid-resident DC subsets and migratory subsets found at

inflammatory zones[46-48]. Based on the high expression of MHC Ⅱ, $CD8^+$ DCs capture antigens and promote T-cell migration at regions of the draining lymph nodes where they mature into functional DCs and present antigens to initiate primary immune responses[49,50]. In the process of maturation and activation of $CD8^+$ DCs, co-stimulatory molecules are highly expressed and include expression of CD205, CD24, CD40 and CD40L[2].

As a symbol of maturation and activation, DCs express co-stimulatory molecules including members of the tumor necrosis factor (TNF)/TNF receptor protein family, CD40/CD40L and OX40/OX40L, and members of the immunoglobulin superfamily including ICAM-1/lymphocyte function-associated antigen (LFA-)1, and CD28/cytotoxic T lymphocyte associated antigen 4/B7. Collectively, these cell-surface expressed protein receptors and their cognate ligands regulate the balance between Th1 and Th2 responses, and were found to be highly expressed in human and animal colitis[51]. For example, CD40/CD40L signaling can stimulate DCs to secrete IL-12, and direct the differentiation of $CD4^+$ T cells into Th1 cells. Similar functions are present in the context of ICAM-1/LFA-1 signaling and the B7-1 molecular signaling pathway (*i.e.*, the B7/CD28 signal)[52,53].

More importantly, $CD8^+$ DCs predominantly produce Th1-promoting cytokines like IL-12 p70 and IL-12 p40, while $CD8^+$ DCs lead to Th1 differentiation with reduced secretion of IFN-γ and IL-10[8,54,55], and enhanced secretion of the proinflammatory cytokine IL-6, which is associated with autoimmunity and chronic inflammatory diseases[56]. These cytokines were previously shown to be closely related to the pathogenesis of IBD[57,58]. Therefore, we have experimental evidence to believe that $CD8^+$ DCs played a critical role in the development of TNBS-induced colitis in our study. This was confirmed by the increased numbers of $CD8^+$ DCs in the spleen and PPs in untreated colitis mice. The results showed high expression of MHC Ⅱ, CD205, CD40, CD40L and ICAM-1. These co-stimulatory molecules and MHC Ⅱ promoted $CD8^+$ DCs to migrate into the colonic mucosa. Here, $CD8^+$ DCs secreted proinflammatory cytokines and suppressed anti-inflammatory cytokine production, and ultimately induced inflammatory injury in the colonic mucosa.

Seven days after administration of Cur, the total number of $CD8^+CD11c^+$ cells was decreased, and the expression of these co-stimulatory molecules of DCs was inhibited. Although it is uncertain that Cur regulated the function of $CD8^+CD11c^+$ cells, Shirley *et al*[23] indicated that Cur prevented DCs from inducing $CD4^+$ T-cell proliferation by blocking maturation marker expression, cytokine and chemokine secretion, and reducing migration and endocytosis of DCs.

The present study suggested that Cur restricted the quantity and activation of $CD8^+CD11c^+$ cells by downregulating expression of the co-stimulatory molecules of DCs in an attempt to improve the level of anti-inflammatory cytokines (*i.e.*, IL-10, IFN-γ and TGF-β1). These data suggest a therapeutic role for Cur as an immunosuppressant in the treatment of IBD. However, the level of TGF-β1 in the colonic mucosa was decreased by Cur, which is contrary to that seen in the spleen. We speculated that overproduction of TGF-β1 in the colonic mucosa was related to the chronicity and fibrosis of experimental colitis. Thus, Cur might inhibit fibroplasia at the base of the colonic ulcer. However, the signaling pathway remains unknown under conditions in which Cur controls maturation and migration of $CD8^+$ DCs. Future work is important in this area in an attempt to explore the pathway that regulates the function of $CD8^+$ DCs by TGF-β1 signaling.

In conclusion, we demonstrated that Cur effectively treated experimental colitis, which was realized by inhibiting $CD8^+CD11c^+$ cells.

COMMENTS

Background

CD11c is a specific marker of dendritic cells (DCs) and is highly expressed in $CD8^+$ and $CD8^-$ DCs. Overaccumulation of $CD8^+$ DCs is seen in colonic mucosa in experimental colitis and patients with inflammatory bowel disease (IBD).

Research frontiers

$CD8^+$ DCs predominantly stimulate T helper (Th)1-inducing cytokines like interleukin (IL)-12p70 and IL-12p40, which can lead to Th1 differentiation, and have been reported to play a key role in controlling viral infection. Overaccumulation of $CD8^+$ DCs induces inflammatory injury in the colonic mucosa when they migrate into Peyer's patches in experimental colitis and in patients with IBD. Thus, $CD8^+$ DCs may be a potential therapeutic target to explore the mechanisms of clinical treatment of IBD.

Innovations and breakthroughs

The present study is believed to be the first to show that curcumin (Cur) can effectively treat experimental colitis, which was realized by inhibiting $CD8^+CD11c^+$ cells.

Applications

It is known that Cur has a long history of effectively treating human IBD and experimental colitis. Cur prevents DC-mediated induction of $CD4^+$ T-cell proliferation by blocking expression of maturation markers, cytokines and chemokines. However, it is unclear whether Cur can regulate expression of $CD8^+CD11c^+$ cells to treat IBD. The present study suggests that Cur can treat experimental colitis, via inhibition of $CD8^+CD11c^+$ cells.

Terminology

CD11c is a type I transmembrane protein that mediates adherence between leukocytes and endothelial cells, and participates in exudation and phagocytosis of leukocytes.

Peer-review

The manuscript is presented in an easy understandable manner. The topic in the manuscript is very well explained. But it requires substantial corrections for the acceptance. According to detailed experimental data and reliable results, the present study had proved that Cur effectively treated experimental colitis, which was realized by inhibiting $CD8^+CD11c^+$ cells.

REFERENCES

1 **Plow EF**, Haas TA, Zhang L, Loftus J, Smith JW. Ligand binding to integrins. *J Biol Chem* 2000; **275**: 21785-21788 [PMID: 10801897 DOI: 10.1074/jbc.R000003200]

2 **Villadangos JA**, Schnorrer P. Intrinsic and cooperative antigen-presenting functions of dendritic-cell subsets in vivo. *Nat Rev Immunol* 2007; **7**: 543-555 [PMID: 17589544 DOI: 10.1038/nri2103]

3 **Belz GT**, Smith CM, Eichner D, Shortman K, Karupiah G, Carbone FR, Heath WR. Cutting edge: conventional CD8 alpha+ dendritic cells are generally involved in priming CTL immunity to viruses. *J Immunol* 2004; **172**: 1996-2000 [PMID: 14764661 DOI: 10.4049/jimmunol.172.4.1996]

4 **Stagg AJ**, Hart AL, Knight SC, Kamm MA. The dendritic cell: its role in intestinal inflammation and relationship with gut bacteria. *Gut* 2003; **52**: 1522-1529 [PMID: 12970149]

5 **Grewal IS**, Flavell RA. CD40 and CD154 in cell-mediated immunity. *Annu Rev Immunol* 1998; **16**: 111-135 [PMID: 9597126 DOI: 10.1146/annurev.immunol.16.1.111]]

6 **Theill LE**, Boyle WJ, Penninger JM. RANK-L and RANK: T cells, bone loss, and mammalian evolution. *Annu Rev Immunol* 2002; **20**: 795-823 [PMID: 11861618]

7 **Vremec D**, Pooley J, Hochrein H, Wu L, Shortman K. CD4 and CD8 expression by dendritic cell subtypes in mouse thymus and spleen. *J Immunol* 2000; **164**: 2978-2986 [PMID: 10706685 DOI: 10.4049/jimmunol.164.6.2978]

8 **Maldonado-López R**, Maliszewski C, Urbain J, Moser M. Cytokines regulate the capacity of CD8alpha(+) and CD8alpha(-) dendritic cells to prime Th1/Th2 cells in vivo. *J Immunol* 2001; **167**: 4345-4350 [PMID: 11591758 DOI: 10.4049/jimmunol.167.8.4345]

9 **Vogt A**, Mahé B, Costagliola D, Bonduelle O, Hadam S, Schaefer G, Schaefer H, Katlama C, Sterry W, Autran B, Blume-Peytavi U, Combadiere B. Transcutaneous anti-influenza vaccination promotes both CD4 and CD8 T cell immune responses in humans. *J Immunol* 2008; **180**: 1482-1489 [PMID: 18209043 DOI: 10.4049/jimmunol.180.3.1482]

10 **Smith CM**, Belz GT, Wilson NS, Villadangos JA, Shortman K, Carbone FR, Heath WR. Cutting edge: conventional CD8 alpha+ dendritic cells are preferentially involved in CTL priming after footpad infection with herpes simplex virus-1. *J Immunol* 2003; **170**: 4437-4440 [PMID: 12707318 DOI: 10.4049/jimmunol.170.9.4437]

11 **Sabado RL**, Bhardwaj N. Directing dendritic cell immunotherapy towards successful cancer treatment. *Immunotherapy* 2010; **2**: 37-56 [PMID: 20473346 DOI: 10.2217/imt.09.43]

12 **Evel-Kabler K**, Song XT, Aldrich M, Huang XF, Chen SY. SOCS1 restricts dendritic cells' ability to break self tolerance and induce antitumor immunity by regulating IL-12 production and signaling. *J Clin Invest* 2006; **116**: 90-100 [PMID: 16357940 DOI: 10.1172/JCI26169]

13 **Guo YM**, Hirokawa M, Takahashi N, Fujishima M, Fujishima N, Komatsuda A, Tagawa H, Ohyagi H, Michishita Y, Ubukawa K, Hebiguchi M, Xiao W, Sawada K. Delayed addition of tumor necrosis factor (TNF) antagonists inhibits the generation of CD11c+ dendritic cells derived from CD34+ cells exposed to TNF-alpha. *Int J Hematol* 2010; **91**: 61-68 [PMID: 20012512 DOI: 10.1007/s12185-009-0456-5]

14 **Castro FV**, Tutt AL, White AL, Teeling JL, James S, French RR, Glennie MJ. CD11c provides an effective immunotarget for the generation of both CD4 and CD8 T cell responses. *Eur J Immunol* 2008; **38**: 2263-2273 [PMID: 18651710 DOI: 10.1002/eji.200838302]

15 **Bachem A**, Güttler S, Hartung E, Ebstein F, Schaefer M, Tannert A, Salama A, Movassaghi K, Opitz C, Mages HW, Henn V, Kloetzel PM, Gurka S, Kroczek RA. Superior antigen cross-presentation and XCR1 expression define human CD11c+CD141+ cells as homologues of mouse CD8+ dendritic cells. *J Exp Med* 2010; **207**: 1273-1281 [PMID: 20479115 DOI: 10.1084/jem.20100348]

16 **Hofmann C**, Dunger N, Grunwald N, Hämmerling GJ, Hoffmann P, Schölmerich J, Falk W, Obermeier F. T cell-dependent protective effects of CpG motifs of bacterial DNA in experimental colitis are mediated by CD11c+ dendritic cells. *Gut* 2010; **59**: 1347-1354 [PMID: 20732920 DOI: 10.1136/gut.2009.193177]

17 **Goel A**, Kunnumakkara AB, Aggarwal BB. Curcumin as "Curecumin": from kitchen to clinic. *Biochem Pharmacol* 2008; **75**: 787-809 [PMID: 17900536]

18 **Salh B**, Assi K, Templeman V, Parhar K, Owen D, Gómez-Muñoz A, Jacobson K. Curcumin attenuates DNB-induced murine colitis. *Am J Physiol Gastrointest Liver Physiol* 2003; **285**: G235-G243 [PMID: 12637253 DOI: 10.1152/ajpgi.00449.2002]

19 **Holt PR**, Katz S, Kirshoff R. Curcumin therapy in inflammatory bowel disease: a pilot study. *Dig Dis Sci* 2005; **50**: 2191-2193 [PMID: 16240238 DOI: 10.1007/s10620-005-3032-8]

20 **Aggarwal BB**, Sung B. Pharmacological basis for the role of curcumin in chronic diseases: an age-old spice with modern targets. *Trends Pharmacol Sci* 2009; **30**: 85-94 [PMID: 19110321 DOI: 10.1016/j.tips.2008.11.002]

21 **Martelli L**, Ragazzi E, di Mario F, Martelli M, Castagliuolo I, Dal Maschio M, Palù G, Maschietto M, Scorzeto M, Vassanelli S, Brun P. A potential role for the vanilloid receptor TRPV1 in the therapeutic effect of curcumin in dinitrobenzene sulphonic acid-induced colitis in mice. *Neurogastroenterol Motil* 2007; **19**: 668-674 [PMID: 17640182 DOI: 10.1111/j.1365]

22 **Hanai H**, Iida T, Takeuchi K, Watanabe F, Maruyama Y, Andoh A, Tsujikawa T, Fujiyama Y, Mitsuyama K, Sata M, Yamada M, Iwaoka Y, Kanke K, Hiraishi H, Hirayama K, Arai H, Yoshii S, Uchijima M, Nagata T, Koide Y. Curcumin maintenance therapy for ulcerative colitis: randomized, multicenter, double-blind, placebo-controlled trial. *Clin Gastroenterol Hepatol* 2006; **4**: 1502-1506 [PMID: 17101300 DOI: 10.1016/j.cgh.2006.08.008]

23 **Shirley SA**, Montpetit AJ, Lockey RF, Mohapatra SS. Curcumin prevents human dendritic cell response to immune stimulants. *Biochem Biophys Res Commun* 2008; **374**: 431-436 [PMID: 18639521 DOI: 10.1016/j.bbrc.2008.07.051]

24 **Zhao HM**, Xu R, Huang XY, Cheng SM, Huang MF, Yue HY, Wang X, Zou Y, Lu AP, Liu DY. Curcumin improves regulatory T cells in gut-associated lymphoid tissue of colitis mice. *World J Gastroenterol* 2016; **22**: 5374-5383 [PMID: 27340353 DOI: 10.3748/wjg.v22.i23.5374]

25 **Huang LY**, He Q, Liang SJ, Su YX, Xiong LX, Wu QQ, Wu QY, Tao J, Wang JP, Tang YB, Lv XF, Liu J, Guan YY, Pang RP, Zhou JG. ClC-3 chloride channel/antiporter defect contributes to inflammatory bowel disease in humans and mice. *Gut* 2014; **63**: 1587-1595 [PMID: 24440986 DOI: 10.1136/gutjnl-2013-305168]

26 **Sałaga M**, Mokrowiecka A, Zakrzewski PK, Cygankiewicz A, Leishman E, Sobczak M, Zatorski H, Małecka-Panas E, Kordek R, Storr M, Krajewska WM, Bradshaw HB, Fichna J. Experimental colitis in mice is attenuated by changes in the levels of endocannabinoid metabolites induced by selective inhibition of fatty acid amide hydrolase (FAAH). *J Crohns Colitis* 2014; **8**: 998-1009 [PMID: 24530133]

27 **Fina D**, Sarra M, Fantini MC, Rizzo A, Caruso R, Caprioli F, Stolfi C, Cardolini I, Dottori M, Boirivant M, Pallone F, Macdonald TT, Monteleone G. Regulation of gut inflammation and th17 cell response by interleukin-21. *Gastroenterology* 2008; **134**: 1038-1048 [PMID: 18395085]

28 **Bai A**, Ma AG, Yong M, Weiss CR, Ma Y, Guan Q, Bernstein CN, Peng Z. AMPK agonist downregulates innate and adaptive immune responses in TNBS-induced murine acute and relapsing colitis. *Biochem Pharmacol* 2010; **80**: 1708-1717 [PMID: 20797389 DOI: 10.1016/j.bcp.2010.08.009]

29 **Ghia JE**, Blennerhassett P, El-Sharkawy RT, Collins SM. The protective effect of the vagus nerve in a murine model of chronic relapsing colitis. *Am J Physiol Gastrointest Liver Physiol* 2007; **293**: G711-G718 [PMID: 17673544 DOI: 10.1152/ajpgi.00240.2007]

30 **Chen Y**, Si JM, Liu WL, Cai JT, Du Q, Wang LJ, Gao M. Induction of experimental acute ulcerative colitis in rats by administration of dextran sulfate sodium at low concentration

followed by intracolonic administration of 30% ethanol. *J Zhejiang Univ Sci B* 2007; **8**: 632-637 [PMID: 17726744 DOI: 10.1631/jzus.2007.B0632]

31 **Schmidt N**, Gonzalez E, Visekruna A, Kühl AA, Loddenkemper C, Mollenkopf H, Kaufmann SH, Steinhoff U, Joeris T. Targeting the proteasome: partial inhibition of the proteasome by bortezomib or deletion of the immunosubunit LMP7 attenuates experimental colitis. *Gut* 2010; **59**: 896-906 [PMID: 20581238 DOI: 10.1136/gut.2009.203554]

32 **Lin Y**, Roberts TJ, Sriram V, Cho S, Brutkiewicz RR. Myeloid marker expression on antiviral CD8+ T cells following an acute virus infection. *Eur J Immunol* 2003; **33**: 2736-2743 [PMID: 14515257 DOI: 10.1002/eji.200324087]

33 **Singh-Jasuja H**, Thiolat A, Ribon M, Boissier MC, Bessis N, Rammensee HG, Decker P. The mouse dendritic cell marker CD11c is down-regulated upon cell activation through Toll-like receptor triggering. *Immunobiology* 2013; **218**: 28-39 [PMID: 22445076 DOI: 10.1016/j.imbio.2012.01.021]

34 **Fujiwara D**, Chen L, Wei B, Braun J. Small intestine CD11c+ CD8+ T cells suppress CD4+ T cell-induced immune colitis. *Am J Physiol Gastrointest Liver Physiol* 2011; **300**: G939-G947 [PMID: 21436315 DOI: 10.1152/ajpgi.00032.2010]

35 **Zhang M**, Deng C, Zheng J, Xia J, Sheng D. Curcumin inhibits trinitrobenzene sulphonic acid-induced colitis in rats by activation of peroxisome proliferator-activated receptor gamma. *Int Immunopharmacol* 2006; **6**: 1233-1242 [PMID: 16782535 DOI: 10.1016/j.intimp.2006.02.013]

36 **Liu L**, Liu YL, Liu GX, Chen X, Yang K, Yang YX, Xie Q, Gan HK, Huang XL, Gan HT. Curcumin ameliorates dextran sulfate sodium-induced experimental colitis by blocking STAT3 signaling pathway. *Int Immunopharmacol* 2013; **17**: 314-320 [PMID: 23856612 DOI: 10.1016/j.intimp.2013.06.020]

37 **Mackern-Oberti JP**, Llanos C, Vega F, Salazar-Onfray F, Riedel CA, Bueno SM, Kalergis AM. Role of dendritic cells in the initiation, progress and modulation of systemic autoimmune diseases. *Autoimmun Rev* 2015; **14**: 127-139 [PMID: 25449681]

38 **Beijer MR**, Molenaar R, Goverse G, Mebius RE, Kraal G, den Haan JM. A crucial role for retinoic acid in the development of Notch-dependent murine splenic CD8- CD4- and CD4+ dendritic cells. *Eur J Immunol* 2013; **43**: 1608-1616 [PMID: 23519987]

39 **Rutella S**, Locatelli F. Intestinal dendritic cells in the pathogenesis of inflammatory bowel disease. *World J Gastroenterol* 2011; **17**: 3761-3775 [PMID: 21987618 DOI: 10.3748/wjg.v17.i33.3761]

40 **Ardavin C**, Wu L, Li CL, Shortman K. Thymic dendritic cells and T cells develop simultaneously in the thymus from a common precursor population. *Nature* 1993; **362**: 761-763 [PMID: 8469288 DOI: 10.1038/362761a0]

41 **Shortman K**, Naik SH. Steady-state and inflammatory dendritic-cell development. *Nat Rev Immunol* 2007; **7**: 19-30 [PMID: 17170756 DOI: 10.1038/nri1996]

42 **Allan RS**, Waithman J, Bedoui S, Jones CM, Villadangos JA, Zhan Y, Lew AM, Shortman K, Heath WR, Carbone FR. Migratory dendritic cells transfer antigen to a lymph node-resident dendritic cell population for efficient CTL priming. *Immunity* 2006; **25**: 153-162 [PMID: 16860764 DOI:]

43 **Langlois RA**, Varble A, Chua MA, García-Sastre A, tenOever BR. Hematopoietic-specific targeting of influenza A virus reveals replication requirements for induction of antiviral immune responses. *Proc Natl Acad Sci USA* 2012; **109**: 12117-12122 [PMID: 22778433 DOI: 10.1073/pnas.1206039109]

44 **Davey GM**, Wojtasiak M, Proietto AI, Carbone FR, Heath WR, Bedoui S. Cutting edge: priming of CD8 T cell immunity to herpes simplex virus type 1 requires cognate TLR3 expression in vivo. *J Immunol* 2010; **184**: 2243-2246 [PMID: 20124105 DOI: 10.4049/jimmunol.0903013]

45 **Waithman J**, Zanker D, Xiao K, Oveissi S, Wylie B, Ng R, Tögel L, Chen W. Resident CD8(+) and migratory CD103(+) dendritic cells control CD8 T cell immunity during acute influenza infection. *PLoS One* 2013; **8**: e66136 [PMID: 23750278 DOI: 10.1371/journal.pone.0066136]

46 **Kim TS**, Braciale TJ. Respiratory dendritic cell subsets differ in their capacity to support the induction of virus-specific cytotoxic CD8+ T cell responses. *PLoS One* 2009; **4**: e4204 [PMID: 19145246 DOI: 10.1371/journal.pone.0004204]

47 **Ballesteros-Tato A**, León B, Lund FE, Randall TD. Temporal changes in dendritic cell subsets, cross-priming and costimulation via CD70 control CD8(+) T cell responses to influenza. *Nat Immunol* 2010; **11**: 216-224 [PMID: 20098442]

48 **Bedoui S**, Whitney PG, Waithman J, Eidsmo L, Wakim L, Caminschi I, Allan RS, Wojtasiak M, Shortman K, Carbone FR, Brooks AG, Heath WR. Cross-presentation of viral and self antigens by skin-derived CD103+ dendritic cells. *Nat Immunol* 2009; **10**: 488-495 [PMID: 19349986 DOI: 10.1038/ni.1724]

49 **Banchereau J**, Steinman RM. Dendritic cells and the control of immunity. *Nature* 1998; **392**: 245-252 [PMID: 9521319 DOI: 10.1038/32588]

50 **Schnorrer P**, Behrens GM, Wilson NS, Pooley JL, Smith CM, El-Sukkari D, Davey G, Kupresanin F, Li M, Maraskovsky E, Belz GT, Carbone FR, Shortman K, Heath WR, Villadangos JA. The dominant role of CD8+ dendritic cells in cross-presentation is not dictated by antigen capture. *Proc Natl Acad Sci USA* 2006; **103**: 10729-10734 [PMID: 16807294 DOI: 10.1073/pnas]

51 **Griseri T**, Asquith M, Thompson C, Powrie F. OX40 is required for regulatory T cell-mediated control of colitis. *J Exp Med* 2010; **207**: 699-709 [PMID: 20368580 DOI: 10.1084/jem.20091618]

52 **Sheng KC**, Pietersz GA, Wright MD, Apostolopoulos V. Dendritic cells: activation and maturation--applications for cancer immunotherapy. *Curr Med Chem* 2005; **12**: 1783-1800 [PMID: 16029147 DOI: 10.2174/0929867054367248]

53 **Vainer B**. Intercellular adhesion molecule-1 (ICAM-1) in ulcerative colitis: presence, visualization, and significance. *APMIS Suppl* 2010; **(129)**: 1-43 [PMID: 20653648]

54 **Kamijo R**, Shapiro D, Gerecitano J, Le J, Bosland M, Vilcek J. Biological functions of IFN-gamma and IFN-alpha/beta: lessons from studies in gene knockout mice. *Hokkaido Igaku Zasshi* 1994; **69**: 1332-1338 [PMID: 7705746]

55 **Khader SA**, Partida-Sanchez S, Bell G, Jelley-Gibbs DM, Swain S, Pearl JE, Ghilardi N, Desauvage FJ, Lund FE, Cooper AM. Interleukin 12p40 is required for dendritic cell migration and T cell priming after Mycobacterium tuberculosis infection. *J Exp Med* 2006; **203**: 1805-1815 [PMID: 16818672 DOI: 10.1084/jem.20052545]

56 **Johnston JA**, O'Shea JJ. Matching SOCS with function. *Nat Immunol* 2003; **4**: 507-509 [PMID: 12774070]

57 **Martins GA**, Cimmino L, Shapiro-Shelef M, Szabolcs M, Herron A, Magnusdottir E, Calame K. Transcriptional repressor Blimp-1 regulates T cell homeostasis and function. *Nat Immunol* 2006; **7**: 457-465 [PMID: 16565721 DOI: 10.1038/ni1320]

58 **Kallies A**, Hawkins ED, Belz GT, Metcalf D, Hommel M, Corcoran LM, Hodgkin PD, Nutt SL. Transcriptional repressor Blimp-1 is essential for T cell homeostasis and self-tolerance. *Nat Immunol* 2006; **7**: 466-474 [PMID: 16565720]

P- Reviewer: Bolboaca SD, Gopu B, Sharaf IA **S- Editor**: Yu J
L- Editor: Ma JY **E- Editor**: Wang CH

World Journal of Gastroenterology

Submit a Manuscript: http://www.wjgnet.com/esps/

World J Gastroenterol 2017 March 14; 23(10): 1816-1827

DOI: 10.3748/wjg.v23.i10.1816

ISSN 1007-9327 (print) ISSN 2219-2840 (online)

ORIGINAL ARTICLE

Basic Study

miR-34a mediates oxaliplatin resistance of colorectal cancer cells by inhibiting macroautophagy *via* transforming growth factor-β/Smad4 pathway

Chen Sun, Fu-Jing Wang, Hao-Gang Zhang, Xun-Zheng Xu, Rui-Chun Jia, Lei Yao, Peng-Fei Qiao

Chen Sun, Fu-Jing Wang, Hao-Gang Zhang, Xun-Zheng Xu, Lei Yao, Peng-Fei Qiao, Department of General Surgery, the Second Affiliated Hospital of Harbin Medical University, Harbin 150086, Heilongjiang Province, China

Rui-Chun Jia, Department of Blood Transfusion, the Second Affiliated Hospital of Harbin Medical University, Harbin 150086, Heilongjiang Province, China

Author contributions: Jia RC, Yao L and Qiao PF should be considered co-corresponding authors; Qiao PF designed the research and analyzed the data; Jia RC and Yao L performed the research; Zhang HG and Xu XZ contributed new reagents or analytic tools; Wang FJ, Yao L and Qiao PF wrote the article.

Supported by Science Foundation of Education Department of Heilongjiang Province, China, No. 12541430.

Institutional review board statement: This study was approved by the Institutional Review Board of Harbin Medical University, and the protocols used in the study were approved by the Committee of Human Subjects Protection of the Second Affiliated Hospital of Harbin Medical University, Harbin, China.

Conflict-of-interest statement: The authors declare that they have no conflicts of interest related to this study.

Data sharing statement: Technical appendices, statistical codes and datasets are available from the corresponding author at lunwenqpf@126.com. Participants gave informed consent for data sharing.

Manuscript source: Unsolicited manuscript

Correspondence to: Dr. Peng-Fei Qiao, Department of General Surgery, the Second Affiliated Hospital of Harbin Medical University, Harbin 150086, Heilongjiang Province, China. lunwenqpf@126.com
Telephone: +86-13895761713
Fax: +86-451-86297283

Received: September 29, 2016
Peer-review started: October 1, 2016
First decision: December 1, 2016
Revised: December 21, 2016
Accepted: February 7, 2017
Article in press: February 8, 2017
Published online: March 14, 2017

Abstract

AIM

To investigate whether microRNA (miR)-34a mediates oxaliplatin (OXA) resistance of colorectal cancer (CRC) cells by inhibiting macroautophagy *via* the transforming growth factor (TGF)-β/Smad4 pathway.

METHODS

miR-34a expression levels were detected in CRC tissues and CRC cell lines by quantitative real-time polymerase chain reaction. Computational search, functional luciferase assay and western blotting were used to demonstrate the downstream target of miR-34a in CRC cells. Cell viability was measured with Cell Counting Kit-8. Apoptosis and macroautophagy of CRC cells were analyzed by flow cytometry and transmission electron microscopy, and expression of beclin I and LC3-II was detected by western blotting.

RESULTS

Expression of miR-34a was significantly reduced while expression of TGF-β and Smad4 was increased in CRC patients treated with OXA-based chemotherapy. OXA treatment also resulted in decreased miR-34a levels and increased TGF-β and Smad4 levels in both parental cells and the OXA-resistant CRC cells. Activation of macroautophagy contributed to OXA resistance in CRC cells. Expression levels of Smad4 and miR-34a in CRC patients had a significant inverse correlation and overexpressing miR-34a inhibited macroautophagy activation by directly targeting Smad4 through the TGF-β/Smad4 pathway. OXA-induced downregulation of miR-34a and increased drug resistance by activating macroautophagy in CRC cells.

CONCLUSION

miR-34a mediates OXA resistance of CRC by inhibiting macroautophagy *via* the TGF-β/Smad4 pathway.

Key words: miR-34a; Oxaliplatin; Colorectal cancer; Macroautophagy; Transforming growth factor-β/Smad pathway

Core tip: This study demonstrated a significant association between microRNA (miR)-34a expression and the acquired chemoresistance to oxaliplatin (OXA) in colorectal cancer (CRC). miR-34a mediates OXA resistance through its inhibitory effects on macroautophagy by the transforming growth factor (TGF)-β/Smad4 pathway. Our findings suggest that miR-34a is a potential therapeutic target for improving the chemotherapeutic effect of OXA in CRC.

Sun C, Wang FJ, Zhang HG, Xu XZ, Jia RC, Yao L, Qiao PF. miR-34a mediates oxaliplatin resistance of colorectal cancer cells by inhibiting macroautophagy *via* transforming growth factor-β/Smad4 pathway. *World J Gastroenterol* 2017; 23(10): 1816-1827 Available from: URL: http://www.wjgnet.com/1007-9327/full/v23/i10/1816.htm DOI: http://dx.doi.org/10.3748/wjg.v23.i10.1816

INTRODUCTION

Colorectal cancer (CRC) is one of the most common causes of cancer-related deaths, leading to approximately 600000 deaths worldwide annually[1,2]. Current standard treatments for CRC include surgical resection, systematic chemotherapy, radiotherapy or a combination of these methods. Oxaliplatin (OXA), a third-generation platinum compound, is the first platinum-based compound to show efficacy in the treatment of CRC[3]. Despite this demonstrated efficacy, the advances in chemotherapy for CRC have been limited because of its resistance to OXA. Therefore, revealing the underlying mechanism for the development of chemoresistance is necessary for developing effective chemotherapeutic agents.

MicroRNAs (miRNAs) are a group of noncoding RNAs that have been highly conserved during evolution and have emerged recently as potent regulators of gene expression, cell proliferation, apoptosis and tumorigenesis[4,5]. Our previous study demonstrated that miR-34a inhibits epithelial mesenchymal transition in human cholangiocarcinoma by targeting Smad4 through the transforming growth factor (TGF)-β/Smad pathway[6]. Recent research has found that miR-34a is one of the well-characterized miRNAs and is consistently downregulated in various types of malignancies, including CRC[7-9]. More importantly, miR-34a has been reported to be involved in drug resistance and regulating chemosensitivity in CRC[10].

Macroautophagy is a catabolic degradation process that is required to maintain cellular homeostasis[11]. Some researchers have shown that macroautophagy is involved in the regulation of chemoresistance. He *et al*[12] found that miR-21 mediates sorafenib resistance of hepatocellular carcinoma cells *via* inhibition of macroautophagy through the PTEN/Akt pathway. Pan *et al*[13] have reported that miR-200b regulates macroautophagy associated with chemoresistance in human lung adenocarcinoma. Whether miR-34a is involved in mediating the chemoresistance of OXA by affecting macroautophagy activity remains unclear.

In the present study, we found that expression of miR-34a was significantly reduced while expression of TGF-β and Smad4 was increased in CRC patients treated with OXA-based chemotherapy. OXA treatment also decreased miR-34a levels and increased TGF-β and Smad4 levels in both parental cells and OXA-resistant CRC cells. Activation of macroautophagy contributed to OXA resistance in CRC cells. In addition, our data indicated that expression of Smad4 and miR-34a in CRC patients had a significant inverse correlation and overexpression of miR-34a inhibited macroautophagy activation by directly targeting Smad4 through the TGF-β/Smad4 pathway. We further demonstrated that OXA-induced downregulation of miR-34a increased drug resistance by activating macroautophagy in CRC cells. We identified a novel mechanism by which miR-34a mediates OXA resistance of CRC by inhibiting autophagy *via* the TGF-β/Smad4 pathway.

MATERIALS AND METHODS

Samples and establishment of chemoresistant cells

We included 30 CRC patients (median age: 61 years, range: 48-75 years) who underwent potentially curative surgery between 2013 and 2015 at the Second Affiliated Hospital of Harbin Medical University (Harbin, China). CRC was verified by a pathologist and patients received OXA-based combination chemotherapy. Blood samples were taken after

obtaining informed consent according to institutional guidelines and the study was approved by the Institutional Review Board of Harbin Medical University, Harbin, China. The protocols used in the study were approved by the Committee of Human Subjects Protection of our hospital.

To establish the chemoresistance model *in vitro*, the human CRC cell line HT29 obtained from the Cell Bank of Chinese Academy of Sciences (Shanghai, China) was seeded in a six-well plate at 10^4 cells/well and 2 μmol/L OXA was added to the medium. The medium was changed after 48 h. The concentration of OXA was increased by 1 μmol/L for each subculture. After subculture and incubation with OXA solution was repeated 10 times, OXA-resistant cell lines were obtained, termed as HT29-OXA, and continuously maintained by culturing them in complete culture medium containing 2 μmol/L OXA[14,15].

Real-time polymerase chain reaction

Real-time polymerase chain reaction (RT-PCR) was used to confirm the expression levels of mRNAs and miRNAs as previously described[6]. For mRNA detection, total RNA from cultured cells and blood samples was extracted using TRIzol (Invitrogen, Carlsbad, CA, United States). Reverse transcription was performed using the High Capacity cDNA Reverse Transcription Kit (Applied Biosystems, Foster City, CA, United States). Total miRNA from cultured cells and fresh surgical tissues was extracted using the mirVana miRNA Isolation Kit (Ambion, Austin, TX, United States). cDNA was synthesized from 2 μg total RNA using the High Capacity cDNA Reverse Transcription Kit (Applied Biosystems). Expression of miRNA and mRNA was assessed with qRT-PCR using Power SYBR Green Master Mix in an Applied Biosystems 7500 Sequence Detection System. The expression level of mRNA and miRNA was defined based on the threshold cycle (Ct), and relative expression levels were calculated using the $2^{-\Delta\Delta Ct}$ method, with the expression level of β-actin mRNA and U6 small nuclear RNA as a reference gene. The names of the genes and the primers are listed in Supplementary Table 1.

Western blotting

Protein lysates were separated using SDS-PAGE and transferred to nitrocellulose membranes (Amersham Pharmacia Biotech, Piscataway, NJ, United States). Membranes were probed with the appropriate primary antibodies (Supplementary Table 2). Alexa Fluor 680 donkey anti-mouse IgG (H + L) or Alexa Fluor 680 donkey anti-rabbit IgG (H + L) were used as secondary antibodies (1:5000; Invitrogen). Fluorophores were detected using the Odyssey Infrared Imaging System (Li-Cor, Lincoln, NE, United States).

Transfection of oligonucleotides

Transfection of pre-miR-34a was conducted as previously described[6]. A synthetic miR-34a mimic (GenePharma, Shanghai, China) was used to increase miR-34a expression. A scrambled oligonucleotide (GenePharma) was used as a control. Transfection was performed using Lipofectamine 2000 transfection reagent (Invitrogen). A mixture of Lipofectamine 2000 and RNA was added to CRC cells, which were 70% confluent, for 4-6 h, and the cells were then incubated for 24 h in fresh medium. The cells were harvested using lysis buffer for luciferase assay. Total RNA and protein were prepared 48 h after transfection and used for qRT-PCR or western blot analysis.

Construction of promoter reporter plasmids and luciferase reporter assays

The luciferase reporter assay was conducted as described previously[6]. The fragment containing miR-34a-binding sites in the Smad4 3′-untranslated region (UTR) was amplified by PCR and inserted downstream of the firefly luciferase gene in a pGL3-promoter vector (Promega, Madison, WI, United States). The mutant reporter plasmids were constructed using the QuikChange mutagenesis kit (Stratagene, La Jolla, CA, United States). These constructed plasmids were all sequenced to confirm their orientation. Luciferase activity was measured with the Dual-Luciferase Reporter Assay System (Promega) as described previously[16]. Promoter activities were expressed as the ratio between firefly luciferase and Renilla luciferase activities.

Cell proliferation analysis

The cells were seeded into a 96-well plate (3×10^3/well) in triplicate and cultured overnight. The culture medium was replaced with fresh fetal-calf-serum-free medium containing vehicle or testing reagents for 24 h. Cell viability was measured with the Cell Counting Kit-8 (CCK-8) (Boster Bio, Wuhan, China). Untreated cells served as controls. Cell viability (%) was calculated according to the formula: experimental OD value/control OD value × 100%.

Evaluation of macroautophagy and apoptosis by flow cytometry

The evaluation of macroautophagy and apoptosis by flow cytometry was performed as previously described[17]. Apoptosis was examined using the Annexin V-FITC/PI Kit (Becton Dickinson, Franklin Lakes, NJ, United States). Cells were collected in 400 mL medium. Following resuspension, approximately 10 mL Annexin V solution and 5 mL propidium iodide were added and incubated for 30 min at room temperature in the dark. The cell suspension was analyzed by flow cytometry (Becton Dickinson). Cell Quest software was used to analyze 10^4 cells.

Cell macroautophagy was detected by monodansylcadaverine (MDC; Sigma-Aldrich, St Louis, MO, United States) staining. Cells were washed with

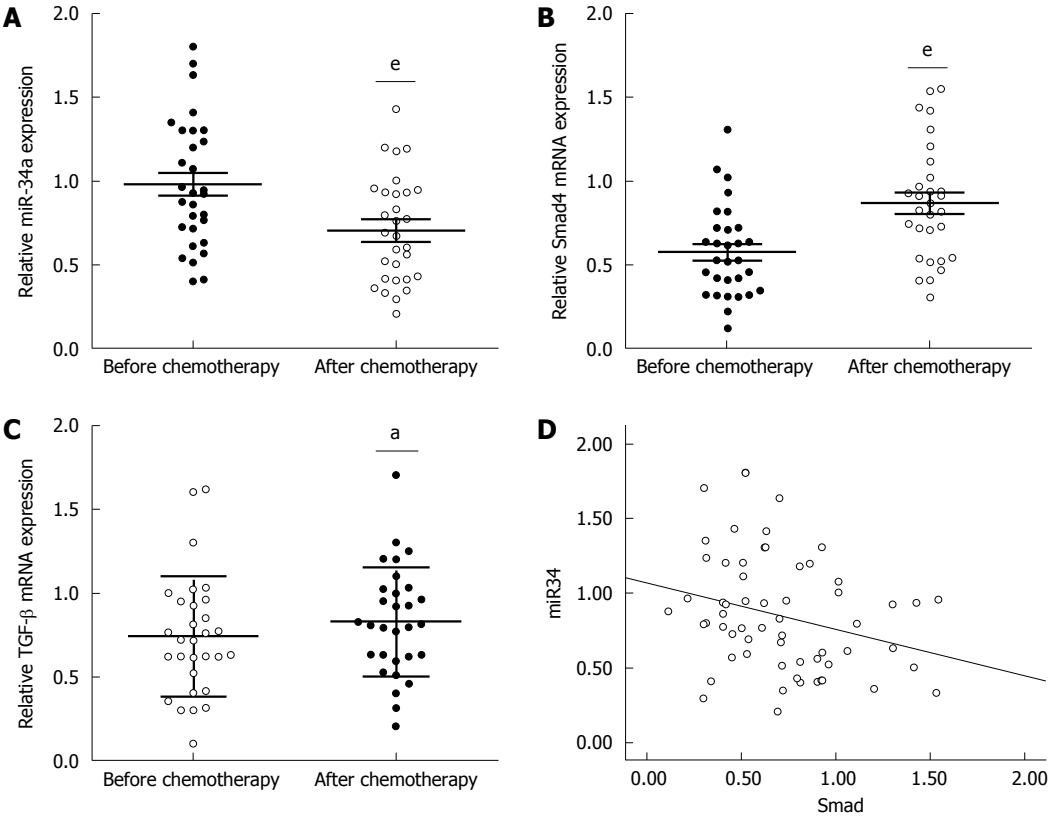

Figure 1 miR-34a levels were significantly decreased after oxaliplatin treatment. A: Analysis of miR-34a expression was performed on blood samples from 30 colorectal cancer (CRC) patients after oxaliplatin (OXA)-based combination chemotherapy. Total RNA was extracted and subjected to qRT-PCR to analyze the expression level of miR-34a in each sample. U6 was used as an internal control; B and C: mRNA expression levels of Smad4 and TGF-β in the blood samples from CRC patients were measured by qRT-PCR. β-actin was used as the internal control ($^aP < 0.05$, $^eP < 0.001$); D: The inverse correlation of miR-34a and Smad4 expression levels was examined by Spearman correlation analysis ($R = -0.283$, $P = 0.029$).

phosphate-buffered saline (PBS) and then incubated with 0.05 mmol/L MDC in PBS at 37 ℃ for 45 min. After incubation, the cells were washed three times with PBS and analyzed by flow cytometry immediately. Cell Quest software was used to analyze 10^4 cells.

Statistical analysis

All the presented data were expressed as the mean ± SD and representative results were from at least three independent experiments. Statistical comparisons were calculated by Student's two-tailed *t* test. When multiple comparisons were possible, ANOVA coupled with Tukey correction was used. Correlation analysis between relative expressions of Smad4 and miR-34a was examined by logistic regression analysis. $P < 0.05$ was considered statistically significant. Statistical analysis was carried out using SPSS version 21 (IBM Corporation, Armonk, NY, United States) or GraphPad Prism version 5.0 (La Jolla, CA, United States).

RESULTS

OXA treatment downregulates miR-34a and upregulates TGF-β/Smad4 in CRC patients

To investigate the underlying mechanism for the resistance of CRC patients to OXA treatment, we focused on identifying the changes in miR-34a and TGF-β/Smad4 pathway expression after OXA-based combination chemotherapy. miR-34a expression was significantly decreased while TGF-β and Smad4 mRNA expression was significantly increased in the blood samples of CRC patients after chemotherapy (Figure 1A-C). Spearman correlation analysis was applied to compare the relative expression levels of Smad4 and miR-34a in CRC patients. We obtained a statistically significant inverse correlation ($R = -0.283$, $P = 0.029$) in 30 CRC patients (Figure 1D). These data suggest that downregulation of miR-34a and upregulation of TGF-β/Smad4 may be related to OXA-based combination chemotherapy.

OXA-resistant CRC cells are insensitive to OXA via inhibition of miR-34a and activation of the TGF-β/Smad4 pathway

To determine further whether miR-34a levels are correlated with chemotherapeutic response, the OXA-resistant cell line, HT29-OXA, was established by chronic exposure of HT29 cells to increasing concentrations of OXA. Incubation of OXA with HT29 cells reduced their viability in a concentration-dependent manner. However, HT29-OXA cells became resistant to OXA as their viability was significantly

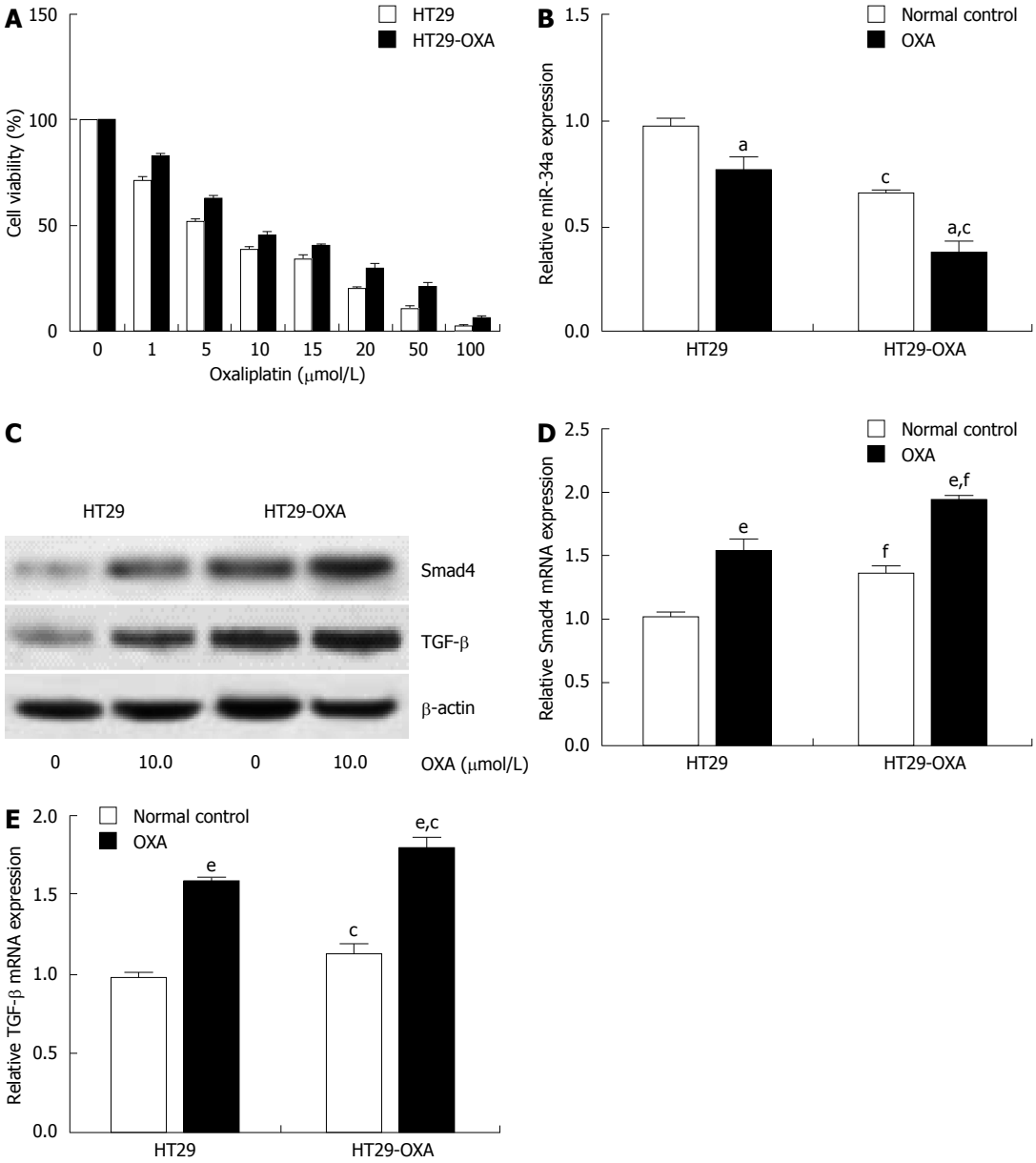

Figure 2 Oxaliplatin treatment inhibited miR-34a expression and activated the TGF-β/Smad4 pathway. A: HT29 and HT29-oxaliplatin (OXA) cells were incubated with serial concentrations of OXA for 48 h and cell viability (%) was measured by CCK-8 kit and normalized with the corresponding untreated cells; B: HT29 and HT29-OXA cells were incubated with OXA (10 μmol/L) for 48 h and expression of miR-34a was determined by qRT-PCR. U6 was used as an internal control; C: The above cells lysates were examined with indicated antibodies by western blotting. β-actin was used as loading control; D and E: The above cells were subjected to qRT-PCR to measure Smad4 and TGF-β mRNA expression levels. β-actin was used as the internal control ($^{a}P < 0.05$, $^{e}P < 0.001$ indicates a significant difference *vs* normal control. $^{c}P < 0.05$, $^{f}P < 0.001$ indicates a significant difference *vs* respective untreated cells).

higher than that of respective parental cells when exposed to the same concentration of OXA (Figure 2A). Expression of miR-34a in HT29 and HT29-OXA cells was downregulated when exposed to 10 μmol/L OXA for 48 h, although HT29-OXA cells expressed lower levels of miR-34a than HT29 cells with or without OXA treatment (Figure 2B).

Smad4 is a known miR-34a target gene in some types of tumor cells. We examined expression of TGF-β and Smad4 in HT29 and HT29-OXA cells in the presence or absence of OXA treatment. Incubation of OXA induced increased expression of TGF-β and Smad4 in HT29 and HT29-OXA cells. HT29-OXA cells expressed higher levels of TGF-β, resulting in upregulation of Smad4 compared with HT29 cells (Figure 2C-E). These results indicate that sustained exposure of CRC cells to OXA could inhibit miR-34a expression and activate the TGF-β/Smad4 pathway.

miR-34a directly regulates Smad4 expression and TGF-β inhibition in CRC cells

To investigate the underlying mechanism of miR-34a in CRC, targetscan (www.targetscan.org) and miRanda (www.microRNA.org) were used to search for potential targets of miR-34a. Consistent with our previous study[6], the result showed that the 3′-UTR of Smad4

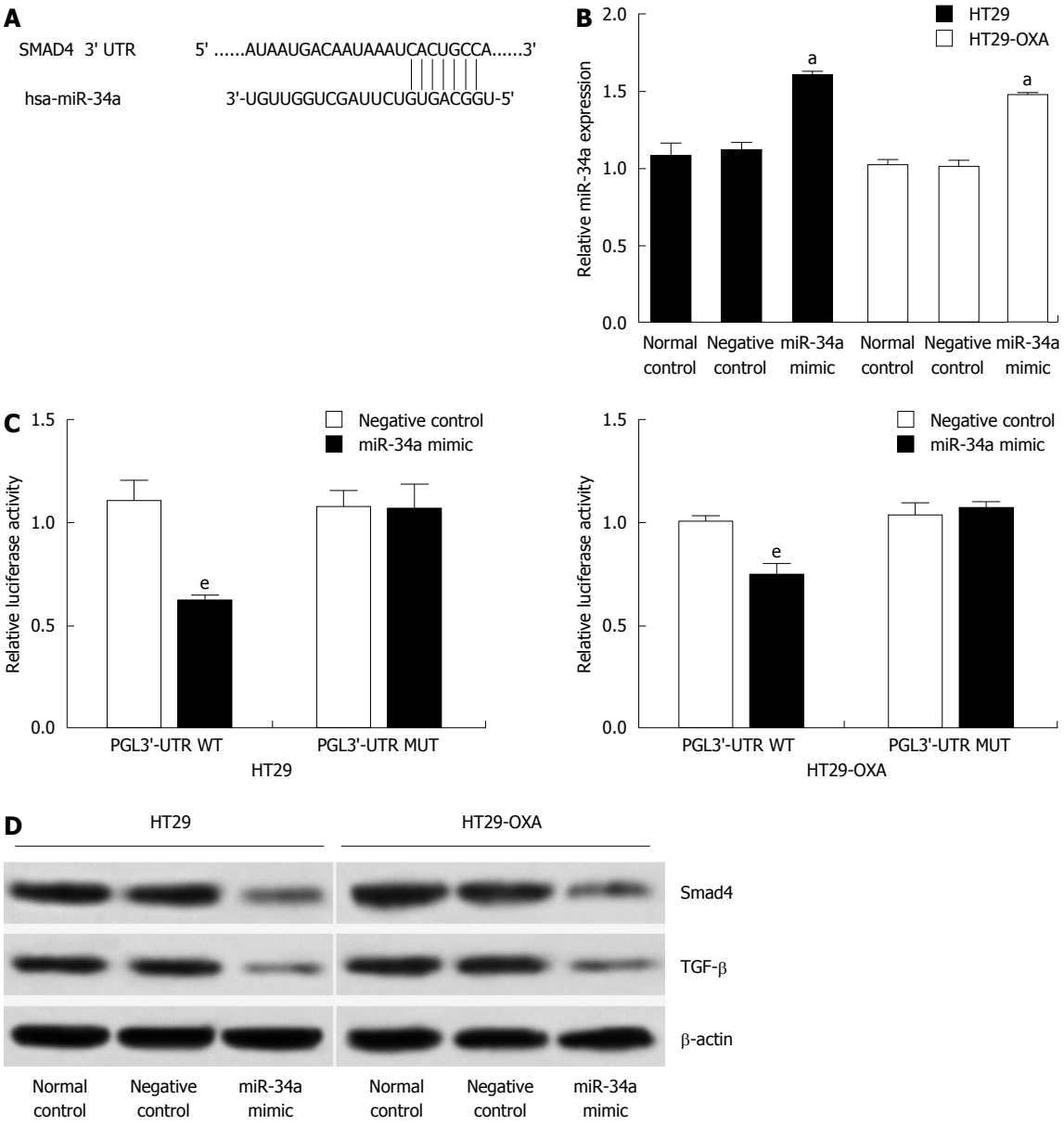

Figure 3 miR-34a directly regulated Smad4 expression and TGF-β inhibition in colorectal cancer cells. A: miRNA target prediction screened one computative miR-34a binding site at Smad4 3'-UTR; B: qRT-PCR analysis of expression of miR-34a treated with miR-34a mimics in HT29 and HT29-OXA cells ($^{a}P < 0.05$). U6 was used as a loading control. Error bars represent mean ± SD from three independent experiments; C: 3'-UTR luciferase reporter assay showed a reduction of relative luciferase activity of wild-type Smad4 3'-UTR by pre-miR-34a in HT29 and HT29-OXA cells ($^{e}P < 0.001$); D: Western blotting of Smad4 and TGF-β expression in HT29 and HT29-OXA cells treated with miR-34a mimic. β-actin expression level was used as internal loading control.

contained the complementary site for the seed region of miR-34a (Figure 3A). To verify that Smad4 is one of the direct targets of miR-34a in OXA-resistant and parental CRC cells, we constructed a reporter vector consisting of the luciferase coding sequence followed by the 3'-UTR of Smad4. A dual luciferase reporter assay was performed in HT29 and HT29-OXA cells. miR-34a significantly decreased the luciferase activity of the wild-type Smad4 3'-UTR compared with the vector-only control (Figure 3B). Additionally, partial mutation of the perfectly complementary sites in the 3'-UTR of Smad4 abolished the suppressive effect due to the disruption of the interaction between miR-34a and Smad4.

miR-34a mimics were transfected into HT29 and HT29-OXA cells to increase the endogenous level of miR-34a to investigate further the biological function of miR-34a in CRC cells (Figure 3C). Compared to the control groups, transfecting with miR-34a mimics downregulated Smad4 and TGF-β expression in HT29 and HT29-OXA cells (Figure 3D). These data suggest that Smad4 is a direct target of miR-34a and miR-34a mediated TGF-β/Smad4 pathway in CRC cell lines.

Activation of macroautophagy contributes to OXA resistance in CRC cells

Macroautophagy is a key regulator of resistance to OXA[18]. We investigated whether activation of

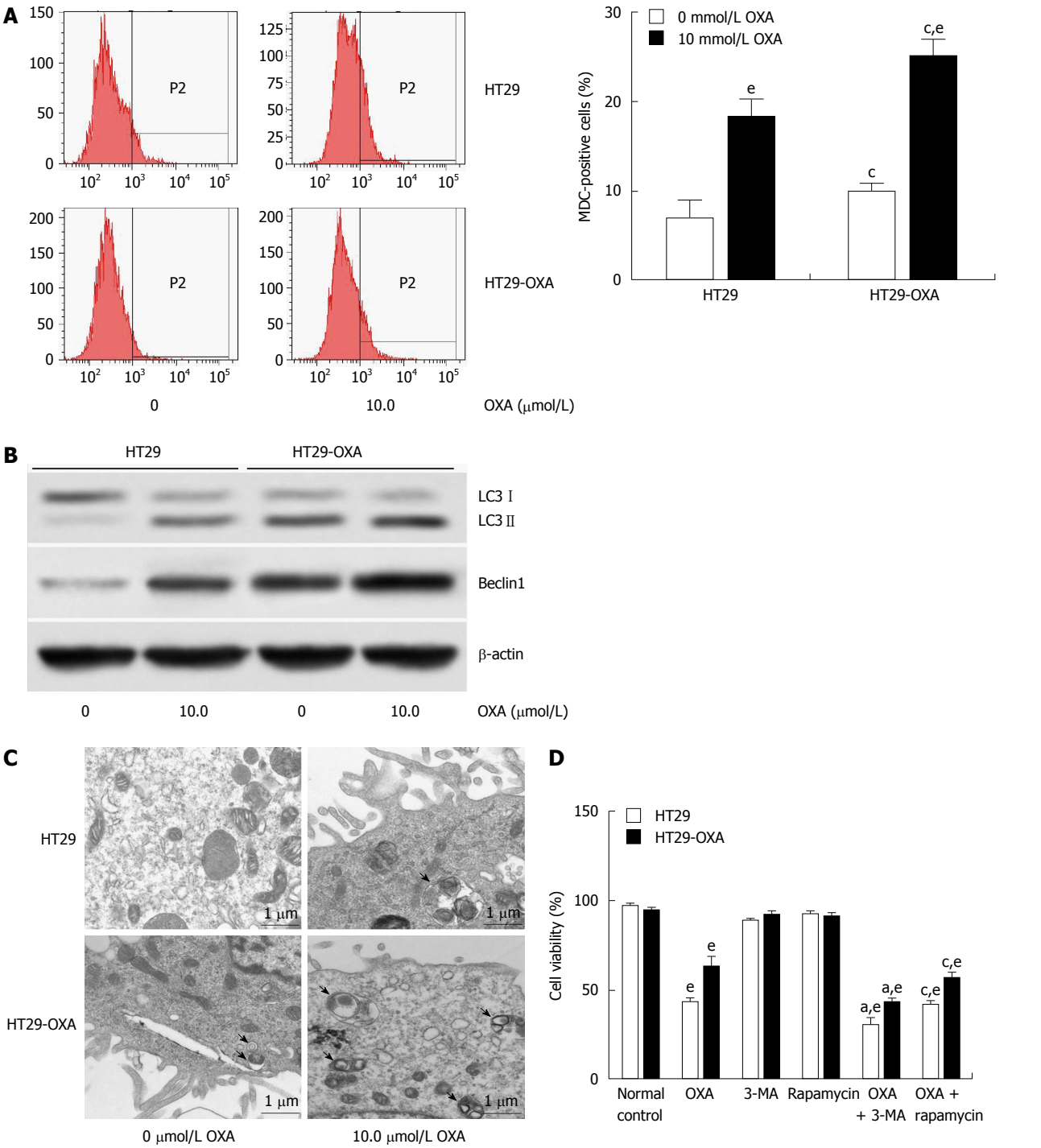

Figure 4 Activation of autophagy contributed to oxaliplatin resistance in colorectal cancer cells. A: HT29 and HT29-oxaliplatin (OXA) cells were incubated with or without 10 μmol/L OXA for 48 h, and autophagy was determined by monodansylcadaverine (MDC)-positive stained cells using flow cytometry; B: Western blotting showed a significant increase in expression of the autophagic markers LC3-II and beclin-1 in HT29 and HT29-OXA cells with or without OXA treatment. The data represent the results of three separate experiments; C: Representative electron micrographs demonstrated autophagic vacuole formation in each group. The arrows indicate the double-membrane vacuoles digesting organelles or cytosolic contents; D: Autophagy regulated chemoresistance of OXA in HT29 and HT29-OXA cells ($^{e}P < 0.001$ indicates a significant difference *vs* normal control; $^{a}P < 0.05$ indicates a significant difference *vs* 3-MA treatment group; $^{c}P < 0.05$ indicates a significant difference *vs* rapamycin treatment group).

macroautophagy contributes to the acquired resistance to OXA. Incubation with OXA led to more MDC-positive HT29 and HT29-OXA cells, but there were more MDC-positive HT29-OXA than HT29 cells in the presence or absence of OXA treatment (Figure 4A). Western blotting confirmed that the HT29-OXA cells had significantly lower LC3-II and beclin 1 intensity than TH29 cells had in the presence or absence of OXA treatment (Figure 4B). Representative electron micrographs demonstrated less autophagic vacuole formation in the HT29-OXA cells than HT29 cells in the presence or absence of OXA treatment (Figure 4C).

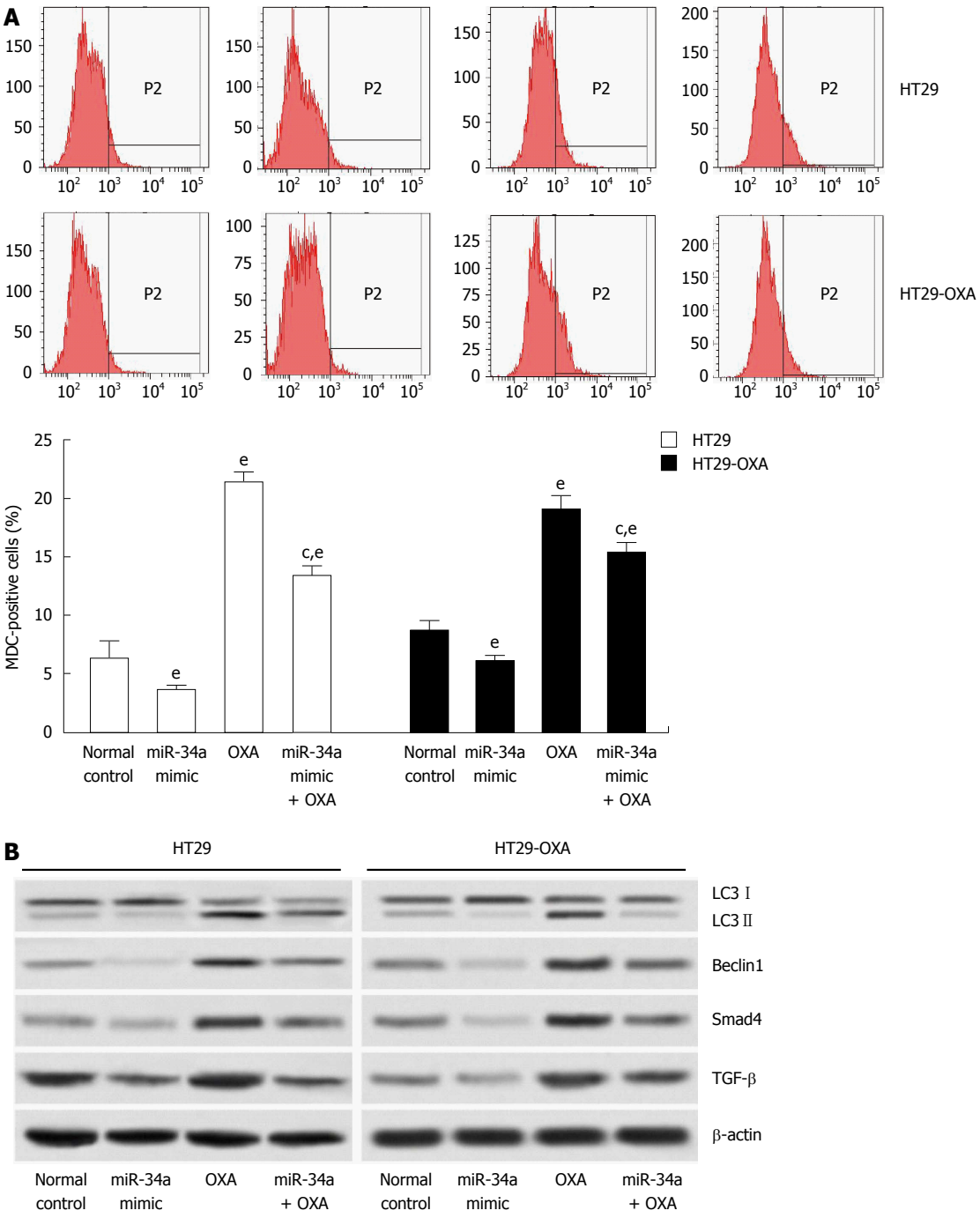

Figure 5 miR-34a inhibited oxaliplatin-induced autophagy in colorectal cancer cells. A: HT29 and HT29-oxaliplatin (OXA) cells were transfected with miR-34a mimics and treated with or without OXA (10 μmol/L) simultaneously. After 48 h, autophagy was determined using a fluorescent dye (monodansylcadaverine, MDC) and flow cytometry; B: The above cell lysates were examined with indicated antibodies by western blotting. β-actin was used as loading control. ($^{e}P < 0.001$ indicates a significant difference *vs* normal control; $^{c}P < 0.05$ indicates a significant difference *vs* transfection with miR-34a mimic group).

Suppression of macroautophagy by 3-methyladenine (3-MA) increased OXA-induced cell death. In contrast, rapamycin, an inhibitor of mammalian target of rapamycin, and positive regulator of macroautophagy, protected OXA-resistant cells against OXA-induced reduction in cell viability (Figure 4D).

miR-34a affects OXA-induced macroautophagy in CRC cells via the TGF-β/Smad4 pathway

Since macroautophagy participates in OXA resistance in CRC cells[19], we investigated the effects of miR-34a on macroautophagy of CRC cells. miR-34a mimics inhibited macroautophagy in parental and OXA-resistant cells, and fewer MDC-stained cells were observed in cells transfected with miR-34a mimics than in normal control cells. OXA treatment increased autophagy of parental and OXA-resistant cells, as shown by the presence of more MDC-stained cells. However, induction of macroautophagy was inhibited by treatment with miR-34a mimics in parental and

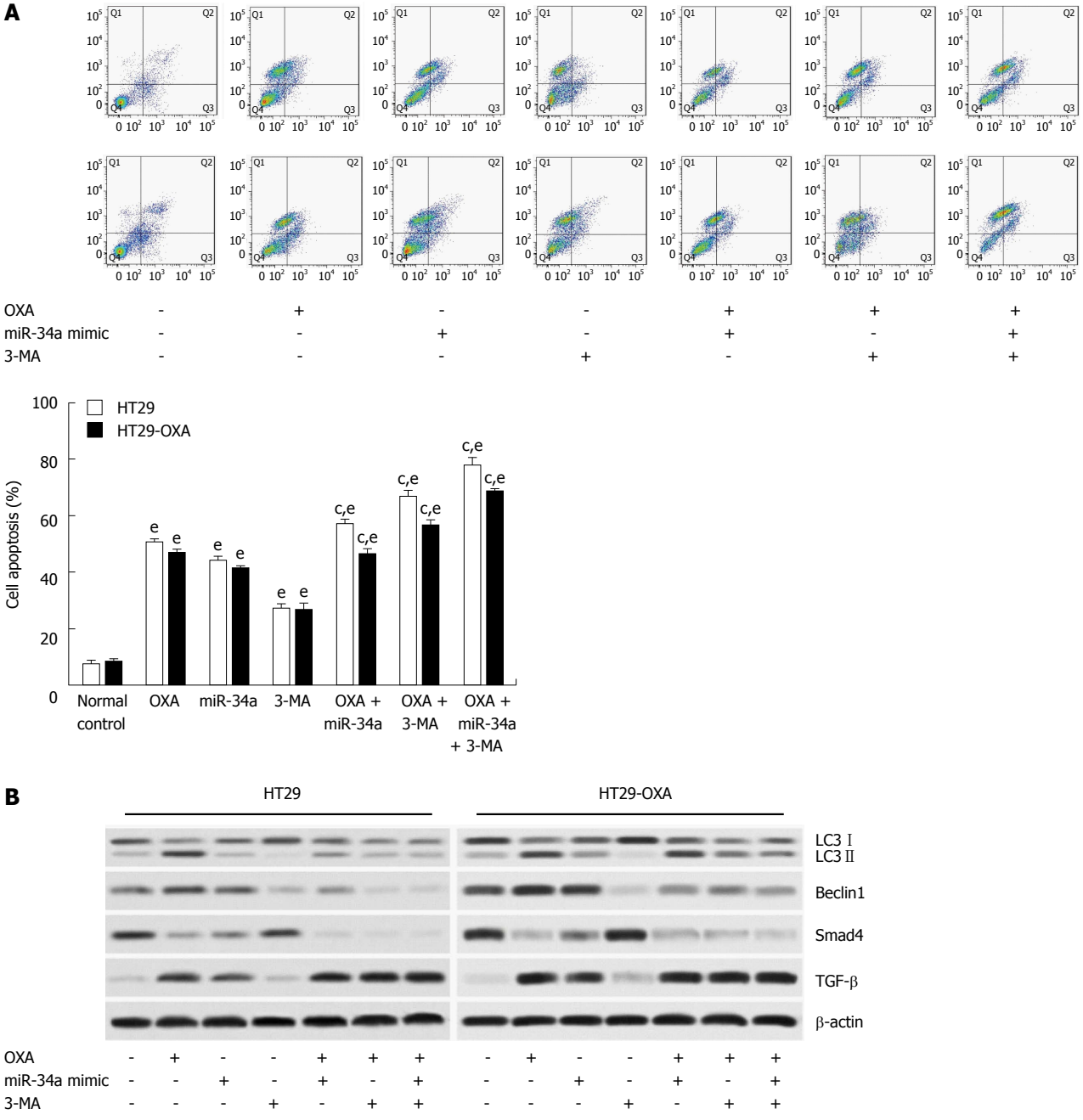

Figure 6 Activation of autophagy protected colorectal cancer cells against oxaliplatin-induced apoptosis by inhibiting miR-34a through the TGF-β/Smad4 pathway. A: HT29 and HT29-oxaliplatin (OXA) cells were transfected with miR-34a mimics and treated with OXA (10 μmol/L) and simultaneously mixed with or without 3-MA. After 48 h, the apoptosis rate was examined by flow cytometry; B: The above cell lysates were examined with the indicated antibodies by western blotting. β-actin was used as loading control. $^{e}P < 0.001$ indicates a significant difference *vs* normal control; $^{c}P < 0.05$ indicates a significant difference *vs* group treated with OXA.

OXA-resistant cells (Figure 5A). miR-34a mimics decreased expression of LC3-II, beclin-1, Smad4 and TGF-β, while OXA treatment increased their expression, and in agreement with quantitative flow cytometry, induction was impaired by treatment with miR-34a mimics mixed with OXA in parental and OXA-resistant cells (Figure 5B). These results indicate that miR-34a participates in the regulation of OXA-induced macroautophagy in CRC cells through downregulation of the TGF-β/Smad4 signaling pathway.

Macroautophagy protection of CRC cells from OXA-induced apoptosis by inhibiting miR-34a through the TGF-β/Smad4 pathway

To determine the mechanism of macroautophagy in OXA-induced apoptosis in CRC cells, we exposed cells to OXA for 48 h with miR-34a mimics or 3-MA and assessed apoptotic rate. 3-MA attenuated the activation of macroautophagy and the anti-apoptotic capacity in HT29 and HT29-OXA cells treated with OXA, as shown by a higher apoptotic rate (Figure

6A). In addition, lower expression of LC3-II, beclin 1, Bax, Smad4 and TGF-β and higher expression of Bcl-2 were found compared with the control group and the OXA treatment group (Figure 6B). Moreover, when treated with OXA, miR-34a mimics and 3-MA, more significantly inhibitory effects on autophagic activity and the anti-apoptotic rate in HT29 and HT29-OXA cells were achieved. These results indicated that the activation of macroautophagy may serve as a protective mechanism against OXA-induced apoptosis by inhibiting miR-34a through the TGF-β/Smad4 pathway in CRC cells.

DISCUSSION

In the present study, we investigated whether miR-34a mediates OXA resistance of colorectal cancer cells by inhibiting macroautophagy *via* the TGF-β/Smad4 pathway. We found that miR-34a levels were significantly decreased in CRC patients after systematic chemotherapy by OXA and in CRC cells treated with OXA. We further demonstrated that miR-34a downregulation increased macroautophagy activation by targeting Smad4. More important, macroautophagy inhibition abolished miR-34a downregulation-induced apoptosis. These data suggest that OXA-induced downregulation of miR-34a increases drug resistance by activating macroautophagy in CRC cells. The TGF-β/Smad4 pathway plays an important role in regulating macroautophagy response[20]. Further investigation found that OXA treatment enhanced macroautophagy *via* inhibiting the expression of miR-34a and activating the TGF-β/Smad4 pathway, which at least partly enacted the protective role of macroautophagy on CRC cell apoptosis induced by OXA.

CRC is a major cause of cancer-related mortality worldwide and its incidence is increasing. Chemotherapy can be used in addition to surgery in certain cases as an adjuvant therapy. However, drug resistance represents a major obstacle for chemotherapy of CRC. OXA is a promising drug for the treatment of advanced CRC. Despite a rapid shrinkage in tumor mass following chemotherapy, the resistance of cancer cells to OXA frequently results in the subsequent recurrence and metastasis of cancer, and the exact mechanism for this effect is still not well understood. Therefore, there is an urgent need to investigate these adverse factors that might help us better understand the mechanism of drug resistance in CRC patients.

Macroautophagy is considered to play a dual role in the regulation of cell fate in the context of cancer treatment[21,22]. Numerous studies have focused on the association between the cytoprotective effects of autophagy and the development of chemoresistance. Sustained drug exposure can induce an imbalance in apoptotic pathways and lead to resistance to apoptosis[23]. Modest macroautophagy is implicated in promoting chemoresistance of cancer cells and attenuating the efficacy of chemotherapy. Lv *et al*[24] have demonstrated that upregulation of CD44v6 contributes to acquired chemoresistance *via* the modulation of macroautophagy in CRC cells. Yang *et al*[14] have reported that macroautophagy contributes to the enrichment and survival of CRC stem cells under OXA treatment. These observations suggest that macroautophagy serves as a pro-survival mechanism that promotes chemoresistance, and selective inhibition of macroautophagy regulators has the potential to improve chemotherapeutic regimens. Here, we found that OXA treatment promoted macroautophagy activation in CRC cells, which protected the cells from OXA-induced apoptosis.

miRNAs are frequently dysregulated in chemoresistant cancers, and they have been shown to target macroautophagy-related genes or modulators[12,13]. It has been well established that miR-34a is an important anti-oncogene by regulation of different downstream targets in various types of cancer[25]. miR-34a has also been identified as one of the molecular species associated with drug resistance in CRC[10]. Here, we reported that miR-34a levels were significantly decreased in CRC patients after systematic chemotherapy by OXA and in CRC cells treated with OXA. Expression of miR-34a was downregulated in OXA-resistant cells. Forced expression of miR-34a promoted OXA-induced apoptosis in parental and OXA-resistant cells.

Among the miR-34a targets, Smad4 is a key regulator of the TGF-β/Smad pathway, which is well characterized as a positive mediator of macroautophagy[6]. Based on our previous study, here we found that mRNA expression of TGF-β and Smad4 was upregulated in CRC patients after OXA chemotherapy. Moreover, expression levels of miR-34a and Smad4 were inversely correlated in human blood samples from CRC patients. Our results showed forced upregulation of miR-34a significantly inhibited protein expression of Smad4 and TGF-β. Contrasting results were observed when the CRC cells were treated with OXA. We have also applied bioinformatic methods to demonstrate that Smad4 is a potential target of miR-34a[6]. Our data reveal that miR-34a directly targets the 3′-UTR of Smad4 and that ectopic expression of miR-34a represses Smad4 and TGF-β protein levels in parental and OXA-resistant CRC cells. Our results demonstrate that the TGF-β/Smad4 pathway at least partly is involved in regulating miR-34a-inhibited macroautophagy and contributes to OXA resistance in CRC.

Our data demonstrate that transfection of miR-34a mimics enhances the therapeutic effect of OXA by inhibition of cell macroautophagy and improves the efficacy of OXA against OXA-resistant CRC cells. The macroautophagy inhibitor, 3-MA, enhances the pro-apoptotic effect in cells treated with OXA or exogenous miR-34a. These data suggest that activation of macroautophagy protects CRC cells from OXA-induced apoptosis by inhibiting miR-34a expression.

In summary, the results of this study demonstrate a significant association between miR-34a expression and the acquired chemoresistance of OXA in CRC. The miR-34a-mediated OXA resistance occurs through its inhibitory effects on macroautophagy *via* regulation of the TGF-β/Smad4 pathway. Our findings suggest that miR-34a could be a potentially therapeutic target for improving the chemotherapeutic effect of OXA in CRC.

COMMENTS

Background

Colorectal cancer (CRC) is one of the most common cancers worldwide. Oxaliplatin (OXA)-based systemic chemotherapy combined with surgical resection plays an important role in the treatment of CRC. However, chemoresistance to OXA is a major limitation in the clinic, and the underlying mechanism is not clear.

Research frontiers

miRNAs have been conserved during evolution and have emerged recently as potent regulators of gene expression, cell proliferation, apoptosis and tumorigenesis. The authors, in a previous study, have demonstrated that miRNA (miR)-34a inhibits epithelial mesenchymal transition in human cholangiocarcinoma by targeting Smad4 through the transforming growth factor (TGF)-β/Smad pathway. More importantly, miR-34a is involved in drug resistance and regulating chemosensitivity in CRC. Some researchers have shown that autophagy is involved in the regulation of chemoresistance. However, whether miR-34a is involved in mediating the chemoresistance of OXA by affecting autophagic activity remained unclear.

Innovations and breakthroughs

This study found that expression of miR-34a was significantly reduced while expression of TGF-β and Smad4 was increased in CRC patients treated with OXA-based chemotherapy. OXA treatment also decreased miR-34a and increased TGF-β and Smad4 levels in parental cells and OXA-resistant CRC cells. Activation of autophagy contributed to OXA resistance in CRC cells. In addition, the data in this study indicated that the relative expression levels of Smad4 and miR-34a in CRC patients had a significant inverse correlation, and overexpression of miR-34a inhibited autophagy activation by directly targeting Smad4 through the TGF-β/Smad4 pathway. The authors further demonstrated that OXA-induced downregulation of miR-34a increased drug resistance by activating autophagy in CRC cells. Moreover, they identified that miR-34a mediated TGF-β/Smad4 pathway induced macroautophagy, which may represent a novel mechanism regulating chemoresistance in CRC.

Applications

The findings in this study suggest that miR-34a could be a potentially therapeutic target for improving the chemotherapeutic effect of OXA in CRC.

Terminology

OXA is a third-generation platinum compound, and is the first platinum-based compound to show efficacy in the treatment of CRC. miRNAs are a group of noncoding RNAs that have been highly conserved during evolution and have emerged recently as potent regulators of gene expression, cell proliferation, apoptosis and tumorigenesis. Macroautophagy is a catabolic degradation process that is required to maintain cellular homeostasis.

Peer-review

In the original article of Sun *et al* the authors demonstrated that a significant association exists between miR-34a expression and the acquired chemo-resistance of OXA in CRC. The miR-34a mediated OXA resistance was found to be mediated by the inhibitory effects of miR34a on autophagy by regulating the TGF-β/Smad4 pathway. Their findings suggest that miR-34a could be a potentially therapeutic target for improving the OXA-based chemotherapeutic effect in CRC. The study is well designed, and moderately presented.

REFERENCES

1 **Ung L**, Lam AK, Morris DL, Chua TC. Tissue-based biomarkers predicting outcomes in metastatic colorectal cancer: a review. *Clin Transl Oncol* 2014; **16**: 425-435 [PMID: 24458880 DOI: 10.1007/s12094-013-1154-6]

2 **Sostres C**, Gargallo CJ, Lanas A. Aspirin, cyclooxygenase inhibition and colorectal cancer. *World J Gastrointest Pharmacol Ther* 2014; **5**: 40-49 [PMID: 24605250 DOI: 10.4292/wjgpt.v5.i1.40]

3 **Meyerhardt JA**, Mayer RJ. Systemic therapy for colorectal cancer. *N Engl J Med* 2005; **352**: 476-487 [PMID: 15689586 DOI: 10.1056/NEJMra040958]

4 **Bartel DP**. MicroRNAs: target recognition and regulatory functions. *Cell* 2009; **136**: 215-233 [PMID: 19167326 DOI: 10.1016/j.cell.2009.01.002]

5 **Matamala N**, Vargas MT, González-Cámpora R, Miñambres R, Arias JI, Menéndez P, Andrés-León E, Gómez-López G, Yanowsky K, Calvete-Candenas J, Inglada-Pérez L, Martínez-Delgado B, Benítez J. Tumor microRNA expression profiling identifies circulating microRNAs for early breast cancer detection. *Clin Chem* 2015; **61**: 1098-1106 [PMID: 26056355 DOI: 10.1373/clinchem.2015.238691]

6 **Qiao P**, Li G, Bi W, Yang L, Yao L, Wu D. microRNA-34a inhibits epithelial mesenchymal transition in human cholangiocarcinoma by targeting Smad4 through transforming growth factor-beta/Smad pathway. *BMC Cancer* 2015; **15**: 469 [PMID: 26077733 DOI: 10.1186/s12885-015-1359-x]

7 **Welch C**, Chen Y, Stallings RL. MicroRNA-34a functions as a potential tumor suppressor by inducing apoptosis in neuroblastoma cells. *Oncogene* 2007; **26**: 5017-5022 [PMID: 17297439 DOI: 10.1038/sj.onc.1210293]

8 **Zhou JY**, Chen X, Zhao J, Bao Z, Chen X, Zhang P, Liu ZF, Zhou JY. MicroRNA-34a overcomes HGF-mediated gefitinib resistance in EGFR mutant lung cancer cells partly by targeting MET. *Cancer Lett* 2014; **351**: 265-271 [PMID: 24983493 DOI: 10.1016/j.canlet.2014.06.010]

9 **Ranadive IN**, Sussman DA. Prevention of Colorectal Cancer: The Future Is Now. *Curr Colorectal Cancer Rep* 2014; **10**: 1-10 [DOI: 10.1007/s11888-013-0201-6]

10 **Toden S**, Tran HM, Tovar-Camargo OA, Okugawa Y, Goel A. Epigallocatechin-3-gallate targets cancer stem-like cells and enhances 5-fluorouracil chemosensitivity in colorectal cancer. *Oncotarget* 2016; **7**: 16158-16171 [PMID: 26930714 DOI: 10.18632/oncotarget.7567]

11 **Duncan C**, Papanikolaou T, Ellerby LM. Autophagy: polyQ toxic fragment turnover. *Autophagy* 2010; **6**: 312-314 [PMID: 20104018]

12 **He C**, Dong X, Zhai B, Jiang X, Dong D, Li B, Jiang H, Xu S, Sun X. MiR-21 mediates sorafenib resistance of hepatocellular carcinoma cells by inhibiting autophagy via the PTEN/Akt pathway. *Oncotarget* 2015; **6**: 28867-28881 [PMID: 26311740 DOI: 10.18632/oncotarget.4814]

13 **Pan B**, Feng B, Chen Y, Huang G, Wang R, Chen L, Song H. MiR-200b regulates autophagy associated with chemoresistance in human lung adenocarcinoma. *Oncotarget* 2015; **6**: 32805-32820 [PMID: 26416454 DOI: 10.18632/oncotarget.5352]

14 **Yang HZ**, Ma Y, Zhou Y, Xu LM, Chen XJ, Ding WB, Zou HB. Autophagy contributes to the enrichment and survival of colorectal cancer stem cells under oxaliplatin treatment. *Cancer Lett* 2015; **361**: 128-136 [PMID: 25749420 DOI: 10.1016/j.canlet.2015.02.045]

15 **Zhou Y**, Wan G, Spizzo R, Ivan C, Mathur R, Hu X, Ye X, Lu J, Fan F, Xia L, Calin GA, Ellis LM, Lu X. miR-203 induces oxaliplatin resistance in colorectal cancer cells by negatively regulating ATM kinase. *Mol Oncol* 2014; **8**: 83-92 [PMID: 24145123 DOI: 10.1016/j.molonc.2013.09.004]

16 **Li G**, Thomas AM, Williams JA, Kong B, Liu J, Inaba Y, Xie W, Guo GL. Farnesoid X receptor induces murine scavenger receptor Class B type I via intron binding. *PLoS One* 2012; **7**: e35895 [PMID: 22540009 DOI: 10.1371/journal.pone.0035895]

17 **Qiao PF**, Yao L, Zhang XC, Li GD, Wu DQ. Heat shock pretreatment improves stem cell repair following ischemia-reperfusion injury via autophagy. *World J Gastroenterol* 2015; **21**: 12822-12834 [PMID: 26668506 DOI: 10.3748/wjg.v21.i45.12822]
18 **Yang AD**, Fan F, Camp ER, van Buren G, Liu W, Somcio R, Gray MJ, Cheng H, Hoff PM, Ellis LM. Chronic oxaliplatin resistance induces epithelial-to-mesenchymal transition in colorectal cancer cell lines. *Clin Cancer Res* 2006; **12**: 4147-4153 [PMID: 16857785 DOI: 10.1158/1078-0432.CCR-06-0038]
19 **Burada F**, Nicoli ER, Ciurea ME, Uscatu DC, Ioana M, Gheonea DI. Autophagy in colorectal cancer: An important switch from physiology to pathology. *World J Gastrointest Oncol* 2015; **7**: 271-284 [PMID: 26600927 DOI: 10.4251/wjgo.v7.i11.271]
20 **Suzuki HI**, Kiyono K, Miyazono K. Regulation of autophagy by transforming growth factor-β (TGF-β) signaling. *Autophagy* 2010; **6**: 645-647 [PMID: 20458184 DOI: 10.4161/auto.6.5.12046]
21 **Kenific CM**, Debnath J. Cellular and metabolic functions for autophagy in cancer cells. *Trends Cell Biol* 2015; **25**: 37-45 [PMID: 25278333 DOI: 10.1016/j.tcb.2014.09.001]
22 **White E**. The role for autophagy in cancer. *J Clin Invest* 2015; **125**: 42-46 [PMID: 25654549 DOI: 10.1172/JCI73941]
23 **Lubner SJ**, Loconte NK, Holen KD, Schelman W, Thomas JP, Jumonville A, Eickhoff JC, Seo S, Mulkerin DL. A phase II study of oxaliplatin, 5-fluorouracil, leucovorin, and high-dose capecitabine in patients with metastatic colorectal cancer. *Clin Colorectal Cancer* 2010; **9**: 157-161 [PMID: 20643620 DOI: 10.3816/CCC.2010.n.021]
24 **Lv L**, Liu HG, Dong SY, Yang F, Wang QX, Guo GL, Pan YF, Zhang XH. Upregulation of CD44v6 contributes to acquired chemoresistance via the modulation of autophagy in colon cancer SW480 cells. *Tumor Biology* 2016; **37**: 8811-8824 [PMID: 26747179 DOI: 10.1007/s13277-015-4755-6]
25 **Li H**, Rokavec M, Hermeking H. Soluble IL6R represents a miR-34a target: potential implications for the recently identified IL-6R/STAT3/miR-34a feed-back loop. *Oncotarget* 2015; **6**: 14026-14032 [PMID: 26091352 DOI: 10.18632/oncotarget.4334]

P- Reviewer: Sipos F **S- Editor**: Gong ZM **L- Editor**: Filipodia
E- Editor: Wang CH

World Journal of Gastroenterology

Submit a Manuscript: http://www.wjgnet.com/esps/ *World J Gastroenterol* 2017 March 14; 23(10): 1828-1835

DOI: 10.3748/wjg.v23.i10.1828 ISSN 1007-9327 (print) ISSN 2219-2840 (online)

ORIGINAL ARTICLE

Basic Study

Experimental porcine model of complex fistula-in-ano

Ma-Mu-Ti-Jiang A Ba-Bai-Ke-Re, Hui Chen, Xue Liu, Yun-Hai Wang

Ma-Mu-Ti-Jiang A Ba-Bai-Ke-Re, Hui Chen, Xue Liu, Yun-Hai Wang, Department of Anorectal Surgery, First Affiliated Hospital, Xinjiang Medical University, Urumqi 830011, Xinjiang Uygur Autonomous Region, China

Author contributions: A Ba-Bai-Ke-Re MMTJ contributed to study conception and design, and surgical technique (critically important intellectual content); Substantial contributions including research, study design, data source, recording, acquisition of data and final approval of the version to be published was carried out by Chen H and Liu X; analysis and interpretation of data was performed by Wang YH.

Supported by the National Natural Science Foundation of China, No. 81460133; Innovation program of regional cooperation of Xinjiang Autonomous Region, China, No. 2016E02063.

Institutional review board statement: This research was reviewed and approved by the Institutional Review Board of The First Affiliated Hospital of Xinjiang Medical University, Urumqi, China.

Institutional animal care and use committee statement: All procedures involving animals in this research were reviewed and approved by the Institutional Animal Care and Use Committee of the First Affiliated Hospital of Xinjiang Medical University, Urumqi, China (IACUC protocol number: 81460133).

Conflict-of-interest statement: The authors declared that there is no conflict of interest related to this research.

Data sharing statement: Technical appendix, statistical code, and dataset of this original article "Experimental Porcine Model of Fistula-In-Ano" is available from the corresponding author at mamutjan206@sina.com. We state that (1) we agree not to further share the data with others; (2) we will not permit the data to be used to set up any form of competing resource; and (3) we will not permit the supplied data to be used in support of any commercial activities.

Manuscript source: Unsolicited manuscript

Correspondence to: Ma-Mu-Ti-Jiang A Ba-Bai-Ke-Re, MD, PhD, Chief Physician, Professor, Department of Anorectal Surgery, First Affiliated Hospital, Xinjiang Medical University, 1 Liyushan Road, Urumqi 830011, Xinjiang Uygur Autonomous Region, China. mamutjan206@sina.com
Telephone: +86-135-79803435
Fax: +86-99-14366938

Received: October 26, 2016
Peer-review started: October 27, 2016
First decision: December 28, 2016
Revised: January 6, 2017
Accepted: January 18, 2017
Article in press: January 18, 2017
Published online: March 14, 2017

Abstract

AIM

To establish and evaluate an experimental porcine model of fistula-in-ano.

METHODS

Twelve healthy pigs were randomly divided into two groups. Under general anesthesia, the experimental group underwent rubber band ligation surgery, and the control group underwent an artificial damage technique. Clinical magnetic resonance imaging (MRI) and histopathological evaluation were performed on the 38th d and 48th d after surgery in both groups, respectively.

RESULTS

There were no significant differences between the experimental group and the control group in general

characteristics such as body weight, gender, and the number of fistula ($P > 0.05$). In the experimental group, 15 fistulas were confirmed clinically, 13 complex fistulas were confirmed by MRI, and 11 complex fistulas were confirmed by histopathology. The success rate in the porcine complex fistula model establishment was 83.33%. Among the 18 fistulas in the control group, 5 fistulas were confirmed clinically, 4 complex fistulas were confirmed by MRI, and 3 fistulas were confirmed by histopathology. The success rate in the porcine fistula model establishment was 27.78%. Thus, the success rate of the rubber band ligation group was significantly higher than the control group ($P < 0.05$).

CONCLUSION

Rubber band ligation is a stable and reliable method to establish complex fistula-in-ano models. Large animal models of complex anal fistulas can be used for the diagnosis and treatment of anal fistulas.

Key words: Complex fistula-in-ano; Animal model; Fistulas

Core tip: Different new surgical methods for fistula-in-ano such as fibrin sealant or AFP plug should be used to establish animal models before a clinical trial begins. We established an experimental porcine anal fistula model using a rubber band ligation method which may provide a possible platform for anorectal fistula research. This surgical method using rubber band ligation is more stable and reliable than an artificial damage technique. Our porcine model of fistula-in-ano was confirmed by histopathology and anatomically similar to humans. This porcine model of fistula-in-ano can be used in the diagnosis and treatment of anal fistulas.

A Ba-Bai-Ke-Re MMTJ, Chen H, Liu X, Wang YH. Experimental porcine model of complex fistula-in-ano. *World J Gastroenterol* 2017; 23(10): 1828-1835 Available from: URL: http://www.wjgnet.com/1007-9327/full/v23/i10/1828.htm DOI: http://dx.doi.org/10.3748/wjg.v23.i10.1828

INTRODUCTION

Fistula-in-ano is a common disorder in general surgery. A simple, open fistulectomy or fistulotomy is effective for simple or low fistulas. However, complex or multiple-tract fistulas are difficult to treat due to a high rate of recurrence and a significant risk of incontinence. Surgery remains the only method of healing anal fistulas. To date, various treatment methods have been used for fistula-in-ano due to the lack of a standard treatment. Numerous surgical procedures including fistulotomy, the Seton cutting procedure, fibrin glue, endoanal advancement flaps, and ligation of the intersphincteric fistula track have been performed. The main aim of anal fistula treatment is to eradicate internal and external openings while preserving anorectal continence. Many treatments can result in sphincter damage and fecal incontinence. For example, use of the Seton cutting procedure is associated with healing rates of approximately 80%-100%, but fecal incontinence rates of up to 60%[1-3]. Fistulotomy results in healing in approximately 75%-100% of patients, but impairs continence in up to 60%, especially in those with a complex fistula[4-6]. Fistulotomy, although extremely effective in treatment of anal fistulas, is not a feasible option when the fistula tract incorporates a significant amount of internal and external anal sphincter, as is the case in many high trans-sphincteric fistulas[7,8]. The mucosal advancement flap, a technically precise operation, is the best established alternative to fistulotomy, with reported success rates ranging from 37% to 89%[9,10] and with incontinence rates ranging from 9% to 21%[9,11]. Fibrin glue injection through the fistula tract is a minimally invasive, sphincter-sparing alternative, but long-term recurrence reaches 69%-100%[12]. To date, there is no standard management method for anal fistulas as none of these procedures has a high chance of success and no risk, and depends on the patients' anatomy, fistula anatomy and the patient's wishes. A variety of new surgical procedures for anorectal fistula or anal gland infection[13] should be performed in animals in order to minimize the possible risk to humans. Small animal models of anal fistula have not been well described in terms of the pathogenesis and healing of anorectal fistulas. Buchanan *et al*[14] successfully established large animal models of anal fistulas and described possible surgical techniques. Although their research provided an important experimental platform for an anal fistula model using large animals, the exact pathogenesis of fistula formation was not described[15]. Different and novel surgical methods, such as fibrin sealant or AFP plug, should be undertaken using animal models before clinical trials are performed. It is necessary to establish large animal models in this research field. Ideal animals used in fistula models are monkeys or dogs[16,17]. However, monkey or dog experiments are not practical. The main purpose of the present prospective study was to establish an experimental porcine anal fistula model using a rubber band ligation method and to provide a possible platform for anorectal fistula research.

MATERIALS AND METHODS

Animal selection and experimental ethics

This research was conducted in accordance with animal ethics regulation laws published in 1986 and an animal protection law of the People's Republic

Table 1 Comparison of the general data between the two groups

	Number of animals	Number of fistulas	Male/female ratio	Average weight
Experimental group	6	18	3/3	39.3 ± 1.1
Control group	6	18	4/2	38.9 ± 1.2
χ^2/t value			0.3429	0.6019
P value			0.5582	0.5606

of China. Care and handling of the animals were in compliance with the "Guide for the Care and Use of Laboratory Animals". Written approval was obtained from the animal experiment ethics committee of The First Affiliated Hospital of Xinjiang Medical University. All aspects of this study, including animal husbandry, were undertaken at the First Affiliated Hospital of Xinjiang Medical University. Considering the similarities of the internal and external sphincter to human anorectal structure, pigs were selected for this research. Twelve healthy pigs (with an average weight of 39-45 kg), chosen from the experimental animal center of the First Affiliated Hospital of Xinjiang Medical University, were used to establish an anal fistula model using rubber band ligation surgery. All pigs were randomly divided into two groups in accordance with a computerized random number table. Under general anesthesia, the experimental group underwent rubber band ligation surgery, and the control group underwent an artificial damage technique. An intramuscular injection of the anesthetic Zoteil 50 at 1 mL/kg was administered. Two mL of lidocaine was administered to the local area for efficient general anesthesia.

Perioperative management

Under general anesthesia, six experimental animals underwent rubber band ligation surgery, and 18 models of fistula-in-ano were created. The control group underwent an artificial damage technique. There were no significant differences between the experimental group and the control group regarding general characteristics such as body weight, gender, and number of fistula ($P > 0.05$) (Table 1). All animals received a visual examination, palpation, and anoscopy in the right lateral position after general anesthesia and disinfection. On the 28th d after surgery, the rubber bands were removed in the experimental group. Clinical magnetic resonance imaging (MRI) and histopathological evaluation were performed on the 38th d and 48th d after surgery in both groups, respectively. Clinical and histopathological evaluations were also carried out in both groups.

Surgical intervention

Modeling methods in the experimental group: All animals in the experimental group underwent regular disinfection, visual anus examination, and diagnostic anoscopy under general anesthesia. A 0.5 cm minimal incision in the anus was made in the lithotomy position at the 3, 9, and 12 o'clock positions. The 6 o'clock position was not used as it was extremely close to the pig's tail and coccyx, and to avoid the risk of sepsis. A rubber band Seton was directly crossed through the anal sphincter and inserted into the sphincter using forceps. The incision was fixed using a gauze bandage. All animals were placed in the postoperative care unit until they regained consciousness. Vital signs were monitored after surgery.

Modeling methods in the control group: All perioperative care, preparation, and incisions in the control group were the same as for the experimental group. Forceps were directly crossed through the anal sphincter and inserted into the sphincter. No additional materials were inserted into this artificial canal. Following the establishment of these two models, all animals received postoperative monitoring and a standard diet.

Postoperative intervention: All wounds in the two groups were observed and dressed daily. All Setons were extracted on the 28th d under general anesthesia. As anus sonography is unstable, all animals underwent anorectal MRI after Seton extraction in order to determine anatomical structure on the 38th d after surgery according to the diagnostic guide for MRI[18]. On the 48th d after surgery, fistulas were resected again and histopathological examinations were performed. Following these procedures, all animals were given their usual diet.

Animal care and use statement

The animal protocol in this research was designed to minimize animal pain and discomfort. The pigs were acclimatized to laboratory conditions (23 ℃, 12h/12h light/dark, 50% humidity, ad libitum access to food and water) for eight weeks prior to experimentation. Intragastric gavage was carried out in conscious animals, using straight gavage needles appropriate for animal size (35-45 g body weight: 22 gauge, 1 inch length, 1.25 mm ball diameter). All animals were euthanized by barbiturate overdose (intravenous injection, 150 mg/kg pentobarbital sodium) for tissue collection.

Outcome measures and statistical analysis

All animals were reexamined under general anesthesia to determine the clinical state of the created fistulas. Fistula creation was considered successful when a clear outer opening on clinical observation or obvious structures on MRI were observed. The basic structure of the fistula and hyperplastic tissue or fibroblast components were considered histopathological confirmation of the fistula model (Figures 1-3). The end point of fistula healing was the disappearance of the

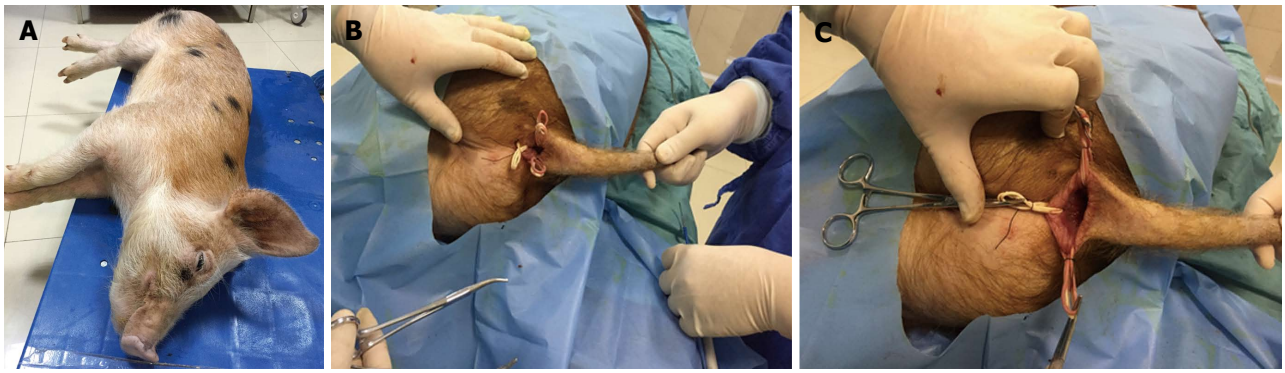

Figure 1 Porcine model creation process. A: Intramuscular injection with anesthetic Zoteil 50 at 1 mL/kg; B: A 0.5 cm minimal incision made in the anus at 3, 9, and 12 o'clock position and ligated rubber used; C: Directly cross through the anal sphincter with rubber band seton.

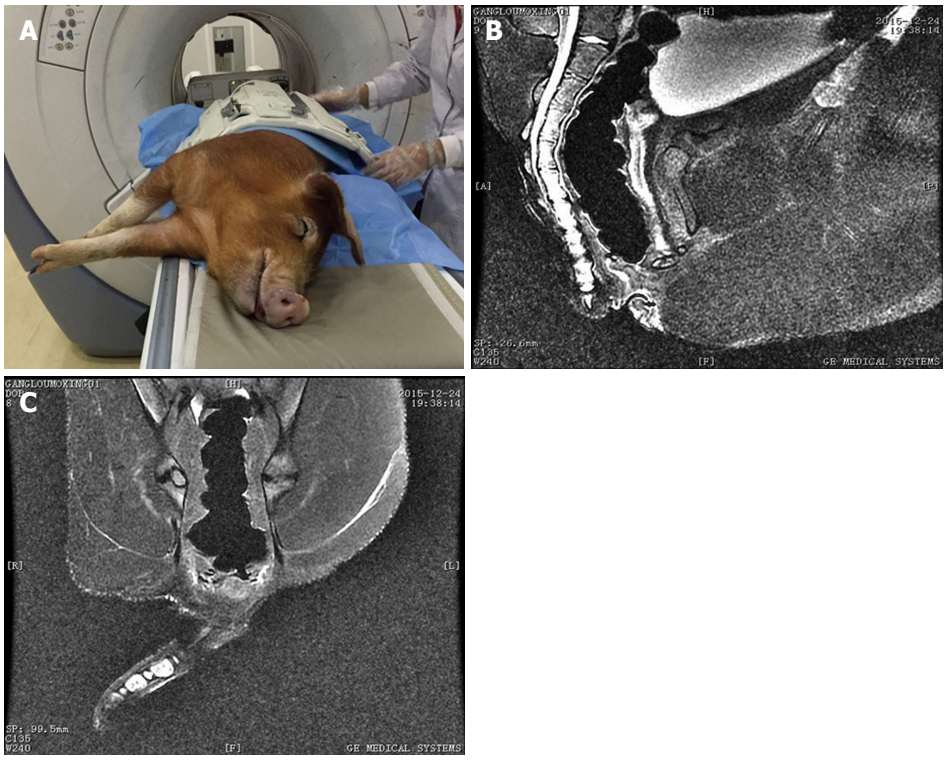

Figure 2 Magnetic resonance imaging evaluation of created fistulas. A: Created fistulas; B and C: Typical fistula imaging was found and it was very similar to human anal fistula imaging of magnetic resonance imaging.

lumen on MRI or clinical observation.

Numerical data were expressed as the median and ranges. Excel data analysis was performed using SPSS 19.0 software. The χ^2 test was used to compare related data. $P < 0.05$ was considered statistically significant.

RESULTS

Following surgery, all animals were alive with no obvious adverse effects and no postoperative complications such as abscess or general infection. There were no significant differences between the experimental group and the control group regarding general characteristics such as body weight, gender, and number of fistulas ($P > 0.05$). In the experimental group, 15 fistulas were confirmed clinically, 13 complex fistulas (7 lower type and 6 hilar type) were confirmed by MRI, and 11 fistulas were confirmed by histopathology. All 11 fistulas assessed histologically had a lumen and surrounding granulation tissue. The granulation tissue was similar to that seen in human fistula-in-ano. The clinical success rate of the porcine fistula model was 83.33%. In the control group of 18 fistulas, 5 fistulas were confirmed clinically, 4 fistulas were confirmed by MRI, and 3 fistulas were confirmed by histopathology. The clinical success rate of the porcine fistula model was 27.78%. The success rate of the rubber band ligation group was significantly better than the control group ($P < 0.05$) (Table 2).

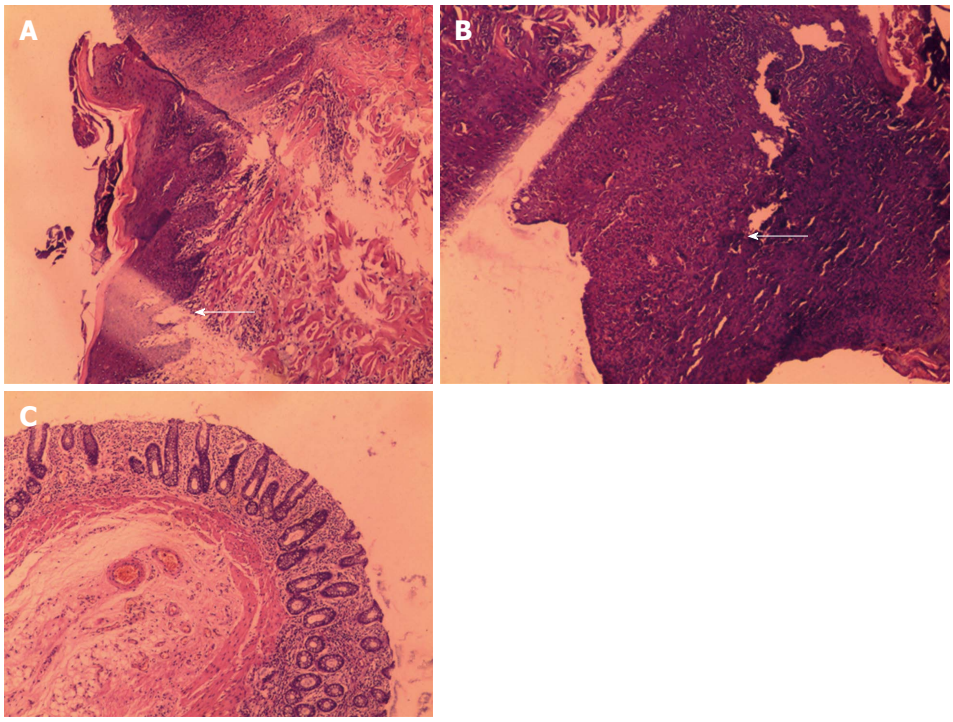

Figure 3 Pathological findings of created fistulas. A: Epithelization in the created fistula tract; B and C: Epithelization and granulation were found in the created fistula tract.

Table 2 Comparison of the characteristics and outcome between the two groups

Group	Animals	No. of fistulas	Number of successful clinical models	MRI showing typical characteristics of complex fistulas	Pathological features showing fixed fistulas
Experimental group	6	18	15	13	11
Control group	6	18	5	4	3
χ^2 value			9.1125	7.1331	7.4805
P value			0.0025	0.0076	0.0062

DISCUSSION

Anorectal fistula is an abnormal channel between the anal canal and perianal skin due to chronic infection, and is also called an anal fistula, or fistula-in-ano. Highly complex anal fistulas are very common and difficult to treat in clinical practice[19-21]. The recurrence rate of highly complex fistulas is high, and the healing time is long. Satisfactory defecation control after traditional open surgery causes major difficulties in the treatment of this disease. Although anal fistulas are caused by chronic infections, it is not the same as a typical superficial chronic infection. The traditional treatment of anal fistulas, such as fistulotomy, fistulectomy, or Seton ligation therapy, can be associated with longer healing time and significant pain in patients. In addition, care can be complicated by anal dysfunction or even fecal incontinence[22,23]. According to previous research, a mucosal advancement flap is an alternative method for repairing fistula-in-ano; however, this procedure requires demanding technical support and has a high postoperative recurrence rate. Although fibrin glue treatment is effective for fistulas, according to a recent meta-analysis, the success rate varies. These surgical procedures have obvious shortcomings, and a standard procedure is needed for treating anal fistulas. Reducing recurrence and avoiding postoperative incontinence are the final objectives of most new minimally invasive surgical methods[24,25]. However, animal experiments should be carried out to confirm the safety and efficacy of the method before it is put into clinical application.

With the application of new concepts in perianal anatomy, anorectal physiology, and the pathogenesis of anal fistulas, there is an increasing tendency to perform new therapeutic methods, and there has been great progress in anorectal studies. Most of the studies on anorectal diseases were based on clinical aspects such as diagnosis or clinical treatment. However, there is less information on basic research, such as animal experiments. Due to technical difficulties and high research cost, it is not easy to carry out basic research on large animals. The purpose of establishing the present animal model was to fill this gap and provide a platform for further research in this field. This study provides a feasible animal model for further study on

the diagnosis and treatment of anal fistulas.

In this study, we confirmed that there were no significant differences between the experimental group and the control group regarding the general characteristics such as body weight, gender, and number of fistulas ($P > 0.05$). In the experimental group, 15 fistulas were confirmed clinically, 13 complex fistulas were confirmed by MRI, and 11 fistulas were confirmed by histopathology. The clinical success rate of the porcine fistula model establishment was 83.33%. This result was encouraging. In the control group of 18 fistulas, 5 fistulas were confirmed clinically, 4 fistulas were confirmed by MRI, and 3 fistulas were confirmed by histopathology. The clinical success rate of the porcine fistula model was 27.78%. The success rate in the rubber band ligation group was significantly higher than that in the control group ($P < 0.05$). The final results indicated that the rubber band ligation method was a better animal model of fistula-in-ano. We consider that use of the rubber band ligation technique is stable and reliable, and better than the artificial damage technique.

As it is impossible to resect the anal canal in humans, the ideal experimental animal is the monkey. These animals have typical anal gland structures similar to humans; however, considering the national animal protection laws, we selected pigs instead and obtained satisfactory models of fistula-in-ano. As shown by MRI and histopathological analysis, we established 15 anal fistula models. We found scar granulation tissue near the fistula. The morphology of the anal muscle was very similar to human internal and external anal sphincter structures. Model fistulas in the experimental group had rich granulation tissue confirmed by MRI and histopathology.

We designed the anal fistula model using pigs as a large animal experimental model of fistula-in-ano is essential when histopathologic evaluations and reproducibility are required. This study presents a successful large animal experimental model of fistula-in-ano, which satisfies the need for new management alternatives such as an anal fistula plug or stem cells.

We believe that the rubber band ligation procedure creates a better fistula model. This model had good tolerance. We observed the experimental animals for 60 d; 15 did not heal naturally, and the three remaining fistulas self-healed. Self-healing may be related to the anti-infection ability of the porcine itself, but the exact mechanism is unclear[26-28] and requires further study. We found that the anal fistulas established using the rubber band ligation method simulated the pathophysiology of a clinical anal fistula. Compared with the animal model using BLAKE silicone drains by Aikawa *et al*[29], the rubber band ligation model was easily created and observed. In the aforementioned research, the authors confirmed the construction of a fistula according to clinical manifestations. However, they did not describe how the animal model was established or observed using measurement methods such as MRI or histopathology. We conclude that the rubber band ligation method was reliable and resulted in less damage to the normal surrounding tissues. Marianas[30] constructed an anal fistula model using steel wire. However, the author was unable to detect possible changes in the surrounding tissues and the state of the sphincter. We believe that steel wire can easily lead to unnecessary damage to normal tissues. In the present study, we also found many epithelial cells, fibroblasts, inflammatory cells, and muscle cell proliferation around the fistula. It is possible that the created porcine fistula model may be associated with the epithelization of chronic inflamed tissue. We also conclude that simple injury does not create a good anal fistula model. It is necessary to provide enough time for the granulation process near the artificial fistula.

With regard to durability and follow-up in this study, we were unable to demonstrate durability (longer length of time, stability without Seton) due to resection of the anus and sphincter at the end of the experiment. Some fistulas healed in the control group; thus, these animals showed good healing of damage in the anorectal area. Therefore, it is difficult to determine whether a stable fistula can be obtained after the Seton is removed. Further investigations are required to obtain satisfactory fistulas. In addition, we were unable to detect the length of the puborectalis muscle which is closely related to the diagnosis of complex fistula-in-ano.

To date, complex human anal fistulas have not been effectively resolved[31-33]. Many anorectal surgeons have attempted to use minimally invasive surgical treatments for anal fistulas, but have failed. Our research team also tried to determine the efficacy of minimally invasive surgery, but the results after a long follow-up period indicated that the final success rate was unsatisfactory[34]. In order to obtain more precise proof regarding pathogenesis, further animal studies and other fundamental researches are required. The porcine anus is anatomically similar to humans, which was confirmed by MRI and histology. We conclude that use of rubber band ligation to establish a complex anorectal fistula was stable and reliable. Rubber band ligation was better than the artificial damage technique. Furthermore, the experimental porcine anal fistula model using rubber band ligation can be used in the diagnosis and treatment of anal fistulas. Large animal models of anal fistula can also be used for other anorectal diseases such as hemorrhoids, anal fissure and anorectal abscess formation.

Compared with the animal model using BLAKE silicone drains by Aikawa *et al*[29], the rubber band ligation model was easily created and observed. We searched for articles on animal anal fistula models using PubMed and Web of Science databases, however, we only identified 4 relevant articles. The researchers in these studies confirmed the establishment of fistula according to clinical manifestations only. They did not describe how the animal model was established or

the measurement methods used such as pathophysiology, MRI and histopathology. In our research, we determined that the rubber band ligation method was reliable using MRI or histopathology. Although we were unable to determine the pathophysiologic evidence of the model, we believe that imaging and pathology assessment were more practical than pathophysiology. In addition, the pathophysiologic determination of fistula is not easy. Anal fistula models established using the rubber band ligation method could simulate the pathophysiology of clinical anal fistulas. We will carry out further studies in order to obtain pathophysiologic evidence of rubber band ligation in the near future.

ACKNOWLEDGMENTS

The authors would like to thank the members of the animal experiment center of Xinjiang Medical University for their technical support; Dr. Turgunjan Tuerxun for his careful language assistance; and Xiang Yan in Xinjiang Medical University for his assistance in careful statistical analysis.

COMMENTS

Background

Fistula-in-ano is a common disorder in general surgery. A simple open fistulectomy or fistulotomy is effective for simple or low fistula. However, complex or multiple tract higher fistulas are difficult to treat due to a high rate of recurrence and a significant risk of incontinence. Different new surgical methods such as fibrin sealant or AFP plug should be carried out using animal models before clinical trials are performed. There is still a need to establish large animal models in this research field.

Research frontiers

The main purpose of this prospective study was to establish an experimental porcine anal fistula model using a rubber band ligation method and to provide a possible platform for anorectal fistula research.

Innovations and breakthroughs

Surgery using rubber band ligation was stable and reliable. This method was better than the artificial damage technique. Fistulas in the experimental group had rich granulation tissue, which was confirmed by magnetic resonance imaging (MRI) and histopathology.

Applications

In order to obtain more precise proof regarding pathogenesis, further animal studies and other fundamental researches are needed. The porcine anus is anatomically similar to humans, which was confirmed by MRI and histology. Furthermore, the experimental porcine or large animal models of anal fistula model can be used in the diagnosis and treatment of anal fistulas.

Terminology

Animal models are a central component of studies aimed at understanding the pathophysiological or anatomical bases of certain diseases, and are essential in the development of new, more effective therapies which are desperately needed.

Peer-review

It is a good original research about the establishment and assess of an experimental porcine model of fistula-in-ano in large animal models. They demonstrate that the surgical method using rubber ligation to establish complex fistula-in-ano was stable and reliable. This method was better than the artificial damage process.

REFERENCES

1 **Rizzo JA**, Naig AL, Johnson EK. Anorectal abscess and fistula-in-ano: evidence-based management. *Surg Clin North Am* 2010; **90**: 45-68 [PMID: 20109632 DOI: 10.1016/j.suc.2009.10.001]
2 **Ho KS**, Tsang C, Seow-Choen F, Ho YH, Tang CL, Heah SM, Eu KW. Prospective randomised trial comparing ayurvedic cutting seton and fistulotomy for low fistula-in-ano. *Tech Coloproctol* 2001; **5**: 137-141 [PMID: 11875680]
3 **Ommer A**, Herold A, Berg E, Fürst A, Sailer M, Schiedeck T. Cryptoglandular anal fistulas. *Dtsch Arztebl Int* 2011; **108**: 707-713 [PMID: 22114639 DOI: 10.3238/arztebl.2011.0707]
4 **Shawki S**, Wexner SD. Idiopathic fistula-in-ano. *World J Gastroenterol* 2011; **17**: 3277-3285 [PMID: 21876614 DOI: 10.3748/wjg.v17.i28.3277]
5 **Whiteford MH**, Kilkenny J, Hyman N, Buie WD, Cohen J, Orsay C, Dunn G, Perry WB, Ellis CN, Rakinic J, Gregorcyk S, Shellito P, Nelson R, Tjandra JJ, Newstead G. Practice parameters for the treatment of perianal abscess and fistula-in-ano (revised). *Dis Colon Rectum* 2005; **48**: 1337-1342 [PMID: 15933794]
6 **Deeba S**, Aziz O, Sains PS, Darzi A. Fistula-in-ano: advances in treatment. *Am J Surg* 2008; **196**: 95-99 [PMID: 18466873 DOI: 10.1016/j.amjsurg.2007.12.047]
7 **Jordán J**, Roig JV, García-Armengol J, García-Granero E, Solana A, Lledó S. Risk factors for recurrence and incontinence after anal fistula surgery. *Colorectal Dis* 2010; **12**: 254-260 [PMID: 19220375 DOI: 10.1111/j.1463-1318.2009.01806.x]
8 **van Koperen PJ**, Safiruddin F, Bemelman WA, Slors JF. Outcome of surgical treatment for fistula in ano in Crohn's disease. *Br J Surg* 2009; **96**: 675-679 [PMID: 19434701 DOI: 10.1002/bjs.6608]
9 **Athanasiadis S**, Köhler A, Nafe M. Treatment of high anal fistulae by primary occlusion of the internal ostium, drainage of the intersphincteric space, and mucosal advancement flap. *Int J Colorectal Dis* 1994; **9**: 153-157 [PMID: 7814990]
10 **van der Hagen SJ**, Baeten CG, Soeters PB, van Gemert WG. Long-term outcome following mucosal advancement flap for high perianal fistulas and fistulotomy for low perianal fistulas: recurrent perianal fistulas: failure of treatment or recurrent patient disease? *Int J Colorectal Dis* 2006; **21**: 784-790 [PMID: 16538494]
11 **Mizrahi N**, Wexner SD, Zmora O, Da Silva G, Efron J, Weiss EG, Vernava AM, Nogueras JJ. Endorectal advancement flap: are there predictors of failure? *Dis Colon Rectum* 2002; **45**: 1616-1621 [PMID: 12473884]
12 **Loungnarath R**, Dietz DW, Mutch MG, Birnbaum EH, Kodner IJ, Fleshman JW. Fibrin glue treatment of complex anal fistulas has low success rate. *Dis Colon Rectum* 2004; **47**: 432-436 [PMID: 14978618]
13 **McColl I**. The comparative anatomy and pathology of anal glands. Arris and Gale lecture delivered at the Royal College of Surgeons of England on 25th February 1965. *Ann R Coll Surg Engl* 1967; **40**: 36-67 [PMID: 6016560]
14 **Buchanan GN**, Sibbons P, Osborn M, Bartram CI, Ansari T, Halligan S, Cohen CR. Experimental model of fistula-in-ano. *Dis Colon Rectum* 2005; **48**: 353-358 [PMID: 15714247 DOI: 10.1007/s10350-004-0769-7]
15 **Harvey CE**. Perianal fistula in the dog. *Vet Rec* 1972; **91**: 25-33 [PMID: 5072622 DOI: 10.1136/vr.91.2.25]
16 **Greiner TP**. Surgical treatment of canine perianal fistulas. *Vet Med Small Anim Clin* 1981; **76**: 663-664 [PMID: 6913298]
17 **PARKS AG**. Pathogenesis and treatment of fistuila-in-ano. *Br Med J* 1961; **1**: 463-469 [PMID: 13732880]
18 **Lunniss PJ**, Armstrong P, Barker PG, Reznek RH, Phillips RK. Magnetic resonance imaging of anal fistulae. *Lancet* 1992; **340**: 394-396 [PMID: 1353557 DOI: 10.1016/0140-6736(92)91472-K]
19 **Lenisa L**, Espìn-Basany E, Rusconi A, Mascheroni L, Escoll-Rufino J, Lozoya-Trujillo R, Vallribera-Valls F, Mégevand J. Anal fistula plug is a valid alternative option for the treatment of complex anal fistula in the long term. *Int J Colorectal Dis* 2010;

25: 1487-1493 [PMID: 20556403]
20 **de la Portilla F**, Rada R, Jiménez-Rodríguez R, Díaz-Pavón JM, Sánchez-Gil JM. Evaluation of a new synthetic plug in the treatment of anal fistulas: results of a pilot study. *Dis Colon Rectum* 2011; **54**: 1419-1422 [PMID: 21979188 DOI: 10.1097/DCR.0b013e31822c4d59]
21 **Ommer A**, Herold A, Joos A, Schmidt C, Weyand G, Bussen D. Gore BioA Fistula Plug in the treatment of high anal fistulas--initial results from a German multicenter-study. *Ger Med Sci* 2012; **10**: Doc13 [PMID: 22984363 DOI: 10.3205/000164]
22 **Ratto C**, Litta F, Parello A, Donisi L, Zaccone G, De Simone V. Gore Bio-A® Fistula Plug: a new sphincter-sparing procedure for complex anal fistula. *Colorectal Dis* 2012; **14**: e264-e269 [PMID: 22288601 DOI: 10.1111/j.1463-1318.2012.02964.x]
23 **Chan S**, McCullough J, Schizas A, Vasas P, Engledow A, Windsor A, Williams A, Cohen CR. Initial experience of treating anal fistula with the Surgisis anal fistula plug. *Tech Coloproctol* 2012; **16**: 201-206 [PMID: 22527917 DOI: 10.1007/s10151-012-0810-0]
24 **Han JG**, Xu HM, Song WL, Jin ML, Gao JS, Wang ZJ, Yang XQ. Histologic analysis of acellular dermal matrix in the treatment of anal fistula in an animal model. *J Am Coll Surg* 2009; **208**: 1099-1106 [PMID: 19476898 DOI: 10.1016/j.jamcollsurg.2009.02.052]
25 **Adedeji OA**, Bailey CA, Varma JS. Porcine dermal collagen graft in abdominal-wall reconstruction. *Br J Plast Surg* 2002; **55**: 85-86 [PMID: 11783979]
26 **O'Riordan JM**, Datta I, Johnston C, Baxter NN. A systematic review of the anal fistula plug for patients with Crohn's and non-Crohn's related fistula-in-ano. *Dis Colon Rectum* 2012; **55**: 351-358 [PMID: 22469804 DOI: 10.1097/DCR.0b013e318239d1e4]
27 **van Koperen PJ**, D'Hoore A, Wolthuis AM, Bemelman WA, Slors JF. Anal fistula plug for closure of difficult anorectal fistula: a prospective study. *Dis Colon Rectum* 2007; **50**: 2168-2172 [PMID: 17701369]
28 **Schwandner O**, Stadler F, Dietl O, Wirsching RP, Fuerst A. Initial experience on efficacy in closure of cryptoglandular and Crohn's transsphincteric fistulas by the use of the anal fistula plug. *Int J Colorectal Dis* 2008; **23**: 319-324 [PMID: 18038233]
29 **Aikawa M**, Miyazawa M, Okada K, Akimoto N, Koyama I, Yamaguchi S, Ikada Y. A newly designed anal fistula plug: clinicopathological study in an experimental iatrogenic fistula model. *Int Surg* 2013; **98**: 122-128 [PMID: 23701146 DOI: 10.9738/CC180]
30 **Arakakia MS**, Henrique C, dos Santos M, Falc GR, Cassinob CP, Nakamurab RK, Gomesb NF, Coutinho Santosb RG. Experimental model of anal fistula in rats. *J Coloproctol* 2013; **33**: 135-138 [DOI: 10.1016/j.jcol.2013.04.005]
31 **Ky AJ**, Sylla P, Steinhagen R, Steinhagen E, Khaitov S, Ly EK. Collagen fistula plug for the treatment of anal fistulas. *Dis Colon Rectum* 2008; **51**: 838-843 [PMID: 18330649 DOI: 10.1007/s10350-007-9191-2]
32 **Lawes DA**, Efron JE, Abbas M, Heppell J, Young-Fadok TM. Early experience with the bioabsorbable anal fistula plug. *World J Surg* 2008; **32**: 1157-1159 [PMID: 18373120 DOI: 10.1007/s00268-008-9504-1]
33 **Christoforidis D**, Etzioni DA, Goldberg SM, Madoff RD, Mellgren A. Treatment of complex anal fistulas with the collagen fistula plug. *Dis Colon Rectum* 2008; **51**: 1482-1487 [PMID: 18521674 DOI: 10.1007/s10350-008-9374-5]
34 **A ba-bai-ke-re MM**, Wen H, Huang HG, Chu H, Lu M, Chang ZS, Ai EH, Fan K. Randomized controlled trial of minimally invasive surgery using acellular dermal matrix for complex anorectal fistula. *World J Gastroenterol* 2010; **16**: 3279-3286 [PMID: 20614483 DOI: 10.3748/wjg.v16.i26.3279]

P- Reviewer: Munoz M, Ren JA **S- Editor**: Qi Y
L- Editor: Ma JY **E- Editor**: Zhang FF

World Journal of Gastroenterology

Submit a Manuscript: http://www.wjgnet.com/esps/

World J Gastroenterol 2017 March 14; 23(10): 1836-1842

DOI: 10.3748/wjg.v23.i10.1836

ISSN 1007-9327 (print) ISSN 2219-2840 (online)

ORIGINAL ARTICLE

Retrospective Cohort Study

Serum HER2 as a predictive biomarker for tissue HER2 status and prognosis in patients with gastric cancer

Hong-Zhi Shi, Yu-Ning Wang, Xiao-Hui Huang, Ke-Cheng Zhang, Hong-Qing Xi, Jian-Xin Cui, Guo-Xiao Liu, Wen-Tao Liang, Bo Wei, Lin Chen

Hong-Zhi Shi, Xiao-Hui Huang, Ke-Cheng Zhang, Hong-Qing Xi, Jian-Xin Cui, Guo-Xiao Liu, Wen-Tao Liang, Bo Wei, Lin Chen, Department of General Surgery, Chinese PLA General Hospital, Beijing 100853, China

Hong-Zhi Shi, Department of General Surgery, General Hospital of Armed Police Force, Beijing 100039, China

Yu-Ning Wang, Department of Surgery, Chinese PLA General Hospital, Beijing 100853, China

Wen-Tao Liang, Institute of General Surgery, Chinese PLA General Hospital, Beijing 100853, China

Author contributions: Shi HZ, Wang YN, Huang XH and Zhang KC contributed equally to this work; Shi HZ, Wang YN, Huang XH and Zhang KC designed the study; Xi HQ, Cui JX and Liu GX conducted the experiments; Liang WT, Wei B and Chen L interpreted the data; all authors approved the final version to be published.

Supported by National Natural Science Foundation of China, No. 81272698, No. 81672319 and No. 81602507.

Institutional review board statement: The study was approved by the Research Ethics Committee of the Chinese People's Liberation Army General Hospital.

Informed consent statement: All study participants provided written consent prior to study enrollment.

Conflict-of-interest statement: All the authors have no conflict of interest.

Data sharing statement: No additional data are available.

Manuscript source: Invited manuscript

Correspondence to: Dr. Lin Chen, Department of General Surgery, Chinese PLA General Hospital, Fuxing Road 28, Beijing 100853, China. chenlinbj301@163.com
Telephone: +86-10-66938128
Fax: +86-10-68181689

Received: October 21, 2016
Peer-review started: October 25, 2016
First decision: December 28, 2016
Revised: January 3, 2017
Accepted: January 17, 2017
Article in press: January 17, 2017
Published online: March 14, 2017

Abstract

AIM

To investigate the association between serum human epidermal growth factor receptor 2 (HER2) extracellular domain (ECD) and tissue HER2 status, and the prognostic value of serum HER2 ECD in patients with gastric cancer.

METHODS

A total of 239 patients with gastric cancer were enrolled from December 2012 to June 2013. Serum HER2 ECD was determined by chemiluminescent assay, and tissue HER2 status was evaluated by immunohistochemistry and fluorescence *in situ* hybridization assay. A receiver operating characteristic (ROC) curve was plotted to identify the optimal cut-off value for serum HER2 ECD assay for predicting survival in gastric cancer patients.

RESULTS

Serum HER2 ECD was significantly correlated with tissue HER2 status ($P < 0.001$), tumor size ($P < 0.001$), and intestinal type of gastric cancer ($P =$

0.021). Serum HER2 ECD levels differed significantly between patients with HER2-positive tissue expression and those with HER2-negative tissue expression. ROC analysis yielded an area under the curve value of 0.79 (95%CI: 0.71-0.87, $P < 0.001$), with a sensitivity and specificity of 0.54 (95%CI: 0.37-0.70) and 0.93 (95%CI: 0.88-0.96), respectively. With a cut-off value of 24.75 ng/mL, high serum HER2 ECD had a negative impact on overall survival of the patients (HR: 1.93, 95%CI: 1.32-4.38, $P = 0.006$).

CONCLUSION

Serum HER2 ECD could be a highly specific surrogate biomarker for tissue HER2 status in gastric cancer. Optimal cut-off criteria for predicting survival should be established.

Key words: Gastric cancer; Serum HER2 extracellular domain; Tissue HER2 status; Prognosis

Core tip: Precise determination of HER2 status is crucial for the appropriate use of HER2-targeted therapy in gastric cancer patients. Our study investigated the association between serum HER2 extracellular domain (ECD) and tissue HER2 status, and also determined the prognostic value of serum HER2 ECD in a large cohort of patients. Serum HER2 ECD could provide an easily accessible surrogate marker for tissue HER2 status, with high specificity. Furthermore, high serum HER2 ECD had a negative impact on overall survival in patients with gastric cancer.

Shi HZ, Wang YN, Huang XH, Zhang KC, Xi HQ, Cui JX, Liu GX, Liang WT, Wei B, Chen L. Serum HER2 as a predictive biomarker for tissue HER2 status and prognosis in patients with gastric cancer. *World J Gastroenterol* 2017; 23(10): 1836-1842 Available from: URL: http://www.wjgnet.com/1007-9327/full/v23/i10/1836.htm DOI: http://dx.doi.org/10.3748/wjg.v23.i10.1836

INTRODUCTION

Patients with advanced gastric cancer positive for human epidermal growth factor receptor 2 (HER2) expression or gene amplification may benefit from HER2-targeted therapy[1]. Accurate determination of HER2 status is therefore crucial for the appropriate use of such therapy, as emphasized in the National Comprehensive Cancer Network Clinical Practice Guidelines in Oncology[2]. These guidelines recommend the use of immunohistochemistry (IHC) and fluorescence *in situ* hybridization (FISH) to assess HER2 overexpression. However, these recommended methods have some limitations. First, a 13% discordancy rate has been reported between the results of IHC and FISH assays[3]. This discrepancy might be partly due to the fact that IHC detects protein expression on the tumor cell surface, while FISH detects gene amplification in the tumor cell nucleus. Second, IHC is semi-quantitative and notoriously subjective, while FISH is time-consuming and relatively expensive. Third, HER2 status might change during trastuzumab therapy[4], and neither IHC nor FISH are effective assays for reflecting the real-time scenario of HER2 status[5]. More convenient and reproducible detection methods are therefore needed to identify HER2-positive gastric cancer, thus facilitating the appropriate and effective use of HER2-targeted therapy[6].

Noninvasive serum HER2 extracellular domain (ECD) assay has the potential to supplement existing HER2 tests[5]. HER2 ECD is the extracellular fragment of the HER2 protein, which is located on the surface of tumor cells and may be released into the circulation by shedding. Detection of serum HER2 ECD could thus provide additional information on HER2 status. Compared with tissue specimens, blood samples are readily accessible and can be obtained repeatedly, making serum HER2 ECD assay an ideal tool for the dynamic monitoring of tumor phenotype. Moreover, the approved automatic detection platforms[7], could be used to measure serum HER2 ECD levels objectively and reliably. The clinical relevance of serum HER2 ECD has been investigated extensively in breast cancer, and good concordance has been reported between serum HER2 ECD levels and HER2 status in the primary tumor site[8-10]. Generally, high serum HER2 ECD levels in patients with metastatic breast cancer were correlated with high risk of disease progression, decreased survival, and reduced response to treatment[11-13]. Several studies have also investigated the clinical significance of serum HER2 ECD in gastric cancer[14-16]. However, differences in detection methods and patient enrollment across studies have led to inconsistent results regarding the associations among serum HER2 ECD concentrations, tissue HER2 status, and patient outcome. Further studies are therefore urgently needed to provide more solid data[17].

Here, we conducted a retrospective study in a large cohort of patients with gastric cancer to investigate the relationship between serum HER2 ECD concentration and tissue HER2 status, and to determine the prognostic value of serum HER2 ECD.

MATERIALS AND METHODS

Patient enrollment

This study was approved by the Research Ethics Committee of the Chinese People's Liberation Army General Hospital. A total of 239 consecutive patients with histologically and pathologically confirmed gastric cancer treated between December 2012 and June 2013 were included. Written informed consent was obtained from the patients. Fasting blood samples

Table 1 Clinicopathological characteristics

Variables	No. of patients	Percent
Age (range, 23-89, yr)		
⩾ 60	126	52.7
< 60	113	47.3
Gender		
Male	167	69.9
Female	72	30.1
Smoking status		
Never	61	25.5
Ever	178	74.5
Tumor location		
GEJ	41	17.2
Non-GEJ	198	82.8
Tumor size		
⩾ 5 cm	102	42.7
< 5 cm	137	57.3
pTNM stage		
Ⅰ	39	16.3
Ⅱ	78	32.6
Ⅲ	102	42.7
Ⅳ	20	8.4
Lauren classification		
Intestinal type	104	43.5
Diffuse type	135	56.5
Tissue HER2 status (IHC/FISH)		
Positive	39	16.3
Negative	200	83.7
Serum HER2 ECD (ng/mL), median (range)	10.5 (4.2-190.2)	

GEJ: Gastroesophageal junction; HER2: Human epidermal growth factor receptor-2; ECD: Extracellular domain; IHC: Immunohistochemistry; FISH: Fluorescence *in situ* hybridization.

were collected the day after admission to hospital, and then stored at -80 ℃ until analysis. Clinicopathological variables including age, gender, tumor location, tumor size, tissue HER2 status, and survival time were collected. Patients were followed up every 3 mo for the first 2 years, every 6 mo for the next 3 years, and every 1 year after 5 years.

Tissue HER2 status evaluated by IHC and FISH

HER2 IHC was performed as described previously[18]. In brief, tumor specimens were fixed in 10% neutral-buffered formalin overnight and embedded in paraffin blocks. Sections (4 μm) were cut from the tissue paraffin blocks, and IHC was performed using HercepTest II™ (Dako, Denmark) according to the manufacturer's instructions. This process was conducted at the Department of Pathology, Chinese People's Liberation Army General Hospital. IHC sections were reviewed by experienced pathologists and were scored for HER2 expression according to the criteria used in the ToGA trial[1]. If tissue HER2 expression was scored as 2+, a further FISH assay was performed with Abbott-Vysis PathVysion™ (Abbott Laboratories, United States) according to the manufacturer's protocol. Tumor specimens with a HER2:CEP17 signal ratio ⩾ 2.0 or 3+ IHC staining intensity were judged as HER2-positive.

Serum HER2 ECD assay

Serum HER2 ECD concentrations were measured by chemiluminescence immunoassays using the ADVIA Centaur System (Siemens Diagnostics, United States) with a detection range of 0.5-350 ng/mL. The assays were conducted in strict adherence with the manufacturer's instructions and blinded to clinical outcomes.

Statistical analysis

Overall survival (OS) was defined as the period from surgery to death from any cause, and patients who were alive were censored at the last follow-up. Survival curves were plotted by the Kaplan-Meier method, and log-rank tests were used to compare curves. Receiver operating characteristic (ROC) curves were plotted to investigate the diagnostic role of serum HER ECD for tissue HER2 status. Youden's index (sensitivity + specificity - 1) was used to determine the optimal cut-off value from the ROC plot. The associations between serum HER2 ECD concentrations and clinicopathological variables were investigated using χ^2 tests. Student's *t* test and Mann-Whitney test were used for analysis of continuous variables. Statistical analyses were performed and presented using GraphPad Prism 6. A two-sided *P* value < 0.05 was considered significant.

RESULTS

Patient characteristics

A total of 239 patients with gastric cancer were enrolled in the study. The patient characteristics are shown in Table 1. The median age was 61 years (range: 23-89 years), and there were 167 (69.9%) men and 72 (30.1%) women. All tumors were adenocarcinomas. According to the American Joint Committee on Cancer 7th edition, 39 (16.3%) patients had stage Ⅰ, 78 (32.6%) had stage Ⅱ, 102 (42.7%) had stage Ⅲ, and 20 (8.4%) had stage Ⅳ tumors. Tumors were classified as intestinal- and diffuse-type in 104 (43.5%) and 135 (56.5%) patients, respectively.

Regarding tissue HER2 status, 150 patients were IHC 1+/0 according to IHC staining, 70 were IHC 2+, and 19 were IHC 3+. Patients with IHC 2+ expression were subjected to FISH assay, and 20 of these patients demonstrated gene amplification (Figure 1). According to the criteria in the ToGA trial, there were 200 (83.7%) HER2-negative and 39 (16.3%) HER2-positive cases.

Predictive performance of serum HER2 ECD for tissue HER2 status

The median serum HER2 ECD concentration among the enrolled patients was 10.5 ng/mL (range: 4.2-190.2 ng/mL). Patients with HER2-positive gastric cancer had significantly higher serum HER2 ECD levels than those with HER2-negative gastric cancer (*P* < 0.001) (Figure 2A). The median serum HER2 ECD concentrations

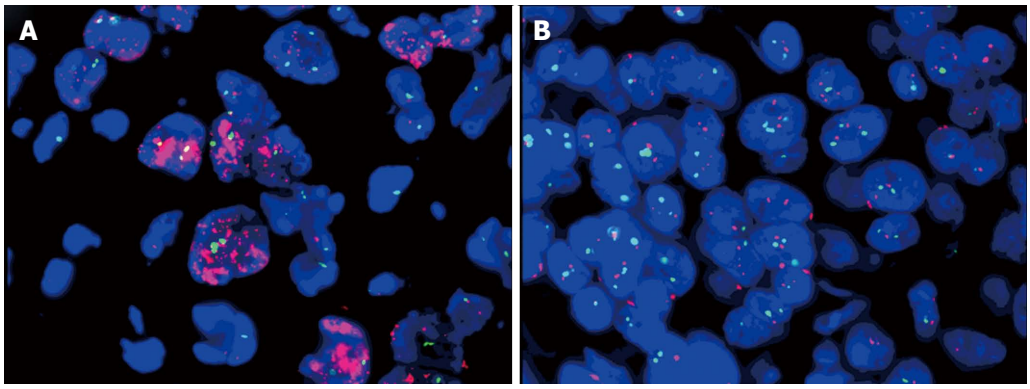

Figure 1 Representative gene amplification results of fluorescence *in situ* hybridization. A: Cases with HER2:CEP17 signal ratio > 2.0; B: Cases with HER2:CEP17 signal ratio < 2.0.

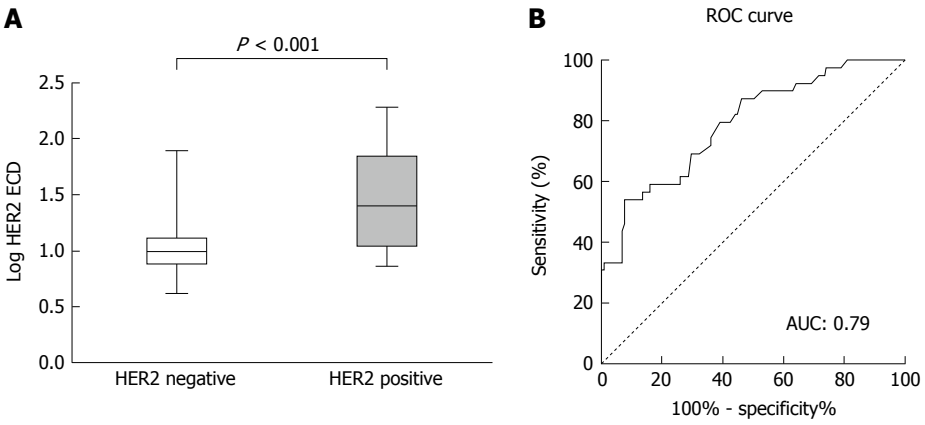

Figure 2 Serum HER2 ECD concentrations in patients with tissue HER2-positive and HER2-negative gastric cancer (A) and receiver operating characteristic curve plot of serum HER2 ECD for tissue HER2 status (B).

in HER2-positive and HER2-negative patients were 25.2 ng/mL (range: 7.3-190.2 ng/mL) and 9.9 ng/mL (range: 4.2-77.7 ng/mL), respectively.

To investigate the predictive potential of serum HER2 ECD for tissue HER2 status, we initially choose a cut-off value of 15.0 ng/mL, as recommended for breast cancer by the Food and Drug Administration (FDA). The sensitivity and specificity were 0.59 (95%CI: 0.42-0.74) and 0.83 (95%CI: 0.77-0.88), respectively (Table 2). The ROC plot showed an area under the curve value of 0.79 (95%CI: 0.71-0.87, $P < 0.001$) (Figure 2B). Youden's index yielded an optimal cut-off value of 24.75 ng/mL, with a sensitivity and specificity of 0.54 (95%CI: 0.37-0.70) and 0.93 (95%CI: 0.88-0.96), respectively.

Survival analysis

There were 93 deaths after a median follow-up time of 33 mo (range: 19-42 mo). The Kaplan-Meier curves are shown in Figure 3. Survival analysis demonstrated no significant difference in survival time between patients with HER2-positive and those with HER2-negative gastric cancer. The median OS in patients with HER2-positive gastric cancer was 37 mo, compared with 38 months in patients with HER2-negative gastric cancer (HR: 1.46 (0.92-2.73), $P = 0.11$) (Figure 3A). There was also no difference in survival time between patients with serum HER2 ECD levels ⩾ 15.0 ng/mL and those with levels < 15.0 ng/mL [median time: 37 mo *vs* 38 mo, HR: 1.37 (0.87-2.36), $P = 0.17$] (Figure 3B). However, using a cut-off point of 24.75 ng/mL (determined by Youden's index in the ROC plot), patients with higher serum HER2 ECD levels had significantly shorter survival compared with patients with lower serum HER2 ECD [median time: 36 mo *vs* 38 mo, HR: 1.93 (1.32-4.38), $P = 0.006$] (Figure 3C).

Correlations between serum HER2 ECD levels and clinicopathological variables

We divided the enrolled patients into high-and low-serum HER2 ECD groups based on the cut-off value of 24.75 ng/mL. High serum HER2 ECD concentrations were significantly correlated with large tumor size ($P < 0.001$), intestinal type ($P = 0.021$), and tissue HER2 status ($P < 0.001$) (Table 3).

DISCUSSION

The clinical application of serum HER2 ECD has been

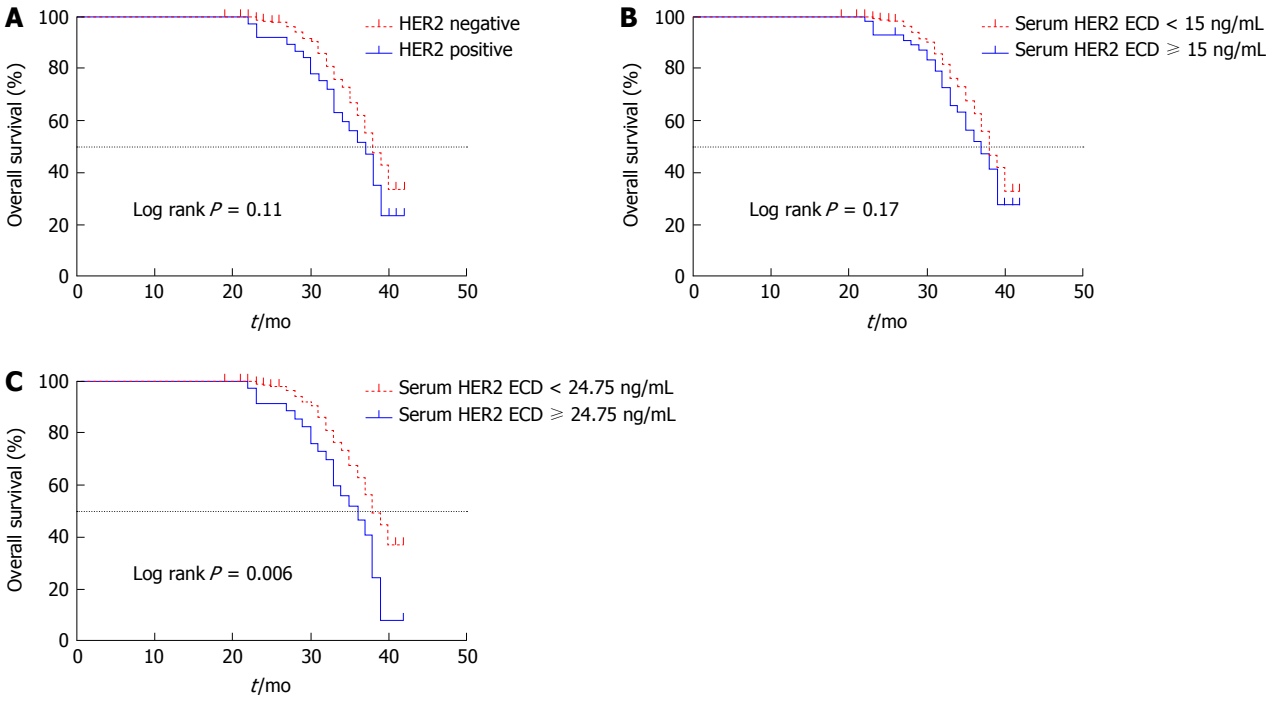

Figure 3 Kaplan-Meier curves for overall survival. A: Overall survival in patients with HER2-positive and HER2-negative gastric cancer; B: Serum HER2 extracellular domain (ECD) level < 15 ng/mL and serum HER2 ECD ⩾ 15.0 ng/mL; and C: Serum HER2 ECD < 24.75 ng/mL and serum HER2 ECD ⩾ 24.75 ng/mL.

Table 2 Diagnostic performance of serum HER2 extracellular domain for tissue HER2 status at different cut-off values

Cut-off values (ng/mL)	True positive	False positive	True negative	False negative	Sensitivity (95%CI)	Specificity (95%CI)
15.00[1]	23	35	165	16	0.59 (0.42-0.74)	0.83 (0.77-0.88)
24.75[2]	21	15	185	18	0.54 (0.37-0.70)	0.93 (0.88-0.96)

[1]Value recommended by FDA for breast cancer; [2]Value determined by Youden's index in ROC plot.

extensively investigated in breast cancer, and has shown promising diagnostic and prognostic potentials[5]. However, investigations of its role in gastric cancer remain in the initial stages, and inconsistent results related to the use of different assays and cut-off values[16] highlight the need for further studies in this field[17].

The current study enrolled 239 patients, which, to the best of our knowledge, comprises the largest cohort to date in studies using the chemiluminescence immunoassay method to determine serum HER2 ECD concentrations. Our results showed that patients with HER2-positive gastric cancer had higher serum HER2 ECD concentrations than patients with HER2-negative gastric cancer. Furthermore, there was a significant association between tissue HER2 status and serum HER2 ECD levels. Moreover, high serum HER2 ECD concentrations were correlated with tumor size, suggesting that circulating HER2 ECD might be released from tumor cells. The ROC plot yielded an optimal sensitivity and specificity of 0.54 and 0.93, respectively, indicating that the serum HER2 ECD assay had high value for identifying patients with HER2-negative expression. Furthermore, our study also showed that serum HER2 ECD concentrations ⩾ 24.75 ng/mL had a negative impact on OS in patients with gastric cancer, and could thus be a useful prognostic indicator.

Using the cut-off value of 15.0 ng/mL recommended for breast cancer by the FDA, we observed no survival difference between patients with high and low serum HER2 ECD concentrations. However, our ROC analysis identified the higher level of 24.75 ng/mL as the optimal cut-off value. A previous study reported similar results, and calculated an optimal cut-off value of > 15.0 ng/mL from an ROC plot[19]. These results suggest that the value of 15.0 ng/mL recommended by the FDA for breast cancer might not be suitable for gastric cancer. There were also different HER2 gene amplification criteria for breast cancer and gastric cancer; a HER2:CEP17 signal ratio > 2.2 was considered to indicate as HER2-positive tumor eligible for trastuzumab therapy in breast cancer patients[20], whereas a HER2:CEP17 signal ratio > 2.0 was considered to indicate HER2-positive gastric cancer in the ToGA trial[1]. The cut-off value of 24.75 ng/mL identified in the current study may therefore be more appropriate for gastric cancer, but more studies in

Table 3 Association between clinicopathological variables and serum HER2 extracellular domain concentrations *n* (%)

Variables	Serum HER2 ECD concentrations		*P* value
	> 24.75 ng/mL (*n* = 36)	⩽ 24.75 ng/mL (*n* = 203)	
Age (yr)			0.474
⩾ 60	17 (47.2)	109 (53.7)	
< 60	19 (52.8)	94 (46.3)	
Gender			0.396
Male	23 (63.9)	144 (70.9)	
Female	13 (36.1)	59 (29.1)	
Smoking status			0.452
Never	11 (30.6)	50 (24.6)	
Ever	25 (69.4)	153 (75.4)	
Tumor location			0.573
GEJ	5 (13.9)	36 (17.7)	
Non-GEJ	31 (86.1)	167 (82.3)	
Tumor size			< 0.001
⩾ 5 cm	27 (75.0)	75 (36.9)	
< 5 cm	9 (25.0)	128 (63.1)	
Type of gastrectomy			0.266
Total	21 (58.3)	98 (48.3)	
Subtotal	15 (41.7)	105 (51.7)	
Type of surgery			0.730
Open	25 (69.4)	135 (66.5)	
MIS	11 (30.6)	68 (33.5)	
Lymph node involvement			0.419
Positive	22 (61.1)	138 (68.0)	
Negative	14 (38.9)	65 (32.0)	
pTNM stage			0.576
Ⅰ	6 (16.7)	33 (16.3)	
Ⅱ	12 (33.3)	66 (32.5)	
Ⅲ	13 (36.1)	89 (43.8)	
Ⅳ	5 (13.9)	15 (7.4)	
Lauren classification			0.021
Intestinal type	22 (61.1)	82 (40.4)	
Diffuse type	14 (38.9)	121 (59.6)	
Tissue HER2 status (IHC/FISH)			< 0.001
Positive	21 (58.3)	18 (8.9)	
Negative	15 (41.7)	185 (91.1)	

GEJ: Gastroesophageal junction; HER2: Human epidermal growth factor receptor-2; ECD: Extracellular domain; MIS: Minimally invasive surgery; IHC: Immunohistochemistry; FISH: Fluorescence in situ hybridization.

clinical settings are needed to confirm the optimal cut-off value.

In addition to its diagnostic and prognostic potentials, serum HER2 ECD levels have other promising clinical values. Because serum HER2 ECD can be measured rapidly and repeatedly, monitoring HER2 ECD levels at different times might yield clinically meaningful data. Oyama *et al*[15] found that changes in serum HER2 ECD levels during chemotherapy were significantly correlated with response to chemotherapy in patients with HER2-positive tumor tissue. More recently, patients with higher baseline serum HER2 ECD were shown to have a better response rate before initiation of trastuzumab treatment[21]. These results demonstrated that serum HER2 ECD could be a predictor of response to chemotherapy. The results of our study showed a significant association between high serum HER2 ECD level and tumor size. It is therefore reasonable to speculate that serum HER2 ECD level might correlate with tumor recurrence. However, no studies have yet reported on this relationship in gastric cancer patients, and we plan to conduct such experiments in the future.

In conclusion, this study showed that serum HER2 ECD could be a highly specific surrogate biomarker for tissue HER2 status in patients with gastric cancer. Furthermore, serum HER2 ECD levels ⩾ 24.75 ng/mL may be associated with poorer OS. Further prospective studies in clinical settings are needed to validate the eligibility of serum HER2 ECD for predicting response to chemotherapy and tumor recurrence in gastric cancer.

COMMENTS

Background

The ToGA trial demonstrated that patients with advanced gastric cancer, positive for human epidermal growth factor receptor 2 (HER2) expression or gene amplification, could benefit from HER2-targeted therapy. However, there are some limitations for current methods to accurately determine HER2 status. More convenient and reproducible detection methods to identify HER2-positive gastric cancer are needed.

Research frontiers

This study investigated the association between serum HER2 extracellular domain (ECD) and tissue HER2 status as well as the prognostic value of serum HER2 ECD in a large cohort of patients.

Innovations and breakthroughs

There were different levels of serum HER2 ECD between patients with HER2-positive tissue expression and those with HER2-negative tissue expression. High serum HER2 ECD had negative impact on patient overall survival [hazard ratio: 1.93 (95%CI: 1.32-4.38), *P* = 0.006].

Applications

Serum HER2 ECD could be a surrogate biomarker for tissue HER2 status with high specificity.

Terminology

The HER2 ECD, the extracellular fragment of HER2 protein, locates on the surface of tumor cells and could be released into the circulation by shedding.

Peer-review

The manuscript is very interesting, and it has several important new findings on gastric cancer therapy. It is of particular notice the use of serum HER2 as a predictive biomarker for tissue HER2 status and prognosis, which seems to be a potential new tool to improve the treatment of gastric cancer.

REFERENCES

1 **Bang YJ**, Van Cutsem E, Feyereislova A, Chung HC, Shen L, Sawaki A, Lordick F, Ohtsu A, Omuro Y, Satoh T, Aprile G, Kulikov E, Hill J, Lehle M, Rüschoff J, Kang YK. Trastuzumab in combination with chemotherapy versus chemotherapy alone for treatment of HER2-positive advanced gastric or gastro-oesophageal junction cancer (ToGA): a phase 3, open-label, randomised controlled trial. *Lancet* 2010; **376**: 687-697 [PMID: 20728210]

2 **Ajani JA**, D'Amico TA, Almhanna K, Bentrem DJ, Chao J, Das P, Denlinger CS, Fanta P, Farjah F, Fuchs CS, Gerdes H, Gibson M, Glasgow RE, Hayman JA, Hochwald S, Hofstetter WL, Ilson DH, Jaroszewski D, Johung KL, Keswani RN, Kleinberg LR, Korn WM, Leong S, Linn C, Lockhart AC, Ly QP, Mulcahy MF,

Orringer MB, Perry KA, Poultsides GA, Scott WJ, Strong VE, Washington MK, Weksler B, Willett CG, Wright CD, Zelman D, McMillian N, Sundar H. Gastric Cancer, Version 3.2016, NCCN Clinical Practice Guidelines in Oncology. *J Natl Compr Canc Netw* 2016; **14**: 1286-1312 [PMID: 27697982]

3 **Yano T**, Doi T, Ohtsu A, Boku N, Hashizume K, Nakanishi M, Ochiai A. Comparison of HER2 gene amplification assessed by fluorescence in situ hybridization and HER2 protein expression assessed by immunohistochemistry in gastric cancer. *Oncol Rep* 2006; **15**: 65-71 [PMID: 16328035]

4 **Pietrantonio F**, Caporale M, Morano F, Scartozzi M, Gloghini A, De Vita F, Giommoni E, Fornaro L, Aprile G, Melisi D, Berenato R, Mennitto A, Volpi CC, Laterza MM, Pusceddu V, Antonuzzo L, Vasile E, Ongaro E, Simionato F, de Braud F, Torri V, Di Bartolomeo M. HER2 loss in HER2-positive gastric or gastroesophageal cancer after trastuzumab therapy: Implication for further clinical research. *Int J Cancer* 2016; **139**: 2859-2864 [PMID: 27578417]

5 **Lam L**, McAndrew N, Yee M, Fu T, Tchou JC, Zhang H. Challenges in the clinical utility of the serum test for HER2 ECD. *Biochim Biophys Acta* 2012; **1826**: 199-208 [PMID: 22521738]

6 **Ross JS**. Update on HER2 testing for breast and upper gastrointestinal tract cancers. *Biomark Med* 2011; **5**: 307-318 [PMID: 21657840]

7 **Carlson RW**, Moench SJ, Hammond ME, Perez EA, Burstein HJ, Allred DC, Vogel CL, Goldstein LJ, Somlo G, Gradishar WJ, Hudis CA, Jahanzeb M, Stark A, Wolff AC, Press MF, Winer EP, Paik S, Ljung BM. HER2 testing in breast cancer: NCCN Task Force report and recommendations. *J Natl Compr Canc Netw* 2006; **4** Suppl 3: S1-S22; quiz S23-S24 [PMID: 16813731]

8 **Colomer R**, Montero S, Lluch A, Ojeda B, Barnadas A, Casado A, Massutí B, Cortés-Funes H, Lloveras B. Circulating HER2 extracellular domain and resistance to chemotherapy in advanced breast cancer. *Clin Cancer Res* 2000; **6**: 2356-2362 [PMID: 10873087]

9 **Ludovini V**, Gori S, Colozza M, Pistola L, Rulli E, Floriani I, Pacifico E, Tofanetti FR, Sidoni A, Basurto C, Rulli A, Crinò L. Evaluation of serum HER2 extracellular domain in early breast cancer patients: correlation with clinicopathological parameters and survival. *Ann Oncol* 2008; **19**: 883-890 [PMID: 18187484]

10 **Farzadnia M**, Meibodi NT, Shandiz FH, Mahmoudi M, Bahar MM, Memar B, Amoian S, Maroozi F, Moheghi N. Evaluation of HER2/neu oncoprotein in serum and tissue samples of women with breast cancer: correlation with clinicopathological parameters. *Breast* 2010; **19**: 489-492 [PMID: 20675140]

11 **Jensen BV**, Johansen JS, Price PA. High levels of serum HER-2/neu and YKL-40 independently reflect aggressiveness of metastatic breast cancer. *Clin Cancer Res* 2003; **9**: 4423-4434 [PMID: 14555515]

12 **Imoto S**, Wada N, Hasebe T, Ochiai A, Kitoh T. Serum c-erbB-2 protein is a useful marker for monitoring tumor recurrence of the breast. *Int J Cancer* 2007; **120**: 357-361 [PMID: 17044019]

13 **Lipton A**, Ali SM, Leitzel K, Demers L, Harvey HA, Chaudri-Ross HA, Brady C, Wyld P, Carney W. Serum HER-2/neu and response to the aromatase inhibitor letrozole versus tamoxifen. *J Clin Oncol* 2003; **21**: 1967-1972 [PMID: 12743150]

14 **Peng Z**, Liu Y, Li Y, Zhang X, Zhou J, Lu M, Li Q, Shen L. Serum HER2 extracellular domain as a potential alternative for tissue HER2 status in metastatic gastric cancer patients. *Biomark Med* 2014; **8**: 663-670 [PMID: 25123035]

15 **Oyama K**, Fushida S, Tsukada T, Kinoshita J, Watanabe T, Shoji M, Nakanuma S, Okamoto K, Sakai S, Makino I, Nakamura K, Hayashi H, Inokuchi M, Nakagawara H, Miyashita T, Tajima H, Takamura H, Ninomiya I, Kitagawa H, Fujimura T, Tajiri R, Ooi A, Ohta T. Evaluation of serum HER2-ECD levels in patients with gastric cancer. *J Gastroenterol* 2015; **50**: 41-45 [PMID: 24557054]

16 **Zhang K**, Cui J, Xi H, Bian S, Ma L, Shen W, Li J, Wang N, Wei B, Chen L. Serum HER2 Is a Potential Surrogate for Tissue HER2 Status in Gastric Cancer: A Systematic Review and Meta-Analysis. *PLoS One* 2015; **10**: e0136322 [PMID: 26292093]

17 **Shimada H**. Is "liquid biopsy" useful for assessing HER2 status in gastric cancer? *J Gastroenterol* 2015; **50**: 119-120 [PMID: 24825793]

18 **Xi HQ**, Cui JX, Shen WS, Wu XS, Bian SB, Li JY, Song Z, Wei B, Chen L. Increased expression of Lgr5 is associated with chemotherapy resistance in human gastric cancer. *Oncol Rep* 2014; **32**: 181-188 [PMID: 24859092]

19 **Dai SQ**, An X, Wang F, Shao Q, Chen YC, Kong YN, Chen C, Li C, Luo HY, Liang Y, Wang FH, Xu RH, Li YH. Serum HER 2 extracellular domain level is correlated with tissue HER 2 status in metastatic gastric or gastro-oesophageal junction adenocarcinoma. *PLoS One* 2013; **8**: e63458 [PMID: 23691049]

20 **Wolff AC**, Hammond ME, Schwartz JN, Hagerty KL, Allred DC, Cote RJ, Dowsett M, Fitzgibbons PL, Hanna WM, Langer A, McShane LM, Paik S, Pegram MD, Perez EA, Press MF, Rhodes A, Sturgeon C, Taube SE, Tubbs R, Vance GH, van de Vijver M, Wheeler TM, Hayes DF. American Society of Clinical Oncology/College of American Pathologists guideline recommendations for human epidermal growth factor receptor 2 testing in breast cancer. *J Clin Oncol* 2007; **25**: 118-145 [PMID: 17159189]

21 **Zhou J**, Peng Z, Liu Y, Gong J, Zhang X, Lu M, Gao J, Li Y, Li Y, Shen L. Predictive value of serum HER2 ECD in patients with HER2-positive advanced gastric cancer treated with trastuzumab plus chemotherapy. *J Gastroenterol* 2015; **50**: 955-961 [PMID: 25702260]

P- Reviewer: Christodoulidis G, Fiorentini G **S- Editor**: Yu J
L- Editor: Ma JY **E- Editor**: Zhang FF

World Journal of Gastroenterology

Submit a Manuscript: http://www.wjgnet.com/esps/

World J Gastroenterol 2017 March 14; 23(10): 1843-1850

DOI: 10.3748/wjg.v23.i10.1843

ISSN 1007-9327 (print) ISSN 2219-2840 (online)

ORIGINAL ARTICLE

Retrospective Cohort Study

Endoscopic submucosal tunnel dissection of upper gastrointestinal submucosal tumors: A comparative study of hook knife *vs* hybrid knife

Jie-Qiong Zhou, Xiao-Wei Tang, Yu-Tang Ren, Zheng-Jie Wei, Si-Lin Huang, Qiao-Ping Gao, Xiao-Feng Zhang, Jian-Feng Yang, Wei Gong, Bo Jiang

Jie-Qiong Zhou, Si-Lin Huang, Qiao-Ping Gao, Wei Gong, Bo Jiang, Guangdong Provincial Key Laboratory of Gastroenterology, Department of Gastroenterology, Nanfang Hospital, Southern Medical University, Guangzhou 510515, Guangdong Province, China

Jie-Qiong Zhou, Yu-Tang Ren, Zheng-Jie Wei, Bo Jiang, Department of Gastroenterology, Beijing Tsinghua Changgung Hospital Medical Center, Tsinghua University, Beijing 102218, China

Xiao-Wei Tang, Xiao-Feng Zhang, Jian-Feng Yang, Department of Gastroenterology, Hangzhou First People's Hospital, Nanjing Medical University, Hangzhou 310006, Zhejiang Province, China

Author contributions: Zhou JQ and Tang XW contributed equally to this work; Zhou JQ, Tang XW and Jiang B designed the research; Ren YT and Gong W performed the research; Wei ZJ, Huang SL, Gao QP, Zhang XF and Yang JF analyzed the data; Gong W and Jiang B supervised the study; Zhou JQ and Tang XW wrote the paper.

Institutional review board statement: The study was reviewed and approved by the Institutional Review Board of Nanfang Hospital, Guangzhou, China.

Informed consent statement: All patients provided informed written consent prior to study enrollment.

Conflict-of-interest statement: The authors declared that there are no conflicts of interest in this study.

Data sharing statement: The original anonymous dataset is available on request from the corresponding author at drjiang@163.com.

Manuscript source: Invited manuscript

Correspondence to: Dr. Bo Jiang, Professor, Guangdong Provincial Key Laboratory of Gastroenterology, Department of Gastroenterology, Nanfang Hospital, Southern Medical University, No.1838, Guangzhou North Ave, Guangzhou 510515, Guangdong Province, China. drjiang@163.com
Telephone: +86-20-61641888
Fax: +86-20-61641541

Received: October 8, 2016
Peer-review started: October 11, 2016
First decision: November 21, 2016
Revised: December 18, 2016
Accepted: January 18, 2017
Article in press: January 18, 2017
Published online: March 14, 2017

Abstract

AIM

To compare the efficacy and safety of a hook knife (HO) with a hybrid knife (HK) during endoscopic submucosal tunnel dissection (ESTD) procedure.

METHODS

Between August 2012 and December 2015, the ESTD procedure was performed for 83 upper GI submucosal lesions, which originated from the muscularis propria layer identified by upper endoscopy and endoscopic ultrasonography. Of these, 34 lesions were treated by a HO, whereas 49 lesions were treated by a HK. Data regarding age, gender, presenting symptoms, tumor

location and size, procedure time, complications, *en bloc* resection rate and others were analyzed and compared between the two groups.

RESULTS

There were no significant differences in the age, gender, presenting symptoms and tumor location between the two groups. ESTD was successfully completed in all the patients, and no case was converted to laparoscopy. The mean procedure time was significantly shorter in the HK group than in the HO group (41.3 ± 20.3 min *vs* 57.2 ± 28.0 min, $P = 0.004$). The mean frequency of device exchange was 1.4 ± 0.6 in the HK group and significantly less than 3.3 ± 0.6 in the HO group ($P < 0.001$). The differences in tumor size and histopathological diagnoses were not significant between the two groups ($P = 0.813$, $P = 0.363$, respectively). Both groups had an equal *en bloc* resection rate and complete resection rate. Additionally, the complication rate was similar between the two groups ($P = 0.901$). During the follow-up, no recurrence occurred in either group.

CONCLUSION

We demonstrate for the first time that HO and HK do not differ in efficacy or safety, but HK reduces the frequency of device exchange and procedure time.

Key words: Endoscopic submucosal tunnel dissection; Submucosal tumor; Hook knife; Hybrid knife; Clinical outcome

Core tip: Settings for the endoscopic submucosal tunnel dissection (ESTD) procedure have not been standardized, and no studies have directly compared ESTD devices in humans. We compared the performance between hook knife (HO) and hybrid knife (HK) in the ESTD procedure for upper gastrointestinal submucosal tumors. Our study demonstrated for the first time that HO and HK do not differ in terms of efficacy or complication rates during ESTD procedure, but HK can significantly reduce the frequency of device exchange and procedure time.

Zhou JQ, Tang XW, Ren YT, Wei ZJ, Huang SL, Gao QP, Zhang XF, Yang JF, Gong W, Jiang B. Endoscopic submucosal tunnel dissection of upper gastrointestinal submucosal tumors: A comparative study of hook knife *vs* hybrid knife. *World J Gastroenterol* 2017; 23(10): 1843-1850 Available from: URL: http://www.wjgnet.com/1007-9327/full/v23/i10/1843.htm DOI: http://dx.doi.org/10.3748/wjg.v23.i10.1843

INTRODUCTION

Although most submucosal tumors (SMTs) are benign, some of them have malignant potential. Resection of SMTs would be helpful in diagnosis and may be curative[1-3]. To date, several therapies have been described to resect SMTs, including open and laparoscopic surgery[4], endoscopic submucosal dissection (ESD)[5-7], endoscopic full-thickness resection (EFR), *etc.*[8,9]. Surgical approaches are more invasive with a longer hospital stay of patients and have greater cost compared with endoscopic methods. However, ESD and EFR also have their limitations, and they can be associated with major complications such as perforation, which may be difficult to close and even require surgery.

More recently, endoscopic submucosal tunnel dissection (ESTD) has been a novel treatment for upper gastrointestinal (GI) SMTs originating from the muscularis propria (MP). Since Inoue *et al*[10] first reported the usefulness of ESTD for SMTs in humans, a number of authors have reported its efficacy and safety. According to a review by Kobara *et al*[11], the complete resection rate of ESTD for upper GI SMTs ranged from 85.7% to 100%, and the complication rate was 0%-16.7%. With regard to the endoscopic devices used in ESTD procedure, there has been wide variability among different centers. A hook knife (HO), a hybrid knife (HK) and an insulated-tip knife were reported in different studies[12-14]. For the two endoscopic devices: HO and HK, no study has assessed and compared their clinical outcomes in the ESTD procedure. Hence, this study was conducted to evaluate the clinical efficacy and safety of HK compared with HO for ESTD.

MATERIALS AND METHODS

Between August 2012 and December 2015, 83 consecutive patients with upper GI SMTs were treated with ESTD at the Department of Gastroenterology, Nanfang Hospital, Southern Medical University, China. The data were prospectively collected and retrospectively reviewed. All the procedures were performed by one experienced endoscopist (Gong W). After the operator performed 15 cases (10 cases were performed by a HO and 5 cases by a HK), the procedure time became stable and the complication rate was low. Therefore, the first 15 cases were not included in our analysis to eliminate the effect of the learning curve. Patients were divided into the following two groups based on the type of endoscopic devices used in ESTD: the hook knife (HO group, $n = 34$) and the hybrid knife (HK group, $n = 49$). Indications for the ESTD procedure were SMTs originating from the MP layer identified by upper endoscopy and endoscopic ultrasonography (EUS), lesions smaller than 4 cm, and patients who can tolerate general anesthesia with tracheal intubation. Data regarding age, gender, presenting symptoms, tumor location and size, procedure time, complications, *en bloc* resection rate and others were analyzed and compared between the

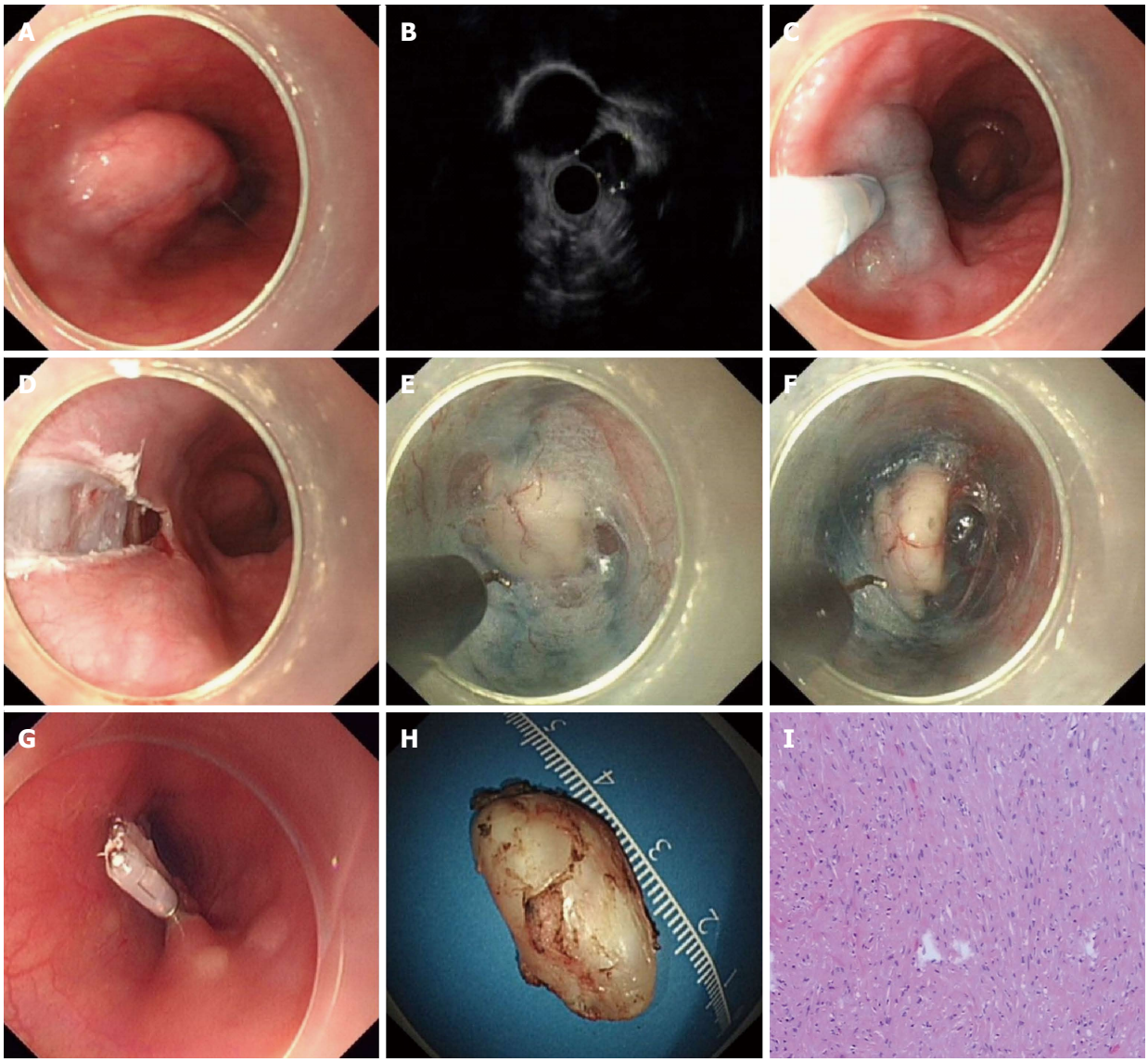

Figure 1 Illustration of endoscopic submucosal tunnel dissection for esophageal submucosal tumor in a patient using a hook knife. A: An submucosal tumor (SMT) located at the left lateral wall of the mid esophagus; B: Endoscopic ultrasonography revealed a 32.8 mm × 14.7 mm hypoechoic submucosal lesion; C and D: A 2-cm longitudinal incision is made into the mucosa after injection of natural saline with indigo carmine and epinephrine; E: After a mucosal incision was made, submucosal dissection was made approximately 4 cm proximal to the SMT with a hook knife, creating a submucosal tunnel until the tumor was visible; F: Dissection was done along the margin of the tumor; G: Endoclips were used to close the entry of the submucosal tunnel; H and I: Pathological examination revealed that the resected specimen was a 28-mm leiomyoma.

two groups. Written informed consent was obtained from all patients before the procedure.

ESTD procedure

A forward-viewing endoscope (GIFQ240Z; Olympus, Tokyo, Japan) was used with a transparent distal cap attachment (MH-588; Olympus). A hook knife (KD-620L; Olympus) and an injection needle (NM-4L-1, Olympus), or a hybrid knife (ERBE, Tübingen, Germany) were used to dissect the submucosal layer and the tumors. A pair of coagulating forceps (Coagrasper, FD-410L; Olympus) was used to coagulate large vessels prior to dissection and for hemostasis. A carbon dioxide (CO_2) insufflator (UCR; Olympus) was used. For electrosurgery, a VIO 200 D electrogenerator (ERBE) was used, and for final closure of the mucosal entry site, hemostatic clips (EZ-CLIP, HX-110QR, Olympus; or Resolution, M00522610; Boston Scientific, Boston, United States) were applied. All the ESTD procedures were performed by a single operator (Gong W).

The patients underwent the procedures under general anesthesia with endotracheal intubation. CO_2 was used during the procedure. The standard steps of the procedure were described previously (Figures 1 and 2)[15].

ESTD devices

The hook knife was developed by Oyama *et al*[16], and the tip of the knife is bent at a right angle for marking

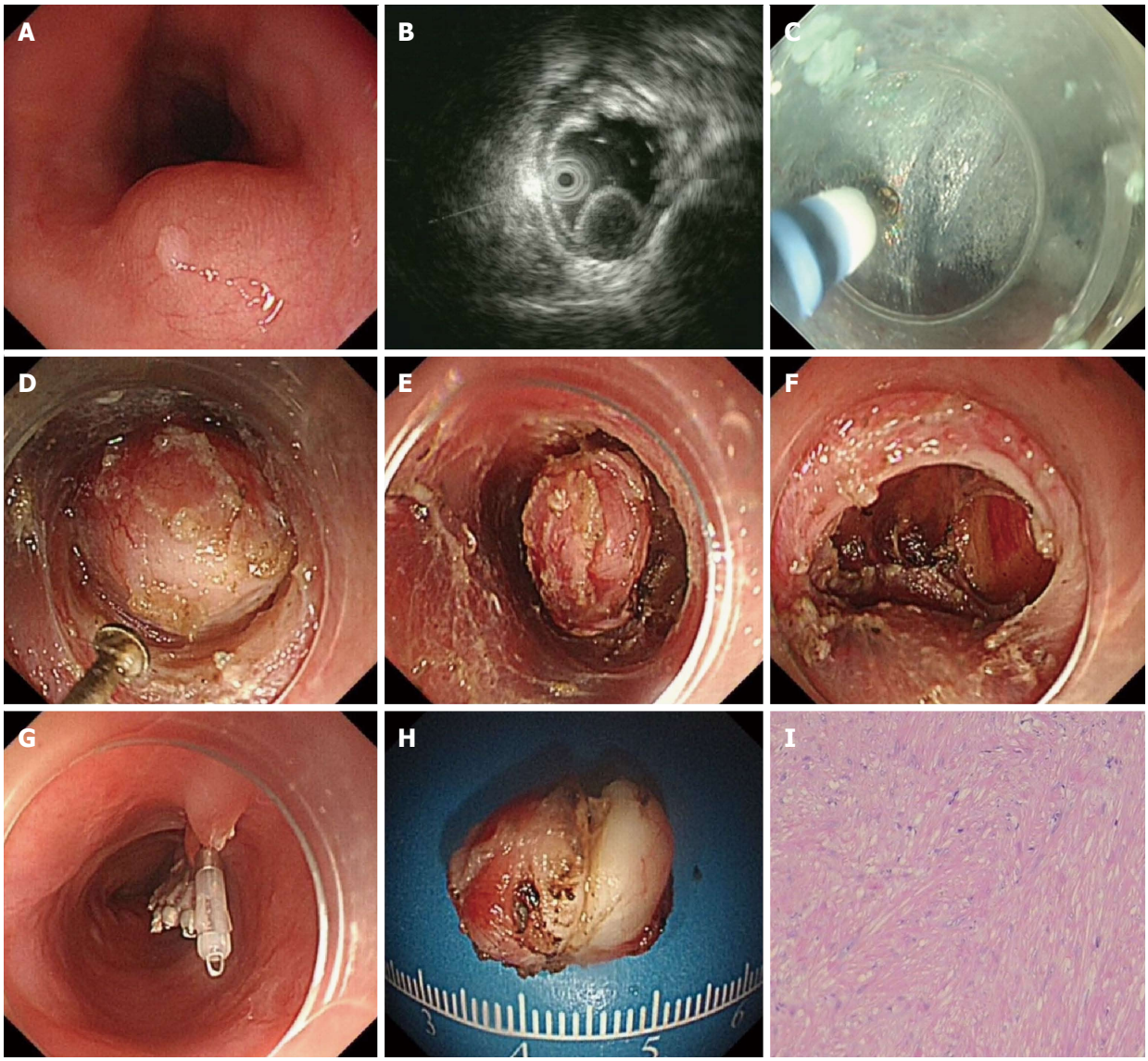

Figure 2 Illustration of endoscopic submucosal tunnel dissection for esophageal submucosal tumor in a patient using a hybrid knife. A: An submucosal tumor (SMT) located at the posterior wall of the mid esophagus; B: Endoscopic ultrasonography revealed a 15.2 mm × 11.4 mm hypoechoic submucosal lesion; C: After a 2-cm longitudinal mucosal incision was made, submucosal dissection was made approximately 4 cm proximal to the SMT with a hybrid knife, creating a submucosal tunnel; D and E: Dissection was done along the margin of the tumor; F: Endoscopic view of submucosal tunnel after removal of the tumor; G: Endoclips were used to close the entry of the submucosal tunnel; H and I: Pathological examination revealed that the resected specimen was a 15-mm leiomyoma.

and cutting mucosa as well as the submucosal fibers. The length of the hook is 1.3 mm and the length of the arm is 4.5 mm. The knife is hosted within an outer sheath.

The hybrid knife has combined capabilities of radiofrequency application and needle-less waterjet injection in a single instrument[17,18]. The outer diameter is 2.1 mm and the lumen is 120 μm. There are two types of hybrid knife: I-type and T-type. In our study, only the T-type was used.

Histopathological evaluation and follow-up

Resected specimens were retrieved and immediately fixed in a 10% buffered formalin solution. Hematoxylin and eosin and immunohistochemical staining (CD34, CD117, actin, S-100, desmin, vimentin, and Ki67) were carried out.

All patients were scheduled for a follow-up visit at 3 and 6 months and 1 year after ESTD for upper endoscopy and EUS. If there is no residual tumor, follow-up is performed annually.

Evaluation of clinical outcomes

The procedure time was defined as from the moment of submucosal injection to closure of mucosal entry after removal of the lesion. *En bloc* resection was defined as resection of the target tumor in one piece. Complete resection was defined as follows: the capsule of the tumor was intact and the basal and lateral margins were free of tumor cells. Complications were defined as bleeding, perforation or subcutaneous emphysema. Bleeding was defined as an oozing or

Table 1 Patient baseline characteristics in hook knife group and hybrid knife group *n* (%)

	HO group (*n* = 34)	HK group (*n* = 49)	*P* value
Gender, female	11 (32.4)	22 (44.9)	0.251
Age, years (range)	50.1 ± 9.4 (27-66)	46.9 ± 12.9 (19-68)	0.195
Presenting symptoms			
Asymptomatic	11 (32.4)	19 (38.8)	
Epigastric discomfort	10 (29.4)	14 (28.6)	
Chest discomfort	8 (23.5)	11 (22.4)	
Dysphagia	3 (8.8)	3 (6.1)	
Regurgitation	2 (5.9)	2 (4.1)	0.965
Tumor location			
Esophagus	23 (67.6)	34 (69.4)	
Cardia	7 (20.6)	10 (20.4)	
Stomach	4 (11.8)	5 (10.2)	0.973

HO group: Hook knife group; HK group: Hybrid knife group.

spurting bleeding observed and requiring the use of coagulating forceps or endoclips. Perforation was defined as having occurred when a hole was easily recognizable by endoscopy during ESTD, or when free air was detected on a plain radiograph taken after ESTD.

Statistical analysis

Continuous variables are presented as the mean ± SD. Categorical variables were expressed as numbers and percentages. Statistical differences were analyzed with Student's *t*-test, χ^2 test or Fisher's exact test. Values of $P < 0.05$ were considered statistically significant. Data were analyzed using commercially available statistical software packages SPSS version 19.0 (SPSS Inc., Chicago, IL, United States).

RESULTS

Patient baseline characteristics

Eighty-three patients with a total of 83 lesions were enrolled in this study. A summary of patient baseline characteristics is shown in Table 1. There were no significant differences in age, gender, presenting symptoms and tumor location between the two groups.

Clinicopathological characteristics

ESTD was successfully completed in all the patients and no case was converted to laparoscopy. The clinicopathological details of patients and lesions are shown in Table 2. The mean size of the resected specimens was 19.7 ± 7.2 mm in the HO group and 19.3 ± 7.5 mm in the HK group. This difference was not significant ($P = 0.813$). The number of tumors larger than 20 mm was 8 (23.5%) in HO group and 13 (26.5%) in HK group ($P = 0.757$). With regard to histopathological results, there were 27 (79.4%) leiomyomas, 6 (17.6%) GISTs and 1 (2.9%) lipoma in the HO group, and there were 42 (85.7%) leiomyomas and 7 (14.3%) GISTs in the HK group. The proportion of tumor pathology was not significantly different between the two groups ($P = 0.363$).

The *en bloc* resection and complete resection were achieved in 32 out of 34 lesions (94.1%) in the HO group and in all 49 lesions (100%) in the HK group, which were similar in the two groups ($P = 0.165$). The mean duration of the hospital stay was 5.6 ± 1.4 d in the HO group and 5.8 ± 1.5 d in the HK group ($P = 0.501$). During the follow-up time, no recurrence occurred in either group.

Procedure time

The total procedure time in the HK group was significantly shorter than in the HO group (41.3 ± 20.3 min *vs* 57.2 ± 28.0 min, $P = 0.004$). The mean frequency of device exchange was 1.4 ± 0.6 in the HK group and 3.3 ± 0.6 in the HO group ($P < 0.001$), and the mean frequency of coagulation forceps use was similar between the two groups ($P = 0.625$).

Complications

Four perforations (two in the HO group and two in the HK group) occurred during ESTD and were closed by endoclips. Intraoperative bleeding occurred in 1 patient of the HO group and was successfully controlled by coagulating forceps. No other complications were recorded during the procedures. Three patients (one in the HO group and two in the HK group) developed subcutaneous emphysema after the procedure, all of which resolved spontaneously after the ESTD.

DISCUSSION

ESTD has been an emerging novel therapeutic option for upper GI SMTs originating from the MP layer. It has several advantages over other treatment modalities, such as ESD and EFR. First, through the submucosal tunnel, SMTs can be dissected and resected under direct endoscopic vision, and the bleeding spot can be detected immediately and managed successfully by hemostasis. Second, the ESTD procedure maintains the mucosa layer above the SMTs intact, thereby maintaining the integrity of the GI tract mucosa. Finally, the entry to the submucosal tunnel can be easily closed with several clips.

For the equipment used in the ESTD procedure, a variety of endoscopic knives were applied in different studies. Li *et al*[12] preferred to use a hook knife or hybrid knife during the procedure, Liu *et al*[13] and Wang *et al*[14] chose to use an insulated-tip knife or a hybrid knife. In our center, a hook knife or hybrid knife was mostly used in ESTD. Different endoscopic devices have various properties and advantages. Therefore, we conducted this study to compare clinical outcomes for upper GI ESTD with the use of HO or HK. Here, we demonstrated for the first time that HK had the advantage of a shorter operation time compared with HO, and the frequency of device exchange in the HK group was less than in the HO group. The complication

Table 2 Clinical outcomes and histopathological results *n* (%)

	HO group (*n* = 34)	HK group (*n* = 49)	*P* value
Procedure time, min (range)	57.2 ± 28.0(30-150)	41.3 ± 20.3 (15-120)	0.004[b]
Frequency of device exchange, *n* (range)	3.3 ± 0.6 (2-5)	1.4 ± 0.6 (1-3)	0.000[b]
Frequency of coagulation forceps use, *n* (range)	0.2 ± 0.4 (0-1)	0.2 ± 0.4 (0-1)	0.625
Tumor size, mm (range)	19.7 ± 7.2 (10-40)	19.3 ± 7.5 (8-40)	0.813
No. of tumors based on size (mm)			
≤ 20	26 (76.5)	36 (73.5)	
> 20	8 (23.5)	13 (26.5)	0.757
Histopathological diagnosis			
Leiomyoma	27 (79.4)	42 (85.7)	
Gastrointestinal stromal tumor	6 (17.6)	7 (14.3)	
Lipoma	1 (2.9)	0 (0)	0.363
En bloc resection	32 (94.1)	49 (100)	0.165
Complete resection	32 (94.1)	49 (100)	0.165
Complications			
Perforation	2 (5.9)	2 (4.1)	
Bleeding	1 (2.9)	0 (0)	
Subcutaneous emphysema	1 (2.9)	2 (4.1)	0.568
Hospital stay, days (range)	5.6 ± 1.4 (3-10)	5.8 ± 1.5 (3-10)	0.501
Mean follow-up time, months (range)	27.2 ± 6.4 (18.9-41.4)	25.5 ± 4.0 (20.6-39.7)	0.175
Recurrence rate, %	0	0	1.000

[b]$P < 0.01$. HO group: Hook knife group; HK group: Hybrid knife group.

rate, *en bloc* resection and complete resection rate were almost the same between the two groups. During the follow-up time, no recurrence occurred in the two groups.

Primarily used in the EMR procedure, HO allows for marking and cutting mucosa, submucosal fibers, and vessels, as well as for hemostasis of minor bleeding[16]. Because the direction of the hook knife can be controlled and held parallel with the muscularis propria layer, it has the advantage of preventing perforation during ESD[16]. However, it is notable that HO does not enable injection of dyed saline to stain submucosal fibers, and it requires a frequent exchange of devices, resulting in prolonged procedural time. Recently, HK was developed to simplify the endoscopic procedure. It is multifunctional with the abilities of submucosal injection, circumferential cutting, dissection of lesions, and coagulation of bleeding[18]. Therefore, the procedure can be performed by the same HK without the need of device exchange.

A few studies have demonstrated that HK can reduce the frequency of device exchange and the procedure time[19,20]. Zhou *et al*[19] compared the procedure time, efficacy, and safety of HK-assisted ESD with the conventional technique in patients with early gastric cancer (EGC) in a randomized controlled trial. They revealed that HK-assisted ESD was as effective and safe as conventional devices (the IT-2 knife, Dual Knife and Hook Knife)-assisted ESD for treating EGC, but the HK group was associated with a shorter procedure time and a lower frequency of device exchange compared with the conventional group[19]. Furthermore, Cai *et al*[20] also demonstrated that HK achieved shorter procedure time, fewer accessory exchanges, less frequent use of coagulation forceps to control bleeding, and a lower bleeding rate in comparison with a triangle knife. Our study found that HK shortened the operation time and required fewer device exchanges in the ESTD procedure, which was comparable to these ESD studies above.

ESTD consisted of 4 standard steps: mucosal incision, creation of the submucosal tunnel, dissection of the lesion and closure of mucosal entry. The step of submucosal tunnel creation was a major and integral part of the whole procedure, which is very time-consuming. In addition to HO, HK, or other endoknives, some novel devices or techniques were also described to facilitate submucosal tunnel creation. Sumiyama *et al*[21] reported using high-pressure carbon dioxide injection and balloon dissection to create a submucosal tunnel, and this was also called the mucosal flap safety valve (SEMF) technique. Khashab *et al*[22] used a novel gel with dissecting properties for facilitating submucosal tunneling during peroral endoscopic myotomy (POEM). The preliminary animal study demonstrated that the gel consistently resulted in efficient auto-tunneling without any complications. The authors suggested that this novel material may replace other endoknives to create submucosal tunnels and has the potential to revolutionize the submucosal tunnel technique and ESD. Moreover, Khashab *et al*[23] also showed that direct jet injection of dyed saline through the dedicated channel of the gastroscope could result in adequate, consistent and reliable staining of submucosal fibers and made submucosal dissection accurate and safe. However, the prerequisite of this method is availability of a gastroscope with a dedicated water jet channel, which may limit its further widespread use. Some chemical agent was also applied to facilitate submucosal tunnel creation. Kawahara *et al*[24] recently demonstrated that submucosal injections of mesna could soften tissues and facilitate POEM.

In the porcine study, submucosal tunneling time was significantly shorter in the mesna group than in the saline group, regardless of the dissection method.

We acknowledge that there are some limitations in the current study. First, it is not a prospectively randomized controlled design. Therefore, the clinical data is not sufficient. The time required for submucosal tunnel creation and tumor dissection during the whole procedure is lacking, so we cannot evaluate in which step of ESTD the HK can reduce operation time. Second, our study only involved a single operator and institution. Finally, the follow-up time was not long enough, hence we cannot comment on long-term efficacy.

In conclusion, our results indicated that a hook knife and a hybrid knife do not differ in terms of efficacy or complication rates, but the hybrid knife can reduce the frequency of device exchange and procedure time. Further randomized controlled trials with large-volume cases are warranted to evaluate the efficacy and safety of these two devices.

ACKNOWLEDGMENTS

We thanked the statistician Xiao-Fei Zhang from Beijing Tsinghua Changgung Hospital for the review and suggestion about our statistics analysis.

COMMENTS

Background

There have been several treatments available for upper gastrointestinal (GI) submucosal tumors (SMTs), which included open and laparoscopic surgery, endoscopic submucosal dissection (ESD), endoscopic full-thickness resection (EFR) and so on. More recently, endoscopic submucosal tunnel resection (ESTD) has been emerging as a novel treatment for upper GI SMTs originating from the muscularis propria (MP). And a number of authors demonstrated the safety and efficacy of ESTD for upper gastrointestinal SMTs. However, settings for ESTD procedure have not been standardized, and no studies have directly compared different ESTD devices in humans.

Research frontiers

ESTD has been an emerging novel therapeutic option for upper GI SMTs originating from the MP layer. It has several advantages over other treatment modalities (ESD and EFR), such as the completed resection, immediate hemostasis and easily closed entry. With regard to the endoscopic devices used in ESTD procedure, there has been wide variability among different centers. Hook knife (HO), hybrid knife (HK) and insulated-tip knife were reported in different studies.

Innovations and breakthroughs

Given settings for ESTD procedure have not been standardized, the authors of this study for the first time compared the application of the HO and the HK during the ESTD procedure. This study demonstrated that HO and HK do not differ in terms of the efficacy or complication rates, but HK can reduce frequency of device exchange and procedure time.

Applications

This study indicated the equal safety and efficacy of HO and HK in the ESTD procedure for upper GI SMTs, and also highlighted the advantage of HK with regard to device exchange times and procedure time. This finding may provide evidences about the setting choice to the endoscopist.

Terminology

ESTD is an emerging endoscopic therapeutic modality. The standard ESTD procedure for GI SMTs includes four major steps: mucosal incision, creation of the submucosal tunnel, dissection of the lesion and closure of mucosal entry. ESTD procedure for GI SMTs has the advantages of high resection rate and the low complication rate.

Peer-review

The manuscript is of interest for a broad readership and the feasibility of ESTD procedures in order to remove upper GI submucosal lesions is highlighted clearly.

REFERENCES

1 **Hwang JH**, Rulyak SD, Kimmey MB. American Gastroenterological Association Institute technical review on the management of gastric subepithelial masses. *Gastroenterology* 2006; **130**: 2217-2228 [PMID: 16762644 DOI: 10.1053/j.gastro.2006.04.033]

2 **Polkowski M**, Butruk E. Submucosal lesions. *Gastrointest Endosc Clin N Am* 2005; **15**: 33-54, viii [PMID: 15555950 DOI: 10.1016/j.giec.2004.07.005]

3 **Ponsaing LG**, Kiss K, Hansen MB. Classification of submucosal tumors in the gastrointestinal tract. *World J Gastroenterol* 2007; **13**: 3311-3315 [PMID: 17659669 DOI: 10.3748/wjg.v13.i24.3311]

4 **von Rahden BH**, Stein HJ, Feussner H, Siewert JR. Enucleation of submucosal tumors of the esophagus: minimally invasive versus open approach. *Surg Endosc* 2004; **18**: 924-930 [PMID: 15108112 DOI: 10.1007/s00464-003-9130-9]

5 **Lee IL**, Lin PY, Tung SY, Shen CH, Wei KL, Wu CS. Endoscopic submucosal dissection for the treatment of intraluminal gastric subepithelial tumors originating from the muscularis propria layer. *Endoscopy* 2006; **38**: 1024-1028 [PMID: 17058168 DOI: 10.1055/s-2006-944814]

6 **Shi Q**, Zhong YS, Yao LQ, Zhou PH, Xu MD, Wang P. Endoscopic submucosal dissection for treatment of esophageal submucosal tumors originating from the muscularis propria layer. *Gastrointest Endosc* 2011; **74**: 1194-1200 [PMID: 21963065 DOI: 10.1016/j.gie.2011.07.039]

7 **Park YS**, Park SW, Kim TI, Song SY, Choi EH, Chung JB, Kang JK. Endoscopic enucleation of upper-GI submucosal tumors by using an insulated-tip electrosurgical knife. *Gastrointest Endosc* 2004; **59**: 409-415 [PMID: 14997145]

8 **Zhou PH**, Yao LQ, Qin XY, Cai MY, Xu MD, Zhong YS, Chen WF, Zhang YQ, Qin WZ, Hu JW, Liu JZ. Endoscopic full-thickness resection without laparoscopic assistance for gastric submucosal tumors originated from the muscularis propria. *Surg Endosc* 2011; **25**: 2926-2931 [PMID: 21424195 DOI: 10.1007/s00464-011-1644-y]

9 **Sun S**, Jin Y, Chang G, Wang C, Li X, Wang Z. Endoscopic band ligation without electrosurgery: a new technique for excision of small upper-GI leiomyoma. *Gastrointest Endosc* 2004; **60**: 218-222 [PMID: 15278048]

10 **Inoue H**, Ikeda H, Hosoya T, Onimaru M, Yoshida A, Eleftheriadis N, Maselli R, Kudo S. Submucosal endoscopic tumor resection for subepithelial tumors in the esophagus and cardia. *Endoscopy* 2012; **44**: 225-230 [PMID: 22354822 DOI: 10.1055/s-0031-1291659]

11 **Kobara H**, Mori H, Rafiq K, Fujihara S, Nishiyama N, Ayaki M, Yachida T, Matsunaga T, Tani J, Miyoshi H, Yoneyama H, Morishita A, Oryu M, Iwama H, Masaki T. Submucosal tunneling techniques: current perspectives. *Clin Exp Gastroenterol* 2014; **7**: 67-74 [PMID: 24741323 DOI: 10.2147/ceg.s43139]

12 **Li QL**, Chen WF, Zhang C, Hu JW, Zhou PH, Zhang YQ, Zhong YS, Yao LQ, Xu MD. Clinical impact of submucosal tunneling endoscopic resection for the treatment of gastric submucosal tumors originating from the muscularis propria layer (with video). *Surg Endosc* 2015; **29**: 3640-3646 [PMID: 25740640 DOI: 10.1007/s00464-015-4120-2]

13 **Liu BR**, Song JT, Kong LJ, Pei FH, Wang XH, Du YJ. Tunneling

endoscopic muscularis dissection for subepithelial tumors originating from the muscularis propria of the esophagus and gastric cardia. *Surg Endosc* 2013; **27**: 4354-4359 [PMID: 23765425 DOI: 10.1007/s00464-013-3023-3]

14 **Wang H**, Tan Y, Zhou Y, Wang Y, Li C, Zhou J, Duan T, Zhang J, Liu D. Submucosal tunneling endoscopic resection for upper gastrointestinal submucosal tumors originating from the muscularis propria layer. *Eur J Gastroenterol Hepatol* 2015; **27**: 776-780 [PMID: 25966671 DOI: 10.1097/meg.0000000000000394]

15 **Gong W**, Xiong Y, Zhi F, Liu S, Wang A, Jiang B. Preliminary experience of endoscopic submucosal tunnel dissection for upper gastrointestinal submucosal tumors. *Endoscopy* 2012; **44**: 231-235 [PMID: 22354823 DOI: 10.1055/s-0031-1291720]

16 **Oyama T**, Tomori A, Hotta K, Morita S, Kominato K, Tanaka M, Miyata Y. Endoscopic submucosal dissection of early esophageal cancer. *Clin Gastroenterol Hepatol* 2005; **3**: S67-S70 [PMID: 16013002]

17 **Yahagi N**, Neuhaus H, Schumacher B, Neugebauer A, Kaehler GF, Schenk M, Fischer K, Fujishiro M, Enderle MD. Comparison of standard endoscopic submucosal dissection (ESD) versus an optimized ESD technique for the colon: an animal study. *Endoscopy* 2009; **41**: 340-345 [PMID: 19340739 DOI: 10.1055/s-0029-1214473]

18 **Neuhaus H**, Wirths K, Schenk M, Enderle MD, Schumacher B. Randomized controlled study of EMR versus endoscopic submucosal dissection with a water-jet hybrid-knife of esophageal lesions in a porcine model. *Gastrointest Endosc* 2009; **70**: 112-120 [PMID: 19286176 DOI: 10.1016/j.gie.2008.10.042]

19 **Zhou PH**, Schumacher B, Yao LQ, Xu MD, Nordmann T, Cai MY, Charton JP, Vieth M, Neuhaus H. Conventional vs. waterjet-assisted endoscopic submucosal dissection in early gastric cancer: a randomized controlled trial. *Endoscopy* 2014; **46**: 836-843 [PMID: 25230136 DOI: 10.1055/s-0034-1377580]

20 **Cai MY**, Zhou PH, Yao LQ, Xu MD, Zhong YS, Li QL, Chen WF, Hu JW, Cui Z, Zhu BQ. Peroral endoscopic myotomy for idiopathic achalasia: randomized comparison of water-jet assisted versus conventional dissection technique. *Surg Endosc* 2014; **28**: 1158-1165 [PMID: 24232052 DOI: 10.1007/s00464-013-3300-1]

21 **Sumiyama K**, Tajiri H, Gostout CJ. Submucosal endoscopy with mucosal flap safety valve (SEMF) technique: a safe access method into the peritoneal cavity and mediastinum. *Minim Invasive Ther Allied Technol* 2008; **17**: 365-369 [PMID: 18972253 DOI: 10.1080/13645700802528512]

22 **Khashab MA**, Sharaiha RZ, Saxena P, Law JK, Singh VK, Lennon AM, Shin EJ, Canto MI, Aguila G, Okolo PI, Stavropoulos SN, Inoue H, Pasricha PJ, Kalloo AN. Novel technique of auto-tunneling during peroral endoscopic myotomy (with video). *Gastrointest Endosc* 2013; **77**: 119-122 [PMID: 23261101 DOI: 10.1016/j.gie.2012.09.011]

23 **Khashab MA**, Messallam AA, Saxena P, Kumbhari V, Ricourt E, Aguila G, Roland BC, Stein E, Nandwani M, Inoue H, Clarke JO. Jet injection of dyed saline facilitates efficient peroral endoscopic myotomy. *Endoscopy* 2014; **46**: 298-301 [PMID: 24338241 DOI: 10.1055/s-0033-1359024]

24 **Kawahara Y**, Sumiyama K, Tajiri H. Chemically assisted peroral endoscopic myotomy with submucosal mesna injection in a porcine model. *Minim Invasive Ther Allied Technol* 2015; **24**: 334-339 [PMID: 25921483 DOI: 10.3109/13645706.2015.1040419]

P- Reviewer: Reinehr R **S- Editor**: Gong ZM **L- Editor**: Ma JY
E- Editor: Wang CH

World Journal of Gastroenterology

Submit a Manuscript: http://www.wjgnet.com/esps/

World J Gastroenterol 2017 March 14; 23(10): 1851-1856

DOI: 10.3748/wjg.v23.i10.1851

ISSN 1007-9327 (print) ISSN 2219-2840 (online)

ORIGINAL ARTICLE

Clinical Trials Study

Percutaneous intraductal radiofrequency ablation for treatment of biliary stent occlusion: A preliminary result

Ning Xia, Ju Gong, Jian Lu, Zhi-Jin Chen, Li-Yun Zhang, Zhong-Min Wang

Ning Xia, Ju Gong, Jian Lu, Zhi-Jin Chen, Li-Yun Zhang, Zhong-Min Wang, Department of Radiology, Ruijin Hospital Luwan Branch, Shanghai Jiao Tong University School of Medicine, Shanghai 200020, China

Zhong-Min Wang, Department of Intervention, Ruijin Hospital, Shanghai Jiao Tong University School of Medicine, Shanghai 200025, China

Author contributions: Xia N, Gong J and Lu J contributed equally to this work; Xia N, Gong J and Wang ZM designed the research; Xia N, Gong J and Wang ZM performed the research; Xia N, Lu J, Chen ZJ and Zhang LY analyzed the data; and Xia N wrote the paper.

Supported by the Youth Foundation of the Shanghai Public Health Bureau, No. 20134Y195; and the Project of Medical Key Specialty of Shanghai Municipality, No. ZK2015A22.

Institutional review board statement: The study was reviewed and approved by the Ruijin Hospital Luwan Branch Review Board.

Informed consent statement: All study participants, or their legal guardian, provided informed written consent prior to study enrollment.

Conflict-of-interest statement: None declared.

Data sharing statement: No additional data are available.

Manuscript source: Unsolicited manuscript

Correspondence to: Zhong-Min Wang, MD, Professor, Department of Intervention, Ruijin Hospital, Shanghai Jiao Tong University School of Medicine, Shanghai 200025, China. james0722@163.com
Telephone: +86-21-63864050
Fax: +86-21-63860461

Received: September 26, 2016
Peer-review started: September 28, 2016
First decision: October 20, 2016
Revised: November 10, 2016
Accepted: January 17, 2017
Article in press: January 17, 2017
Published online: March 14, 2017

Abstract

AIM

To assess the feasibility and effectiveness of a novel application of percutaneous intraductal radiofrequency (RF) for the treatment of biliary stent obstruction.

METHODS

We specifically report a retrospective study presenting the results of percutaneous intraductal RF in patients with biliary stent occlusion. A total of 43 cases involving biliary stent obstruction were treated by placing an EndoHPB catheter and percutaneous intraductal RF was performed to clean stents. The stent patency was evaluated by cholangiography and follow-up by contrast enhanced computed tomography or ultrasound after the removal of the drainage catheter.

RESULTS

Following the procedures, of the 43 patients, 40 survived and 3 died with a median survival of 80.5 (range: 30-243) d. One patient was lost to follow-up. One patient had the stent patent at the time of last follow-up. Two patients with stent blockage at 35 d and 44 d after procedure underwent percutaneous

transhepatic drain insertion only. The levels of bilirubin before and after the procedure were 128 ± 65 μmol/L and 63 ± 29 μmol/L, respectively. There were no related complications (haemorrhage, bile duct perforation, bile leak or pancreatitis) and all patients' stent patency was confirmed by cholangiography after the procedure, with a median patency time of 107 (range: 12-180) d.

CONCLUSION

This preliminary clinical study demonstrated that percutaneous intraductal RF is safe and effective for the treatment of biliary stent obstruction, increasing the duration of stent patency, although randomized controlled trials are needed to confirm the effectiveness of this approach.

Key words: Percutaneous transhepatic cholangiography; Intraductal radiofrequency; Malignant obstructive jaundice

Core tip: This study sought to assess the feasibility and effectiveness of a novel application of percutaneous radiofrequency ablation in the treatment of biliary stent obstruction. We report a retrospective study with the results of percutaneous intraductal radiofrequency ablation in patients with biliary stent occlusion.

Xia N, Gong J, Lu J, Chen ZJ, Zhang LY, Wang ZM. Percutaneous intraductal radiofrequency ablation for treatment of biliary stent occlusion: A preliminary result. *World J Gastroenterol* 2017; 23(10): 1851-1856 Available from: URL: http://www.wjgnet.com/1007-9327/full/v23/i10/1851.htm DOI: http://dx.doi.org/10.3748/wjg.v23.i10.1851

INTRODUCTION

The use of biliary self-expanding metallic stents (SEMSs) is an effective method for treating malignant biliary obstruction. However, with excessive tumor growth, tumor ingrowth, epithelial hyperplasia, biological film deposition and biliary sludge formation, the patency time of SEMSs is approximately 120 d[1]. The current management approaches for occluded SEMSs include mechanical cleaning and the insertion of a second stent (a covered SEMS, uncovered SEMS or plastic stent) *via* an endoscopic or percutaneous approach[2].

Recently, numerous clinical reports have demonstrated the safety and efficacy of using a novel radiofrequency (RF) ablation (RFA) catheter for endoscopic palliative procedures[3,4]. There is a clinical need for an effective method of re-opening biliary stents that accounts for the limitations of an endoscope, particularly in cases involving hepatic hilar tumors or after gastrointestinal operations. Therefore, our research group investigated the treatment of biliary stent occlusion by percutaneous biliary RF.

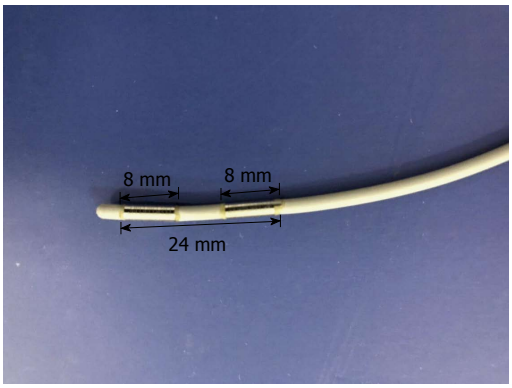

Figure 1 The Habib EndoHPB bipolar radiofrequency ablation catheter with two bare metal electrodes 8 mm apart and the catheter head located 5 mm from the distal electrode.

MATERIALS AND METHODS

The Habib EndoHPB RF catheter for bipolar RFA (EMcision, United States) has a bipolar RF probe diameter of 8 Fr (2.6 mm), a length of 1.8 m, and a distance of 0.035 (COOK, United States) that allows to pass over a guide wire. The catheter has two ring electrodes separated by a distance of 8 mm and a leading edge that extends 5 mm beyond the distal electrode, and it can produce focal coagulation necrosis with a long diameter of more than 2.5 cm (Figure 1). This catheter can be used in the treatment of intraductal RF.

Patient characteristics

From July 2012 to March 2014, 43 patients with malignant biliary obstruction were recruited to this study. These patients underwent biliary stent (SEMSs, length 6-8 cm, diameter 1 cm, BARD, United States) treatment by percutaneous puncture (n = 24; stent patency range: 72-145 d) or endoscopic retrograde cholangiopancreatography (n = 19; stent patency range: 69-139 d). After treatment, the patients had fever, jaundice or symptoms of abdominal pain again (15-110 d). All patients underwent evaluation by CT or ultrasound to confirmed the proximal stent dilatation of the bile duct, an assessment of biliary stent occlusion, and dilatation of the intrahepatic bile duct, and routine preoperative examinations (routine blood parameters, liver function, renal function, and blood coagulation function). There were 24 cases of pancreatic carcinoma, 8 cases of bile duct carcinoma, 6 cases of hepatocellular carcinoma, and 5 cases of gallbladder cancer. The mean of patients' ages was 62 (47-82) years, and the male:female ratio was 26:17. Severe coagulopathy, heart failure and cardiac pacemaker implantation were contraindications for the procedures of this study. All patients signed an informed consent form before undergoing these procedures, which were

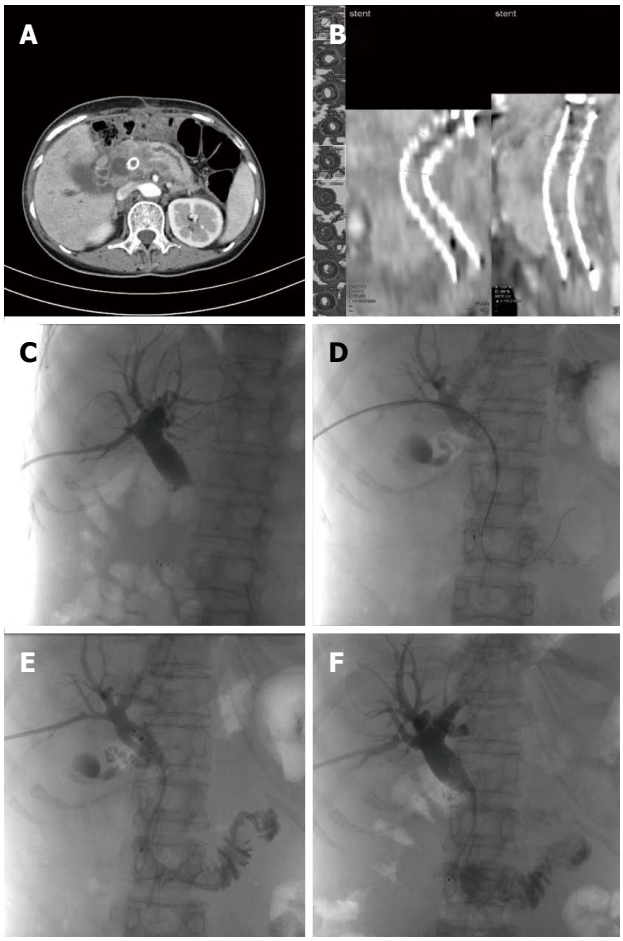

Figure 2 Images for a 53-year-old female with carcinoma of the pancreatic head and a biliary stent implanted to treat obstructive jaundice 3.5 mo prior to this study for obstructive jaundice. An enhanced computed tomography (CT) scan showing bile duct obstruction (A); CT coronal reconstruction clearly showing stent obstruction (B); cholangiography revealing the complete obstruction of the biliary stent (C), the intraductal radiofrequency (RF) catheter in the position of obstruction (D), and internal and external drainage tube after RF (E); angiography indicating stent patency after procedure (F).

approved by the relevant ethics committee.

Procedure details

An Innova 3100 DSA (GE, United States) system was used for image-guided applications. A RITA 1500X RF generator (AngioDynamics, United States) was used for energy output. Under DSA guidance, contrast agent was injected into the bile duct, and the length of the stenosis was accurately determined by cholangiography. Using a guidewire technique, the catheter (C3 COOK, United States) was positioned in the area of the occlusion. In cases of complete biliary occlusion, it was necessary to form the guide wire into a loop using vascular catheters and a 5 Fr sheath (Terumo Japan) for support before passing the wire through the occlusion. If the 0.035 guide wire (Terumo Japan) remained unable to pass through the obstruction, the 0.018 guidewire (Boston, United States) was used. The location of the RF catheter was confirmed to avoid contact with the intestine. The RF generator was then connected using the following parameters: a frequency of 400 KHz, a power of 710 W, the mean ablation time of 90 s (range from 60 to 120 s), a stop time of 60 s, and a total output energy of 1200-3600 J (Figure 2). The ablation procedure was repeated 2 to 3 times across the length of the obstruction, and the catheter was removed simultaneously (Table 1).

Table 1 Procedure details

Ablation time (s)	90 (62-150)
Ablation repeats	3 (2-5)
Ablation energy (J)	2474 (1200-3600)
Stenosis length (mm)	35 (20-55)

Data are expressed as medians (range).

The RFA catheter was then withdrawn. A drainage tube was implanted, stent patency was confirmed by angiography, and the bile duct was flushed with 0.9% saline to avoid stents restenosis. The indwelling drainage tube was removed 2-3 d after the operation, after which biliary stent patency was reconfirmed by cholangiography and the tract was plugged.

Evaluation and follow-up

All patients underwent routine blood tests, liver and kidney function assessments, and determinations of serum amylase and C-reactive protein (CRP). And relevant data were recorded. Biliary tract dilatation was determined by CT, and biliary stent stenosis measurements, the number of ablations, and the ablation power output were recorded. The indwelling biliary drainage tube was removed 2 d after the procedures, and the tract was plugged with a gelatin sponge to prevent bile leakage into the peritoneal cavity. During the first week of follow-up, the patients were subjected to liver function tests and determinations of serum amylase and CRP. At 2 or 3 wk of follow-up, the patients were examined either as outpatients or during hospitalization, and liver function and bilirubin concentration changes were recorded. Ultrasound or low-dose CT was also performed to evaluate biliary tract dilatation, and survival times were recorded. Additionally, stent patency was evaluated by ultrasound or CT scan, with continuous bilirubin increase or pneumobilia considered to indicate stent obstruction.

Statistical analysis

All study data were analyzed using SPSS 17.0 and GraphPad Prism 5 statistical software. The data are expressed as the median (range) or mean (± SD). Measurement and count data were evaluated using *t*-tests and χ^2 tests, respectively. $P < 0.05$ was regarded as statistically significant.

RESULTS

All patients underwent successful intraductal RF in the

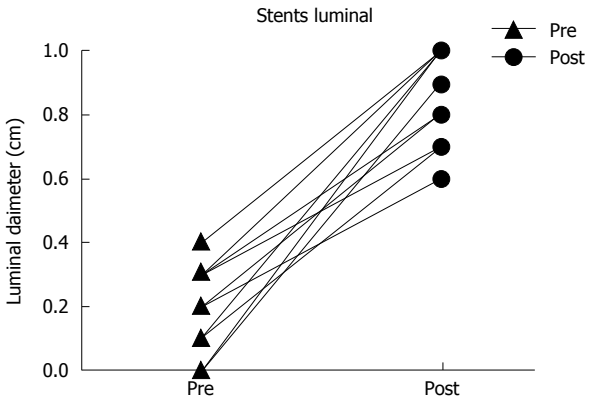

Figure 3 Stent patency trends after procedure.

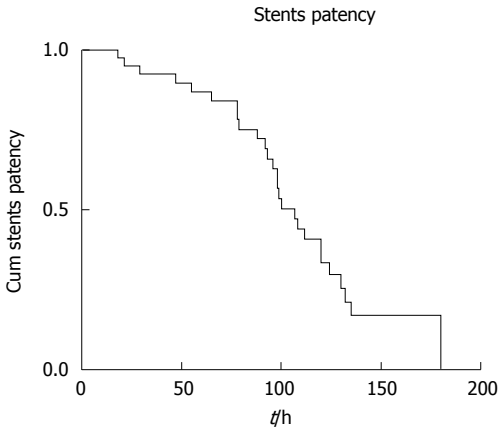

Figure 4 Luminal diameters before and after the procedure.

stents, and cholangiography was performed to ensure stent patency after the procedure. The indwelling drainage tube was retained for 7 d after procedures in 2 cases, because of necrosis and cholestasis after procedure, and in the remaining 41 cases, the biliary drainage tube was removed 2 d after the procedure. Post-procedure cholangiography revealed stent patency. There were no cases requiring implanting another biliary stent or further percutaneous transhepatic drainage.

There were no procedure related complications per SIR reporting standards. And no cases of hemorrhage, bile duct perforation, bile leak, or pancreatitis were observed after the intraductal RF. Mild abdominal pain (n = 16) was the main symptom after procedure, and it can subside spontaneously in 36 h. One patient was lost to follow-up, and 3 patients with cachexia due to multiple organ failure died 1 mo after ablation. Intraoperative angiography indicated that the median length of the biliary stricture was 35 mm (range: 20-55 mm). The median number of intraductal RF was 3 times (range: 2-5 times), which was based on the location and degree of obstruction of the biliary stent. The median output power for the intraductal RF was 2474 J (range: 1200-3600 J), and cholangiography was used to measure the diameter of the biliary tract. The median diameter of the biliary stricture before and after procedure was 1 mm (range: 0-4 mm) *vs* 8.0 mm (range: 6.0-10.0 mm). The median stent patency duration was 107 d (range: 12-180 d). Figure 3 presents Kaplan-Meier curves that reveal stent patency trends. Figure 4 indicates pre- and post-procedure luminal diameters. The bilirubin levels before and after procedure were 63 ± 29 μmol/L *vs* 128 ± 65 μmol/L (P < 0.05). Table 2 showed details about hepatic function metrics changes before and after procedure.

Table 2 Biochemical parameters before and after the procedure

Parameters	Pre-ablation	Post-ablation (day 3)	Normal
Bilirubin (μmol/L)	128 ± 65	63 ± 29	0-21
ALP (IU/L)	1240 ± 865	1032 ± 790	30-130
ALT (IU/L)	105 ± 58	79 ± 40	< 40
GGT (IU/L)	747 ± 729	720 ± 625	< 55
LDH (IU/L)	60 ± 84	311 ± 45	0-250
AST (IU/L)	98 ± 49	65 ± 34	< 40
CRP (mg/L)	15 ± 8	12 ± 7	0-5
Amylase (IU/L)	80 ± 15	79 ± 12	0-90

DISCUSSION

Obviously, with lengthened patient survival times, SEMS occlusion has become a common clinical situation. Although organic polymer-packaged SEMSs or methods to coat stents with nickel titanium alloy or other alloys could potentially be used instead of stainless steel or covered stents to address the issue of stent restenosis, experimental data have not supported this possibility[5,6]. Rather, the data have indicated that these novel types of stents increase the incidence of pancreatitis and cholecystitis, leading to long-term inflammation and bile duct bleeding[7-9]. Khashab *et al*[10] tried to extend the stent patency time by changing the shape of the stent, but the results were not different from those for a conventional stent.

Once a stent is placed in the bile duct, an encrustation of amorphous material and bacteria (sludge) begins to accumulate on its surface. The major limitation to long-term biliary stenting is thus early stent occlusion, although early symptoms of stent obstruction are not typical. Pneumobilia in the intrahepatic biliary tree is present when there is reflux of gas from the bowel and can also be present after biliary stent occlusion. In this context, early improvement of biliary drainage is particularly important[11].

RF has been widely used to treat malignant solid tumors and has even become a standard treatment for certain inoperable tumors, such as liver cancer and lung cancer. Its safety and efficacy are well established. However, restricted to the traditional RF structure, the RF technology has never been used to treat malignant biliary obstruction. The use of this catheter risks indirect injury to adjacent organs and electrode-induced skin burns. In addition, the

unpredictability of the electric current path reduces the ablation area. The use of RFA in the biliary tract is also limited due to the possibility of biliary fistulas and bile duct adhesion. A new bipolar catheter can avoid the aforementioned problems and has been demonstrated to be successful and safe for palliative therapy for malignant biliary occlusion[12].

Intraductal RF can delay tumor growth and retain the patency of SEMSs for a prolonged duration. In turn, the successful drainage leads to prolongation of survival time[13]. Khorsandi *et al*[14] subjected the EndoHPB catheter to extensive *in vivo* preclinical testing. A preliminary study using a pig model indicated that this catheter can be safely deployed in the context of SEMSs. In particular, intraductal RF treatment using this catheter causes the coagulative burning of intraductal tissues, but the heat associated with this burning will not damage surrounding tissue[15,16]. Another single published ex-vivo porcine study sought to systematically evaluate the effect of intraductal RF at various power settings (5, 10, 15 and 20 W) and durations of treatment (60, 90 and 120 s) on freshly resected porcine livers[17]. In practice, setting the output power to 10 W and ablation time for 90 s, it performed safe and efficient (Table 1). In the current study, none of patients exhibited pancreatitis or a biliary fistula due to heating.

An examination of endoscopic biliary RFA treatment in cases of malignant biliary obstruction and stent restenosis has confirmed the efficacy and safety of biliary RF technology[18]. Steel *et al*[3] specifically reported the endoscopic intraductal RF in 22 patients with malignant biliary obstruction. The examined cases included 10 patients with biliary SEMS restenosis (6 pancreatic cancer patients, 2 bile duct carcinoma patients, and 2 metastatic liver cancer patients) who underwent 13 intraductal RF treatments. The luminal diameter of the stenosis increased from a preoperative value of 1 mm to 5 mm after intraductal RF. The biliary stents remained open with a median patency duration of 119 d after procedures. Clinical research results have also demonstrated the effectiveness and safety of RF therapy for stent restenosis treatment in the biliary tract[19]. For patients with a history of gastrointestinal surgery, ERCP is considered a contraindication, but PTCD has no such limitation.

Intraductal RF *via* endoscopy has been used in the treatment of SEMS obstruction because of tumour ingrowth or overgrowth, which is a frequent complication. Mukund *et al*[19] specifically used intraductal RF to clear obstructed SEMSs. Both cases had extensive disease and showed radiological and biochemical evidence of improved drainage after intraductal RF application. However, the number of cases was too small to draw a definitive conclusion. Complication rates with both approaches appear to be comparable with those with the current standard ERC/PTD insertion and stenting in patients with malignant biliary disease[20,21].

Research has indicated that RF technology has potential clinical applications in treating stenosis of the biliary tract, and endoscopic RFA treatment in cases of malignant biliary obstruction and in-stent restenosis has confirmed the efficacy and safety of intraductal RF technology[22]. Furthermore, in the case of obstruction of a previously deployed metal stent, which cannot be removed, this intraductal RF approach can clear the occlusion and restore the biliary flow without the insertion of a new stent inside the obstructed stent, thereby saving the cost of a second stent[23]. Intraductal RF also has the advantageous characteristics of being a repeatable procedure by ERCP and PTCD. Moreover, for obstructive jaundice with a history of gastrointestinal surgery, it is difficult to reach the site of bile duct obstruction by endoscopy[24].

There were no major complications in our patients. The RF catheter can be easily introduced to the biliary tract and accurately positioned at the stricture lesion. However, the dispute is that how to apply intraductal RF for different stent locations (the hilum or ampulla) and how to choose an appropriate approach (percutaneous RFA or endoscopic RFA) to avoid injury to the bile duct and surrounding structures[21,25]. More clinical studies are required to guide clinical application.

The present study was a pilot feasibility study with obvious limitations. The number of patients enrolled was small. The follow-up duration may have been inadequate to demonstrate the long-term efficacy of this novel technique. Further studies are required to confirm our results.

COMMENTS

Background

The use of biliary self-expanding metallic stents is an effective method for treating malignant biliary obstruction. There is a clinical need for an effective method of re-opening biliary stents that accounts for the limitations of an endoscope, particularly in cases involving hepatic hilar tumors or after gastrointestinal operations. Therefore, our research group investigated the treatment of biliary stent occlusion by percutaneous biliary radiofrequency ablation (RFA).

Innovations and breakthroughs

To assess the feasibility and effectiveness of a novel application of percutaneous RF for the treatment of biliary stents obstruction, the authors specifically report a retrospective study presenting the results of percutaneous intraductal RF in patients with biliary stent occlusion.

Applications

This preliminary clinical study demonstrated that percutaneous intraductal RF is safe and effective for the treatment of biliary stent obstruction, increasing the duration of stent patency, although randomized controlled trials are needed to confirm the effectiveness of this approach.

Peer-review

In this manuscript, a total of 43 cases involving biliary obstruction caused by biliary stent stenosis were treated by placing an EndoHPB catheter into the stenosis and performing percutaneous transhepatic biliary RFA. The authors found that percutaneous internal biliary RFA is safe and effective for the treatment of biliary stent obstruction and increases the accumulation of stent patency time, although randomized controlled trials are needed to confirm the

effectiveness of this approach.

REFERENCES

1 **Shepherd HA**, Royle G, Ross AP, Diba A, Arthur M, Colin-Jones D. Endoscopic biliary endoprosthesis in the palliation of malignant obstruction of the distal common bile duct: a randomized trial. *Br J Surg* 1988; **75**: 1166-1168 [PMID: 2466520 DOI: 10.1002/bjs.1800751207]

2 **Ridtitid W**, Rerknimitr R. Management of an occluded biliary metallic stent. *World J Gastrointest Endosc* 2012; **4**: 157-161 [PMID: 22624066 DOI: 10.4253/wjge.v4.i5.157]

3 **Steel AW**, Postgate AJ, Khorsandi S, Nicholls J, Jiao L, Vlavianos P, Habib N, Westaby D. Endoscopically applied radiofrequency ablation appears to be safe in the treatment of malignant biliary obstruction. *Gastrointest Endosc* 2011; **73**: 149-153 [PMID: 21184881 DOI: 10.1016/j.gie.2010.09.031]

4 **Monga A**, Gupta R, Ramchandani M, Rao GV, Santosh D, Reddy DN. Endoscopic radiofrequency ablation of cholangiocarcinoma: new palliative treatment modality (with videos). *Gastrointest Endosc* 2011; **74**: 935-937 [PMID: 21168839 DOI: 10.1016/j.gie.2010.10.018]

5 **Andersen JR**, Sørensen SM, Kruse A, Rokkjaer M, Matzen P. Randomised trial of endoscopic endoprosthesis versus operative bypass in malignant obstructive jaundice. *Gut* 1989; **30**: 1132-1135 [PMID: 2475392 DOI: 10.1136/gut.30.8.1132]

6 **Elwir S**, Sharzehi K, Veith J, Moyer MT, Dye C, McGarrity T, Mathew A. Biliary stenting in patients with malignant biliary obstruction: comparison of double layer, plastic and metal stents. *Dig Dis Sci* 2013; **58**: 2088-2092 [PMID: 23456505 DOI: 10.1007/s10620-013-2607-z]

7 **Loew BJ**, Howell DA, Sanders MK, Desilets DJ, Kortan PP, May GR, Shah RJ, Chen YK, Parsons WG, Hawes RH, Cotton PB, Slivka AA, Ahmad J, Lehman GA, Sherman S, Neuhaus H, Schumacher BM. Comparative performance of uncoated, self-expanding metal biliary stents of different designs in 2 diameters: final results of an international multicenter, randomized, controlled trial. *Gastrointest Endosc* 2009; **70**: 445-453 [PMID: 19482279 DOI: 10.1016/j.gie.2008.11.018]

8 **Cariati A**, Piromalli E. Prevention of biliary stent occlusion. *Dig Dis Sci* 2012; **57**: 1971; author reply 1971-1972 [PMID: 22395960 DOI: 10.1007/s10620-012-2109-4]

9 **Cui PJ**, Yao J, Zhao YJ, Han HZ, Yang J. Biliary stenting with or without sphincterotomy for malignant biliary obstruction: a meta-analysis. *World J Gastroenterol* 2014; **20**: 14033-14039 [PMID: 25320543 DOI: 10.3748/wjg.v20.i38.14033]

10 **Khashab MA**, Hutfless S, Kim K, Lennon AM, Canto MI, Jagannath SB, Okolo PI, Shin EJ, Singh VK. A comparative evaluation of early stent occlusion among biliary conventional versus wing stents. *Dig Dis Sci* 2012; **57**: 1708-1716 [PMID: 22262198 DOI: 10.1007/s10620-012-2048-0]

11 **Thomas S**, Patel RP, Oto A. Resolution of pneumobilia as a predictor of biliary stent occlusion. *Clin Imaging* 2015; **39**: 650-653 [PMID: 25892599 DOI: 10.1016/j.clinimag.2015.03.010]

12 **Eum YO**, Kim YT, Lee SH, Park SW, Hwang JH, Yoon WJ, Ryu JK, Yoon YB, Han JK, Yoon CJ, Cho JH, Choi Y. Stent patency using competing risk model in unresectable pancreatic cancers inserted with biliary self-expandable metallic stent. *Dig Endosc* 2013; **25**: 67-75 [PMID: 23286259 DOI: 10.1111/j.1443-1661.2012.01335.x]

13 **Sugiyama G**, Okabe Y, Ishida Y, Saitou F, Kawahara R, Ishikawa H, Horiuchi H, Kinoshita H, Tsuruta O, Sata M. Evaluation of endoscopic biliary stenting for obstructive jaundice caused by hepatocellular carcinoma. *World J Gastroenterol* 2014; **20**: 6968-6973 [PMID: 24944490 DOI: 10.3748/wjg.v20.i22.6968]

14 **Khorsandi SE**, Zacharoulis D, Vavra P, Navarra G, Kysela P, Habib N. The modern use of radiofrequency energy in surgery, endoscopy and interventional radiology. *Eur Surg* 2008; **40**: 204-210 [DOI: 10.1007/s10353-008-0427-8]

15 **Ortner MA**. Photodynamic therapy for cholangiocarcinoma: overview and new developments. *Curr Opin Gastroenterol* 2009; **25**: 472-476 [PMID: 19550314 DOI: 10.1097/MOG.0b013e32832e6e1f]

16 **Itoi T**, Isayama H, Sofuni A, Itokawa F, Tamura M, Watanabe Y, Moriyasu F, Kahaleh M, Habib N, Nagao T, Yokoyama T, Kasuya K, Kawakami H. Evaluation of effects of a novel endoscopically applied radiofrequency ablation biliary catheter using an ex-vivo pig liver. *J Hepatobiliary Pancreat Sci* 2012; **19**: 543-547 [PMID: 22038500 DOI: 10.1007/s00534-011-0465-7]

17 **Branovan DI**, Fridman M, Krasko O, Lushchik M, Drozd V, Shiglik N, Danilova L, Demidchik Y. Bipolar radiofrequency ablation for thyroid nodules with effective induction of sufficiently large lesions without danger to surrounding structures (ex vivo morphological evaluation). *Pathology* 2016; **48** Suppl 1: S119 [PMID: 27772831 DOI: 10.1016/j.pathol.2015.12.314]

18 **Wadsworth CA**, Westaby D, Khan SA. Endoscopic radiofrequency ablation for cholangiocarcinoma. *Curr Opin Gastroenterol* 2013; **29**: 305-311 [PMID: 23449026 DOI: 10.1097/MOG.0b013e32835faacc]

19 **Mukund A**, Arora A, Rajesh S, Bothra P, Patidar Y. Endobiliary radiofrequency ablation for reopening of occluded biliary stents: a promising technique. *J Vasc Interv Radiol* 2013; **24**: 142-144 [PMID: 23273706 DOI: 10.1016/j.jvir.2012.09.018]

20 **Mulier S**, Ruers T, Jamart J, Michel L, Marchal G, Ni Y. Radiofrequency ablation versus resection for resectable colorectal liver metastases: time for a randomized trial? An update. *Dig Surg* 2008; **25**: 445-460 [PMID: 19212117 DOI: 10.1159/000184736]

21 **Kobayashi N**, Watanabe S, Hosono K, Kubota K, Nakajima A, Kaneko T, Sugimori K, Tokuhisa M, Goto A, Mori R, Taniguchi K, Matsuyama R, Endo I, Maeda S, Ichikawa Y. Endoscopic inside stent placement is suitable as a bridging treatment for preoperative biliary tract cancer. *BMC Gastroenterol* 2015; **15**: 8 [PMID: 25649526 DOI: 10.1186/s12876-015-0233-2]

22 **Kogure H**, Isayama H, Nakai Y, Tsujino T, Matsubara S, Yashima Y, Ito Y, Hamada T, Takahara N, Miyabayashi K, Mizuno S, Mohri D, Kawakubo K, Sasaki T, Yamamoto N, Hirano K, Sasahira N, Tada M, Koike K. High single-session success rate of endoscopic bilateral stent-in-stent placement with modified large cell Niti-S stents for malignant hilar biliary obstruction. *Dig Endosc* 2014; **26**: 93-99 [PMID: 23517109 DOI: 10.1111/den.12055]

23 **Wu TT**, Li WM, Li HC, Ao GK, Zheng F, Lin H. Percutaneous Intraductal Radiofrequency Ablation for Extrahepatic Distal Cholangiocarcinoma: A Method for Prolonging Stent Patency and Achieving Better Functional Status and Quality of Life. *Cardiovasc Intervent Radiol* 2017; **40**: 260-269 [PMID: 27743089 DOI: 10.1007/s00270-016-1483-2]

24 **Alvarez-Sánchez MV**, Napoléon B. Review of endoscopic radiofrequency in biliopancreatic tumours with emphasis on clinical benefits, controversies and safety. *World J Gastroenterol* 2016; **22**: 8257-8270 [PMID: 27729733 DOI: 10.3748/wjg.v22.i37.8257]

25 **Kato H**, Tsutsumi K, Harada R, Okada H, Yamamoto K. Endoscopic bilateral deployment of multiple metallic stents for malignant hilar biliary strictures. *Dig Endosc* 2013; **25** Suppl 2: 75-80 [PMID: 23617654 DOI: 10.1111/den.12061]

P- Reviewer: Musquer N, Seo DW **S- Editor**: Yu J
L- Editor: Wang TQ **E- Editor**: Wang CH

World Journal of Gastroenterology

Submit a Manuscript: http://www.wjgnet.com/esps/

World J Gastroenterol 2017 March 14; 23(10): 1857-1865

DOI: 10.3748/wjg.v23.i10.1857

ISSN 1007-9327 (print) ISSN 2219-2840 (online)

ORIGINAL ARTICLE

Observational Study

Hospital resource intensity and cirrhosis mortality in United States

Amit K Mathur, Apurba K Chakrabarti, Jessica L Mellinger, Michael L Volk, Ryan Day, Andrew L Singer, Winston R Hewitt, Kunam S Reddy, Adyr A Moss

Amit K Mathur, Ryan Day, Andrew L Singer, Winston R Hewitt, Kunam S Reddy, Adyr A Moss, Division of Transplant Surgery, Department of Surgery, Mayo Clinic Arizona, Phoenix, AZ 85054, United States

Amit K Mathur, Robert D and Patricia E Kern Center for the Science of Healthcare Delivery, Mayo Clinic, Phoenix, AZ 85054, United States

Apurba K Chakrabarti, Jessica L Mellinger, Department of Medicine, University of Michigan, Ann Arbor, MI 48109, United States

Michael L Volk, Department of Medicine, Loma Linda University, Loma Linda, CA 92350, United States

Author contributions: Mathur AK, Chakrabarti AK, Mellinger JL and Volk ML designed the study and acquired the data; Mathur AK, Chakrabarti AK, Mellinger JL, Volk ML, Day R and Singer AL analyzed and interpreted the data; Mathur AK, Chakrabarti AK, Mellinger JL, Volk ML, Day R, Singer AL, Hewitt WR, Reddy KS and Moss AA drafted and performed critical revisions of the manuscript.

Institutional review board statement: The study employed data from publicly available data sources and was therefore exempt from Institutional Review Board approval at the University of Michigan.

Informed consent statement: Humans subjects were not involved in this project and so informed consent was waived.

Conflict-of-interest statement: The authors have no conflicts of interest to disclose.

Manuscript source: Invited manuscript

Correspondence to: Amit K Mathur, MD, MS, Assistant Professor, Division of Transplant Surgery, Department of Surgery, Mayo Clinic Arizona, 5777 East Mayo Boulevard, Phoenix, AZ 85054, United States. mathur.amit@mayo.edu
Telephone: +1-480-3420437
Fax: +1-480-3422324

Received: November 5, 2016
Peer-review started: November 8, 2016
First decision: December 19, 2016
Revised: January 4, 2017
Accepted: February 7, 2017
Article in press: February 8, 2017
Published online: March 14, 2017

Abstract

AIM

To determine whether hospital characteristics predict cirrhosis mortality and how much variation in mortality is attributable to hospital differences.

METHODS

We used data from the 2005-2011 Nationwide Inpatient Sample and the American Hospital Association Annual survey to identify hospitalizations for decompensated cirrhosis and corresponding facility characteristics. We created hospital-specific risk and reliability-adjusted odds ratios for cirrhosis mortality, and evaluated patient and facility differences based on hospital performance quintiles. We used hierarchical regression models to determine the effect of these factors on mortality.

RESULTS

Seventy-two thousand seven hundred and thirty-three cirrhosis admissions were evaluated in 805 hospitals. Hospital mean cirrhosis annual case volume was 90.4

(range 25-828). Overall hospital cirrhosis mortality rate was 8.00%. Hospital-adjusted odds ratios (aOR) for mortality ranged from 0.48 to 1.89. Patient characteristics varied significantly by hospital aOR for mortality. Length of stay averaged 6.0 ± 1.6 days, and varied significantly by hospital performance ($P < 0.001$). Facility level predictors of risk-adjusted mortality were higher Medicaid case-mix (OR = 1.00, $P = 0.029$) and LPN staffing (OR = 1.02, $P = 0.015$). Higher cirrhosis volume (OR = 0.99, $P = 0.025$) and liver transplant program status (OR = 0.83, $P = 0.026$) were significantly associated with survival. After adjusting for patient differences, era, and clustering effects, 15.3% of variation between hospitals was attributable to differences in facility characteristics.

CONCLUSION

Hospital characteristics account for a significant proportion of variation in cirrhosis mortality. These findings have several implications for patients, providers, and health care delivery in liver disease care and inpatient health care design.

Key words: Cirrhosis; Mortality; Hospital variation; Resource utilization; Quality; Outcomes

Core tip: Cirrhosis mortality varies across hospitals, but it is not well-understood what differences between hospitals contribute to this variation. In our study, using administrative data on cirrhosis discharges and a national dataset on hospital structural characteristics, we found that several hospital factors including payer-mix and staffing patterns were associated with risk-adjusted mortality, but hospital experience with cirrhosis and presence of a liver transplant program were associated with survival. Structural factors are vital components to cirrhosis care delivery, and account for a significant proportion of the variation in cirrhosis mortality observed between hospitals. Future research should focus on other areas of variation, including differences in processes of cirrhosis care.

Mathur AK, Chakrabarti AK, Mellinger JL, Volk ML, Day R, Singer AL, Hewitt WR, Reddy KS, Moss AA. Hospital resource intensity and cirrhosis mortality in United States. *World J Gastroenterol* 2017; 23(10): 1857-1865 Available from: URL: http://www.wjgnet.com/1007-9327/full/v23/i10/1857.htm DOI: http://dx.doi.org/10.3748/wjg.v23.i10.1857

INTRODUCTION

Cirrhosis is the final common pathway for chronic liver disease, which predisposes patients to life-threatening complications. These complications - including ascites, spontaneous bacterial peritonitis, hepatic hydrothorax, variceal hemorrhage, hepatic encephalopathy, and hepatocellular carcinoma - require significant inpatient resources for appropriate and timely management to ensure good clinical outcomes[1]. Inpatient admissions for cirrhosis represent a critical juncture in the con tinuum of care of liver disease, because hospitals differ in their ability to care for these patients. We have previously demonstrated that hospitals differ 14-fold in mortality rates for cirrhosis[1], but the mechanism behind these differences is relatively unknown.

A major impediment to improving mortality in cirrhosis is a lack of national-level clinical registry data, which obligates providers to utilizing inferential studies from a variety of data sources to change practices[1]. Conceptually, variation in cirrhosis mortality between hospitals, using the Donabedian model of health care quality, are attributable to differences in: (1) patient characteristics and severity of disease; (2) the structure of health care facilities; and (3) processes of cirrhosis care[1]. Two hospitals can only have different clinical outcomes if they differ in these factors. Processes of care are the way in which care is delivered in a particular context and how prevailing structural re-sources are used for patients. These are of critical importance, but cirrhosis quality measures are not tracked nationally[1]. However, facility resources create the context for these processes, and are easily measured. For inpatient cirrhosis care, these resources include hospital bed capacity, staffing patterns of physicians and nurses, teaching status, endoscopic and imaging services, critical care and transplant personnel, and other specialized services.

In this study, we aimed to further evaluate the mechanism behind hospital variation in cirrhosis mortality by evaluating structural differences while controlling for patient differences. Specifically, we aimed to identify specific factors that were different between hospitals based on their risk-adjusted performance, whether these factors were associated with survival, and to what extent did they explain variation in cirrhosis mortality across hospitals. This approach would therefore allow us to "partition the total variance" in cirrhosis outcomes among patient differences, which are largely immutable, and modifiable factors such as hospital resource intensity, and, by exclusion, processes of care.

MATERIALS AND METHODS

Data sources

We captured admissions from the Nationwide Inpatient Sample (NIS) from the years 2005-2011. The NIS is the largest publicly available inpatient care database in the United States. It is sponsored by the Agency for Healthcare Research and Quality (AHRQ) through the Healthcare Cost and Utilization Project (HCUP). It contains clinical and resource utilization information for over 7 million admissions per year from a stratified

sample of 20% of discharges from US acute care hospitals. Facility characteristics were derived from the American Hospital Association (AHA) Annual Survey. This survey contains data on approximately 6500 hospitals nationwide with over 1000 elements covering hospital facilities, services, organization, and personnel. We merged NIS and AHA data using a common hospital identifier for each cirrhosis admission in each year.

Admission selection

We utilized admissions from NIS that contained an AHA Annual Survey identifier and had corresponding data in the AHA Survey. We captured cirrhotic admissions as previously described[1,2]. Briefly, we included admissions with a primary or secondary diagnosis of cirrhosis (alcoholic, non-alcoholic, or biliary) or a complication of cirrhosis (ascites, hepatic encephalopathy, hepatorenal syndrome, portal hypertension, or variceal bleed). We excluded admissions to hospitals with a cirrhotic volume less than 25 patients annually as well as admissions missing data on sex, insurance type, hospital bed size, or had inconsistent or undefined liver transplant program status across the study period[1,2].

Statistical analysis

We first created a risk and reliability-adjusted logistic regression model for mortality for any given hospital compared to an average hospital. We did this by first creating a hierarchical logistic regression model where patient covariates and year of admission were treated as fixed effects (level 1 variables) and hospital (level 2 variables) was treated as a random effect. Patient covariates included age, sex, race/ethnicity, cause of cirrhosis including hepatitis C virus positivity, alcoholic liver disease, or other, and presence of cirrhotic complications including ascites, variceal bleed, hepatic encephalopathy, portal hypertension, hepatorenal syndrome, liver transplant, hepatocellular carcinoma, requirement of paracentesis or esophagogastroduodenoscopy. Further adjustment for clinical co-morbidities was included in the model using the all patient refined-diagnosed related group (APR-DRG) risk of mortality[2,3].

Using this model, we then used the empirical Bayes technique to estimate a risk and reliability adjusted odds ratio for mortality via the random effects estimate[4,5]. Of note, this method is considered to be a relatively conservative one, as it "shrinks" variation towards the mean. This estimate incorporated the above fixed effects for risk adjustment and the hospital cirrhosis volume to adjust for reliability of the mortality measurement. We then partitioned hospital into quintiles based on the adjusted OR for mortality (quintile 1 included highest performing hospitals (lowest adjusted OR's for mortality) and quintile 5 included lowest performing (highest adjusted OR's for mortality).

We subsequently examined whether patient covariates and key hospital characteristics varied across quintiles. Hospital characteristics representing several structural domains including organizational structure, personnel, hospital facilities and services, and financial performance were selected based on previous literature[6] and included liver transplant program status, cirrhosis volume, the number of ICU beds, teaching status (number of resident full-time equivalents), and payer mix (the number of yearly Medicaid days), clinical staffing (licensed practical nurses (LPNs), and physicians per adjusted facility patient days). These structural variables were based on previous studies on the role of hospital structure on clinical outcomes[6], but were further expanded to include clinical resources specifically relevant to the management of cirrhotic patients.

We designed the statistical models to conceptually understand what factors account for differences in the mortality rate (risk and reliability-adjusted) between hospitals. Specifically, we assumed that variance in mortality was attributable to (1) clinical differences between patients; (2) hospital differences (further delineated by differences in structural variables); and (3) unmeasured factors (differences in unmeasured processes of care, other factors, and random error. We created a cumulative hierarchical logistic regression model that added these structural variables sequentially to calculate the fraction of inter-hospital variance in adjusted mortality explained by each structural variable. The baseline model adjusted for clinical differences between patients, and we evaluated the change in the calculated variance of the model with the sequential addition of specific structural characteristics. These were selected from the factors significantly different across mortality quintiles on univariate analysis. This approach assumed that structural factors contribute to variation in mortality between hospitals, and adjusting for them would attenuate the measured variance, *i.e.,* more of the differences between hospitals would be explained by the model as more significant structural factors were included.

These data were publicly available administrative data and were exempt from Institutional Review Board approval at the University of Michigan. All statistical analyses were performed using Stata 13 (Stata Corp, College Station, TX, United States). Statistical significance was considered at the $P = 0.05$ level.

RESULTS

Figure 1 demonstrates the range of risk and reliability-adjusted odds ratios (aOR) for in-hospital mortality, or hospital performance in cirrhosis. The demographic characteristics of the study cohort are included in Table 1 and stratified by aOR quintiles. The study cohort included 72733 hospital admissions from 2005-2011 that were divided amongst 805 hospitals. 29.6% of hospitalizations occurred in the lowest-mortality 20%

Table 1 Patient and hospital characteristics by hospital performance quintile in risk and reliability-adjusted cirrhosis mortality

	Q1 (highest performance)	Q2	Q3	Q4	Q5 (lowest performance)	Overall	*P* value
Patient characteristics							
Patients	21524	11117	12427	12648	15017	72733	-
Demographics							
Age							
Mean age (yr)	56.8	57.5	57.6	57.3	57.4	57.2	< 0.00001
Sex							
Female (%)	36.4	36.7	35.9	35.0	35.3	35.9	0.01381
Race							
White (%)	59.9	55.6	54.8	51.7	52.6	55.4	< 0.00001
Black (%)	5.8	7.7	5.6	5.7	9.0	6.7	
Hispanic (%)	15.2	20.2	21.5	17.4	20.3	18.5	
Asian or Pacific Islander (%)	1.6	1.8	2.3	1.3	2.2	1.8	
Native American (%)	1.6	0.5	0.8	1.1	0.9	1.1	
Other (%)	1.6	2.0	2.6	3.3	3.1	2.4	
Missing (%)	14.4	12.1	12.4	19.6	12.0	14.1	
Insurance							
Medicare (%)	36.1	37.2	38.0	36.9	37.3	37.0	< 0.00001
Medicaid (%)	22.9	24.5	24.8	23.8	26.5	24.4	
Private Insurance (%)	27.4	26.5	25.2	25.3	22.5	25.5	
Self-Pay (%)	7.5	7.4	7.3	8.4	7.8	7.7	
No Charge (%)	1.0	0.4	0.6	0.5	1.5	0.9	
Other (%)	5.0	4.0	4.0	5.0	4.3	4.6	
Cause of cirrhosis[1]							
Alcoholic liver disease (%)	61.0	62.5	61.0	60.8	60.3	61.1	0.00880
Alcoholic cirrhosis (%)	60.9	62.4	60.9	60.6	60.2	60.9	0.00589
Non-alcoholic cirrhosis (%)	38.0	36.9	38.0	38.6	39.0	38.1	0.00762
Biliary cirrhosis (%)	2.3	1.5	2.0	1.7	1.6	1.9	< 0.00001
HCV positive (%)	25.3	23.0	22.1	25.1	26.4	24.6	< 0.00001
Unspecified liver disease or cirrhosis (%)	2.7	2.0	2.0	2.0	1.8	2.2	< 0.00001
A1AT, Cu, Fe disease (%)	0.89	0.65	0.64	0.74	0.68	0.74	0.04067
Complications of Cirrhosis							
Ascites (%)	31.8	27.5	30.2	30.3	26.9	29.6	< 0.00001
Variceal bleed (%)	9.6	10.3	9.6	9.3	9.4	9.6	0.05605
Hepatic Encephalopathy (%)	53.7	55.2	52.5	54.1	55.7	54.2	< 0.00001
Portal HTN (%)	44.3	41.1	44.9	42.7	41.5	43.0	< 0.00001
Hepatorenal syndrome (%)	9.3	7.8	8.2	8.3	8.9	8.6	0.00003
Hepatocellular carcinoma (%)	3.9	2.7	3.1	3.1	3.2	3.3	< 0.00001
Procedures							
Liver transplant	2.7	0.6	1.0	1.1	2.4	1.7	< 0.00001
Esophagogastroduodenoscopy	18.1	19.0	20.4	19.3	18.3	18.9	< 0.00001
Paracentesis	32.9	29.7	30.0	29.7	29.2	30.6	< 0.00001
Mortality characteristics							
APR-DRG Risk of Mortality							
Minor risk of mortality (%)	5.9	7.8	6.8	6.5	9.1	7.1	< 0.00001
Moderate risk of mortality (%)	31.3	34.1	34.4	33.2	34.0	33.2	
Major risk of mortality (%)	41.0	39.4	39.4	39.5	37.0	39.4	
Extreme risk of mortality (%)	21.8	18.7	19.4	20.7	19.9	20.3	
Mortality							
Expired during admission (%)	5.1	6.0	7.5	9.8	12.3	7.9	< 0.00001
Hospital characteristic							
Number of hospitals	161	161	161	161	161	805	-
Region							
Northeast hospital region (%)	19.3	25.5	27.3	24.8	34.2	26.2	0.06961
Midwest hospital region (%)	18.6	13.7	17.4	13.0	9.3	14.4	
South hospital region (%)	29.2	32.3	19.9	29.2	26.7	27.5	
West hospital region (%)	32.9	28.6	35.4	32.9	29.8	31.9	
Bed capacity							
Small bedsize (%)	23.0	41.0	36.6	33.5	32.3	33.3	0.05554
Medium bedsize (%)	37.9	31.7	32.9	34.2	29.8	33.3	
Large bedsize (%)	39.1	27.3	30.4	32.3	37.9	33.4	
Hospital ICU beds (mean)	24.3	19.1	20.1	19.9	20.8	20.8	0.04608
Patient casemix							
Hospital Cirrhosis Annual Volume (mean)	133.7	69.0	77.2	78.6	93.3	90.4	< 0.00001
Medicaid Days (mean)	18139	15339	18158	18699	22662	18599	0.18260
Admission characteristics							
Length of stay (days) (mean)	5.9	5.7	5.9	6.2	6.4	6.0	0.00019

Total charges ($ mean)[2]	43391	36593	40500	43389	40340	40877	0.19458
Expired during admission (%)	4.0	5.3	7.3	10.1	13.2	8.0	< 0.00001
Staffing characteristics							
Full-time LPN's[3] (mean)	1.65	2.18	2.18	1.94	2.34	2.06	0.03218
Full-time MD's[3] (mean)	2.74	2.02	2.55	1.88	1.8	2.2	0.27122
Teaching Status							
Teaching hospital[4] (%)	42.9	32.9	38.5	39.8	41.6	39.1	0.40386
Resident FTE's (mean)	79.2	40.7	57.7	59.0	65.7	60.5	0.33158
Specialty Services							
Liver transplant hospital (%)	15.5	5.0	5.0	5.6	4.3	7.1	0.00020

[1]Patients have multiple diagnoses; [2]19 hospitals missing total charge data on 1751 patients; [3]per 10000 Adjusted Patient days; [4]43 hospitals that changed teaching status during the study period were considered teaching if 50% or more of patients were admitted while a teaching hospital.

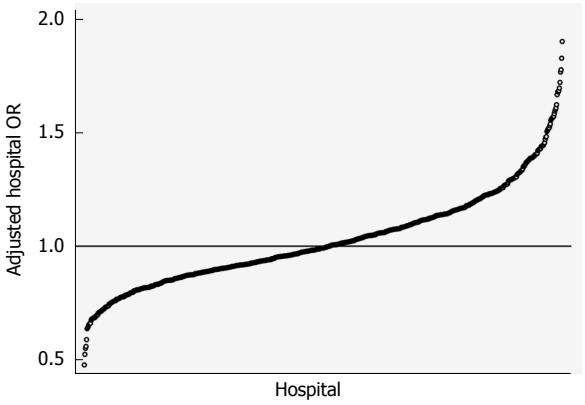

Figure 1 Variation in risk and reliability-adjusted mortality for cirrhosis admissions. The 805 hospitals in the analysis demonstrated tremendously variable mortality risk, even after risk adjusting for clinical and demographic differences between patients and accounting for differences in the reliability of the estimate for a given hospital, which is driven by institutional cirrhosis volume. Cirrhosis mortality odds ratios ranged from nearly 50% lower than the average hospital to 200% higher for some hospitals.

of hospitals, and 20.6% of hospitalizations occurred in the highest-mortality 20%. Patient demographic distributions varied significantly across quintiles, including age, sex, race, and payer mix. The mean age of the cohort was 57.2 years and was nearly 65% male. White patients had a higher proportion of admissions in the lowest-mortality hospitals, and minority race patients had higher relative proportions in the highest-mortality hospitals. Insurance status also varied significantly - the lowest performing hospitals had the highest relative proportions of government-paid admissions and the lowest proportions of privately insured patients. Differences in causes of cirrhosis were statistically significant, but absolute differences were quite small from a clinical standpoint. From a case mix perspective, the lowest performing hospitals had a greater proportion of the relatively lower risk patients (APR-DRG minor and moderate), whereas the highest performing hospitals had a greater proportion of the highest mortality risk patients (APR-DRG major and extreme). Within quintiles, the mean crude mortality rate ranged from 5.1%-12.3%.

Facility characteristics differed by hospital performance quintile in cirrhosis on univariate analysis (Table 1). Cirrhosis volume had a U-shaped distribution when distributed across mortality quintiles - the highest and lowest performing quintiles had an average of 20.8%-73.2% more cirrhosis admissions compared to the average performing hospitals (Table 1). The lowest quintile had nearly 25% greater Medicaid case-mix than the other groups. There were no significant differences in total bed capacity, but ICU bed capacity was roughly 20% larger in the highest quintile compared to the other groups. Staffing patterns were significantly different as well. Nurse staffing with LPNs was 40% greater in low performing hospitals compared to the highest quintile, however physician staffing was similar. 15.5% of the highest performing hospitals were liver transplant centers, which was three-fold greater than average or low performing hospitals. While not statistically significant, the geographic make-up of each performance quintile was also asymmetric. The highest performing group had more Western and Midwestern hospitals, and less Northeastern and Southern hospitals. This distribution was reversed in the lowest performing group - Northeastern hospitals made up more than 34% of this group.

In a multivariable risk-adjusted model evaluating predictors of cirrhosis mortality, both patient and facility factors were significant (Table 2). At the patient level, individual cirrhosis complications and co-morbidities were significant predictors of mortality - clinical presentation of hemorrhage, documented portal hypertension, hepatitis C status, alcoholic liver disease, and APR-DRG risk score were significant predictors of mortality (all, $P \leqslant 0.005$). Invasive diagnostic and therapeutic procedures including endoscopy, paracentesis, and liver transplantation were significantly protective (all, $P < 0.01$). There was also a significant era effect, as each successive year was independently associated with lower mortality (all, $P < 0.001$). At the facility level, each additional cirrhosis admission was associated with 0.05% lower odds of mortality. Liver transplant centers had 17% lower odds of mortality non-transplant facilities across all cirrhosis admissions. Medicaid payer-mix and more LPN nurse staffing were also associated with higher mortality.

To better understand the magnitude of between-hospital variation in cirrhosis mortality further, we

Table 2 Risk-adjusted effects of patient factors, era, and hospital resources on in-patient cirrhosis mortality

Characteristic	OR	95%CI	*P* value
Patient covariates			
Age	1.00	0.97-1.01	0.592
Female	1.05	0.93-1.06	0.753
Ascites	1.79	0.96-1.15	0.262
Variceal hemorrhage	1.26	1.64-1.95	< 0.001
Hepatic encephalopathy	0.63	1.18-1.34	< 0.001
Portal hypertension	1.16	0.59-0.68	< 0.001
Hepatorenal syndrome	0.20	1.07-1.25	< 0.001
Received liver transplant	0.83	0.15-0.26	< 0.001
HCV positive	1.43	1.33-1.54	< 0.001
Alcoholic liver disease	1.23	1.33-1.54	< 0.001
Paracentesis during admission	0.76	0.71-0.82	0.006
EGD during admission	0.81	0.75-0.88	< 0.001
Co-morbidity burden (APR DRG risk of mortality)			
Minor	Reference		
Moderate	1.54	1.14-2.07	0.005
Major	6.02	4.55-7.96	< 0.001
Extreme	58.8	44.5-77.8	< 0.001
Era (year of admission)			
2005	Reference		
2006	0.89	0.79-1.00	0.053
2007	0.79	0.70-0.89	< 0.001
2008	0.75	0.66-0.85	< 0.001
2009	0.68	0.60-0.78	< 0.001
2010	0.51	0.56-0.59	< 0.001
2011	0.49	0.42-0.56	< 0.001
Hospital resources (hospital structural factors)			
Hospital cirrhosis volume	1.01	1.00-1.01	0.025
Hospital medicaid days	1.01	1.00-1.01	0.029
Hospital liver transplant program	0.83	0.71-0.98	0.026
Full-time LPN's	1.02	1.00-1.04	0.015
Full-time MD's	0.99	0.98-1.00	0.140
Resident FTE's	1.00	1.00-1.00	0.115
ICU beds	1.00	1.00-1.00	0.446

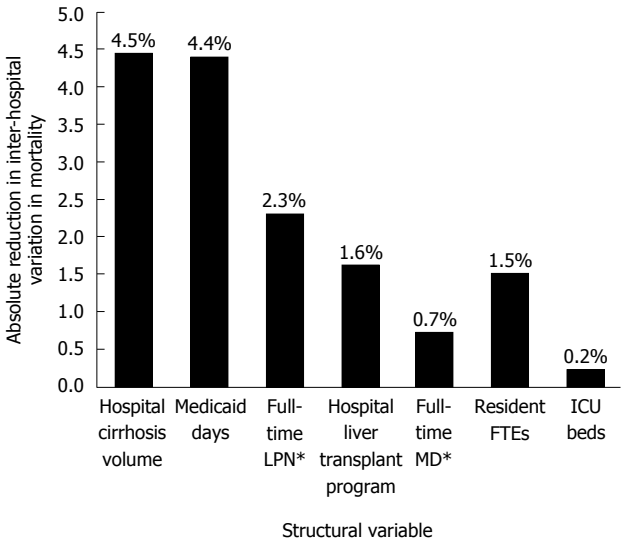

Figure 2 Inter-hospital variation in cirrhosis mortality explained by individual facility characteristics. Across the 72733 cirrhosis admissions in 805 hospitals, the regression model including clinical risk adjustors, era effects, and facility characteristics explained approximately 15.3% of the total variation in cirrhosis mortality between hospitals. This figure demonstrates the specific hospital factors that additively accounted for this measured variation. Annual cirrhosis volume, case mix, nurse staffing, liver transplant services, and other facility characteristics accounted for this variation, but it is notable that the majority of variation between hospitals remains unexplained.

evaluated how individual facility characteristics cumulatively affected measured mortality (Figure 2). With the cumulative effect of all structural variables added into the model, overall, 15.3% of the total variation is related to these parameters. The remaining variation remains unmeasured.

DISCUSSION

Recent data suggest that cirrhosis mortality differs widely across hospitals in the United States. This alarming phenomenon naturally lends itself to questions about what factors within hospitals contribute to this variation. For decades, variation in health care quality has been tied, in part, to differences in structure responsible for health care delivery[7]. In this analysis, we sought to better understand to what extent hospital facility characteristics affect the outcomes of patients admitted with cirrhosis to United States hospitals. Our study demonstrates that several hospital structural domains - case mix, payer mix, staffing patterns, and the presence of specialty liver transplant service line - are predictors of inpatient cirrhosis outcomes, account for a sizable fraction (15%) of the overall variation in mortality.

Recent data have demonstrated that cirrhosis mortality for hospitalized patients has improved over time[8,9], which we also observed in our analysis. While inpatient care in cirrhosis seems to be improving over time overall, nearly 40% of patients with life-threatening cirrhotic complications were admitted to hospitals with higher than expected risk-adjusted mortality rates. Even after adjusting for this era effect, our findings add to a growing body of work that show the importance of specific hospital resources in the care of patients with liver disease, surgical diseases, and malignancy[6,9-20]. Hospitals with higher than expected risk-adjusted cirrhosis mortality have less resources than those performing better. Resource intensity remains a predictor of survival which is likely driven by the development of care processes based on the local care environment within hospitals.

The specific hospital resources associated with cirrhosis mortality were interesting and speak to a structural footprint for quality cirrhosis care. High cirrhosis volume was significant, and the volume-outcome relationship has long been established in the health services research literature[15,21,22]. In the current study, higher Medicaid payer-mix and higher utilization of LPNs (*vs* RNs) were responsible for a significant portion of the total variation attributable to structural differences. These metrics may be proxies for financial difficulties in resource-strapped facilities that may not have services available that complicated cirrhosis patients require. The presence of a liver transplant program was significant in reducing mortality, but establishing these programs may be a significant hurdle for hospitals and may not be warranted based on current estimates of liver disease mortality nationally. Interestingly, ICU bed capacity, teaching status, and physician staffing were important but not as relevant as the aforementioned factors. This may be related to the near ubiquity of these resources across the population of hospitals in this study. From a clinical perspective, providers understand the ideal structural footprint of a hospital managing advanced cirrhosis- multi-specialty physician staffing, quality nursing, intensive care beds, radiological and endoscopy capacity, and many other services. This notion and some of the findings of this study naturally imply that further capital investments by hospitals may improve clinical outcomes in cirrhosis.

However, boosting resource intensity everywhere is neither the entire solution nor is it financially realistic[16,17,23]. The residual variation in cirrhosis mortality across hospitals remained vast even after accounting for structural differences, implying that unmeasured sources of variation likely account for major differences in clinical performance. By exclusion, based on our conceptual model, this residual variation can be attributable to processes of care and random error. Processes of cirrhosis care were not directly evaluated in this study. Kanwal *et al*[16,18,19] have outlined usable process of care measures for cirrhosis, but there neither is a national impetus to adopt these, nor is there a platform to track this data on a population level. Based on our findings, it is possible that differences in adherence to quality practices could account for a significant degree of variation. However, since nearly 85% of the variation was attributable to processes of care, care innovation in average and low performing hospitals may demonstrate immediate benefits. Recent initiatives to develop cirrhosis quality improvement programs by the sharing of regional or national data between hospitals holds significant promise, particularly for hospitals with higher than expected mortality.

These findings also have implications for developing care processes beyond the local hospital environment. The hospital characteristic that had the largest effect size in favor of survival was the presence of a liver transplant program. In fact, the beneficial effect of a liver transplant program was observed in non-transplant cases within that facility. In the interest of population health management, our findings imply that liver transplant programs should partner with providers in resource-poor institutions in order to improve care. The development of robust care networks between hospitals may, for example, help expedite transfers of critically ill patients who require liver transplant evaluation, optimize care for those patients who may not be liver transplant candidates, and improve quality of care in cirrhosis in general. There are obvious incentives for creating these networks for both resource-intense and resource-poor institutions, and has been alluded to in centralizing care for other conditions including cancer[24-26].

Based on our study, resource intensity seems to be responsible for some of this variation, but the totality of differences between hospitals was not completely adjusted for in the analysis. The limitations of this study are related to the inherent nature of the data source - administrative hospital discharge data - which do not adequately capture hospital-specific processes of care in cirrhosis, which are poorly defined in general[16,18,19]. Unmeasured structural variables, unmeasured processes of care, and unmeasured clinical granularity at the patient level may have affected the estimate of mortality risk during a given cirrhosis hospitalization, and so these results have to considered in that context. The statistical approach and study design cannot be used to determine causality, and population-based conclusions can lead to incorrect inferences when applied to individual patient treatments.

Given these limitations, the contribution of resource intensity to hospital variation in cirrhosis mortality is an important consideration for patients, providers, and payers despite secular improvements in inpatient mortality in general. Quality improvement within hospitals and collaboration between centers hold the

most promise to address these differences over time.

COMMENTS

Background

Hospitals vary significantly in cirrhosis mortality which can be attributable to multiple factors, which can be considered in the context of structural factors, processes of care, and patient differences.

Research frontiers

Hospital structural characteristics are a marker of hospital resources and affect outcomes. The effect of hospital resource differences on cirrhosis mortality has never been studied in a population context.

Innovations and breakthroughs

The authors were able to merge the Healthcare Cost and Utilization Project' s Nationwide Inpatient Sample data on hospital discharges with the American Hospital Association Annual Survey data on hospital structural resources to create a hierarchical logistic regression model to better understand hospital-level predictors of risk-adjusted mortality and how much hospital factors contribute to the overall variation in cirrhosis mortality between hospitals.

Applications

This analysis indicates that specific hospital resources are associated with mortality in cirrhosis, including staffing patterns and a shift in payer-mix toward public payers. However, hospital cirrhosis volume and liver transplant program status were independently associated with survival. These findings should help design cirrhosis care protocols and encourage care-networking between hospitals that have vast resource differences.

Peer-review

It is interesting to explore the relationship between the hospital characteristics and mortality. This article entitled "Hospital resource intensity and cirrhosis mortality in United States" by Mathur *et al* showed that "Hospital characteristics account for a significant proportion of variation in cirrhosis mortality". This paper provides readers new insight of the health care and management in patients with cirrhosis.

REFERENCES

1 **Nguyen GC**, Segev DL, Thuluvath PJ. Nationwide increase in hospitalizations and hepatitis C among inpatients with cirrhosis and sequelae of portal hypertension. *Clin Gastroenterol Hepatol* 2007; **5**: 1092-1099 [PMID: 17625983 DOI: 10.1016/j.cgh.2007.04.027]

2 **Mellinger JL**, Richardson CR, Mathur AK, Volk ML. Variation among United States hospitals in inpatient mortality for cirrhosis. *Clin Gastroenterol Hepatol* 2015; **13**: 577-584; quiz e30 [PMID: 25264271 DOI: 10.1016/j.cgh.2014.09.038]

3 **Iezzoni LI**, Ash AS, Shwartz M, Daley J, Hughes JS, Mackiernan YD. Judging hospitals by severity-adjusted mortality rates: the influence of the severity-adjustment method. *Am J Public Health* 1996; **86**: 1379-1387 [PMID: 8876505 DOI: 10.2105/AJPH.86.10.1379]

4 **Rabe-Hesketh S**, Skrondal A. Multilevel and longitudinal modeling using Stata. 3rd ed. College Station, Tex: Stata Press Publication, 2012

5 **Hosmer DW**, Lemeshow S, Sturdivant RX. Applied logistic regression. 3rd ed. Hoboken: John Wiley & Sons, Inc, 2013 [DOI: 10.1002/9781118548387]

6 **Ghaferi AA**, Osborne NH, Birkmeyer JD, Dimick JB. Hospital characteristics associated with failure to rescue from complications after pancreatectomy. *J Am Coll Surg* 2010; **211**: 325-330 [PMID: 20800188 DOI: 10.1016/j.jamcollsurg.2010.04.025]

7 **Donabedian A**. Evaluating the quality of medical care. *Milbank Mem Fund Q* 1966; **44**: Suppl: 166-206 [PMID: 5338568]

8 **Schmidt ML**, Barritt AS, Orman ES, Hayashi PH. Decreasing mortality among patients hospitalized with cirrhosis in the United States from 2002 through 2010. *Gastroenterology* 2015; **148**: 967-977.e2 [PMID: 25623044 DOI: 10.1053/j.gastro.2015.01.032]

9 **Kanwal F**. Decreasing mortality in patients hospitalized with cirrhosis. *Gastroenterology* 2015; **148**: 897-900 [PMID: 25805421 DOI: 10.1053/j.gastro.2015.03.023]

10 **Reames BN**, Ghaferi AA, Birkmeyer JD, Dimick JB. Hospital volume and operative mortality in the modern era. *Ann Surg* 2014; **260**: 244-251 [PMID: 24368634 DOI: 10.1097/SLA.0000000000000375]

11 **Ghaferi AA**, Birkmeyer JD, Dimick JB. Hospital volume and failure to rescue with high-risk surgery. *Med Care* 2011; **49**: 1076-1081 [PMID: 22002649 DOI: 10.1097/MLR.0b013e3182329b97]

12 **Hollenbeck BK**, Wei Y, Birkmeyer JD. Volume, process of care, and operative mortality for cystectomy for bladder cancer. *Urology* 2007; **69**: 871-875 [PMID: 17482924 DOI: 10.1016/j.urology.2007.01.040]

13 **Birkmeyer JD**, Sun Y, Goldfaden A, Birkmeyer NJ, Stukel TA. Volume and process of care in high-risk cancer surgery. *Cancer* 2006; **106**: 2476-2481 [PMID: 16634089 DOI: 10.1002/cncr.21888]

14 **Goodney PP**, Stukel TA, Lucas FL, Finlayson EV, Birkmeyer JD. Hospital volume, length of stay, and readmission rates in high-risk surgery. *Ann Surg* 2003; **238**: 161-167 [PMID: 12894006 DOI: 10.1097/01.SLA.0000081094.66659.c3]

15 **Birkmeyer JD,** Siewers AE, Finlayson EV, Stukel TA, Lucas FL, Batista I, Welch HG, Wennberg DE. Hospital volume and surgical mortality in the United States. *N Eng J Med* 2002; **346**:1128-1137 [PMID: 11948273 DOI: 10.1056/NEJMsa012337]

16 **Kanwal F**, Volk M, Singal A, Angeli P, Talwalkar J. Improving quality of health care for patients with cirrhosis. *Gastroenterology* 2014; **147**: 1204-1207 [PMID: 25449026 DOI: 10.1053/j.gastro.2014.10.029]

17 **Kanwal F**. Coordinating care in patients with cirrhosis. *Clin Gastroenterol Hepatol* 2013; **11**: 859-861 [PMID: 23542329 DOI: 10.1016/j.cgh.2013.03.015]

18 **Kanwal F**, Kramer JR, Buchanan P, Asch SM, Assioun Y, Bacon BR, Li J, El-Serag HB. The quality of care provided to patients with cirrhosis and ascites in the Department of Veterans Affairs. *Gastroenterology* 2012; **143**: 70-77 [PMID: 22465432 DOI: 10.1053/j.gastro.2012.03.038]

19 **Kanwal F**, Kramer J, Asch SM, El-Serag H, Spiegel BM, Edmundowicz S, Sanyal AJ, Dominitz JA, McQuaid KR, Martin P, Keeffe EB, Friedman LS, Ho SB, Durazo F, Bacon BR. An explicit quality indicator set for measurement of quality of care in patients with cirrhosis. *Clin Gastroenterol Hepatol* 2010; **8**: 709-717 [PMID: 20385251 DOI: 10.1016/j.cgh.2010.03.028]

20 **Mathur A**, Luberice K, Ross S, Choung E, Rosemurgy A. Pancreaticoduodenectomy at High-volume Centers: Surgeon Volume Goes Beyond the Leapfrog Criteria. *Ann Surg* 2015; **262**: e37-e39 [PMID: 26164432 DOI: 10.1097/SLA.0000000000001330]

21 **Finlayson EV**, Birkmeyer JD. Effects of hospital volume on life expectancy after selected cancer operations in older adults: a decision analysis. *J Am Coll Surg* 2003; **196**: 410-417 [PMID: 12648693 DOI: 10.1016/S1072-7515(02)01753-2]

22 **Birkmeyer JD**, Finlayson SR, Tosteson AN, Sharp SM, Warshaw AL, Fisher ES. Effect of hospital volume on in-hospital mortality with pancreaticoduodenectomy. *Surgery* 1999; **125**: 250-256 [PMID: 10076608 DOI: 10.1016/S0039-6060(99)70234-5]

23 **Mellinger JL**, Volk ML. Multidisciplinary management of patients with cirrhosis: a need for care coordination. *Clin Gastroenterol Hepatol* 2013; **11**: 217-223 [PMID: 23142204 DOI: 10.1016/j.cgh.2012.10.040]

24 **Stitzenberg KB**, Sigurdson ER, Egleston BL, Starkey RB, Meropol NJ. Centralization of cancer surgery: implications for patient access to optimal care. *J Clin Oncol* 2009; **27**: 4671-4678

[PMID: 19720926 DOI: 10.1200/JCO.2008.20.1715]
25 **DeMeester S**. Centralization of esophageal cancer surgery: the right thing to do is seldom easy. *Ann Surg Oncol* 2009; **16**: 1760-1761 [PMID: 19352775 DOI: 10.1245/s10434-009-0464-y]
26 **Greenberg CC**, Ashley SW, Schrag D. Centralization of cancer surgery: what does it mean for surgical training? *J Clin Oncol* 2009; **27**: 4637-4639 [PMID: 19720900 DOI: 10.1200/JCO.2009.23.0052]

P- Reviewer: Giorgio A, Kreisel W, Zheng SJ **S- Editor**: Qi Y
L- Editor: A **E- Editor**: Wang CH

World Journal of Gastroenterology

Submit a Manuscript: http://www.wjgnet.com/esps/

World J Gastroenterol 2017 March 14; 23(10): 1866-1871

DOI: 10.3748/wjg.v23.i10.1866

ISSN 1007-9327 (print) ISSN 2219-2840 (online)

ORIGINAL ARTICLE

Observational Study

Mortality associated with hepatitis C and hepatitis B virus infection: A nationwide study on multiple causes of death data

Ugo Fedeli, Enrico Grande, Francesco Grippo, Luisa Frova

Ugo Fedeli, Epidemiological Department, Veneto Region, 35131 Padova, Italy

Enrico Grande, Francesco Grippo, Luisa Frova, Italian National Institute of Statistics, 00184 Roma, Italy

Author contributions: All authors contributed equally to this work, designed the study, performed analyses, and wrote the manuscript.

Institutional review board statement: Mortality data are routinely collected by the National Institute of Statistics. All analyses were carried out on aggregated data without any possibility of identification of individuals; therefore, the study was exempt from institutional review board approval.

Informed consent statement: Since analyses were carried out on retrospective, routinely collected aggregated data, the informed consent was not required.

Conflict-of-interest statement: The authors declare that they have no conflict of interest.

Data sharing statement: No additional data are available.

Manuscript source: Invited manuscript

Correspondence to: Ugo Fedeli, MD, Epidemiological Department, Veneto Region, Passaggio Gaudenzio 1, 35131 Padova, Italy. ugo.fedeli@regione.veneto.it
Telephone: +39-49-8778251
Fax: +39-49-8778235

Received: November 15, 2016
Peer-review started: November 16, 2016
First decision: December 28, 2016
Revised: January 16, 2017
Accepted: February 16, 2017
Article in press: February 17, 2017
Published online: March 14, 2017

Abstract

AIM

To analyze mortality associated with hepatitis C virus (HCV) and hepatitis B virus (HBV) infection in Italy.

METHODS

Death certificates mentioning either HBV or HCV infection were retrieved from the Italian National Cause of Death Register for the years 2011-2013. Mortality rates and proportional mortality (percentage of deaths with mention of HCV/HBV among all registered deaths) were computed by gender and age class. The geographical variability in HCV-related mortality rates was investigated by directly age-standardized rates (European standard population). Proportional mortality for HCV and HBV among subjects aged 20-59 years was assessed in the native population and in different immigrant groups.

RESULTS

HCV infection was mentioned in 1.6% (n = 27730) and HBV infection in 0.2% (n = 3838) of all deaths among subjects aged $\geqslant$ 20 years. Mortality rates associated with HCV infection increased exponentially with age in both genders, with a male to female ratio close to unity among the elderly; a further peak was observed in the 50-54 year age group especially among male subjects. HCV-related mortality rates were higher

in Southern Italy among elderly people (45/100000 in subjects aged 60-79 and 125/100000 in subjects aged ⩾ 80 years), and in North-Western Italy among middle-aged subjects (9/100000 in the 40-59 year age group). Proportional mortality was higher among Italian citizens and North African immigrants for HCV, and among Sub-Saharan African and Asian immigrants for HBV.

CONCLUSION

Population ageing, immigration, and new therapeutic approaches are shaping the epidemiology of virus-related chronic liver disease. In spite of limits due to the incomplete reporting and misclassification of the etiology of liver disease, mortality data represent an additional source of information for surveillance.

Key words: Hepatitis C virus; Hepatitis B virus; Mortality; Epidemiology; Immigrants

Core tip: Multiple causes of death analyses carried out on the Italian National Cause of Death Register showed that 1.6% and 0.2% of all deaths in 2011-2013 were associated with hepatitis C virus (HCV) and hepatitis B virus (HBV) infection, respectively. HCV-associated mortality followed a bimodal distribution, increasing exponentially among the elderly in both genders, with a minor peak in middle-aged subjects, especially among males. The proportion of viral hepatitis-related deaths was higher among Italian citizens and North African immigrants for HCV, and among Sub-Saharan African and Asian immigrants for HBV.

Fedeli U, Grande E, Grippo F, Frova L. Mortality associated with hepatitis C and hepatitis B virus infection: A nationwide study on multiple causes of death data. *World J Gastroenterol* 2017; 23(10): 1866-1871 Available from: URL: http://www.wjgnet.com/1007-9327/full/v23/i10/1866.htm DOI: http://dx.doi.org/10.3748/wjg.v23.i10.1866

INTRODUCTION

Viral hepatitis is one of the leading causes of death and disability worldwide, with a greater burden of disease associated with hepatitis C virus (HCV) infection in Europe, the Middle East, the Americas and North-Africa, and with hepatitis B virus (HBV) infection in sub-Saharan Africa and most of Asia[1].

Within Europe, Italy is affected by the highest prevalence of HCV infection, as well as by high rates of liver cancer mortality[2]. According to a recent systematic review, the prevalence of anti-HCV antibodies in other European countries ranges from 0.1% to 3.2%, whereas it has been estimated to be 5.9% in Italy[3]. HCV prevalence shows a steep increase with age in subjects born before 1950, and a marked geographical trend with higher rates in Southern compared to Northern regions[2].

The available data suggest unique features in the epidemiology of HCV infection in Italy with at least two different epidemic waves experienced during the past century. The first wave, which likely peaked in the 1950s and 1960s, mostly affected people born during the 1920s to 1930s and was probably associated with the widespread use of minor invasive procedures performed with improperly sterilized, non-disposable instruments. The second wave affected young adults in the 1970s and 1980s who suffered the largest impact of intravenous drug use-related HCV infections[4,5].

The vanishing effect of the first epidemic may have a profound impact on the burden of liver disease in Italy[5]: HCV infection might be considered mostly a feature of elderly subjects, and the mortality of HCV-related liver cancer is expected to decline in the years to come, which is line with the current observable trend[6].

The epidemiology of HBV has shown a progressive reduction in the endemicity levels with less than 1% of subjects in the overall population currently being HBsAg positive[7]. Similar to HCV, the burden of HBV infection could further decline given that the overall vaccination coverage rate is approximately 95% and nearly all Italian individuals under 35 years have now been vaccinated against HBV[7].

However, such favorable trends observed in more recent years could be impaired by the increasing number of immigrants living in Italy not vaccinated against HBV[7], and by a rising burden of HCV-associated disease with ageing of the cohort affected by the more recent HCV epidemic. In Italy, HBV and HCV testing has been so far carried out for high-risk or convenience groups (including intravenous drug users, blood donors, pregnant women, hospitalized patients), whereas there have not been national or regional testing strategies at the population level. Current population-based epidemiological figures on virus-related chronic liver disease in Italy are based mainly on local studies, whereas nationwide data are lacking. The aim of this study was to assess the burden and variability of mortality associated with HBV and HCV infection by analyzing the data obtained by the national database of causes of death.

MATERIALS AND METHODS

All analyses were carried out on the Italian National Cause of Death Register, managed by the Italian National Institute of Statistics (ISTAT). Data are based on the information reported on death certificates; all the diseases mentioned in the certificate are coded according to the International Classification of Diseases, 10th Edition (ICD-10 2009 version). Standard mortality statistics are usually based on internationally adopted algorithms that identify a single underlying

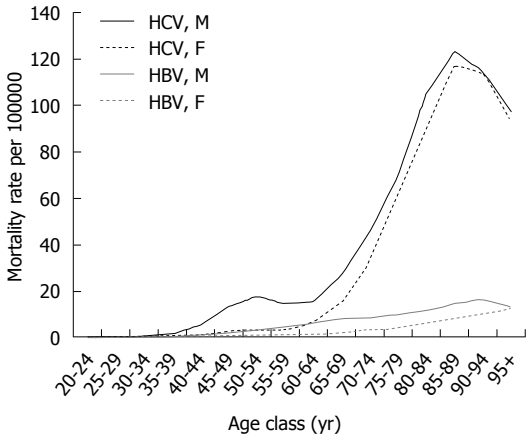

Figure 1 Mortality associated with hepatitis C virus and hepatitis B virus infection: Age and gender-specific mortality rates, Italy 2011-2013. HBV: Hepatitis B virus; HCV: Hepatitis C virus.

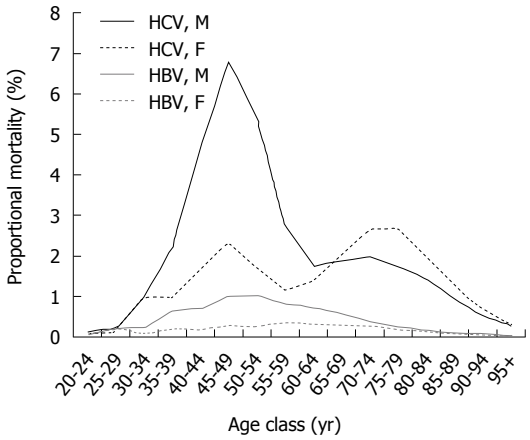

Figure 2 Mortality associated with hepatitis C virus and hepatitis B virus infection: Age and gender-specific proportional mortality, Italy 2011-2013. HBV: Hepatitis B virus; HCV: Hepatitis C virus.

cause of death (UCOD) from all the conditions reported in the certificate. Analyses based on any mention of a disease irrespective of its selection as the UCOD, the so-called multiple causes of death approach (MCOD), can more fully describe the burden of mortality associated with chronic diseases[8].

All deaths from January 1, 2011 to December 31, 2013 of subjects resident in Italy and aged ⩾ 20 years with any mention in the death certificate of HCV (ICD-10 codes B17.1, B18.2) or HBV infection (ICD-10 B16.0-B16.9, B17.0, B18.0, B18.1) were extracted. Age and gender-specific mortality rates were computed for the whole nation as well as by area of residence (North-West, North-East, Centre, South, Islands). The geographical variability in HCV-related mortality rates was summarized by directly age-standardized rates (European standard population) both for the whole population aged ⩾ 20 years, and for broad age classes. Proportional mortality was defined as the percentage of deaths with any mention of HCV or HBV out of all registered deaths, and was computed by age, gender, and immigrant status based on the country of citizenship. To deal with larger numbers, non-Italian countries of citizenship were grouped by area of provenance on the basis of macro-geographical regions and sub-regions: North Africa, Sub-Saharan Africa, South Asia (Indian subcontinent), other Asian countries, Central and South America, EU15 and other developed countries. Furthermore, analyses were restricted to the 20-59-year age band, where the immigrant population is more represented[9]. Among deaths with mention of HCV or HBV infection, the selected UCOD was analyzed by age class according to broad nosological sectors: viral hepatitis, liver cancer, and chronic liver diseases (ICD-10 B15-B19, C22, K70, K73, K74), acquired immunodeficiency syndrome (AIDS, B20-B24), neoplasms other than liver cancer (C00-D48, except for C22), circulatory diseases (I00-I99), and a residual category including all other diseases.

RESULTS

Out of 1787434 deaths of subjects aged ⩾ 20 years in the causes of death registry, HCV infection was mentioned in 1.6% (n = 27730) and HBV infection in 0.2% (n = 3838). These two groups included 647 decedents presenting with HBV-HCV co-infection. Figure 1 shows that the mortality rate associated with HCV infection increased exponentially with age in both genders, and among the elderly, the male to female ratio was close to unity. A further peak was observed in the 50-54-year age-group, especially among males, with a male to female ratio equal to 5.3. Mortality rates associated with HBV infection increased slowly with age and were always higher in the male gender. Proportional mortality figures (Figure 2) confirmed the bimodal distribution of HCV-related deaths. The selected UCOD was a liver disease (cirrhosis, liver cancer, viral hepatitis) in the majority of deaths with mention of HCV or HBV infection. This was observed especially in subjects aged 50-79 years (Figure 3). Among younger decedents a large proportion was represented by AIDS, whereas among the very elderly the UCOD was more evenly distributed across different nosological sectors.

The overall age-standardized HCV-related mortality rate was higher in Southern Italy (Table 1). However, the findings were observed to vary depending on the age class. The peak in mortality among people aged ⩾ 60 years was higher in Southern Italy, whereas mortality rates in the 40-59-year age band, corresponding to the lower peak registered among middle-aged subjects, was more pronounced in the North-Western and Central regions of the country.

In analyses restricted to the 20-59-year band, HCV infection was mentioned in 4092 Italian and 120 immigrant decedents, and HBV infection in 757 Italian and 78 immigrant decedents; information

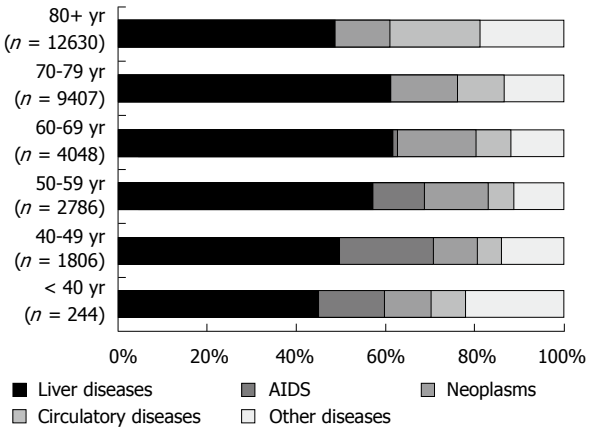

Figure 3 Distribution of the underlying cause of death among decedents with mention of hepatitis C or hepatitis B infection, by age class, Italy, 2011-2013.

Table 1 Mortality associated with hepatitis C virus infection across Italian areas: age-standardized mortality rates per 100000 (European standard population), 2011-2013

	Italy	North-West	North-East	Centre	South	Islands
20-39 yr	0.4	0.4	0.4	0.5	0.4	0.5
40-59 yr	7.7	9.1	6.8	8.7	6.5	6.7
60-79 yr	30.9	31.1	22.8	21.9	45.0	34.5
80+ yr	106.1	120.3	99.9	80.1	125	95.2
All ages 20+	17.7	19.1	14.8	14.0	22.1	17.6

on citizenship was missing for 8 and 6 subjects with HCV and HBV infection, respectively. In spite of low numbers among immigrants, Figure 4 shows that proportional mortality for HCV infection was higher among Italian citizens and immigrants from North Africa. In the case of HBV infection, the proportional mortality was higher among immigrants from Sub-Saharan Africa and Asian countries.

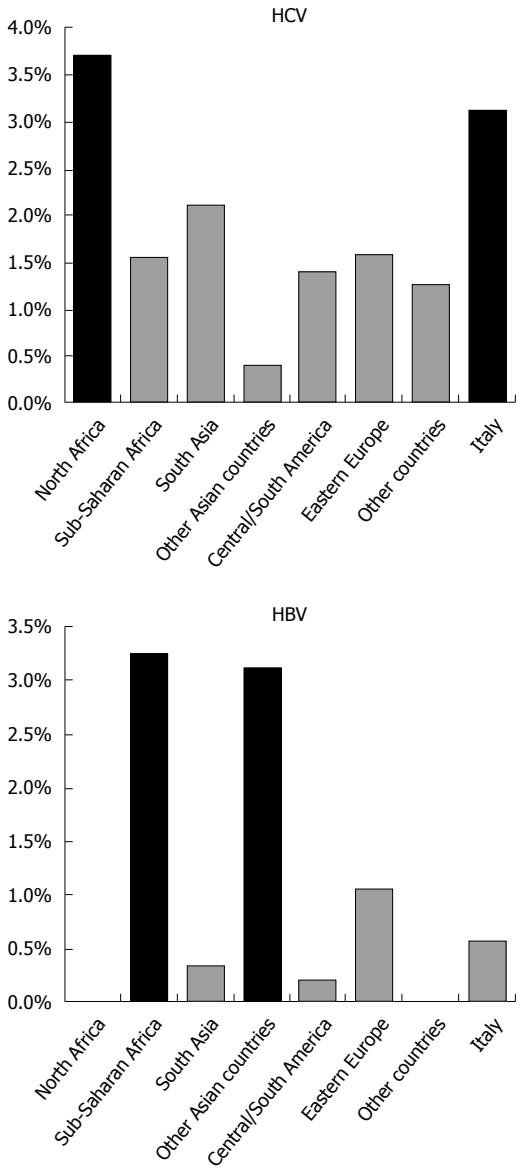

Figure 4 Mortality associated with hepatitis C virus and hepatitis B virus infection by country of citizenship: Proportional mortality among decedents aged 20-59 years, Italy 2011-2013. HBV: Hepatitis B virus; HCV: Hepatitis C virus.

DISCUSSION

Analyses of death certificates are known to be affected by incomplete reporting and misclassification of the etiology of liver diseases, leading to an underestimation of the true mortality burden associated with chronic viral infection[10]. The physicians filling in death certificates may be unaware of HCV or HBV infection in the patient or may not consider that the disease contributed to the death. Furthermore, among elderly patients affected by multiple comorbidities, there may be no simple etiologic chain leading to the identification of a single underlying cause; especially in the contest of ageing populations like in Italy, death often results from a complex interaction between multiple factors. As a consequence, instead of relying only on the underlying cause of death, the MCOD approach allows a more complete identification of the burden of mortality attributable to viral hepatitis infection. The MCOD methodology has been applied in the United States to monitor time trends in HCV-related mortality[10,11], and to assess the burden of HCV-related deaths in high-risk populations such as prison inmates[12]. In Italy, MCOD analyses of virus-related liver diseases have been carried out only at the regional level[13]. This first nationwide report allows for the investigation of variations in mortality by age, gender, area of residence, and immigrant status, thereby providing a raw but comprehensive picture of the contemporary burden of HCV and HBV-related mortality in Italy.

Repeated surveys carried out in a small town in Southern Italy suggest a decreasing prevalence of HCV infection, being mostly confined to the oldest age groups[14]. Moreover, clinical studies found that, although HCV infection still represents the main

etiology for chronic liver disease in Italy, its role is declining in more recent years[15,16]. The present data suggest that the current burden of HCV-related disease among elderly Italians is still large, especially in Southern regions. These figures must be interpreted within the frame of the recent availability of safe and effective drugs that will change the approach to the aged HCV patient, with an increasing number of treatment candidates[17]. Furthermore, mortality data confirm the presence of two distinct epidemic waves that have partly been associated with different HCV subtypes[18]. A bimodal distribution of HCV infection has been previously reported by seroprevalence surveys conducted both in Northern[19] as well as in Southern Italy[20], and by analyses of the mention of HCV infection in records from a sample of Italian general practitioners[21]. The peak in middle-aged subjects is most likely associated with intravenous drug abuse as well as with other risk factors (including tattoos and piercing) typical of younger generations[19]. Such a peak is well-recognizable from mortality rates at least in the male gender, and must strictly be monitored in the future: HCV-related liver disease progresses faster with aging, extra-hepatic manifestations of HCV infection are probably worse in the elderly, and the risk of hepatocellular carcinoma increases with age[17]. In the United States, where HCV infection is mostly restricted to the 1945-1965 birth cohort, HCV-related mortality assessed with the MCOD methodology is steeply increasing[10]. The HCV-related mortality wave is rapidly rising in the United States as the age of the affected birth cohort is increasing[22]; a similar unfavorable trend could be observed in Italy in the near future. Furthermore, mortality data suggest that the geographical variation in the burden of HCV differs across age groups, with higher rates observed among middle-aged subjects residing in Northern and Central Italy with respect to the Southern regions.

Mortality among immigrants mirrors the available data on the global epidemiology of viral hepatitis. Estimates for the prevalence of HCV infection range from < 1.0% in Northern Europe to > 2.9% in Northern Africa, with the highest prevalence (15%-20%) reported from Egypt[23]. Similar to Italy, other countries with high HCV prevalence suffered from iatrogenic spread around the middle of the past century. In Egypt, this was due to parenteral antischistosomal therapy through 1961-1986[24]; mass trypanosomiasis therapy before 1951 in the Central Africa Republic, and intravenous treatment with antimalarial drugs and other medical interventions in Cameroon, also caused iatrogenic transmission of HCV[25]. Data on HBV-related mortality are consistent with the rates that have been reported from the countries of origin and with previous studies on immigrants in Italy. Among undocumented immigrants in a city in Northern Italy, 6% tested positive for HBsAg; the only independent predictor was the prevalence of HBV infection in the area of provenance, with higher rates for subjects from Sub-Saharan Africa and Asia[26]. The present mortality analysis was carried out on legal residents with foreign citizenship, representing about 5000000 subjects (8.3% of all residents in Italy, 10.9% in the 20-59-year age band), and was not restricted to selected high-risk groups like undocumented immigrants or asylum seekers. All of the above evidence should guide a re-appraisal of strategies tailored according to the area of provenance for screening, HBV vaccination, HBV and HCV infection treatment of the immigrant population.

In conclusion, population ageing, an increase in the number of immigrants from countries with high HBV and HCV prevalence, and changes in the therapeutic approaches are re-shaping the epidemiology of virus-related chronic liver disease. MCOD data are a useful tool among the multiple information sources needed to monitor this rapidly evolving scenario.

COMMENTS

Background

Within Europe, Italy is affected by the highest prevalence of hepatitis C virus (HCV) infection. HCV prevalence shows a steep increase with age in subjects born before 1950, and a marked geographical trend with higher rates in Southern compared to Northern regions.

Research frontiers

Population-based epidemiological figures on virus-related chronic liver disease in Italy are based mainly on local studies. Mortality records can provide a nationwide estimate of the impact of hepatitis B virus (HBV) and HCV infection.

Innovations and breakthroughs

Mortality rates associated with HCV infection increased exponentially with age in both genders. A further peak was observed in the 50-54-year age class, especially among males. HCV-related mortality rates were higher in Southern Italy among elderly subjects, and in North-Western Italy among middle-aged subjects.

Applications

Despite the limit of incomplete reporting of the etiology of liver disease, the analysis of mortality data represents an additional tool for investigating the impact of HBV and HCV infection.

Terminology

Multiple causes of death approach: the analysis of mortality records based not only on the selected underlying cause of death, but on any mention of a disease in the death certificate.

Peer-review

As the authors acknowledge, death certificates provide incomplete or misclassified health condition data. Hence, their data likely underestimates HBV and HCV prevalence. Despite these limitations, the study provides data not currently available in the literature which is immediately useful for clinicians and public health authorities to follow trends in HBV and HCV disease-related mortality.

REFERENCES

1 **Stanaway JD**, Flaxman AD, Naghavi M, Fitzmaurice C, Vos T, Abubakar I, Abu-Raddad LJ, Assadi R, Bhala N, Cowie B, Forouzanfour MH, Groeger J, Mohd Hanafiah K, Jacobsen KH, James SL, MacLachlan J, Malekzadeh R, Martin NK, Mokdad

AA, Mokdad AH, Murray CJ, Plass D, Rana S, Rein DB, Richardus JH, Sanabria J, Saylan M, Shahraz S, So S, Vlassov VV, Weiderpass E, Wiersma ST, Younis M, Yu C, El Sayed Zaki M, Cooke GS. The global burden of viral hepatitis from 1990 to 2013: findings from the Global Burden of Disease Study 2013. *Lancet* 2016; **388**: 1081-1088 [PMID: 27394647 DOI: 10.1016/S0140-6736(16)30579-7]

2 **European Centre for Disease Prevention and Control**. Hepatitis B and C in the EU neighbourhood: prevalence, burden of disease and screening policies. Stockholm: ECDC, 2010

3 **European Centre for Disease Prevention and Control**. Systematic review on hepatitis B and C prevalence in the EU/EEA. Stockholm: ECDC, 2016

4 **Mariano A**, Scalia Tomba G, Tosti ME, Spada E, Mele A. Estimating the incidence, prevalence and clinical burden of hepatitis C over time in Italy. *Scand J Infect Dis* 2009; **41**: 689-699 [PMID: 19579149 DOI: 10.1080/00365540903095358]

5 **Puoti M**, Girardi E. Chronic hepatitis C in Italy: the vanishing of the first and most consistent epidemic wave. *Dig Liver Dis* 2013; **45**: 369-370 [PMID: 23567493 DOI: 10.1016/j.dld.2013.02.012]

6 **Cazzagon N**, Trevisani F, Maddalo G, Giacomin A, Vanin V, Pozzan C, Poggio PD, Rapaccini G, Nolfo AM, Benvegnù L, Zoli M, Borzio F, Giannini EG, Caturelli E, Chiaramonte M, Foschi FG, Cabibbo G, Felder M, Ciccarese F, Missale G, Baroni GS, Morisco F, Pecorelli A, Farinati F. Rise and fall of HCV-related hepatocellular carcinoma in Italy: a long-term survey from the ITA.LI.CA centres. *Liver Int* 2013; **33**: 1420-1427 [PMID: 23758775 DOI: 10.1111/liv.12208]

7 **Sagnelli E**, Sagnelli C, Pisaturo M, Macera M, Coppola N. Epidemiology of acute and chronic hepatitis B and delta over the last 5 decades in Italy. *World J Gastroenterol* 2014; **20**: 7635-7643 [PMID: 24976701 DOI: 10.3748/wjg.v20.i24.7635]

8 **Frova L**, Salvatore MA, Pappagallo M, Egidi V. Multiple cause of death approach to analyze mortality patterns. *Genus* 2009; **65**: 1-21 [DOI: 10.4402/genus-10]

9 **Fedeli U**, Ferroni E, Pigato M, Avossa F, Saugo M. Causes of mortality across different immigrant groups in Northeastern Italy. *PeerJ* 2015; **3**: e975 [PMID: 26038730 DOI: 10.7717/peerj.975]

10 **Ly KN**, Hughes EM, Jiles RB, Holmberg SD. Rising Mortality Associated With Hepatitis C Virus in the United States, 2003-2013. *Clin Infect Dis* 2016; **62**: 1287-1288 [PMID: 26936668 DOI: 10.1093/cid/ciw111]

11 **Ly KN**, Xing J, Klevens RM, Jiles RB, Ward JW, Holmberg SD. The increasing burden of mortality from viral hepatitis in the United States between 1999 and 2007. *Ann Intern Med* 2012; **156**: 271-278 [PMID: 22351712 DOI: 10.7326/0003-4819-156-4-201202210-00004]

12 **Harzke AJ**, Baillargeon JG, Kelley MF, Diamond PM, Goodman KJ, Paar DP. HCV-related mortality among male prison inmates in Texas, 1994-2003. *Ann Epidemiol* 2009; **19**: 582-589 [PMID: 19443239 DOI: 10.1016/j.annepidem.2009.03.009]

13 **Fedeli U**, Avossa F, Goldoni CA, Caranci N, Zambon F, Saugo M. Education level and chronic liver disease by aetiology: A proportional mortality study. *Dig Liver Dis* 2015; **47**: 1082-1085 [PMID: 26315625 DOI: 10.1016/j.dld.2015.07.154]

14 **Guadagnino V**, Stroffolini T, Caroleo B, Menniti Ippolito F, Rapicetta M, Ciccaglione AR, Chionne P, Madonna E, Costantino A, De Sarro G, Focà A, Lentini M, Staltari O. Hepatitis C virus infection in an endemic area of Southern Italy 14 years later: evidence for a vanishing infection. *Dig Liver Dis* 2013; **45**: 403-407 [PMID: 23199596 DOI: 10.1016/j.dld.2012.10.014]

15 **Stroffolini T**, Sagnelli E, Gaeta GB, Sagnelli C, Andriulli A, Brancaccio G, Pirisi M, Colloredo G, Morisco F, Furlan C, Almasio PL. Characteristics of liver cirrhosis in Italy: Evidence for a decreasing role of HCV aetiology. *Eur J Intern Med* 2017; **38**: 68-72 [PMID: 27836249 DOI: 10.1016/j.ejim.2016.10.012]

16 **Saracco GM**, Evangelista A, Fagoonee S, Ciccone G, Bugianesi E, Caviglia GP, Abate ML, Rizzetto M, Pellicano R, Smedile A. Etiology of chronic liver diseases in the Northwest of Italy, 1998 through 2014. *World J Gastroenterol* 2016; **22**: 8187-8193 [PMID: 27688660 DOI: 10.3748/wjg.v22.i36.8187]

17 **Vespasiani-Gentilucci U**, Galati G, Gallo P, De Vincentis A, Riva E, Picardi A. Hepatitis C treatment in the elderly: New possibilities and controversies towards interferon-free regimens. *World J Gastroenterol* 2015; **21**: 7412-7426 [PMID: 26139987 DOI: 10.3748/wjg.v21.i24.7412]

18 **Ansaldi F**, Bruzzone B, Salmaso S, Rota MC, Durando P, Gasparini R, Icardi G. Different seroprevalence and molecular epidemiology patterns of hepatitis C virus infection in Italy. *J Med Virol* 2005; **76**: 327-332 [PMID: 15902713 DOI: 10.1002/jmv.20376]

19 **Fabris P**, Baldo V, Baldovin T, Bellotto E, Rassu M, Trivello R, Tramarin A, Tositti G, Floreani A. Changing epidemiology of HCV and HBV infections in Northern Italy: a survey in the general population. *J Clin Gastroenterol* 2008; **42**: 527-532 [PMID: 18277889 DOI: 10.1097/MCG.0b013e318030e3ab]

20 **Polilli E**, Tontodonati M, Flacco ME, Ursini T, Striani P, Di Giammartino D, Paoloni M, Vallarola L, Pressanti GL, Fragassi G, Accorsi P, Manzoli L, Parruti G. High seroprevalence of HCV in the Abruzzo Region, Italy: results on a large sample from opt-out pre-surgical screening. *Infection* 2016; **44**: 85-91 [PMID: 26363567 DOI: 10.1007/s15010-015-0841-3]

21 **Lapi F**, Capogrosso Sansone A, Mantarro S, Simonetti M, Tuccori M, Blandizzi C, Rossi A, Corti G, Bartoloni A, Bellia A, Baiocchi L, Cricelli I, Cricelli C. Hepatitis C virus infection: opportunities for an earlier detection in primary care. *Eur J Gastroenterol Hepatol* 2017; **29**: 271-276 [PMID: 27849644 DOI: 10.1097/MEG:0000000000000785]

22 **Fedeli U**, Schievano E. Mortality Waves Related to Hepatitis C Virus Infection: Multiple Causes of Death Data From the United States and Northern Italy Compared. *Clin Infect Dis* 2016; **63**: 849-850 [PMID: 27329234 DOI: 10.1093/cid/ciw421]

23 **Alter MJ**. Epidemiology of hepatitis C virus infection. *World J Gastroenterol* 2007; **13**: 2436-2441 [PMID: 17552026 DOI: 10.3748/WJG.v13.i17.2436]

24 **Frank C**, Mohamed MK, Strickland GT, Lavanchy D, Arthur RR, Magder LS, El Khoby T, Abdel-Wahab Y, Aly Ohn ES, Anwar W, Sallam I. The role of parenteral antischistosomal therapy in the spread of hepatitis C virus in Egypt. *Lancet* 2000; **355**: 887-891 [PMID: 10752705 DOI: 10.1016/S0140-6736(99)06527-7]

25 **Strickland GT**. An epidemic of hepatitis C virus infection while treating endemic infectious diseases in Equatorial Africa more than a half century ago: did it also jump-start the AIDS pandemic? *Clin Infect Dis* 2010; **51**: 785-787 [PMID: 20735241 DOI: 10.1086/656234]

26 **El-Hamad I**, Pezzoli MC, Chiari E, Scarcella C, Vassallo F, Puoti M, Ciccaglione A, Ciccozzi M, Scalzini A, Castelli F. Point-of-care screening, prevalence, and risk factors for hepatitis B infection among 3,728 mainly undocumented migrants from non-EU countries in northern Italy. *J Travel Med* 2015; **22**: 78-86 [PMID: 25424439 DOI: 10.1111/jtm.12176]

P- Reviewer: Hunt CM, Makara M, Morikawa K **S- Editor**: Yu J
L- Editor: A **E- Editor**: Wang CH

World Journal of Gastroenterology

Submit a Manuscript: http://www.wjgnet.com/esps/

World J Gastroenterol 2017 March 14; 23(10): 1872-1880

DOI: 10.3748/wjg.v23.i10.1872

ISSN 1007-9327 (print) ISSN 2219-2840 (online)

ORIGINAL ARTICLE

Observational Study

Prognostic value of site-specific metastases in pancreatic adenocarcinoma: A Surveillance Epidemiology and End Results database analysis

Hani Oweira, Ulf Petrausch, Daniel Helbling, Jan Schmidt, Meinrad Mannhart, Arianeb Mehrabi, Othmar Schöb, Anwar Giryes, Michael Decker, Omar Abdel-Rahman

Hani Oweira, Anwar Giryes, Omar Abdel-Rahman, Swiss Cancer Institute, 6330 Cham, Switzerland

Hani Oweira, Arianeb Mehrabi, Department of General, Visceral and Transplant Surgery, University of Heidelberg, 69120 Heidelberg, Germany

Ulf Petrausch, Swiss Tumor Immunology Institute, 8001 Zurich, Switzerland

Daniel Helbling, Gastrointestinal Tumor Center Zurich, 8001 Zurich, Switzerland

Hani Oweira, Jan Schmidt, Othmar Schöb, Surgical center Zurich - Hirslanden Hospital Zurich, 8001 Zurich, Switzerland

Meinrad Mannhart, Department of Oncology, Center of Zug, 6301 Zug, Switzerland

Michael Decker, Zentrum für Integrative Onkologie, 8001 Zurich, Switzerland

Omar Abdel-Rahman, Clinical Oncology Department, Faculty of Medicine, Ain Shams University, Cairo 11511, Egypt

Author contributions: Abdel-Rahman O conducted the analyses and wrote the manuscript; all other authors contributed to the idea of the manuscript and approved the final version.

Institutional review board statement: This article does not contain any studies with human participants or animals performed by any of the authors.

Informed consent statement: As this study is based on a publicly available database without identifying patient information, informed consent was not needed.

Conflict-of-interest statement: The authors declare they have no conflicts of interest.

Data sharing statement: Technical appendix, statistical code, and dataset available from the corresponding author at omar.abdelrhman@med.asu.edu.eg. Consent was not obtained but the presented data are anonymized and risk of identification is low.

Manuscript source: Invited manuscript

Correspondence to: Dr. Omar Abdel-Rahman, Clinical Oncology Department, Faculty of Medicine, Ain Shams University, Cairo 11511, Egypt. omar.abdelrhman@med.asu.edu.eg
Telephone: +2-100-8541806
Fax: +2-100-6858397

Received: October 9, 2016
Peer-review started: October 11, 2016
First decision: December 19, 2016
Revised: December 20, 2016
Accepted: February 7, 2017
Article in press: February 8, 2017
Published online: March 14, 2017

Abstract

AIM

To evaluate the prognostic value of site-specific metastases among patients with metastatic pancreatic

carcinoma registered within the Surveillance, Epidemiology and End Results (SEER) database.

METHODS

SEER database (2010-2013) has been queried through SEER*Stat program to determine the presentation, treatment outcomes and prognostic outcomes of metastatic pancreatic adenocarcinoma according to the site of metastasis. In this study, metastatic pancreatic adenocarcinoma patients were classified according to the site of metastases (liver, lung, bone, brain and distant lymph nodes). We utilized chi-square test to compare the clinicopathological characteristics among different sites of metastases. We used Kaplan-Meier analysis and log-rank testing for survival comparisons. We employed Cox proportional model to perform multivariate analyses of the patient population; and accordingly hazard ratios with corresponding 95%CI were generated. Statistical significance was considered if a two-tailed *P* value < 0.05 was achieved.

RESULTS

A total of 13233 patients with stage Ⅳ pancreatic cancer and known sites of distant metastases were identified in the period from 2010-2013 and they were included into the current analysis. Patients with isolated distant nodal involvement or lung metastases have better overall and pancreatic cancer-specific survival compared to patients with isolated liver metastases (for overall survival: lung *vs* liver metastases: $P < 0.0001$; distant nodal *vs* liver metastases: $P < 0.0001$) (for pancreatic cancer-specific survival: lung *vs* liver metastases: $P < 0.0001$; distant nodal *vs* liver metastases: $P < 0.0001$). Multivariate analysis revealed that age < 65 years, white race, being married, female gender; surgery to the primary tumor and surgery to the metastatic disease were associated with better overall survival and pancreatic cancer-specific survival.

CONCLUSION

Pancreatic adenocarcinoma patients with isolated liver metastases have worse outcomes compared to patients with isolated lung or distant nodal metastases. Further research is needed to identify the highly selected subset of patients who may benefit from local treatment of the primary tumor and/or metastatic disease.

Key words: Pancreatic cancer; Liver metastases; Lung metastases; Bone metastases; Surveillance Epidemiology and End Results database

Core tip: Pancreatic adenocarcinoma patients with isolated liver metastases have worse outcomes compared to patients with isolated lung or distant nodal metastases. Further research is needed to identify the highly selected subset of patients who may benefit from local treatment of the primary tumor and/or metastatic disease.

Oweira H, Petrausch U, Helbling D, Schmidt J, Mannhart M, Mehrabi A, Schöb O, Giryes A, Decker M, Abdel-Rahman O. Prognostic value of site-specific metastases in pancreatic adenocarcinoma: A Surveillance Epidemiology and End Results database analysis. *World J Gastroenterol* 2017; 23(10): 1872-1880 Available from: URL: http://www.wjgnet.com/1007-9327/full/v23/i10/1872.htm DOI: http://dx.doi.org/10.3748/wjg.v23.i10.1872

INTRODUCTION

Pancreatic cancer is a global health burden with a poor prognosis and a difficult to treat biology in the majority of cases[1]. Histologically, pancreatic adenocarcinoma represents the majority of pancreatic cancer cases; and unfortunately the worst prognosis[2].

Treatment decisions for pancreatic adenocarcinoma differ according to patient- and disease-related factors. For fit patients with localized disease, surgical resection should always be considered, to be followed by or preceded by systemic chemotherapy[3]; while for locally advanced disease, personalized multimodality treatment strategies may be proposed[4]. For patients with metastatic disease, the primary treatment is systemic therapy (which may include systemic chemotherapy and more recently targeted therapy)[5].

Unfortunately, population-based studies in many parts of the world have shown a limited improvement in survival for non metastatic pancreatic cancer patients over years[6]. The situation is even worse for advanced stages of the disease[7]; and this calls for reconsideration of the current therapeutic strategies for this disease.

In the setting of metastatic pancreatic adenocarcinoma, liver is the most common site of metastasis. However, some cases may experience a change of the metastatic pattern and involve other distant organs without involving the liver. These cases may represent a different subset of patients with different biology and prognosis and subsequently different therapeutic approach[8-10].

Population-based data on the prognostic value of site-specific metastases for pancreatic adenocarcinoma are lacking. And thus, the objective of this study is to review the presentation and treatment trends of metastatic pancreatic cancer patients registered within the Surveillance Epidemiology and End Results (SEER) database with a particular focus on the prognostic value of different sites of metastases.

MATERIALS AND METHODS

This study was based on the publicly available SEER-18 registry of the United States national cancer institute[11]. We retrieved data using the SEER*Stat software Version 8.3.2. Because this study is based on a publicly available database, it was exempted from

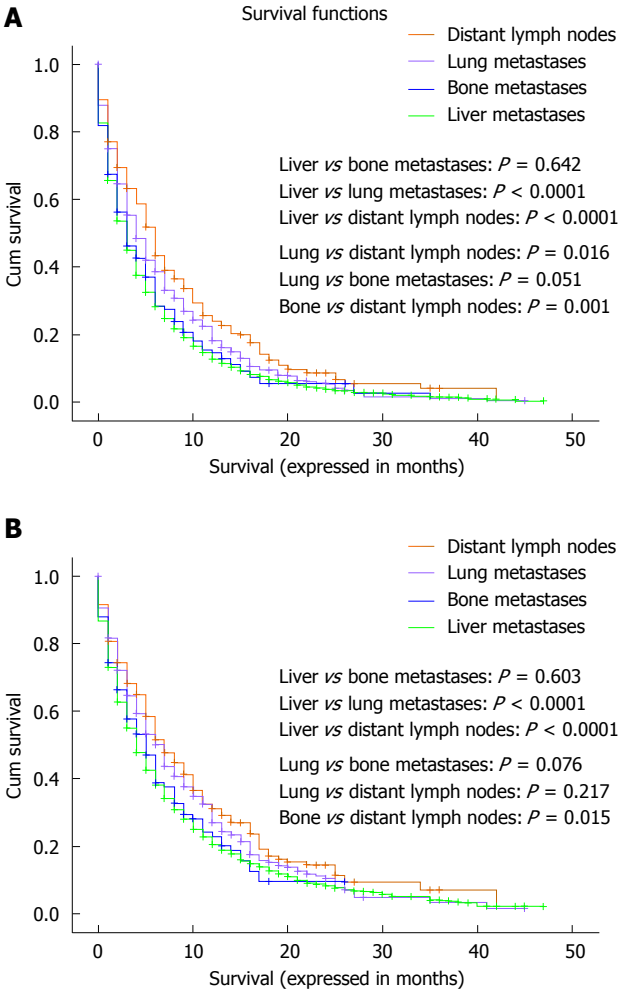

Figure 1 Kaplan-Meier curve of: overall survival (A), and pancreatic cancer-specific survival (B) according to the site of single site metastases.

IRB approval.

Data collection

We restricted our search to SEER database (2010-2013) because detailed information about the site of distant metastases was not available before 2010.

To identify metastatic pancreatic cancer patients, we included cases with a primary site of "pancreas", with ICD-O-Histology/behavior codes of 8140/3, 8141/3, 8142/3, 8143/3, 8144/3 and 8145/3 (variants of adenocarcinoma) and with AJCC stage Ⅳ. We excluded patients without sufficient survival data or data about the site of the metastases.

Data extracted for each case included age at diagnosis, gender, race, marital status, T stage, N stage, site of metastases, surgery to the primary and metastases, cause-specific death classification, survival months and vital status. For the sake of the current analysis, pancreatic cancer-specific survival was defined as time from diagnosis to death from pancreatic adenocarcinoma. Data about systemic therapy were not available in the SEER database.

Statistical analysis

In this study, metastatic pancreatic adenocarcinoma patients were classified according to the site of metastases (liver, lung, bone, brain and distant lymph nodes). We utilized chi-square test to compare the clinicopathological characteristics among different sites of metastases. We used Kaplan-Meier analysis and log-rank testing for survival comparisons.

We employed Cox proportional model to perform multivariate analyses of the patient population; and accordingly hazard ratios with corresponding 95%CI were generated. Statistical significance was considered if a two-tailed P value < 0.05 was achieved. All of the statistical analyses were performed using SPSS Statistics 20.0 (IBM, NY, United States).

RESULTS

Patients' characteristics

A total of 13233 patients with stage Ⅳ pancreatic cancer at the time of initial diagnosis and known sites of distant metastases were identified in the period from 2010-2013 and they were included into the current study. Table 1 summarizes the distribution of different metastatic sites for all included patients. 10088 (76%) patients were diagnosed with liver metastases, 2638 (19.9%) patients were diagnosed with lung metastases, and 910 (6.8%) patients were diagnosed with bone metastases, 90 (0.6%) patients were diagnosed with brain metastases, 1246 (9.4%) patients were diagnosed with distant (non regional) lymph nodes. 8786 (66.3%) patients have a single organ site of metastases while 4447 patients (33.7%) patients have multi-organ metastases. Statistically significant correlations between different baseline characteristics and different sites of metastases are shown in Table 1.

Surgical resection of the primary tumor was performed in 225 (1.7%) patients while surgical resection of the metastatic lesions was performed in 572 (4.3%). No information was provided in the SEER database about systemic treatment.

Survival outcomes

Overall and pancreatic cancer-specific survival were compared according to the site of metastases; for both endpoints, patients with isolated distant lymph node involvement or lung metastases have better outcomes compared to patients with isolated liver metastases (for overall survival: lung *vs* liver metastases: P < 0.0001; distant nodal *vs* liver metastases: P < 0.0001; lung *vs* bone metastases: P = 0.051; distant nodal *vs* bone metastases: P = 0.001) (for pancreatic cancer-specific survival: lung *vs* liver metastases: P < 0.0001; distant nodal *vs* liver metastases: P < 0.0001; lung *vs* bone metastases: P = 0.076; distant nodal *vs* bone metastases: P = 0.015) (Figure 1A and B).

Table 1 Clinical features and metastatic sites *n* (%)

Features	Bone metastases		*P* value	Liver metastases		*P* value	Lung metastases		*P* value	Distant lymph nodes		*P* value	Brain metastases		*P* value
	Yes	No		Yes	No		Yes	No		Yes	No		Yes	No	
Age (yr)			0.002			< 0.0001			0.008			< 0.0001			0.636
< 65	396 (7.7)	4724 (92.3)		3996 (78.0)	1124 (22.0)		961 (18.8)	4159 (81.2)		569 (11.1)	4551 (88.9)		37 (0.7)	5083 (99.3)	
⩾ 65	514 (6.3)	7599 (93.7)		6092 (75.1)	2021 (24.9)		1677 (20.7)	6463 (79.3)		677 (8.3)	7436 (91.7)		53 (0.7)	8060 (99.3)	
Race			0.076			0.001			0.312			0.059			0.314
White	727 (9.6)	9734 (93.1)		7974 (76.2)	2487 (23.8)		2106 (20.1)	8355 (79.9)		1005 (9.6)	9456 (90.4)		71 (0.7)	10390 (99.3)	
Black	105 (5.9)	1661 (94.1)		1388 (78.6)	378 (21.4)		329 (18.6)	1437 (81.4)		140 (7.9)	1626 (92.1)		16 (0.9)	1750 (99.1)	
Others	928 (93)	78 (7.0)		726 (73.0)	280 (27.0)		203 (19.0)	803 (81.0)		905 (90.0)	101 (10.0)		3 (0.2)	1003 (99.8)	
Gender			0.002			< 0.0001			0.020			0.028			0.770
Male	636 (7.5)	6613 (92.5)		5565 (77.8)	1584 (22.2)		1372 (19.2)	5777 (80.8)		710 (9.9)	6439 (90.1)		50 (0.7)	7099 (99.3)	
Female	374 (6.1)	5710 (93.9)		4523 (74.3)	1561 (25.7)		1266 (20.8)	4818 (79.2)		536 (8.8)	5548 (91.2)		40 (0.7)	6044 (99.3)	
Location of the primary			0.001			0.084			< 0.0001			0.003			0.024
Head	269 (5.8)	4387 (94.2)		3580 (76.9)	1076 (23.1)		828 (17.2)	3828 (82.2)		480 (10.3)	4176 (89.7)		21 (0.5)	4635 (99.5)	
Body/tail	340 (7.2)	4408 (92.8)		3638 (76.6)	1110 (23.4)		961 (20.2)	3787 (79.8)		394 (8.3)	4354 (91.7)		33 (0.7)	4715 (99.3)	
Unknown	301 (7.9)	3528 (92.1)		2870 (75.0)	959 (25.0)		849 (22.2)	2980 (77.8)		372 (9.7)	3457 (90.3)		36 (0.9)	3793 (99.1)	
Marital status			0.083			0.895			0.083			0.014			0.189
Married	512 (7.1)	6720 (92.9)		5510 (76.2)	1722 (23.8)		1402 (19.4)	5830 (80.6)		722 (10.0)	6510 (90.0)		43 (0.6)	7189 (99.4)	
Unmarried	398 (6.6)	5603 (93.4)		4578 (76.3)	1423 (23.7)		1236 (20.6)	4765 (79.4)		524 (8.7)	5477 (91.3)		47 (0.8)	5954 (99.2)	
T stage			< 0.0001			< 0.0001			0.003			< 0.0001			< 0.0001
T1	29 (8.9)	296 (91.1)		242 (74.5)	83 (25.5)		59 (18.2)	266 (81.8)		23 (7.1)	302 (92.9)		3 (0.9)	322 (99.1)	
T2	209 (6.7)	3079 (93.6)		2705 (82.3)	583 (17.7)		595 (18.1)	2693 (81.9)		277 (8.4)	3011 (91.6)		17 (0.5)	3271 (99.5)	
T3	200 (5.5)	3460 (94.5)		2699 (73.7)	961 (26.3)		711 (19.4)	2949 (80.6)		345 (9.4)	3315 (90.6)		11 (0.3)	3649 (99.7)	
T4	153 (6.8)	2106 (93.2)		1611 (71.3)	648 (28.7)		504 (22.3)	1755 (77.7)		278 (12.3)	1981 (87.7)		13 (0.6)	2246 (99.4)	
Tx	319 (9.0)	3382 (91.0)		2831 (76.0)	870 (24.0)		769 (20.5)	2932 (79.5)		323 (10.0)	3378 (90.0)		46 (1.2)	3655 (98.8)	
N stage			< 0.0001			0.788			< 0.0001			< 0.0001			0.089
N0	395 (5.8)	6424 (94.2)		5210 (76.4)	1609 (23.6)		1143 (16.8)	5676 (83.2)		310 (4.5)	6509 (95.5)		36 (0.5)	6783 (99.5)	
N1	354 (8.7)	3729 (91.3)		3097 (75.9)	986 (24.1)		1018 (24.9)	3065 (75.1)		811 (19.9)	3272 (80.1)		34 (0.8)	4049 (99.2)	
Nx	161 (6.9)	2170 (93.1)		1781 (76.4)	550 (23.6)		477 (20.5)	1854 (79.5)		125 (5.4)	2206 (94.5)		20 (0.9)	2311 (99.1)	
Surgery of the primary			0.035			< 0.0001			0.006			0.265			0.422
Yes	7 (3.1)	218 (96.9)		112 (49.8)	113 (50.2)		26 (11.6)	199 (88.4)		15 (6.7)	210 (93.3)		0 (0)	225 (100.0)	
No	903 (7.0)	12105 (93.0)		9976 (76.7)	3033 (23.3)		2612 (20.1)	10369 (79.9)		1231 (9.5)	11777 (90.5)		90 (0.7)	12918 (99.3)	
Surgery of the metastases			0.808			< 0.0001			0.002			< 0.0001			0.503
Yes	38 (6.6)	534 (93.4)		288 (50.3)	284 (49.7)		81 (14.2)	491 (85.8)		91 (15.9)	481 (84.1)		6 (1.0)	566 (99.0)	
No	872 (6.7)	11789 (93.3)		9800 (77.4)	2861 (22.6)		2557 (20.2)	10104 (79.8)		1155 (9.1)	11506 (90.9)		84 (0.7)	12577 (99.3)	

Moreover, patients with isolated distant lymph node involvement but not those with lung metastases have better outcomes compared to patients with isolated bone metastases (for overall survival: lung *vs* bone metastases: $P = 0.051$; distant nodal *vs* bone metastases: $P = 0.001$) (for pancreatic cancer-specific survival: lung *vs* bone metastases: $P = 0.076$; distant nodal *vs* bone metastases: $P = 0.015$) (Figure 1A and B). Because of the very small number of patients with brain metastases (90 patients), they were not included in this analysis.

Overall survival was assessed according to whether or not surgery to the primary tumor was performed in patients with isolated liver, lung and distant nodal metastases. There was evidence of benefit for patients with isolated liver or distant nodal metastases but not for patients with isolated lung metastases (Figure 2A-C).

Overall survival was also evaluated according to whether or not surgery to the metastatic disease was performed in patients with isolated liver, lung or distant nodal

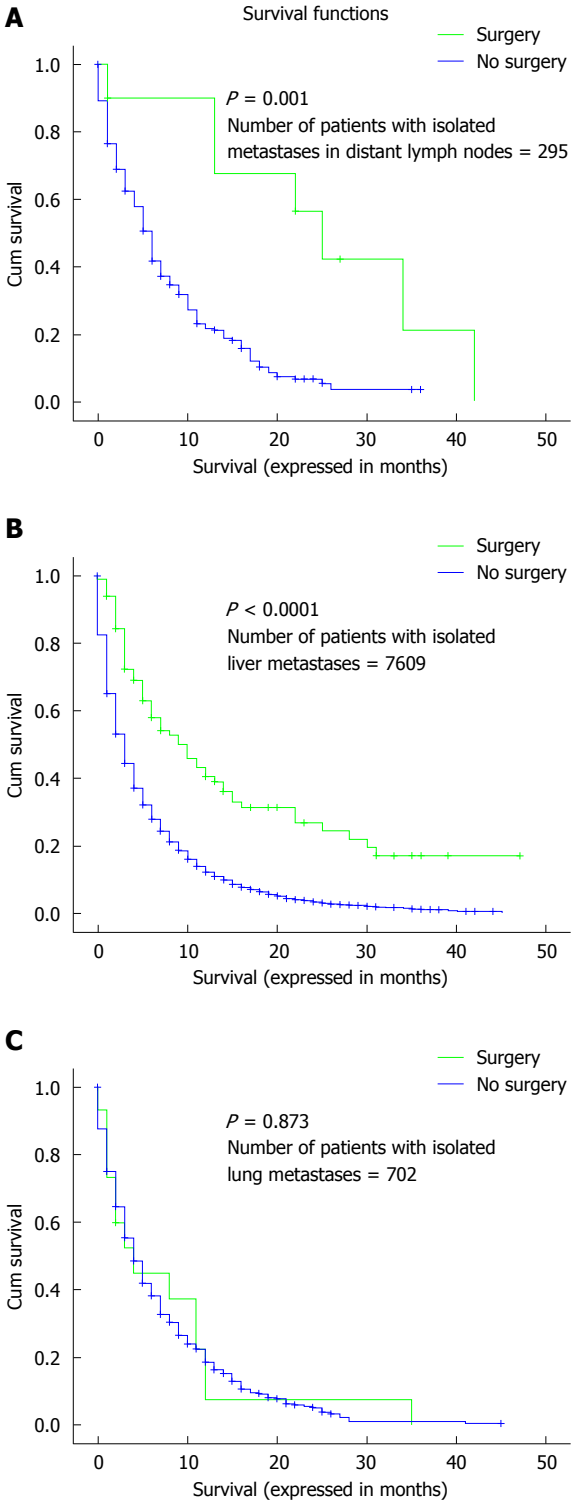

Figure 2 Kaplan-Meier curve of overall survival according to whether or not surgery to the primary has been done: (A) patients with isolated distant nodal deposits; (B) patients with isolated liver metastases; (C) patients with isolated lung metastases.

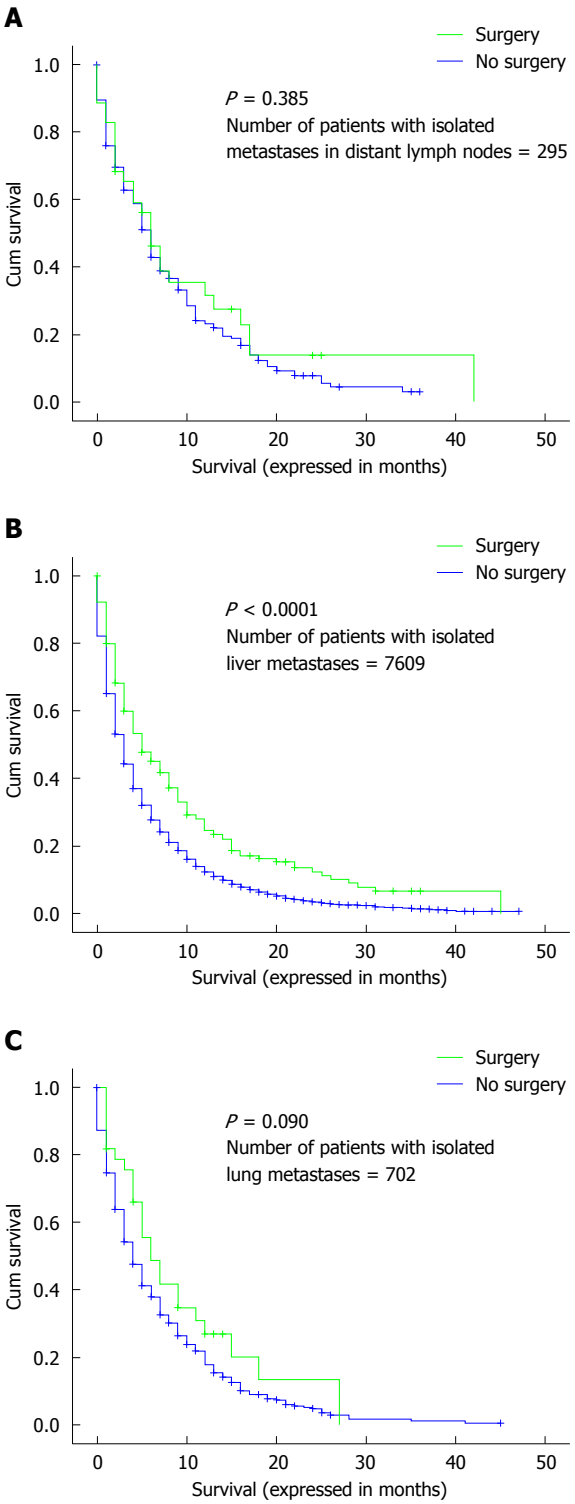

Figure 3 Kaplan-Meier curve of overall survival according to whether or not surgery to the metastatic disease has been done: (A) patients with isolated distant nodal deposits; (B) patients with isolated liver metastases; (C) patients with isolated lung metastases.

metastases. There was evidence of benefit for patients with isolated liver metastases but not for patients with isolated lung or distant nodal metastases (Figure 3A-C).

Multivariate analysis revealed that age < 65 years, white race, being married, female gender; surgery to the primary tumor and surgery to the metastatic disease were associated with better overall survival and pancreatic cancer-specific survival (Table 2).

Table 2 Multivariate analyses of overall survival and pancreatic cancer-specific survival in metastatic pancreatic cancer patients

Features	Overall survival		Pancreatic cancer-specific survival	
	Hazard ratio(95%CI)	*P* value	Hazard ratio (95%CI)	*P* value
Age (yr)				
< 65	1.00 (reference)		1.00 (reference)	
> 65	1.343 (1.292-1.396)	< 0.0001	1.131 (1.083-1.181)	< 0.0001
Race				
Black	1.00 (reference)		1.00 (reference)	
White	0.913 (0.865-0.965)	0.001	0.924 (0.869-0.983)	0.013
Others	0.891 (0.818-0.971)	0.009	0.956 (0.870-1.052)	0.360
Gender				
Female	1.00 (reference)		1.00 (reference)	
Male	1.117 (1.075-1.160)	< 0.0001	1.087 (1.042-1.135)	< 0.0001
Marital status				
Married	1.00 (reference)		1.00 (reference)	
Unmarried	1.243 (1.196-1.291)	< 0.0001	1.222 (1.170-1.276)	< 0.0001
T stage				
T1	1.00 (reference)		1.00 (reference)	
T2	1.151 (1.015-1.304)	0.028	1.170 (1.015-1.349)	0.030
T3	1.014 (0.895-1.149)	0.826	1.033 (0.896-1.191)	0.652
T4	0.974 (0.857-1.107)	0.688	0.986 (0.853-1.141)	0.851
N stage				
N0	1.00 (reference)		1.00 (reference)	
N1	1.004 (0.962-1.049)	0.841	1.001 (0.954-1.051)	0.958
Surgery of the primary				
No	1.00 (reference)		1.00 (reference)	
Yes	0.573 (0.489-0.671)	< 0.0001	0.537 (0.448-0.643)	< 0.0001
Surgery of the metastases				
No	1.00 (reference)		1.00 (reference)	
Yes	0.773 (0.703-0.851)	< 0.0001	0.782 (0.703-0.871)	< 0.0001
Distant metastases				
Multiple metastases	1.00 (reference)		1.00 (reference)	
Single metastasis	1.080 (0.900-1.297)	0.409	1.049 (0.867-1.270)	0.619

DISCUSSION

The main findings of this study are: (1) patients with distant nodal and lung metastases from pancreatic adenocarcinoma have a statistically significant better prognosis than patients with liver metastases; and (2) surgical resection could play a role in the management of a highly selected subset of patients with pancreatic adenocarcinoma and isolated resectable liver or distant nodal metastases.

Knowledge of the prognostic consequences of having one site of metastases rather than the other may help in the informed discussion with the patients about the overall outlook of their disease; moreover, this could help tailor systemic therapy strategies for this disease.

Despite the differences in our analysis between patients affected with different isolated sites of metastases, there was no difference in general between patients affected with single site versus multiple sites of metastases. This is in contrast to lung cancer where prognostic differences have been found according to this parameter[12,13].

The current analysis showed that married patients have better overall and pancreatic cancer specific survival compared to unmarried patients. This is in line with previous SEER analyses for pancreatic cancer patients[14] as well as for many other solid tumors[15,16]. Moreover, the current analysis showed an evidence for age and racial differences in survival outcomes. This confirms the findings from previous SEER analyses[17-19] and the racial differences may be explained by disparities in the access to care; while the impact of age may be explained by differences in baseline co morbid conditions. Our analysis showed also that male patients have poorer survival outcomes compared to female patients. This may be explained by unreported differences in co-morbid conditions.

Value of local treatment of the primary in cases of a metastatic solid tumor has been shown for metastatic renal cell carcinoma[20], metastatic non-functioning pancreatic neuroendocrine tumors[21,22] and hepatocellular carcinoma[23]. Similar strategy is currently being explored in a number of ongoing studies for patients with metastatic breast cancer[24,25].

For pancreatic adenocarcinoma, there is no evidence-based consensus about whether and when to use surgery in the setting of metastatic disease. While older retrospective studies suggested no benefit from surgical resection to the primary tumor and synchronous liver metastases[26,27], more recent retrospective studies suggested that primary tumor resection following favorable response to systemic chemotherapy in stage Ⅳ patients may be considered in highly selected patients[28,29]. However, the number of patients in all these studies was not large enough to

derive clear recommendations. Moreover, these studies still carry the methodological defects of a retrospective analysis.

The presence of liver metastases was shown in our analysis as a poor prognostic factor compared to lung or distant nodal metastases. This result is in line with the post-hoc analysis of the MPACT phase Ⅲ study as well as another retrospective study[30,31]. However, our analysis differs in being on a much larger sample size which may give a more representative picture of the routine daily practice.

The results of this analysis have to be interpreted with caution given the inherent difficulties in conducting retrospective studies in general and SEER analyses in particular; most notably the lack of information about the co-morbidities in evaluated patients as well as the absence of systemic therapy information. Patients who are offered surgical resection are more likely to have better general health and less co- morbidities; thus, potential selection bias could not be totally excluded. Moreover, an important site of metastasis from pancreatic cancer-that is peritoneal deposits- is not detailed in the SEER database which may confound further the conclusions from this analysis.

Prospective controlled studies are thus needed in order to evaluate the best way to integrate local and systemic therapies in the management of pancreatic cancer patients with good general condition and limited resectable extrapancreatic disease. This is especially important given the plethora of newer systemic therapy agents approved or evaluated in the management of this disease.

The current analysis evaluated surgical options for metastatic patients; however, other local therapies (which are not detailed in the SEER database) should also be evaluated within clinical trials in these patients including interventional radiology ablative techniques (*e.g.,* radiofrequency or microwave ablation) as well as stereotactic body radiotherapy.

The biological behavior of pancreatic cancer patients presenting with a first site of metastasis other than the liver needs to be interpreted in light of our recent understanding of the different molecular subtypes of pancreatic cancer[32]. Those patients may have a peculiar molecular phenotype and thus may benefit from a different course of systemic therapy.

In conclusion, based on the SEER analysis, pancreatic adenocarcinoma patients with isolated liver metastases have worse outcomes compared to patients with isolated lung or distant nodal metastases. Further research is needed to identify the highly selected subset of patients who may benefit from local treatment of the primary tumor and/or metastatic disease.

COMMENTS

Background

Population-based data on the prognostic value of site-specific metastases for pancreatic adenocarcinoma are scarce. The authors sought to evaluate this parameter in patients registered within the Surveillance Epidemiology and End Results database (SEER) database.

Research frontiers

SEER database (2010-2013) has been queried through SEER*Stat program to determine the presentation, treatment outcomes and prognostic outcomes of metastatic pancreatic adenocarcinoma according to the site of metastasis.

Innovations and breakthroughs

Patients with isolated distant nodal involvement or lung metastases have better overall and pancreatic cancer-specific survival compared to patients with isolated liver metastases (for overall survival: lung *vs* liver metastases: $P < 0.0001$; distant nodal *vs* liver metastases: $P < 0.0001$) (for pancreatic cancer-specific survival: lung *vs* liver metastases: $P < 0.0001$; distant nodal *vs* liver metastases: $P < 0.0001$).

Applications

Pancreatic adenocarcinoma patients with isolated liver metastases have worse outcomes compared to patients with isolated lung or distant nodal metastases.

Peer-review

This is a straightforward manuscript in which, based on the SEER analysis, the authors have shown that pancreatic adenocarcinoma patients with isolated liver metastases have worse outcomes compared to patients with isolated lung or distal nodal metastases. The paper reports a potentially interesting, practically important and original data. The authors provided sufficient methodological detail. Statistical analysis is well done. The claims are appropriately discussed. Overall, the paper is clear and well written.

REFERENCES

1 **Ma J**, Jemal A. The rise and fall of cancer mortality in the USA: why does pancreatic cancer not follow the trend? *Future Oncol* 2013; **9**: 917-919 [PMID: 23837751 DOI: 10.2217/fon.13.76]

2 **Simard EP**, Ward EM, Siegel R, Jemal A. Cancers with increasing incidence trends in the United States: 1999 through 2008. *CA Cancer J Clin* 2012; **62**: 118-128 [PMID: 22281605 DOI: 10.3322/caac.20141]

3 **Steen W**, Blom R, Busch O, Gerhards M, Besselink M, Dijk F, Festen S. Prognostic value of occult tumor cells obtained by peritoneal lavage in patients with resectable pancreatic cancer and no ascites: A systematic review. *J Surg Oncol* 2016; **114**: 743-751 [PMID: 27642007 DOI: 10.1002/jso.24402]

4 **Chen Y**, Che X, Zhang J, Huang H, Zhao D, Tian Y, Li Y, Feng Q, Zhang Z, Jiang Q, Zhang S, Tang X, Huang X, Chu Y, Zhang J, Sun Y, Zhang Y, Wang C. Long-term results of intraoperative electron beam radiation therapy for nonmetastatic locally advanced pancreatic cancer: Retrospective cohort study, 7-year experience with 247 patients at the National Cancer Center in China. *Medicine* (Baltimore) 2016; **95**: e4861 [PMID: 27661028 DOI: 10.1097/md.0000000000004861]

5 **Varghese AM**, Lowery MA, Yu KH, O'Reilly EM. Current management and future directions in metastatic pancreatic adenocarcinoma. *Cancer* 2016; **122**: 3765-3775 [PMID: 27649047 DOI: 10.1002/cncr.30342]

6 **Sirri E**, Castro FA, Kieschke J, Jansen L, Emrich K, Gondos A, Holleczek B, Katalinic A, Urbschat I, Vohmann C, Brenner H. Recent Trends in Survival of Patients With Pancreatic Cancer in Germany and the United States. *Pancreas* 2016; **45**: 908-914 [PMID: 26745860 DOI: 10.1097/mpa.0000000000000588]

7 **Worni M**, Guller U, White RR, Castleberry AW, Pietrobon R, Cerny T, Gloor B, Koeberle D. Modest improvement in overall survival for patients with metastatic pancreatic cancer: a trend analysis using the surveillance, epidemiology, and end results registry from 1988 to 2008. *Pancreas* 2013; **42**: 1157-1163 [PMID: 23867367 DOI: 10.1097/MPA.0b013e318291fbc5]

8 **Deeb A**, Haque SU, Olowokure O. Pulmonary metastases in

pancreatic cancer, is there a survival influence? *J Gastrointest Oncol* 2015; **6**: E48-E51 [PMID: 26029466 DOI: 10.3978/j.issn.2078-6891.2014.114]

9 **Lemke J**, Scheele J, Kapapa T, Wirtz CR, Henne-Bruns D, Kornmann M. Brain metastasis in pancreatic cancer. *Int J Mol Sci* 2013; **14**: 4163-4173 [PMID: 23429199 DOI: 10.3390/ijms14024163]

10 **Kumar A**, Dagar M, Herman J, Iacobuzio-Donahue C, Laheru D. CNS involvement in pancreatic adenocarcinoma: a report of eight cases from the Johns Hopkins Hospital and review of literature. *J Gastrointest Cancer* 2015; **46**: 5-8 [PMID: 25451139 DOI: 10.1007/s12029-014-9667-y]

11 **Surveillance, Epidemiology and End Results Program**. About the SEER Program. Accessed June 25, 2016. Available from: URL: http://seer.cancer.gov/about

12 **Ren Y**, Dai C, Zheng H, Zhou F, She Y, Jiang G, Fei K, Yang P, Xie D, Chen C. Prognostic effect of liver metastasis in lung cancer patients with distant metastasis. *Oncotarget* 2016; **7**: 53245-53253 [PMID: 27449299 DOI: 10.18632/oncotarget.10644]

13 **Riihimäki M**, Hemminki A, Fallah M, Thomsen H, Sundquist K, Sundquist J, Hemminki K. Metastatic sites and survival in lung cancer. *Lung Cancer* 2014; **86**: 78-84 [PMID: 25130083 DOI: 10.1016/j.lungcan.2014.07.020]

14 **Wang XD**, Qian JJ, Bai DS, Li ZN, Jiang GQ, Yao J. Marital status independently predicts pancreatic cancer survival in patients treated with surgical resection: an analysis of the SEER database. *Oncotarget* 2016; **7**: 24880-24887 [PMID: 27036036 DOI: 10.18632/oncotarget.8467]

15 **He XK**, Lin ZH, Qian Y, Xia D, Jin P, Sun LM. Marital status and survival in patients with primary liver cancer. *Oncotarget* 2016; Epub ahead of print [PMID: 27527862 DOI: 10.18632/oncotarget.11066]

16 **Jin JJ**, Wang W, Dai FX, Long ZW, Cai H, Liu XW, Zhou Y, Huang H, Wang YN. Marital status and survival in patients with gastric cancer. *Cancer Med* 2016; **5**: 1821-1829 [PMID: 27264020 DOI: 10.1002/cam4.758]

17 **Cheung R**. Racial and social economic factors impact on the cause specific survival of pancreatic cancer: a SEER survey. *Asian Pac J Cancer Prev* 2013; **14**: 159-163 [PMID: 23534717]

18 **Amin S**, Lucas AL, Frucht H. Evidence for treatment and survival disparities by age in pancreatic adenocarcinoma: a population-based analysis. *Pancreas* 2013; **42**: 249-253 [PMID: 22836862 DOI: 10.1097/MPA.0b013e31825f3af4]

19 **Murphy MM**, Simons JP, Ng SC, McDade TP, Smith JK, Shah SA, Zhou Z, Earle CC, Tseng JF. Racial differences in cancer specialist consultation, treatment, and outcomes for locoregional pancreatic adenocarcinoma. *Ann Surg Oncol* 2009; **16**: 2968-2977 [PMID: 19669839 DOI: 10.1245/s10434-009-0656-5]

20 **Heng DY**, Wells JC, Rini BI, Beuselinck B, Lee JL, Knox JJ, Bjarnason GA, Pal SK, Kollmannsberger CK, Yuasa T, Srinivas S, Donskov F, Bamias A, Wood LA, Ernst DS, Agarwal N, Vaishampayan UN, Rha SY, Kim JJ, Choueiri TK. Cytoreductive nephrectomy in patients with synchronous metastases from renal cell carcinoma: results from the International Metastatic Renal Cell Carcinoma Database Consortium. *Eur Urol* 2014; **66**: 704-710 [PMID: 24931622 DOI: 10.1016/j.eururo.2014.05.034]

21 **Keutgen XM**, Nilubol N, Glanville J, Sadowski SM, Liewehr DJ, Venzon DJ, Steinberg SM, Kebebew E. Resection of primary tumor site is associated with prolonged survival in metastatic nonfunctioning pancreatic neuroendocrine tumors. *Surgery* 2016; **159**: 311-318 [PMID: 26453135 DOI: 10.1016/j.surg.2015.05.042]

22 **Hüttner FJ**, Schneider L, Tarantino I, Warschkow R, Schmied BM, Hackert T, Diener MK, Büchler MW, Ulrich A. Palliative resection of the primary tumor in 442 metastasized neuroendocrine tumors of the pancreas: a population-based, propensity score-matched survival analysis. *Langenbecks Arch Surg* 2015; **400**: 715-723 [PMID: 26198970 DOI: 10.1007/s00423-015-1323-x]

23 **Abdel-Rahman O**. Role of liver-directed local tumor therapy in the management of hepatocellular carcinoma with extrahepatic metastases: a SEER database analysis. *Expert Rev Gastroenterol Hepatol* 2017; **11**: 183-189 [PMID: 27830958 DOI: 10.1080/17474124.2017.1259563]

24 **Shien T**, Nakamura K, Shibata T, Kinoshita T, Aogi K, Fujisawa T, Masuda N, Inoue K, Fukuda H, Iwata H. A randomized controlled trial comparing primary tumour resection plus systemic therapy with systemic therapy alone in metastatic breast cancer (PRIM-BC): Japan Clinical Oncology Group Study JCOG1017. *Jpn J Clin Oncol* 2012; **42**: 970-973 [PMID: 22833684 DOI: 10.1093/jjco/hys120]

25 **Ruiterkamp J**, Voogd AC, Tjan-Heijnen VC, Bosscha K, van der Linden YM, Rutgers EJ, Boven E, van der Sangen MJ, Ernst MF. SUBMIT: Systemic therapy with or without up front surgery of the primary tumor in breast cancer patients with distant metastases at initial presentation. *BMC Surg* 2012; **12**: 5 [PMID: 22469291 DOI: 10.1186/1471-2482-12-5]

26 **Gleisner AL**, Assumpcao L, Cameron JL, Wolfgang CL, Choti MA, Herman JM, Schulick RD, Pawlik TM. Is resection of periampullary or pancreatic adenocarcinoma with synchronous hepatic metastasis justified? *Cancer* 2007; **110**: 2484-2492 [PMID: 17941009 DOI: 10.1002/cncr.23074]

27 **Dünschede F**, Will L, von Langsdorf C, Möhler M, Galle PR, Otto G, Vahl CF, Junginger T. Treatment of metachronous and simultaneous liver metastases of pancreatic cancer. *Eur Surg Res* 2010; **44**: 209-213 [PMID: 20571276 DOI: 10.1159/000313532]

28 **Wright GP**, Poruk KE, Zenati MS, Steve J, Bahary N, Hogg ME, Zuriekat AH, Wolfgang CL, Zeh HJ, Weiss MJ. Primary Tumor Resection Following Favorable Response to Systemic Chemotherapy in Stage IV Pancreatic Adenocarcinoma with Synchronous Metastases: a Bi-institutional Analysis. *J Gastrointest Surg* 2016; **20**: 1830-1835 [PMID: 27604886 DOI: 10.1007/s11605-016-3256-2]

29 **Crippa S**, Bittoni A, Sebastiani E, Partelli S, Zanon S, Lanese A, Andrikou K, Muffatti F, Balzano G, Reni M, Cascinu S, Falconi M. Is there a role for surgical resection in patients with pancreatic cancer with liver metastases responding to chemotherapy? *Eur J Surg Oncol* 2016; **42**: 1533-1539 [PMID: 27423449 DOI: 10.1016/j.ejso.2016.06.398]

30 **Tabernero J**, Chiorean EG, Infante JR, Hingorani SR, Ganju V, Weekes C, Scheithauer W, Ramanathan RK, Goldstein D, Penenberg DN, Romano A, Ferrara S, Von Hoff DD. Prognostic factors of survival in a randomized phase III trial (MPACT) of weekly nab-paclitaxel plus gemcitabine versus gemcitabine alone in patients with metastatic pancreatic cancer. *Oncologist* 2015; **20**: 143-150 [PMID: 25582141 DOI: 10.1634/theoncologist.2014-0394]

31 **Suenaga M**, Fujii T, Kanda M, Takami H, Okumura N, Inokawa Y, Kobayashi D, Tanaka C, Yamada S, Sugimoto H, Nomoto S, Fujiwara M, Kodera Y. Pattern of first recurrent lesions in pancreatic cancer: hepatic relapse is associated with dismal prognosis and portal vein invasion. *Hepatogastroenterology* 2014; **61**: 1756-1761 [PMID: 25436375]

32 **Bailey P**, Chang DK, Nones K, Johns AL, Patch AM, Gingras MC, Miller DK, Christ AN, Bruxner TJ, Quinn MC, Nourse C, Murtaugh LC, Harliwong I, Idrisoglu S, Manning S, Nourbakhsh E, Wani S, Fink L, Holmes O, Chin V, Anderson MJ, Kazakoff S, Leonard C, Newell F, Waddell N, Wood S, Xu Q, Wilson PJ, Cloonan N, Kassahn KS, Taylor D, Quek K, Robertson A, Pantano L, Mincarelli L, Sanchez LN, Evers L, Wu J, Pinese M, Cowley MJ, Jones MD, Colvin EK, Nagrial AM, Humphrey ES, Chantrill LA, Mawson A, Humphris J, Chou A, Pajic M, Scarlett CJ, Pinho AV, Giry-Laterriere M, Rooman I, Samra JS, Kench JG, Lovell JA, Merrett ND, Toon CW, Epari K, Nguyen NQ, Barbour A, Zeps N, Moran-Jones K, Jamieson NB, Graham JS, Duthie F, Oien K, Hair J, Grützmann R, Maitra A, Iacobuzio-Donahue CA, Wolfgang CL, Morgan RA, Lawlor RT, Corbo V, Bassi C, Rusev B, Capelli P, Salvia R, Tortora G, Mukhopadhyay D, Petersen GM, Munzy DM, Fisher WE, Karim SA, Eshleman JR, Hruban

RH, Pilarsky C, Morton JP, Sansom OJ, Scarpa A, Musgrove EA, Bailey UM, Hofmann O, Sutherland RL, Wheeler DA, Gill AJ, Gibbs RA, Pearson JV, Waddell N, Biankin AV, Grimmond SM. Genomic analyses identify molecular subtypes of pancreatic cancer. *Nature* 2016; **531**: 47-52 [PMID: 26909576 DOI: 10.1038/nature16965]

P- Reviewer: Seicean A, Swierczynski JT, Yang F
S- Editor: Gong ZM **L- Editor**: A **E- Editor**: Wang CH

World Journal of Gastroenterology

Submit a Manuscript: http://www.wjgnet.com/esps/

World J Gastroenterol 2017 March 14; 23(10): 1881-1890

DOI: 10.3748/wjg.v23.i10.1881

ISSN 1007-9327 (print) ISSN 2219-2840 (online)

ORIGINAL ARTICLE

Observational Study

Role of illness perception and self-efficacy in lifestyle modification among non-alcoholic fatty liver disease patients

Shira Zelber-Sagi, Shiran Bord, Gali Dror-Lavi, Matthew Lee Smith, Samuel D Towne Jr, Assaf Buch, Muriel Webb, Hanny Yeshua, Assy Nimer, Oren Shibolet

Shira Zelber-Sagi, Assaf Buch, Muriel Webb, Hanny Yeshua, Oren Shibolet, Liver Unit, Department of Gastroenterology, Tel-Aviv Medical Center, Tel-Aviv 6423906, Israel

Shira Zelber-Sagi, Shiran Bord, Gali Dror-Lavi, School of Public Health, University of Haifa, Haifa 3498838, Israel

Matthew Lee Smith, Institute of Gerontology, College of Public Health, The University of Georgia, Athens, GA 30602, United States

Matthew Lee Smith, Samuel D Towne Jr, Texas A&M University, School of Public Health, College Station, TX 77843, United States

Assaf Buch, Muriel Webb, Hanny Yeshua, Oren Shibolet, The Sackler Faculty of Medicine, Tel-Aviv University, Tel-Aviv 6423906, Israel

Hanny Yeshua, Family Medicine Department, Tel-Aviv and Dan Petach-Tikva, Clalit Health Services, Rabin Medical Center, Tel-Aviv 49100, Israel

Assy Nimer, Internal medicine A Galler medical Center, Bar-Ilan University, Ramat-Gan 5290002, Israel

Author contributions: Zelber-Sagi S and Bord S contributed equally to this study; Zelber-Sagi S conceived the study; Zelber-Sagi S, Bord S and Dror-Lavi G designed the study; Zelber-Sagi S, Dror-Lavi G, Buch A, Webb M and Yeshua H performed the data collection; Shibolet O conducted on data collection; Zelber-Sagi S, Bord S, Smith ML and Towne SD Jr wrote the manuscript; Nimer A and Shibolet O critically reviewed the manuscript.

Institutional review board statement: The study was approved by the institutional review board of Tel Aviv medical center.

Informed consent statement: All participants signed an informed consent.

Conflict-of-interest statement: We declare that in this manuscript there was no Conflict of interest and no financial support.

Data sharing statement: Technical appendix, statistical code, and dataset available from the corresponding author at zelbersagi@bezeqint.net.

Manuscript source: Unsolicited manuscript

Correspondence to: Dr. Shira Zelber-Sagi, RD, PhD, Liver Unit, Department of Gastroenterology, Tel-Aviv Medical Center, Tel-Aviv 6423906, Israe. zelbersagi@bezeqint.net
Telephone: +972-3-6973984
Fax: +972-3-6966286

Received: December 3, 2016
Peer-review started: December 6, 2016
First decision: December 28, 2016
Revised: January 9, 2017
Accepted: February 6, 2017
Article in press: February 8, 2017
Published online: March 14, 2017

Abstract

AIM

To describe the relationships between non-alcoholic fatty-liver disease (NAFLD) patient's disease consequences and treatment perceptions, self-efficacy, and healthy lifestyle maintenance.

METHODS

A cross-sectional study among 146 ultrasound diagnosed

NAFLD patients who visited the fatty liver clinic at the Tel-Aviv Medical Center. Eighty-seven of these individuals, participated in a clinical trial of physical activity and underwent fasting blood tests, analyzed at the same lab. Exclusion criteria included positivity for serum HBsAg or anti-HCV antibodies; fatty liver suspected to be secondary to hepatotoxic drugs; excessive alcohol consumption ($\geqslant$ 30 g/d in men or $\geqslant$ 20 g/d in women) and positive markers of genetic or immune-mediated liver diseases. Patients were asked to complete a self-report structured questionnaire, assembled by the Israeli Center for Disease Control. Nutrition habits were measured using six yes/no questions (0 = no, 1 = yes) adopted from the national survey questionnaire. Participants in the clinical trial completed a detailed semi-quantitative food frequency questionnaire (FFQ) reporting their habitual nutritional intake during the past year. Self-efficacy was assessed by the Self-Efficacy Scale questionnaire, emotional representation, degree of illness understanding, timeline perception, treatment perception and symptoms were measured by the Brief Illness Perception questionnaire. Illness consequences were measured by the Personal Models of Diabetes Interview questionnaire. A path analysis was performed to describe the interrelationships between the patients' illness perceptions, and assess the extent to which the data fit a prediction of nutritional habits.

RESULTS

The study sample included 54.1% men, with a mean age of 47.76 ± 11.68 years (range: 20-60) and mean body mass index of 31.56 ± 4.6. The average perceived nutrition habits score was 4.73 ± 1.45 on a scale between 0-6, where 6 represents the healthiest eating habits. Most of the study participants (57.2%) did not feel they fully understood what NAFLD is. Better nutritional habits were positively predicted by the degree of illness understanding (β = 0.26; P = 0.002) and self-efficacy (β = 0.25; P = 0.003). Perceptions of more severe illness consequences were related with higher emotional representation (β = 0.55; P < 0.001), which was related with lower self-efficacy (β = -0.17; P = 0.034). The perception of treatment effectiveness was positively related with self-efficacy (β = 0.32; P < 0.001). In accordance with the correlation between self-efficacy and the perceived nutrition habits score, self-efficacy was also correlated with nutrient intake evaluated by the FFQ; negatively with saturated fat (percent of saturated fat calories from total calories) (r = -0.28, P = 0.010) and positively with fiber (r = 0.22, P = 0.047) and vitamin C intake (r = 0.34, P = 0.002). In a sub analysis of the clinical trial participants, objectively measured compliance to physical activity regimen was positively correlated with the self-efficacy level (r = 0.34, P = 0.046).

CONCLUSION

Self-efficacy and illness understanding are major determinants of lifestyle-modification among NAFLD patients. This information can assist clinicians in improving compliance with lifestyle changes among these patients.

Key words: Non-alcoholic fatty-liver disease; Physical activity; Diet; Illness perception; Self-efficacy

Core tip: Dietary modification is a main route of treatment in non-alcoholic fatty liver disease (NAFLD), however it is difficult to maintain in the long term and better ways for implementation are needed. Higher perceptions of understanding the illness and a higher self-efficacy are positively related to better nutritional habits, and therefore its enhancement should be part of the behavioral treatment. Emphasizing to patients that although NAFLD is a chronic condition, it is effectively treatable by diet, increases their self-efficacy. "Scaring" the patients and leading them to believe that NAFLD has severe consequences may lead to the undesirable outcome of reduced self-efficacy and worse dietary habits.

Zelber-Sagi S, Bord S, Dror-Lavi G, Smith ML, Towne SD Jr, Buch A, Webb M, Yeshua H, Nimer A, Shibolet O. Role of illness perception and self-efficacy in lifestyle modification among non-alcoholic fatty liver disease patients. *World J Gastroenterol* 2017; 23(10): 1881-1890 Available from: URL: http://www.wjgnet.com/1007-9327/full/v23/i10/1881.htm DOI: http://dx.doi.org/10.3748/wjg.v23.i10.1881

INTRODUCTION

Non-alcoholic fatty liver disease (NAFLD) is emerging globally as the most prevalent liver disease. Its prevalence is strongly related to growing obesity rates, adoption of a sedentary lifestyles and the globalization of a Western diet[1]. NAFLD is a leading cause for chronic liver disease, cirrhosis and hepatocellular carcinoma[2], and is an independent risk factor for diabetes and cardiovascular disease[3].

Poor dietary habits represent a main modifiable target for the primary prevention and treatment of NAFLD and the more advanced form of non-alcoholic steatohepatitis (NASH)[4]. Weight reduction is the most established treatment for both NAFLD and NASH[5], but changing dietary composition without reducing caloric intake may offer a more feasible alternative to treat NAFLD patients. Maintaining or striving towards healthier dietary composition is crucial regardless of body fatness, as indicated by several epidemiological studies[6,7] demonstrating that normal weight NAFLD patients are more likely to consume an unhealthy diet compared to controls. Thus, efficient and sustainable lifestyle modification programs are needed for NAFLD patients. However, building and implementing such programs may be difficult without adequate knowledge about disease and treatment perceptions among this patient group. This is particularly important in the

context of an asymptomatic disease such as NAFLD, which has no accepted pharmacological treatment, although under intensive investigation including antihypertensive and antidiabetic medications[4,8]. Our group recently showed that NAFLD patients do not think of themselves as sick and accordingly do not utilize more health services[9]. Not surprisingly, NAFLD patients were found to have limited readiness to lifestyle changes[10].

It is generally accepted that self-efficacy, defined as "beliefs in one's capabilities to organize and execute the courses of action required for producing given attainments", is an important component in health promotion including lifestyle modification[11,12]. Importantly, self-efficacy was demonstrated to be low among NAFLD patients as compared to patients with other liver diseases[13]. However, the factors associated with self-efficacy among NAFLD patients have never been tested. Furthermore, the association between self-efficacy, along with disease and treatment perceptions, and keeping a healthy lifestyle among NAFLD patients has not been studied. Understanding NAFLD patients' cognitive representations of their disease, which may underlie individual differences in illness-related behaviors[14], and the relationship of these representations to diet maintenance may help in developing NAFLD-tailored lifestyle interventions.

The current study aim was to describe, for the first time, the relationships between NAFLD patient's perceptions regarding disease consequences and treatment, self-efficacy, and lifestyle habits maintenance.

MATERIALS AND METHODS

Study population

A cross-sectional survey was conducted among ultrasound diagnosed adult (above the age of 18) NAFLD patients who visited the fatty liver clinic at the Tel Aviv Medical Center during 2011 and 2012. Eighty-seven of these individuals participated in a clinical trial testing the effect of resistance training (RT) *vs* stretching on NAFLD[15]. Exclusion criteria included positivity for serum HBsAg or anti-HCV antibodies; fatty liver suspected to be secondary to hepatotoxic drugs; known diabetes treated by medications other than Metformin; cancer; renal failure; heart disease; non-compensated cirrhosis; inflammatory bowel disease; excessive alcohol consumption ($\geqslant$ 30 g/d in men or $\geqslant$ 20 g/d in women)[2]; positive markers of genetic or immune-mediated liver diseases.

The study conformed to the ethical guidelines of the 1975 Declaration of Helsinki, and was approved by the Tel-Aviv Medical Center ethics committee. All patients signed an informed consent. The clinical trial was pre-registered in the NIH registration website (TRIAL no. NCT01264198).

Data collection

Patients were asked to complete a self-report structured questionnaire. The questionnaire was assembled by the Israeli Center for Disease Control and was used in the first Israeli National Health Survey (MABAT)[16]. Following a 12-h fast, each participant of the clinical trial underwent blood tests, analyzed at the same lab.

Nutrition habits were measured using six yes/no questions (0 = no, 1 = yes) adopted from the national survey questionnaire tailored for the Israeli population[17]. Individuals' nutritional habits score was calculated based on the patient's answers (0-6, where 0 represents poor nutritional habits and 6 represents excellent nutritional habits). Participants in the clinical trial completed a detailed semi-quantitative food frequency questionnaire (FFQ) reporting their habitual nutritional intake during the past year. The FFQ was assembled by the Food and Nutrition Administration, Ministry of Health as previously described[18].

The main independent variables were measured by questions adopted from validated questionnaires as follows (the questions included are specified in Table 1): Self-efficacy was measured by adopting the Self-Efficacy Scale questionnaire[11,19], which was modified for the aims of the current study, referring to both physical activity and healthy dietary habits and keeping a food diary. The questions included "how confident you are that you could do things like these consistently, for at least six months. Ratings were made on a 5-point Likert-type scale ranging from "Sure I could not do it" (1) to "Sure I can do it" (5). The patient's self-efficacy rating was calculated as the mean of 7 questions on a scale from 1 to 5 (α = 0.785, 5 represents high level of self-efficacy).

The questions regarding disease and treatment perceptions were adopted from the brief illness perception questionnaire[20], including: emotional representation (mean of 2 questions number 5, 6), illness understanding degree (a single question number 4), timeline perception (a single statement number 1), treatment perception (a single statement number 2) and symptoms (a single question number 3).

In addition, Illness consequences were measured based on questions adopted from the Personal Models of Diabetes Interview (PMDI) questionnaire[14], which is based on the Health Belief Model (HBM)[21,22] and the Self-Regulation Model of illness (SRM)[22,23] (mean of 4 questions number 7-10, α = 0.722).

All questions were measured using a scale from 1 to 5 (*e.g.*, 5 represents: high level of illness emotional representation, high level of perceived understanding, perceiving NAFLD as a long-term disease, a high level of symptoms experienced severe perceived consequences and high belief in treatment). In addition, the questionnaire included an open-ended question[20], "Please list in rank-order the three most important factors that you believe caused your

Table 1 Description of disease perceptions, illness emotional representation, perceived illness consequences, self-efficacy and reported nutritional habits among non-alcoholic fatty liver disease patients

Variable (n = 146)	Items	% of patients who responded 4 and above (range 1-5)
Disease perceptions		
Time line perception	1. How long do you think your NAFLD will continue?	53.6%
Treatment perception	2. How much do you believe that there is a treatment that can help in reducing or healing NAFLD	72.6%
Symptoms	3. How much do you experience symptoms due to NAFLD?	9.0%
Illness understanding degree	4. How well do you feel that you understand what NAFLD is?	42.8%
Emotional representation	5. How concerned are you about having NAFLD?	60.0%
	6. How much does your illness (NAFLD) affect you emotionally? (*e.g.*, does it make you angry, scared, upset or depressed?)	20.0%
Illness consequences	7. To what extent having a NAFLD affects your everyday life?	13.7%
	8. To what extent do you believe that NAFLD is a severe health problem?	59.6%
	9. To what extent do you believe that NAFLD is a disease?	50.0%
	10. To what extent do you anticipate having medical complications due to NAFLD?	46.6%
Self-efficacy	11. I'm sure that I can make the time and persist in performing physical activity even if I'm very busy at work or at home	63.0%
	12. I'm sure that I can persist keeping low fat diet	71.9%
	13. I'm sure that I can persist in keeping low sugar diet	67.1%
	14. I'm sure that I can persist in keeping low sodium diet	72.6%
	15. I'm sure that I can persist in eating smaller portions during my meals	64.1%
	16. I'm sure that I can avoid buying snacks and candies	61.0%
	17. I'm sure that I can persist in keeping a food diary	51.7%
Nutrition habits[1]	18. I make an effort to reduce the amount of fat in my diet	88.8%
	19. I make an effort to reduce the amount of calories in my diet	67.5%
	20. I make an effort to reduce the amount of sugar and sweats in my diet	83.3%
	21. I make an effort to reduce soft drinks consumption (with sugar not diet)	89.5%
	22. I make an effort to reduce red meat and sausages consumption	65.1%
	23. I make an effort to increase vegetables consumption	79.4%

[1]Percent of respondents that answered YES to each item. NAFLD: Non-alcoholic fatty liver disease.

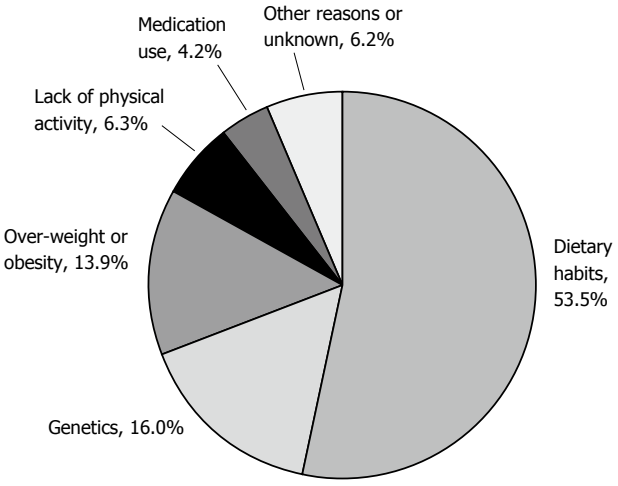

Figure 1 Patients' perceptions regarding the main reasons for non-alcoholic fatty liver disease.

NAFLD". Respondents' answers were categorized into six main reasons (see Figure 1).

Statistical analysis

Statistical analyses were performed using SPSS version 22 (SPSS Inc., Chicago, IL, United States). Continuous variables are presented as mean ± SD. Independent samples *t*-test were performed to test differences in continuous variables between the two groups. The Mann-Whitney test was used if non-parametric tests were required based on data distribution. Pearson's χ^2 tests were performed to examine associations between nominal variables. Pearson or Spearmen correlations were used to test correlations between the diet score, self-efficacy and disease perception.

A path analysis was performed, using AMOS version 22 software (IBM Corp., SPSS, 2013), to describe the interrelationships between the study variables and assess the extent to which the data fit a predicted model associated with nutritional habits. This is a useful methodological and statistical tool to assess the fit between a set of variables and a theory. This method estimates the unidirectional relationship between a set of independent predictors and a set of dependent criteria. A model-modification approach is used to estimate existing relationships and to evaluate and improve them. The final result is a model that, on the one hand, is theoretically based and, on the other, fits the specific set of data.

Model fit was assessed with NFI, NNFI, CFI, and RMSEA. Usually, two statistical criteria are applied: a measure of the model fit (represented by χ^2 and its derivates) and significant estimates of the interrelationship of the model variables (represented by Bs) (Arbuckle, 2013). The most common measures of model fit, χ^2, should be non-significant in order to represent a non-significant departure from the best

Table 2 Description of the study sample (mean ± SD unless otherwise stated)

Variable (units; normal range)	Total (n = 146)
Gender (%; males)	54.1
Nutrition habits (score)	4.73 ± 1.45
BMI (kg/m^2; 20-25)	31.56 ± 4.62
Age (yr)	47.76 ± 11.68
Education (%; high school and above)	66.7
Smoking (%; current smoker)	12.3
Time since diagnosis (%; one year or less)	36.0
HOMA-IR (score)	6.10 ± 2.79
HbA1C (%; 3.9-6)	5.65 ± 0.46
AST (U/L; 5-40)	32.66 ± 14.95
Glucose (mg/dL; 70-110)	85.62 ± 10.63
ALT (U/L; 5-39)	50.16 ± 34.12
GGT (U/L; 6-28)	48.29 ± 50.60
Albumin (g/L; 35-50)	45.05 ± 2.75
Total Cholesterol (mg/dL; 150-200)	187.97 ± 38.08
Ferritin (ng/mL; 7.1-151)	148.77 ± 129.31
Metabolic syndrome (%)	28.7
Lipid-lowering medications (%)	28.8
Antihypertensive medications (%)	20.5

Blood tests were available to 87 subjects.

model possible; the Fit Indexes (NFI - normal fit index, NNFI - non-normal fit index, CFI - comparative fit index) should be close to a value of 1. RMSEA (Root mean standard error of approximation) should be lower than 0.05. Estimates given by the model (β) should be significant[24]. P < 0.05 was considered statistically significant for all analyses.

RESULTS

Description of the study population

The study sample included 146 NAFLD patients, 54.1% men, with a mean age of 47.76 ± 11.68 years (range 19-72), mean body mass index (BMI) of 31.56 ± 4.62, 25 patients (28.7% out of the 87 subjects with blood tests) had the metabolic syndrome according to the accepted criteria[25] and 13 patients (8.9%) had type-2 diabetes, all were treated solely by Metformin. The average nutrition habits score was 4.73 ± 1.45 on a scale between 0-6, where 6 represents the healthiest eating habits. Table 2 describes the study sample characteristics.

Description of disease perceptions, illness emotional representation, perceived illness consequences, self-efficacy and reported nutritional habits among NAFLD patients

Table 1 presents the patients' perceptions regarding different aspects of having NAFLD. Most of the study participants (57.2%) did not feel they fully understood what having a NAFLD really meant. Only a little more than half of the patients (53.6%) perceived NAFLD as a long-term condition. The majority (72.6%) believed there was some form of treatment that could help healing or reducing the severity of NAFLD.

With regard to emotional representation, 60% of the patients reported high levels of concern regarding having a NAFLD, but only 20% reported that having a NAFLD greatly affected them emotionally. In addition, with regard to illness consequences, almost 60% believed that NAFLD is a severe health problem, but only half of the patients believed NAFLD is a disease. Furthermore, only a little more than half of the patients (53.4%) anticipated having medical complications due to NAFLD. Only 13.7% felt that having NAFLD severely affected their everyday life.

The majority of the patients reported relatively high self-efficacy regarding their ability to maintain a healthy diet. For instance, 72.6% of participants reported high levels of self-efficacy to maintain a low sodium diet, 71.9% reported high levels of self-efficacy to maintain a low fat diet, and 67.1% reported high levels of self-efficacy to maintain a low sugar diet. The overall self-efficacy mean rating of the patients was 3.76 ± 0.72 on a scale of 1-5, which indicates medium-high self-efficacy rating.

The majority of the patients reported maintaining healthy eating habits. Most patients reported making efforts to reduce dietary intake of fat (88.8%), calories (67.5%), sugar (83.3%), soft drinks (89.5%), and red meat (65.1%), and to increase intake of vegetables (79.4%).

Perceptions regarding the main reasons for NAFLD among patients

Figure 1 presents the distribution of the perceived main reasons for having NAFLD. Most patients (73.7%) believed that behavioral factors were the most important reasons for NAFLD; approximately 54% reporting dietary habits as the main reason for fatty liver, followed by 13.9% who reported overweight or obesity and 6.3% who reported lack of physical activity. The second most prevalent perceived reason was genetics at 16%. Medication use was cited as the main reason for fatty liver by 4.2% of respondents.

Bivariate correlations between illness perception, emotional representation, self-efficacy and perceived nutritional habits

Table 3 presents bivariate correlations between the study variables. Maintaining healthy nutritional habits was significantly positively correlated with the patients' perceptions regarding their illness consequences (r_s = 0.19; P = 0.035), the degree of understanding their illness (r_s = 0.27; P = 0.003) and their self-efficacy (r_s = 0.20; P = 0.028). Self-efficacy was significantly negatively correlated with timeline perceptions (r_s = -0.27; P = 0.001).

There was a significant, strong positive correlation between the perception of illness consequences and high emotional representation (reflecting the extent by which the patients were afraid or concerned about having NAFLD; r_s = 0.58; $P \leqslant 0.001$), timeline

Table 3 Bivariate correlations between variables of illness perception, emotional representation, self-efficacy and perceived nutritional habits (n = 146)

		1	2	3	4	5	6	7
1	Nutrition habits	-						
2	Illness consequences perception	0.19[a]	-					
3	Emotional representation	-0.05	0.58[b]	-				
4	Self efficacy	0.20[a]	-0.02	-0.09	-			
5	Treatment perception	-0.02	0.06	0.26[b]	0.27[b]	-		
6	Symptoms	0.13	0.45[b]	0.24[b]	-0.14[a]	-0.10	-	
7	Time line perception	0.12	0.21[a]	0.09	-0.27[b]	-0.32[b]	0.19[a]	-
8	Illness understanding degree	0.27[b]	0.38[b]	0.22[b]	0.03	0.00	0.04	0.05
	mean	4.73	3.19	3.03	3.76	3.97	1.80	3.14
	SD	1.45	0.73	1.06	0.72	0.99	1.08	1.14

[a]$P < 0.05$; [b]$P < 0.01$.

perceptions (reflecting the extent by which the patients perceived NAFLD as a long term illness, r_s = 0.21; P = 0.011), symptoms perception (r_s = 0.45; $P \leqslant 0.001$) and perceived Illness understanding degree (r_s = 0.38; $P \leqslant 0.001$).

Path analysis model for the prediction of nutritional habits

A path model was developed to describe the interrelationships between the study variables and assess the extent by which nutritional habits can be predicted by them.

The model was found to fit the data: NFI = 0.870, NNFI = 0.985, CFI = 0.992, RMSEA = 0.018, and $\chi^2(29) = 30.413$, P = 0.394, as shown in Figure 2 and in Supplementary Table.

Better nutritional habits were positively and directly predicted by illness understanding degree (β = 0.26; P = 0.002), self-efficacy (β = 0.25; P = 0.003) and timeline perception (longer-term illness) (β = 0.17; P = 0.036).

Several indirect significant associations were observed. First, male gender was negatively related with illness understanding (β = -0.46; P = 0.014) and self-efficacy (β = -0.24; P = 0.031). Meaning that, women perceived higher illness understanding and higher self-efficacy. Second, BMI was positively related with a perception of more severe illness consequences (β = 0.27; P = 0.002). The latter was related with a higher perception of illness understanding and a perception of a longer term illness, both of which were positively predictive of better nutrition habits. However, perceptions of more severe illness consequences were strongly related with higher emotional representation (β = 0.55; P < 0.001), which in turn was related with lower self-efficacy (β = -0.17; P = 0.034), predicting worse nutritional habits. Third, although the perceptions of a longer term illness were directly related with better nutritional habits, these perceptions were also negatively related with the perception of effective treatment (β = -0.31; P < 0.001). The perception of treatment effectiveness was positively related with self-efficacy (β = 0.32; P < 0.001), which predicts better nutritional habits. Fourth, experiencing many symptoms was related with lower perceptions of illness understanding (β = -0.19; P = 0.026) and may lead indirectly to a higher illness emotional representation. However, only 9% of the sample experienced significant NAFLD-related symptoms.

The accordance between perceived nutritional habits and reported nutritional intake

A sub-sample of the study population (n = 84) completed FFQ. There was a positive correlation between healthy eating habits scores and fiber intake (r = 0.26, P = 0.027), and there was a negative correlation between healthy eating habits scores and saturated fat intake (percent of saturated fat calories from total calories) (r = -0.43, P < 0.001).

The association between self-efficacy and reported nutritional intake and actual compliance with physical activity regimen

In accordance with the correlation between self-efficacy and the perceived diet score, self-efficacy was also correlated with nutrient intake evaluated by the FFQ; negatively with saturated fat (percent of saturated fat calories from total calories) (r = -0.28, P = 0.010) and positively with fiber (r = 0.22, P = 0.047) and vitamin C intake (r = 0.34, P = 0.002).

In a sub analysis of RCT participants who in the intervention arm (resistance training) who had regular training sessions at the gym (n = 34). The number of training sessions at the gym was automatically recorded every time a patient entered the gym with his/her personal chip. Compliance was defined as the number of recorded training sessions divided by the recommended number of sessions (*i.e.*, 3 times a week during the 12-wk trial). This objective compliance measure was positively correlated with the self-efficacy level (r = 0.34, P = 0.046).

DISCUSSION

In the present study, we demonstrated that nutritional habits and lifestyle modification among NAFLD patients may be associated with the patients' perceptions concerning their illness, and with their self-efficacy regarding their ability to change their lifestyle. Our results highlight the impotence and the complexity of achieving NAFLD patient's adherence to healthy nutritional habits. The model suggests ways by which clinicians can improve NAFLD patient's eating habits,

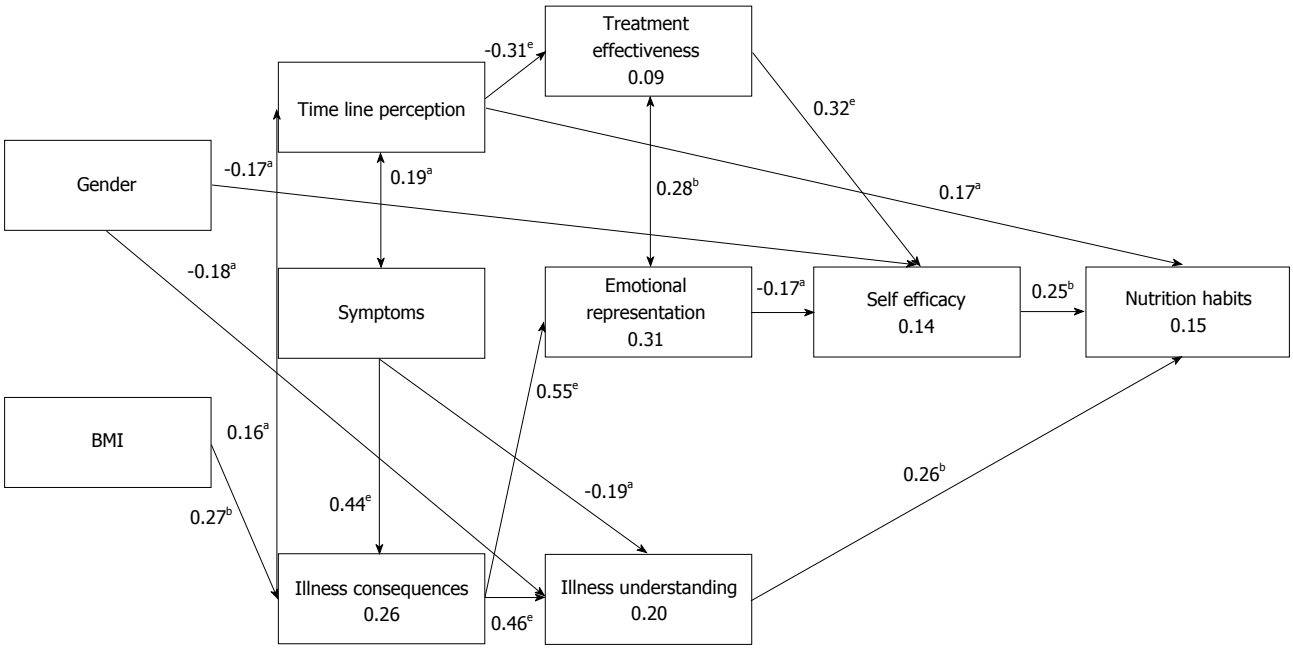

Figure 2 Path model for the study variables predicting nutritional habits. Values attached to the arrows represent regression standardized coefficients (β values), with significance levels in asterisks. Values within the rectangles represent the explained variance by the variable (R^2). NFI = 0.870, NNFI = 0.985, CFI = 0.992, RMSEA = 0.018, $\chi^2(29) = 30.413$, $P = 0.394$. $^aP < 0.05$, $^bP < 0.01$, $^eP < 0.001$ NFI: Normal fit index; NNFI: Non-normal fit index; CFI: Comparative fit index; RMSEA: Root mean standard error of approximation.

or, on the other hand, may unintentionally discourage them from trying. The main conclusions that can be drawn are that higher perceptions of understanding the illness and a higher self-efficacy are positively related to better nutritional habits, and therefore its enhancement should be part of the behavioral treatment. Conversely, "scaring" the patients and leading them to believe that NAFLD has severe consequences may lead to the undesirable outcome of greater disease-related emotional stress, which, in turn, reduces self-efficacy and thus may lead to worse nutritional habits. In addition, although the patients should know that NAFLD is a chronic disease, a perception of a longer-term illness was related with a perception of a less effective treatment and lower self-efficacy. Therefore, it may be important to emphasize to patients that although NAFLD is a chronic condition, it is still treatable and even reversible if diet is maintained[5]. Our results emphasize the importance of explaining patients the effectiveness of dietary treatment in NAFLD, a step that may increase their self-efficacy and compliance.

In support of our results, the Health Belief Model (HBM)[22], indicates that perceived risk, severity, or threat of disease among patients as well as their confidence to make lifestyle changes may be critical to motivate patients into chancing their eating and physical activity habits. The HBM was never tested in the context of improving eating habits among NAFLD patients. However, several studies have tested patients' perceptions according to the HBM among diabetic patients, and the similarity between diabetes and NAFLD may help in the interpretation of the current study results. In a recent study among type-2 diabetes patients, both self-efficacy and perceived medication benefits were significant HBM predictors for medication adherence[26].

The current study results shows that perceptions of more severe illness consequences were related with higher emotional representation, which in turn was related with lower self-efficacy, predicting poor nutritional habits. We believe that this is a very crucial finding for care-givers treating NAFLD patients. Understanding of the emotional aspects of having a NAFLD may be a key element in a successful treatment and a better modification of healthy lifestyle. The impotence of the illness emotional representation and the patients' emotional status among chronic patients is well documented. For instance, higher emotional representation was negatively correlated with well-being among patients with chronic kidney disease[27]. Among type-2 diabetes patients, it was suggested that patients construct their own individual self-management from an emotional base. Therefore, balanced emotional status can contribute to a better self-management[28].

The current study suggests that the mechanism by which emotional representation affect the health outcomes, may be through the patients' self- efficacy. Patients with a better balanced emotional status may be less emotionally distressed, and therefore may have higher self-efficacy related to their ability to make the changes needed in their life. A previous study showed that lower illness-associated emotional representation is associated with a better sense of control among haemodialysis patients[29].

The positive association between perceived understanding of NAFLD and maintaining healthy nutritional habits is another important finding. This may indicate that patients who feel they understand their illness will make more efforts or will have better self-efficacy to maintain healthy eating habits[30-32]. In patients with alcohol-related liver disease, illness understanding made a significant contribution to their self-management confidence[33].

Our study highlights the major role of self-efficacy as a determinant of lifestyle modification maintenance. This is consistent with past research supporting the role of self-efficacy in lifestyle modification[34,35]. Furthermore, we demonstrated a positive association between self-efficacy and actual compliance with a physical activity regimen, as measured by an objective tool of automatically recorded number of training sessions at the gym. This finding further supports the importance of self-efficacy in lifestyle-modification demonstrated in our study as well as in previous study which demonstrated a particularly low self-efficacy to perform physical activity among NAFLD patients[13]. Interestingly, low parental self-efficacy for lifestyle modification was demonstrated among parents to obese children with NAFLD[36]. Indeed, similarly to the treatment of obesity and other metabolic disorders, the promotion of self-efficacy as part of behavioral therapy should be adopted in the treatment of NAFLD as well[12].

This study provides critical information that can be used and disseminated among interventionists, clinicians, and other key stakeholders. This study may also serve as a model to other studies seeking to identify targets for lifestyle interventions among this relatively understudied group.

Our study has several limitations to consider. First, nutritional habits relied on self-report, which may lead to report bias. This bias is most likely non-differential and thus can only weaken the observed associations. To provide construct validity to the eating habits score, we correlated it with another type of nutritional assessment, based on a detailed FFQ, indicating correlations between reported nutritional habits and calculated nutrients consumption, as expected. Furthermore, self-efficacy was positively correlated with the FFQ-estimated fiber and vitamin C intake, which are indicators for fruit and vegetable intake, and negatively with saturated fat.

Second, generalization to other populations needs to be validated, especially given the potential for cultural differences in health beliefs[37]. Lastly, the cross-sectional design of the study prevents the determination of the directions of associations, and is insufficient to determine causality.

In conclusion, complex relationships exist between disease perception, knowledge, emotional stress, self-efficacy and nutritional habits in NAFLD patients. The identification of these relationships may help tailor behavioral interventions delivered by clinicians treating NAFLD patients. Self-efficacy enhancement seems to be a key-factor, along with believing in treatment effectiveness and improving illness understanding. Focusing on these parameters is likely to enhance effective lifestyle interventions achieving long term engagement of NAFLD patients.

COMMENTS

Background

Non-alcoholic fatty liver disease (NAFLD) is emerging globally as the most prevalent liver disease. Poor dietary habits represent a main modifiable target for the primary prevention and treatment of NAFLD. Thus, efficient and sustainable lifestyle modification programs are needed for NAFLD patients. However, building and implementing such programs may be difficult without adequate knowledge about disease and treatment perceptions of NAFLD patients and their association with self-efficacy to execute lifestyle changes.

Research frontiers

The factors associated with self-efficacy among NAFLD patients have never been tested. Furthermore, the association between self-efficacy, along with disease and treatment perceptions, and keeping a healthy lifestyle among NAFLD patients has not been studied.

Innovations and breakthroughs

In the present study, the authors demonstrated that nutritional habits and lifestyle modification among NAFLD patients may be associated with the patients' perceptions concerning their illness, and with their self-efficacy regarding their ability to change their lifestyle. Current results highlight the importance and the complexity of achieving NAFLD patient's adherence to healthy nutritional habits.

Applications

Understanding NAFLD patients' cognitive representations of their disease can help in developing NAFLD-tailored lifestyle interventions. The model suggests ways by which clinicians can improve NAFLD patient's eating habits, or, on the other hand, may unintentionally discourage them from trying. The main conclusions that can be drawn are that higher perceptions of understanding the illness and a higher self-efficacy are positively related to better nutritional habits, and therefore its enhancement should be part of the behavioral treatment. Conversely, "scaring" the patients and leading them to believe that NAFLD has severe consequences may lead to the undesirable outcome of lower self-efficacy. In addition, it may be important to emphasize to patients that although NAFLD is a chronic condition, it is still treatable and even reversible if diet is maintained.

Terminology

Self-efficacy, defined as beliefs in one's capabilities to organize and execute the courses of action required for producing given attainments. The health Belief Model (HBM), indicates that perceived risk, severity, or threat of disease among patients as well as their confidence to make lifestyle changes may be critical to motivate patients into chancing their eating and physical activity habits.

Peer-review

The topic is quite interesting and the paper is very well written, with clear language and discussion consistent with the results obtained. The study by Zelber-Sagi *et al* has investigated the relation between illness perception and dietary modification among 146 patients with NAFLD. The study has shown significant correlations between disease perception and dietary habits among NAFLD patients, suggesting self-efficacy enhancement as an effective tool for improving illness understanding, thus treatment effectiveness. Aim of the study has been clearly stated. Data relevant to the topic have been precisely presented and discussed in detail. Statistical methods have been meticulously

mentioned in the text.

REFERENCES

1 **Loomba R**, Sanyal AJ. The global NAFLD epidemic. *Nat Rev Gastroenterol Hepatol* 2013; **10**: 686-690 [PMID: 24042449 DOI: 10.1038/nrgastro.2013.171]

2 **Chalasani N**, Younossi Z, Lavine JE, Diehl AM, Brunt EM, Cusi K, Charlton M, Sanyal AJ. The diagnosis and management of non-alcoholic fatty liver disease: practice Guideline by the American Association for the Study of Liver Diseases, American College of Gastroenterology, and the American Gastroenterological Association. *Hepatology* 2012; **55**: 2005-2023 [PMID: 22488764 DOI: 10.1002/hep.25762]

3 **Lonardo A**, Sookoian S, Pirola CJ, Targher G. Non-alcoholic fatty liver disease and risk of cardiovascular disease. *Metabolism* 2016; **65**: 1136-1150 [PMID: 26477269 DOI: 10.1016/j.metabol.2015.09.017]

4 **European Association for the Study of the Liver (EASL)**; European Association for the Study of Diabetes (EASD); European Association for the Study of Obesity (EASO). EASL-EASD-EASO Clinical Practice Guidelines for the management of non-alcoholic fatty liver disease. *J Hepatol* 2016; **64**: 1388-1402 [PMID: 27062661 DOI: 10.1016/j.jhep.2015.11.004]

5 **Vilar-Gomez E**, Martinez-Perez Y, Calzadilla-Bertot L, Torres-Gonzalez A, Gra-Oramas B, Gonzalez-Fabian L, Friedman SL, Diago M, Romero-Gomez M. Weight Loss Through Lifestyle Modification Significantly Reduces Features of Nonalcoholic Steatohepatitis. *Gastroenterology* 2015; **149**: 3673-3678.e5; quiz e14-15 [PMID: 25865049 DOI: 10.1053/j.gastro.2015.04.005]

6 **Musso G**, Gambino R, De Michieli F, Cassader M, Rizzetto M, Durazzo M, Fagà E, Silli B, Pagano G. Dietary habits and their relations to insulin resistance and postprandial lipemia in nonalcoholic steatohepatitis. *Hepatology* 2003; **37**: 909-916 [PMID: 12668986 DOI: 10.1053/jhep.2003.50132]

7 **Yasutake K**, Nakamuta M, Shima Y, Ohyama A, Masuda K, Haruta N, Fujino T, Aoyagi Y, Fukuizumi K, Yoshimoto T, Takemoto R, Miyahara T, Harada N, Hayata F, Nakashima M, Enjoji M. Nutritional investigation of non-obese patients with non-alcoholic fatty liver disease: the significance of dietary cholesterol. *Scand J Gastroenterol* 2009; **44**: 471-477 [PMID: 19058085]

8 **Souza-Mello V**, Gregório BM, Cardoso-de-Lemos FS, de Carvalho L, Aguila MB, Mandarim-de-Lacerda CA. Comparative effects of telmisartan, sitagliptin and metformin alone or in combination on obesity, insulin resistance, and liver and pancreas remodelling in C57BL/6 mice fed on a very high-fat diet. *Clin Sci* (Lond) 2010; **119**: 239-250 [PMID: 20415664 DOI: 10.1042/CS20100061]

9 **Mlynarsky L**, Schlesinger D, Lotan R, Webb M, Halpern Z, Santo E, Shibolet O, Zelber-Sagi S. Non-alcoholic fatty liver disease is not associated with a lower health perception. *World J Gastroenterol* 2016; **22**: 4362-4372 [PMID: 27158205 DOI: 10.3748/wjg.v22.i17.4362]

10 **Centis E**, Moscatiello S, Bugianesi E, Bellentani S, Fracanzani AL, Calugi S, Petta S, Dalle Grave R, Marchesini G. Stage of change and motivation to healthier lifestyle in non-alcoholic fatty liver disease. *J Hepatol* 2013; **58**: 771-777 [PMID: 23201248 DOI: 10.1016/j.jhep.2012.11.031]

11 **Kroll T**, Kehn M, Ho PS, Groah S. The SCI Exercise Self-Efficacy Scale (ESES): development and psychometric properties. *Int J Behav Nutr Phys Act* 2007; **4**: 34 [PMID: 17760999 DOI: 10.1186/1479-5868-4-34]

12 **Bellentani S**, Dalle Grave R, Suppini A, Marchesini G. Behavior therapy for nonalcoholic fatty liver disease: The need for a multidisciplinary approach. *Hepatology* 2008; **47**: 746-754 [PMID: 18098321 DOI: 10.1002/hep.22009]

13 **Frith J**, Day CP, Robinson L, Elliott C, Jones DE, Newton JL. Potential strategies to improve uptake of exercise interventions in non-alcoholic fatty liver disease. *J Hepatol* 2010; **52**: 112-116 [PMID: 19897272 DOI: 10.1016/j.jhep.2009.10.010]

14 **Hampson SE**, Glasgow RE, Toobert DJ. Personal models of diabetes and their relations to self-care activities. *Health Psychol* 1990; **9**: 632-646 [PMID: 2226390]

15 **Zelber-Sagi S**, Buch A, Yeshua H, Vaisman N, Webb M, Harari G, Kis O, Fliss-Isakov N, Izkhakov E, Halpern Z, Santo E, Oren R, Shibolet O. Effect of resistance training on non-alcoholic fatty-liver disease a randomized-clinical trial. *World J Gastroenterol* 2014; **20**: 4382-4392 [PMID: 24764677 DOI: 10.3748/wjg.v20.i15.4382]

16 **Kaluski DN**, Goldsmith R, Arie OM, Mayer C, Green M. The first Israeli national health and nutrition survey (MABAT) as a policy maker. *Public Health Rev* 2000; **28**: 23-26 [PMID: 11411274]

17 **Niskar A**, Baron-Epel O, Garty-Sandalon N, Keinan-Boker L. Body weight dissatisfaction among Israeli Jewish and Arab women with normal or overweight-obese body mass index, Israeli INHIS-1, 2003-2004. *Prev Chronic Dis* 2009; **6**: A51 [PMID: 19288994]

18 **Zelber-Sagi S**, Nitzan-Kaluski D, Goldsmith R, Webb M, Blendis L, Halpern Z, Oren R. Long term nutritional intake and the risk for non-alcoholic fatty liver disease (NAFLD): a population based study. *J Hepatol* 2007; **47**: 711-717 [PMID: 17850914]

19 **Hofstetter CR**, Sallis JF, Hovell MF. Some health dimensions of self-efficacy: analysis of theoretical specificity. *Soc Sci Med* 1990; **31**: 1051-1056 [PMID: 2255964]

20 **Broadbent E**, Petrie KJ, Main J, Weinman J. The brief illness perception questionnaire. *J Psychosom Res* 2006; **60**: 631-637 [PMID: 16731240 DOI: 10.1016/j.jpsychores.2005.10.020]

21 **Mirotznik J**, Ginzler E, Zagon G, Baptiste A. Using the health belief model to explain clinic appointment-keeping for the management of a chronic disease condition. *J Community Health* 1998; **23**: 195-210 [PMID: 9615295]

22 **Harvey JN**, Lawson VL. The importance of health belief models in determining self-care behaviour in diabetes. *Diabet Med* 2009; **26**: 5-13 [PMID: 19125754 DOI: 10.1111/j.1464-5491.2008.02628.x]

23 **Heijmans M**, de Ridder D. Assessing illness representations of chronic illness: explorations of their disease-specific nature. *J Behav Med* 1998; **21**: 485-503 [PMID: 9836133]

24 **Bentler PM**. Comparative fit indexes in structural models. *Psychol Bull* 1990; **107**: 238-246 [PMID: 2320703]

25 **National Cholesterol Education Program (NCEP) Expert Panel on Detection, Evaluation, and Treatment of High Blood Cholesterol in Adults (Adult Treatment Panel III)**. Third Report of the National Cholesterol Education Program (NCEP) Expert Panel on Detection, Evaluation, and Treatment of High Blood Cholesterol in Adults (Adult Treatment Panel III) final report. *Circulation* 2002; **106**: 3143-3421 [PMID: 12485966]

26 **Alatawi YM**, Kavookjian J, Ekong G, Alrayees MM. The association between health beliefs and medication adherence among patients with type 2 diabetes. *Res Social Adm Pharm* 2015; **12**: 914-925 [PMID: 26706405 DOI: 10.1016/j.sapharm.2015.11.006]

27 **Fowler C**, Baas LS. Illness representations in patients with chronic kidney disease on maintenance hemodialysis. *Nephrol Nurs J* 2006; **33**: 173-174, 179-186 [PMID: 16613412]

28 **Furler J**, Walker C, Blackberry I, Dunning T, Sulaiman N, Dunbar J, Best J, Young D. The emotional context of self-management in chronic illness: A qualitative study of the role of health professional support in the self-management of type 2 diabetes. *BMC Health Serv Res* 2008; **8**: 214 [PMID: 18928555 DOI: 10.1186/1472-6963-8-214]

29 **Covic A**, Seica A, Gusbeth-Tatomir P, Gavrilovici O, Goldsmith DJ. Illness representations and quality of life scores in haemodialysis patients. *Nephrol Dial Transplant* 2004; **19**: 2078-2083 [PMID: 15213317 DOI: 10.1093/ndt/gfh254]

30 **AbuSabha R**, Achterberg C. Review of self-efficacy and locus of control for nutrition- and health-related behavior. *J Am Diet Assoc* 1997; **97**: 1122-1132 [PMID: 9336559 DOI: 10.1016/S0002-8223(97)00273-3]

31 **Kelly RB**, Zyzanski SJ, Alemagno SA. Prediction of motivation and behavior change following health promotion: role of health beliefs, social support, and self-efficacy. *Soc Sci Med* 1991; **32**: 311-320 [PMID: 2024141]

32 **Adams RJ**. Improving health outcomes with better patient understanding and education. *Risk Manag Healthc Policy* 2010; **3**:

61-72 [PMID: 22312219 DOI: 10.2147/RMHP.S7500]
33 **Lau-Walker M**, Presky J, Webzell I, Murrells T, Heaton N. Patients with alcohol-related liver disease--beliefs about their illness and factors that influence their self-management. *J Adv Nurs* 2016; **72**: 173-185 [PMID: 26446497 DOI: 10.1111/jan.12826]
34 **Dalle Grave R**, Calugi S, Centis E, Marzocchi R, El Ghoch M, Marchesini G. Lifestyle modification in the management of the metabolic syndrome: achievements and challenges. *Diabetes Metab Syndr Obes* 2010; **3**: 373-385 [PMID: 21437107 DOI: 10.2147/DMSOTT.S13860]
35 **Bandura A**. Self-efficacy: toward a unifying theory of behavioral change. *Psychol Rev* 1977; **84**: 191-215 [PMID: 847061]
36 **Iñiguez IR**, Yap J, Mager DR. Parental perceptions regarding lifestyle interventions for obese children and adolescents with nonalcoholic fatty liver disease. *Paediatr Child Health* 2014; **19**: e24-e29 [PMID: 24855432]
37 **Betancourt JR**, Green AR, Carrillo JE, Ananeh-Firempong O. Defining cultural competence: a practical framework for addressing racial/ethnic disparities in health and health care. *Public Health Rep* 2003; **118**: 293-302 [PMID: 12815076]

P- Reviewer: Emre A, Gregorio BM **S- Editor**: Yu J
L- Editor: A **E- Editor**: Wang CH

World Journal of Gastroenterology

Submit a Manuscript: http://www.wjgnet.com/esps/

World J Gastroenterol 2017 March 14; 23(10): 1891-1898

DOI: 10.3748/wjg.v23.i10.1891

ISSN 1007-9327 (print) ISSN 2219-2840 (online)

ORIGINAL ARTICLE

Observational Study

Validation of the chinese version of the EORTC QLQ-CR29 in patients with colorectal cancer

Jin-Bo Lin, Lei Zhang, Dong-Wen Wu, Zhou-Huan Xi, Xue-Jun Wang, Yun-Shou Lin, Wakana Fujiwara, Jing-Ru Tian, Min Wang, Peng Peng, Ai Guo, Zhen Yang, Le Luo, Ling-Ya Jiang, Qia-Qia Li, Xue-Ying Zhang, Yun-Feng Zhang, Hou-Wei Xu, Bing Yang, Xun-Lin Li, Yi-Xiong Lei

Jin-Bo Lin, Yi-Xiong Lei, School of Public Health, Guangzhou Medical University, Guangzhou 511436, Guangdong Province, China

Jin-Bo Lin, Bing Yang, Longgang Central Hospital of Shenzhen, Shenzhen 518116, Guangdong Province, China

Lei Zhang, Department of Thoracic Surgery, Tianjin Medical University Cancer Institute and Hospital, National Clinical Research Center for Cancer, Key Laboratory of Cancer Prevention and Therapy, Tianjin Lung Cancer Center, Tianjin 300060, China

Dong-Wen Wu, Zhou-Huan Xi, Jing-Ru Tian, Zhen Yang, Ling-Ya Jiang, Qia-Qia Li, Xue-Ying Zhang, Xiangya School of Medicine, Central South University, Changsha 410013, Hunan Province, China

Xue-Jun Wang, Department of Gastrointestinal Surgery, Tianjin Medical University Cancer Institute and Hospital, National Clinical Research Center for Cancer, Key Laboratory of Cancer Prevention and Therapy, Tianjin Lung Cancer Center, Tianjin 300060, China

Yun-Shou Lin, Min Wang, Peng Peng, Ai Guo, Xun-Lin Li, Tianjin Medical University, Tianjin 300060, China

Wakana Fujiwara, School of Medicine, Georgetown University, N.W., Washington D.C. 20057, United States

Le Luo, Department of Radiation Oncology, Tumor Hospital, Xiangya School of Medicine of Central South University, Changsha 410013, Hunan Province, China

Yun-Feng Zhang, Longgang District Peoples Hospital of Shenzhen, Shenzhen 518172, Guangdong Province, China

Hou-Wei Xu, Cancer Center of Guangzhou Medical University, Guangzhou 510182, Guangdong Province, China

Author contributions: Lin JB, Zhang L, Wu DW and Xi ZH designed the research; Wang XJ, Lin YS, Tian JR and Guo A performed data analysis and interpretation; Wang M and Peng P wrote the paper; Yang Z, Luo L, Jiang LY, Li QQ, Zhang XY, Zhang YF, Xu HW, Yang B and Li XL collected the data; Fujiwara W and Lei YX revised the article; all authors have approved the final version to be published.

Supported by Science & Technology Innovation Commission of Shenzhen (to Lin JB), No. 201404113000346 and No. JCYJ20140411150916744; and the Science & Technology Project of Shenzhen Longgang District, No. 201406063001007 and No. YLWS20140606101914846; and the Science & Technology Project of Shenzhen Longgang District, No. 20160607153104624 (to Zhang YF).

Institutional review board statement: The study was reviewed and approved by the Institutional Review Boards of the Third Xiangya Hospital of Central South University, the Affiliated Tumor Hospital of Central South University, the Longgang Central Hospital of Shenzhen, and the Affiliated Tumor Hospital of Guangzhou Medical University.

Informed consent statement: All study participants, or their legal guardian, provided informed written consent prior to study enrollment.

Conflict-of-interest statement: There is no conflict of interest related to this study.

Data sharing statement: The datasets in the current study are available from the corresponding author on reasonable request at colorectum@163.com.

Manuscript source: Unsolicited manuscript

Correspondence to: Yi-Xiong Lei, PhD, School of Public Health, Guangzhou Medical University, Xinzao, Panyu District, Guangzhou 511436, Guangdong Province, China. colorectum@163.com
Telephone: +86-755-84802448
Fax: +86-755-84816979

Received: December 11, 2016
Peer-review started: December 12, 2016
First decision: December 29, 2016
Revised: January 19, 2017
Accepted: February 16, 2017
Article in press: February 17, 2017
Published online: March 14, 2017

Abstract

AIM

To assess the validity and reliability of the European Organization for Research and Treatment of Cancer Quality of Life Questionnaire-Colorectal Cancer 29 (EORTC QLQ-CR29) in Chinese patients with colorectal cancer (CRC).

METHODS

From March 2014 to January 2015, 356 patients with CRC from four different hospitals in China were enrolled in the study, and all patients self-administered the EORTC QLQ-CR29 and the quality of life core questionnaire (EORTC QLQ-C30). Evaluation of the scores was based on the Karnofsky Performance Scale (KPS). The reliability and validity of the questionnaires were assessed by Cronbach's α coefficient, the Spearman correlation test and Wilcoxon rank sum test.

RESULTS

The EORTC QLQ-CR29 showed satisfactory reliability ($\alpha > 0.7$), although the urinary frequency and blood and mucus in stool dimensions had only moderate reliability ($\alpha = 0.608$). The multitrait scaling analyses showed good convergent ($r > 0.4$) and discriminant validity. Significant differences were obtained for each item in the different KPS subgroups (KPS $\leqslant$ 80; KPS > 80). Body image and most single-item dimensions showed statistically significant differences in patients with a stoma compared with the rest of the patients.

CONCLUSION

The EORTC QLQ-CR29 exhibits high validity and reliability in Chinese patients with CRC, and can therefore be recommended as a valuable tool for the assessment of quality of life in these patients.

Key words: Colorectal cancer; Health-related quality of life; EORTC QLQ-CR29; Mainland China

Core tip: This is the first study to examine the reliability and validity of the Chinese version of the EORTC QLQ-CR29 in patients with colorectal cancer in mainland China. The EORTC QLQ-CR29 exhibits high validity and reliability in Chinese patients with CRC, and can therefore be recommended as a valuable tool for the assessment of quality of life in these patients.

Lin JB, Zhang L, Wu DW, Xi ZH, Wang XJ, Lin YS, Fujiwara W, Tian JR, Wang M, Peng P, Guo A, Yang Z, Luo L, Jiang LY, Li QQ, Zhang XY, Zhang YF, Xu HW, Yang B, Li XL, Lei YX. Validation of the Chinese version of the EORTC QLQ-CR29 in patients with colorectal cancer. *World J Gastroenterol* 2017; 23(10): 1891-1898 Available from: URL: http://www.wjgnet.com/1007-9327/full/v23/i10/1891.htm DOI: http://dx.doi.org/10.3748/wjg.v23.i10.1891

INTRODUCTION

Colorectal cancer (CRC) is the third most common cancer and the fourth leading cause of cancer death worldwide. According to the latest data, almost 1.4 million people were diagnosed with CRC and 700000 people died of CRC worldwide in 2012[1]. Moreover, the number of newly diagnosed CRC patients in China in 2012 was estimated to be 331 300, which accounted for approximately 24% of all cases in the world[2]. Therefore, it is important to prolong the lives of CRC patients and improve their quality of life.

The EORTC QLQ-CR29 questionnaire was developed by the European Organization for Research and Treatment of Cancer (EORTC) to evaluate the quality of life in CRC patients. It has already been validated in Holland, Spain, Poland and several other countries[3-8]. However, the dietary and cultural differences between China and Western countries may lead to different interpretations of quality of life. Therefore, it is essential to test the reliability and validity of the Chinese version of the EORTC QLQ-CR29 in patients with CRC, which has never been done in mainland China.

MATERIALS AND METHODS

Patients

A total of 356 patients with CRC in the Third Xiangya Hospital of Central South University, the Affiliated Tumor Hospital of Central South University, the Longgang Central Hospital of Shenzhen, and the Affiliated Tumor Hospital of Guangzhou Medical University were recruited between March 2014 and January 2015. Patients were included in the study if they were older than 18 years and had histological confirmation of colon or rectal cancer. Patients who had complications or who had been diagnosed with a cognitive disorder or psychonosema were excluded.

All participants completed the Chinese version of the EORTC QLQ-C30 and EORTC QLQ-CR29 during the 11-mo recruitment period.

Instruments

EORTC QLQ-C30: The EORTC QLQ-C30 is the core questionnaire designed by the European Organization for Research and Treatment of Cancer, and has five functional dimensions: physical functioning (PF), role functioning (RF), cognitive functioning (CF), emotional functioning (EF) and social functioning (SF); three symptom scales: fatigue (FA), pain (PA), and nausea/vomiting (NV); six single items addressing various symptoms and perceived financial impact, and a global health-related quality of life (HRQOL) subscale. Among the 30 items, 29 have seven possible responses and are awarded a score of 1 to 7 points according to the answer; the other has a four-point answer scale: 1, Not at all; 2, A little; 3, Quite a bit; 4, Very much[9,10]. The reliability and validity of C30 have already been verified in China[11].

EORTC QLQ-CR29: The EORTC QLQ-CR29 was specifically designed by the EORTC QL Group (The European Organization for Research and Treatment of Cancer Quality of Life Group) as the QLQ-C30 supplement for the evaluation of HRQOL in CRC patients. This combination has already been widely used in both clinical and basic research[12-14].

The QLQ-CR29 includes 29 items that evaluate symptoms (gastrointestinal, urinary, pain and others) and functional areas (sexual, body image and others) that are associated with CRC and its treatments. There are separate items for patients with and without a stoma (items 49 to 54, with item 55 only for patients with a stoma) and separate items to evaluate the sexual function of men and women. The questionnaires ask for all items in the past week except those pertaining to sexuality, which request the patients to evaluate the items in the past four weeks. Similar to the EORTC QLQ-C30, the QLQ-CR29 has a Likert scale of four response categories (item 48 requires a yes or no answer)[5,8,9]. All patient-rated scores are linearly converted into a scale from 0 to 100 for both the QLQ-C30 and QLQ-CR29[7,15].

According to the EORTC guidelines[16], two translators first translated EORTC QLQ-CR29 into Chinese (Simplified Chinese), then another two translators translated the Chinese version of the EORCT QLQ-CR29 into English and compared it with the original questionnaire to verify whether it fully reflected the contents of the original questionnaire. After several amendments, we then selected 20 female and 20 male patients (both male and female patients included 3 stoma patients) to determine if the questionnaire was easy to understand. According to the feedback, we finally developed the Chinese version of the EORTC QLQ-CR29.

Karnofsky performance scale

The Karnofsky performance scale (KPS) was determined by physicians according to the condition of the patient with respect to illness, self-care ability and daily activities. The total score of 100 was graded by 10 and the higher the score, the better the patient's health[17,18].

Ethics

Approval for this study was obtained from the Ethics Committees of the four participating hospitals. Before the investigation, we asked patients to provide a signed informed consent, and confirmed their consent to participate in the study to protect their voluntary participation, right to know, and right of privacy.

Statistical analysis

We selected nurses on duty in the relevant departments as investigators in this study. After training, the investigators explained and introduced the protocol to the participants, and obtained basic information and KPS scores. Each participant completed the EORTC QLQ-CR29 and EORTC QLQ-C30 independently. Each scale score was converted based on standard formula, and the points ranged from 0 points (the worst) to 100 points (best).

All data were analyzed using SPSS17.0 software. Numbers (percentages) were used to describe numerical data and the mean ± SD was adopted to describe measured data.

The internal consistency of the questionnaire was assessed using Cronbach's α coefficient ($\alpha > 0.7$ was considered acceptable).

Multitrait scaling analysis was used to assess the module structure. The convergent validity of each item was determined by calculating the correlation between each item and its own dimension ($r > 0.40$ was considered acceptable). For discriminant validity, we expected the correlation between each item and its own dimension to be greater than the correlation between the item and the other dimensions.

Correlations between all of the EORTC QLQ-CR29 and the EORTC QLQ-C30 areas were calculated based on the Spearman correlation coefficient ($r > 0.4$ was considered strongly correlated).

Known-groups validity was assessed by making comparisons between subgroups based on the presence of a stoma and KPS score (KPS $\leqslant$ 80; KPS > 80) using the Wilcoxon rank sum test.

The acceptability was evaluated by the completion ratio of the questionnaires and the miss rate of each item.

RESULTS

Patient characteristics and compliance

A total of 356 patients were enrolled in the study and no one declined the invitation to participate. The study

Table 1 Sociodemographic and clinical characteristics of the patients (*n* = 356) *n* (%)

Characteristics	No. of patients[1]
Age (yr, mean ± SD)	54.5 ± 13.5
Sex	341[2]
Male	213 (62.5)
Female	128 (37.5)
Educational status	341[2]
Junior high school	182 (53.4)
Senior high school	107 (31.4)
University	47 (13.8)
Postgraduate and above	5 (1.5)
Marital status	340[2]
Single	5 (1.5)
Married	334 (98.2)
Divorced	1 (0.3)
Employment	343[2]
Yes	268 (78.1)
No	75 (21.9)
Location of tumor	342[2]
Colon	193 (56.4)
Rectum	147 (43.0)
Both	2 (0.6)
Metastasis	343[2]
Yes	102 (29.7)
No	215 (62.7)
Unknown	26 (7.6)
Time from first diagnosis (wk) Median (interquartile range)	16.0 (33.8)

[1]All percentages are valid; [2]There are missing data.

group included 213 men and 128 women with an average age of 54.5 (±13.5) years. Of the participants, 193 patients had colon cancer, 147 patients had rectal cancer and three had both colon and rectal cancer, and 102 patients had metastasis (Table 1).

Reliability

Internal consistency: Reliability was assessed using Cronbach's α coefficient. The correlations between the items showed that the body image and stool frequency dimensions had high reliability (α > 0.7), while the urinary frequency and blood and mucus in the stool dimensions had lower, but still moderate reliability (0.608 and 0.641). Except for the urinary frequency dimension (0.608 with *vs* 0.363 without), the reliability of other dimensions in patients without a stoma was higher than that in patients with a stoma (Table 2).

Validity

Multitrait scaling analyses: The correlations between all dimensions and their sub-items were higher than 0.4. In addition to the finding that the correlation between item 28 for the patients with a stoma and blood and mucus in stool dimension was 1, the correlations between other dimensions and their sub-items were all greater than their correlations with other items (Table 2).

Correlations with the EORTC QLQ-C30: The dimensions and the single items included in the CR29 had correlations of 0.004-0.648 with the C30. Abdominal pain and pain showed a good correlation (r = 0.648), while the correlation between abdominal pain and fatigue was 0.411. The correlations between the anxiety dimension and the four dimensions of the C30 (role functioning, emotional functioning, social functioning and financial problems) were all greater than 0.4. The correlations between the blood and mucus in the stool dimension and three dimensions of the C30 (quality of life, pain and diarrhea) were all greater than 0.4. Seven dimensions (body image, buttock pain, hair loss, bloating, fecal incontinence, sore skin and dyspareunia) had correlation coefficients with nausea/vomiting that were higher than 0.4, and the correlations between the stool frequency and diarrhea as well as taste and appetite loss were also greater than 0.4 (Table 3).

Known-groups validity: The differences between the CR29 and C30 scores are shown in Table 4, where the data are grouped based on the clinical parameters. In addition to items such as abdominal pain, dry mouth and stoma care problems (0.059, 0.170, and 0.941) and dimensions such as urinary frequency and body image (0.098 and 0.589), other areas in subgroups divided by the KPS scores (KPS ≤ 80; KPS > 80) also showed statistical significance (P < 0.05). As for patients with or without a stoma, body image and most single-item dimensions from the CR29 and only role, social as well as nausea and vomiting dimensions from the C30 showed statistically significant differences.

Acceptability

In the survey, 285 of 356 patients (80.1%) completed the EORTC (C30 and CR29) questionnaires, and a total of 265 patients (74.4%) completed the basic status questionnaire and the measurement questionnaires. The lowest response rates were associated with sexual problems, with a miss rate of 3.4% (12 cases). Overall, the questionnaire completion rate was higher than 90%, which shows that over 90% of the items were answered.

DISCUSSION

Due to improvements in curative therapy, doctors have started to pay more attention to HRQOL in CRC patients[13,19-23]. In this study, we selected the EORTC QLQ-CR29 and EORTC QLQ-C30, and examined their reliability, validity, and acceptability in terms of assessing the quality of life in patients with CRC in mainland China. The overall goal of the study was to determine the feasibility of these instruments in the clinical setting in China.

The analysis of internal consistency showed that, regardless of whether a stoma was present, Cronbach'

Table 2 Item convergent and discriminant validity for the EORTC QLQ-CR29 scales, and for patients with and without a stoma

QLQ-CR29 scales	Total sample (n = 354)[1]			Without a stoma (n = 298)			With a stoma (n = 56)		
	Convergent	Discriminant	α	Convergent	Discriminant	α	Convergent	Discriminant	α
Urinary frequency	0.589-0.923	0.004-0.306	0.406	0.588-0.924	0.002-0.321	0.363	0.587-0.919	0.017-0.333	0.608
Blood or mucus in stools	0.794-0.886	0.004-0.712	0.641	0.790-0.891	0.002-0.738	0.638	0.815-0.829	0.037-1.000	0.632
Stool frequency	0.689-0.965	0.003-0.641	0.679	0.696-0.967	0.001-0.669	0.716	0.645-0.957	0.003-0.389	0.423
Body image	0.628-0.826	0.060-0.405	0.715	0.614-0.839	0.039-0.422	0.718	0.703-0.792	0.004-0.504	0.676

[1]Two are missing.

Table 3 Correlations between the EORTC QLQ-CR29 and the QLQ-C30

	EORTC-QLQ-C30														
	QOL	PF	RF	EF	CF	SF	FA	NV	PA	DY	SL	AP	CO	DI	FI
CR29 scales															
Urinary frequency	0.004	-0.071	-0.111[a]	-0.083	-0.163[b]	-0.159[b]	0.107[a]	-0.130[a]	-0.033	-0.046	0.061	0.023	-0.131[a]	-0.022	0.063
Blood and mucus in stool	-0.412[b]	-0.320[b]	-0.074	-0.091	-0.166[b]	0.077	0.296[b]	0.383[b]	0.451[b]	0.166[b]	0.190[b]	0.120[a]	0.321[b]	0.526[b]	-0.141[a]
Stool frequency	-0.322[b]	-0.236[b]	-0.075	-0.132[a]	-0.115[a]	-0.026	0.268[b]	0.340[b]	0.349[b]	0.212[b]	0.188[b]	0.120[a]	0.247[b]	0.492[b]	-0.113[a]
Body image	0.254[b]	0.179[b]	-0.052	0.051	0.100	-0.172[b]	-0.303[b]	-0.485[b]	-0.363[b]	-0.251[b]	-0.185[b]	-0.279[b]	-0.240[b]	-0.224[b]	0.132[a]
CR29 single items															
Urinary incontinence	0.084	0.040	0.237[b]	0.203[b]	-0.071	0.171[b]	-0.038	0.270[b]	0.125[a]	0.311[b]	0.080	0.040	0.135[a]	0.139[b]	-0.291[b]
Dysuria	0.032	0.101	0.223[b]	0.210[b]	-0.185[b]	0.288[b]	0.053	0.330[b]	0.272[b]	0.296[b]	0.133[a]	0.003	0.279[b]	0.158[b]	-0.294[b]
Abdominal pain	-0.357[b]	-0.399[b]	-0.149[b]	-0.086	-0.245[b]	0.097	0.411[b]	0.342[b]	0.648[b]	0.321[b]	0.307[b]	0.241[b]	0.375[b]	0.381[b]	-0.118[a]
Buttock pain	-0.114[a]	-0.105	0.129[a]	0.056	-0.138[a]	0.271[b]	0.131[a]	0.487[b]	0.343[b]	0.224[b]	0.178[b]	0.139[b]	0.278[b]	0.160[b]	-0.273[b]
Bloating	-0.261[b]	-0.233[b]	-0.277[b]	-0.302[b]	-0.129[a]	-0.206[b]	0.213[b]	0.080	0.240[b]	0.130[a]	0.221[b]	0.183[b]	0.207[b]	0.252[b]	0.125[a]
Dry mouth	-0.117[a]	-0.074	0.181[b]	0.120[a]	-0.104	0.216[b]	0.152[b]	0.321[b]	0.262[b]	0.358[b]	0.134[a]	0.110[a]	0.218[b]	0.122[a]	-0.163[b]
Hair loss	-0.112[a]	-0.085	0.167[b]	0.037	-0.131[a]	0.222[b]	0.184[b]	0.486[b]	0.286[b]	0.276[b]	0.108[a]	0.127[a]	0.232[b]	0.155[b]	-0.200[b]
Taste	-0.218[b]	-0.238[b]	-0.214[b]	-0.278[b]	-0.222[b]	-0.107[a]	0.266[b]	0.137[a]	0.102	0.088	0.294[b]	0.459[b]	0.013	0.163[b]	0.083
Anxiety	-0.233[b]	-0.147[b]	-0.425[b]	-0.547[b]	-0.033	-0.412[b]	0.150[b]	-0.272[b]	-0.103	-0.095	0.011	0.134[a]	-0.089	0.066	0.449[b]
Weight	-0.217[b]	-0.266[b]	-0.346[b]	-0.371[b]	-0.175[b]	-0.244[b]	0.287[b]	0.042	0.103	0.026	0.202[b]	0.287[b]	0.005	0.184[b]	0.306[b]
Flatulence	-0.057	-0.094	0.170[b]	0.039	-0.115[a]	0.159[b]	0.092	0.433[b]	0.206[b]	0.180[b]	0.106[a]	0.180[b]	0.200[b]	0.236[b]	-0.166[b]
Fecal incontinence	-0.017	-0.032	0.275[b]	0.218[b]	-0.129[a]	0.320[b]	0.049	0.447[b]	0.284[b]	0.252[b]	0.163[b]	0.055	0.229[b]	0.257[b]	-0.350[b]
Sore skin	-0.052	-0.132[a]	0.208[b]	0.170[b]	-0.094	0.296[b]	0.081	0.497[b]	0.205[b]	0.130[a]	0.160[b]	0.123[a]	0.106[a]	0.194[b]	-0.271[b]
Embarrassment	-0.049	-0.041	0.200[b]	0.085	-0.019	0.209[b]	0.036	0.317[b]	0.167[b]	-0.006	0.027	0.059	0.070	0.088	-0.209[b]
Stoma care problems	-0.184	0.210	0.224	-0.254	0.044	0.064	-0.025	0.019	-0.033	-0.265	-0.059	0.007	-0.161	0.073	0.175
Sexual interest (men)	-0.108	-0.177[a]	-0.051	0.041	-0.276[b]	-0.184[b]	0.142[a]	-0.089	0.051	0.119	0.112	0.004	-0.010	0.039	0.092
Impotence	-0.026	-0.102	0.189[b]	0.177[a]	-0.212[b]	0.243[b]	0.105	0.242[b]	0.082	0.155[a]	0.175[a]	0.157[a]	0.069	0.093	-0.256[b]
Sexual interest (women)	-0.319[b]	-0.213[a]	-0.092	0.030	-0.386[b]	-0.006	0.091	-0.099	0.044	0.194	0.270[b]	0.056	0.176	-0.010	0.215[a]
Dyspareunia	0.026	0.003	0.213[b]	0.322[b]	-0.129	0.258[b]	-0.094	0.423[b]	0.185	0.227[a]	0.005	0.090	0.312[b]	0.117	-0.193

[a]$P < 0.05$, [b]$P < 0.01$, EORTC QLQ-CR29 *vs* the QLQ-C30. QOL: Quality of life; PF: Physical functioning; RF: Role functioning; EF: Emotional functioning; CF: Cognitive functioning; SF: Social functioning; FA: Fatigue; NV: Nausea/vomiting; PA: Pain; DY: Dyspnea; SL: Insomnia; AP: Appetite loss; CO: Constipation; DI: Diarrhea; FI: Financial problems.

s α coefficient in each dimension was satisfactory or near-satisfactory. In the original EORTC study, Cronbach's α coefficients were greater than or almost equal to 0.7[9]. Our data mainly showed lower Cronbach's α coefficients than those in a similar study by Nowak *et al*[8], particularly in the urinary frequency dimension (0.363-0.608). Of note, in the studies by Arraras *et al*[5], Nowak *et al*[8] and Arraras Urdaniz *et al*[24], Cronbach's α coefficients below 0.7 were also obtained for the abdominal pain and blood and mucus in the stool dimensions. The differences between our findings and those of previous studies may be due to differences in the perceptions of quality of life in patients from different regions; however, the differences were still in the acceptable range. In addition, the reliability of the dimensions related to body image and stool frequency in patients without a stoma was higher than that in patients with a stoma, which is different from the studies reported by Nowak *et al*[8] and Whistance *et al*[9].

In agreement with the results reported by Whistance, the correlations between the EORTC

Table 4 Known group comparisons: scales and items in the QLQ-C30 and CR29 for clinically distinct groups

	Stoma (n = 56)	No stoma (n = 298)	P value[1]	KPS ≤ 80 (n = 162)	KPS > 80 (n = 177)	P value[1]
CR29 scales						
Urinary frequency	6.5 ± 14.5	6.1 ± 13.5	0.856	6.7 ± 12.3	5.8 ± 14.9	0.098
Blood and mucus in stool	18.9 ± 25.9	10.3 ± 16.3	0.160	13.8 ± 19.7	7.3 ± 12.7	0.019
Stool frequency	8.0 ± 13.2	8.4 ± 14.8	0.960	11.2 ± 18.2	5.1 ± 9.6	0.017
Body image	81.7 ± 18.9	88.6 ± 14.7	0.004	87.7 ± 17.7	89.0 ± 11.9	0.589
CR29 single items						
Urinary incontinence	7.7 ± 4.2	1.6 ± 7.1	< 0.001	0.8 ± 0.7	4.2 ± 11.1	0.001
Dysuria	7.7 ± 16.8	5.4 ± 12.3	0.444	3.2 ± 11.2	8.0 ± 14.7	< 0.001
Abdominal pain	11.9 ± 21.5	12.0 ± 18.7	0.651	13.5 ± 21.0	9.0 ± 16.1	0.059
Buttock pain	10.7 ± 15.7	5.4 ± 13.2	0.005	2.5 ± 8.8	9.0 ± 16.1	< 0.001
Bloating	16.1 ± 16.8	20.9 ± 21.4	0.183	25.2 ± 23.9	15.0 ± 16.6	< 0.001
Dry mouth	11.9 ± 17.3	7.2 ± 15.1	0.025	6.0 ± 14.4	8.0 ± 15.1	0.170
Hair loss	14.3 ± 18.9	9.6 ± 16.6	0.058	7.7 ± 17.2	11.1 ± 16.2	0.010
Taste	15.5 ± 22.9	23.8 ± 21.7	0.002	26.0 ± 25.0	18.8 ± 18.4	0.015
Anxiety	31.0 ± 31.0	44.6 ± 23.7	< 0.001	52.1 ± 22.6	35.1 ± 24.1	< 0.001
Weight	22.6 ± 21.2	44.6 ± 23.7	0.032	32.3 ± 19.9	21.6 ± 16.8	< 0.001
Flatulence	14.3 ± 17.8	5.0 ± 13.4	< 0.001	4.5 ± 14.6	7.0 ± 13.6	0.012
Fecal incontinence	15.5 ± 20.1	4.4 ± 11.9	< 0.001	2.5 ± 10.2	8.0 ± 15.1	< 0.001
Sore skin	26.2 ± 23.5	3.1 ± 10.1	< 0.001	3.5 ± 12.7	9.7 ± 17.5	< 0.001
Embarrassment	25.0 ± 20.4	2.3 ± 8.4	< 0.001	4.1 ± 12.8	7.1 ± 14.6	0.019
Stoma care problems	/	/	/	18.8 ± 20.8	19.8 ± 25.2	0.941
Sexual interest (men)	74.4 ± 23.5	69.8 ± 25.5	0.333	76.3 ± 22.8	66.0 ± 26.0	0.020
Impotence	9.4 ± 17.0	8.5 ± 20.2	0.364	6.5 ± 19.2	10.7 ± 19.9	0.021
Sexual interest (women)	81.0 ± 17.8	77.1 ± 22.5	0.749	83.7 ± 16.8	71.2 ± 25.0	0.005
Dyspareunia	9.5 ± 16.3	4.3 ± 14.1	0.172	2.7 ± 15.0	6.5 ± 13.4	0.012
QLQ-C30 scales						
Physical	85.5 ± 12.4	82.9 ± 16.5	0.335	77.6 ± 18.3	89.4 ± 10.7	< 0.001
Role	84.8 ± 17.2	69.4 ± 20.6	< 0.001	61.7 ± 20.6	81.2 ± 16.4	< 0.001
Emotional	80.5 ± 17.7	74.4 ± 14.0	0.001	69.3 ± 14.4	81.2 ± 11.9	< 0.001
Cognitive	79.5 ± 20.5	80.7 ± 20.0	0.397	75.4 ± 34.9	85.9 ± 14.6	< 0.001
Social	60.0 ± 22.4	45.7 ± 25.5	< 0.001	38.5 ± 24.9	55.7 ± 23.5	< 0.001
Overall quality of life	67.9 ± 21.4	67.8 ± 17.4	0.636	59.5 ± 16.5	76.4 ± 14.4	< 0.001
Fatigue	18.8 ± 18.2	22.8 ± 19.9	0.108	30.5 ± 20.3	13.2 ± 13.8	< 0.001
Nausea and vomiting	11.6 ± 13.8	6.1 ± 14.4	< 0.001	4.7 ± 15.7	8.1 ± 12.5	< 0.001
Pain	13.0 ± 16.6	12.0 ± 17.3	0.427	13.3 ± 19.1	9.4 ± 13.8	0.211

[1]Wilcoxon rank sum test.

QLQ-CR29 items and their dimensions were greater than the correlation coefficients of other dimensions, suggesting that the EORTC QLQ-CR29 has great convergent validity and discriminant validity[9]. Item 28 was examined only in females. In this subgroup, there were 10 women, five of whom answered one survey, while the other five answered two surveys. The correlation coefficient between item 28 in the stoma group and the presence of blood and mucus in the stool was 1, probably due to the small number of cases in the sample. A similar finding was noted in the study by Arraras *et al*[5].

The correlation coefficients between the EORTC QLQ-CR29 and EORTC QLQ-C30 scales showed that similar dimensions of QLQ had high correlations, while unrelated dimensions were only weakly correlated, demonstrating the validity of the QLQ-CR29 and indicating that the two questionnaires had different points of emphasis.

A comparison of the results showed that there were different QLQ-CR29 dimension scores among the groups divided by the KPS scores (KPS ≤ 80; KPS > 80) and whether the patients had a stoma or not, which signified that the QLQ-CR29 had good clinical validity and can be used to measure different patients with different conditions. These results are consistent with those reported by Whistance and other foreign validity tests[5,8,9]. In addition, this study showed that patients with a KPS > 80 had higher scores in functional dimensions, but lower scores in the symptom dimensions, and those patients with a KPS ≤ 80 had a poorer quality of life. Statistically significant differences existed in numerous dimensions in groups divided by the KPS score (*e.g.*, stool frequency, P = 0.017). Due to the impact of disease or treatment, sexual function in patients was significantly inhibited, similar to the findings in previous reports by other groups[5,6,24]. The studies by Song *et al*[25] and Peng *et al*[26] revealed that treatment of CRC may lead to impotence. However, this was not found in our study, probably because different countries perform different types of surgery, which result in different types of complications. In addition, compared with patients with a stoma, patients without a stoma had

lower scores in the symptom dimensions, and higher scores in the functional dimensions, which indicated better quality of life. Moreover, in our study, the scope of the scores was wide in each dimension of the questionnaire, indicating that the Chinese version of the CR29 had good clinical validity.

People of different cultures often have a different understanding of quality of life. After adequate translation, the EORTC QLQ-CR29 was also proved to be suitable for Chinese patients. When Arraras performed research on a Spanish version of the survey, 4.7% of patients considered some of the items in the questionnaire to be difficult to understand or answer, or unrelated to quality of life[5]. In our study, few patients had such problems and there was a high compliance rate (with a low miss rate), both of which indicate that the Chinese version of the EORTC QLQ-CR29 had great acceptability. Compared with the studies by Arraras *et al*[5] and Whistance *et al*[9], the sexual dimension in our study had a higher miss rate (2.9% and 2.3% *vs* 3.4%). This may be due to the fact that Asians are more reticent when talking about sex than Western patients, and were not willing to tell the truth to doctors[26]. In order to address this problem and obtain a more accurate and comprehensive evaluation, a more detailed explanation from medical professionals is required when patients complete the questionnaire.

There are a few limitations in our study. Firstly, the subgroups were only segregated by the score on the Karnofsky Performance Scale, the presence of a stoma had more clinical significance than previously thought, and increased bias should not be ignored. In addition, the representativeness of our study should be treated cautiously due to the deficiency of larger cross-regional multicenter studies in mainland China. To obtain more rigorous results, we will pay more attention to these limitations in future studies.

In conclusion, the present study showed that the EORT QLQ-C29 (Chinese version) is a valid and reliable instrument for assessing the quality of life of patients with CRC in mainland China.

COMMENTS

Background

Colorectal cancer (CRC) is the third most common cancer and the fourth leading cause of cancer death. In 2012, almost 1.4 million people were diagnosed with CRC and 700 000 people died of CRC worldwide, of which China accounted for approximately 24%. Therefore, assessing and improving the quality of life of patients with CRC have become more important in these patients. The EORTC QLQ-CR29 questionnaire was developed by the European Organization for Research and Treatment of Cancer (EORTC) to evaluate quality of life in CRC patients.

Research frontiers

The EORTC QLQ-CR29 questionnaire has already been validated in Spain, Poland and several other countries. However, the dietary and cultural differences between China and Western countries may lead to different interpretations of quality of life. Therefore, it is essential to test the reliability and validity of the Chinese version of the EORTC QLQ-CR29 in patients with CRC, which has never been done in mainland China.

Innovations and breakthroughs

In the past few decades, advances in medical technology have made it possible for CRC patients to live longer. More attention has been paid to the quality of life of these patients; thus, questionnaires that can accurately assess quality of life have been developed, of which the series of EORTC questionnaires play very important roles. The EORTC developed sub-questionnaires, including the core questionnaire QLQ-C30 for all cancers, the BR-23 for breast cancer, the CX-24 for cervical cancer and the CR-29 for CRC.

Applications

Due to improvements in curative therapy, doctors have started to pay more attention to health-related quality of life in CRC patients. In this study, the authors selected the EORTC QLQ-CR29 and EORTC QLQ-C30 and examined their reliability, validity, and acceptability in terms of assessing the quality of life in patients with CRC in mainland China. The overall goal of the study was to determine the feasibility of these instruments in the clinical setting in China.

Terminology

The EORTC QLQ-C30 is the core questionnaire designed by the European Organization for Research and Treatment of Cancer, which can be used for all types of cancer. Based on the QLQ-C30, the EORTC QLQ-CR29 was specifically designed by the EORTC QL Group (The European Organization for Research and Treatment of Cancer Quality of Life Group) as a QLQ-C30 supplement for the evaluation of health-related quality of life in CRC patients.

Peer-review

By now, available papers have shown the EORTC QLQ-C30 combined the EORTC QLQ-CR29 can assess the quality of life of patients with CRC in Spanish, Polish and Malaysia. And this combination has already been widely used in both clinical and basic research.

REFERENCES

1 **Torre LA**, Bray F, Siegel RL, Ferlay J, Lortet-Tieulent J, Jemal A. Global cancer statistics, 2012. *CA Cancer J Clin* 2015; **65**: 87-108 [PMID: 25651787 DOI: 10.3322/caac.21262]

2 **Chen W**, Zheng R, Zuo T, Zeng H, Zhang S, He J. National cancer incidence and mortality in China, 2012. *Chin J Cancer Res* 2016; **28**: 1-11 [PMID: 27041922 DOI: 10.3978/j.issn.1000-9604.2016.02.08]

3 **Gujral S**, Conroy T, Fleissner C, Sezer O, King PM, Avery KN, Sylvester P, Koller M, Sprangers MA, Blazeby JM. Assessing quality of life in patients with colorectal cancer: an update of the EORTC quality of life questionnaire. *Eur J Cancer* 2007; **43**: 1564-1573 [PMID: 17521904 DOI: 10.1016/j.ejca.2007.04.005]

4 **Stiggelbout AM**, Kunneman M, Baas-Thijssen MC, Neijenhuis PA, Loor AK, Jägers S, Vree R, Marijnen CA, Pieterse AH. The EORTC QLQ-CR29 quality of life questionnaire for colorectal cancer: validation of the Dutch version. *Qual Life Res* 2016; **25**: 1853-1858 [PMID: 26711791 DOI: 10.1007/s11136-015-1210-5]

5 **Arraras JI**, Suárez J, Arias de la Vega F, Vera R, Asín G, Arrazubi V, Rico M, Teijeira L, Azparren J. The EORTC Quality of Life questionnaire for patients with colorectal cancer: EORTC QLQ-CR29 validation study for Spanish patients. *Clin Transl Oncol* 2011; **13**: 50-56 [PMID: 21239355 DOI: 10.1007/s12094-011-0616-y]

6 **Arraras Urdaniz JI**, Vera García R, Martínez Aguillo M, Manterola Burgaleta A, Arias de la Vega F, Salgado Pascual E. Quality of Life assessment through the EORTC questionnaires of colorectal cancer patients in advanced disease stages. *Clin Transl Oncol* 2006; **8**: 664-671 [PMID: 17005468]

7 **Magaji BA**, Moy FM, Roslani AC, Sagap I, Zakaria J, Blazeby JM, Law CW. Health-related quality of life among colorectal cancer patients in Malaysia: a study protocol. *BMC Cancer* 2012; **12**: 384 [PMID: 22937765 DOI: 10.1186/1471-2407-12-384]

8 **Nowak W**, Tobiasz-Adamczyk B, Brzyski P, Sałówka J, Kuliś D, Richter P. Adaptation of quality of life module EORTC QLQ-CR29 for Polish patients with rectal cancer: initial assessment of

validity and reliability. *Pol Przegl Chir* 2011; **83**: 502-510 [PMID: 22166739 DOI: 10.2478/v10035-011-0078-5]

9 **Whistance RN**, Conroy T, Chie W, Costantini A, Sezer O, Koller M, Johnson CD, Pilkington SA, Arraras J, Ben-Josef E, Pullyblank AM, Fayers P, Blazeby JM. Clinical and psychometric validation of the EORTC QLQ-CR29 questionnaire module to assess health-related quality of life in patients with colorectal cancer. *Eur J Cancer* 2009; **45**: 3017-3026 [PMID: 19765978 DOI: 10.1016/j.ejca.2009.08.014]

10 **Borghede G**, Sullivan M. Measurement of quality of life in localized prostatic cancer patients treated with radiotherapy. Development of a prostate cancer-specific module supplementing the EORTC QLQ-C30. *Qual Life Res* 1996; **5**: 212-222 [PMID: 8998490]

11 **Zhao H**, Kanda K. Translation and validation of the standard Chinese version of the EORTC QLQ-C30. *Qual Life Res* 2000; **9**: 129-137 [PMID: 10983477]

12 **Ward WL**, Hahn EA, Mo F, Hernandez L, Tulsky DS, Cella D. Reliability and validity of the Functional Assessment of Cancer Therapy-Colorectal (FACT-C) quality of life instrument. *Qual Life Res* 1999; **8**: 181-195 [PMID: 10472150]

13 **Zolciak A**, Bujko K, Kepka L, Oledzki J, Rutkowski A, Nowacki MP. Abdominoperineal resection or anterior resection for rectal cancer: patient preferences before and after treatment. *Colorectal Dis* 2006; **8**: 575-580 [PMID: 16919109 DOI: 10.1111/j.1463-1318.2006.01000.x]

14 **Uwer L**, Rotonda C, Guillemin F, Miny J, Kaminsky MC, Mercier M, Tournier-Rangeard L, Leonard I, Montcuquet P, Rauch P, Conroy T. Responsiveness of EORTC QLQ-C30, QLQ-CR38 and FACT-C quality of life questionnaires in patients with colorectal cancer. *Health Qual Life Outcomes* 2011; **9**: 70 [PMID: 21859485 DOI: 10.1186/1477-7525-9-70]

15 **Blazeby JM**, Hall E, Aaronson NK, Lloyd L, Waters R, Kelly JD, Fayers P. Validation and reliability testing of the EORTC QLQ-NMIBC24 questionnaire module to assess patient-reported outcomes in non-muscle-invasive bladder cancer. *Eur Urol* 2014; **66**: 1148-1156 [PMID: 24612661 DOI: 10.1016/j.eururo.2014.02.034]

16 **Sprangers MA**, Cull A, Bjordal K, Groenvold M, Aaronson NK. The European Organization for Research and Treatment of Cancer. Approach to quality of life assessment: guidelines for developing questionnaire modules. EORTC Study Group on Quality of Life. *Qual Life Res* 1993; **2**: 287-295 [PMID: 8220363]

17 **Yates JW**, Chalmer B, McKegney FP. Evaluation of patients with advanced cancer using the Karnofsky performance status. *Cancer* 1980; **45**: 2220-2224 [PMID: 7370963]

18 **Friendlander AH**, Ettinger RL. Karnofsky performance status scale. *Spec Care Dentist* 2009; **29**: 147-148 [PMID: 19573040 DOI: 10.1111/j.1754-4505.2009.00088.x]

19 **Färkkilä N**, Sintonen H, Saarto T, Järvinen H, Hänninen J, Taari K, Roine RP. Health-related quality of life in colorectal cancer. *Colorectal Dis* 2013; **15**: e215-e222 [PMID: 23351057 DOI: 10.1111/codi.12143]

20 **Fenech DS**, Takahashi T, Liu M, Spencer L, Swallow CJ, Cohen Z, Macrae HM, McLeod RS. Function and quality of life after transanal excision of rectal polyps and cancers. *Dis Colon Rectum* 2007; **50**: 598-603 [PMID: 17309002 DOI: 10.1007/s10350-006-0865-y]

21 **Hendren SK**, O'Connor BI, Liu M, Asano T, Cohen Z, Swallow CJ, Macrae HM, Gryfe R, McLeod RS. Prevalence of male and female sexual dysfunction is high following surgery for rectal cancer. *Ann Surg* 2005; **242**: 212-223 [PMID: 16041212]

22 **Pietrzak L**, Bujko K, Nowacki MP, Kepka L, Oledzki J, Rutkowski A, Szmeja J, Kladny J, Dymecki D, Wieczorek A, Pawlak M, Lesniak T, Kowalska T, Richter P. Quality of life, anorectal and sexual functions after preoperative radiotherapy for rectal cancer: report of a randomised trial. *Radiother Oncol* 2007; **84**: 217-225 [PMID: 17692977 DOI: 10.1016/j.radonc.2007.07.007]

23 **Tofthagen C**, Donovan KA, Morgan MA, Shibata D, Yeh Y. Oxaliplatin-induced peripheral neuropathy's effects on health-related quality of life of colorectal cancer survivors. *Support Care Cancer* 2013; **21**: 3307-3313 [PMID: 23903798 DOI: 10.1007/s00520-013-1905-5]

24 **Arraras Urdaniz JI**, Arias de la Vega F, Vera García R, Manterola Burgaleta A, Martínez Aguillo M, Villafranca Iturre E, Salgado Pascual E. Quality of Life assessment through the EORTC questionnaires of locally advanced rectal cancer patients treated with preoperative chemo-radiotherapy. *Clin Transl Oncol* 2006; **8**: 423-429 [PMID: 16790395]

25 **Song PH**, Yun SM, Kim JH, Moon KH. Comparison of the erectile function in male patients with rectal cancer treated by preoperative radiotherapy followed by surgery and surgery alone. *Int J Colorectal Dis* 2010; **25**: 619-624 [PMID: 20169350 DOI: 10.1007/s00384-010-0879-8]

26 **Peng J**, Shi D, Goodman KA, Goldstein D, Xiao C, Guan Z, Cai S. Early results of quality of life for curatively treated rectal cancers in Chinese patients with EORTC QLQ-CR29. *Radiat Oncol* 2011; **6**: 93 [PMID: 21835046 DOI: 10.1186/1748-717X-6-93]

P- Reviewer: Hoensch HPP, Pellino G **S- Editor**: Ma YJ
L- Editor: Ma JY **E- Editor**: Wang CH

World Journal of Gastroenterology

Submit a Manuscript: http://www.wjgnet.com/esps/

World J Gastroenterol 2017 March 14; 23(10): 1899-1908

DOI: 10.3748/wjg.v23.i10.1899

ISSN 1007-9327 (print) ISSN 2219-2840 (online)

SYSTEMATIC REVIEWS

Microbiome and pancreatic cancer: A comprehensive topic review of literature

Natalie Ertz-Archambault, Paul Keim, Daniel Von Hoff

Natalie Ertz-Archambault, Department of Internal Medicine, Mayo School of Graduate Medical Education, Mayo Clinic Arizona, Scottsdale, AZ 85259, United States

Paul Keim, Pathogen Genomics Division, Translational Genomics Institute and Regents Northern Arizona University, Flagstaff, AZ 86001, United States

Daniel Von Hoff, Translational Genomics Institute (TGen), Mayo Clinic Arizona, Scottsdale, AZ 85259, United States

Author contributions: Von Hoff D served as principal investigator, project visionary, and reviewed several drafts of this manuscript; Keim P reviewed manuscript drafts and edited each revision; Ertz-Archambault N performed the background literature research and wrote the manuscript.

Conflict-of-interest statement: All the authors declare that they have no competing interests.

Data sharing statement: This manuscript represents comprehensive topic review from published manuscript on topic as indicated in methods section. Prior drafts and PDF versions of articles utilized as referenced in citation section are available with first author on request ertz-archambault.natalie@mayo.edu. No additional data are available.

Manuscript source: Unsolicited manuscript

Correspondence to: Natalie Ertz-Archambault, MD, Department of Internal Medicine, Mayo School of Graduate Medical Education, Mayo Clinic Arizona, 13400 E Shea Blvd, Scottsdale, AZ 85259, United States. ertz.natalie@mayo.edu

Telephone: +1-480-3019824
Fax: +1-480-3014171

Received: October 4, 2016
Peer-review started: October 7, 2016
First decision: October 28, 2016
Revised: December 6, 2016
Accepted: December 21, 2016
Article in press: December 21, 2016
Published online: March 14, 2017

Abstract

AIM

To review microbiome alterations associated with pancreatic cancer, its potential utility in diagnostics, risk assessment, and influence on disease outcomes.

METHODS

A comprehensive literature review was conducted by all-inclusive topic review from PubMed, MEDLINE, and Web of Science. The last search was performed in October 2016.

RESULTS

Diverse microbiome alterations exist among several body sites including oral, gut, and pancreatic tissue, in patients with pancreatic cancer compared to healthy populations.

CONCLUSION

Pilot study successes in non-invasive screening strategies warrant further investigation for future translational application in early diagnostics and to learn modifiable risk factors relevant to disease prevention. Pre-clinical investigations exist in other tumor types that suggest microbiome manipulation provides opportunity to favorably transform cancer response to existing

treatment protocols and improve survival.

Key words: Pancreatic Cancer; Human microbiome; Biomarkers, cancer; Cancer screening tests; Treatment effectiveness

Core tip: Recent literature reports influences of microbiome alterations contributing to carcinogenesis of pancreatic cancer. The poor prognostics of pancreatic cancer are related to late recognition and treatment resistance, thus warranting investigations for modifiable risk factors, early screening biomarkers, and microenvironment elements that affect outcomes. Learning the role of microbiome in carcinogenesis may lead to identifying reliable, non-invasive screening strategies, and additional modifiable risk factors. Microbiome studies in pancreatic cancer could offer therapeutic targets and an extraordinary opportunity to favorably transform cancer response to existing treatment protocols and improve survival by reduction of cancer-related cachexia by manipulating human gut microbiota.

Ertz-Archambault N, Keim P, Von Hoff D. Microbiome and pancreatic cancer: A comprehensive topic review of literature. *World J Gastroenterol* 2017; 23(10): 1899-1908 Available from: URL: http://www.wjgnet.com/1007-9327/full/v23/i10/1899.htm DOI: http://dx.doi.org/10.3748/wjg.v23.i10.1899

INTRODUCTION

A commensal microbiome, by definition maintains a symbiotic relationship in healthy individuals, offering protection from disease by nutritive, inflammatory-modulating activity, hormonal homeostasis, detoxification, and metabolic effects of bacterial metabolites[1-3]. Dysbiosis is the manifestation of a corrupt, imbalanced microbiome, which contributes to pathogenesis of several diseased states[2]. Recently, there are literature reports on influences of microbiome alteration contributing to carcinogenesis of multiple malignancies[1,2,4-6]. A classic pathogen in the literature is *Helicobacter pylori* (*H. pylori*), which has revealed inconsistent and paradoxical associations pending the body site studied[7,8]. *H. pylori* has been extensively scrutinized as a risk factor for development of pancreatic cancer and an association is controversial[9-12]. Pancreatic cancer often denotes a poor clinical prognosis in part due to late recognition and treatment resistance, warranting investigations for modifiable risk factors, early screening biomarkers, and microenvironment elements that affect outcomes[13,14].

MATERIALS AND METHODS

Search methods: PubMed, MEDLINE, and Web of Science for medical search terms: "pancreatic cancer" and "microbiome," "carcinogenesis," antibiotic," "probiotic," "microorganism," "bacteria," "colonization," "cachexia," or "infection." The relevant articles reference lists were also searched manually for additional articles. The last search was performed in October 2016.

Selection criteria: Manuscripts and abstracts describing pre-clinical studies, animal models, epidemiological studies, case series, case-control, retrospective chart reviews, prospective studies, pilot, meta-analysis, and literature topic reviews were included. There were no randomized clinical trials identified from these search terms. Articles were limited to abstract and manuscript publications in the English written language.

RESULTS

Characterization of the healthy microbiome spectrum is ongoing. In 2012, the NIH Human Microbiome Project[3], demonstrated no microbial taxa were universally present across all humans in a single body site. The oral cavity contains an extensive reservoir of bacteria with more than 700 species observed, most of which have not been cultured in a laboratory[15,16]. Healthy oral habitats are dominated by Streptococcus, followed by Haemophilus in the buccal mucosa, Actinomyces in the supragingival plaque, and Prevotella in adjacent, low-oxygen subgingival region[3].

Oral microbiome and pancreatic cancer

Alterations in the ecological balance of the microbiome exist during diseased oral cavity states including gingivitis and periodontal disease compared to a healthy oral cavity[16-20]. Periodontal disease, manifested by an inflamed oral activity, pathogenic oral flora, and tooth loss are well-established independent risk factors associated with development of pancreatic cancer[21-23]. Therefore, the shifts in taxa dominance and diversity of bacterial communities that deviate from an established healthy microbiome may be reflective of disease states[2,3]. Pilot studies have proposed a role in oral pathogenic bacteria in periodontal disease as an early screening test and as a biomarker of pancreatic cancer[12,24,25]. Several dedicated studies have aimed to define microbiome changes in the oral cavity associated with pancreatic cancer, results are summarized in Table 1.

Oral microbiome and pancreatic cancer summary

Oral flora alterations exist in pancreatic cancer patients compared to healthy populations. Salivary RNA studies reveal *bacteroides* genus and *Granulicatella adiacens* are more common in pancreatic cancer patients than healthy subjects[12,24]. However, *Neisseria elongata*, *Streptococcus mitis*, *Corynebacterium* genus, and the *Aggregatibacter* genus are present in lower concentrations in pancreatic cancer than

Table 1 Oral microbiome and pancreatic cancer

Ref.	Study design	Case No.	Control No.	Detection Method	Bacteria association	Outcome	Author conclusion
Michaud *et al*[18], 2013, Western Europe	Prospective	405	416	Plasma IgG	*Porphyromonas gingivalis* ATTC 53978	High titer *P. gingivalis* (IgG > 200 ng/mL) OR 2.14 *P* = 0.05	Two fold increase in pancreatic cancer among individuals with high titer *P. gingivalis*
					High titer, *commensal* bacteria	OR = 0.55 95%CI: 0.36-0.83	45% lower risk of pancreatic cancer compared to individuals with lower antibody levels
Farrell *et al*[12], 2012, United States	Case-control	28	28	Salivary qPCR, Microarray	*Neisseria elongata* and *Streptococcus mitis*	*N. elongata* and *S. mitis* significantly decreased ROC-plot AUC 0.90; 95%CI: 0.78-0.96, *P* < 0.0001	*N. elongate* and *S. mitis* combination ROC plot AUC 0.90 serves as 96% sensitive, 82% specific biomarker for pancreatic ca *vs*. healthy subjects
					Granulicatella adiacens	*G. adiacens* Significantly elevated compared to healthy control	
Lin *et al*[24], 2013, United States	Pilot	13	12	Salivary rRNA	*Bacteroides genus*	More common pancreatic cancer patient *vs* healthy subjects *P* = 0.002	Oral flora alterations in microbiome in pancreatic cancer exist compared to healthy individuals
					Corynebacterium genus *Aggregatibacter* genus	Less common in pancreatic cancer *vs* healthy subjects *P* = 0.033 and 0.019	
Torres *et al*[25], 2015 United States	Cross-sectional	8	22	Salivary rRNA, PCR	Higher *Leptotrichia* and lower *Porphyromonas* colonization	*Lepotrichia:Porphyromonas* ratio elevated in pancreatic cancer *vs* healthy control *P* = 0.001	L:P ratio may be reliable biomarker for pancreatic cancer diagnosis
Fan *et al*[26], 2016 United States	Nested Case control	361	371	Salivary rRNA gene sequencing	Oral pathogens *P. gingivalis*, *A. actinomycetemcomitans*	*P. gingivalis* AOR = 1.60 (95%CI: 1.15-2.22) *A. actinomycetes* OR = 2.20 (95%CI: 1.16-4.18)	Presence of oral pathogens are related to subsequent increased risk of pancreatic cancer. On contrary, *Fusobacteria* and *Leptotrichia* are associated with dose or concentration dependent decrease risk of pancreatic cancer
					Fusobacteria and *Leptotrichia*	*Fusobacteria* decreased risk OR per percent increase of relative Abundance OR = 0.94 (95%CI: 0.89-0.99) *Lepotrichia* OR = 0.87 (95%CI: 0.79-0.95)	

healthy subjects[12,24]. Combining salivary RNA biomarkers for *N. elongata* and *S. mitis* yielded an ROC-plot AUC value of 0.90 with 96.4% sensitivity and 82.1% specificity in distinguishing patients with pancreatic cancer from healthy subjects[12]. A cross-sectional study[25] identified of a significantly higher *Leptotrichia* and lower *Porphyromonas* colonization in pancreatic cancer patient saliva, translating to an *Leptotrichia:Porphyromonas* (L:P) ratio of biomarker significance. In this same study, a patient classified with an unknown digestive disease presented with an elevated L:P ratio that led to dedicated workup revealing a new diagnosis of pancreatic cancer[25]. Pilot successes deserve further exploration into utilizing salivary markers as potentially valuable non-invasive, economical screening strategies.

Interestingly, the highest concentration of plasma antibodies *to Porphyromonas gingivalis* (strain ATTC 53978), a pathogenic bacteria associated with periodontal disease, was linked with a 2-fold increased risk of pancreatic cancer[18]. The association was amplified over time, with the addition of 5 or 7 year lag[18]. Similar to case control studies of saliva samples revealing oral pathogens, *P. gingivalis* and *A. actinomycetemcomitans* are associated with increased risk for subsequent development of pancreatic cancer[26]. This finding is consistent with epidemiologic data that periodontal disease is an independent risk factor for pancreatic cancer development[20,23,27]. Alternatively, high antibody titers against non-pathogenic, commensal bacteria were associated with 45% decreased risk of pancreatic cancer compared to those with a lower antibody level profile[18]. Similarly *Fusobacterium* and *Lepotrichia* are protective and decreases risk, also in a dose dependent relationship[26]. *Lactobacillus* is a commensal oral cavity bacterium that diminishes gingival inflammation and cariogenic periodontal pathogenic bacteria[28]. Thus,

with the clearly established role of periodontal disease and associated periodontal pathogens for pancreatic cancer risk profiles, any measures to prevent periodontal pathogens may serve protective role to prevent pancreatic cancer, but has not been studied on this topic specifically.

H. pylori and pancreatic cancer

There is literature that illustrates a paradoxical nature of microorganisms relative to by site and tumor studied. For example, eradication of *H. pylori* causes regression of MALT lymphoma and decreases risk of metachronous gastric carcinoma after endoscopic resection for early stage gastric cancer[1,29]. However, *H. pylori* gastric colonization decreases the risk of oesophageal adenocarcinoma that does not involve the gastric cardia[30]. *H. pylori* is a diverse bacteria with several virulent strain variations. Among the best studied are *Cytotoxin-associated gene A* (*Cag-A*) positive strains that express Cag-A virulence factor, which is linked to gastric inflammation, ulceration, and promoting malignant transformation in gastric cancer[31,32]. *H. pylori* and *Cag-A* dominate microbiome studies in pancreatic cancer. Study results are variable and complex, as is noted in Table 2[9-11,33-42].

H. pylori and pancreatic cancer summary

Results from *H. pylori* case studies in pancreatic cancer reveals complex mixed results pending virulence strain *cag-A* status. Consensus from recent meta-analysis is that there is a modestly significant increased risk associated with development of pancreatic cancer for *cag-A*-negative *H. pylori* strain[9-11,39], with positive correlated adjustment factors including non-O blood type[37,43] and active smoking status[34,36]. The general literature trend summarized in Table 2 is *cag-A*-positive strains results in decreased risk or non-significant association with pancreatic cancer. Notable global population differences exist as the majority of studies highlighted in this review are mainly relevant to Western European or North American ethnic groups. The results of one meta-analysis addressing global studies[41] and pancreatic cancer risk including two Eastern Asian population case-cohorts that suggest a decreased risk of pancreatic cancer risk for *H. pylori* seropositivity overall, including *Cag-A*-positive strains in Eastern Asian ethnic region[41].

Tissue microbiome and pancreatic cancer

We found three human pancreatic adenocarcinoma tissue studies dedicated to microbiome alterations or their effect on the tumor microenvironment (Table 3[44-46]).

Tissue microbiome and pancreatic cancer summary

In one case control study, enteric strains of *Helicobacter* DNA were demonstrated to colonize the pancreas in 75% of adenocarcinoma patients but not in pancreatic controls with benign disease[44]. Among proposed mechanisms for dissemination may result from hepatobiliary translocation or hematogenous seeding[44,46]. However, DNA of different *Helicobacter* species is mutually exclusive by sampled site[44]. For example, *Helicobacter* identified in the pancreas compared with *Helicobacter* of gastroduodenal tissue of the same patient were different *Helicobacter* subspecies[44]. Thus, dissemination of *H. pylori* from the stomach to the pancreas is unlikely, instead a subspecies tissue tropism may exist[44].

Both direct microbe colonization and downstream proliferative metabolic affects may promote tumor-associated inflammation preserved by low-grade chronic inflammation[6,29,47]. Evidence of this effect in a pre-clinical study of human a pancreatic cell line showed *H. pylori* colonization of a human pancreatic cell line expressed increased factors for malignant potential including proliferative factors, NF-kappa-B, activator protein-1, proflammatory IL-8 activity, vascular endothelial growth factor secretion, and the growth factor promoter, serum response element[45]. The overall result is activation of molecular pathways for tumor growth and progression in the setting of *H. pylori* infection[45].

Fusobacterium is an anaerobic, oral bacterium that has been identified in pancreatic abscesses and carries unfavorable prognostic implications in some gastrointestinal cancers[46]. To explore a role for *Fusobacterium* in pancreatic cancer, surgical specimens of pancreatic adenocarcinoma were analyzed for presence of this bacterium. Only 8% of specimens in this cohort contained *Fusobacterium* colonization[46]. However, pancreatic ductal adenocarcinoma surgical specimens with presence of *Fusobacterium* colonization was identified as an independent predictive factor for shorter survival compared to *Fusobacterium* negative tumors[46]. The *fusobacterium* positive sample group also demonstrated 28% detection of paired normal tissue[46]. The presence of *Fusobacterium* in normal tissue margin suggests it may contribute to malignant potential, but this theory requires further exploration[46].

DISCUSSION

The oral microbiome has a protective role against pancreatic cancer in a healthy, commensal state, but may promote malignancy in a pathologic state[1,2,4-6,12,18,24,25]. Shifts in taxa dominance and diversity of oral bacterial communities, especially those reflective of periodontal disease are associated with increased pancreatic cancer risk[12,18,24,25]. This correlates clinically with periodontal disease status, a validated independent risk factor for development of pancreatic cancer[21-23]. Bacterial markers of periodontal disease[18] and shifts in microbial taxa diversity[12,24,25] have promising potential to serve as non-invasive screening biomarkers of pancreatic cancer. The evidence is strong enough to

Table 2 ***Helicobacter pylori*** **and pancreatic cancer**

Ref.	Study Design	Case No.	Control No.	Detection Method	Bacteria association	Outcome	Author conclusion
Raderer *et al*[33], 1998, Austria	Case-control	92	27	Plasma IgG ELISA	*H. pylori*	OR = 2.1 95%CI: 1.1-4.1 *P* = 0.035	*H. pylori* seropositivity prominent in pancreatic cancer patients compared with colorectal cancer combined with normal controls
Stolzenberg-Solomon *et al*[34] 2001, Finland	Nested case-control	121	226	Plasma IgG ELISA	cytotoxin-associated gene-A (CagA) virulence factor and *H. pylori*	*H. pylori* OR = 1.87; 95%CI: 1.05-3.34 CagA+ strains OR = 2.01; 95%CI: 1.09-3.70	Male smokers seropositive for *H. pylori* were nearly twice as likely to develop pancreatic cancer compared to seronegative. Stronger influence adjusting for years of smoking
de Martel *et al*[35], 2008, United States	Nested Case-control	104	262	Plasma IgG ELISA	cytotoxin-associated gene-A (CagA) virulence factor and *H. pylori*	*H. pylori* OR = 0.85; 95%CI: 0.49-1.48 CagA+ OR = 0.96; 95%CI: 0.48-1.92	*H. pylori* infection is not associated with development of pancreatic cancer
Lindkvist *et al*[36], 2008, Sweden	Nested Case-control	87	263	Plasma IgG ELISA	*H. pylori*	*H. pylori* overall OR = 1.25 95%CI: 0.75-2.09 *H. pylori* in Never smokers AOR = 3.81 95%CI: 1.06-13.63	Adjusted risk for development of pancreatic cancer highly increased in never-smokers seropositive for *H. pylori*
Risch *et al*[37] 2010, United States	Case-control	373	690	Plasma IgG ELISA	cytotoxin-associated gene-A (CagA) virulence factor and *H. pylori*	CagA negative *H. pylori* non-O blood group OR = 2.78, 95%CI: 1.49-5.20, *P* = 0.0014; CagA negative *H. pylori* O-blood group OR = 1.28, 95%CI: 0.62-2.64, *P* = 0.51	CagA-negative *H. pylori* seropositivity is a risk factor for pancreatic cancer among individuals with non–O blood type
Trikudanathan *et al*[11], 2011	Meta-analysis	822	1513	meta-analysis of 6 case control studies	*H. pylori*	AOR = 1.38, 95%CI: 1.08-1.75	Significant positive association between the presence of *H. pylori* infection and pancreatic cancer.
Gawin *et al*[38], 2012, Poland	Case-control	139	177	Plasma IGg, ELISA, western blot	cytotoxin-associated gene-A (CagA) virulence factor and *H. pylori*	*H. pylori* OR = 1.27; 95%CI: 0.64-2.61 *P* = 0.514 CagA+ OR = 0.90; 95%CI: 0.46-1.73, *P* = 0.744	No association between seropositivity of *H. pylori* or CagA with development of pancreatic cancer
Xiao *et al*[39], 2013	Meta-analysis	1083	1950	meta-analysis of 9 case-control studies	cytotoxin-associated gene-A (CagA) virulence factor and *H. pylori*	*H. pylori* Overall OR = 1.47 95%CI: 1.22-1.77 Adjusted for "High quality" studies AOR = 1.28; 95%CI: 1.01-1.63 Adjusted for CagA positive AOR = 1.47; 95%CI: 0.79-2.57	Borderline positive association *H. pylori* seropositivity overall. Adjusted risk for high quality studies revealed a significant, but modest association. CagA virulence seropositivity was not associated with pancreatic cancer
Yu *et al*[40], 2013, Finland	Case-control	353	353	multiplex serology to 4 *H. pylori* antigens	*H. pylori*	OR = 0.85; 95%CI: 0.49 -1.49	No association between seropositivity of *H. pylori* with development of pancreatic cancer

Wang *et al*[41], 2014	Meta-analysis	2049	2861	Meta-analysis of 9 case-control studies (2 non- English language)	cytotoxin-associated gene-A (CagA) virulence factor and *H. pylori*	*H. pylori* overall OR = 1.06, 95%CI: 0.74-1.37 Eastern Asian Population *H. pylori* OR = 0.62, 95%CI: 0.49-0.76 Cag-A positive OR = 0.66, 95%CI: 0.52-0.80 Western European population *H. pylori* OR = 1.14 95%CI: 0.89-1.40 Cag-A positive OR = 0.84 95%CI: 0.63-1.04	Eastern Asian populations demonstrate significant decreased risk pancreatic cancer associated with *H. pylori* seropositivity. No association present in Western populations
Risch *et al*[42], 2014, Shanghai	Case-control	761	794	Plasma IGg, ELISA	cytotoxin-associated gene-A (CagA) virulence factor and *H. pylori*	Cag-A positive *H. pylori* AOR = 0.68; 95%CI: 0.54-0.84 Cag-A negative *H. pylori* AOR = 1.28; 95%CI: 0.76-2.13	Decreased pancreas-cancer risk was seen for CagA positive *H. pylori* compared to seronegativity for both *H. pylori* and CagA. A modest increased risk for CagA-negative *H. pylori* seropositivity
Chen *et al*[9], 2015	Meta-analysis	1446	2236	meta-analysis of 5 case control studies	cytotoxin-associated gene-A (CagA) virulence factor and *H. pylori*	Overall OR = 0.99; 95%CI: 0.65-1.50 CagA+ OR = 0.92; 95%CI: 0.65 -1.3 Virulent strain infection OR = 0.97 95%CI: 0.50-1.89 Nonvirulent infection OR = 1.47 95%CI: 1.11-1.96	CagA-negative, nonvirulent strains of *H. pylori* may be a risk factor for pancreatic cancer. No association with seropositivity for *H. pylori* infection overall, nor when adjusted for CagA or virulent strain infection
Schulte *et al*[10], 2015	Combination Case-control and meta-analysis	580	626	Plasma IGg, ELISA and meta-analysis of 10 case-control studies	cytotoxin-associated gene-A (CagA) virulence factor and *H. pylori*	*H. pylori* overall OR = 1.00 95%CI: 0.74-1.35 Cag-A negative AOR = 1.23 95%CI: 0.83-1.82 Cag-A positive OR = 0.74 95%CI: 0.48-1.15	No overall association observed for *H. pylori* seropositivity and risk of pancreatic cancer, but evidence of non-significant CagA strain-specific associations

warrant targeted risk reduction strategies in patient education and modifiable lifestyle counseling regarding maintenance of oral hygiene.

A directly carcinogenic role for *H. pylori* has been explored after discovering enteric strains of *Helicobacter* DNA demonstrated to colonize the pancreas in a majority of sampled pancreatic adenocarcinoma but not in patients with benign disease[44]. A preclinical study[45] examined direct *H. pylori* colonization and associated activation of molecular pathways for tumor growth and progression[45]. These downstream molecular effects highlight oncogenic potential with microbiome influence that promotes tumor-associated inflammation preserved by low-grade chronic inflammation[6,29,47]. Despite the existence of several proposed carcinogenic mechanisms of dysbiosis, inflammation is a central facilitator illustrated in pancreatic cancer murine models, human cell lines, and tumor translational expression profiles[6].

Future directions

There have been studies that indicate the microbiome and antibiotics modulate tumor response to chemotherapy[48,49]. Germ-free and antibiotic treated murine models highlight the protective effect of commensal bacteria by shaping the inflammatory network required for favorable response to anti-tumor therapy[48]. In murine models, platinum therapy eliminated most subcutaneous lymphoma tumors and prolonged survival in control mice[48]. However, antibiotic-treated and germ free mice failed to respond to platinum-treatment, in part by decreasing reactive oxygen species[48]. Similarly, CTLA-4 inhibitor treated murine models with sarcoma suggest that gut microbiota, specifically *bacteroides* subspecies, are required for the successful anti-tumor effects

Table 3 Tissue microbiome and pancreatic cancer

Ref.	Study design	Case sample size	Detection method and sample	Bacteria association	Outcome	Author conclusion
Nilsson *et al*[44], 2006, Sweden	Case-control	84	DNA genus specific PCR, surgical specimen	*H. pylori*	*Helicobacter* DNA detected in pancreas of 75% patients with adenocarcinoma, but not detected in any control	*Helicobacter* DNA, mostly *H. pylori* genus, commonly detected in pancreatic cancer
Takayama *et al*[45], 2007, Japan	Abstract	-	ELISA and western blot, Pre-clinical cell line	*H. pylori*	IL-8 and VEGF secretion and proliferation factors NF-kappa-B, AP-1, and serum response element of human pancreatic cells increased by *H. pylori* infection	*H. pylori* infection of human pancreatic cells may increase malignant potential of pancreatic cells
Mitsuhashi *et al*[46], 2015, Japan	Case-control	283	PCR, surgical specimen	Fusobacterium	Detected in 8.8% cases. Median cancer-survival (mo) positive *vs* negative detection 17.2 *vs* 32.5 for log-rank $P = 0.021$	significantly shorter survival observed in the *Fusobacterium* species-positive group

of CTLA-4 blockade[49]. Notably, antibiotic and germ free mice with sarcomas do not respond to CTLA-4 inhibitor at baseline, but recover antitumor activity with recolonization of gut commensals by human fecal microbiota transplantation of specific *bacteroides* subspecies[49]. Oral administration of *Bifidobacterium* in murine models with melanoma augments the immune response to tumor cells, in part by dendritic cell activation of the innate immune system[49]. This effect was not observed with administration of *lactobacillus* species, suggesting a complex, species specific modulation of the immune system *in vivo*[49]. The potential to utilize probiotics in humans to amplify antitumor response to existing chemotherapy and immunotherapy protocols requires further investigation[50].

Anti-tumor therapy and commensal flora collaborate in part, by loss of TNF-dependent early tumor necrosis response, down-regulation of inflammatory cytokines, phagocytosis, antigen presentation, and adaptive immune response gene expression controlling tissue development and cancer[48]. The loss of commensal organisms by antibiotics and the possibility of carcinogenic promoting effects of antibiotics have been explored. The risk related to pancreatic cancer seems limited to the penicillin class, especially with more than five courses, but this risk diminishes over time[51]. Macrolides, cephalosporins, tetracyclines, antivirals, and antifungals were not associated with increased risk of pancreatic cancer[51]. The impact of antibiotics on commensal framework may explain the need for repeated antibiotic exposures, leading to an enduring change in bacterial community diversity[51]. Murine models demonstrate *lactobacillus* was among quickest flora to recover in the gut after antibiotic therapy. However, the effect of antibiotics on the gut microbiome is enduring at four weeks after exposure; the population is deficient, and not reflective of its healthy, baseline, pre-antibiotic diversity[48].

Commensal bacteria offer protection from disease by inflammatory-modulating activity as above, but also by hormonal homeostasis, detoxification, and metabolic effects of bacterial metabolites. For example, murine models show *lactobacilli* are consistently reduced in cachectic mouse models[52]. A *lactobacilli* cocktail combination with prebiotic substrate that supports growth of microorganisms, changes the dysbiotic populations of cecal microbiota composition in murine models, clinically resulting in improved survival and reduction of cachexia[53]. These are highly important implications in pancreatic adenocarcinoma population since these patients carry the strongest burden of cancer cachexia among all malignancies, present in up to 80% of patients[54,55] resulting in reduced survival and progressive disease[55-57]. Weight stabilization alone significantly proven to improve survival in pancreatic adenocarcinoma patients with unresectable disease[58].

In conclusion, the initial motive to explore microbiome role in carcinogenesis may lead to identifying reliable non-invasive screening strategies and discern additional modifiable risk factors. With further investigation, potentially microbiome studies in pancreatic cancer could offer therapeutic targets. Perhaps the most extraordinary opportunity is to favorably transform cancer response to existing treatment protocols and improve survival by reduction of cancer-related cachexia by manipulating human gut microbiota.

COMMENTS

Background

Recently, there are literature reports on influences of microbiome alteration contributing to carcinogenesis of multiple malignancies. Among the most controversial is dysbiosis related to pancreatic cancer. Pancreatic cancer often denotes a poor clinical prognosis in part due to late recognition and treatment resistance, warranting investigations for modifiable risk factors, early screening biomarkers, and microenvironment elements that affect patient outcomes.

Research frontiers

Murine models demonstrate commensal microbiome taxa modulates a favorable tumor response to chemotherapy in multiple tumor types In addition, manipulation of cecal microbiome composition with lactobacillus in murine models, have resulted in improved survival and reduction of cachexia a clinically significant burden in the majority of pancreatic cancer patients.

Innovations and breakthroughs

This review article serves to update literature on microbiome alterations associated with pancreatic cancer, its potential utility as an early screening biomarker, examine the influence of the microbiome in antitumor therapy, and the potential impact of microbiome manipulation to affect pancreatic cancer patient outcomes.

Applications

Exploring the microbiome role in carcinogenesis may lead to identifying reliable non-invasive screening strategies and discern additional modifiable risk factors. With further investigation, potentially microbiome studies in pancreatic cancer could offer therapeutic targets. Perhaps the most extraordinary opportunity is to favorably transform cancer response to existing treatment protocols and improve survival by reduction of cancer-related cachexia by manipulating human gut microbiota.

Peer-review

This review describes the relationships between microbiome and pancreatic cancer. The data in this report is of considerable importance in investigations for modifiable risk factors of pancreatic cancer.

REFERENCES

1 **Vogtmann E**, Goedert JJ. Epidemiologic studies of the human microbiome and cancer. *Br J Cancer* 2016; **114**: 237-242 [PMID: 26730578 DOI: 10.1038/bjc.2015.465]

2 **Sheflin AM**, Whitney AK, Weir TL. Cancer-promoting effects of microbial dysbiosis. *Curr Oncol Rep* 2014; **16**: 406 [PMID: 25123079]

3 **Human Microbiome Project Consortium**. Structure, function and diversity of the healthy human microbiome. *Nature* 2012; **486**: 207-214 [PMID: 22699609 DOI: 10.1038/nature11234]

4 **Sears CL**, Pardoll DM. Perspective: alpha-bugs, their microbial partners, and the link to colon cancer. *J Infect Dis* 2011; **203**: 306-311 [PMID: 21208921 DOI: 10.1093/jinfdis/jiq061]

5 **Zhu Q**, Gao R, Wu W, Qin H. The role of gut microbiota in the pathogenesis of colorectal cancer. *Tumour Biol* 2013; **34**: 1285-1300 [PMID: 23397545 DOI: 10.1007/s13277-013-0684-4]

6 **Zambirinis CP**, Pushalkar S, Saxena D, Miller G. Pancreatic cancer, inflammation, and microbiome. *Cancer J* 2014; **20**: 195-202 [PMID: 24855007 DOI: 10.1097/PPO.0000000000000045]

7 **Fukase K**, Kato M, Kikuchi S, Inoue K, Uemura N, Okamoto S, Terao S, Amagai K, Hayashi S, Asaka M. Effect of eradication of Helicobacter pylori on incidence of metachronous gastric carcinoma after endoscopic resection of early gastric cancer: an open-label, randomised controlled trial. *Lancet* 2008; **372**: 392-397 [PMID: 18675689 DOI: 10.1016/S0140-6736(08)61159-9]

8 **Pakodi F**, Abdel-Salam OM, Debreceni A, Mózsik G. Helicobacter pylori. One bacterium and a broad spectrum of human disease! An overview. *J Physiol Paris* 2000; **94**: 139-152 [PMID: 10791696]

9 **Chen XZ**, Wang R, Chen HN, Hu JK. Cytotoxin-Associated Gene A-Negative Strains of Helicobacter pylori as a Potential Risk Factor of Pancreatic Cancer: A Meta-Analysis Based on Nested Case-Control Studies. *Pancreas* 2015; **44**: 1340-1344 [PMID: 26390415 DOI: 10.1097/MPA.0000000000000414]

10 **Schulte A**, Pandeya N, Fawcett J, Fritschi L, Risch HA, Webb PM, Whiteman DC, Neale RE. Association between Helicobacter pylori and pancreatic cancer risk: a meta-analysis. *Cancer Causes Control* 2015; **26**: 1027-1035 [PMID: 25951801 DOI: 10.1007/s10552-015-0595-3].]

11 **Trikudanathan G**, Philip A, Dasanu CA, Baker WL. Association between Helicobacter pylori infection and pancreatic cancer. A cumulative meta-analysis. *JOP* 2011; **12**: 26-31 [PMID: 21206097]

12 **Farrell JJ**, Zhang L, Zhou H, Chia D, Elashoff D, Akin D, Paster BJ, Joshipura K, Wong DT. Variations of oral microbiota are associated with pancreatic diseases including pancreatic cancer. *Gut* 2012; **61**: 582-588 [PMID: 21994333 DOI: 10.1136/gutjnl-2011-300784]

13 **Whatcott CJ**, Han H, Von Hoff DD. Orchestrating the Tumor Microenvironment to Improve Survival for Patients With Pancreatic Cancer: Normalization, Not Destruction. *Cancer J* 2015; **21**: 299-306 [PMID: 26222082 DOI: 10.1097/PPO.0000000000000140]

14 **Von Hoff DD**, Korn R, Mousses S. Pancreatic cancer--could it be that simple? A different context of vulnerability. *Cancer Cell* 2009; **16**: 7-8 [PMID: 19573807 DOI: 10.1016/j.ccr.2009.06.011]

15 **Meurman JH**. Oral microbiota and cancer. *J Oral Microbiol* 2010; **2** [PMID: 21523227 DOI: 10.3402/jom.v2i0.5195]

16 **Aas JA**, Paster BJ, Stokes LN, Olsen I, Dewhirst FE. Defining the normal bacterial flora of the oral cavity. *J Clin Microbiol* 2005; **43**: 5721-5732 [PMID: 16272510 DOI: 10.1128/JCM.43.11.5721-5732.2005]

17 **Michaud DS**, Izard J. Microbiota, oral microbiome, and pancreatic cancer. *Cancer J* 2014; **20**: 203-206 [PMID: 24855008 DOI: 10.1097/PPO.0000000000000046]

18 **Michaud DS**, Izard J, Wilhelm-Benartzi CS, You DH, Grote VA, Tjønneland A, Dahm CC, Overvad K, Jenab M, Fedirko V, Boutron-Ruault MC, Clavel-Chapelon F, Racine A, Kaaks R, Boeing H, Foerster J, Trichopoulou A, Lagiou P, Trichopoulos D, Sacerdote C, Sieri S, Palli D, Tumino R, Panico S, Siersema PD, Peeters PH, Lund E, Barricarte A, Huerta JM, Molina-Montes E, Dorronsoro M, Quirós JR, Duell EJ, Ye W, Sund M, Lindkvist B, Johansen D, Khaw KT, Wareham N, Travis RC, Vineis P, Bueno-de-Mesquita HB, Riboli E. Plasma antibodies to oral bacteria and risk of pancreatic cancer in a large European prospective cohort study. *Gut* 2013; **62**: 1764-1770 [PMID: 22990306 DOI: 10.1136/gutjnl-2012-303006]

19 **Berezow AB**, Darveau RP. Microbial shift and periodontitis. *Periodontol 2000* 2011; **55**: 36-47 [PMID: 21134227 DOI: 10.1111/j.1600-0757.2010.00350.x]

20 **Ahn J**, Segers S, Hayes RB. Periodontal disease, Porphyromonas gingivalis serum antibody levels and orodigestive cancer mortality. *Carcinogenesis* 2012; **33**: 1055-1058 [PMID: 22367402 DOI: 10.1093/carcin/bgs112]

21 **Hujoel PP**, Drangsholt M, Spiekerman C, Weiss NS. An exploration of the periodontitis-cancer association. *Ann Epidemiol* 2003; **13**: 312-316 [PMID: 12821269]

22 **Stolzenberg-Solomon RZ**, Dodd KW, Blaser MJ, Virtamo J, Taylor PR, Albanes D. Tooth loss, pancreatic cancer, and Helicobacter pylori. *Am J Clin Nutr* 2003; **78**: 176-181 [PMID: 12816788]

23 **Michaud DS**, Joshipura K, Giovannucci E, Fuchs CS. A prospective study of periodontal disease and pancreatic cancer in US male health professionals. *J Natl Cancer Inst* 2007; **99**: 171-175 [PMID: 17228001 DOI: 10.1093/jnci/djk021]

24 **Lin IH**, Wu J, Cohen SM, Chen C, Bryk D, Marr M, Melis M, Newman E, Pachter HL, Alekseyenko AV, Hayes RB, Ahn J. Pilot study of oral microbiome and risk of pancreatic cancer. *Cancer Res* 2013; **73** [DOI: 10.1158/1538-7445.AM2013-101]

25 **Torres PJ**, Fletcher EM, Gibbons SM, Bouvet M, Doran KS, Kelley ST. Characterization of the salivary microbiome in patients with pancreatic cancer. *PeerJ* 2015; **3**: e1373 [PMID: 26587342 DOI: 10.7717/peerj.1373]

26 **Fan X**, Alekseyenko AV, Wu J, Peters BA, Jacobs EJ, Gapstur SM, Purdue MP, Abnet CC, Stolzenberg-Solomon R, Miller G, Ravel J, Hayes RB, Ahn J. Human oral microbiome and prospective risk for pancreatic cancer: a population-based nested case-control study. *Gut* 2016; Epub ahead of print [PMID: 27742762 DOI: 10.1136/gutjnl-2016-312580]

27 **Meyer MS**, Joshipura K, Giovannucci E, Michaud DS. A review of the relationship between tooth loss, periodontal disease, and cancer. *Cancer Causes Control* 2008; **19**: 895-907 [PMID: 18478344 DOI: 10.1007/s10552-008-9163-4]

28 **Di Cerbo A**, Palmieri B, Aponte M, Morales-Medina JC, Iannitti T. Mechanisms and therapeutic effectiveness of lactobacilli. *J Clin Pathol* 2016; **69**: 187-203 [PMID: 26578541 DOI: 10.1136/jclinpath-2015-202976]

29 **Suerbaum S**, Michetti P. Helicobacter pylori infection. *N Engl J Med* 2002; **347**: 1175-1186 [PMID: 12374879 DOI: 10.1056/NEJMra020542]

30 **Anderson LA**, Murphy SJ, Johnston BT, Watson RG, Ferguson HR, Bamford KB, Ghazy A, McCarron P, McGuigan J, Reynolds JV, Comber H, Murray LJ. Relationship between Helicobacter pylori infection and gastric atrophy and the stages of the oesophageal inflammation, metaplasia, adenocarcinoma sequence: results from the FINBAR case-control study. *Gut* 2008; **57**: 734-739 [PMID: 18025067 DOI: 10.1136/gut.2007.132662]

31 **Kalaf EA**, Al-Khafaji ZM, Yassen NY, Al-Abbudi FA, Sadwen SN. Study of the cytoxin-associated gene a (CagA gene) in Helicobacter pylori using gastric biopsies of Iraqi patients. *Saudi J Gastroenterol* 2013; **19**: 69-74 [PMID: 23481132 DOI: 10.4103/1319-3767.108474]

32 **Chen S**, Duan G, Zhang R, Fan Q. Helicobacter pylori cytotoxin-associated gene A protein upregulates α-enolase expression via Src/MEK/ERK pathway: implication for progression of gastric cancer. *Int J Oncol* 2014; **45**: 764-770 [PMID: 24841372 DOI: 10.3892/ijo.2014.2444]

33 **Raderer M**, Wrba F, Kornek G, Maca T, Koller DY, Weinlaender G, Hejna M, Scheithauer W. Association between Helicobacter pylori infection and pancreatic cancer. *Oncology* 1998; **55**: 16-19 [PMID: 9428370]

34 **Stolzenberg-Solomon RZ**, Blaser MJ, Limburg PJ, Perez-Perez G, Taylor PR, Virtamo J, Albanes D. Helicobacter pylori seropositivity as a risk factor for pancreatic cancer. *J Natl Cancer Inst* 2001; **93**: 937-941 [PMID: 11416115]

35 **de Martel C**, Llosa AE, Friedman GD, Vogelman JH, Orentreich N, Stolzenberg-Solomon RZ, Parsonnet J. Helicobacter pylori infection and development of pancreatic cancer. *Cancer Epidemiol Biomarkers Prev* 2008; **17**: 1188-1194 [PMID: 18483341 DOI: 10.1158/1055-9965.EPI-08-0185]

36 **Lindkvist B**, Johansen D, Borgström A, Manjer J. A prospective study of Helicobacter pylori in relation to the risk for pancreatic cancer. *BMC Cancer* 2008; **8**: 321 [PMID: 18986545 DOI: 10.1186/1471-2407-8-321]

37 **Risch HA**, Yu H, Lu L, Kidd MS. ABO blood group, Helicobacter pylori seropositivity, and risk of pancreatic cancer: a case-control study. *J Natl Cancer Inst* 2010; **102**: 502-505 [PMID: 20181960 DOI: 10.1093/jnci/djq007]

38 **Gawin A**, Wex T, Ławniczak M, Malfertheiner P, Starzyńska T. [Helicobacter pylori infection in pancreatic cancer]. *Pol Merkur Lekarski* 2012; **32**: 103-107 [PMID: 22590913]

39 **Xiao M**, Wang Y, Gao Y. Association between Helicobacter pylori infection and pancreatic cancer development: a meta-analysis. *PLoS One* 2013; **8**: e75559 [PMID: 24086571 DOI: 10.1371/journal.pone.0075559]

40 **Yu G**, Murphy G, Michel A, Weinstein SJ, Männistö S, Albanes D, Pawlita M, Stolzenberg-Solomon RZ. Seropositivity to Helicobacter pylori and risk of pancreatic cancer. *Cancer Epidemiol Biomarkers Prev* 2013; **22**: 2416-2419 [PMID: 24089457 DOI: 10.1158/1055-9965.EPI-13-0680]

41 **Wang Y**, Zhang FC, Wang YJ. Helicobacter pylori and pancreatic cancer risk: a meta- analysis based on 2,049 cases and 2,861 controls. *Asian Pac J Cancer Prev* 2014; **15**: 4449-4454 [PMID: 24969867]

42 **Risch HA**, Lu L, Kidd MS, Wang J, Zhang W, Ni Q, Gao YT, Yu H. Helicobacter pylori seropositivities and risk of pancreatic carcinoma. *Cancer Epidemiol Biomarkers Prev* 2014; **23**: 172-178 [PMID: 24234587 DOI: 10.1158/1055-9965.EPI-13-0447]

43 **Risch HA**. Pancreatic cancer: Helicobacter pylori colonization, N-nitrosamine exposures, and ABO blood group. *Mol Carcinog* 2012; **51**: 109-118 [PMID: 22162235 DOI: 10.1002/mc.20826]

44 **Nilsson HO**, Stenram U, Ihse I, Wadstrom T. Helicobacter species ribosomal DNA in the pancreas, stomach and duodenum of pancreatic cancer patients. *World J Gastroenterol* 2006; **12**: 3038-3043 [PMID: 16718784 DOI: 10.3748/wjg.v12.i19.3038]

45 **Takayama S**, Takahashi H, Matsuo Y, Okada Y, Manabe T. Effects of Helicobacter pylori infection on human pancreatic cancer cell line. *Hepatogastroenterology* 2007; **54**: 2387-2391 [PMID: 18265671]

46 **Mitsuhashi K**, Nosho K, Sukawa Y, Matsunaga Y, Ito M, Kurihara H, Kanno S, Igarashi H, Naito T, Adachi Y, Tachibana M, Tanuma T, Maguchi H, Shinohara T, Hasegawa T, Imamura M, Kimura Y, Hirata K, Maruyama R, Suzuki H, Imai K, Yamamoto H, Shinomura Y. Association of Fusobacterium species in pancreatic cancer tissues with molecular features and prognosis. *Oncotarget* 2015; **6**: 7209-7220 [PMID: 25797243 DOI: 10.18632/oncotarget.3109]

47 **Bongers G**, Pacer ME, Geraldino TH, Chen L, He Z, Hashimoto D, Furtado GC, Ochando J, Kelley KA, Clemente JC, Merad M, van Bakel H, Lira SA. Interplay of host microbiota, genetic perturbations, and inflammation promotes local development of intestinal neoplasms in mice. *J Exp Med* 2014; **211**: 457-472 [PMID: 24590763 DOI: 10.1084/jem.20131587]

48 **Iida N**, Dzutsev A, Stewart CA, Smith L, Bouladoux N, Weingarten RA, Molina DA, Salcedo R, Back T, Cramer S, Dai RM, Kiu H, Cardone M, Naik S, Patri AK, Wang E, Marincola FM, Frank KM, Belkaid Y, Trinchieri G, Goldszmid RS. Commensal bacteria control cancer response to therapy by modulating the tumor microenvironment. *Science* 2013; **342**: 967-970 [PMID: 24264989 DOI: 10.1126/science.1240527]

49 **Vétizou M**, Pitt JM, Daillère R, Lepage P, Waldschmitt N, Flament C, Rusakiewicz S, Routy B, Roberti MP, Duong CP, Poirier-Colame V, Roux A, Becharef S, Formenti S, Golden E, Cording S, Eberl G, Schlitzer A, Ginhoux F, Mani S, Yamazaki T, Jacquelot N, Enot DP, Bérard M, Nigou J, Opolon P, Eggermont A, Woerther PL, Chachaty E, Chaput N, Robert C, Mateus C, Kroemer G, Raoult D, Boneca IG, Carbonnel F, Chamaillard M, Zitvogel L. Anticancer immunotherapy by CTLA-4 blockade relies on the gut microbiota. *Science* 2015; **350**: 1079-1084 [PMID: 26541610 DOI: 10.1126/science.aad1329]

50 **Sivan A**, Corrales L, Hubert N, Williams JB, Aquino-Michaels K, Earley ZM, Benyamin FW, Lei YM, Jabri B, Alegre ML, Chang EB, Gajewski TF. Commensal Bifidobacterium promotes antitumor immunity and facilitates anti-PD-L1 efficacy. *Science* 2015; **350**: 1084-1089 [PMID: 26541606 DOI: 10.1126/science.aac4255]

51 **Boursi B**, Mamtani R, Haynes K, Yang YX. Recurrent antibiotic exposure may promote cancer formation--Another step in understanding the role of the human microbiota? *Eur J Cancer* 2015; **51**: 2655-2664 [PMID: 26338196 DOI: 10.1016/j.ejca.2015.08.015]

52 **Bindels LB**, Beck R, Schakman O, Martin JC, De Backer F, Sohet FM, Dewulf EM, Pachikian BD, Neyrinck AM, Thissen JP, Verrax J, Calderon PB, Pot B, Grangette C, Cani PD, Scott KP, Delzenne NM. Restoring specific lactobacilli levels decreases inflammation and muscle atrophy markers in an acute leukemia mouse model. *PLoS One* 2012; **7**: e37971 [PMID: 22761662 DOI: 10.1371/journal.pone.0037971]

53 **Bindels LB**, Neyrinck AM, Claus SP, Le Roy CI, Grangette C, Pot B, Martinez I, Walter J, Cani PD, Delzenne NM. Synbiotic approach restores intestinal homeostasis and prolongs survival in leukaemic mice with cachexia. *ISME J* 2016; **10**: 1456-1470 [PMID: 26613342 DOI: 10.1038/ismej.2015.209]

54 **Fearon KC**, Baracos VE. Cachexia in pancreatic cancer: new treatment options and measures of success. *HPB (Oxford)* 2010; **12**: 323-324 [PMID: 20590907 DOI: 10.1111/j.1477-2574.2010.00178.x]

55 **Ronga I**, Gallucci F, Riccardi F, Uomo G. Anorexia-cachexia syndrome in pancreatic cancer: recent advances and new pharmacological approach. *Adv Med Sci* 2014; **59**: 1-6 [PMID: 24797965 DOI: 10.1016/j.advms.2013.11.001]

56 **Mueller TC**, Burmeister MA, Bachmann J, Martignoni ME. Cachexia and pancreatic cancer: are there treatment options? *World J Gastroenterol* 2014; **20**: 9361-9373 [PMID: 25071331 DOI: 10.3748/wjg.v20.i28.9361]
57 **Bachmann J**, Büchler MW, Friess H, Martignoni ME. Cachexia in patients with chronic pancreatitis and pancreatic cancer: impact on survival and outcome. *Nutr Cancer* 2013; **65**: 827-833 [PMID: 23909726 DOI: 10.1080/01635581.2013.804580]
58 **Davidson W**, Ash S, Capra S, Bauer J. Weight stabilisation is associated with improved survival duration and quality of life in unresectable pancreatic cancer. *Clin Nutr* 2004; **23**: 239-247 [PMID: 15030964 DOI: 10.1016/j.clnu.2003.07.001]

P- Reviewer: Kimura K, MatsudaY, Wei DY **S- Editor**: Qi Y
L- Editor: A **E- Editor**: Wang CH

World Journal of Gastroenterology

Submit a Manuscript: http://www.wjgnet.com/esps/

World J Gastroenterol 2017 March 14; 23(10): 1909-1919

DOI: 10.3748/wjg.v23.i10.1909

ISSN 1007-9327 (print) ISSN 2219-2840 (online)

META-ANALYSIS

Markers of systemic inflammation and colorectal adenoma risk: Meta-analysis of observational studies

Justyna Godos, Antonio Biondi, Fabio Galvano, Francesco Basile, Salvatore Sciacca, Edward L Giovannucci, Giuseppe Grosso

Justyna Godos, Salvatore Sciacca, Giuseppe Grosso, Integrated Cancer Registry of Catania-Messina-Siracusa-Enna, Azienda Ospedaliero Universitaria Policlinico Vittorio Emanuele, 95123 Catania, Italy

Antonio Biondi, Francesco Basile, Department of General Surgery, Section of General Surgery and Oncology, University of Catania, 95123 Catania, Italy

Fabio Galvano, Department of Biomedical and Biotechnological Sciences, University of Catania, 95123 Catania, Italy

Edward L Giovannucci, Department of Epidemiology, Harvard TH Chan School of Public Health, Boston, MA 02115, United States

Edward L Giovannucci, Department of Nutrition, Harvard TH Chan School of Public Health, Boston, MA 02115, United States

Edward L Giovannucci, Channing Division of Network Medicine, Department of Medicine, Brigham and Women's Hospital and Harvard Medical School, Boston, MA 02115, United States

Author contributions: Godos J performed the search, the analysis, and wrote the manuscript; Biondi A, Galvano F, Basile F and Sciacca S provided critical revision; Giovannucci EL and Grosso G designed the study, and provided insights on methodology, data interpretation and manuscript drafting (equal contribution).

Conflict-of-interest statement: The authors deny any conflict of interest.

Data sharing statement: No additional data are available.

Manuscript source: Invited manuscript

Correspondence to: Giuseppe Grosso, MD, PhD, Integrated Cancer Registry of Catania-Messina-Siracusa-Enna, Azienda Ospedaliero Universitaria Policlinico Vittorio Emanuele, 95123 Catania, Italy. giuseppe.grosso@studium.unict.it
Telephone: +39-95-3782110
Fax: +39-95-3782110

Received: December 11, 2016
Peer-review started: December 12, 2016
First decision: January 10, 2017
Revised: January 20, 2017
Accepted: February 16, 2017
Article in press: February 17, 2017
Published online: March 14, 2017

Abstract

AIM

To perform a meta-analysis of observational studies on inflammatory markers levels and occurrence of colorectal adenoma.

METHODS

PubMed and EMBASE databases were searched until March 2016 for the articles reporting on the circulating levels of inflammatory markers, including: C-reactive protein (CRP), interleukin-6 (IL-6), and tumor necrosis factor-alpha (TNF-α) and risk of colorectal adenoma. Random-effects models were used to calculate summary odds ratios (ORs) with 95%CIs for the highest *vs* lowest category of exposure. Heterogeneity was assessed by using the Q test and I^2 statistic. Subgroup analyses were also performed to test for potential source of heterogeneity.

RESULTS

A total of 14 case-control studies were included. Ten studies on CRP including a total of 3350 cases and 4168 controls showed non-significant summary (OR = 1.23, 95%CI: 0.98-1.54; I^2 = 54%, $P_{heterogeneity}$ = 0.01) in the general analysis, but significant increased odds when considering only advanced adenoma (OR = 1.59, 95%CI: 1.09-2.32; I^2 = 44%, $P_{heterogeneity}$ = 0.15). Subgroup and stratified analyses revealed a potential influence of smoking status and aspirin use on the association between CRP levels and colorectal adenoma. Five studies examined the association between circulating levels of TNF-α and colorectal adenoma risk, including a total of 1,568 cases and 2,832 controls. The summary OR for the highest *vs* the lowest category of exposure was 1.00 (95%CI: 0.77-1.29). The relationship between circulating IL-6 levels and colorectal adenoma risk was investigated in 7 studies including a total of 1936 cases and 3611 controls. The summary OR for the highest *vs* the lowest category of exposure was 1.19 (95%CI: 0.92-1.55).

CONCLUSION

Summary of current evidence suggests a positive association of CRP levels and advanced colorectal adenoma risk. The role of potential confounding factors should be further evaluated.

Key words: Inflammatory markers; Meta-analysis; Colorectal adenoma; C-reactive protein; Tumor necrosis factor-alpha; Interleukin-6

Core tip: The present study investigated the association between inflammatory markers and risk of colorectal adenoma. Ten studies on C-reactive protein (CRP) showed non-significant summary odds ratios in the general analysis. However, CRP was significantly correlated with increased risk of advanced adenoma. Subgroup and stratified analyses revealed a potential influence of smoking status and aspirin use on the association between CRP levels and colorectal adenoma risk. The results of the study may have practical value for clinicians screening for colorectal cancer.

Godos J, Biondi A, Galvano F, Basile F, Sciacca S, Giovannucci EL, Grosso G. Markers of systemic inflammation and colorectal adenoma risk: Meta-analysis of observational studies. *World J Gastroenterol* 2017; 23(10): 1909-1919 Available from: URL: http://www.wjgnet.com/1007-9327/full/v23/i10/1909.htm DOI: http://dx.doi.org/10.3748/wjg.v23.i10.1909

INTRODUCTION

Colorectal cancer represents one of the most common cancers diagnosed in developed countries and the fourth leading cause of cancer-related death globally. Chronic inflammation has been hypothesized to play an important role in several aspects of cancer initiation, promotion, and progression[1]. Indeed, existence of chronic inflammatory bowel diseases (such as Crohn's colitis or ulcerative colitis) or regular use of anti-inflammatory medications has been demonstrated to affect risk of colorectal cancer[2,3] and colorectal adenoma, the precursor of most colorectal cancers[4,5]. However, despite evidence on potential involvement of inflammatory processes in colorectal carcinogenesis, epidemiological data regarding markers of systemic inflammation and colorectal neoplasia risk are conflicting.

Tumor necrosis factor-alpha (TNF-α) and interleukin-6 (IL-6) are pro-inflammatory cytokine involved in cell growth, differentiation, and apoptosis, and are altered within adenoma tissues reflecting an inflammatory state[6]. C-reactive protein (CRP) is a non-specific marker of systemic inflammation produced and released into the circulation primarily by hepatocytes in response to elevations in IL-6 and TNF-α[6]. Elevated levels of CRP are typically associated with acute inflammatory conditions, such as infections, trauma, or acute flares of autoimmune diseases, and with a variety of chronic conditions[6]. Current evidence suggests that pre-diagnostic circulating CRP levels may be associated with increased risk of colorectal cancer[7]. In addition, serum levels of TNF-α have been associated with increased risk of this malignancy[8]. Results on IL-6 are inconclusive, suggesting that it is not associated with colorectal cancer risk, but the evidence is weakened by a limited number of studies[7,8]. Overall, existing summary of evidence rely on colorectal cancer risk, but findings on colorectal adenoma have not been meta-analyzed yet. Thus, the aim of this study was to systematically review and perform a meta-analysis of studies examining the association between circulating levels of CRP, TNF-α, and IL-6 and risk of colorectal adenoma.

MATERIALS AND METHODS

The design, analysis, and reporting of this study followed the meta-analysis of Observational Studies in Epidemiology (MOOSE) guidelines (Online Resource 3). The reporting of this work is compliant with PRISMA guidelines.

Literature search and study selection

We performed a systematic search on PubMed (http://www.ncbi.nlm.nih.gov/pubmed/) and EMBASE (http://www.embase.com/) databases of all English language studies published up to March 2016. The search terms used are shown in Online Resource 4. Inclusion criteria for the studies were: (1) having a cross-sectional, case-control, or prospective design; (2) evaluating

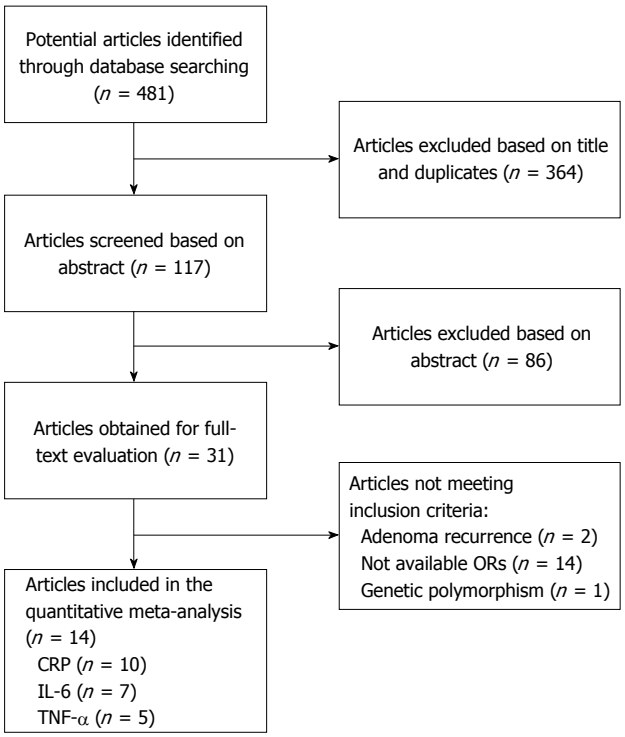

Figure 1 Study selection process. CRP: C-reactive protein; IL-6: Interleukin-6; TNF-α: Tumor necrosis factor-alpha.

the association between CRP, TNF-α, or IL-6 levels and colorectal adenoma comparing the highest *vs* the lowest category of exposure; and (3) assessing and reporting odds ratios (ORs) and the corresponding 95%CIs. Reference lists of included studies were examined for any additional article not previously identified. If more than one study was conducted on the same cohort, only the most comprehensive or most updated was included in the meta-analysis. The selection process was independently performed by two authors (Godos J and Grosso G).

Data extraction and study quality assessment

Data were abstracted from each identified study by using a standardized extraction form. The following information was collected: (1) author name; (2) year of publication; (3) country; (4) number, gender, and age of participants; (5) main characteristics related to markers; (6) OR and 95%CI for the highest *vs* the lowest category of exposure; and (7) covariates used in adjustments.

The Newcastle-Ottawa Quality Assessment Scale was used to assess the quality of each study[9]. The instrument consists of 3 domains indicating the study quality as follows: selection (4 points), comparability (2 points), and outcome (3 points) for a total score of 9 points (9 representing the highest quality). Studies scoring 7-9 points, 3-6 points, and 0-3 points were identified as high, moderate, and low quality, respectively.

Statistical analysis

Random-effects models were used to calculate summary ORs with 95% CIs for the highest *vs* lowest category of exposure. The risk estimate from the most fully adjusted models in the analysis of the pooled RR was used. Heterogeneity was assessed by using the *Q* test and I^2 statistic. The level of significance for the *Q* test was defined as $P < 0.10$. The I^2 statistic represented the amount of total variation that could be attributed to heterogeneity. I^2 values $\leqslant$ 25%, $\leqslant$ 50%, $\leqslant$ 75%, and > 75% indicated no, small, moderate, and significant heterogeneity, respectively. A sensitivity analysis by exclusion of one study at a time was performed to assess the stability of results and potential sources of heterogeneity. Separate analyses were conducted on adenoma advancement based on availability of datasets. According to literature investigated, advanced adenoma was defined as having diameter > 1 cm or containing villous/tubulovillous characteristics, or severe dysplasia. Subgroup analyses were also performed to test for potential source of heterogeneity according to geographical area, gender, study design, sample fasting status, measurement methods, and adjustment for main confounding factors (BMI or obesity, smoking status, family history of colorectal neoplasia, aspirin or NSAIDs use, energy intake or physical activity, and alcohol consumption). Stratified analyses were conducted by smoking status (non/former *vs* current), NSAIDs use (non/former *vs* current), and adenoma location. Publication bias was evaluated by a visual investigation of funnel plots for potential asymmetry. All analyses were performed with Review Manager (RevMan) software version 5.2 (The Nordic Cochrane Centre, The Cochrane Collaboration). Artwork was created using RevMan software. Statistical analysis was reviewed by a biostatistician (Grosso G).

RESULTS

Study characteristics

The process of identification and study selection is summarized in Figure 1. Among the initial 481 articles screened on the basis of title, 31 articles were screened for full-text examination. Seventeen studies were excluded because they assessed adenoma recurrence (*n* = 2), did not report risk estimates (*n* = 14), and reported information only on genetic polymorphisms (*n* = 1). A final number of 14 studies[10-23] were included for the quantitative meta-analysis (Table 1). Four studies were nested case-control studies, 9 had a case-control design, and one was cross-sectional. The studies were conducted in the United States[10,11,13,16,18,19,21-23], Japan[12,14,15,17], and the United Kingdom[20]. Four studies investigated advanced and 4 studies non-advanced adenoma. Measurements methods varied greatly between studies, including INA (Immunonephelometric

Table 1 Characteristics of the studies included in the meta-analysis

Ref.	Study design	Study population	No. of controls; No of controls; gender; age	Assay method, sample type, fasting status	Exposure *vs* reference category	Matching factors	Adjusting factors
Kim *et al*[10]	Case-control	Patients who underwent colonoscopy and/or patients who underwent screening colonoscopy	631; 242; M and F > 30 yr	CRP (ELISA), IL-6 (ELISA), TNF-α (ELISA), plasma, fasting	T3 (≥ 12013.1 ng/mL) *vs* T1 (< 2916.03 ng/mL) for CRP; T3 (≥ 0.3571 pg/mL) *vs* T1 (0 pg/mL) for IL-6; T3 (≥ 2.2358 pg/mL) *vs* T1 (< 1.3877 pg/mL) for TNF-α	NA	Age, sex, obesity
Tsilidis *et al*[11]	Nested case-control	Subjects who undergone sigmoidoscopy or colonoscopy	269; 135, M and F 45-65 yr	CRP (Dade-Behring method), plasma, NR	Q4 (> 2.95 mg/L) *vs* Q1 (< 0.65 mg/L)	Age, sex, race, date of blood draw, time since last meal, type of endoscopy	Cigarette smoking status, BMI at baseline, BMI at age 21, ever use of estrogen or progesterone (women), use of aspirin or non-steroidal anti-inflammatory drugs, use of diabetes medications, family history of colorectal cancer
Otake *et al*[12]	Case-control	Subjects who underwent colonoscopy for health checkup	635; 646; M 50-53 yr	CRP(INA), plasma/serum, fasting	Q4 (≥ 1541 ng/mL) *vs* Q1 (< 206 ng/mL)	NA	Age, hospital, plasma/serum status, rank in the Self Defense Forces, cigarette smoking, alcohol use, BMI, physical activity, parental colorectal cancer
Ognjanovic *et al*[13]	Case-control	Subjects who undergone screening sigmoidoscopy	539; 271; M and F 55-69 yr	CRP (ITA), IL-6 (ELISA), serum, fasting	Q4 (> 2.00 mg/L) *vs* Q1 (> 0.30 mg/L) for CRP; Q4 (> 2.79 pg/mL) *vs* Q1 (> 1.09 pg/mL) for IL-6	Age, sex, ethnicity, screening date, recruitment clinic	Sex, age, race, smoking status, BMI
Otake *et al*[14]	Cross-sectional	Patients who underwent colonoscopy	26; 47; M 53-80 yr	CRP (INA), plasma, fasting	high (≥ 500 ng/mL) *vs* low (< 500 ng/mL)	NA	None
Yamaji *et al*[15]	Case-control	Healthy subjects who underwent screening colonoscopy	735; 778; M 50-79 yr; F 40-79 yr	TNF-α (Cytokine/ Chemokine Magnetic Bead Panel Assay), plasma, fasting	Q3 (≥ 2.98 pg/mL) *vs* Q1 (≤ 2.38 pg/mL)	Age, two screening periods	Age, sex, screening period, duration of fasting, cigarette smoking, alcohol drinking, family history of colorectal cancer, nonsteroidal anti-inflammatory drug use, BMI
Gunter *et al*[16]	Nested case-control	Subjects who undergone screening sigmoidoscopy	396; 356; M and F 55-74 yr	CRP (Chemiluminescent Immunometric Assay), serum, NR	Q4 (≥ 4.0 mg/L) *vs* Q1 (< 0.8 mg/L)	Age at study entry, gender, fiscal year at study entry, race, screening center, study protocol, season of blood draw	Cigarette smoking status, BMI, use of non-steroidal anti-inflammatory drugs, diabetes, use of hormone therapy (females only), family history of colorectal cancer, educational attainment
Sasaki *et al*[17]	Case-control	Subjects who underwent colonoscopy for health checkup	218; 118; M 52 yr cases, 51 yr controls (median)	IL-6 (ELISA), serum, fasting	Q4 (≥ 1.619 pg/mL) *vs* Q1 (< 0.804 pg/mL)	Age	Age, current smoking, alcohol consumption, family history of CRC, BMI, HOMA-IR, insulin
Vaughn *et al*[18]	Case-control	Patients who underwent routine colonoscopy	1050; 401; M and F 46-66 yr	IL-6 (ELISA), TNF-α (Cytokine/ Chemokine Magnetic Bead Panel Assay), serum, fasting	T3 (> 2.71 pg/mL) *vs* T1 (< 1.44 pg/mL) for IL-6; T3 (> 4.46 pg/mL) *vs* T1 (< 3.01 pg/mL) for TNF-α	NA	Age, sex, non-steroidal anti-inflammatory use, BMI, family history of colorectal cancer, smoking status, race
Kong *et al*[19]	Case-control	Patients who underwent colonoscopy	201; 139; M and F 46-66 yr	CRP (INA), plasma, NR	high (> 6.2 mikrog/mL) *vs* low (< 6.2 mikrog/mL)	NA	Age, race, sex, BMI, total energy intake, plasma cholesterol, family history of colorectal cancer in a first degree relative, hormone replacement therapy, dietary fiber, physical activity, study

Basavaraju *et al*[20]	Case-control	Patients who undergone screening colonoscopy	319; 50; M and F 64 yr	CRP (INA), IL-6 (Cytometric Bead Array), TNF-α (Cytometric Bead Array), serum (CRP), plasma (IL-6, TNF-α), fasting	high (> 1.88) *vs* low (≤ 1.88) units NR for CRP; high (> 3.32) *vs* low (≤ 3.32) units NR for IL-6; high (> 3.53) *vs* low (≤ 3.53) units NR for TNF-α	NA	Time of recruitment, age, sex, BMI, alcohol consumption, exercise, smoking, diverticular disease, exercise, aspirin use
Davenport *et al*[21]	Case-control	Patients who underwent colonoscopy	395; 707; M and F 49-67 yr	CRP (ITA), plasma, NR	single small tubular adenoma T3 (> 5.97 mg/L) *vs* T1 (< 1.59 mg/L); multiple small tubular adenoma T3 (> 6.96 mg/L) *vs* T1 (< 1.82 mg/L); advanced adenoma T3 (> 7.16 mg/L) *vs* T1 (< 1.69 mg/L)	Age, sex, race, and matched at least one of the following factors: study site, collection date of plasma, NSAID use for a minimum of three times per week for at least one year	Age, educational attainment, study site
Henry *et al*[22]	Nested case-control	Subjects who undergone colonoscopy	97; 97; M and F ≥ 50 yr	IL-6 (Cytokine/Chemokine Magnetic Bead Panel Assay), TNF-α (Cytokine/Chemokine Magnetic Bead Panel Assay), serum, fasting	T3 *vs* T1 for IL-6; T3 *vs* T1 for TNF-α	NA	Age, sex, previous screening
Song *et al*[23]	Nested case-control	Subjects who undergone sigmoidoscopy or colonoscopy	757; 757; F 30-55 yr	CRP (ITA), IL-6 (ELISA), plasma, fasting/non-fasting	Q5 (6.32 mg/L - median) *vs* Q1 (0.43 mg/L - median) for CRP; Q5 (2.64 ng/l - median) *vs* Q1 (0.42 ng/l - median) for IL-6	Date of endoscopy, birth year, indication for endoscopy, time period of any prior endoscopy, month and year of blood draw, fasting status	Family history of colorectal cancer, multivitamin use, pack-years of smoking before age 30, alcohol consumption, BMI, physical activity, regular aspirin/NSAID use, postmenopausal status and hormone use, calcium intake, and Alternative Healthy Eating Index

BMI: Body mass index; ELISA: Enzyme-linked immunosorbent assay; NA: Not applicable; NR: Not reported; NSAIDs: Non-steroidal anti-inflammatory drugs; INA: Immunonephelometric assay; ITA: Immunoturbidimetric assay; CRP: C-reactive protein; IL-6: Interleukin-6; TNF-α: Tumor necrosis factor-alpha.

Assay)[12,14,19,20], ITA (Immunoturbidimetric Assay)[13,21,23], ELISA[10,13,17,18,23], DADE-Behring method[11], Chemiluminescent Immunometric Assay[16], Cytometric Bead Array[20], Cytokine/Chemokine Magnetic Bead Panel Assay[15,18,22]. Seven studies tested markers of inflammation in plasma, 5 in serum, and 2 in serum and plasma. 10 studies collected overnight fasting samples while 4 studies did not specified fasting status. The overall quality of the studies included was high (Online Resource 5).

CRP and adenoma risk

The association between CRP levels and colorectal adenoma risk was examined in 10 studies including a total of 3350 cases and 4168 controls. The summary OR for the highest *vs* the lowest category of exposure was 1.23 (95%CI: 0.98-1.54) with evidence of heterogeneity (I^2 = 54%, $P_{heterogeneity}$ = 0.01; Figure 2). Publication bias was not evident based on the symmetrical shape of funnel plot (Online Resource 1). Sensitivity analysis by excluding one study at a time showed that one study, which showed a suggestive inverse association, contributed largely to the heterogeneity[16]; after exclusion of this study, the summary OR = 1.31, 95%CI: 1.06-1.61; I^2 = 40%; $P_{heterogeneity}$ = 0.08). Subgroup analyses are presented in Table 2. Grouping studies by fasting status and measurement method showed statistically significant results when considering studies that collected fasting blood samples (OR = 1.38, 95%CI: 1.02-1.88; I^2 = 32%, $P_{heterogeneity}$ = 0.21) and INA measurement (OR = 1.54, 95%CI: 1.06-2.23; I^2 = 29%, $P_{heterogeneity}$ = 0.24). Moreover, including one study[23] in which blood analyses were not uniformly conducted on fasting samples but risk estimates were adjusted for fasting/non-fasting, did not change markedly results (OR = 1.29, 95%CI: 1.01-1.64; I^2 = 25%, $P_{heterogeneity}$ = 0.25). No significant confounders were detected when grouping by gender, sample size, geographical location, and quality score. In contrast, subgroup analysis showed significant results only for the studies not adjusting for potential confounding factors of BMI, smoking status, aspirin/NSAIDs use, and family history of colorectal neoplasia showed significant results (Table 2).

Stratified analyses for such potential confounding factors were limited[12,21] but showed significant interaction with smoking status and use of aspirin/NSAIDs, whereby associations were only observed in heavy smokers and non-regular aspirin users (Online Resource 2). A stratified analysis was also conducted according to

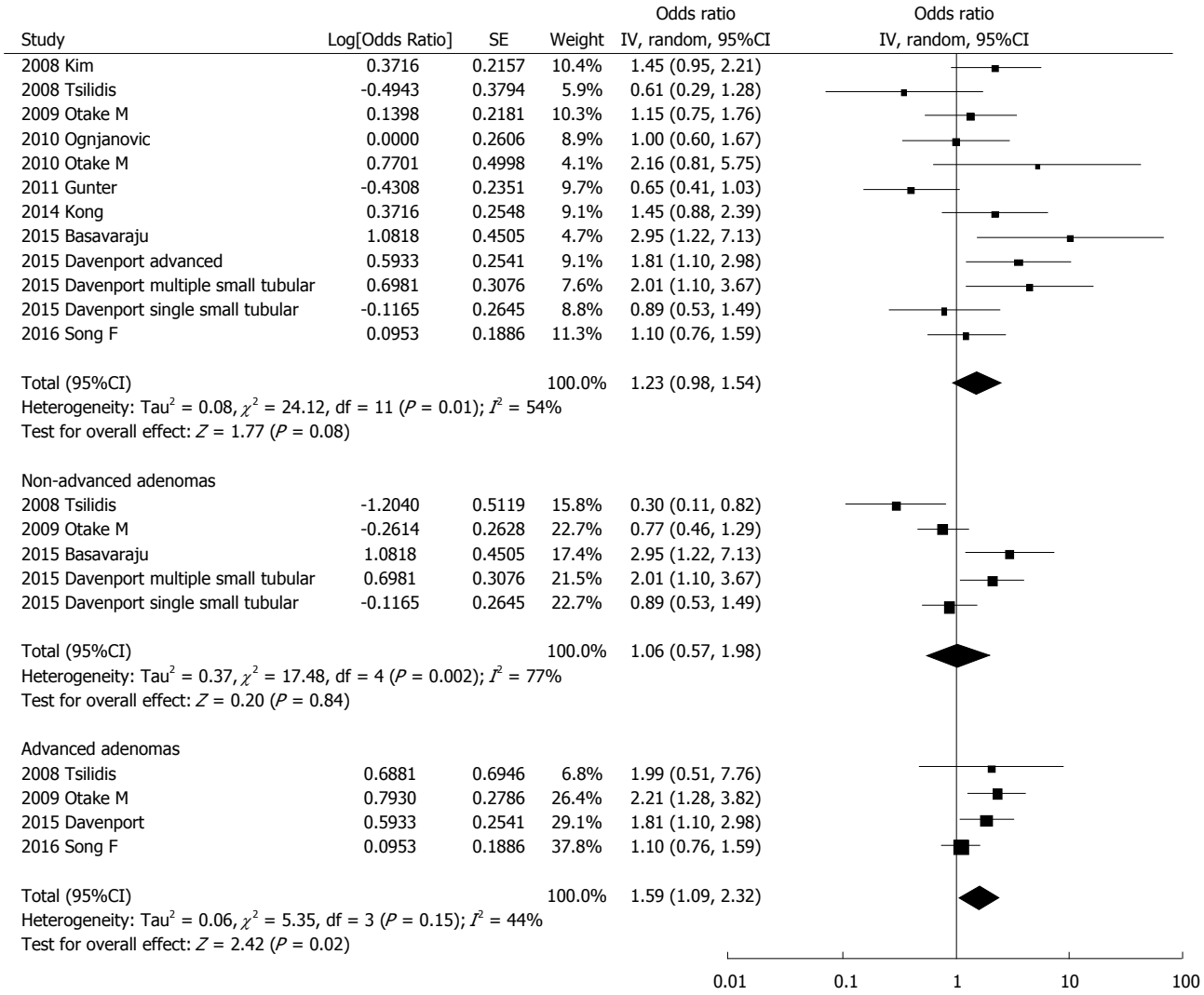

Figure 2 Meta-analysis of highest *vs* lowest category of C-reactive protein and risk of colorectal adenoma, total and by advancement status. CRP: C-reactive protein.

adenoma localization. No significant results for were observed for adenoma of proximal or distal colon (Online Resource 1) and for non-advanced adenoma (Figure 2). In contrast, separate analysis of the highest *vs* lowest CRP levels showed a significant association with increased advanced adenoma risk (OR = 1.59, 95%CI: 1.09-2.32; I^2 = 44%, $P_{heterogeneity}$ = 0.15; Figure 2).

IL-6 and adenoma risk

The relationship between circulating IL-6 levels and colorectal adenoma risk was investigated in 7 studies including a total of 1936 cases and 3611 controls. The summary OR for the highest *vs* the lowest category of exposure was 1.19 (95%CI: 0.92-1.55) with no evidence of publication bias (Online Resource 1) and little evidence of heterogeneity (I^2 = 46%, $P_{heterogeneity}$ = 0.09, Figure 3) and no evidence of asymmetry at funnel plot (Online Resource 1). Subgroup analyses are presented in Table 2. Grouping studies by adjustment for smoking status showed significant results for the studies that did not adjust for smoking and not significant for those that did adjust (Table 2). However, subgroup analysis for the adjustment for confounding factors, such as BMI, aspirin use, family history of colorectal cancer, and physical activity showed not-significant results. Similar results were observed for subgroup analysis controlling for IL-6 measurement.

TNF-α and adenoma risk

Five studies examined the association between circulating levels of TNF-α and colorectal adenoma risk, including a total of 1568 cases and 2832 controls. The summary OR for the highest *vs* the lowest category of exposure was 1.00 (95%CI: 0.77-1.29) with no evidence of publication bias (Online Resource 1) and little evidence of heterogeneity (I^2 = 49%, $P_{heterogeneity}$ = 0.08; Figure 4). Subgroup analyses showed significant results for the studies that did not adjust for smoking status while those studies adjusting did not show significant results (Table 2). Similar results were observed when pooling studies that did not adjust for aspirin/NSAIDs use (Table 2). The summary OR for the highest *vs* the lowest

Table 2 Subgroup analyses of studies reporting risk of colorectal adenomas for the highest *vs* lowest (reference) category of markers of inflammation

Subgroup	CRP				IL-6				TNF-α			
	No. of datasets	RR (95%CI)	I^2	Pheterogeneity	No. of datasets	RR (95%CI)	I^2	Pheterogeneity	No. of datasets	RR (95%CI)	I^2	Pheterogeneity
Total	12	1.23 (0.98, 1.54)	54%	0.01	7	1.19 (0.92, 1.55)	46%	0.09	6	1.00 (0.77, 1.29)	49%	0.08
Study design												
Nested case-control	3	0.81 (0.54, 1.21)	49%	0.14	2	1.02 (0.72, 1.45)	0%	0.47	1	1.14 (0.55, 2.36)	NA	NA
Case-control	8	1.39 (1.11, 1.74)	34%	0.16	5	1.25 (0.89, 1.78)	59%	0.04	5	0.98 (0.73, 1.31)	59%	0.05
Cross-sectional	1	2.16 (0.81, 5.75)	NA	NA	0	NA	NA	NA	0	NA	NA	NA
Gender												
Men	2	1.34 (0.79, 2.28)	25%	0.25	1	2.06 (1.02, 4.16)	NA	NA	1	0.94 (0.68, 1.30)	NA	NA
Women	1	1.10 (0.76, 1.59)	NA	NA	1	0.96 (0.65, 1.42)	NA	NA	1	0.65 (0.41, 1.03)	NA	NA
Geographical location												
United States	9	1.14 (0.89, 1.47)	57%	0.02	5	1.14 (0.86, 1.52)	52%	0.08	3	1.23 (0.87, 1.72)	44%	0.17
United Kingdom	1	2.95 (1.22, 7.13)	NA	NA	1	1.00 (0.44, 2.27)	NA	NA	1	0.73 (0.32, 1.67)	NA	NA
Japan	2	1.34 (0.79, 2.28)	25%	0.25	1	2.06 (1.02, 4.16)	NA	NA	2	0.81 (0.57, 1.16)	39%	0.20
By adjustment for confounders												
BMI/obesity												
Yes	8	1.12 (0.86, 1.45)	54%	0.03	6	1.19 (0.89, 1.58)	55%	0.05	5	0.98 (0.73, 1.31)	59%	0.05
No	4	1.54 (1.01, 2.37)	49%	0.12	1	1.35 (0.58, 3.14)	NA	NA	1	1.14 (0.55, 2.36)	NA	NA
Smoking												
Yes	6	1.01 (0.73, 1.40)	56%	0.04	5	1.03 (0.83, 1.29)	9%	0.35	4	0.90 (0.74, 1.09)	0%	0.42
No	6	1.48 (1.17, 1.88)	15%	0.32	2	1.74 (1.22, 2.49)	0%	0.52	2	1.51 (1.05, 2.16)	0%	0.39
Aspirin/NSAIDs use												
Yes	4	1.00 (0.58, 1.72)	72%	0.01	3	0.99 (0.78, 1.26)	0%	0.98	4	0.90 (0.74, 1.09)	0%	0.42
No	8	1.35 (1.10, 1.65)	17%	0.30	4	1.43 (0.93, 2.21)	58%	0.07	2	1.51 (1.05, 2.16)	0%	0.39
Alcohol consumption												
Yes	3	1.32 (0.87, 2.03)	53%	0.12	3	1.20 (0.75, 1.92)	44%	0.17	3	0.82 (0.64, 1.06)	0%	0.42
No	9	1.19 (0.89, 1.59)	60%	0.01	4	1.20 (0.83, 1.73)	60%	0.06	3	1.23 (0.87, 1.72)	44%	0.17
Energy/physical activity												
Yes	4	1.32 (0.97, 1.79)	34%	0.21	2	0.97 (0.68, 1.38)	0%	0.93	1	0.73 (0.32, 1.67)	NA	NA
No	8	1.16 (0.84, 1.61)	63%	0.008	5	1.30 (0.92, 1.84)	58%	0.05	5	1.02 (0.78, 1.35)	56%	0.06
Family history of colorectal neoplasia												
Yes	5	0.98 (0.73, 1.32)	49%	0.10	3	1.13 (0.80, 1.61)	47%	0.15	3	0.90 (0.71, 1.13)	22%	0.28
No	7	1.49 (1.11, 1.99)	43%	0.11	4	1.24 (0.81, 1.90)	53%	0.10	3	1.24 (0.78, 1.97)	38%	0.20
Sample fasting status												
Yes	6	1.29 (1.01, 1.64)	25%	0.25	7	1.19 (0.92, 1.55)	46%	0.09	6	1.00 (0.77, 1.29)	49%	0.08
No	6	1.12 (0.75, 1.68)	70%	0.005	0	NA	NA	NA	0	NA	NA	NA
Measurement method												
ELISA	1	1.45 (0.95, 2.21)	NA	NA	5	1.21 (0.88, 1.67)	63%	0.03	1	1.65 (1.09, 2.50)	NA	NA
INA	4	1.54 (1.06, 2.23)	29%	0.24	0	NA	NA	NA	0	NA	NA	NA
ITA	5	1.26 (0.94, 1.69)	45%	0.12	0	NA	NA	NA	0	NA	NA	NA
Cytokine/Chemokine Magnetic Bead Panel Assay	0	NA	NA	NA	1	1.35 (0.58, 3.14)	NA	NA	4	0.92 (0.76, 1.11)	0%	0.41

Cytometric Bead Assay	0	NA	NA	NA	1	1.00 (0.44, 2.27)	NA	NA	1	0.73 (0.32, 1.67)	NA	NA
Dade-Behring method	1	0.61 (0.29, 1.28)	NA	NA	0	NA	NA	NA	0	NA	NA	NA
Chemiluminescent Immunometric Assay	1	0.65 (0.41, 1.03)	NA	NA	0	NA	NA	NA	0	NA	NA	NA

BMI: Body mass index; ELISA: Enzyme-linked immunosorbent assay; NA: Not applicable; NSAIDs: Non-steroidal anti-inflammatory drugs; INA: Immunonephelometric assay; ITA: Immunoturbidimetric assay; CRP: C-reactive protein; IL-6: Interleukin-6; TNF-α: Tumor necrosis factor-alpha.

category of exposure, when grouping studies by other confounding factors (BMI, family history of colorectal cancer, physical activity, alcohol consumption) showed no significant evidence.

DISCUSSION

In this meta-analysis, circulating levels of CRP, TNF-α, and IL-6 were not appreciable associated with the risk of colorectal adenoma. Significant positive associations were observed, especially for CRP, in studies that did not adjust for smoking, aspirin use, BMI and family history. Stratified analyses also showed significant associations for CRP in the strata of heavy smokers and non-users of aspirin. In addition, CRP was significantly associated with occurrence of advanced adenoma, irrespectively of the group. These findings suggest a potential role of subclinical inflammation driven by the aforementioned factors in increasing risk of colorectal adenoma, which may be accentuated in more advanced stages of adenoma.

Experimental studies on animals have shown that colonic epithelial dysplasia provokes a cytokine-driven inflammatory response that up-regulates circulatory inflammatory markers such as TNF-α, IL-6, and, consequently, CRP production[24,25]. Thus, it is biologically plausible that an inflammatory state would occur in patients with adenoma, possibly reflected in an increase in systemic inflammatory markers. However, results observed in the studies reviewed were inconsistent. The results appeared to differ depending on whether the studies adjusted for potentially confounding factors, such as smoking, BMI, aspirin use and family history. Smoking[26], high BMI[27], and non-use of aspirin would be expected to increase levels of inflammatory markers, and these are associated with increased risk of colorectal adenoma (and cancer)[28]. Studies that did not adjust for these factors tended to show associations with inflammatory markers, whereas those that did adjust showed not significant results. This pattern suggests that uncontrolled confounding by these factors could have caused the positive associations, when observed. On the other hand, inflammation could possibly be a mediator of the effects of some of these factors. Further, when considering studies that reported fasting sample, results were significant in favor of an increased risk of colorectal adenoma for higher levels of CRP. Markers of subclinical systemic inflammatory state, especially CRP, have been hypothesized to be influenced by fasting[29] and that diet may also impact level and direction of modification[30]. Nevertheless, number of studies for such stratified analyses were limited, thus the specific role that known risk factors associated with systemic subclinical inflammation will require further investigation.

There are at least three ways that systemic inflammation may relate to colorectal adenoma. First, inflammation in the pre-neoplastic colorectal tissue (*i.e.*, as in ulcerative colitis) could directly predispose to risk of colorectal neoplasia. Second, a neoplastic lesion (adenoma, cancer) could induce inflammation and increase inflammatory markers. Thirdly, systemic inflammation could reflect various processes, some of which may be directly or indirectly (*i.e.*, by different mechanisms) be associated with colorectal adenoma risk (*i.e.*, smoking habits or obesity). The first possibility is difficult to demonstrate because the studies cannot distinguish the source of the inflammation, and in most cases the adenomas were present at the time of blood draw, so a temporal relationship could not be established. The second explanation is supported by the stratified analysis that we conducted including only advanced adenoma that resulted in increased risk of disease for higher CRP levels. Most of studies combined all adenomas into an individual condition, which likely included a significant proportion of single small tubular adenoma that may not provoke an inflammatory response sufficient to raise inflammatory markers levels[10,13-19,22]. Studies exploring inflammatory markers levels over different phases of tumor progression showed increasing concentrations of several cytokines (including TNF-α) in normal mucosa, adenoma, hyperplastic polyp, and serrated adenoma[31]. Interestingly, habitual use of aspirin and NSAIDs interact with COX-2 activation that has been suggested to occur as a carcinogenic mechanism within the colonic epithelium[32]. Also, CRP and IL-6 levels have been demonstrated to vary not only between colorectal adenoma and cancer, but also by cancer stage[33]. However,

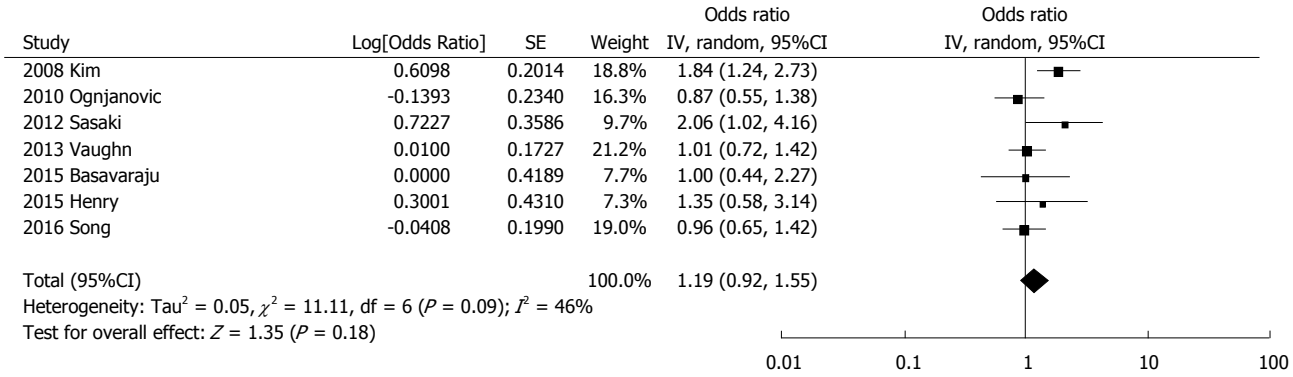

Figure 3 Meta-analysis of highest *vs* lowest category of interleukin-6 and risk of colorectal adenoma. IL-6: Interleukin-6.

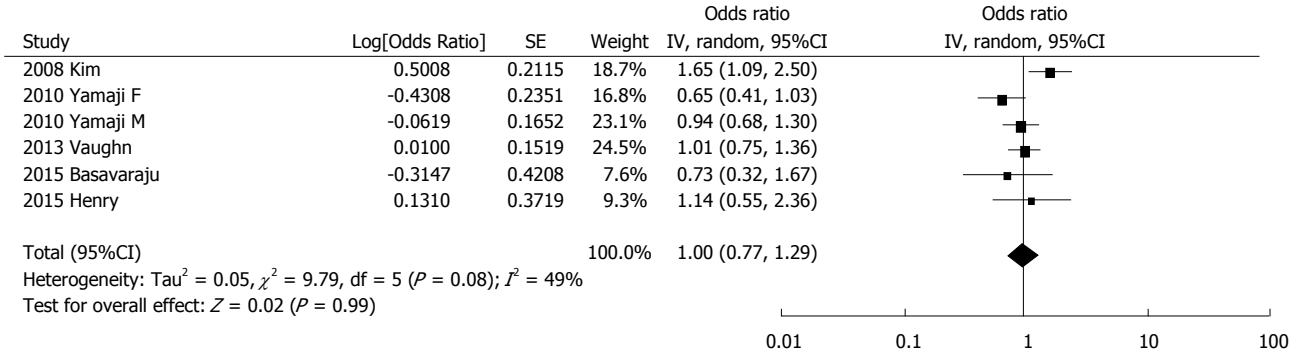

Figure 4 Meta-analysis of highest *vs* lowest category of tumor necrosis factor-alpha and risk of colorectal adenoma. TNF-α: Tumor necrosis factor-alpha.

evidence for markers of inflammation other than CRP was limited and future studies exploring this issue are needed.

The results of the present meta-analysis should be considered in light of some limitations. First, our meta-analysis was conducted on blood/serum markers of inflammation, but the biological effects of circulating *vs* local inflammatory makers may differ, and how circulating inflammation is reflecting etiologically relevant tissue inflammation will vary by factors in the study population, and by stratification of relevant factors. Second, although we included in our analyses the most adjusted models for various potential confounding factors, residual or unknown confounding may still exist. For instance, differences in the definition of advanced adenomas among study may have led to misclassification. Moreover, due to study design, results may be affected by reverse causation depending on timing of measurements. Third, number of studies and information retrieved were limited for some potential important characteristics that should be taken into account, such as adenoma location (presented in 2 studies[11,12]), multiplicity and size (not investigated in the present meta-analysis).

In conclusion, inflammation may play an important role in colorectal cancer development. Discrepancy between biological plausibility and lack of strong epidemiological difference may depend on inadequate methods of assessing inflammatory markers, with special regard to existing confounders. Although findings from this meta-analysis suggest an involvement of CRP in the early stage of colorectal cancer (*i.e.*, advanced adenoma risk), final conclusions cannot be drawn given the nature of the studies (observational non prospective), heterogeneous determinants of systemic inflammatory markers, and the limited number of investigations involved. Future studies estimating pre-diagnostic serum/plasma markers of inflammation and sequent adenoma incidence are needed to better assess the role of chronic inflammation in malignancy development. The potentiality of using CRP as a marker to distinguish between advanced and non-advanced adenoma could be also studies to improve surveillance strategies.

COMMENTS

Background

Colorectal cancer represents one of the most common cancers diagnosed in developed countries and the fourth leading cause of cancer-related death globally. Chronic inflammation has been hypothesised to play an important role in the initiation and progression of colorectal cancer. Patients with ulcerative colitis and Crohn's colitis demonstrate chronic inflammation in the gastrointestinal mucosa and are at higher risk of developing cancer. On the contrary, regular use of anti-inflammatory drugs such as aspirin has been associated with lower risk of colorectal cancer as well as colorectal adenomas, precursors of most colorectal cancer.

Research frontiers

Regardless the fact, that the majority of evidence implicates chronic inflammation in colorectal carcinogenesis, epidemiological data remain inconclusive about the association between systemic inflammatory markers and colorectal neoplasia risk.

Innovations and breakthroughs

The present study investigate the associations between inflammatory markers and risk of colorectal adenoma. The authors found that C-reactive protein (CRP) was significantly correlated with increased risk of advanced adenoma.

Applications

The results of the study may contribute to the improvement of the detection of advanced premalignant lesions during colorectal cancer screening.

Terminology

Colorectal adenoma is a benign glandular tumour of the colon and the rectum. It is a precursor lesion of the colorectal cancer.

Peer-review

This systematic review and meta-analysis represents an interesting collation of evidence to date on three inflammatory markers (CRP, IL-6 and TNF-α) in relation to colorectal adenoma risk. The review is also largely well conducted and written.

REFERENCES

1 **Terzić J**, Grivennikov S, Karin E, Karin M. Inflammation and colon cancer. *Gastroenterology* 2010; **138**: 2101-2114.e5 [PMID: 20420949 DOI: 10.1053/j.gastro.2010.01.058]

2 **Algra AM**, Rothwell PM. Effects of regular aspirin on long-term cancer incidence and metastasis: a systematic comparison of evidence from observational studies versus randomised trials. *Lancet Oncol* 2012; **13**: 518-527 [PMID: 22440112 DOI: 10.1016/S1470-2045(12)70112-2]

3 **Itzkowitz SH**, Yio X. Inflammation and cancer IV. Colorectal cancer in inflammatory bowel disease: the role of inflammation. *Am J Physiol Gastrointest Liver Physiol* 2004; **287**: G7-G17 [PMID: 15194558 DOI: 10.1152/ajpgi.00079.2004]

4 **Cole BF**, Logan RF, Halabi S, Benamouzig R, Sandler RS, Grainge MJ, Chaussade S, Baron JA. Aspirin for the chemoprevention of colorectal adenomas: meta-analysis of the randomized trials. *J Natl Cancer Inst* 2009; **101**: 256-266 [PMID: 19211452 DOI: 10.1093/jnci/djn485]

5 **Wanders LK**, Dekker E, Pullens B, Bassett P, Travis SP, East JE. Cancer risk after resection of polypoid dysplasia in patients with longstanding ulcerative colitis: a meta-analysis. *Clin Gastroenterol Hepatol* 2014; **12**: 756-764 [PMID: 23920032 DOI: 10.1016/j.cgh.2013.07.024]

6 **Pepys MB**, Hirschfield GM. C-reactive protein: a critical update. *J Clin Invest* 2003; **111**: 1805-1812 [PMID: 12813013 DOI: 10.1172/JCI18921]

7 **Sinha RA**, Farah BL, Singh BK, Siddique MM, Li Y, Wu Y, Ilkayeva OR, Gooding J, Ching J, Zhou J, Martinez L, Xie S, Bay BH, Summers SA, Newgard CB, Yen PM. Caffeine stimulates hepatic lipid metabolism by the autophagy-lysosomal pathway in mice. *Hepatology* 2014; **59**: 1366-1380 [PMID: 23929677 DOI: 10.1002/hep.26667]

8 **Joshi RK**, Kim WJ, Lee SA. Association between obesity-related adipokines and colorectal cancer: a case-control study and meta-analysis. *World J Gastroenterol* 2014; **20**: 7941-7949 [PMID: 24976730 DOI: 10.3748/wjg.v20.i24.7941]

9 **Wells GA**, Shea BJ, O'Connell D, Peterson J, Welch V, Losos M, Tugwell P. The Newcastle-Ottawa Scale (NOS) for assessing the quality of nonrandomised studies in meta-analyses. Proceedings of the Ottawa (Canada): Ottawa Health Research Institute; 1999. Available from: URL: https://www.mendeley.com/catalog/newcastleottawa-scale-nos-assessing-quality-nonrandomized-studies-metaanalyses/

10 **Kim S**, Keku TO, Martin C, Galanko J, Woosley JT, Schroeder JC, Satia JA, Halabi S, Sandler RS. Circulating levels of inflammatory cytokines and risk of colorectal adenomas. *Cancer Res* 2008; **68**: 323-328 [PMID: 18172326 DOI: 10.1158/0008-5472.CAN-07-2924]

11 **Tsilidis KK**, Erlinger TP, Rifai N, Hoffman S, Hoffman-Bolton J, Helzlsouer KJ, Platz EA. C-reactive protein and colorectal adenoma in the CLUE II cohort. *Cancer Causes Control* 2008; **19**: 559-567 [PMID: 18214695 DOI: 10.1007/s10552-008-9117-x]

12 **Otake T**, Uezono K, Takahashi R, Fukumoto J, Tabata S, Abe H, Tajima O, Mizoue T, Ohnaka K, Kono S. C-reactive protein and colorectal adenomas: Self Defense Forces Health Study. *Cancer Sci* 2009; **100**: 709-714 [PMID: 19469014]

13 **Ognjanovic S**, Yamamoto J, Saltzman B, Franke A, Ognjanovic M, Yokochi L, Vogt T, Decker R, Le Marchand L. Serum CRP and IL-6, genetic variants and risk of colorectal adenoma in a multiethnic population. *Cancer Causes Control* 2010; **21**: 1131-1138 [PMID: 20333461 DOI: 10.1007/s10552-010-9540-7]

14 **Otake S**, Takeda H, Fujishima S, Fukui T, Orii T, Sato T, Sasaki Y, Nishise S, Kawata S. Decreased levels of plasma adiponectin associated with increased risk of colorectal cancer. *World J Gastroenterol* 2010; **16**: 1252-1257 [PMID: 20222170 DOI: 10.3748/wjg.v16.i10.1252]

15 **Yamaji T**, Iwasaki M, Sasazuki S, Tsugane S. Interaction between adiponectin and leptin influences the risk of colorectal adenoma. *Cancer Res* 2010; **70**: 5430-5437 [PMID: 20516125 DOI: 10.1158/0008-5472.CAN-10-0178]

16 **Gunter MJ**, Cross AJ, Huang WY, Stanczyk FZ, Purdue M, Xue X, Schoen R, Limburg PJ, Schatzkin A, Sinha R, Hayes RB. A prospective evaluation of C-reactive protein levels and colorectal adenoma development. *Cancer Epidemiol Biomarkers Prev* 2011; **20**: 537-544 [PMID: 21212059 DOI: 10.1158/1055-9965.EPI-10-1099]

17 **Sasaki Y**, Takeda H, Sato T, Orii T, Nishise S, Nagino K, Iwano D, Yaoita T, Yoshizawa K, Saito H, Tanaka Y, Kawata S. Serum Interleukin-6, insulin, and HOMA-IR in male individuals with colorectal adenoma. *Clin Cancer Res* 2012; **18**: 392-399 [PMID: 22048241 DOI: 10.1158/1078-0432.CCR-11-0896]

18 **Vaughn CB**, Ochs-Balcom HM, Nie J, Chen Z, Thompson CL, Tracy R, Li L. No Association between Circulating Levels and Genetic Variants of IL-6 and TNF-α and Colon Adenoma. *Gastroenterology Res* 2013; **6**: [PMID: 24235998 DOI: 10.4021/gr529w]

19 **Kong SY**, Bostick RM, Flanders WD, McClellan WM, Thyagarajan B, Gross MD, Judd S, Goodman M. Oxidative balance score, colorectal adenoma, and markers of oxidative stress and inflammation. *Cancer Epidemiol Biomarkers Prev* 2014; **23**: 545-554 [PMID: 24443405 DOI: 10.1158/1055-9965.EPI-13-0619]

20 **Basavaraju U**, Shebl FM, Palmer AJ, Berry S, Hold GL, El-Omar EM, Rabkin CS. Cytokine gene polymorphisms, cytokine levels and the risk of colorectal neoplasia in a screened population of Northeast Scotland. *Eur J Cancer Prev* 2015; **24**: 296-304 [PMID: 25350634 DOI: 10.1097/CEJ.0000000000000087]

21 **Davenport JR**, Cai Q, Ness RM, Milne G, Zhao Z, Smalley WE, Zheng W, Shrubsole MJ. Evaluation of pro-inflammatory markers plasma C-reactive protein and urinary prostaglandin-E2 metabolite in colorectal adenoma risk. *Mol Carcinog* 2016; **55**: 1251-1261 [PMID: 26333108 DOI: 10.1002/mc.22367]

22 **Henry CJ**, Sedjo RL, Rozhok A, Salstrom J, Ahnen D, Levin TR, D'Agostino R, Haffner S, DeGregori J, Byers T. Lack of significant association between serum inflammatory cytokine profiles and the presence of colorectal adenoma. *BMC Cancer* 2015; **15**: 123 [PMID: 25884547 DOI: 10.1186/s12885-015-1115-2]

23 **Song M**, Mehta RS, Wu K, Fuchs CS, Ogino S, Giovannucci EL, Chan AT. Plasma Inflammatory Markers and Risk of Advanced Colorectal Adenoma in Women. *Cancer Prev Res* (Phila) 2016; **9**: 27-34 [PMID: 26511487 DOI: 10.1158/1940-6207.CAPR-15-0307]

24 **Grivennikov S**, Karin E, Terzic J, Mucida D, Yu GY, Vallabhapurapu S, Scheller J, Rose-John S, Cheroutre H, Eckmann L,

Karin M. IL-6 and Stat3 are required for survival of intestinal epithelial cells and development of colitis-associated cancer. *Cancer Cell* 2009; **15**: 103-113 [PMID: 19185845 DOI: 10.1016/j.ccr.2009.01.001]

25 **Popivanova BK**, Kitamura K, Wu Y, Kondo T, Kagaya T, Kaneko S, Oshima M, Fujii C, Mukaida N. Blocking TNF-alpha in mice reduces colorectal carcinogenesis associated with chronic colitis. *J Clin Invest* 2008; **118**: 560-570 [PMID: 18219394 DOI: 10.1172/JCI32453]

26 **Tonstad S**, Cowan JL. C-reactive protein as a predictor of disease in smokers and former smokers: a review. *Int J Clin Pract* 2009; **63**: 1634-1641 [PMID: 19732183 DOI: 10.1111/j.1742-1241.2009.02179.x]

27 **Choi J**, Joseph L, Pilote L. Obesity and C-reactive protein in various populations: a systematic review and meta-analysis. *Obes Rev* 2013; **14**: 232-244 [PMID: 23171381 DOI: 10.1111/obr.12003]

28 **Keum N**, Lee DH, Kim R, Greenwood DC, Giovannucci EL. Visceral adiposity and colorectal adenomas: dose-response meta-analysis of observational studies. *Ann Oncol* 2015; **26**: 1101-1109 [PMID: 25480876 DOI: 10.1093/annonc/mdu563]

29 **Myers GL**, Rifai N, Tracy RP, Roberts WL, Alexander RW, Biasucci LM, Catravas JD, Cole TG, Cooper GR, Khan BV, Kimberly MM, Stein EA, Taubert KA, Warnick GR, Waymack PP. CDC/AHA Workshop on Markers of Inflammation and Cardiovascular Disease: Application to Clinical and Public Health Practice: report from the laboratory science discussion group. *Circulation* 2004; **110**: e545-e549 [PMID: 15611379 DOI: 10.1161/01.CIR.0000148980.87579.5E]

30 **Smidowicz A**, Regula J. Effect of nutritional status and dietary patterns on human serum C-reactive protein and interleukin-6 concentrations. *Adv Nutr* 2015; **6**: 738-747 [PMID: 26567198 DOI: 10.3945/an.115.009415]

31 **Szylberg Ł**, Janiczek M, Popiel A, Marszałek A. Expression of COX-2, IL-1β, TNF-α and IL-4 in epithelium of serrated adenoma, adenoma and hyperplastic polyp. *Arch Med Sci* 2016; **12**: 172-178 [PMID: 26925134 DOI: 10.5114/aoms.2016.57594]

32 **Greenhough A**, Smartt HJ, Moore AE, Roberts HR, Williams AC, Paraskeva C, Kaidi A. The COX-2/PGE2 pathway: key roles in the hallmarks of cancer and adaptation to the tumour microenvironment. *Carcinogenesis* 2009; **30**: 377-386 [PMID: 19136477 DOI: 10.1093/carcin/bgp014]

33 **Groblewska M**, Mroczko B, Wereszczyńska-Siemiatkowska U, Kedra B, Lukaszewicz M, Baniukiewicz A, Szmitkowski M. Serum interleukin 6 (IL-6) and C-reactive protein (CRP) levels in colorectal adenoma and cancer patients. *Clin Chem Lab Med* 2008; **46**: 1423-1428 [PMID: 18844497 DOI: 10.1515/CCLM.2008.278]

P- Reviewer: Coleman HGG **S- Editor**: Ma YJ **L- Editor**: A
E- Editor: Wang CH

World Journal of Gastroenterology

Submit a Manuscript: http://www.wjgnet.com/esps/

World J Gastroenterol 2017 March 14; 23(10): 1920-1924

DOI: 10.3748/wjg.v23.i10.1920

ISSN 1007-9327 (print) ISSN 2219-2840 (online)

CASE REPORT

Supraclavicular lymph node metastases from malignant gastrointestinal stromal tumor of the jejunum: A case report with review of the literature

Chi Ma, Shao-Long Hao, Xin-Cheng Liu, Jin-Yao Nin, Guo-Chang Wu, Li-Xin Jiang, Alessandro Fancellu, Alberto Porcu, Hai-Tao Zheng

Chi Ma, Jin-Yao Nin, Guo-Chang Wu, Li-Xin Jiang, Hai-Tao Zheng, Department of Gastrointestinal and Thyroid Surgery, Yuhuangding Hospital Affiliated to Qingdao University, Yantai 264000, Shandong Province, China

Shao-Long Hao, Xin-Cheng Liu, Qingdao University Medical College, Qingdao 266021, Shandong Province, China

Alessandro Fancellu, Alberto Porcu, Unit of General Surgery, Department of Clinical and Experimental Medicine, University of Sassari, 07100 Sassari, Italy

Author contributions: Ma C drafted the manuscript, and contributed to acquisition of material; Hao SL and Liu XC collected material; Ning JY collected patient's information; Wu GC revised the manuscript, collected patient's information; Jiang LX revised the manuscript; Fancellu A and Porcu A revised the manuscript and modified the language; Zheng HT drafted the manuscript, and contributed to the acquisition of patient's information.

Institutional review board statement: Approved by the Yuhuangding Hospital Affiliated to Qingdao University Institutional Review Board.

Informed consent statement: All study participants, or their legal guardian, provided informed written consent prior to study enrollment.

Conflict-of-interest statement: There is no conflict of interest.

Manuscript source: Unsolicited manuscript

Correspondence to: Hai-Tao Zheng, PhD, Department of Gastrointestinal and Thyroid Surgery, Yuhuangding Hospital Affiliated to Qingdao University, No. 20 Yuhuangdingdong Road, Zhifu District, Yantai 264000, Shandong Province, China. machi_sdu@163.com
Telephone: +86- 535-6691999

Received: October 26, 2016
Peer-review started: October 28, 2016
First decision: December 19, 2017
Revised: January 5, 2017
Accepted: January 18, 2017
Article in press: January 18, 2017
Published online: March 14, 2017

Abstract

Gastrointestinal stromal tumors (GISTs) represent the most common mesenchymal tumors of the alimentary tract. These tumors may have different clinical and biological behaviors. Malignant forms usually spread via a hematogenous route, and lymph node metastases rarely occur. Herein, we report a patient with a jejunal GIST who developed supraclavicular lymph node metastasis. We conclude that lymphatic diffusion via the mediastinal lymphatic station to the supraclavicular lymph nodes can be a potential metastatic route for GISTs.

Key words: Gastrointestinal stromal tumor; Metastasis; Lymph nodes

Core tip: Unlike gastrointestinal carcinomas, lymph node metastases rarely develop in patients with malignant gastrointestinal stromal tumors (GISTs). We

report a patient with a jejunal GIST who developed supraclavicular lymph nodes metastasis and review the related literature. We conclude that lymphatic diffusion *via* mediastinal lymphatic station to the supraclavicular lymph nodes can be a potential metastatic route of GISTs.

Ma C, Hao SL, Liu XC, Nin JY, Wu GC, Jiang LX, Fancellu A, Porcu A, Zheng HT. Supraclavicular lymph node metastases from malignant gastrointestinal stromal tumor of the jejunum: A case report with review of the literature. *World J Gastroenterol* 2017; 23(10): 1920-1924 Available from: URL: http://www.wjgnet.com/1007-9327/full/v23/i10/1920.htm DOI: http://dx.doi.org/10.3748/wjg.v23.i10.1920

INTRODUCTION

Gastrointestinal stromal tumors (GISTs) represent the most common mesenchymal tumors of the alimentary tract. These tumors may have different clinical and biological behavior. Malignant forms usually spread *via* hematogenous route, and lymph nodes metastases rarely occur. Herein, we report a patient with jejunal GIST who developed supraclavicular lymph nodes metastasis.

CASE REPORT

A 56-year-old man with a 24-h history of melena was admitted to the gastrointestinal department of the Yuhuangding Hospital affiliated to Qingdao University, China. Laboratory assessment revealed a hemoglobin level of 8 g/dL. Urgent gastroduodenoscopy, colonoscopy, and enhanced computed tomography (CT) did not reveal any source of bleeding. During the next 24 h, the patient had further episodes of melena and became hemodynamically unstable after receiving a transfusion of 5 units of packed red blood cells and hemostatic agents. Therefore, emergency laparotomy was performed. Upon surgical exploration, a bleeding solid mass was found in the jejunum. Resection of a small bowel loop measuring 20 cm in length was performed. Gross examination revealed a nodular well-encapsulated tumor measuring 2 cm. Histologic sections showed a GIST infiltrating through all bowel layers, and it had features of mixed spindle and epithelioid types of cells. The mitotic index was > 5/50 high-power fields (HPFs). There was no infiltration of the surgical margins, and two harvested lymph nodes were free of metastases (Figure 1). CD117, CD34, and Dog-1 were positive in immunohistochemical studies; the Ki67 index was 20%. A diagnosis of GIST of the small intestine with high-grade malignancy was established based on the modified NIH GIST criteria[1]. Postoperative total body CT scan and positron emission tomography-computed tomography (PET-CT) were negative for metastatic disease. Adjuvant imatinib therapy was prescribed, but he declined it due to family and economic reasons.

One year later, the patient was admitted to the thyroid department at same hospital complaining of a left cervical mass that had been gradually enlarging over one month. Ultrasound revealed a hypoechoic mass above the left clavicle, measuring 3.1 cm x 4.6 cm; this mass was unenhanced in a contrast-enhanced CT scan (Figures 2 and 3). Interestingly,

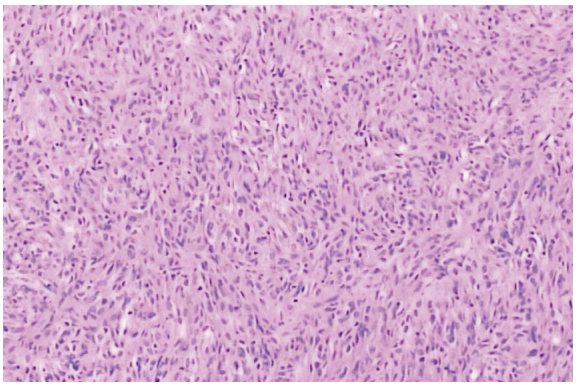

Figure 1 Histopathologic section of the primary tumor. The tumor was composed of spindle and epithelioid cells, which were predominantly arranged in spiral and lace-like shape (HE staining × 400).

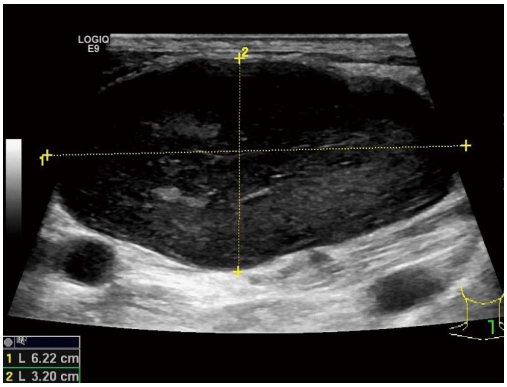

Figure 2 Ultrasonography of cervical mass: The mass was hypoechoic, with a smooth border and un-even internal echo.

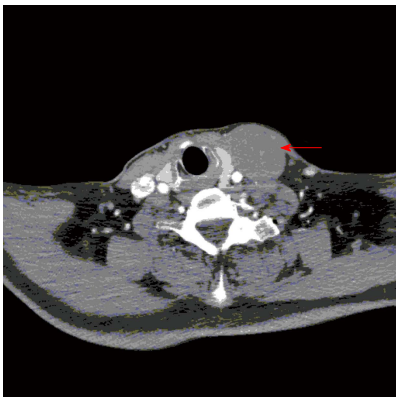

Figure 3 Computed tomography: The mass appeared as a low density cyst with clear edge without contrast enhancement.

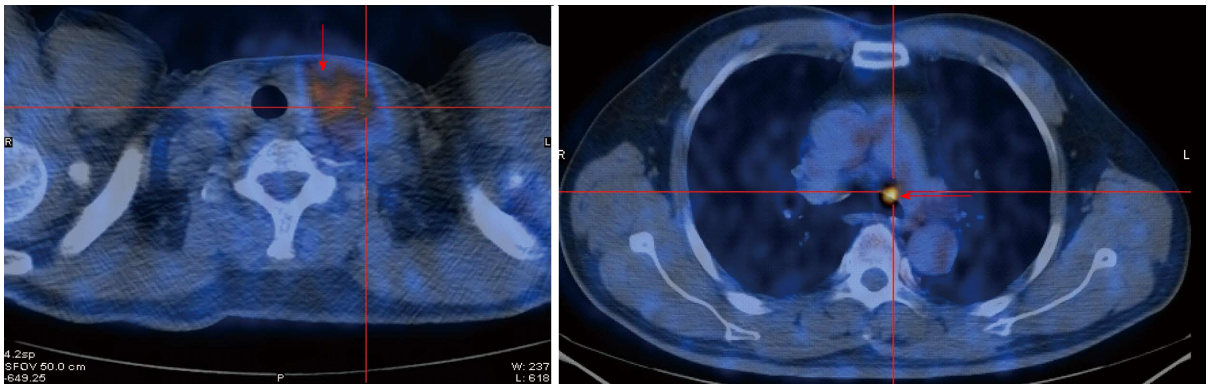

Figure 4 Positron emission tomography-computed tomography: FDG accumulated unevenly in the cervical mass and multiple lymph nodes in mediastinum.

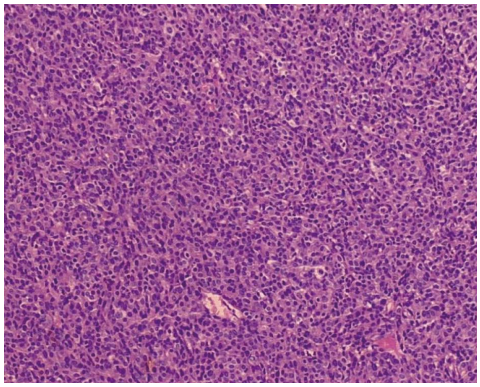

Figure 5 Histopathologic section of the cervical tumor (HE staining). The epithelioid cells were arranged in sheets, with abundant eosinophilic cytoplasm and prominent nuclei (HE staining × 400).

there were no alterations of the thyroid in imaging studies. Core needle biopsy was performed, and histopathological examination with hematoxylin-eosin staining revealed lymph node metastasis from a GIST. In immunohistochemical studies, CD117, CD34, and vim were positive, whereas calponin, estrogen, progesterone, and thyroglobulin were negative. A PET-CT scan showed uneven 18F-fluorodeoxyglucose (FDG) uptake in the cervical mass and multiple lymph nodes in the mediastinum (Figure 4). The patient underwent surgical removal of the cervical mass. Gross examination of the excised lymph node demonstrated that it measured 5 cm x 6 cm x8 cm and appeared irregular, smooth, and well encapsulated. Histopathologic examination again confirmed a metastasis from a GIST (Figure 5). Immunohistochemical studies of the resected lymph node showed positivity for CD117 and CD34 and negativity for Dog-1 and S-100. The Ki67 index was 30%. Insertion of GCC TAT in exon 9 of the c-KIT gene was identified with mutation analysis. Exons 11, 13, and 17 and the PDGFRα gene were wild type. After the second operation, the patient was regularly given imatinib at a dose of 400 mg per day. At 1 year following the surgery, the patient was asymptomatic, and there were no signs of tumor recurrence or progression (Table 1).

DISCUSSION

GISTs represent the most common neoplasms of mesenchymal origin of the gastrointestinal tract. GISTs may have different clinical and biological behavior, ranging from small benign tumors to aggressive forms that have a dismal prognosis. Approximately 20%-25% of GISTs are located in the stomach, and 40%-50% of those located in the small intestine were malignant neoplasms with features such as local recurrence after surgical removal, intraperitoneal dissemination and distant metastases[2]. However, unlike gastrointestinal carcinomas, lymph node metastases (LNMs) rarely develop in patients with malignant GISTs. The mainstay of treatment for GISTs is complete surgical resection without a regional lymph adenectomy[3,4].

The rates of LNMs from GISTs range from 0% to 5%[3,5,6]. A few studies reporting on this subject are summarized in Table 1[5,7-19]. Most of the reported cases are peritumoral lymph nodes metastases, which have occasionally been discovered with histopathological examination of surgical specimens. We found only 3 cases that could be defined as distant LNMs[14,18], including 2 inguinal lymph nodes and 1 axillary lymph node. In our case, LNMs developed in the left supraclavicular and mediastinal basins. This behavior is similar to that observed in malignant gastrointestinal tumors of an epithelial origin. To the best of our knowledge, this is the first case report of the lymphatic spread of a gastric GIST to supraclavicular and mediastinum lymph nodes. This might indicate that a particular subgroup of GISTs has biological characteristics similar to carcinomas.

According to the modified NIH GIST criteria, our case was a high-grade malignancy[1]. Ki67 expression changed from 20% in the primary tumor to 30% in the supraclavicular metastasis. Interestingly, Dog-1

Table 1 Clinical characteristics of cases reported

Ref.	Primary site	HPF	T size (cm)	Treatment	LNM site	LNM time	Gene mutation
Sato *et al*[7]	Gastric		4	Proximal gastrectomy	Right cardia	Pre	deletion mutation in exon 11
	Gastric		2.5	Wedge resection + partial hepatectomy	Adjacent to the tumor	Pre	No mutation
El Demellawy *et al*[8]	Small bowel				Mesenteric	Pre	
Hu *et al*[9]	Hepatic	4/10	15 × 10	Right hepatic lobectomy	Hilar	Post	
Canda *et al*[12]	Gastric	25/50	8 × 8 × 4	Distal gastrectomy + perigastric LN dissection	Perigastric	Pre	No mutation
Kong *et al*[13]	Small intestinal	2/50	6 × 7	Partial resection of the ileum	Peri-intestine	Pre	deletion 559-569 in exon 11
	Small intestinal	2/50	5 × 5	Partial resection of the ileum	Peri-intestine	Pre	Deletion 559-565 in exon 11
Zhang *et al*[14]	Gastric			Distal gastrectomy, perigastriclymphadenectomy and hepatectomy	Inguinal LN	Post	deletion 557/558 in exon 11
Yamada *et al*[15]	Gastric	> 5/50	4.5 × 3.5	Gastrectomy + lymph node dissection	Perigastric	Pre	
Catani *et al*[19]	Gastric			Gastrectomy + resection of the tail of the pancreas, the spleen, and the transverse colon	Perigastric	Pre	
Masuda *et al*[16]	Esophagus	15/50	9.5	Subtotal esophagectomy	Periesophagus	Pre	
Shafizad *et al*[17]	Gastric		8	Total gastrectomy and omentectomy	Perigastric	Pre	
Vassos *et al*[18]	Ileum			Partial resection of the ileum	Inguinal	Pre	
	Gastric			Extended gastrectomy, atypical liver resection, splenectomy	Auxiliary	Post	
Sakurai *et al*[10]	Esophagus			Middle and lower esophagectomy	Multiple	Post	
Asakage *et al*[11]	Gastric			Total gastrectomy with distal pancreatosplenectomy and segmental liver resection	Perigastric	Pre	
Tashiro *et al*[5]	Gastric		1-5				No mutation
	Gastric	Ki67 10%	2.5	Proximal gastrectomy with sampling of the regional LNs			Exon 11

HPF: High-power fields; LNM: Lymph node metastases; Pre: Before or during operation; Post: After operation.

was negative in the LNM, whereas it was positive in primary tumor. It could be speculated that the Ki67 and Dog-1 levels may be markers of a primary tumor de-differentiation tendency.

Activating mutations of the c-kit gene (especially exons 11 and 9) are present in most GISTs and probably play a fundamental role in the development of these tumors. Among the reported cases of LNMs from GISTs, few gene detection results have been described, most of which are exon 11 mutations[5,7,13,14]. In the study by Kong *et al*[13], the exon 11 mutation was linked to the likelihood of LNMs. However, in our case, we found an exon 9 mutation. This genetic mutation in the LNMs from GISTs has not been reported to date. The relationship between gene mutations and LNMs is still not clear, but many authors have stated that KIT exon 9-mutant tumors developed imatinib resistance more frequently than exon 11-mutant tumors[20,21]. Cases with exon 9-mutant tumors should be treated with increased imatinib doses. Because the patient declined imatinib treatment after the first surgery, he was treated with 400 mg of imatinib per day after the second operation.

In conclusion, complete surgical resection remains the mainstay of treatment for resectable GISTs. Imatinib is currently indicated for the first-line treatment of patients with metastatic or unresectable KIT-positive GISTs. Adjuvant therapy with imatinib was deemed necessary for this patient following complete resection of a primary jejunual tumor because it was an aggressive, high-risk form of GIST. Unfortunately, he did not take imatinib after his first operation, and distant lymph node metastases occurred after 12 months. Following the second operation, the patient received imatinib treatment and had survived without disease progression at the 1-year follow up.

This case confirms that LNMs in the mediastinum and supraclavicular lymph nodes is a potential metastatic route for malignant GISTs. Further studies are needed to clarify the mechanism of lymph node metastases in patients with GISTs.

COMMENTS

Case characteristics

The patient was admitted to hospital, complaining of a left cervical mass, which had been diagnosed as a jejunum gastrointestinal stromal tumor (GIST) and cured by surgery 1 year before.

Clinical diagnosis

For the differential diagnoses of thyroid tumor, lymphoma, or metastatic carcinoma, the patient underwent computed tomography (CT), ultrasound (US), positron emission tomography-computed tomography (PET-CT) and biopsy. US, CT and PET-CT revealed a hypoechoic, unenhanced and uneven FDG uptake mass above the left clavicle measuring 3.1 cm × 4.6 cm.

Laboratory diagnosis

After a biopsy of the cervical mass, this patient was diagnosed as having supraclavicular lymph node metastases from GISTs.

Pathological diagnosis

Core needle biopsy was carried out, and the histopathological examination using hematoxylin-eosin stain showed lymph node metastasis from GIST.

Treatment

The patient underwent surgical removal of the cervical mass and was regularly given imatinib 400 mg per day after the second operation.

Experiences and lessons

This case confirms that LNM in the mediastinum and supraclavicular lymph nodes are a potential metastatic route of malignant GISTs. Physicians should be aware of this during operation and chemotherapy. In this case report, we tried to give some but not sufficient evidence of the possible mechanisms of the supraclavicular lymph node metastasis.

Peer-review

This case report is well organized and had much information including genetic analysis data on primary GIST and metastatic lesion.

REFERENCES

1 **Joensuu H**. Risk stratification of patients diagnosed with gastrointestinal stromal tumor. *Hum Pathol* 2008; **39**: 1411-1419 [PMID: 18774375 DOI: 10.1016/j.humpath.2008.06.025]

2 **Miettinen M**, Lasota J. Gastrointestinal stromal tumors: review on morphology, molecular pathology, prognosis, and differential diagnosis. *Arch Pathol Lab Med* 2006; **130**: 1466-1478 [PMID: 17090188 DOI: 10.1043/1543-2165(2006)130]

3 **DeMatteo RP**, Lewis JJ, Leung D, Mudan SS, Woodruff JM, Brennan MF. Two hundred gastrointestinal stromal tumors: recurrence patterns and prognostic factors for survival. *Ann Surg* 2000; **231**: 51-58 [PMID: 10636102]

4 **Pierie JP**, Choudry U, Muzikansky A, Yeap BY, Souba WW, Ott MJ. The effect of surgery and grade on outcome of gastrointestinal stromal tumors. *Arch Surg* 2001; **136**: 383-389 [PMID: 11296107]

5 **Tashiro T**, Hasegawa T, Omatsu M, Sekine S, Shimoda T, Katai H. Gastrointestinal stromal tumour of the stomach showing lymph node metastases. *Histopathology* 2005; **47**: 438-439 [PMID: 16178904 DOI: 10.1111/j.1365-2559.2005.02133.x]

6 **Aparicio T**, Boige V, Sabourin JC, Crenn P, Ducreux M, Le Cesne A, Bonvalot S. Prognostic factors after surgery of primary resectable gastrointestinal stromal tumours. *Eur J Surg Oncol* 2004; **30**: 1098-1103 [PMID: 15522557 DOI: 10.1016/j.ejso.2004.06.016]

7 **Sato T**, Kanda T, Nishikura K, Hirota S, Hashimoto K, Nahagawa S, Ohashi M, Hatakeyama K. Two cases of gastrointestinal stromal tumor of the stomach with lymph node metastasis. *Hepatogastroenterology* 2007; **54**: 1057-1060 [PMID: 17629038]

8 **El Demellawy D**, Shokry P, Ing A, Khalifa M. Polypoid gastrointestinal stromal tumor of small bowel metastasizing to mesenteric lymph nodes: a case report. *Pathol Res Pract* 2008; **204**: 197-201 [PMID: 18096326 DOI: 10.1016/j.prp.2007.10.007]

9 **Hu X**, Forster J, Damjanov I. Primary malignant gastrointestinal stromal tumor of the liver. *Arch Pathol Lab Med* 2003; **127**: 1606-1608 [PMID: 14632569 DOI: 10.1043/1543-2165(2003)127<1606:pmgsto>2.0.co;2]

10 **Sakurai N**, Yamauchi J, Shibuma H, Ikeda E, Sasou S. [A case of recurrent GIST of the esophagus which completely responded to imatinib mesilate]. *Gan To Kagaku Ryoho* 2007; **34**: 237-240 [PMID: 17301535]

11 **Asakage N**, Kobayashi S, Gotou T, Sasaki M, Tsukada K, Suzuki T, Yamamoto T, Sekine M, Miyazaki E, Hirai S, Yamasaki S. [Two cases of gastrointestinal stromal tumor (GIST) of the stomach and a consideration of its malignancy potential and treatment strategy - report of two cases]. *Gan To Kagaku Ryoho* 2007; **34**: 919-923 [PMID: 17565257]

12 **Canda AE**, Ozsoy Y, Nalbant OA, Sagol O. Gastrointestinal stromal tumor of the stomach with lymph node metastasis. *World J Surg Oncol* 2008; **6**: 97 [PMID: 18775061 DOI: 10.1186/1477-7819-6-97]

13 **Kong M**, Wang YL, Xu LJ, Teng XD. [Gastrointestinal stromal tumor of small intestine associated with lymph node metastasis: a report of 2 cases with review of literatures]. *Zhonghua Bing Li Xue Za Zhi* 2009; **38**: 617-620 [PMID: 20079191]

14 **Zhang Q**, Yu JW, Yang WL, Liu XS, Yu JR. Gastrointestinal stromal tumor of stomach with inguinal lymph nodes metastasis: a case report. *World J Gastroenterol* 2010; **16**: 1808-1810 [PMID: 20380018 DOI: 10.3748/wjg.v16.i14.1808]

15 **Yamada E**, Oyaizu T, Miyashita T. [A case of gastrointestinal stromal tumor of the stomach with lymph node metastasis followed up for 7 years without evidence of recurrence after surgery]. *Nihon Shokakibyo Gakkai Zasshi* 2010; **107**: 743-749 [PMID: 20460848]

16 **Masuda T**, Toh Y, Kabashima A, Aoki Y, Harimoto N, Ito S, Taomoto J, Ikeda O, Ohga T, Adachi E, Sakaguchi Y, Hirahashi M, Nishiyama K, Okamura T. Overt lymph node metastases from a gastrointestinal stromal tumor of the esophagus. *J Thorac Cardiovasc Surg* 2007; **134**: 810-811 [PMID: 17723845 DOI: 10.1016/j.jtcvs.2007.06.002]

17 **Shafizad A**, Mohammadianpanah M, Nasrolahi H, Mokhtari M, Mousavi SA. Lymph Node Metastasis in Gastrointestinal Stromal Tumor (GIST): to Report a Case. *Iran J Cancer Prev* 2014; **7**: 171-174 [PMID: 25250169]

18 **Vassos N**, Agaimy A, Hohenberger W, Croner RS. Extraabdominal lymph node metastasis in gastrointestinal stromal tumors (GIST). *J Gastrointest Surg* 2011; **15**: 1232-1236 [PMID: 21336495 DOI: 10.1007/s11605-011-1464-3]

19 **Catani M**, De Milito R, Simi M. [New orientations in the management of advanced, metastatic gastrointestinal stromal tumors (GIST): combination of surgery and systemic therapy with imatinib in a case of primary gastric location]. *Chir Ital* 2005; **57**: 127-133 [PMID: 15832750]

20 **Heinrich MC**, Owzar K, Corless CL, Hollis D, Borden EC, Fletcher CD, Ryan CW, von Mehren M, Blanke CD, Rankin C, Benjamin RS, Bramwell VH, Demetri GD, Bertagnolli MM, Fletcher JA. Correlation of kinase genotype and clinical outcome in the North American Intergroup Phase III Trial of imatinib mesylate for treatment of advanced gastrointestinal stromal tumor: CALGB 150105 Study by Cancer and Leukemia Group B and Southwest Oncology Group. *J Clin Oncol* 2008; **26**: 5360-5367 [PMID: 18955451 DOI: 10.1200/jco.2008.17.4284]

21 **Lee JH**, Kim Y, Choi JW, Kim YS. Correlation of imatinib resistance with the mutational status of KIT and PDGFRA genes in gastrointestinal stromal tumors: a meta-analysis. *J Gastrointestin Liver Dis* 2013; **22**: 413-418 [PMID: 24369323]

P- Reviewer: Alimehmeti RH, Kim ST **S- Editor**: Qi Y
L- Editor: Ma JY **E- Editor**: Wang CH

Published by **Baishideng Publishing Group Inc**
8226 Regency Drive, Pleasanton, CA 94588, USA
Telephone: +1-925-223-8242
Fax: +1-925-223-8243
E-mail: bpgoffice@wjgnet.com
Help Desk: http://www.wjgnet.com/esps/helpdesk.aspx
http://www.wjgnet.com

ISSN 1007-9327